Serological Analysis to Accompany Clinical Research, Vaccination and Evolution of the COVID-19 Pandemic

Dissertation

der Mathematisch-Naturwissenschaftlichen Fakultät

der Eberhard Karls Universität Tübingen

zur Erlangung des Grades eines

Doktors der Naturwissenschaften

(Dr. rer. nat.)

vorgelegt von

Matthias Becker

aus Tübingen

Tübingen

2022

Gedruckt mit Genehmigung der Mathematisch-Naturwissenschaftlichen Fakultät der Eberhard Karls Universität Tübingen.

"It is the power of the mind to be unconquerable."

- Seneca.

Table of Contents

Abstract

The COVID-19 pandemic is resulting in a constantly fluctuating and challenging field of research, where public health and socioeconomic decisions must be accompanied by hard scientific evidence. In the work of this thesis, we developed, validated and applied MULTICOV-AB, a multiplex serological assay as a tool for in-depth analysis of the SARS-CoV-2 humoral immune response.

In our clinical assay validation, we achieved improved sensitivity and specificity over widely used commercial assays for classification of previous infection. Although initially hypothesized, we found no evidence of cross-protection from endemic human coronaviruses. During the first wave of the pandemic, children were found to get infected at a lower than average rate and were more often asymptomatic, which we were able to associate with increased antibody formation over adults. Furthermore, we found seroconversion to be independent of a symptomatic course of infection in children and adults.

COVID-19 vaccines were developed and widely disseminated in the population at an unprecedented pace. With the developed assay, we verified early on that mRNA vaccines, which saw their first widespread use during the COVID-19 pandemic, were able to induce a strong humoral immune response. We further found that homologous vector based vaccination elicited an inferior humoral response, in terms of titre and neutralizing activity. In addition, we showed that the humoral immune response peaked roughly 28 days post immunisation and steadily declined over six months, which was compensated by booster vaccinations. Furthermore, we found vaccines to introduce an inferior humoral immune response in patients on haemodialysis and observed fast decreasing antibody levels.

Rapid evolution of SARS-CoV-2 resulted in the emergence of virus variants with key mutations, which called into question the effectiveness of vaccine protection. In response, we expanded MULTICOV-AB to include variant-specific antigens. We could show that some virus variants like Alpha and Delta exhibited mild to moderate levels of immune evasion, while others were associated with heavily diminished antibody binding, such as the Omicron sub-lineages. Overall, we were able to deliver data on vaccines, virus variants and groups of special interest such as children or haemodialysis patients in a time sensitive manner, thereby expediting adaption of official recommendations for vaccination regimens as and furthering the understanding of the immunity towards SARS-CoV-2.

IV

Zusammenfassung

Die COVID-19-Pandemie führt zu einem sich ständig verändernden und herausfordernden Forschungsbereich, in dem Entscheidungen im Bereich der öffentlichen Gesundheit und der Sozioökonomie durch belastbare wissenschaftliche Beweise begleitet werden müssen. Im Rahmen dieser Arbeit haben wir MULTICOV-AB, einen serologischen Multiplex-Assay als Methode für die eingehende Analyse der humoralen Immunantwort auf SARS-CoV-2 entwickelt, validiert und angewandt.

In der klinischen Assay Validierung erzielten wir für die Klassifizierung einer zurückliegenden Infektion eine verbesserte Sensitivität und Spezifität im direkten Vergleich mit weit verbreiteten kommerziellen Assays. Obgleich initial vermutet, fanden wir keine Hinweise auf eine Kreuzprotektivität durch endemische humane Coronaviren. Während der ersten Welle der Pandemie infizierten sich Kinder unterdurchschnittlich oft und waren häufiger asymptomatisch, was wir mit einer erhöhten Antikörperbildung im Vergleich zu Erwachsenen assoziieren konnten. Des Weiteren konnten wir feststellen, dass die Serokonversion bei Kindern und Erwachsenen unabhängig von einem symptomatischen Verlauf der Infektion ist.

COVID-19 Impfstoffe wurden in einem beispiellosen Tempo entwickelt und in der Bevölkerung angewandt. Mit dem entwickelten Assay konnten wir schon früh verifizieren, dass mRNA-Impfstoffe, die erstmals während der COVID-19-Pandemie in großem Umfang eingesetzt wurden, eine starke humorale Immunantwort induzieren. Wir haben außerdem festgestellt, dass die homologe Impfung mit Vektor-basierten Impfstoffen in Bezug auf Titer und neutralisierende Aktivität eine schwächere humorale Immunantwort hervorruft. Zudem haben wir gezeigt, dass die humorale Immunantwort etwa 28 Tage nach der Immunisierung ihren Höhepunkt erreicht und danach über sechs Monate hinweg stetig abnimmt, was durch Auffrischungsimpfungen kompensiert werden konnte. Außerdem stellten wir fest, dass Impfstoffe bei Personen auf Hämodialyse eine schwächere humorale Immunantwort auslösen, und beobachteten schnell abnehmende Antikörperspiegel.

Die rapide Evolution von SARS-CoV-2 führte zum Auftreten von Virusvarianten mit Schlüsselmutationen, die die Wirksamkeit des Impfschutzes in Frage stellten. Daraufhin haben wir MULTICOV-AB mit variantenspezifischen Antigenen erweitert. Wir konnten zeigen, dass einige Virusvarianten wie Alpha und Delta nur geringe bis mittelstarke Immunevasion aufweisen, während andere, wie die Omicron-Subtypen, mit einer stark verminderten Antikörperbindung verbunden sind. Zusammenfassend konnten wir Daten über Impfstoffe, Virusvarianten und Gruppen von besonderem Interesse, wie Kinder oder Personen auf Hämodialyse zeitnah liefern und konnten so die Anpassung der offiziellen Empfehlungen für Impfschemata beschleunigten und das Verständnis der Immunität gegen SARS-CoV-2 voranbringen.

Abbreviations

%CV   Coefficient of Variation in Percent (For a set of values defined as the standard deviation divided by the Mean and multiplied by 100)

AZE   COVID-19 vaccine Vaxzevria from AstraZeneca AB

Beads   xMAP magnetic microspheres

BNT   COVID-19 vaccine BNT162b2 / Comirnaty by BioNTech Manufacturing GmbH

COVID-19   Coronavirus Disease 2019

ELISA   Enzyme-linked immunosorbent assay

EMA   European Medicines Agency

FDA   United States Food and Drug Administration

hCoV   Endemic human coronavirus

IgA   Immunoglobulin A

IgG   Immunoglobulin G

IgM   Immunoglobulin M

JJ   COVID-19 vaccine Jcovden by Janssen-Cilag International NV

MOD   COVID-19 vaccine mRNA-1273 / Spikevax from Moderna Biotech Spain, S.L.

QC   Quality control

RBD   SARS-CoV-2 Spike protein receptor binding domain

STIKO   German Standing Committee on Vaccination

VoC   SARS-CoV-2 Variant of Concern

VoI   SARS-CoV-2 Variant of Interest

WHO   World Health Organisation

List of Figures

x

List of Tables

List of Publications

Key publications for this thesis

 * = Authors contributed equally

1. **Matthias Becker***, Monika Strengert*, Daniel Junker, Philipp D. Kaiser, Tobias Kerrinnes, Bjoern Traenkle, Heiko Dinter, Julia Häring, Stéphane Ghozzi, Anne Zeck, Frank Weise, Andreas Peter, Sebastian Hörber, Simon Fink, Felix Ruoff, Alex Dulovic, Tamam Bakchoul, Armin Baillot, Stefan Lohse, Markus Cornberg, Thomas Illig, Jens Gottlieb, Sigrun Smola, André Karch, Klaus Berger, Hans-Georg Rammensee, Katja Schenke-Layland, Annika Nelde, Melanie Märklin, Jonas S. Heitmann, Juliane S. Walz, Markus Templin, Thomas O. Joos, Ulrich Rothbauer, Gérard Krause & Nicole Schneiderhan-Marra, **Exploring beyond clinical routine SARS-CoV-2 serology using MultiCoV-Ab to evaluate endemic coronavirus cross-reactivity**, *Nature Communications*, https://doi.org/10.1038/s41467-021-20973-3

2. **Matthias Becker***, Alex Dulovic*, Daniel Junker, Natalia Ruetalo, Philipp D. Kaiser, Yudi T. Pinilla, Constanze Heinzel, Julia Haering, Bjoern Traenkle, Teresa R. Wagner, Mirjam Layer, Martin Mehrlaender, Valbona Mirakaj, Jana Held, Hannes Planatscher, Katja Schenke-Layland, Gérard Krause, Monika Strengert, Tamam Bakchoul, Karina Althaus, Rolf Fendel, Andrea Kreidenweiss, Michael Koeppen, Ulrich Rothbauer, Michael Schindler & Nicole Schneiderhan-Marra, **Immune response to SARS-CoV-2 variants of concern in vaccinated individuals**, *Nature Communications*, https://doi.org/10.1038/s41467-021-23473-6

3. Hanna Renk*, Alex Dulovic*, Alina Seidel*, **Matthias Becker**, Dorit Fabricius, Maria Zernickel, Daniel Junker, Rüdiger Groß, Janis Müller, Alexander Hilger, Sebastian F. N. Bode, Linus Fritsch, Pauline Frieh, Anneke Haddad, Tessa Görne, Jonathan Remppis, Tina Ganzemueller, Andrea Dietz, Daniela Huzly, Hartmut Hengel, Klaus Kaier, Susanne Weber, Eva-Maria Jacobsen, Philipp D. Kaiser, Bjoern Traenkle, Ulrich Rothbauer, Maximilian Stich, Burkhard Tönshoff, Georg F. Hoffmann, Barbara Müller, Carolin Ludwig, Bernd Jahrsdörfer, Hubert Schrezenmeier, Andreas Peter, Sebastian Hörber, Thomas Iftner, Jan Münch, Thomas Stamminger, Hans-Jürgen Groß, Martin Wolkewitz, Corinna Engel, Weimin Liu, Marta Rizzi, Beatrice H. Hahn, Philipp Henneke, Axel R. Franz, Klaus-Michael Debatin, Nicole Schneiderhan-Marra, Ales Janda & Roland Elling, **Robust and durable serological response following pediatric SARS-CoV-2 infection**, *Nature Communications*, https://doi.org/10.1038/s41467-021-27595-9

4. Alex Dulovic*, Barbora Kessel*, Manuela Harries*, **Matthias Becker**, Julia Ortmann, Johanna Griesbaum, Jennifer Jüngling, Daniel Junker, Pilar Hernandez, Daniela Gornyk, Stephan Glöckner, Vanessa Melhorn, Stefanie Castell, Jana-Kristin Heise, Yvonne Kemmling, Torsten Tonn, Kerstin Frank, Thomas Illig, Norman Klopp, Neha Warikoo, Angelika Rath, Christina Suckel, Anne Ulrike Marzian, Nicole Grupe, Philipp D. Kaiser, Bjoern Traenkle, Ulrich Rothbauer, Tobias Kerrinnes, Gérard Krause, Berit Lange, Nicole Schneiderhan-Marra & Monika Strengert, **Comparative Magnitude and Persistence of Humoral SARS-CoV-2 Vaccination Responses in the Adult population in Germany**, *Frontiers in Immunology*, https://doi.org/10.3389/fimmu.2022.828053

5. Daniel Junker*, **Matthias Becker***, Teresa R. Wagner*, Philipp D. Kaiser, Sandra Maier, Tanja M. Grimm, Johanna Griesbaum, Patrick Marsall, Jens Gruber, Bjoern Traenkle, Constanze Heinzel, Yudi T. Pinilla, Jana Held, Rolf Fendel, Andrea Kreidenweiss, Annika Nelde, Yacine Maringer, Sarah Schroeder, Juliane S. Walz, Karina Althaus, Gunalp Uzun, Marco Mikus, Tamam Bakchoul, Katja Schenke-Layland, Stefanie Bunk, Helene Haeberle, Siri Göpel, Michael Bitzer, Hanna Renk, Jonathan Remppis, Corinna Engel, Axel R. Franz, Manuela Harries, Barbora Kessel, Berit Lange, Monika Strengert, Gerard Krause, Anne Zeck, Ulrich Rothbauer & Alex Dulovic, **Antibody binding and ACE2 binding inhibition is significantly reduced for both the BA.1 and BA.2 omicron variants**, *Clinical Infectious Diseases*, https://doi.org/10.1093/cid/ciac498

6. Monika Strengert*, **Matthias Becker***, Gema Morillas Ramos*, Alex Dulovic, Jens Gruber, Jennifer Juengling, Karsten Lürken, Andrea Beigel, Eike Wrenger, Gerhard Lonnemann, Anne Cossmann, Metodi V. Stankov, Alexandra Dopfer-Jablonka, Philipp D. Kaiser, Bjoern Traenkle, Ulrich Rothbauer, Gérard Krause, Nicole Schneiderhan-Marra & Georg M.N. Behrens, **Cellular and humoral immunogenicity of a SARS-CoV-2 mRNA vaccine in patients on haemodialysis**, *eBioMedicine*, *https://doi.org/10.1016/j.ebiom.2021.103524*

7. Alex Dulovic*, Monika Strengert*, Gema Morillas Ramos*, **Matthias Becker**, Johanna Griesbaum, Daniel Junker, Karsten Lürken, Andrea Beigel, Eike Wrenger, Gerhard Lonnemann, Anne Cossmann, Metodi V. Stankov, Alexandra Dopfer-Jablonka, Philipp D. Kaiser, Bjoern Traenkle, Ulrich Rothbauer, Gérard Krause, Nicole Schneiderhan-Marra & Georg M.N. Behrens, **Diminishing Immune Responses against Variants of Concern in Dialysis Patients 4 Months after SARS-CoV-2 mRNA Vaccination**, *Emerging Infectious Diseases*, https://doi.org/10.3201/eid2804.211907

8. **Matthias Becker***, Anne Cossmann*, Karsten Lürken, Daniel Junker, Jens Gruber, Jennifer Juengling, Gema Morillas Ramos, Andrea Beigel, Eike Wrenger, Gerhard Lonnemann, Metodi V. Stankov, Alexandra Dopfer-Jablonka, Philipp D. Kaiser, Bjoern Traenkle, Ulrich Rothbauer, Gérard Krause, Nicole Schneiderhan-Marra, Monika Strengert, Alex Dulovic & Georg M.N. Behrens, **Longitudinal cellular and humoral immune responses after triple BNT162b2 and fourth full-dose mRNA-1273 vaccination in haemodialysis patients**, *Frontiers in Immunology*, https://doi.org/10.3389/fimmu.2022.1004045

Author contribution

Manuscript Number	1	2	3	4	5	6	7	8
Accepted for publication	yes	yes	yes	yes	yes	yes	yes	yes
Number of authors	36	26	50	32	40	19	19	20
Position of candidate in list of authors	1	1	4	4	1	1	4	1
Scientific ideas by candidate (%)	50	50	10	10	40	20	20	20
Data generation by candidate (%)	50	50	30	10	20	40	10	20
Interpretation and analysis by candidate (%)	70	70	50	50	50	60	50	60
Paper writing by candidate (%)	70	30	10	20	30	20	10	30

Publications with Co-Authorship that are not part of this thesis

9. Annika Nelde*, Tatjana Bilich*, Jonas S. Heitmann*, Yacine Maringer, Helmut R. Salih, Malte Roerden, Maren Lübke, Jens Bauer, Jonas Rieth, Marcel Wacker, Andreas Peter, Sebastian Hörber, Bjoern Traenkle, Philipp D. Kaiser, Ulrich Rothbauer, **Matthias Becker**, Daniel Junker, Gérard Krause, Monika Strengert, Nicole Schneiderhan-Marra, Markus F. Templin, Thomas O. Joos, Daniel J. Kowalewski, Vlatka Stos-Zweifel, Michael Fehr, Armin Rabsteyn, Valbona Mirakaj, Julia Karbach, Elke Jäger, Michael Graf, Lena-Christin Gruber, David Rachfalski, Beate Preuß, Ilona Hagelstein, Melanie Märklin, Tamam Bakchoul, Cécile Gouttefangeas, Oliver Kohlbacher, Reinhild Klein, Stefan Stevanović, Hans-Georg Rammensee & Juliane S. Walz, **SARS-CoV-2-derived peptides define heterologous and COVID-19-induced T cell recognition**, *Nature Immunology*, https://doi.org/10.1038/s41590-020-00808-x

10. Luciano F. Huergo, Khaled A. Selim, Marcelo S. Conzentino, Edileusa C. M. Gerhardt, Adrian R. S. Santos, Berenike Wagner, Janette T. Alford, Nelli Deobald, Fabio O. Pedrosa, Emanuel M. de Souza, Meri B. Nogueira, Sônia M. Raboni, Dênio Souto, Fabiane G. M. Rego, Dalila L. Zanette, Mateus N. Aoki, Jeanine M. Nardin, Bruna Fornazari, Hugo M. P. Morales, Vânia A. Borges, Annika Nelde, Juliane S. Walz, **Matthias Becker**, Nicole Schneiderhan-Marra, Ulrich Rothbauer, Rodrigo A. Reis, & Karl Forchhammer, **Magnetic Bead-Based Immunoassay Allows Rapid, Inexpensive, and Quantitative Detection of Human SARS-CoV-2 Antibodies**, *ACS Sensors*, https://doi.org/10.1021/acssensors.0c02544

11. Simon Fink*, Felix Ruoff*, Aaron Stahl, **Matthias Becker**, Philipp Kaiser, Bjoern Traenkle, Daniel Junker, Frank Weise, Natalia Ruetalo, Sebastian Hörber, Andreas Peter, Annika Nelde, Juliane Walz, Gérard Krause, Armin Baillot, Katja Schenke-Layland, Thomas O. Joos, Ulrich Rothbauer, Nicole Schneiderhan-Marra, Michael Schindler & Markus F. Templin, **Multiplexed Serum Antibody Screening Platform Using Virus Extracts from Endemic Coronaviridae and SARS-CoV-2**, *ACS Infectious Diseases*, https://doi.org/10.1021/acsinfecdis.0c00725

12. Teresa R. Wagner*, Elena Ostertag*, Philipp D. Kaiser, Marius Gramlich, Natalia Ruetalo, Daniel Junker, Julia Haering, Bjoern Traenkle, **Matthias Becker**, Alex Dulovic, Helen Schweizer, Stefan Nueske, Armin Scholz, Anne Zeck, Katja Schenke-Layland, Annika Nelde, Monika Strengert, Juliane S. Walz, Georg Zocher, Thilo Stehle, Michael Schindler, Nicole Schneiderhan-Marra & Ulrich Rothbauer, **NeutrobodyPlex— monitoring SARS-CoV-2 neutralizing immune responses using nanobodies**, *EMBO Reports*, https://doi.org/10.15252/embr.202052325

13. Teresa R. Wagner*, Daniel Schnepf*, Julius Beer*, Natalia Ruetalo*, Karin Klingel, Philipp D. Kaiser, Daniel Junker, Martina Sauter, Bjoern Traenkle, Desiree I. Frecot, **Matthias Becker**, Nicole Schneiderhan-Marra, Annette Ohnemus, Martin Schwemmle, Michael Schindler & Ulrich Rothbauer, **Biparatopic nanobodies protect mice from lethal challenge with SARS-CoV-2 variants of concern**, *EMBO Reports*, https://doi.org/10.15252/embr.202153865

14. Daniel Junker, Alex Dulovic, **Matthias Becker**, Teresa R. Wagner, Philipp D. Kaiser, Bjoern Traenkle, Katharina Kienzle, Stefanie Bunk, Carlotta Struemper, Helene Haeberle, Kristina Schmauder, Natalia Ruetalo, Nisar Malek, Karina Althaus, Michael Koeppen, Ulrich Rothbauer, Juliane S. Walz, Michael Schindler, Michael Bitzer, Siri Göpel & Nicole Schneiderhan-Marra, **COVID-19 patient serum less potently inhibits ACE2-RBD binding for various SARS-CoV-2 RBD mutants**, *Scientific Reports*, https://doi.org/10.1038/s41598-022-10987-2

Chapter 1: Introduction

1.1. The COVID-19 Pandemic and SARS-CoV-2

1.1.1.   The Beginning of the COVID-19 Pandemic

In late 2019, a localised outbreak characterised by heavy and often fatal pneumatic disease symptoms was reported in Wuhan, China[1,2]. The causative agent was identified to be a novel Coronavirus, which is now believed to have spilled over from its animal reservoir to humans via bats[2,3]. Within weeks of the first reported cases, a full genome sequence was made available[4,5]. The novel virus revealed a striking homology to the causative agent of Severe Acute Respiratory Syndrome or SARS, named SARS-CoV (assigned SARS-CoV-1 in this thesis), which saw an outbreak with more than 750 deaths in 2003[6,7].
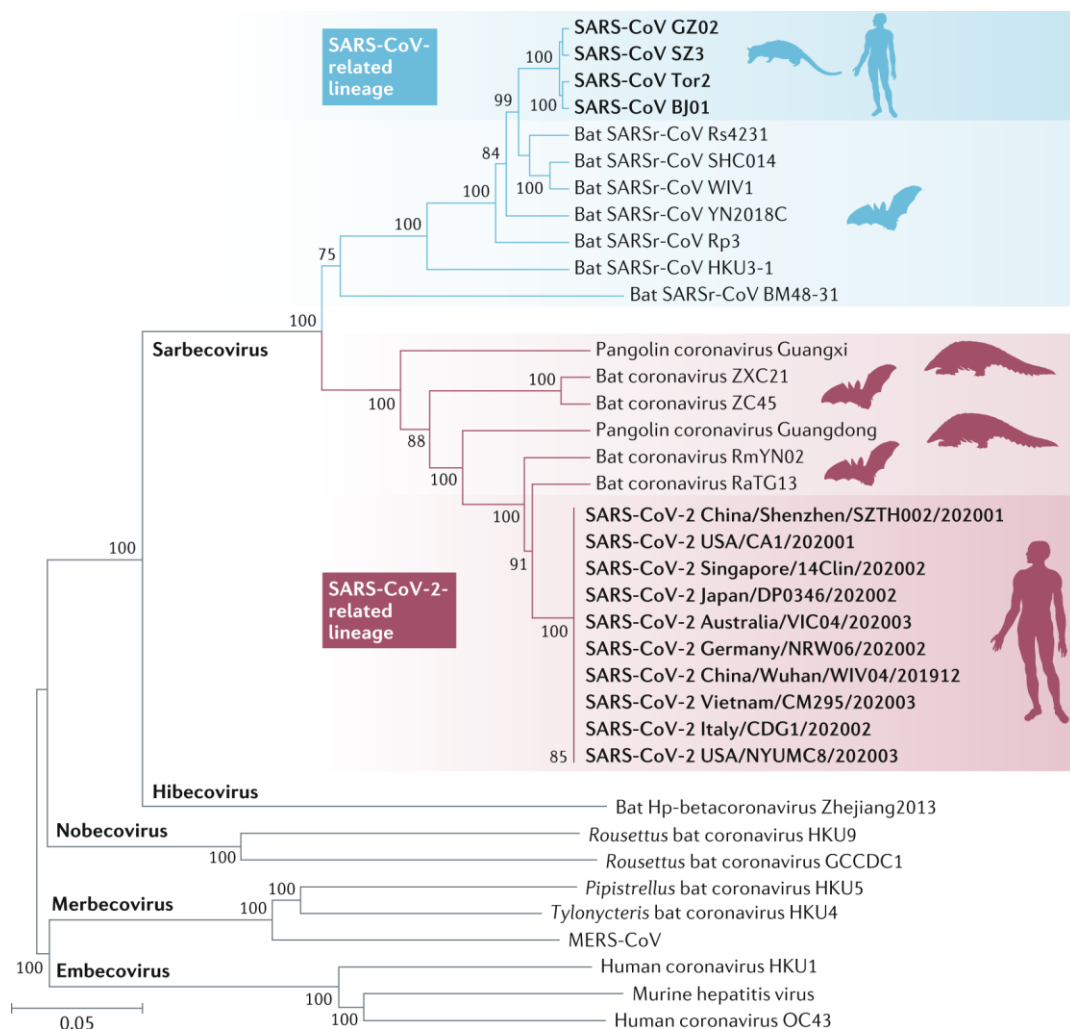
Figure 1: SARS-CoV-2 phylogenetic tree
Phylogenetic tree of early SARS-CoV-2 genome sequences and other betacoronaviruses, highlighting likely bat origin and relation to SARS-CoV-1. Reprinted by permission from Springer Nature Customer Service Centre GmbH: Springer Nature Reviews Microbiology (Characteristics of SARS-CoV-2 and COVID-19, Ben Hu et al.[8]), © (2020).

The novel disease was termed Coronavirus Disease 2019 (COVID-19) and the virus was initially designated 2019-nCoV[1,2], which was later changed to SARS-CoV-2[9]. A phylogenetic tree highlighting early SARS-CoV-2 genome sequences in within the genus of betacoronaviruses is shown in **Figure 1**.

Within weeks, SARS-CoV-2 spread throughout the Wuhan province and China, with 125 infections reported by January 19th 2020[10]. Shortly afterwards, more and more countries began to report cases, with the first case in Germany officially confirmed on January 27th 2020[11]. In response to the growing global spread, the World Health Organisation (WHO) declared a pandemic on 11th March of 2020, by which point the infection had spread to 114 countries and the global death toll was estimated over 4,000[12]. Deaths from SARS-CoV-2 increased more than tenfold by the end of the month and reached almost 2 million deaths reported by the end of 2020[10]. **Figure 2** shows an overview of events surrounding the outbreak of SARS-CoV-2.
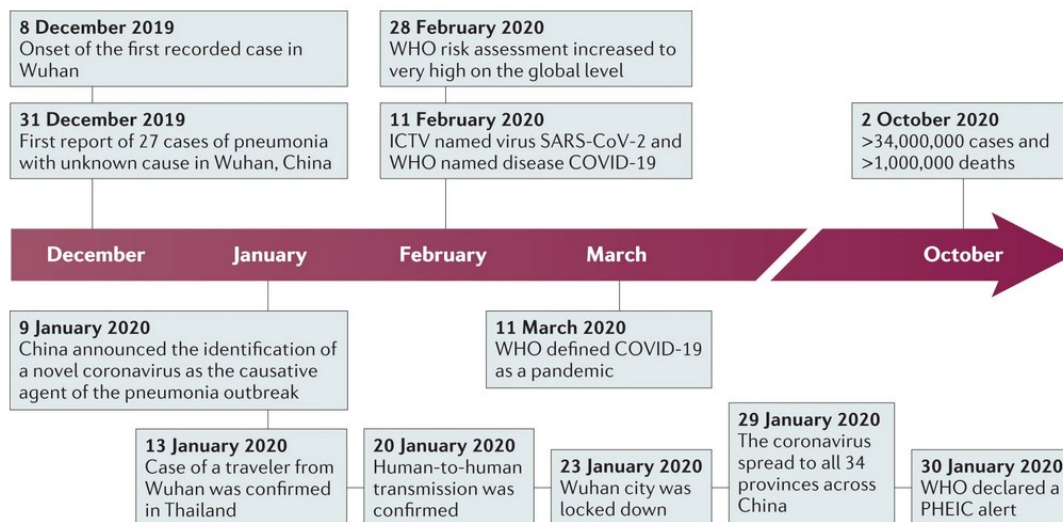
Figure 2: Pandemic outbreak timeline
Timeline of the outbreak of SARS-CoV-2, highlighting key events throughout the beginning of 2020. Reprinted by permission from Springer Nature Customer Service Centre GmbH: Springer Nature Reviews Microbiology (Characteristics of SARS-CoV-2 and COVID-19, Ben Hu et al. [8]), © (2020).

1.1.2. COVID-19 Transmission and Symptoms

COVID-19 disease is transmitted from person to person primarily by droplets and aerosols, the latter of which can penetrate deep into the lungs[13-16]. Infection occurs at the entry points of the human airway system[17,18], after which the virus quickly multiples and spreads throughout the body. Symptoms occur roughly 5 days after initial infection[19]. In contrast, viral loads are reported to already peak 1-3 days before symptom onset, which can lead to people spreading the disease before developing symptoms[20,21]. This was a major contributing factor to the rapid spread of COVID-19[21,22].

Symptoms of COVID-19 are diverse but the three most common symptoms are cough, fever and shortness of breath[23]. Less common symptoms include diarrhoea, myalgia and headache[23-25], although anosmia and dysguesia (loss of smell and taste) are also reported in some individuals[23,26-28]. A significant fraction of infected individuals remain asymptomatic, although estimates of the proportion of this group vary with reports ranging from 4% to 31%[23,29-31]. Spread of COVID-19 happens independently of symptoms, making asymptomatic infections especially critical for containment of the pandemic[29]. Severe symptoms commonly seen in hospitalized patients may include hypoxemia and lymphopenia leading to acute respiratory distress syndrome, requiring invasive ventilation in severe cases, potentially resulting in multiple organ failure and death[25,32,33].

Disease severity strongly varies between different groups of individuals. Immunocompromised individuals such as organ transplant recipients[34], haemodialysis or cancer patients[35,36] are particularly severely affected, which makes them an at-risk group during the pandemic. Increasing age is considered a strong risk factor for severe COVID-19 disease, so the elderly population in general is another at-risk group, where notably males are more commonly hospitalized[37]. In constrast, children are less often infected, develop symptoms less frequently and have milder disease course[38-40]. Overall, COVID-19 had a world-wide fatality rate of roughly 2.3% in 2020 (calculated using data provided by WHO[10]), however fatality rates are increased with age and reach 4.6% at age 75 and 15% at age 85 according to a large meta study[41].

The changing of predominant virus variants, which is discussed at a later point in this thesis, has also had an influence on symptoms of COVID-19. During the Alpha and Delta variant infection waves, COVID-19 infections were more often associated with anosmia and dysguesia compared to before[42,43] and the following Omicron variant had a higher prevalence of sore throat and hoarse voice, while anosmia and dysguesia were much more uncommon again[42,44,45].

It must be noted, that a small percentage of infected individuals develop a long-lasting disease stage characterized among other symptoms by general fatigue, shortness of breath and decreased cognitive status[46]. This prolonged affliction, which is often summarized under the term "long COVID" is difficult to define clinically, since symptoms are variable and very general and therefore difficult to attribute specifically to COVID-19[47]. More research on this topic is needed to identify causes and biomarkers for diagnosis[48], however in this thesis, COVID-19 infection and disease progression is discussed in the context of the acute infection and immunity and not in the context of "long COVID".

1.1.3.   SARS-CoV-2 Structure and Life Cycle

SARS-CoV-2 is a coronavirus of the genus betacoronavirus subgenus sarbecovirus[9]. The virus particle of SARS-CoV-2 is schematically depicted in **Figure 3** and is made up of a lipid membrane containing three membrane-bound proteins (Spike, Envelope and Membrane). Of these, the Spike Protein forms trimers and is crucial to viral cell entry, while the Envelope and Membrane proteins are thought to play a role in virus particle assembly[49,50]. The Nucleocapsid protein is located within the membrane and stabilizes the single-stranded, linear RNA genome within the virus particle. Additionally, the genome encodes for two large polyproteins, which are proteolytically processed into 16 proteins, relevant for virus replication[51]. Several other non-structural proteins are encoded interlaced with the other open reading frames on the SARS-CoV-2 genome[51].
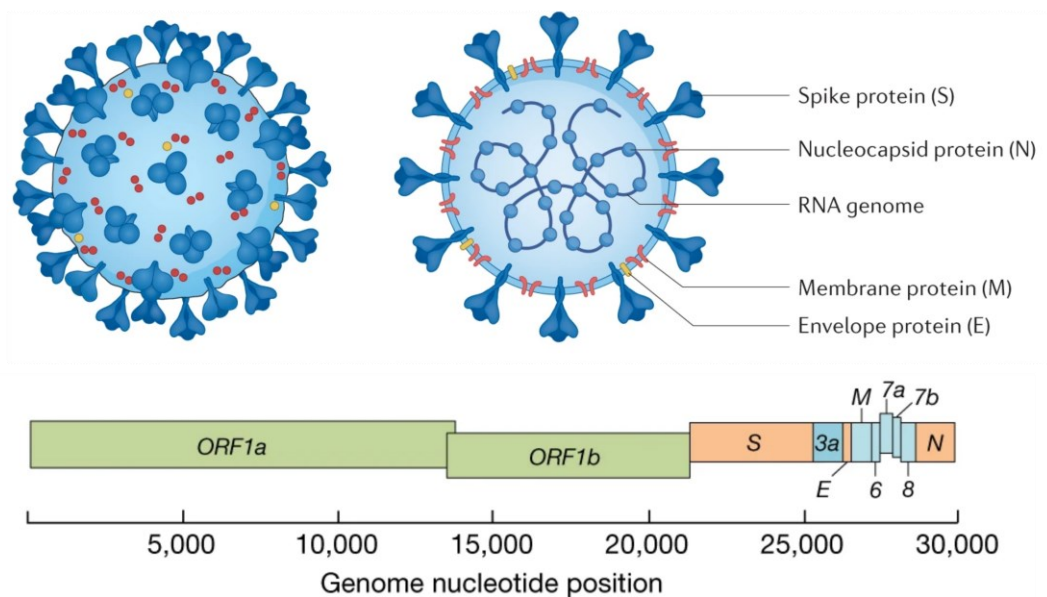
Figure 3: SARS-CoV-2 virus particle
Schematic illustration of the SARS-CoV-2 virus particle with all proteins contained in the virus particle highlighted. Open reading frames in the SARS-CoV-2 RNA genome are shown below. Virus schematic adapted by permission from Springer Nature Customer Service Centre GmbH: Springer Nature Reviews Microbiology (SARS-CoV-2 pathogenesis, Mart M. Lamers et al.[52]), © (2022) and genome illustration adapted from Zhou et al.[2].

Figure 4 is an illustration of the life virus cycle of SARS-CoV-2. The virus particle is able to latch onto human cells via the interaction of the trimeric Spike protein and the human ACE2 receptor[54,55]. The Spike protein is subsequently activated by protease cleavage via human serine protease TMPRSS2 at the S2 region[56], which then mediates fusion of the virus particle with the host cell membrane. In humans, ACE2 and TMPRSS2 are co-expressed in nasal and bronchial epithelial cells, making these cell types the primary target of viral entry into the host, thus causing predominance of infection at entry points of the airway system and droplet spread of SARS-CoV-2[57,58]. The proteases Furin and Capthepsin L have also been associated with SARS-CoV-2 cell entry, the latter in an alternate entry pathway via endosomal escape[59-61].
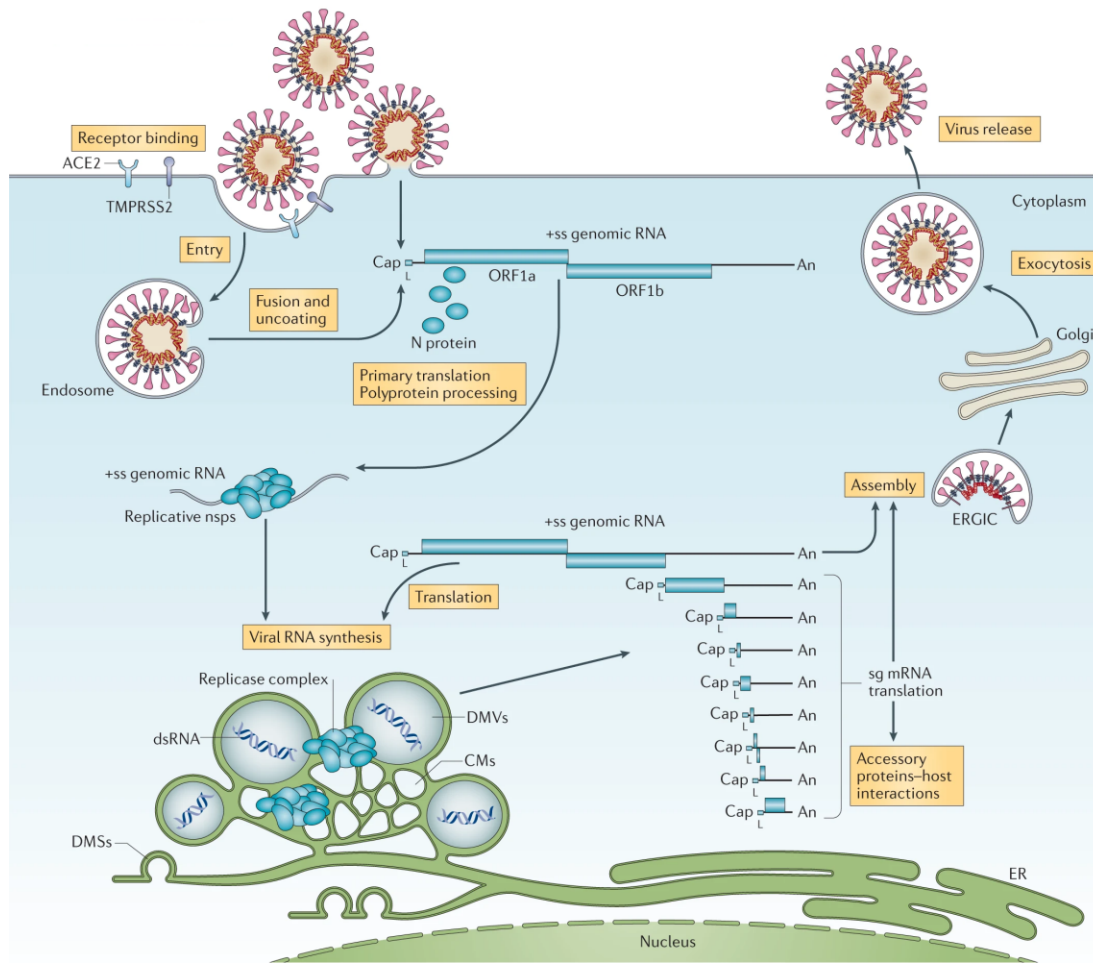
Figure 4: SARS-CoV-2 life cycle
Schematic overview of the SARS-CoV-2 life cycle. Viral cell entry is followed by endosomal escape, viral RNA synthesis in virus replication organelles, assembly of new virus particles and viral egress by exocytosis. Adapted by permission from Springer Nature Customer Service Centre GmbH: Springer Nature Reviews Microbiology (Coronavirus biology and replication: implications for SARS-CoV-2, Philip V'kovski et al.[53]), © (2020).

Upon membrane fusion, the viral protein-RNA complex is released into the host cell cytoplasm, where the viral RNA is translated using cap-dependent translation of the host. The polyproteins are subsequently processed and virus replication organelles are formed at the endoplasmic reticulum resulting in double membrane vesicles as centres for viral replication[62-64]. Assembly of new virus particles occurs at the endoplasmic reticulum-golgi intermediate compartment, where budding is facilitated by Spike, Membrane and Envelope proteins[64]. Newly formed virus particles egress the infected cell via lysosomes[65].

1.2. Serology

1.2.1. Overview of the Humoral Immune Response

When the human immune system comes into contact with a previously not encountered pathogen, it raises a polyclonal set of antibodies which can with high avidity bind to pathogen-specific structures, also called antigens. The human immune response is highly individual and varies for each pathogen and antigen. Antigens can be parts of proteins carried by the pathogen, and although they can be linear epitopes, the majority of antigens that the human immune system responds to are believed to be folded, conformational epitopes[66]. Furthermore, many pathogens are highly glycosylated either at the protein levels or at their membrane. These glycan structures can also serve as antigens to the human immune system as was for example shown in tuberculosis[67].

An antigen is processed by professional antigen presenting cells, which then present it to naïve B-cells at germinal centres, such as lymph nodes[68]. These B-cells undergo a selection process which involves improving avidity towards presented antigens and excluding reactivity to endogenous structures[68]. After stimulation by immune system contact with their antigen, B cells differentiate into antibody-producing plasma cells or memory B cells, the latter representing a diverse group of long-lived B cells that contribute to an enhanced response upon re-exposure to the same antigen[69]. Each plasma cell specifically produces monoclonal antibodies of one of several immunoglobulin classes. Immunoglobulin G (IgG) constitute by far the largest fraction of antibodies in serum and have the strongest binding affinity to their target[70]. Besides IgG, immunoglobulin M (IgM) and immunoglobulin A (IgA) are the other major antibody types found in serum[70]. IgM is mostly produced in the early phase of the immune reaction and has low affinity but high avidity due to its pentameric structure[70]. While present in serum, IgA is mainly found in body secretions such as breast milk or sputum and functions to protect mucosal membranes[70,71]. One of the modes of action of antibodies is to directly disrupt entry of the pathogen into human cells by binding to and thus blocking epitopes on specific pathogen structures[72]. This activity is also called neutralization[72]. Only a fraction of the polyclonal antibodies generated upon exposure to a pathogen are neutralizing[73]. Antibodies in blood have a half-life of 1 to 4 weeks, depending on the subclass, as shown for immunoglobulin G (IgG)[74]. However, they are persistently replenished by plasma cells, resulting in a constant total concentration of antibodies in human blood. Antigens-specific antibody levels could be detected in serum for up to 50 years after a pathogen encounter in some cases[75]. While plasma cells do not proliferate, they can persist for long times in specialized niches in the bone marrow as memory plasma cells[69]. When the immune system re-encounters a pathogen, its response is much faster, since

memory plasma cells as well as memory B-cells can be re-activated[68]. Multiple exposures to the same antigens are thought to iteratively improve antibody affinity[68].

In addition to the previously described humoral immune response, the immune system also mounts an adaptive cellular immune response, characterized by the activity of T-cells. In brief, T-cells are activated by professional antigen presenting cells, if their T-cell receptor can bind to the presented antigen[68]. After activation, the diverse set of CD4+ helper cells fulfil multiple roles in the adaptive cellular immune response such as stimulating macrophage and B cell activity[68]. CD8+ cytotoxic cells can recognize and kill cells that are infected by the pathogen matching their respective T cell receptor[68]. As part of their effector function, T-cells secrete specific sets of cytokines, which are small peptide molecules used in cellular signalling[68]. Therefore, the presence of cytokines such as Interferon gamma can serve as a correlate for activity of the cellular immune response[76].

1.2.2.   Applications of Serology

Serology is the study of serum and other bodily fluids, usually referring to the identification of antibodies. In the context of this thesis, serology will explicitly refer to the study of pathogen-specific antibodies in human bodily fluids such as blood (serum and plasma) and saliva. An excellent overview of the current state and challenges in serology is given by Wine and colleagues[77].

Overall, the encounter with a pathogen leaves a specific "imprint" in the human immune system, which can be read, among other things, from the antibodies. While other methods of detecting infection, such as genome sequencing or detection of antigens in samples, are better suited for diagnosing active infection, antibodies can be detected long after infection and are an indirect measure of a person's immunity.

Serological assays are scientific methods for measuring the levels of antigen-specific antibodies, usually in blood derivatives such as serum or plasma, but also in other fluids such as saliva or cerebrospinal fluid. The most commonly measured class of antibodies is IgG, which makes up the majority of antibodies in blood[69,70]. Besides, IgA and IgM are often measured. IgM can serve as a marker of recent infection, as its half-life is reduced compared to IgG[70]. IgA can be used as a correlate of mucosal protection[70,71]. In addition to directly measuring the presence of antibodies, another approach is to estimate their capacity to act as neutralizing antibodies. In such surrogate neutralization tests, an infection is mimicked and a particular set of antibodies, e.g., from serum, can be assessed for its capacity to disrupt the infection and thereby provide protection against the pathogen. These assays can range from complex systems such as models of infection in cell culture using live pathogens to reductionist models that rely on protein-protein interaction to mimic infection.

1.2.3. Multiplex Assays and xMAP Technology

Multiplexing of antigens is to simultaneously measure reactivity from a sample towards a multitude of antigens. This approach is especially well suited to capturing the aforementioned "imprint", which a pathogen leaves on the human immune system as accurately and broadly as possible.
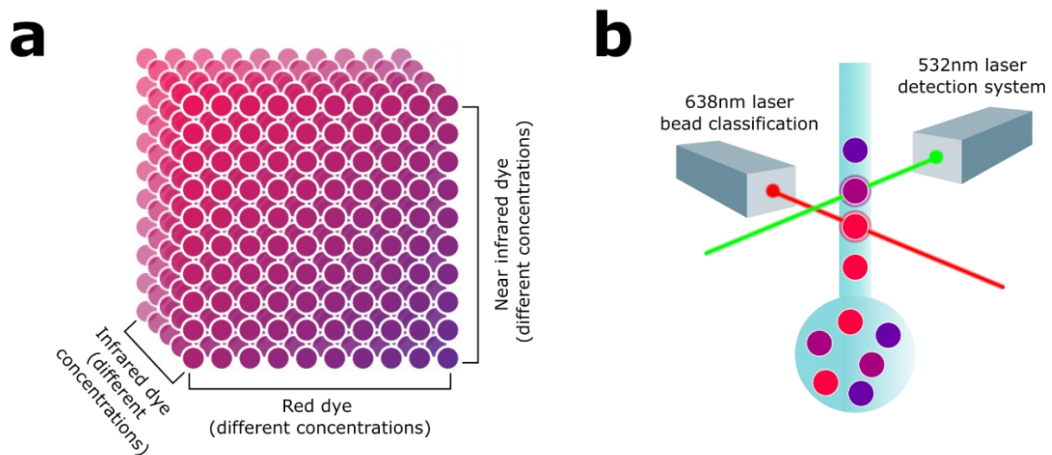
Figure 5: xMAP technology
(a) Combination of different concentrations of three fluorescent dyes within the xMAP microspheres allows to distinguish a total of 500 different emission profiles and enables multiplexing. **(b)** In the FLEXMAP3D instrument system, microspheres are singled out and classified with a red laser, while a green laser can be used to measure fluorescence intensity on the surface of the bead. Figure modified and used with permission from Luminex, a Diasorin Company[78].

Figure 5 displays the principles of the xMAP technology (Luminex Corp.). Instead of being coated to a well surface, as is the case in classical serological enzyme-linked immunosorbent assay (ELISA), antigens are immobilized on xMAP magnetic microspheres (beads). Beads have a combination of three internal dyes at different concentrations in a total of 500 unique combinations, also called bead regions (**Figure 5a**). A different antigen can be immobilized on each bead region allowing a combination of up to 500 different antigens which can be analysed simultaneously. The measurement device singles out beads and determines the bead region with its red laser (638 nm wavelength), while detecting a signal for the bead with its green laser (532 nm wavelength) for which phycoerythrin is a common chromophore (**Figure 5b**).
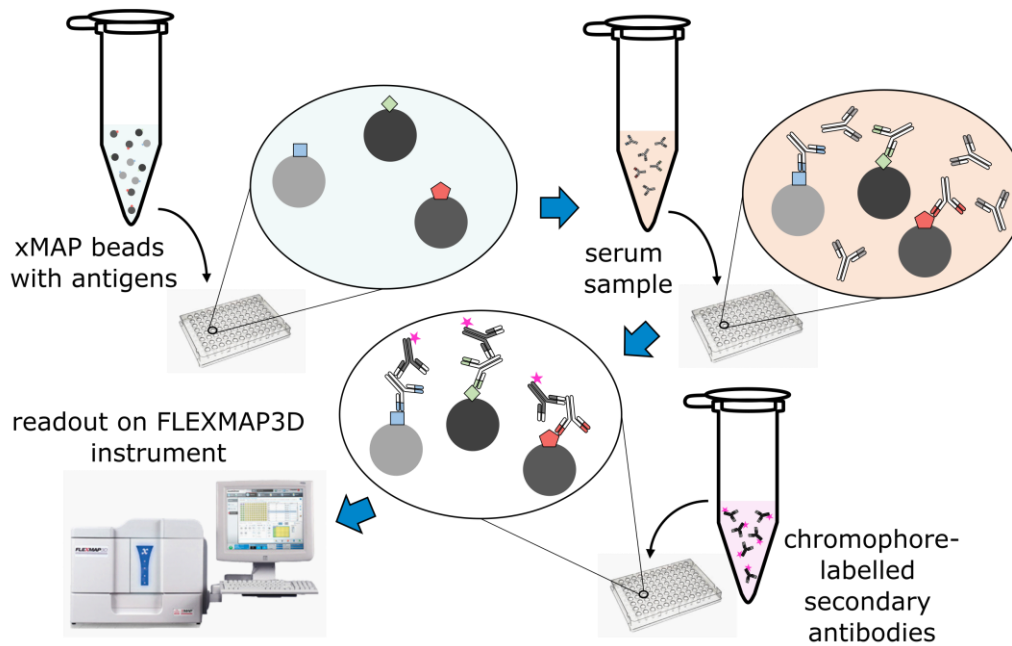
Figure 6: Multiplex serological assay
Schematic representation of a serological assay using xMAP technology. Beads with immobilized antigens are incubated with samples containing antibodies, reaching a steady state of antibodies binding to the antigens on the bead surface. Unbound antibodies are then washed off and a chromophore-conjugated secondary antibody is added. After washing off unbound secondary antibody, the fluorescence of every single bead is measured in the measurement device, e.g. a FLEXMAP3D instrument. The fluorescence signal of the chromophore is a direct correlate with the amount of antibody bound to each antigen. At least 35 beads are counted and the median fluorescence intensity is reported per region per sample as the primary read-out of the assay.

Figure 6 is a schematic representation of a standard protocol for a serological assay based on xMAP technology. The assay is performed in a 96-well format, allowing for high-throughput processing of samples. The modular assay setup allows to easily adapt protocols to change the primary readout by adding alternate secondary antibodies. These can be specific for any species of immunoglobulin, e.g. IgG or IgA. Multiplexing of serological assays allows to save processing time and costs. The bead format also enables to work with high sample dilutions and for serum, sample volumes of 5 µL are often sufficient for measurement. However, the amount of antigens that can be assessed simultaneously can lead to very complex data sets and requires careful planning for analysis and interpretation.

1.2.4. Coronavirus Serology Prior to the COVID-19 Pandemic

SARS-CoV-2 and SARS-CoV-1 have moderately conserved genomes (79% sequence identity)[79], with the Nucleocapsid (90%), Envelope (95%) and Membrane (90%) proteins being well conserved on an amino acid level, whereas the Spike protein is more divergent (76%)[79]. It was therefore clear that the results of research on SARS-CoV-1 could be used as a basis for SARS-CoV-2 serology. For SARS-CoV-1, the major antigens were Spike and Nucleocapsid, with B- and T-Cell epitopes within these proteins being used to predict corresponding SARS-CoV-2 epitopes[80]. Most serological assays for SARS-CoV-1 were directed towards either the Spike or Nucleocapsid and detected IgG from human serum[81]. Both antigens exhibited similar levels of sensitivity and specificity and have therefore been the focus of SARS-CoV-2 serological assay development. However, it was shown that neutralizing antibodies were exclusively directed towards Spike[82]. In contrast to the SARS-CoV-1 epidemic, the global pandemic for SARS-CoV-2 enabled significantly larger sample cohorts to become available, allowing a thorough evaluation of individual antigen performance.

The presence of SARS-CoV-1 in the human body could most reliably be diagnosed by sequencing of the viral RNA from specimens of the lower respiratory tracts or nasopharyngeal swabs, due to viral loads increasing to detectable levels before seroconversion. However, sequencing methods often suffered from poor sensitivity and serological assays were recommended as confirmatory test in diagnosis of SARS-CoV-1[6,83,84]. SARS-CoV-1 patients developed IgG, IgA and IgM levels between two and four weeks after disease onset[85,86]. While IgM is generally considered to be an early marker for infection, it was not detected earlier than IgG or IgA for SARS-CoV-1 and further proved to have a higher cross-reactivity due to its low affinity[81,85]. IgA and IgM titres decreased more rapidly, while IgG titres were more stable over time[85]. SARS-CoV-1 infections could therefore reliably be detected with serological assays for 8 months via IgG, while IgM and IgA added additional value in detecting whether an infection occurred recently. **Figure 7** is a schematic representation of the dynamics of viral loads and antibody formation during a SARS-CoV-2 infection.
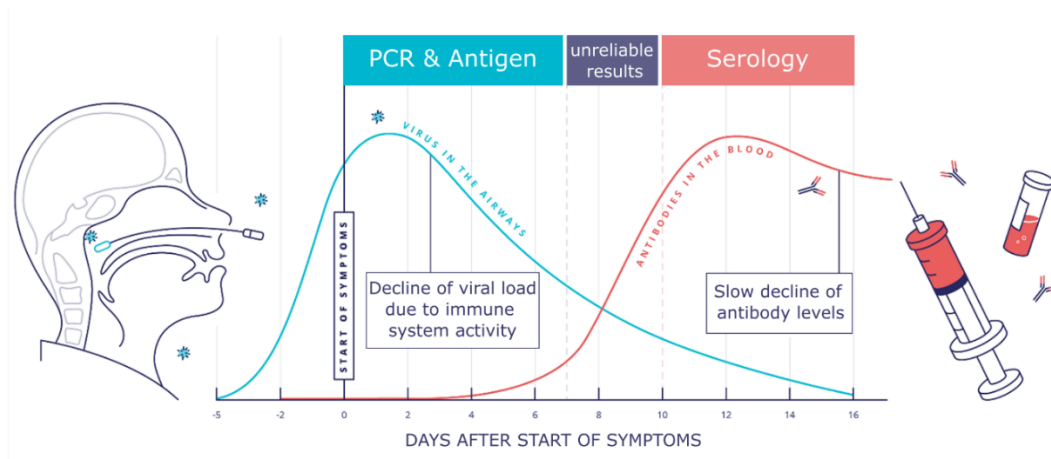
Figure 7: Detection of COVID-19
Schematic illustration of viral load and antibody formation over COVID-19 disease course. Initially, infection can only be detected by the presence of SARS-CoV-2 using PCR or antigen testing. Antibodies can be reliably detected with serology after approximately one week, depending on assay sensitivity. There may be a period where either test principle is unreliable, depending on the course of disease and the individual immune response. Adapted from UK Research and Innovation[87].

During the SARS-CoV-1 epidemic, the WHO recommended the use of virus neutralization tests to eliminate cross-reactive effects and directly measure inhibition of virus infection[84]. However such assays are not widely applicable due to safety requirements for live virus cultures of minimum biosafety level 3, nor are they suitable to high-throughput screenings, due to high time and costs of cell culture. As a result, virus neutralization tests were considered best suited as a tool to confirm results and to evaluate serological assay performance[84].

In addition to the coronaviruses SARS-CoV-1 and MERS-CoV, both of which caused epidemics with high mortality rates but then disappeared, there are four species of seasonal coronaviruses that infect humans. Namely these are 229E and NL63 of the genus alphacoronavirus, as well as OC43 and HKU1 which like SARS-CoV-2 are betacoronaviruses[88]. All four viruses cause seasonal cold-like symptoms, with the majority of humans being infected at least once in their lifetime[89,90]. Together they are therefore often referred to as endemic human coronaviruses (hCoVs). The viral proteins of hCoVs and SARS-CoV-2 are related and have conserved stretches within immunodominant regions[81]. For the Spike protein, these stretches are mainly located within the S2 domain, whereas the Nucleocapsid is more conserved overall[81]. An immune response towards hCoVs may therefore confer some form of immune protection from SARS-CoV-2 via cross reactive antibodies and conserved epitopes, as was demonstrated for SARS-CoV-1[89,91]. However, there are indications that the immunity to hCoVs may be short lived, as re-infections often occur 12 months after infection[92]. Therefore, the relevance of cross-protection from SARS-CoV-2 through hCoV-induced immunity was uncertain and an important research topic in the COVID-19 pandemic.

1.3. Emerging Topics During the COVID-19 Pandemic

1.3.1. SARS-CoV-2 Vaccination

Shortly after the outbreak of SARS-CoV-2, many pharmaceutical and biotechnology companies announced they were beginning pre-clinical development of a SARS-CoV-2 vaccination. Within a year, and following accelerated approval of the first generation of vaccines in fast-track system[93,94], several SARS-CoV-2 vaccinations became publically available. Governments and public health bodies around the world subsequently issued different vaccination regimens, based on clinical trial studies and vaccine availability. In the first half of 2021, four different vaccines were approved for use in Germany. These were BNT162b2, later marketed as Comirnaty by BioNTech Manufacturing GmbH (BNT); mRNA-1273, later marketed as Spikevax from Moderna Biotech Spain, S.L. (MOD); Vaxzevria from AstraZeneca AB (AZE) and Jcovden by Janssen-Cilag International NV (JJ)[95]. While other vaccines have been developed worldwide and some were approved for use in Germany in 2022, the aforementioned four vaccines together make up nearly 100% of all administered vaccine doses in Germany by July 1st of 2022[96] and are the focus of this thesis. An overview is also presented in **Table 1**.

Table 1: Overview of COVID-19 vaccines in Germany

Name (Commercial name)[95]	Abbre-viation	Manu-facturer[95]	Type[95]	Dosage (Number of vaccinations)[97]	Licensing Date in Germany[95]	% of Doses administered in Germany as of 01.07.2022[96]
BNT162b2 (Comirnaty)	BNT	BioNTech Manufac-turing GmbH	mRNA	30 μg RNA (2x)	21.12.2020	73.8 %
mRNA-1273 (Spikevax)	MOD	Moderna Biotech Spain, S.L.	mRNA	100 μg RNA (2x)	06.01.2021	17.1 %
ChAdOx1-S (Vaxzeriva)	AZE	Astra-Zeneca AB	Vector-based	5×10^{10} adenovirus vector particles (2x)	29.01.2021	7.0%
Ad26.COV2.S (Jcovden)	JJ	Janssen-Cilag Inter-national NV	Vector-based	5×10^{10} adenovirus vector particles (1x)	11.03.2021	2.0%

The COVID-19 pandemic led to the use of relatively novel vaccination methods, as they proved more flexible and had short development times compared to conventional methods[97]. All four vaccines utilize the Spike protein as their antigen, as the Spike protein receptor binding domain (RBD) is the target for the majority of neutralizing activity towards SARS-CoV-2[98]. MOD and BNT are mRNA vaccines, while AZE and JJ are vector-based vaccines.

The urgent need for vaccines during the pandemic triggered to the first use of mRNA vaccines outside of clinical trial studies. In this approach, vaccine formulations contain mRNA encoding for a target antigen packaged in lipid-nanoparticles[97]. After an intramuscular injection, the mRNA is delivered to cells and subsequently uses the translation machinery of host cells to produce the antigen[97]. The mRNA contains modulated 5′ and 3′ untranslated regions including 3′-polyadenylation and a 5′-cap structure[97]. Furthermore, Uridines in the mRNA of MOD and BNT are replaced by N1-methylpseudouridine, which increases stability and improves tolerability by suppressing innate immune responses[99-101]. One of their main differences is the amount of mRNA in one dose, where BNT contains only 30µg, compared to 100µg for MOD[102,103].

Other vaccine developers decided to utilize adenovirus vectors, which have seen wide use in basic research and gene therapy studies[104]. Although vector-based vaccines were used during emergency situations in the Ebola outbreaks of the 2010s[105], they have never been administered as widely as during the COVID-19 pandemic. Vector-based vaccines contain a modified adenovirus as a carrier for DNA encoding for the target protein[97]. Two vector-based SARS-CoV-2 vaccines were approved for usage in Germany. AZE utilizes chimpanzee adenovirus Y25, while JJ uses human adenovirus 26[97]. The vaccine delivery process is more complex than in mRNA vaccines. The adenovirus infects host cells, but its genome is altered to contain the SARS-CoV-2 Spike protein, while viral factors for genome replication are deleted[106-108]. Once inside cells, the DNA is transcribed to mRNA in the nucleus and subsequently SARS-CoV-2 Spike protein is translated and induced an immune response, likely by exposure on the plasma membrane of the cell[97].

Vaccine efficacy is the metric describing the actual protection from pathogen infection, conferred by vaccination. This is assessed in double-blind clinical trials and is an essential step in vaccine approval. For SARS-CoV-2, the WHO had set a goal of 50% vaccine efficacy for vaccines in development, meaning that COVID-19 should be prevented in 50% of all vaccinated individuals[109]. Clinical trials of the four vaccines in use in Germany reported different efficacies, where the mRNA vaccines performed superior to vector-based vaccines, with efficacies of 94% for MOD[103] and 95% for BNT[102], while AZE had 70%[110] and JJ 67%[111]. Of the four vaccines described, JJ is the only one for which the vaccination schedule of the original marketing authorization only requires administration of a single dose of the vaccine for complete immunisation[111]. All four vaccines were shown to be safe and rare adverse effects such as myocarditis were outweighed by conferred protection from COVID-19, which carries substantially increased risks for the same adverse events[112,113].

By contrast to the above discussed vaccines, many vaccine developers utilised more conventional systems based on direct delivery of antigens[114], which are proven in vaccines against many other pathogens[115]. However, they were met with limited success. One approach that promised straightforward and fast generation of vaccines was the use of attenuated, live viruses, as used in measles vaccination for example[115]. However, this approach did not lead to a vaccine approved by WHO, as of July 2022[116]. Vaccines using inactivated whole virus have been developed, however while they saw application in some countries[116], none of the developed vaccines was approved by the European Medicines Agency (EMA) and subsequently recommended for use in Germany in 2021[95]. Subunit vaccines based on recombinant proteins ultimately proved successful but were slow in development, likely due to more complicated production and required optimisation[117]. Overall, vaccines that were not based the delivery of genetic material were by comparison slow in development or not widely approved by public health authorities, such as the EMA. Two further SARS-CoV-2 vaccines have been approved for use in Germany, as of July 2022[95]. Nuvaxovid (Novavax CZ a.s.) is a subunit vaccine based on SARS-CoV-2 Spike protein[118] and COVID-19 Vaccine Valneva (Valneva Austria GmbH) is a inactivated virus vaccine[119]. Their late arrival on the market has however lead to limited use in Germany[96] and future usage will ultimately depend on pandemic development and political decisions.

Serological assays are utilised in vaccine trials, to assess the generation and duration of the immunological response[100,101,106,120]. They are well suited for monitoring and comparing vaccination outcomes across different vaccination regimens and between different population groups. While vaccine effectiveness and safety were shown in the clinical trial studies themselves, it was crucial to rapidly generate independent data on the vaccine-induced immune response to inform public health strategies. Throughout the pandemic the German Standing Committee on Vaccination (STIKO) constantly evaluated the pandemic situation and adapted their recommendations accordingly. For example, an additional dose of vaccine to boost declining immunity levels was recommended for the general population at the end of 2021[121], but in the vaccine trials before approval, a third vaccination was never investigated.

In Germany, among many other countries, a risk-based priority system was established, in which older citizens, healthcare workers and immunocompromised were offered a vaccination first[122]. Immunocompromised individuals are particularly vulnerable during a pandemic because they are more susceptible to infection and often have more severe courses of illness[36,123,124]. Haemodialysis patients are often transplant recipients or have insufficient kidney function and belong to the group of immunocompromised individuals. During haemodialysis, a patient's blood is filtered outside their body and soluble components are largely removed to eliminate toxic waste products that have accumulated, for example, due to reduced kidney function[125]. Patients on haemodialysis are often poor vaccine responders and require adjusted vaccination regimens for many vaccine-preventable diseases[126,127]. Therefore, it is critical to monitor the SARS-CoV-2 vaccine immune response in this group and adjust their vaccination regimen accordingly to protect them from infection.

1.3.2. SARS-CoV-2 Variants

In a pandemic scenario, due to the sheer number of infections and the changing immunity landscape, driven for example by vaccination, a pathogen can undergo rapid evolution to optimize and adapt to its circumstances. While certain countries initially sequenced a fraction of their positive PCR samples, some countries and research groups sequenced significantly more and began to identify the presence of clusters of distinct viral strains. Genome sequences were collected in databases and assigned clades based on divergence, allowing to track the evolution of SARS-CoV-2[128,129]. Over the course of 2021, several major SARS-CoV-2 variants emerged with the first occurrence of mutations in key regions of their genome. Mutations in the RBD of the Spike protein were considered critical due to the use of this antigen in vaccines. Major variants were categorized as SARS-CoV-2 Variants of Concern (VoC) or Variants of Interest (VoI) by the WHO, based on worldwide spread and number of recorded infections[130,131].

Table 2: SARS-CoV-2 variants of concern designated by the WHO

WHO label[131]	Pango Lineage[131]	Earliest occurrence[131]	Earliest occurrence[131]	Date designated VoC[131]	Increased transmissibility compared to non VoC variants[132]
Alpha	B.1.1.7	09.2020	United Kingdom	18.12.2020	29%
Beta	B.1.351	05.2020	South Africa	18.12.2020	25%
Gamma	P.1	11.2020	Brazil	11.01.2021	38%
Delta	B.1.617.2	10.2020	India	11.05.2021	97%
Omicron*	B.1.1.529	11.2021	Multiple countries	26.11.2021	*

The WHO definition of Omicron represents all Omicron sub lineages, which is an as of July 2022 still evolving group

An overview of variants that have been assigned VoCs over the course of the pandemic as of July 2022 is given in **Table 2**. It should be noted that the WHO assigned Omicron as a general label for all circulating Omicron sub-lineages. Notably, the VoCs all carried one or more mutations inside the RBD which re-occurred at several distinct amino acid positions (**Figure 8a**). Through accumulated mutations, the VoCs gained fitness advantages over other circulating variants and became predominant locally or globally[132].

Notable global Variants in 2021 included the Alpha and Delta variant. The Alpha variant was the first variant to dominate infection events worldwide and made up more than 90% of fully sequenced infections in Germany from March 2021 to May 2021[129,133]. It carried the key mutation N501Y in the ACE2 binding interface of the RBD, which is associated with increased binding to ACE2[134]. In the first half of 2021, there were two more designated VoCs beside Alpha. The Beta and Gamma variant dominated in South Africa and Brazil, respectively, but were not successful globally. In addition to the N501Y mutation, they each carried two more mutations in the RBD at positions 417 and 484, which were associated with increased ACE2 binding and immune escape[134,135]. The previously circulating variants were displaced by the Delta variant in the second half of 2021, which became almost solely dominant worldwide and made up over 99% of fully sequenced infections in Germany from August 2021 to December 2021[129,133]. The Delta variant developed a different set of mutations in the Spike protein compared to the previous VOCs, such as L452R, which is a mutation associated with increased viral shedding and infectivity[136,137]. A visualisation of Spike mutations and variant frequencies is provided in **Figure 8**.
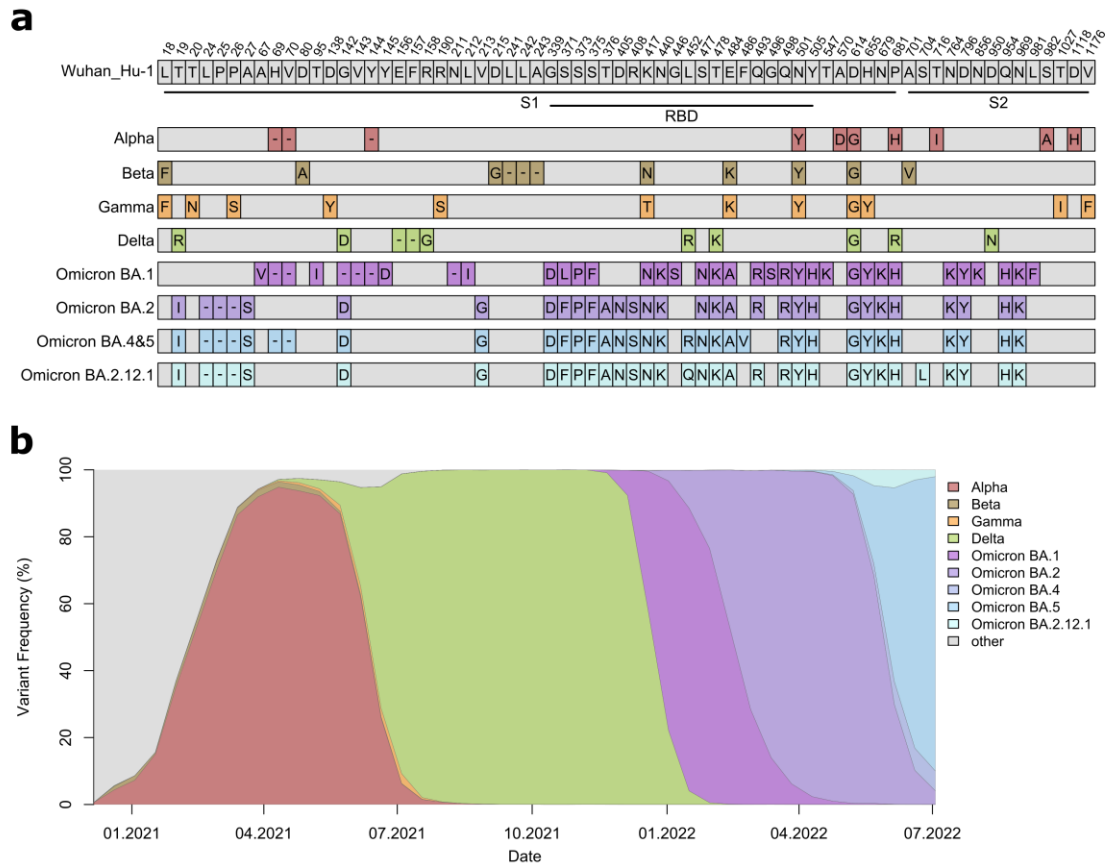
Figure 8: Overview of SARS-CoV-2 variants of concern
(a) Defining mutations of VoC in the Spike protein compared to the original Wuhan_Hu-1 strain. Amino acid positions and Spike subdomains are indicated in reference to Wuhan_Hu-1 strain. **(b)** Relative variant frequency in Germany over the course of the pandemic is shown. The number of sequenced genomes of a specific variant in relation to all sequenced genomes in a respective periods of 14 days was calculated. Figures were generated from CoVariants data provided by Hodcroft and colleagues[133] using source data from GISAID[129].

Infectivity was increased from the original Wuhan Hu1 isolate to Alpha, and from Alpha in turn to Delta, which enabled their global spread over competing variants[132]. Compared to infections with the original Wuhan Hu1 isolate, infections with VoCs were associated with higher risks of hospitalisation and death[138,139]. These effects were, however, mitigated by vaccination in countries where vaccination campaigns could be rolled out quickly in 2021. A significant amount of breakthrough infections occurred with VoCs in individuals convalescing after previous infections and in vaccinated individuals, indicating immune escape properties of SARS-CoV-2 VoCs[140-142]. It was therefore crucial to generate data on immune response towards VoCs rapidly.

2022 saw the rise of the Omicron VoC, which quickly replaced Delta as the globally dominant SARS-CoV-2 variant. Several sub lineages have developed during this wave of infection, which is still ongoing as of July 2022[143,144]. The Omicron infection wave started out with the BA.1 sub lineage, followed by BA.2. As of July 2022, there are three major circulating Omicron sub lineages (BA.4, BA.5, and BA.2.12.1) and it is not quite clear which will prevail, although it appears that BA.5 is developing into the major variant[133]. While previous VoCs had few mutations, Omicron BA.1 had developed an unprecedented number of mutations in the spike protein (**Figure 8a**). Despite a vaccine coverage of around 70 % by the end of 2021 in Germany[96], 18 million infections have been recorded between February and July of 2022, which means roughly one fifth of the population have been infected with an Omicron sub lineage over the span of 6 months[10]. This indicates significant immune escape from vaccine-elicited immunity by the Omicron sub lineages. The increase in incidences was unprecedented within the pandemic so far. Many people, who had been infected in 2020 or 2021 were reinfected with Omicron VoC in 2022[140,145]. At the same time disease severity was strongly reduced, especially in vaccinated individuals, even though the vaccines were all directed towards the Wuhan Hu-1 Spike protein[146]. The Omicron sub lineages therefore present a major change in the SARS-CoV-2 pandemic and understanding alterations of the immune response towards them is essential for adjustment of vaccines as well as public health and political decisions.

As of July 2022, more than 500 million infections with SARS-CoV-2 have been recorded worldwide and the total number of deaths associated with SARS-CoV-2 is estimated to be above 6 million[10]. The true costs of the COVID-19 pandemic in damages to the socioeconomic landscape cannot be estimated.

Chapter 2: Objective of the Thesis

This thesis aims to develop a multiplex serological assay for SARS-CoV-2, the causative agent for COVID-19 and apply it to generate scientific evidence to accompany the real-world pandemic situation and support critical decisions for public health and socioeconomics.

In a first step, we evaluated candidate SARS-CoV-2 antigens and set a core antigen panel. We subsequently established a system to classify SARS-CoV-2 infection in serum and plasma samples with high clinical sensitivity and specificity.

In addition, we investigated whether cross-reactivity to endemic human coronaviruses (hCoVs) is a relevant factor in SARS-CoV-2 immunity and hence extended our antigen panel to include antigens from all four known hCoVs.

Next, we used our assay to assess why SARS-CoV-2 infection in children was less common and more often associated with a milder course of disease, by comparing the humoral immune response after infection in children and adults within a multi-centric cohort study.

The development of vaccines was a key step towards managing infections and stabilizing health infrastructure in the COVID-19 pandemic. We compared different vaccination regimens in a large population-based cohort and investigated the kinetics of the associated humoral immune response, with the aim of providing evidence for health authorities to evaluate and adjust vaccination recommendations.

Immunocompromised patients, such as patients on haemodialysis are an at-risk group in a pandemic setting. We accompanied a cohort of patients on haemodialysis at multiple time points throughout the pandemic and assessed whether they responded to the vaccines and whether they required an adjusted vaccination regimen compared to healthy individuals.

The evolution of SARS-CoV-2 over the course of the pandemic has led to emergence of several virus variants with mutations in key antigens. We therefore iteratively expanded our assay to include variant-specific antigens to be able to generate data relevant to the real-world situation. Shortly after the first SARS-CoV-2 variants of concern (VoCs) emerged, we analysed whether VoCs were able to evade the vaccine induced immune response. Most recently, the emergence of the Omicron variant has led to an unprecedented number of vaccine breakthrough infections. In order to better understand this shift in the pandemic landscape and to inform future development of vaccines, we investigated its immune escape potential and compared it to the previously circulating variants.

Chapter 3: Results and Discussion

Parts of this thesis have been previously published. A full list of the publications of this thesis is shown below. Publications including supplementary material have been reprinted in **Appendix I-VIII**.

The content of this chapter is based the following publications:

1. **Matthias Becker***, Monika Strengert*, Daniel Junker, Philipp D. Kaiser, Tobias Kerrinnes, Bjoern Traenkle, Heiko Dinter, Julia Häring, Stéphane Ghozzi, Anne Zeck, Frank Weise, Andreas Peter, Sebastian Hörber, Simon Fink, Felix Ruoff, Alex Dulovic, Tamam Bakchoul, Armin Baillot, Stefan Lohse, Markus Cornberg, Thomas Illig, Jens Gottlieb, Sigrun Smola, André Karch, Klaus Berger, Hans-Georg Rammensee, Katja Schenke-Layland, Annika Nelde, Melanie Märklin, Jonas S. Heitmann, Juliane S. Walz, Markus Templin, Thomas O. Joos, Ulrich Rothbauer, Gérard Krause & Nicole Schneiderhan-Marra, **Exploring beyond clinical routine SARS-CoV-2 serology using MultiCoV-Ab to evaluate endemic coronavirus cross-reactivity**, *Nature Communications*, https://doi.org/10.1038/s41467-021-20973-3

2. **Matthias Becker***, Alex Dulovic*, Daniel Junker, Natalia Ruetalo, Philipp D. Kaiser, Yudi T. Pinilla, Constanze Heinzel, Julia Haering, Bjoern Traenkle, Teresa R. Wagner, Mirjam Layer, Martin Mehrlaender, Valbona Mirakaj, Jana Held, Hannes Planatscher, Katja Schenke-Layland, Gérard Krause, Monika Strengert, Tamam Bakchoul, Karina Althaus, Rolf Fendel, Andrea Kreidenweiss, Michael Koeppen, Ulrich Rothbauer, Michael Schindler & Nicole Schneiderhan-Marra, **Immune response to SARS-CoV-2 variants of concern in vaccinated individuals**, *Nature Communications*, https://doi.org/10.1038/s41467-021-23473-6

3. Hanna Renk*, Alex Dulovic*, Alina Seidel*, **Matthias Becker**, Dorit Fabricius, Maria Zernickel, Daniel Junker, Rüdiger Groß, Janis Müller, Alexander Hilger, Sebastian F. N. Bode, Linus Fritsch, Pauline Frieh, Anneke Haddad, Tessa Görne, Jonathan Remppis, Tina Ganzemueller, Andrea Dietz, Daniela Huzly, Hartmut Hengel, Klaus Kaier, Susanne Weber, Eva-Maria Jacobsen, Philipp D. Kaiser, Bjoern Traenkle, Ulrich Rothbauer, Maximilian Stich, Burkhard Tönshoff, Georg F. Hoffmann, Barbara Müller, Carolin Ludwig, Bernd Jahrsdörfer, Hubert Schrezenmeier, Andreas Peter, Sebastian Hörber, Thomas Iftner, Jan Münch, Thomas Stamminger, Hans-Jürgen Groß, Martin Wolkewitz, Corinna Engel, Weimin Liu, Marta Rizzi, Beatrice H. Hahn, Philipp Henneke, Axel R. Franz, Klaus-Michael Debatin, Nicole Schneiderhan-Marra, Ales Janda & Roland Elling, **Robust and durable serological response following pediatric SARS-CoV-2 infection**, *Nature Communications*, https://doi.org/10.1038/s41467-021-27595-9

4. Alex Dulovic*, Barbora Kessel*, Manuela Harries*, **Matthias Becker**, Julia Ortmann, Johanna Griesbaum, Jennifer Jüngling, Daniel Junker, Pilar Hernandez, Daniela Gornyk, Stephan Glöckner, Vanessa Melhorn, Stefanie Castell, Jana-Kristin Heise, Yvonne Kemmling, Torsten Tonn, Kerstin Frank, Thomas Illig, Norman Klopp, Neha Warikoo, Angelika Rath, Christina Suckel, Anne Ulrike Marzian, Nicole Grupe, Philipp D. Kaiser, Bjoern Traenkle, Ulrich Rothbauer, Tobias Kerrinnes, Gérard Krause, Berit Lange, Nicole Schneiderhan-Marra & Monika Strengert, **Comparative Magnitude and Persistence of Humoral SARS-CoV-2 Vaccination Responses in the Adult population in Germany**, *Frontiers in Immunology*, https://doi.org/10.3389/fimmu.2022.828053

5. Daniel Junker*, **Matthias Becker***, Teresa R. Wagner*, Philipp D. Kaiser, Sandra Maier, Tanja M. Grimm, Johanna Griesbaum, Patrick Marsall, Jens Gruber, Bjoern Traenkle, Constanze Heinzel, Yudi T. Pinilla, Jana Held, Rolf Fendel, Andrea Kreidenweiss, Annika Nelde, Yacine Maringer, Sarah Schroeder, Juliane S. Walz, Karina Althaus, Gunalp Uzun, Marco Mikus, Tamam Bakchoul, Katja Schenke-Layland, Stefanie Bunk, Helene Haeberle, Siri Göpel, Michael Bitzer, Hanna Renk, Jonathan Remppis, Corinna Engel, Axel R. Franz, Manuela Harries, Barbora Kessel, Berit Lange, Monika Strengert, Gerard Krause, Anne Zeck, Ulrich Rothbauer & Alex Dulovic, **Antibody binding and ACE2 binding inhibition is significantly reduced for both the BA.1 and BA.2 omicron variants**, *Clinical Infectious Diseases*, https://doi.org/10.1093/cid/ciac498

6. Monika Strengert*, **Matthias Becker***, Gema Morillas Ramos*, Alex Dulovic, Jens Gruber, Jennifer Juengling, Karsten Lürken, Andrea Beigel, Eike Wrenger, Gerhard Lonnemann, Anne Cossmann, Metodi V. Stankov, Alexandra Dopfer-Jablonka, Philipp D. Kaiser, Bjoern Traenkle, Ulrich Rothbauer, Gérard Krause, Nicole Schneiderhan-Marra & Georg M.N. Behrens, **Cellular and humoral immunogenicity of a SARS-CoV-2 mRNA vaccine in patients on haemodialysis**, *eBioMedicine*, *https://doi.org/10.1016/j.ebiom.2021.103524*

7. Alex Dulovic*, Monika Strengert*, Gema Morillas Ramos*, **Matthias Becker**, Johanna Griesbaum, Daniel Junker, Karsten Lürken, Andrea Beigel, Eike Wrenger, Gerhard Lonnemann, Anne Cossmann, Metodi V. Stankov, Alexandra Dopfer-Jablonka, Philipp D. Kaiser, Bjoern Traenkle, Ulrich Rothbauer, Gérard Krause, Nicole Schneiderhan-Marra & Georg M.N. Behrens, **Diminishing Immune Responses against Variants of Concern in Dialysis Patients 4 Months after SARS-CoV-2 mRNA Vaccination**, *Emerging Infectious Diseases*, https://doi.org/10.3201/eid2804.211907

8. **Matthias Becker***, Anne Cossmann*, Karsten Lürken, Daniel Junker, Jens Gruber, Jennifer Juengling, Gema Morillas Ramos, Andrea Beigel, Eike Wrenger, Gerhard Lonnemann, Metodi V. Stankov, Alexandra Dopfer-Jablonka, Philipp D. Kaiser, Bjoern Traenkle, Ulrich Rothbauer, Gérard Krause, Nicole Schneiderhan-Marra, Monika Strengert, Alex Dulovic & Georg M.N. Behrens, **Longitudinal cellular and humoral immune responses after triple BNT162b2 and fourth full-dose mRNA-1273 vaccination in haemodialysis patients**, *Frontiers in Immunology*, https://doi.org/10.3389/fimmu.2022.1004045

3.1. Development of MULTICOV-AB

3.1.1. Purpose and Development of the Assay

In early 2020, prior to first confirmed cases being detected in Europe, we began the development of a SARS-CoV-2 serological immunoassay utilizing highly sensitive Luminex xMAP technology, which we later named MULTICOV-AB. The purpose of MULTICOV-AB initially was to assess human serum for antibody binding to multiple SARS-CoV-2 antigens, thereby providing a broad overview of the humoral immune response in infected individuals.

As part of the development process for MULTICOV-AB, we evaluated the performance of several antigens, spanning the range of proteins found in SARS-CoV-2. Using a set of infected samples, we initially assessed whether we could detect binding of IgG, IgA or IgM towards the antigens. We excluded proteins based on SARS-CoV-2 Envelope and Matrix proteins, as we could not detect a specific antibody response. Therefore, we focussed on different constructs of SARS-CoV-2 Spike and Nucleocapsid for further development. These antigens are detailed in **Figure 9** and were used as the SARS-CoV-2 core panel of MULTICOV-AB throughout all studies described in this thesis. In addition, we excluded detection of antigen specific IgM, as we observed high background levels in serum samples from uninfected individuals.
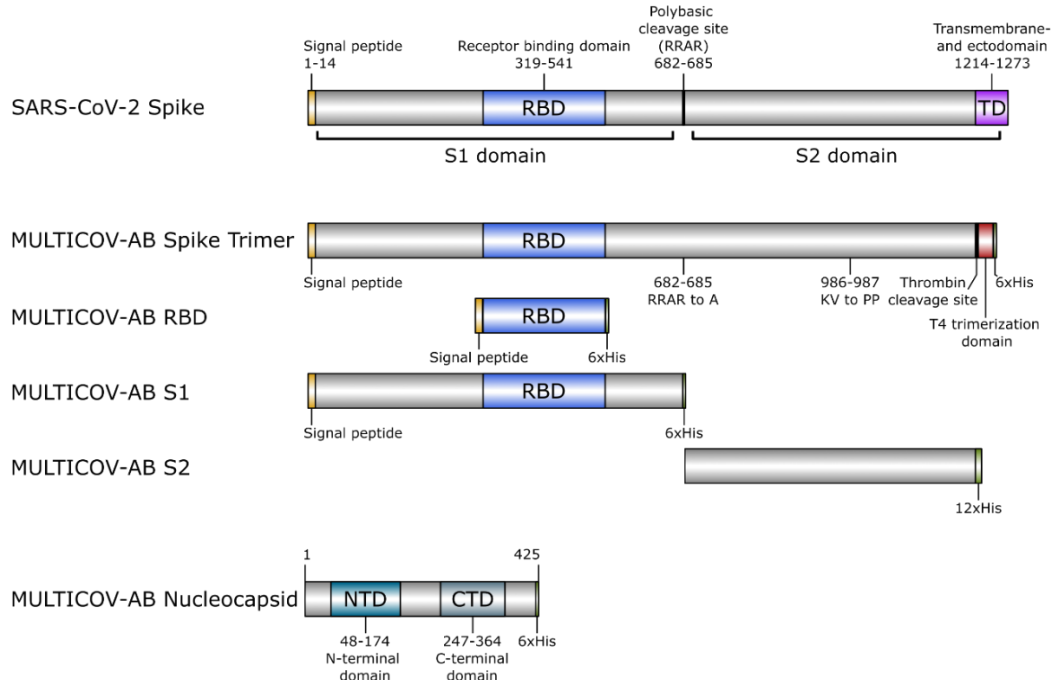

Figure 9: MULTICOV-AB SARS-CoV-2 antigen panel
Sequences of the MULTICOV-AB core antigen panel for SARS-CoV-2 are schematically displayed. Spike-based antigens are shown in reference to the original Whuan-Hu1 sequence (above) and divergences are annotated. Sequences are shown from N-terminus (left) to C-terminus (right). Positions and domains are drawn to scale.

Commercial vendors quickly developed SARS-CoV-2 serological assays on established high-throughput platforms. However, these assays were optimized for clinical routine laboratories and mostly focussed on single antigens only[147,148]. Most commonly, single-antigen assays utilized constructs of Spike protein for detection of SARS-CoV-2 specific antibodies, but in some cases Nucleocapsid was also used as the antigen, which is in line with our initial assessment of suitable antigens. Other groups also developed serological assays for SARS-CoV-2 research, which also simultaneously assess IgG levels to multiple SARS-CoV-2 antigens using Luminex xMAP technology, but also alternate methods, such as a spotted electrochemiluminescence ELISA or proteome microarrays[149-153].

3.1.2.   Clinical Assay Validation

Following the initial development cycle, we screened a large set of serum and plasma samples from 310 infected and 866 uninfected individuals, as described in Becker & Strengert et al. (**Appendix I**). From our pre-selected set of antigens, Spike Trimer and RBD stood out in their ability to distinguish infected from uninfected individuals as displayed in **Figure 10a**. The Spike Trimer is a construct spanning the entire ectodomain of the Spike protein, which mimics the virus Spike proteins natural trimerization with an inserted C-terminal T4 trimerization-domain. It contains stabilizing mutations in the S2 region and additionally the polybasic cleavage site, where virus Spike protein is naturally cleaved to initiate viral fusion is deleted (see **Figure 9**). The RBD utilized construct spans only the Receptor Binding Domain of the Spike protein, which enables to isolate the faction of antibodies directed towards the primary attachment site for SARS-COV-2 on human cells. These antigens were previously described for their excellent performance in ELISA[154]. We were able to achieve a greatly improved specificity for our assay by integrating the information from both antigens into a combined cut-off for sample classification (Becker & Strengert et al., **Appendix I: Figure 2a**). Through combining IgG and IgA detection, we could achieve a sensitivity and specificity of 90 and 100% respectively (Becker & Strengert et al., **Appendix I: Figure 2b, Table 3**). Additionally, we compared MULTICOV-AB performance to a selection of widely-used commercial immunoassays for a subset of 205 infected and 72 uninfected samples. MULTICOV-AB had improved sensitivity over all assays as shown in **Figure 10b** and Becker & Strengert et al. (**Appendix I: Table 1, Supplementary Figure 3**). The determined cut-off for IgG was used to define samples as seropositive to determine seroconversion events in infected or vaccinated individuals in following studies.
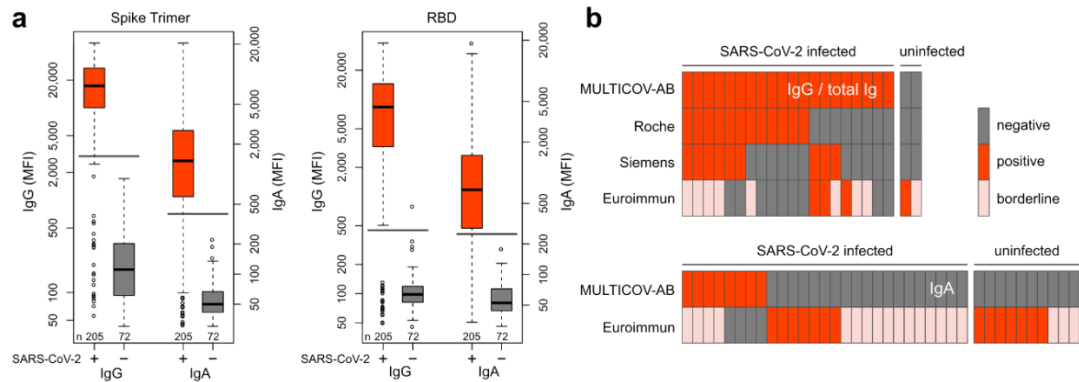
Figure 10: MULTICOV-AB, a sensitive and specific tool to monitor SARS-CoV-2 antibody responses

Control sera (grey, n = 72) and sera from individuals with PCR-confirmed SARS-CoV-2 infection (red, n = 205) were screened with MULTICOV-AB and commercially available single analyte SARS-CoV-2 IVD assays. **(a)** Reactivity towards Spike Trimer or RBD were found to be the best predictors of SARS-CoV-2 infection. Data are presented as Box-Whisker plots of a sample's MFI on a logarithmic scale. Box represents the median and the 25th and 75th percentiles, whiskers show the largest and smallest values. Outliers as determined by 1.5 times IQR of log-transformed data are depicted as circles. Cut-off values for classification for single antigens are displayed as horizontal lines (Spike Trimer IgG: 3,000 MFI, IgA: 400 MFI; RBD IgG: 450 MFI, IgA: 250 MFI). **(b)** Comparison of assay performance between MULTICOV-AB and commercial assays which detect total Ig (Elecsys Anti-SARS-CoV-2 (Roche); ADVIA Centaur SARS-CoV-2 Total (COV2T) (Siemens Healthineers)) or IgG (Anti-SARS-CoV-2-ELISA - IgG (Euroimmun)) or IgA (Anti-SARS-CoV-2-ELISA - IgA (Euroimmun)). SARS-CoV-2 infection status of samples based on PCR diagnostic is indicated as SARS-CoV-2 positive or negative. Results were classified as negative (grey), positive (red), or borderline (light red) as per the manufacturer's definition. Only samples with divergent antibody test results are shown. Figure adapted from Becker & Strengert et al. (**Appendix I: Figure 1**).

Classification with MULTICOV-AB was optimized for specificity so as to avoid false-positive results more than false-negative. Serology aims to detect antibodies, which inherently imply immune protection or reactivity of the immune system and it is therefore crucial to avoid falsely attributing immune protection to individuals, who may be insufficiently protected. This is in contrast to methods for detection of the virus itself such a PCR, where the cut-offs are optimized towards sensitivity, as the aim is to detect and prevent the spread of infection. Since PCR status was used as gold standard for whether a person was infected or not, this difference in assay cut-off optimisation can also explain why we were unable to reach a specificity of over 90%, which was in line with studies reporting that up 10% of SARS-CoV-2 positive individuals do not develop measureable antibody levels[149,155]. Other research groups taking similar approaches to develop SARS-CoV-2 serological assays reached comparable assay performances[149,151].

An intriguing point was the superior performance of Spike antigens over Nucleocapsid (Becker & Strengert et al., **Appendix I: Supplementary Figure 4**). An early study comparing serological assays reported, that combinatory use of antigens may improve assay performance, since some individuals showed a better reaction in Nucleocapsid based assays[147]. While samples from infected individuals showed high signals for SARS-CoV-2 Nucleocapsid in our study, we also found high signals in a significant proportion of pre-pandemic samples, which can be attributed to cross-reactive antibodies. We therefore had to exclude the Nucleocapsid from our classification in order to avoid false-positive results. Other groups were in agreement with our findings that Spike antigens perform superior to Nucleocapsid for tracking of SARS-CoV-2 infections[150,152,156], while others showed that detecting antibodies against Nucleocapsid was more specific[157]. Among the commercial assays we compared in our study, the best performing assay was based on Nucleocapsid instead of a Spike construct, however, it utilized a different means of antibody detection. In that assay, serum antibodies bridge between two Nucleocapsid proteins, one of which is bound to a bead and the other is bound to a fluorophore, thereby also being not selective for antibody classes[158]. Because the antibody must facilitate two binding events to the Nucleocapsid, this assay better filters out low-affinity binders compared to the classical detection with a secondary, species-specific antibody used in MULTICOV-AB. However, this bridging approach is less suitable for multiplexing because with a higher number of antigens, cross-reactivities of nonspecific binders become more likely and in addition it requires fluorophore-labelled antigens, driving the assay costs. Overall this demonstrates that the performance of antigens heavily depends on the specific assay setup.

3.1.3.   Technical Assay Validation

As part of the technical assay validation, we established quality control (QC) samples to be processed with every assay run in order to track performance. MULTICOV-AB was validated in a fit-for-purpose approach, which oriented itself on guidelines given by the EMA[159] and United States Food and Drug Administration (FDA)[160]. We assessed intra-assay variance, inter-assay variance, limit of detection, parallelism and matrix effects from serum or plasma samples as described in Becker & Strengert et al. (**Appendix I**). Overall the assay proved to deliver reliable results for IgG and IgA detection in serum and plasma samples with coefficients of variation (%CV) values of no larger than 8.5 % for SARS-CoV-2 antigens intra- or inter-assay variance (Becker & Strengert et al., **Appendix I: Supplementary Figure 2, Supplementary Table 1**). Reagent stability was not shown for prolonged periods, which is being addressed by current efforts for an extended validation.

3.1.4. Adaption of MULTICOV-AB During the COVID-19 Pandemic

In response to an evolving pandemic, MULTICOV-AB was also continually developed and adapted as show in **Figure 11**. In a rapidly changing landscape of vaccination recommendations and emerging virus variants, there was an urgent need for feedback from the scientific community to inform policy decisions.
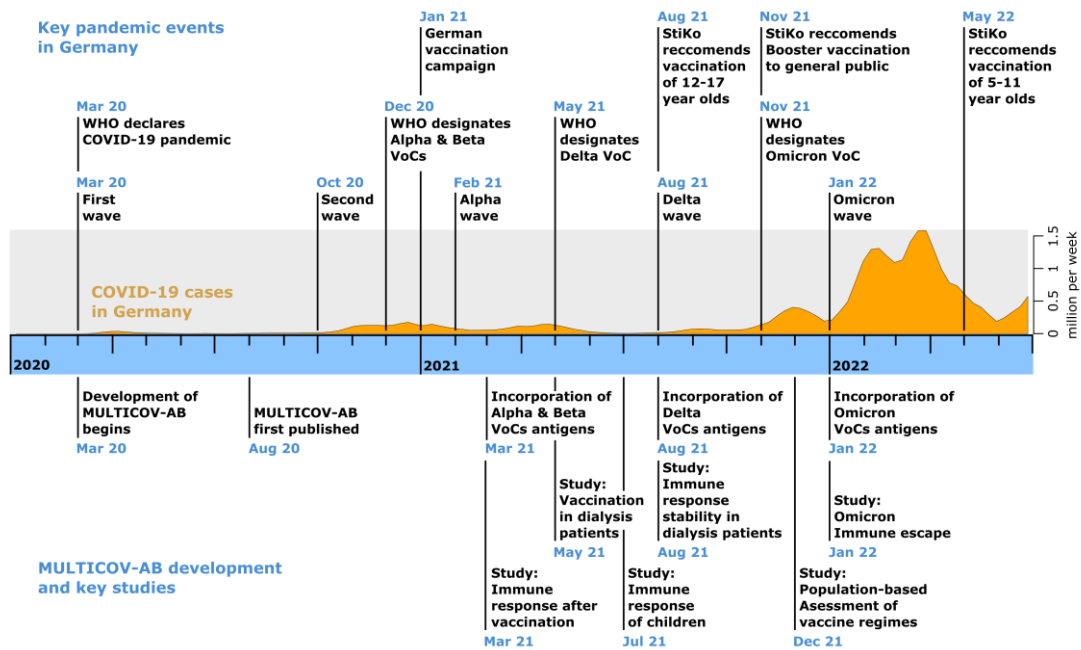
Figure 11: MULTICOV-AB adaption and key studies throughout the COVID-19 pandemic
A timeline of pandemic events for vaccination policies in Germany and SARS-CoV-2 VoCs is shown on top. Infection waves and numbers of cases per week are indicated for Germany. MULTICOV-AB assay development and adaption, as well as key studies are shown below. For studies and assay adaptions the first date of publication in preprint was used. Data for weekly cases in Germany was collected by WHO[10].

Through the flexibility of the multiplex technology we were able to rapidly adapt our antigen repertoire for MULTICOV-AB to include Spike and RBD constructs of SARS-CoV-2 VoCs and VoIs as they arose throughout the pandemic. For example, VoCs were first addressed by WHO in mid-December 2020, and we were able to publish data on changes in the immune response to them just three months later (Becker & Dulovic et al., **Appendix II**), delivering critical data which was used in official WHO reports[161]. For Delta and Omicron VoCs, we were already able to publish results at the beginning of the infection waves in Germany (Dulovic, Strengert & Morillas Ramos et al., **Appendix VII**; Junker, Becker & Wagner et al., **Appendix V**). We took advantage of the broad antigen spectrum of MULTICOV-AB to conduct a number of studies on topical issues during the pandemic, such as comparative analysis of vaccine regimens (Dulovic, Kessel & Harries et al., **Appendix IV**), changes in the SARS-CoV-2 immune response in children compared to adults (Renk, Dulovic & Seidel et al., **Appendix III**), and longevity of the vaccine-induced immune response in dialysis patients (Strengert, Becker & Morillas Ramos et al., **Appendix VI**; Dulovic, Strengert & Morillas Ramos et al., **Appendix VII**; Becker & Cossmann et al., **Appendix VIII**). Our findings in these studies are discussed in the following sections. In addition, we established semi-automated high-throughput measurements in 384-well format using a pipetting robot (Renk, Dulovic & Seidel et al., **Appendix III: Methods section**) and adapted our protocol for measuring IgG in saliva samples, which provides insights into the humoral immune response in the first line of defence against infection (Becker & Dulovic et al., **Appendix II: Figure 2**).

For future developments, the usage of dried blood spots as samples would enable the use of MULTICOV-AB in a broader range of studies, as was demonstrated for SARS-CoV-2 in multiple studies[150,162]. Dried blood spots have the advantage that no invasive venipuncture is required and sample collection is less skill and labour intensive[163]. Furthermore, building on MULTICOV-AB, we have developed an assay to measure surrogate neutralization for SARS-CoV-2 using the same RBD constructs as in MULTICOV-AB[164].

3.2. Humoral Immune Response to SARS-CoV-2

3.2.1. Distinguishing Vaccination from Natural Infection

Distinguishing between the humoral responses generated vaccination or infection was important to assess the performance of different vaccines. Moreover, it was crucial for use in epidemiological studies to understand the true infection rate by detecting unnoticed seroconversions, since in a significant proportion of individuals the disease is either asymptomatic or even completely undetected[22,41,165]. This differentiation was not possible with the majority commercial available antibody assays that used the Spike protein (or parts of it) as their single analyte. Our multiplex-based platform allowed the inclusion of a wide variety of antigens, enabling distinction between individuals with a vaccine-induced immune response and those that had been infected by SARS-CoV-2. We could show that only in an infection, a humoral immune response towards SARS-CoV-2 Nucleocapsid occurs, whereas it is absent in BNT vaccinated individuals as shown in **Figure 12**. We were later able to confirm the absence of a Nucleocapsid response for MOD, AZE and JJ vaccines as well (Dulovic, Kessel & Harries et al., **Appendix IV**). This was expected, as the in 2021 available COVID-19 vaccines in Germany were all formulated against the Spike protein only and do not contain any other parts of the virus. Due to the multiplex design of our assay, these data can all be collected at once from the same well, allowing for higher throughput and more comparable results in contrast to corresponding data from conventional ELISA formats.
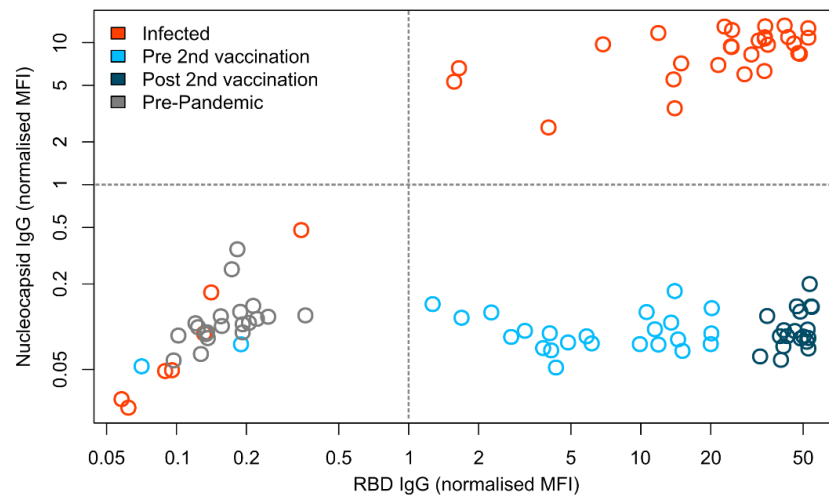
Figure 12: Distinguishing between vaccinated and infected donors
IgG response in sera from BNT162b2 vaccinated (pre second vaccination (light blue, n = 25), post second vaccination (dark blue, n = 20)), infected (red) (n = 35), and negative (grey) (n = 20) individuals were measured with MULTICOV-AB. IgG response is shown as normalized MFI for RBD (Wuhan strain) versus normalized Nucleocapsid MFI values allowing for visualization of separation between the different groups. Figure adapted from Becker & Dulovic et al. (**Appendix II: Figure 1**).

3.2.2.   The Unique SARS-CoV-2 Immune Response of Children

Through the early stages of the pandemic, study cohorts and testing strategy were targeted almost exclusively towards adults. As a result, it meant that there was very little understanding of the immune response following infection in children. As part of a multicentre study with the children's hospitals of Freiburg, Tübingen, Ulm and Heidelberg, we analysed the specific humoral response in a large longitudinal cohort of 548 children and 717 adults for up to a year post-infection (Renk, Dulovic & Seidel et al., **Appendix III**). Key to this study was the recruitment of all members of the same household, allowing for differences in humoral response, symptoms experienced and disease progression to be evaluated between individuals with comparable exposure risk. Children had a significantly lower seroprevalence compared to adults, with the majority of infections also being asymptomatic. This pattern of increased asymptomatic infections with lower age is in line with other studies[40,166]. However, SARS-CoV-2-specific IgG titres for Spike Trimer, S1, RBD and Nucleocapsid were all significantly increased in children as shown in **Figure 13**. Interestingly, titres themselves were not associated with symptomatic course of disease in exposed individuals overall, but we identified dysguesia as the best indicator of seropositivity in adults and children. These findings pointed towards children, whilst often having asymptomatic courses of disease, being better protected against SARS-CoV-2 than adults and might explain why COVID-19 affects the adult population much more heavily.
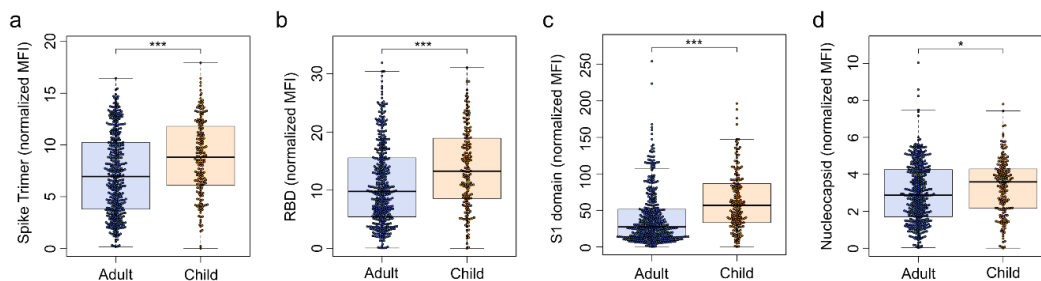
Figure 13: Children have a significantly higher humoral response to SARS-CoV-2 than adults
The humoral response generated following SARS-CoV-2 household exposure with seroconversion was examined using MULTICOV-AB. Children (orange, n = 181) produced significantly more antibodies against the Spike (**(a)** $p = 6.00 \times 10^{-6}$), Receptor Binding Domain (RBD) (**(b)** $p = 2.86 \times 10^{-6}$), S1 domain (**(c)** $p = 3.00 \times 10^{-14}$) and Nucleocapsid (**(d)** $p = 1.76 \times 10^{-2}$) than adults (blue, n = 414). Only samples from study time point 1 with a seropositive status are shown. Box and whisker plots with the box representing the median, 25th and 75th percentiles, while whiskers show the largest and smallest non-outlier values. Outliers were identified using upper/lower quartile ±1.5 times IQR. Statistical significance was calculated using Mann–Whitney-U (two-sided) with significance defined as being *<0.05, ***<0.001. Figure adapted from Renk, Dulovic & Seidel et al. (**Appendix III: Figure 1**).

This study was the first to associate the often milder symptoms in children with an improved humoral immune response and was included as part of the CDC report on COVID[167]. It occurred during the period of prolonged school closures within Germany and demonstrated clearly that using symptoms to identify potential infections was unreliable within children. At the time of publication on a pre-print server, debates as to whether or not to vaccinate children were ongoing and our results were featured in the eventual scientific justification of vaccination in children between ages 12 and 17 in Germany[168]. In agreement of our findings, other studies were also able to show a higher and more stable antibody response in children compared to adults[169,170]. Vaccination of children under 12 years of age has only recently been recommended by STIKO in Germany, but for the time being only with a single dose[171]. It will therefore be important to monitor the extent and stability of the induced humoral immune response in children after vaccination and inform further recommendations.

3.2.3.   The Vaccine-Induced Humoral Immune Response

Following the licencing of SARS-CoV-2 vaccinations within the EU, distribution began in the last few weeks of 2020. Initial studies, all provided by the manufacturers themselves, identified strong efficacy[102,103,110]. As antibody levels have been shown to correlate well with immunity for SARS-CoV-2[172,173], we independently investigated the humoral response following BNT two-dose vaccination. We identified that the BNT mRNA vaccine induced a humoral immune response to Spike protein on par or even stronger than infection (Becker & Dulovic et al., **Appendix II**). Due to vaccine shortage, it was politically debated whether to perform a single dose vaccination in a broader population instead of prioritizing completing vaccinations. Importantly, we demonstrated that a second dose of vaccine significantly boosted serum IgG as well as IgA antibody levels (Becker & Dulovic et al., **Appendix II: Figure 1c-d**) and was furthermore required to raise neutralizing antibodies towards SARS-CoV-2 in a virus neutralization test, as well as our surrogate neutralization assay (Becker & Dulovic et al., **Appendix II: Figure 4**).

Later in 2021, as part of the Germany-wide SARS-CoV-2 seroprevalence survey MuSPAD[174], we compared different vaccine regimens and their outcome on the humoral immune response (Dulovic, Kessel & Harries et al., **Appendix IV**). We found that Spike-specific IgG levels were lower in individuals vaccinated twice with AZE compared to homologous vaccination with either mRNA vaccine as shown in **Figure 14a** and Dulovic, Kessel & Harries et al. (**Appendix IV: Figure 1**). This finding is consistent with studies that showed reduced humoral as well as cellular responses of vector based vaccines compared with mRNA vaccines[175,176].

Particularly with respect to emerging VoCs these findings called into question the protective efficacy of AZE. However, we found that a heterologous vaccination regimen of AZE and an mRNA vaccine lead to comparable levels to homologous mRNA vaccination. A mixed vaccination regimen was later recommended in Germany to those who received a single dose of AZE, which our data supported[177].
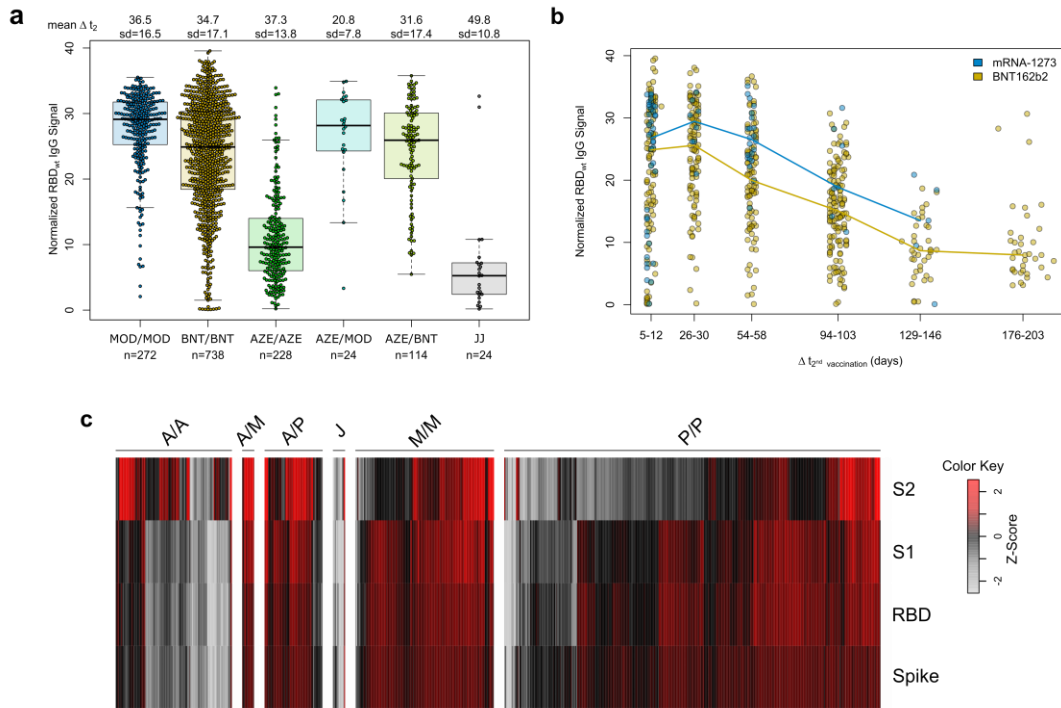
Figure 14: Vaccine response of different regimens and kinetics of antibody titres
(a) IgG antibody levels against RBD were measured with MULTICOV-AB. Individuals received either homologous mRNA-1273 (MOD/MOD, blue, n = 272), BNT162b2 (BNT/BNT, orange, n = 738) or ChAdOx1-S (AZE/AZE, green, n = 228), heterologous ChAdOx1-S-mRNA-1273 (AZE/MOD, light blue, n = 24), ChAdOx1-S-BNT162b2 (AZE/BNT, light green, n = 114), or a single dose of Ad26.CoV2.S (JJ, grey, n = 24). Raw MFI values were normalised against QC samples to generate signal ratios for each antigen. Data is shown as box and whisker plots overlaid with strip charts. Boxes represent medians, 25th and 75th percentiles and whiskers show the largest and smallest non-outlier values based on 1.5 IQR calculation. Time between sampling and full vaccination is displayed as mean and SD for each group. Number of samples per vaccination scheme are stated below. **(b)** Antibody kinetic up to 7 months after SARS-CoV-2 mRNA vaccination. Humoral vaccine response in independent donors was assessed by MULTICOV-AB. Samples were either 5 to 12, 26 to 30, 54 to 58, 94 to 103, 129 to 146 or 176 to 203 days post-second dose of either a two-dose BNT162b2 (yellow, n = 515) or mRNA-1273 (blue, n = 82) vaccination. Coloured line connects median response per time point and vaccine. Data is displayed as normalised IgG RBD ratio. **(c)** Antigen-specific antibody titres measured with MULTICOV-AB were scaled and centred per antigen. Resulting values greater than 2.5 and smaller than -2.5 were set to these extreme values instead. Samples were then clustered within their subgroups based on immunisation scheme and are displayed as a heat map. Negative values represent below average titres and positive values represent positive above average titres per antigen. Groups are annotated as in (a). Figure adapted from Dulovic, Kessel & Harries et al. (**Appendix IV: Figure 1, Figure 2, Figure 6)**.

At a later point in 2021, the JJ vaccine was introduced in Germany, which as per the manufacturer's specifications only required a single dose for immunisation, in contrast to all other then-licenced vaccines which required at least two doses. Like others[178,179], we found that the humoral immune response was significantly lower compared to the other vaccine regimens (Dulovic, Kessel & Harries et al., **Appendix IV: Figure 1**), with the majority of individuals who had received only this vaccine being classified as non-responsive. Subsequently, STIKO recommendations were adjusted to no longer accept a single dose of JJ as effective immunisation[180]. Notably, while both homologous vector-based vaccinations resulted in lower responses towards the Spike trimer, the S1 domain and the RBD, the response towards the S2 domain was comparable (**Figure 14c**). Considering that neutralizing antibodies are mostly binding the RBD, which is part of the S1 domain of the virus Spike protein[98], this observed bias towards generating S2-specific antibodies may explain the reduced vaccine efficacies for the vector-based vaccines compared to the mRNA vaccines.

Interestingly, homologous MOD vaccination induced significantly higher IgG levels compared to BNT. It is notable that the dosage of mRNA in MOD is higher than in BNT and that MOD vaccination was more often associated with adverse reactions than BNT[181,182]. However, recent findings indicate that MOD also confers a slightly better protection from breakthrough infections compared to BNT[183]. The dosage of mRNA in the formulation may therefore play a crucial role for future optimisations.

When analysing Saliva of BNT vaccinated donors, we found increased levels of Spike protein specific IgG 2-4 weeks after second vaccination, but no increase in IgA (Becker & Dulovic et al., **Appendix II: Figure 2**), which is in line with the findings of a more recent study[184]. The presence of salivary IgG indicates protection against virus spread by droplet infection in newly vaccinated individuals. However, the absence of IgA leaves open the question of whether the IgG levels, which are likely of serum origin[114,185] are sufficient and stable for prolonged periods of time after vaccination. Novel COVID-19 vaccination approaches utilizing the oral or nasal route[186] may induce a broader mucosal immune response including formation of mucosal IgA and provide improved protection at the entry site of SARS-COV-2.

In addition to efficacy of different vaccines and vaccine combinations, data on the longevity of the induced immune response were urgently needed to adjust public health recommendations over the course of the pandemic. When comparing samples with different time after initial immunisation, we could determine that the humoral immune response peaked after approximately 28 days and declined steadily afterwards for eight months after homologous mRNA vaccination as shown in **Figure 14b** and Dulovic, Kessel & Harries et al. (**Appendix IV: Figure 6**). In other sample sets, we also saw a steep decline in healthy donors from 3 to 16 weeks (Dulovic, Strengert & Morillas Ramos et al., **Appendix VII: Figure 1**) and from 5 to 35 weeks post initial immunisation (Becker & Cossmann et al., **Appendix VIII: Figure 2**). Our study findings are in agreement with others describing similar kinetics for the decline of the humoral immune response and associated protection from breakthrough infections[187-190]. It has also been shown that delaying the second dose of an mRNA vaccine can improve the magnitude and longevity of the humoral immune response[191]. Importantly, while antibody levels decline after vaccination, it was shown that the COVID-19 mRNA vaccines are able to induce germinal centre B cells, which persist after decline of circulating B cells and will contribute to long-term immunity[192].

Furthermore our results indicated, that convalescent individuals who were vaccinated had an immune response which was improved over individuals with the same vaccination regimen and no infection (Dulovic, Kessel & Harries et al., **Appendix IV: Figure 5**). This is in line with recent reports stating that breakthrough infections occurred less frequently in recovered and vaccinated individuals than in just vaccinated ones[193,194].

Between December 2021 and July 2022, two further SARS-CoV-2 vaccines have been approved for use in Germany[95]. Nuvaxovid (Novavax CZ a.s.) a protein-based vaccine, contains recombinant SARS-CoV-2 Spike protein equivalent to the original Wuhan-Hu 1 isolate[118], while COVID-19 Vaccine Valneva (Valneva Austria GmbH), an inactivated virus vaccine, utilizes a Wuhan virus strain, produced in cell culture[119]. Due to the pandemic situation and high percentage of recently infected or boosted population, these vaccines have not been administered widely in Germany as of July 2022[96]. However, ours and other studies have shown that a heterologous vaccine regimen is comparable or even superior, depending on the vaccines[175,176,195]. With constantly evolving recommendations based on emerging evidence, mixed vaccination regimens including newer vaccines will likely become standard in the future and it will be interesting to monitor their effects in comparison to the mRNA and Vector based vaccines. It is also likely, that the COVID-19 Vaccine Valneva will generate a Nucleocapsid response, due to containing a full virus particle, which may compromise the ability of MULTICOV-AB to distinguish the vaccine response from the infection.

3.2.4.   Vaccine Effectiveness Against SARS-CoV-2 VoCs

In 2021, the first major SARS-CoV-2 VoC spread worldwide and became the prevalent strains. We could show early on that VoCs and VoIs had evolved different levels of immune evasion by employing variant specific RBD and Spike proteins in MULTICOV-AB. Across multiple studies (Becker & Dulovic et al., **Appendix II**; Strengert, Becker & Morillas Ramos et al., **Appendix VI**; Dulovic, Strengert & Morillas Ramos et al., **Appendix VII**), we found IgG binding and virus neutralization in infected and vaccinated individuals greatly reduced for the Beta and Gamma variant, whereas it was only very slightly reduced compared to the original Wuhan isolate for the Alpha variant. This is highlighted in **Figure 15**, as well as in Becker & Dulovic et al. (**Appendix II: Figure 3, Figure 4**), Strengert, Becker & Morillas Ramos et al. (**Appendix VI: Figure 1**) and Dulovic, Strengert & Morillas Ramos et al. (**Appendix VII: Figure 2**).
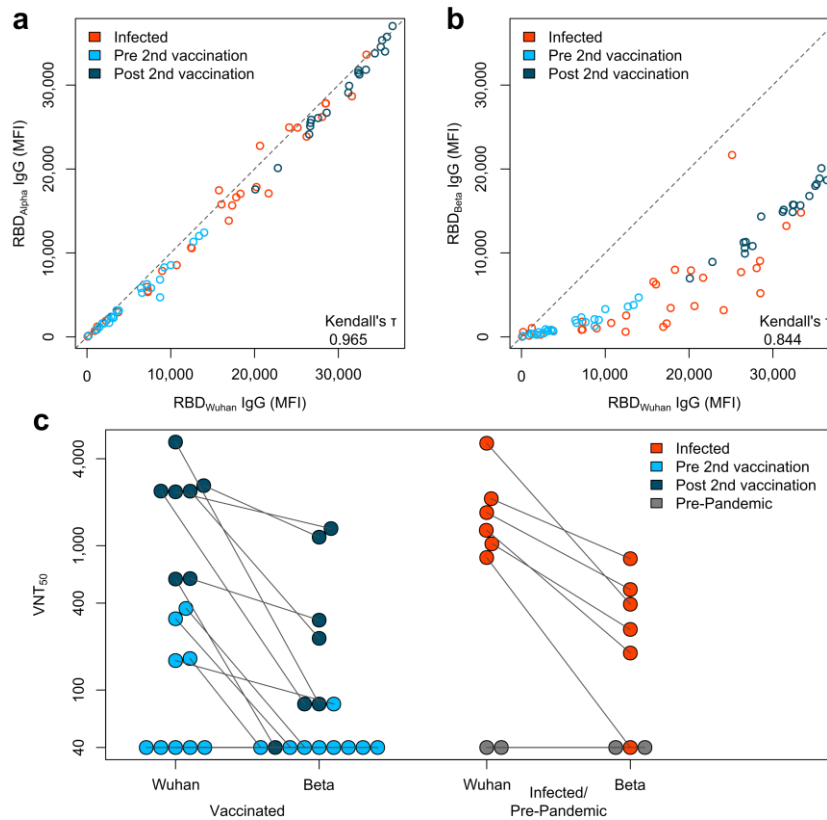
Figure 15: Humoral immune response towards Alpha and Beta VoCs
Variant RBD antigens for Alpha **(a)** and Beta **(b)** were generated and added to MULTICOV-AB to measure the immune response towards them in sera from BNT162b2 vaccinated pre-second dose (light blue, n = 25), post second dose (dark blue, n= 20), and infected (red, n = 35) individuals, compared to the Wuhan strain RBD. A linear curve (y = x) is shown as a dashed grey line to indicate an identical response between Wuhan strain and variant RBD. Kendall's tau was calculated to measure the ordinal association between the mutant and Wuhan strain. Neutralization for the Beta variant **(c)** displayed as virus neutralizing titres (VNT50) was measured in a virus neutralization assay compared to Wuhan strain with sera from BNT162b2 vaccinated (pre second vaccination (light blue, n =9), post second vaccination (dark blue, n = 7)), infected (red, n = 6), and negative (pre-pandemic) (grey, n = 2) individuals. Lines indicate unique samples. Figure adapted from Becker & Dulovic et al. (**Appendix II: Figure 3, Figure 4**).

Our results are in line with the findings of other groups, confirming immune escape properties for Beta and Gamma variants, but not for the Alpha variant[196-199]. Nonetheless, the Alpha variant proved better fit for spreading worldwide in the first half of 2021, where Beta and Gamma variants were only able to dominate single regions[133]. Due to low vaccine coverage at the time, the immune escape properties likely did not give enough of a significant advantage over the Alpha variant.

In the second half of 2021, the Delta variant became globally dominant. In vaccinated individuals, we found that the immune response was slightly reduced compared to the Alpha variant, but not to the same extent as for the Beta and Gamma variant (Dulovic, Kessel & Harries et al., **Appendix IV: Supplementary Figure 2**; Dulovic, Strengert & Morillas Ramos et al., **Appendix VII: Figure 2**). The findings of other studies in vaccinated and infected individuals varied from neutralizing activity being mostly retained against the Delta variant[164,200], to moderate loss of neutralizing activity and vaccine effectiveness[201,202]. From these results and given the increased infectivity of the Delta variant[132], the massive global increase in infections that came with the Delta wave in the second half of 2021 can be attributed to a combination of general increase in infectivity, but also immune escape properties of the Delta variant, especially in the light of the improved vaccine coverage in the second half of 2021.

We were also able to show, that Wuhan strain infection-induced immune responses followed the same patterns for different variants as shown previously for vaccinations (Renk, Dulovic & Seidel et al., **Appendix III: Figure 3**) and therefore likely offered no better protection from VoCs on the humoral level than vaccinations. We also could confirm that kinetics of the decrease in humoral immune response were comparable among SARS-CoV-2 variants (Dulovic, Kessel & Harries et al., **Appendix IV: Figure 7**).

The immune escape variants Beta and Gamma carry the RBD mutations K417T or K17N and E484K within the ACE2 binding interface, as well as the N510Y, which is also present in Alpha. In contrast, the Delta variant, which exhibits less immune evasion, but vastly superior infectivity over other VoCs instead carries L452R and T478K mutations, both of which are also within the ACE2 binding interface. VoC mutations in the RBD can drive virus immune evasion by inhibiting binding of neutralizing antibodies to RBD and enhance ACE2 binding affinity of RBD. This is supported by structural and computational studies of the RBD-ACE2 binding interface[135,203,204], as well as correlations of the mutations with variant immune escape based on data from studies such as ours.

SARS-CoV-2 omicron variant became globally dominant shortly after its identification at the end of 2021[143,144]. The first globally dominant Omicron variant belonged to sub-lineage BA.1, but was quickly superseded by sub-lineage BA.2, which in turn was superseded by three simultaneously dominant sub-linages BA.2.12.1, BA.4, and BA.5, of which it is unclear as of July 2022 which will prevail[133] (see also **Figure 8**). It was crucial for us to be flexible and not fall behind in this constant fluctuation of variants in order to generate relevant data to inform public health decisions and vaccine developments. We were able to rapidly implement RBD and Spike proteins for the BA.1 and BA.2 variants in MULTICOV-AB, as well as our surrogate neutralization assay[164]. We found a drastic reduction in the humoral immune response compared to previously circulating variants in vaccinated and infected individuals (Junker, Becker & Wagner et al., **Appendix V: Figure 1**). Booster vaccination has proven to be an effective tool in managing the pandemic, as shown by data from Israel, where it was the key factor in containing infections during the Delta wave[205]. In our study, the identified pattern of immune escape between SARS-CoV-2 variants persisted after booster vaccinations, but while booster vaccinations were effective against the Delta variant, they elicited a significantly lower immune response against Omicron BA.1 or BA.2 as shown in **Figure 16**. Other recent studies report that mRNA booster immunization does confer effective protection from Omicron, albeit to a lesser extent than other VoCs[206] and that boosted individuals are less often hospitalized[207]. Furthermore, hybrid immunity of vaccination and infection may be superior to pure vaccination[208,209], which is what our results with limited samples also indicated (Junker, Becker & Wagner et al., **Appendix V: Figure 2**).
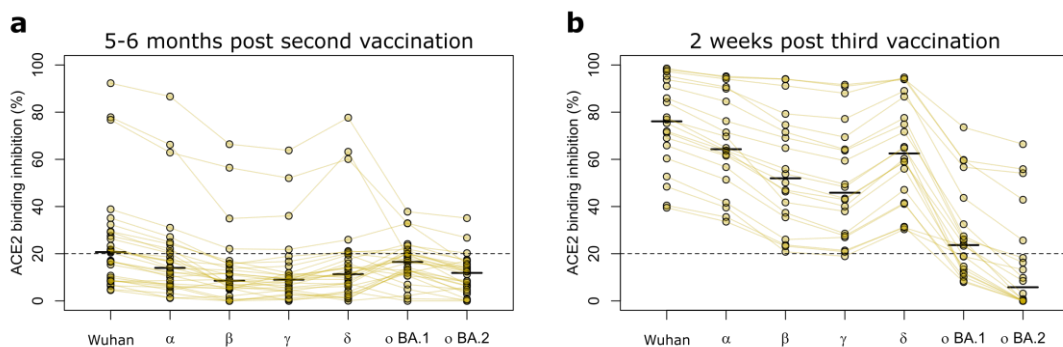
Figure 16: Effect on booster vaccination on ACE2 binding inhibition toward VoCs
Changes in ACE2 binding inhibition following the third dose of BNT162b2 for VoCs in serum samples from donors 5–6 months post–second dose of BNT162b2 (**(a)**, n= 20) and boosted donors (**(b)**, n=20, median 14 days post boost). Individual samples are highlighted by connected lines with bars representing medians. A value below 20% value indicates non responders and is shown by the dashed line. Figure adapted from Junker, Becker & Wagner et al. (**Appendix V: Figure 4**).

The Omicron waves so far (as of July 2022) have been characterized by large amounts of re-infections from convalescent individuals[140,145] and breakthrough infections in vaccinated individuals[210], which combined with the dramatic increase in COVID-19 cases emphasizes the unprecedented immune escape potential of the Omicron sub lineages. The Omicron variant therefore proved to be the first variant with strong immune escape properties which could spread and dominate globally. This was likely aided by rising vaccination coverage and the effect of booster vaccinations, which proved effective in restricting Delta variant spread and therefore benefitted spread of immune escape variants. Other studies also found diminished vaccine effectiveness and reduced binding of neutralizing antibodies[178,209,211-213]. Despite the large amount of mutations in the RBD the virus has evolved to retain its affinity for the ACE2 receptor (Junker, Becker & Wagner et al., **Appendix V: Supplementary Figure 2**). It has even been suggested that the Omicron sub lineages are to be considered a new virus serotype[214], supported by studies finding limited cross- neutralisation between Omicron and other VoCs[215-217].

3.2.5. Vaccine Response in Haemodialysis Patients

Immunocompromised patients were among the first to be vaccinated against SARS-CoV-2, due to their underlying conditions resulting in them having an increased risk of severe infection[36,123,124]. Haemodialysis patients are due to their treatment required to regularly attend hospitals/outpatient clinics, increasing their exposure risk towards the virus, while they have been previously shown to be poor responders for a variety of other vaccinations[126,127]. However, throughout the pandemic, official recommendations and guidelines for this group have always lagged behind the ongoing situation, meaning that attending physicians had to decide to the best of their knowledge how to proceed. To help guide these decisions, we followed a cohort of haemodialysis patients through their vaccination regimes (Strengert, Becker & Morillas Ramos et al., **Appendix VI**; Dulovic, Strengert & Morillas Ramos et al., **Appendix VII**; Becker & Cossmann et al., **Appendix VIII**). An overview of cohort sampling is shown in **Figure 17**.
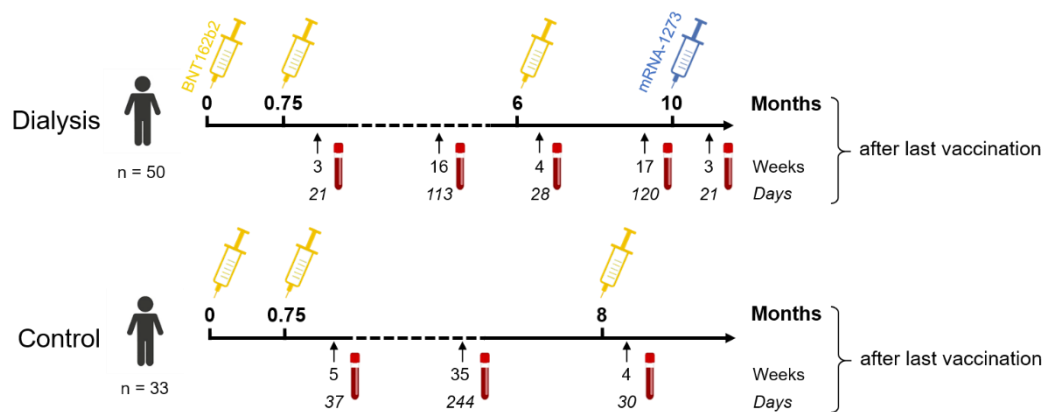
Figure 17: Participant recruitment scheme for longitudinal vaccination response analysis in haemodialysis patients after triple BNT162b2 and fourth full-dose mRNA-1273
Patients on haemodialysis (n=50) and healthcare workers as controls (n=33) were triple-vaccinated with BNT162b2 (yellow syringe) followed by a 100 μg (full) dose of mRNA-1273 (blue syringe) for dialysed individuals only. Samples were collected at multiple time points (red serum tubes). Sampling and vaccination schedule is given in days and weeks. Figure adapted from Becker & Cossmann et al. (**Appendix VIII: Figure 1**).

Initially, we found that although the vaccines had an effect in haemodialysis patients, they developed significantly lower levels of SARS-CoV-2-specific IgG in their serum and saliva 3 weeks after initial immunisation with two doses of BNT (Strengert, Becker & Morillas Ramos et al., **Appendix VI: Figure 1**). This reduction was also reflected in their IgG binding towards VoCs. The T-cell response was also reduced in haemodialysis patients, as measured by interferon gamma release upon stimulation of blood with SARS-CoV-2 Spike peptides (Strengert, Becker & Morillas Ramos et al., **Appendix VI: Figure 2**). However, on the individual level this did not correlate well with the reduction in the humoral immune response (Strengert, Becker & Morillas Ramos et al., **Appendix VI: Figure 3**), suggesting that for the vaccine response, the balance of humoral and cellular level is highly individual. Following up 16 weeks after first immunisation, we observed drastically reduced antibody levels in both dialysis patients and the control group (Dulovic, Strengert & Morillas Ramos et al., **Appendix VII: Figure 1**). We therefore then concluded that a third vaccination would be required, especially for the group of haemodialysis patients.

Subsequently, a third dose of BNT was administered during the Delta wave in Germany, followed by a fourth dose of MOD during the Omicron wave. For booster vaccinations, a MOD dosage of 50μg was recommended by STIKO for the general population[121]. However, in light of early data on the Omicron VoC indicating its potential for immune escape, the decision was taken to administer a full 100μg dose of MOD for the fourth vaccination, as is recommended for immunodeficient individuals[121].

We were able to show that the immune response towards Delta VoC upon initial vaccination was severely diminished in both the control group and dialysis patients (Dulovic, Strengert & Morillas Ramos et al., **Appendix VII: Figure 2**). However, the third vaccination was able to introduce a significant response towards the Delta variant, but not Omicron in dialysis patients (Becker & Cossmann et al., **Appendix VIII: Figure 3**).

As shown in **Figure 18**, only administration of a fourth vaccination dose was able to confer a significant humoral immune response toward the Omicron variant. Conversely to the observed fluctuations for the humoral immune response, the cellular response remained relatively constant and was dominated by individual high and low-responders throughout the study (Becker & Cossmann et al., **Appendix VIII: Figure 4**). In line with this finding, the cellular immune response to SARS-CoV-2 vaccines was found more stable in immunocompromised individuals, such as transplant recipients[218].
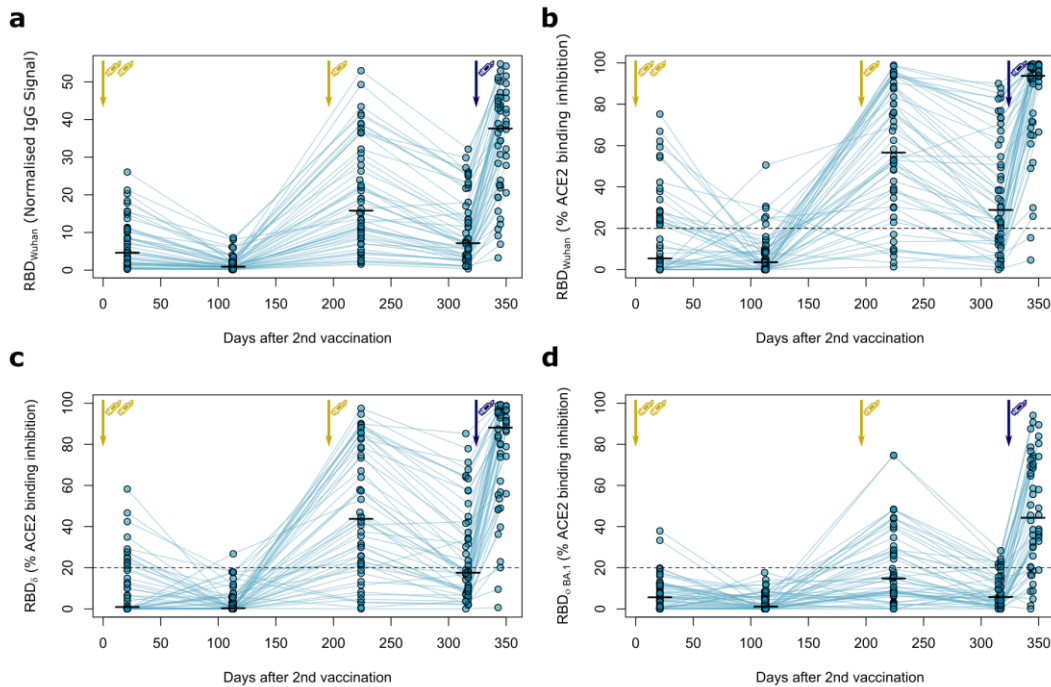
Figure 18: Longitudinal humoral immune response in haemodialysis patients after a triple vaccination with BNT162b2 and a fourth full-dose of mRNA-1273
IgG response **(a)** and ACE2 binding inhibition **(b, c, d)** towards the SARS-CoV-2 RBD of Wuhan strain **(a, b)**, Delta (δ, **(c)**) and Omicron BA.1 (o BA.1, **(d)**) isolates were measured in plasma from haemodialysis patients (n=50) using MULTICOV-AB **(a)** or an ACE2-RBD competition assay **(b, c, d)** after immunisation with a triple dose of BNT162b2 (yellow syringe) and a fourth full-dose of mRNA-1273 (blue syringe). Data is displayed as normalised median fluorescence intensity (MFI) signal for IgG binding **(a)** or as % ACE2 binding inhibition where 100% indicates maximum inhibition and 0% no inhibition **(b, c, d)**. Samples with an ACE2 binding inhibition of less than 20% (dashed line) are classified as non-responders **(b, c, d)**. Interconnecting lines represent samples from the same individual. Sampling time points in days after the standard complete two-dose BNT162b2 vaccination is stated below the graph. Figure adapted from Becker & Cossmann et al. (**Appendix VIII: Figure 3**).

Vaccines have been found to be less effective in immunocompromised individual[34,35], which is reflected in our findings of a reduced humoral immune response upon vaccination compared to healthy individuals. Furthermore, our findings are in line with reports that a third dose of vaccine is an effective boost of the immune response in immunocompromised individuals, such as patients receiving immunosuppressive medication[219] and cancer patients[220]. We showed that a third dose of the vaccine could elicit a significant immune response against the Delta variant, which is in line with other reports[221], whereas a fourth dose was required against the omicron variant for a majority of our study population. Similarly, others found that a fourth vaccination was required for an immune response towards Omicron in dialysis patients[222], but neutralizing antibodies towards Delta and Omicron were significantly reduced compared to the original virus isolate[223]. Another study found that a large portion of kidney transplant recipients with low immune response after third vaccination developed a neutralizing immune response after a fourth dose, while only a small portion that showed no response after three vaccinations developed a neutralizing response[224]. Taken together, the findings of our studies and others have highlighted that the SARS-CoV-2 vaccine response in immunocompromised individuals such as haemodialysis patients is highly individual, but overall inferior compared to healthy individuals. This at-risk group therefore requires adjusted vaccination regimes to compensate. It remains to be seen, how the immune response declines after a fourth dose, but from the decline we observed after second and third doses it is likely that immunocompromised individuals will have to be regularly vaccinated throughout the pandemic, where serological assays can serve as tools to identify individuals with insufficient responses for targeted vaccinations. The upcoming new generation of variant-adjusted vaccines[225] may improve response rates further. Although there are indications of improved protection, there are no are no population based data on efficacy available as of July 2022 and no EMA approval has been granted.

3.3. Cross Protection from hCoVs

3.3.1. High hCoV Response Rate Throughout the Population

As part of our routine SARS-CoV-2 measurements, we also assessed humoral responses towards the hCoVs, aiming to identify if cross-reactive or cross-protective patterns existed. We therefore included Spike S1 and Nucleocapsid antigens from all four hCoVs in the MULTICOV-AB antigen panel in addition to the previously described SARS-CoV-2 core panel. We identified that almost all individuals had an immune response towards the hCoVs, characterized by specific IgG binding to hCoV S1 and Nucleocapsid (Becker & Strengert et al., **Appendix I**; Becker & Dulovic et al., **Appendix II**; Renk, Dulovic & Seidel et al., **Appendix III**), suggesting that there is a high level of pre-exposure to hCoVs among the population. The only exception to this was in children under the age of five, where we identified a relatively high proportion of naïve individuals (Renk, Dulovic & Seidel et al., **Appendix III**). This is in agreement with previous seroprevalence data, where hCoV infection and corresponding ubiquitous seropositivity is on average found from the age of 5 onwards[88]. It was therefore difficult to study the effects of SARS-CoV-2 infection in hCoV naïve individuals. Given these limitations, another approach is to study large sample sets for associations of SARS-CoV-2 infection with hCoV infection or longitudinally follow individuals after SARS-CoV-2 infection to capture alterations in hCoV antibody titres.

3.3.2. Correlation of SARS-CoV-2 Seroconversion and hCoV Immune Response

Initially, we examined potential correlations between pre-existing hCoV titre and SARS-CoV-2 infection status to identify potential cross-protective effects (Becker & Strengert et al., **Appendix I**). We found that there was no clear association of the hCoV-specific humoral immune response with SARS-CoV-2 infection (Becker & Strengert et al., **Appendix I: Figure 4b-c**), indicating no cross-protective effect. Using clustering analysis, we found that the immune response towards the different hCoV antigens correlated best within the clusters of alpha- or beta-hCoVs (Becker & Strengert et al., **Appendix I: Figure 4a**), indicating that there is cross-reactivity within these genuses of coronaviruses, but not between them or to SARS-CoV-2. We did, however, find a slight ordinal association of a high response towards alpha and beta hCoVs with infection (Becker & Strengert et al., **Appendix I: Figure 5**), meaning that SARS-CoV-2 infected individuals were more likely to be hCoV high-responders, although the diverse sample set limited the extent by which this data set could be used for further analyses.
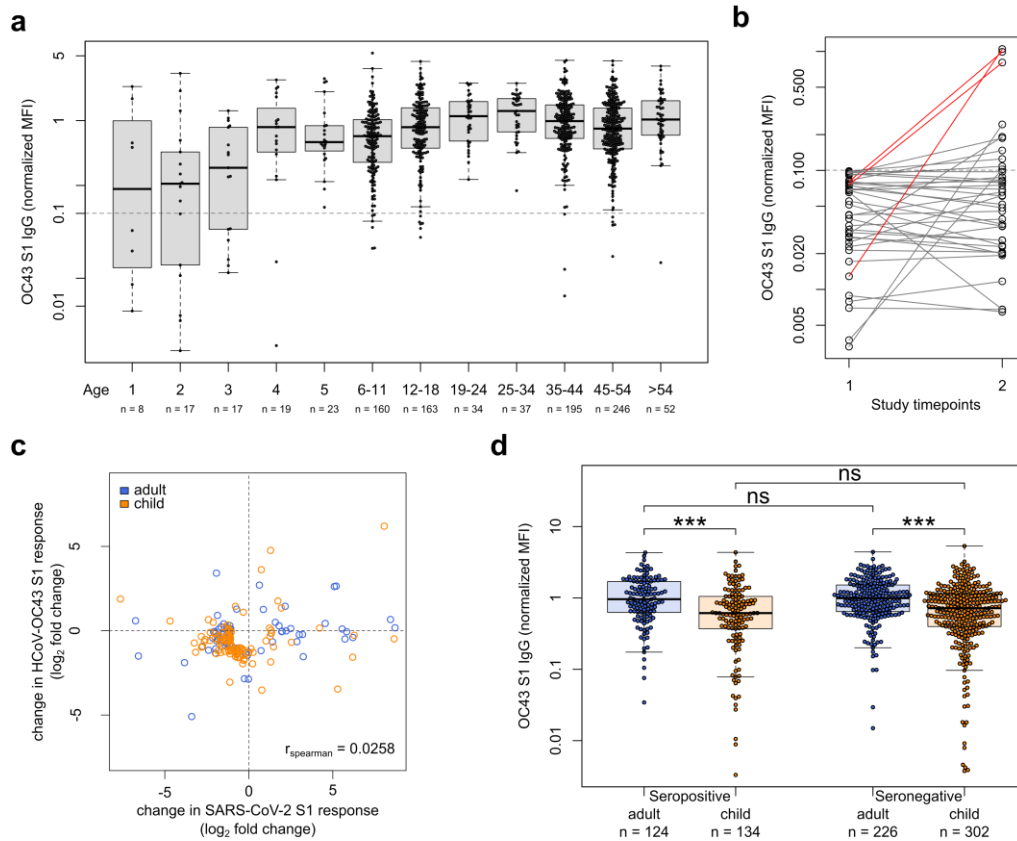
Figure 19: hCoVs offer no protection against SARS-CoV-2, nor do they show a boost-back antibody response following SARS-CoV-2 infection
Samples from households with a known index case (n = 971) were examined with MULTICOV-AB to determine whether the antibody response to hCoVs (exemplified by OC43 S1 IgG titres) provides any protection against infection with SARS-CoV-2. **(a)** Initial screening of the population showed that seroprevalence increases with age, although several samples were within the blank range of the hCoV assays, indicating the presence of naïve samples. Naïve samples were defined as those having less than one-tenth the mean antibody response (indicated by dotted line), with the majority of these samples occurring in children under the age of five. Boxes represent the median, 25th and 75th percentiles, while whiskers show the largest and smallest non-outlier values. Outliers were identified using upper/lower quartile ±1.5 times IQR. **(b)** Line graph showing the longitudinal response of these naïve samples from study time point 1 to 2 (median 231 days), with new infections with OC43 shown in red. **(c)** When comparing paired samples longitudinally within the SARS-CoV-2 seropositive subgroup, there was no increase in hCoV-OC43 S1 response in either adults (blue, n = 76) or children (orange, n = 103) following SARS-CoV-2 infection. Change in response is presented as log2-fold change from study time point 1 to 2 and only samples with either log2-fold change greater than 1 or smaller than −1 are shown. Spearman's rank was used to calculate the ordinal association between the change in response for HCoV-OC43 and SARS-CoV-2. **(d)** Box and whisker plot showing there is no significant difference in OC43 S1 IgG antibody titre between SARS-CoV-2 seropositive and seronegative individuals, among either adults (blue, n = 440, p = 0.974) or children (orange, n = 436, p= 0·214). Boxes represent the median, 25th and 75th percentiles, while whiskers show the largest and smallest non-outlier values. Outliers were identified using upper/lower quartile ±1.5 times IQR. Statistical significance was calculated by Mann–Whitney-U (two-sided) with *** indicating a p value < 0.001 and ns indicating a p value > 0.05. Figure adapted from Renk, Dulovic & Seidel et al. (**Appendix III: Figure 4**).

In another study, we followed children that had been exposed to or infected by SARS-CoV-2 (Renk, Dulovic & Seidel et al., **Appendix III**). In this cohort we were able to identify hCoV-seronegative children (**Figure 19a**), mostly aged three and below. In our analysis of longitudinal samples from these hCoV-naïve children, we identified hCoV infection events that lead to seroconversion as displayed in **Figure 19b**. We interpreted these as a first contact of hCoVs with an immune system, however, the increase in hCoV titres did not coincide with and increase SARS-CoV-2 titres (**Figure 19c**). We further found no association of hCoV titres with overall SARS-CoV-2 seropositivity across the study cohort of 548 children and 717 adults, as shown in **Figure 19d**. Moreover, when analysing the effects of vaccination, we found that SARS-CoV-2 seroconversion induced by BNT vaccination also did not affect hCoV S1 titres, as shown in **Figure 20**.
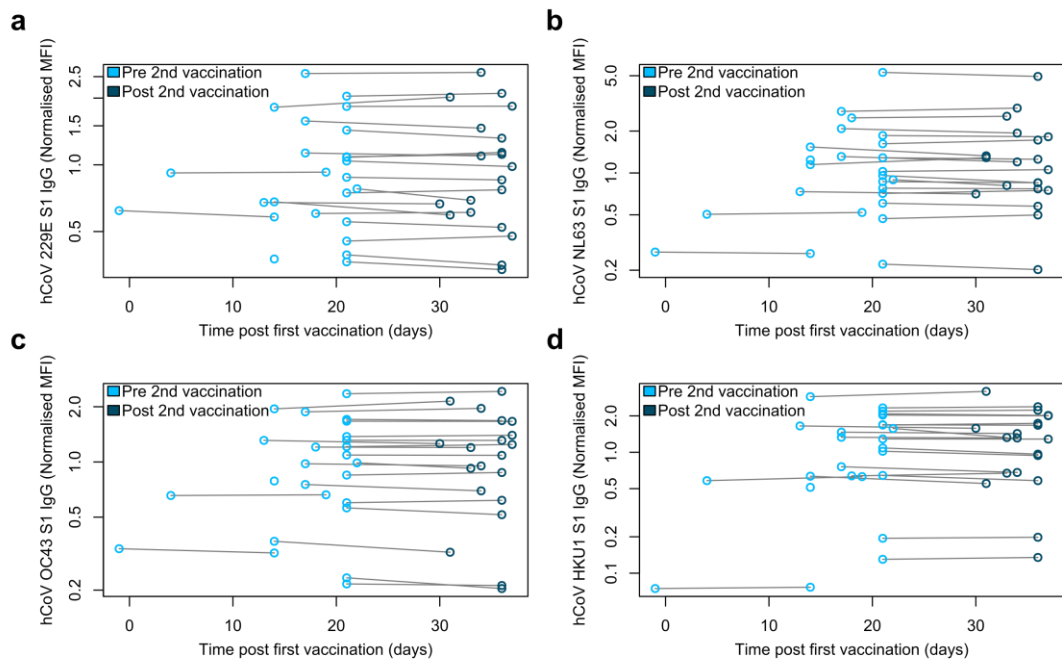
Figure 20: Cross-reactivity of antibodies to endemic coronaviruses in vaccinated individuals:
BNT162b2 vaccinated individuals did not have an increased antibody response towards S1 proteins of the endemic coronaviruses 229E **(a)**, NL63 **(b)**, OC43 **(c)** and HKU1 **(d)**. hCoV S1 IgG titres are displayed against time after first vaccination dose in days. All samples were measured using MULTICOV-AB. Light blue (n=25) indicates samples are pre second vaccination, while dark blue (n=20) indicates samples are post second vaccination. Lines indicated paired samples from the same donor. Figure adapted from Becker & Dulovic et al. (**Appendix II: Supplementary Figure 3**).

Overall, our findings with MULTICOV-AB suggest, that there is no association of SARS-CoV-2 infection or seroconversion with hCoV infection or seroconversion. Other studies using different serological methods also found no association of SARS-CoV-2 specific antibody levels with hCoV infected sera or vice versa[149,226,227].

In contrast to these findings, other groups have identified cross reactivity stemming from the S2 region in the Spike protein, where conservation among coronaviruses is higher than in the S1 region[169,192,228,229]. One study found cross-reactivity to the betacoronaviruses HKU1 and OC43 in the serum of children, but not in adults[169], which was in line with the findings of a second study, that found children to have hCoV mediated neutralizing activity towards SARS-CoV-2[228]. Another study found a boost of hCoV reactivity in the first week after COVID-19 hospitalisation[229]. Furthermore, a small portion of Spike reactive germinal centre B cells which exhibit cross-specificity with HKU1 and OC43 were found in vaccinated individuals in another study[192] and a small portion of monoclonal antibodies isolated from SARS-CoV-2 infected donors was found to be cross reactive to hCoV Spike proteins, but did not target the RBD[203].

In MULTICOV-AB we employed only hCoV S1 and Nucleocapsid antigens and were therefore unable to evaluate these effects, which appear to be limited to the S2 region of Spike. The limitation of this cross reactivity to the S2 region is congruent with our initial characterisation of the MULTICOV-AB SARS-CoV-2 S2 antigen, where we found a large amount of false-positive IgG binding from uninfected donors, leading to reduced sensitivity and ultimately excluding S2 from our classification (Becker & Strengert et al., **Appendix I: Figure 2c**). Despite being unable to assess antibody binding towards hCoV S2, our finding that an hCoV infection was not associated with SARS-CoV-2 seroconversion remains valid because an hCoV infection would be reflected in our antigens as we demonstrated using naïve sera.

While our studies are focussed on the humoral immune response, there are findings which suggest that a level of cross-protection may be conferred via the cellular immune response through hCoV-induced T-cells in SARS-CoV-2 naïve individuals[230-232]. Therefore, cross-protection via hCoV infection may not be ruled out by our findings. The only way to definitely confirm this would be to study a large cohort with a known history of hCoV infection throughout the pandemic and determine whether hCoVs infection does confer additional protection from SARS-CoV-2.

Chapter 4: Conclusion and Outlook

In this thesis, we developed MULTICOV-AB, one of the first published multiplex SARS-CoV-2 serological assays and thereby generated a tool to study the humoral immune response towards SARS-CoV-2 in-depth. This development formed the basis for a multitude of studies about ongoing topics within the COVID-19 pandemic.

Initially, we evaluated a set of SARS-CoV-2 antigens to form a core antigen panel and determined an optimal cut-off for classification of serum and plasma samples from infected individuals. We reached a sensitivity of 90% while retaining 100% specificity for MULTICOV-AB in a sample set from over 300 infected and over 850 uninfected individuals, using detection of IgG and IgA, which we were later able to confirm with other large sample sets. We found Spike based antigens to allow for more specific classification than those based on Nucleocapsid. MULTICOV-AB had an improved classification over widely used commercial assays.

Although initially hypothesized, we found no evidence of cross-protection from seasonal hCoVs across the studies of this thesis. This may in part be due to our selection of hCoV antigens, as other groups have shown that cross-reactivity can stem from the virus Spike S2 domain, which we did not include in our hCoV antigen panel. However, the presence of cross-reactive antibodies does not confirm an actual impact on cross protective immunity, especially as antibodies binding to the Spike S2 domain are seldom neutralizing in human coronaviruses. It is possible that hCoV cross-protection may be conferred on the level of the cellular immune response instead, as recent findings are suggesting.

The development of vaccines was a key step in managing infection rates and stabilizing health systems. Vaccines were developed and approved in a fast-track system by authorities. Although safety and efficacy had been well documented in clinical trials, the development of COVID-19 vaccines proceeded at an unprecedentedly rapid pace, while at the same time achieving broad dissemination in the population. It was therefore crucial to independently monitor the outcome of vaccinations to ensure efficacy and longevity of the induced protective immune response. Using MULTICOV-AB, we could verify that mRNA vaccines, which saw their first widespread use during the COVID-19 pandemic, were able to induce a strong humoral immune response on par or exceeding the response in COVID-19 convalescent individuals. We further showed that administering a second vaccine dose led to greatly improved antibody formation and was required to induce a neutralizing antibody response.

In a population based study, we compared different vaccine regimens and found homologous vector based vaccination to induce an inferior humoral immune response compared to homologous mRNA vaccination, which is also reflected in retrospective studies of vaccine efficacy over the pandemic. A heterologous regimen of vector based and mRNA vaccination was able to confer an immune response on par with a homologous mRNA regimen, which was subsequently also recommended by German health authorities for individuals who had received a single dose of vector based vaccine. In addition we showed that the humoral immune response peaked roughly 28 days post immunisation and steadily declined over six months for homologous mRNA vaccination, which called into question the longevity of vaccine protection.

In the initial pandemic stages, children were found to get infected at a lower than average rate and were more often asymptomatic. We therefore studied the immune response upon virus exposure in children as compared to adults and found children to form higher antibody levels, which was accompanied by a general milder course of disease observed by us and others. Seroconversion did not coincide with symptomatic course of infection in children and adults, meaning that asymptomatic individuals did not necessarily have worse protection.

The sheer volume of reinfections and the presence of separate virus reservoirs in different countries led to rapid evolution of SARS-CoV-2, and the first major SARS-CoV-2 variants emerged in late 2020. Vaccine trial studies for the most widely used COVID-19 vaccines were all performed in 2020 whilst the prevalent virus strains had not yet evolved any key RBD mutations. However, vaccines were administered to the general population in 2021, where the globally predominant variants were Alpha and Delta, which were characterized by increased infection rates and mutations in the RBD, raising concerns of virus immune escape capabilities. We were able to adjust our assay systems and add variant RBD proteins to our antigen panel corresponding to the virus variants, which enabled us to study how mutations affected the potency of the immune response elicited by vaccines and infections. Across several studies, we found varying levels of immune escape for different variants ranging from virtually none in the Alpha variant to significant reduction in Beta and Gamma variants.

The observed diminished response against SARS-CoV-2 variants as well as the general decline of the humoral immune response observed by us and others led health authorities to recommend a third, booster vaccination towards the end of 2021. We found the booster vaccination to compensate for diminishing antibody levels as well as for immune escape by the Delta variant, which was prevalent at the time. In 2022 the Omicron variant has become dominant worldwide and introduced a dramatic increase in worldwide infections and vaccine breakthroughs. We and others

showed that the Omicron variant is capable of immune escape to an extent beyond what was observed for previously circulating variants.

We further studied the immune response in patients on haemodialysis, who are an at-risk group in a pandemic setting. We found vaccination to induce an inferior humoral immune response and observed rapidly decreasing antibody levels in a haemodialysis cohort, whilst the cellular immune response remained more constant. A booster vaccination was able to confer an improved immune response towards Delta variant, but only a fourth dose elicited any significant response towards the Omicron variant. These patients will be continually monitored, but it is likely that they will have to be constantly re-vaccinated so long as the pandemic persists.

As of July 2022, the Omicron wave is still ongoing and it is unclear how infections rates and further virus mutations will develop in the future. The COVID-19 pandemic will remain a constantly evolving field, where conclusions and decisions may have to be revised within months for example due to emergence of a new virus variant. The implementation of variant adjusted vaccines and recommendations by health authorities for further booster vaccination campaigns will likely play a key part in the outcome of the COVID-19 pandemic.

Our research focussed mainly on the humoral immune response. However, immunity to SARS-CoV-2 is also conferred on the level of the cellular immune response. To provide a complete picture, findings regarding the cellular immune response must also always be considered. Future research with MULTICOV-AB will aim to characterize the more recent Omicron sub-lineages BA.4, BA.5 and BA.2.12.1 and any new emerging variants. The multiplex assay platform allows to rapidly integrate new antigens as we have shown in this thesis. Finally, developments in the vaccination landscape should be followed closely to confirm their outcomes, with special focus on new vaccines and vaccine regimens. Here, MULTICOV-AB can serve as a tool for vaccine manufacturers to aid in development with in-depth analysis of the antibody response.

Critical decisions for public health and socioeconomics need to be accompanied by hard scientific evidence, if the pandemic is to be overcome. The work of this thesis was aimed at generating relevant data to inform such critical decisions. Overall, we were able to deliver data on vaccines, virus variants and groups of special interest such as children or haemodialysis patients in a time sensitive manner and contributed towards a better understanding of the immunity towards SARS-CoV-2.

References

1   Zhu, N. *et al.* A Novel Coronavirus from Patients with Pneumonia in China, 2019. *New England Journal of Medicine* **382**, 727-733, doi:10.1056/NEJMoa2001017 (2020).

2   Zhou, P. *et al.* A pneumonia outbreak associated with a new coronavirus of probable bat origin. *Nature* **579**, 270-273, doi:10.1038/s41586-020-2012-7 (2020).

3   Wacharapluesadee, S. *et al.* Evidence for SARS-CoV-2 related coronaviruses circulating in bats and pangolins in Southeast Asia. *Nature Communications* **12**, 972, doi:10.1038/s41467-021-21240-1 (2021).

4   Wu, F. *et al.* A new coronavirus associated with human respiratory disease in China. *Nature* **579**, 265-269, doi:10.1038/s41586-020-2008-3 (2020).

5   Wu, A. *et al.* Genome Composition and Divergence of the Novel Coronavirus (2019-nCoV) Originating in China. *Cell Host & Microbe* **27**, 325-328, doi:10.1016/j.chom.2020.02.001 (2020).

6   Drosten, C. *et al.* Identification of a Novel Coronavirus in Patients with Severe Acute Respiratory Syndrome. *New England Journal of Medicine* **348**, 1967-1976, doi:10.1056/NEJMoa030747 (2003).

7   Peiris, J. S. M., Guan, Y. & Yuen, K. Y. Severe acute respiratory syndrome. *Nature Medicine* **10**, S88-S97, doi:10.1038/nm1143 (2004).

8   Hu, B., Guo, H., Zhou, P. & Shi, Z.-L. Characteristics of SARS-CoV-2 and COVID-19. *Nature Reviews Microbiology* **19**, 141-154, doi:10.1038/s41579-020-00459-7 (2021).

9   Gorbalenya, A. E. *et al.* The species Severe acute respiratory syndrome-related coronavirus: classifying 2019-nCoV and naming it SARS-CoV-2. *Nature Microbiology* **5**, 536-544, doi:10.1038/s41564-020-0695-z (2020).

10   World Health Organization. *WHO COVID-19 Dashboard* (2020), https://covid19.who.int/, accessed 17.07.2022.

11   Böhmer, M. M. *et al.* Investigation of a COVID-19 outbreak in Germany resulting from a single travel-associated primary case: a case series. *The Lancet Infectious Diseases* **20**, 920-928, doi:10.1016/S1473-3099(20)30314-5 (2020).

12   World Health Organization. *WHO Director-General's opening remarks at the media briefing on COVID-19-11 March 2020, Geneva, Switzerland* (2020).

13   Chan Jasper, F.-W. *et al.* Improved Molecular Diagnosis of COVID-19 by the Novel, Highly Sensitive and Specific COVID-19-RdRp/Hel Real-Time Reverse Transcription-PCR Assay Validated In Vitro and with Clinical Specimens. *Journal of Clinical Microbiology* **58**, e00310-00320, doi:10.1128/JCM.00310-20 (2020).

14   Stadnytskyi, V., Bax Christina, E., Bax, A. & Anfinrud, P. The airborne lifetime of small speech droplets and their potential importance in SARS-CoV-2 transmission. *Proceedings of the National Academy of Sciences* **117**, 11875-11877, doi:10.1073/pnas.2006874117 (2020).

15   Meselson, M. Droplets and Aerosols in the Transmission of SARS-CoV-2. *New England Journal of Medicine* **382**, 2063-2063, doi:10.1056/NEJMc2009324 (2020).

16   van Doremalen, N. *et al.* Aerosol and Surface Stability of SARS-CoV-2 as Compared with SARS-CoV-1. *New England Journal of Medicine* **382**, 1564-1567, doi:10.1056/NEJMc2004973 (2020).

17   Khan, M. *et al.* Visualizing in deceased COVID-19 patients how SARS-CoV-2 attacks the respiratory and olfactory mucosae but spares the olfactory bulb. *Cell* **184**, 5932-5949.e5915, doi:10.1016/j.cell.2021.10.027 (2021).

18   Meinhardt, J. *et al.* Olfactory transmucosal SARS-CoV-2 invasion as a port of central nervous system entry in individuals with COVID-19. *Nature Neuroscience* **24**, 168-175, doi:10.1038/s41593-020-00758-5 (2021).

19   Lauer, S. A. *et al.* The Incubation Period of Coronavirus Disease 2019 (COVID-19) From Publicly Reported Confirmed Cases: Estimation and Application. *Annals of Internal Medicine* **172**, 577-582, doi:10.7326/M20-0504 (2020).

20   Marks, M. *et al.* Transmission of COVID-19 in 282 clusters in Catalonia, Spain: a cohort study. *The Lancet Infectious Diseases* **21**, 629-636, doi:10.1016/S1473-3099(20)30985-3 (2021).

21   Jones Terry, C. *et al.* Estimating infectiousness throughout SARS-CoV-2 infection course. *Science* **373**, eabi5273, doi:10.1126/science.abi5273 (2021).

22   Li, R. *et al.* Substantial undocumented infection facilitates the rapid dissemination of novel coronavirus (SARS-CoV-2). *Science* **368**, 489-493, doi:10.1126/science.abb3221 (2020).

23   Stokes, E. K. *et al.* Coronavirus Disease 2019 Case Surveillance - United States, January 22-May 30, 2020. *MMWR Morb Mortal Wkly Rep* **69**, 759-765, doi:10.15585/mmwr.mm6924e2 (2020).

24   Chen, N. *et al.* Epidemiological and clinical characteristics of 99 cases of 2019 novel coronavirus pneumonia in Wuhan, China: a descriptive study. *The Lancet* **395**, 507-513, doi:10.1016/S0140-6736(20)30211-7 (2020).

25   Wang, D. *et al.* Clinical Characteristics of 138 Hospitalized Patients With 2019 Novel Coronavirus–Infected Pneumonia in Wuhan, China. *JAMA* **323**, 1061-1069, doi:10.1001/jama.2020.1585 (2020).

26   Giacomelli, A. *et al.* Self-reported Olfactory and Taste Disorders in Patients With Severe Acute Respiratory Coronavirus 2 Infection: A Cross-sectional Study. *Clinical Infectious Diseases* **71**, 889-890, doi:10.1093/cid/ciaa330 (2020).

27   Tong, J. Y., Wong, A., Zhu, D., Fastenberg, J. H. & Tham, T. The Prevalence of Olfactory and Gustatory Dysfunction in COVID-19 Patients: A Systematic Review and Meta-analysis. *Otolaryngology–Head and Neck Surgery* **163**, 3-11, doi:10.1177/0194599820926473 (2020).

28   Yan, C. H., Faraji, F., Prajapati, D. P., Boone, C. E. & DeConde, A. S. Association of chemosensory dysfunction and COVID-19 in patients presenting with influenza-like symptoms. *Int Forum Allergy Rhinol* **10**, 806-813, doi:10.1002/alr.22579 (2020).

29   Gao, Z. *et al.* A systematic review of asymptomatic infections with COVID-19. *Journal of Microbiology, Immunology and Infection* **54**, 12-16, doi:10.1016/j.jmii.2020.05.001 (2021).

30   Mizumoto, K., Kagaya, K., Zarebski, A. & Chowell, G. Estimating the asymptomatic proportion of coronavirus disease 2019 (COVID-19) cases on board the Diamond Princess cruise ship, Yokohama, Japan, 2020. *Euro Surveill* **25**, doi:10.2807/1560-7917.Es.2020.25.10.2000180 (2020).

31   Nishiura, H. *et al.* Estimation of the asymptomatic ratio of novel coronavirus infections (COVID-19). *International Journal of Infectious Diseases* **94**, 154-155, doi:10.1016/j.ijid.2020.03.020 (2020).

32   Goh, K. J. *et al.* Rapid Progression to Acute Respiratory Distress Syndrome: Review of Current Understanding of Critical Illness from Coronavirus Disease 2019 (COVID-19) Infection. *Ann Acad Med Singap* **49**, 108-118 (2020).

33   Zhou, F. *et al.* Clinical course and risk factors for mortality of adult inpatients with COVID-19 in Wuhan, China: a retrospective cohort study. *The Lancet* **395**, 1054-1062, doi:10.1016/S0140-6736(20)30566-3 (2020).

34   Manothummetha, K. *et al.* Immunogenicity and Risk Factors Associated With Poor Humoral Immune Response of SARS-CoV-2 Vaccines in Recipients of Solid Organ Transplant: A Systematic Review and Meta-Analysis. *JAMA Network Open* **5**, e226822-e226822, doi:10.1001/jamanetworkopen.2022.6822 (2022).

35   Galmiche, S. *et al.* Immunological and clinical efficacy of COVID-19 vaccines in immunocompromised populations: a systematic review. *Clinical Microbiology and Infection* **28**, 163-177, doi:10.1016/j.cmi.2021.09.036 (2022).

36   Kuderer, N. M. & Lyman, G. H. COVID-19 vaccine effectiveness in patients with cancer: remaining vulnerabilities and uncertainties. *Lancet Oncol* **23**, 693-695, doi:10.1016/s1470-2045(22)00252-2 (2022).

37   Grasselli, G. *et al.* Baseline Characteristics and Outcomes of 1591 Patients Infected With SARS-CoV-2 Admitted to ICUs of the Lombardy Region, Italy. *JAMA* **323**, 1574-1581, doi:10.1001/jama.2020.5394 (2020).

38   Viner, R. M. *et al.* Susceptibility to SARS-CoV-2 Infection Among Children and Adolescents Compared With Adults: A Systematic Review and Meta-analysis. *JAMA Pediatrics* **175**, 143-156, doi:10.1001/jamapediatrics.2020.4573 (2021).

39   Wu, Z. & McGoogan, J. M. Characteristics of and Important Lessons From the Coronavirus Disease 2019 (COVID-19) Outbreak in China: Summary of a Report of 72 314 Cases From the Chinese Center for Disease Control and Prevention. *JAMA* **323**, 1239-1242, doi:10.1001/jama.2020.2648 (2020).

40   Lu, X. *et al.* SARS-CoV-2 Infection in Children. *New England Journal of Medicine* **382**, 1663-1665, doi:10.1056/NEJMc2005073 (2020).

41   Levin, A. T. *et al.* Assessing the age specificity of infection fatality rates for COVID-19: systematic review, meta-analysis, and public policy implications. *European Journal of Epidemiology* **35**, 1123-1138, doi:10.1007/s10654-020-00698-1 (2020).

42   Butowt, R., Bilińska, K. & von Bartheld, C. Why Does the Omicron Variant Largely Spare Olfactory Function? Implications for the Pathogenesis of Anosmia in Coronavirus Disease 2019. *The Journal of Infectious Diseases*, jiac113, doi:10.1093/infdis/jiac113 (2022).

43   Schulze, H. & Bayer, W. Changes in Symptoms Experienced by SARS-CoV-2-Infected Individuals – From the First Wave to the Omicron Variant. *Frontiers in Virology* **2**, doi:10.3389/fviro.2022.880707 (2022).

44   Menni, C. *et al.* Symptom prevalence, duration, and risk of hospital admission in individuals infected with SARS-CoV-2 during periods of omicron and delta variant dominance: a prospective observational study from the ZOE COVID Study. *The Lancet* **399**, 1618-1624, doi:10.1016/S0140-6736(22)00327-0 (2022).

45   Whitaker, M. *et al.* Variant-specific symptoms of COVID-19 among 1,542,510 people in England. *Preprint at medRxiv*, doi:10.1101/2022.05.21.22275368 (2022).

46   van Kessel, S. A. M., Olde Hartman, T. C., Lucassen, P. L. B. J. & van Jaarsveld, C. H. M. Post-acute and long-COVID-19 symptoms in patients with mild diseases: a systematic review. *Family Practice* **39**, 159-167, doi:10.1093/fampra/cmab076 (2022).

47   Matta, J. *et al.* Association of Self-reported COVID-19 Infection and SARS-CoV-2 Serology Test Results With Persistent Physical Symptoms Among French Adults During the COVID-19 Pandemic. *JAMA Internal Medicine* **182**, 19-25, doi:10.1001/jamainternmed.2021.6454 (2022).

48   Berlit, P. Wir brauchen Biomarker. *DGNeurologie* **5**, 175-176, doi:10.1007/s42451-022-00435-w (2022).

49   Mariano, G., Farthing, R. J., Lale-Farjat, S. L. M. & Bergeron, J. R. C. Structural Characterization of SARS-CoV-2: Where We Are, and Where We Need to Be. *Frontiers in Molecular Biosciences* **7**, doi:10.3389/fmolb.2020.605236 (2020).

50   Masters, P. S. *The Molecular Biology of Coronaviruses* in *Advances in Virus Research* Vol. 66 193-292 (Academic Press, 2006).

51   Chan, J. F.-W. *et al.* Genomic characterization of the 2019 novel human-pathogenic coronavirus isolated from a patient with atypical pneumonia after visiting Wuhan. *Emerging Microbes & Infections* **9**, 221-236, doi:10.1080/22221751.2020.1719902 (2020).

52   Lamers, M. M. & Haagmans, B. L. SARS-CoV-2 pathogenesis. *Nature Reviews Microbiology* **20**, 270-284, doi:10.1038/s41579-022-00713-0 (2022).

53   V'kovski, P., Kratzel, A., Steiner, S., Stalder, H. & Thiel, V. Coronavirus biology and replication: implications for SARS-CoV-2. *Nature Reviews Microbiology* **19**, 155-170, doi:10.1038/s41579-020-00468-6 (2021).

54   Tai, W. *et al.* Characterization of the receptor-binding domain (RBD) of 2019 novel coronavirus: implication for development of RBD protein as a viral attachment inhibitor and vaccine. *Cellular & Molecular Immunology* **17**, 613-620, doi:10.1038/s41423-020-0400-4 (2020).

55   Beumer, J. *et al.* A CRISPR/Cas9 genetically engineered organoid biobank reveals essential host factors for coronaviruses. *Nature Communications* **12**, 5498, doi:10.1038/s41467-021-25729-7 (2021).

56 Hoffmann, M. *et al.* SARS-CoV-2 Cell Entry Depends on ACE2 and TMPRSS2 and Is Blocked by a Clinically Proven Protease Inhibitor. *Cell* **181**, 271-280.e278, doi:10.1016/j.cell.2020.02.052 (2020).

57 Sungnak, W. *et al.* SARS-CoV-2 entry factors are highly expressed in nasal epithelial cells together with innate immune genes. *Nature Medicine* **26**, 681-687, doi:10.1038/s41591-020-0868-6 (2020).

58 Lukassen, S. *et al.* SARS-CoV-2 receptor ACE2 and TMPRSS2 are primarily expressed in bronchial transient secretory cells. *The EMBO Journal* **39**, e105114, doi:10.15252/embj.20105114 (2020).

59 Bestle, D. *et al.* TMPRSS2 and furin are both essential for proteolytic activation of SARS-CoV-2 in human airway cells. *Life Science Alliance* **3**, e202000786, doi:10.26508/lsa.202000786 (2020).

60 Laporte, M. *et al.* The SARS-CoV-2 and other human coronavirus spike proteins are fine-tuned towards temperature and proteases of the human airways. *PLOS Pathogens* **17**, e1009500, doi:10.1371/journal.ppat.1009500 (2021).

61 Zhao, M.-M. *et al.* Cathepsin L plays a key role in SARS-CoV-2 infection in humans and humanized mice and is a promising target for new drug development. *Signal Transduction and Targeted Therapy* **6**, 134, doi:10.1038/s41392-021-00558-8 (2021).

62 Snijder, E. J. *et al.* A unifying structural and functional model of the coronavirus replication organelle: Tracking down RNA synthesis. *PLOS Biology* **18**, e3000715, doi:10.1371/journal.pbio.3000715 (2020).

63 Kung, Y.-A. *et al.* Molecular Virology of SARS-CoV-2 and Related Coronaviruses. *Microbiology and Molecular Biology Reviews* **86**, e00026-00021, doi:10.1128/mmbr.00026-21 (2022).

64 Mendonça, L. *et al.* Correlative multi-scale cryo-imaging unveils SARS-CoV-2 assembly and egress. *Nature Communications* **12**, 4629, doi:10.1038/s41467-021-24887-y (2021).

65 Ghosh, S. *et al.* Beta-Coronaviruses Use Lysosomes for Egress Instead of the Biosynthetic Secretory Pathway. *Cell* **183**, 1520-1535.e1514, doi:10.1016/j.cell.2020.10.039 (2020).

66 Van Regenmortel, M. H. V. *What Is a B-Cell Epitope?* in *Epitope Mapping Protocols: Second Edition* 3-20 (Humana Press, 2009).

67 Choudhary, A. *et al.* Characterization of the Antigenic Heterogeneity of Lipoarabinomannan, the Major Surface Glycolipid of *Mycobacterium tuberculosis*, and Complexity of Antibody Specificities toward This Antigen. *The Journal of Immunology*, ji1701673, doi:10.4049/jimmunol.1701673 (2018).

68 Murphy, K. & Weaver, C. *Janeway's immunobiology*. 9 edn (Garland science, 2016).

69 Yoshida, T. *et al.* Memory B and memory plasma cells. *Immunol Rev* **237**, 117-139, doi:10.1111/j.1600-065X.2010.00938.x (2010).

70 Schroeder, H. W., Jr. & Cavacini, L. Structure and function of immunoglobulins. *J Allergy Clin Immunol* **125**, S41-52, doi:10.1016/j.jaci.2009.09.046 (2010).

71 Underdown, B. J. & Schiff, J. M. Immunoglobulin A: Strategic Defense Initiative at the Mucosal Surface. *Annual Review of Immunology* **4**, 389-417, doi:10.1146/annurev.iy.04.040186.002133 (1986).

72 Forthal Donald, N. Functions of Antibodies. *Microbiology Spectrum* **2**, 2.4.21, doi:10.1128/microbiolspec.AID-0019-2014 (2014).

73 Walker, L. M. & Burton, D. R. Passive immunotherapy of viral infections: 'super-antibodies' enter the fray. *Nature Reviews Immunology* **18**, 297-308, doi:10.1038/nri.2017.148 (2018).

74 Spiegelberg, H. L. & Fishkin, B. G. The catabolism of human G immunoglobulins of different heavy chain subclasses. 3. The catabolism of heavy chain disease proteins and of Fc fragments of myeloma proteins. *Clin Exp Immunol* **10**, 599-607 (1972).

75 Amanna, I. J., Carlson, N. E. & Slifka, M. K. Duration of Humoral Immunity to Common Viral and Vaccine Antigens. *New England Journal of Medicine* **357**, 1903-1915, doi:10.1056/NEJMoa066092 (2007).

76 Finco, D. *et al.* Cytokine release assays: Current practices and future directions. *Cytokine* **66**, 143-155, doi:10.1016/j.cyto.2013.12.009 (2014).

77   Wine, Y., Horton, A. P., Ippolito, G. C. & Georgiou, G. Serology in the 21st century: the molecular-level analysis of the serum antibody repertoire. *Curr Opin Immunol* **35**, 89-97, doi:10.1016/j.coi.2015.06.009 (2015).

78   Luminex Corporation. *MagPlex® Microspheres*, https://www.luminexcorp.com/magplex-microspheres/, accessed 09.08.2022.

79   Lu, R. *et al.* Genomic characterisation and epidemiology of 2019 novel coronavirus: implications for virus origins and receptor binding. *The Lancet* **395**, 565-574, doi:10.1016/S0140-6736(20)30251-8 (2020).

80   Grifoni, A. *et al.* A Sequence Homology and Bioinformatic Approach Can Predict Candidate Targets for Immune Responses to SARS-CoV-2. *Cell Host & Microbe* **27**, 671-680.e672, doi:10.1016/j.chom.2020.03.002 (2020).

81   Meyer, B., Drosten, C. & Müller, M. A. Serological assays for emerging coronaviruses: Challenges and pitfalls. *Virus Research* **194**, 175-183, doi:10.1016/j.virusres.2014.03.018 (2014).

82   Buchholz, U. J. *et al.* Contributions of the structural proteins of severe acute respiratory syndrome coronavirus to protective immunity. *Proceedings of the National Academy of Sciences* **101**, 9804-9809, doi:10.1073/pnas.0403492101 (2004).

83   Poon, L. L. M., Guan, Y., Nicholls, J. M., Yuen, K. Y. & Peiris, J. S. M. The aetiology, origins, and diagnosis of severe acute respiratory syndrome. *The Lancet Infectious Diseases* **4**, 663-671, doi:10.1016/S1473-3099(04)01172-7 (2004).

84   World Health Organization. WHO guidelines for the global surveillance of severe acute respiratory syndrome (SARS). WHO/CDS/CSR/ARO/2004.1 (2004), https://www.who.int/publications/i/item/who-guidelines-for-the-global-surveillance-of-severe-acute-respiratory-syndrome-(-sars), accessed 25.07.2022.

85   Woo, P. C. *et al.* Longitudinal profile of immunoglobulin G (IgG), IgM, and IgA antibodies against the severe acute respiratory syndrome (SARS) coronavirus nucleocapsid protein in patients with pneumonia due to the SARS coronavirus. *Clin Diagn Lab Immunol* **11**, 665-668, doi:10.1128/cdli.11.4.665-668.2004 (2004).

86   Li, G., Chen, X. & Xu, A. Profile of Specific Antibodies to the SARS-Associated Coronavirus. *New England Journal of Medicine* **349**, 508-509, doi:10.1056/NEJM200307313490520 (2003).

87   UK Research and Innovation. *What is the purpose of testing for COVID-19?* (2020), https://coronavirusexplained.ukri.org/en/article/vdt0006/, accessed 08.08.2022.

88   Huang, A. T. *et al.* A systematic review of antibody mediated immunity to coronaviruses: kinetics, correlates of protection, and association with severity. *Nature Communications* **11**, 4704, doi:10.1038/s41467-020-18450-4 (2020).

89   Che, X.-y. *et al.* Antigenic Cross-Reactivity between Severe Acute Respiratory Syndrome—Associated Coronavirus and Human Coronaviruses 229E and OC43. *The Journal of Infectious Diseases* **191**, 2033-2037, doi:10.1086/430355 (2005).

90   Dijkman, R. *et al.* The dominance of human coronavirus OC43 and NL63 infections in infants. *Journal of Clinical Virology* **53**, 135-139, doi:10.1016/j.jcv.2011.11.011 (2012).

91   Patrick, D. M. *et al.* An Outbreak of Human Coronavirus OC43 Infection and Serological Cross-Reactivity with SARS Coronavirus. *Canadian Journal of Infectious Diseases and Medical Microbiology* **17**, 152612, doi:10.1155/2006/152612 (2006).

92   Edridge, A. W. D. *et al.* Seasonal coronavirus protective immunity is short-lasting. *Nature Medicine* **26**, 1691-1693, doi:10.1038/s41591-020-1083-1 (2020).

93   European Medicines Agency. *COVID-19: how EMA fast-tracks development support and approval of medicines and vaccines* (2020), https://www.ema.europa.eu/en/news/covid-19-how-ema-fast-tracks-development-support-approval-medicines-vaccines, accessed 28.07.2022.

94   U.S. Food and Drug Administration. *Development and Licensure of Vaccines to Prevent COVID-19* (2020), https://www.fda.gov/regulatory-information/search-fda-guidance-documents/development-and-licensure-vaccines-prevent-covid-19, accessed 28.07.2022.

95   Paul-Ehrlich-Institut. *List of COVID-19 Vaccines with a marketing authorisation*, https://www.pei.de/EN/medicinal-products/vaccines-human/covid-19/covid-19-node.html, accessed 29.07.2022.

96   Bundesministerium für Gesundheit (BMG). *COVID-19 Impfdashboard*, https://impfdashboard.de/, accessed 29.07.2022.

97   Heinz, F. X. & Stiasny, K. Distinguishing features of current COVID-19 vaccines: knowns and unknowns of antigen presentation and modes of action. *npj Vaccines* **6**, 104, doi:10.1038/s41541-021-00369-6 (2021).

98   Piccoli, L. *et al.* Mapping Neutralizing and Immunodominant Sites on the SARS-CoV-2 Spike Receptor-Binding Domain by Structure-Guided High-Resolution Serology. *Cell* **183**, 1024-1042.e1021, doi:10.1016/j.cell.2020.09.037 (2020).

99   Nelson, J. *et al.* Impact of mRNA chemistry and manufacturing process on innate immune activation. *Science Advances* **6**, eaaz6893, doi:doi:10.1126/sciadv.aaz6893 (2020).

100   Corbett, K. S. *et al.* SARS-CoV-2 mRNA vaccine design enabled by prototype pathogen preparedness. *Nature* **586**, 567-571, doi:10.1038/s41586-020-2622-0 (2020).

101   Vogel, A. B. *et al.* BNT162b vaccines protect rhesus macaques from SARS-CoV-2. *Nature* **592**, 283-289, doi:10.1038/s41586-021-03275-y (2021).

102   Polack, F. P. *et al.* Safety and Efficacy of the BNT162b2 mRNA Covid-19 Vaccine. *New England Journal of Medicine* **383**, 2603-2615, doi:10.1056/NEJMoa2034577 (2020).

103   Baden, L. R. *et al.* Efficacy and Safety of the mRNA-1273 SARS-CoV-2 Vaccine. *New England Journal of Medicine* **384**, 403-416, doi:10.1056/NEJMoa2035389 (2020).

104   Mendonça, S. A., Lorincz, R., Boucher, P. & Curiel, D. T. Adenoviral vector vaccine platforms in the SARS-CoV-2 pandemic. *npj Vaccines* **6**, 97, doi:10.1038/s41541-021-00356-x (2021).

105   Woolsey, C. & Geisbert, T. W. Current state of Ebola virus vaccines: A snapshot. *PLOS Pathogens* **17**, e1010078, doi:10.1371/journal.ppat.1010078 (2021).

106   van Doremalen, N. *et al.* ChAdOx1 nCoV-19 vaccine prevents SARS-CoV-2 pneumonia in rhesus macaques. *Nature* **586**, 578-582, doi:10.1038/s41586-020-2608-y (2020).

107   Folegatti, P. M. *et al.* Safety and immunogenicity of the ChAdOx1 nCoV-19 vaccine against SARS-CoV-2: a preliminary report of a phase 1/2, single-blind, randomised controlled trial. *The Lancet* **396**, 467-478, doi:10.1016/S0140-6736(20)31604-4 (2020).

108   Mercado, N. B. *et al.* Single-shot Ad26 vaccine protects against SARS-CoV-2 in rhesus macaques. *Nature* **586**, 583-588, doi:10.1038/s41586-020-2607-z (2020).

109   World Health Organisation. Considerations for the Assessment of COVID-19 Vaccines for Listing by WHO. (2020), https://www.who.int/publications/m/item/considerations-for-the-assessment-of-covid-19-vaccines-for-listing-by-who, accessed 11.09.2022.

110   Voysey, M. *et al.* Safety and efficacy of the ChAdOx1 nCoV-19 vaccine (AZD1222) against SARS-CoV-2: an interim analysis of four randomised controlled trials in Brazil, South Africa, and the UK. *The Lancet* **397**, 99-111, doi:10.1016/S0140-6736(20)32661-1 (2021).

111   Sadoff, J. *et al.* Safety and Efficacy of Single-Dose Ad26.COV2.S Vaccine against Covid-19. *New England Journal of Medicine* **384**, 2187-2201, doi:10.1056/NEJMoa2101544 (2021).

112   Barda, N. *et al.* Safety of the BNT162b2 mRNA Covid-19 Vaccine in a Nationwide Setting. *New England Journal of Medicine* **385**, 1078-1090, doi:10.1056/NEJMoa2110475 (2021).

113   Xie, Y., Xu, E., Bowe, B. & Al-Aly, Z. Long-term cardiovascular outcomes of COVID-19. *Nature Medicine* **28**, 583-590, doi:10.1038/s41591-022-01689-3 (2022).

114   Krammer, F. SARS-CoV-2 vaccines in development. *Nature* **586**, 516-527, doi:10.1038/s41586-020-2798-3 (2020).

115   Pollard, A. J. & Bijker, E. M. A guide to vaccinology: from basic principles to new developments. *Nature Reviews Immunology* **21**, 83-100, doi:10.1038/s41577-020-00479-7 (2021).

116   World Health Organization. *COVID19 Vaccine Tracker*, https://covid19.trackvaccines.org/, accessed 11.09.2022.

117   Tian, J.-H. *et al.* SARS-CoV-2 spike glycoprotein vaccine candidate NVX-CoV2373 immunogenicity in baboons and protection in mice. *Nature Communications* **12**, 372, doi:10.1038/s41467-020-20653-8 (2021).

118 Heath, P. T. *et al.* Safety and Efficacy of NVX-CoV2373 Covid-19 Vaccine. *New England Journal of Medicine* **385**, 1172-1183, doi:10.1056/NEJMoa2107659 (2021).

119 Lazarus, R. *et al.* Immunogenicity and safety of an inactivated whole-virus COVID-19 vaccine (VLA2001) compared with the adenoviral vector vaccine ChAdOx1-S in adults in the UK (COV-COMPARE): interim analysis of a randomised, controlled, phase 3, immunobridging trial. *The Lancet Infectious Diseases* **online before print**, doi:10.1016/S1473-3099(22)00502-3.

120 Logunov, D. Y. *et al.* Safety and immunogenicity of an rAd26 and rAd5 vector-based heterologous prime-boost COVID-19 vaccine in two formulations: two open, non-randomised phase 1/2 studies from Russia. *The Lancet* **396**, 887-897, doi:10.1016/S0140-6736(20)31866-3 (2020).

121 Ständige Impfkommission. Beschluss der STIKO zur 14. Aktualisierung der COVID-19-Impfempfehlung. *Epidemiologisches Bulletin*, 3-14, doi:10.25646/9326 (2021).

122 Vygen-Bonnet, S. *et al.* Beschluss und Wissenschaftliche Begründung der Ständigen Impfkommission (STIKO) für die COVID-19-Impfempfehlung. *Epidemiologisches Bulletin*, 3-63, doi:10.25646/7755.2 (2020).

123 Tian, Y. *et al.* Cancer associates with risk and severe events of COVID-19: A systematic review and meta-analysis. *International Journal of Cancer* **148**, 363-374, doi:10.1002/ijc.33213 (2021).

124 Raja, M. A. *et al.* COVID-19 in solid organ transplant recipients: A systematic review and meta-analysis of current literature. *Transplantation Reviews* **35**, 100588, doi:10.1016/j.trre.2020.100588 (2021).

125 Jablonski, K. L. & Chonchol, M. Recent advances in the management of hemodialysis patients: a focus on cardiovascular disease. *F1000Prime Rep* **6**, 72, doi:10.12703/p6-72 (2014).

126 Krueger, K. M., Ison, M. G. & Ghossein, C. Practical Guide to Vaccination in All Stages of CKD, Including Patients Treated by Dialysis or Kidney Transplantation. *American Journal of Kidney Diseases* **75**, 417-425, doi:10.1053/j.ajkd.2019.06.014 (2020).

127 Reddy, S., Chitturi, C. & Yee, J. Vaccination in Chronic Kidney Disease. *Advances in Chronic Kidney Disease* **26**, 72-78, doi:10.1053/j.ackd.2018.10.002 (2019).

128 O'Toole, Á. *et al.* Assignment of epidemiological lineages in an emerging pandemic using the pangolin tool. *Virus Evolution* **7**, veab064, doi:10.1093/ve/veab064 (2021).

129 Khare, S. *et al.* GISAID's role in pandemic response. *China CDC Weekly* **3**, 1049 (2021).

130 World Health Organization. *WHO announces simple, easy-to-say labels for SARS-CoV-2 variants of interest and concern* (2021), https://www.who.int/news/item/31-05-2021-who-announces-simple-easy-to-say-labels-for-sars-cov-2-variants-of-interest-and-concern, accessed 02.08.2022.

131 World Health Organization. *Tracking SARS-CoV-2 variants*, https://www.who.int/activities/tracking-SARS-CoV-2-variants, accessed 02.08.2022.

132 Campbell, F. *et al.* Increased transmissibility and global spread of SARS-CoV-2 variants of concern as at June 2021. *Eurosurveillance* **26**, 2100509, doi:10.2807/1560-7917.ES.2021.26.24.2100509 (2021).

133 Hodcroft, E. B. *CoVariants: SARS-CoV-2 Mutations and Variants of Interest* (2021), https://covariants.org/, accessed 02.08.2022.

134 Starr, T. N. *et al.* Deep Mutational Scanning of SARS-CoV-2 Receptor Binding Domain Reveals Constraints on Folding and ACE2 Binding. *Cell* **182**, 1295-1310.e1220, doi:10.1016/j.cell.2020.08.012 (2020).

135 Zahradník, J. *et al.* SARS-CoV-2 variant prediction and antiviral drug design are enabled by RBD in vitro evolution. *Nature Microbiology* **6**, 1188-1198, doi:10.1038/s41564-021-00954-4 (2021).

136 Deng, X. *et al.* Transmission, infectivity, and neutralization of a spike L452R SARS-CoV-2 variant. *Cell* **184**, 3426-3437.e3428, doi:10.1016/j.cell.2021.04.025 (2021).

137 Chen, J., Wang, R., Wang, M. & Wei, G.-W. Mutations Strengthened SARS-CoV-2 Infectivity. *Journal of Molecular Biology* **432**, 5212-5226, doi:10.1016/j.jmb.2020.07.009 (2020).

138   Funk, T. *et al.* Characteristics of SARS-CoV-2 variants of concern B.1.1.7, B.1.351 or P.1: data from seven EU/EEA countries, weeks 38/2020 to 10/2021. *Eurosurveillance* **26**, 2100348, doi:10.2807/1560-7917.ES.2021.26.16.2100348 (2021).

139   Ong, S. W. X. *et al.* Clinical and Virological Features of Severe Acute Respiratory Syndrome Coronavirus 2 (SARS-CoV-2) Variants of Concern: A Retrospective Cohort Study Comparing B.1.1.7 (Alpha), B.1.351 (Beta), and B.1.617.2 (Delta). *Clinical Infectious Diseases*, doi:10.1093/cid/ciab721 (2021).

140   Özüdoğru, O., Bahçe, Y. G. & Acer, Ö. SARS CoV-2 reinfection rate is higher in the Omicron variant than in the Alpha and Delta variants. *Ir J Med Sci*, doi:10.1007/s11845-022-03060-4 (2022).

141   Levine-Tiefenbrun, M. *et al.* Viral loads of Delta-variant SARS-CoV-2 breakthrough infections after vaccination and booster with BNT162b2. *Nat Med* **27**, 2108-2110, doi:10.1038/s41591-021-01575-4 (2021).

142   Chau, N. V. V. *et al.* An observational study of breakthrough SARS-CoV-2 Delta variant infections among vaccinated healthcare workers in Vietnam. *eClinicalMedicine* **41**, 101143, doi:https://doi.org/10.1016/j.eclinm.2021.101143 (2021).

143   Paton, R. S., Overton, C. E. & Ward, T. The rapid replacement of the SARS-CoV-2 Delta variant by Omicron (B.1.1.529) in England. *Science Translational Medicine* **14**, eabo5395, doi:doi:10.1126/scitranslmed.abo5395 (2022).

144   Xia, S., Wang, L., Zhu, Y., Lu, L. & Jiang, S. Origin, virological features, immune evasion and intervention of SARS-CoV-2 Omicron sublineages. *Signal Transduction and Targeted Therapy* **7**, 241, doi:10.1038/s41392-022-01105-9 (2022).

145   Pulliam, J. R. C. *et al.* Increased risk of SARS-CoV-2 reinfection associated with emergence of Omicron in South Africa. *Science* **376**, eabn4947, doi:doi:10.1126/science.abn4947 (2022).

146   Sheikh, A. *et al.* Severity of omicron variant of concern and effectiveness of vaccine boosters against symptomatic disease in Scotland (EAVE II): a national cohort study with nested test-negative design. *The Lancet Infectious Diseases* **22**, 959-966, doi:10.1016/S1473-3099(22)00141-4 (2022).

147   Schnurra, C. *et al.* Comparison of the diagnostic sensitivity of SARS-CoV-2 nucleoprotein and glycoprotein-based antibody tests. *Journal of Clinical Virology* **129**, 104544, doi:10.1016/j.jcv.2020.104544 (2020).

148   Naaber, P. *et al.* Evaluation of SARS-CoV-2 IgG antibody response in PCR positive patients: Comparison of nine tests in relation to clinical data. *PLOS ONE* **15**, e0237548, doi:10.1371/journal.pone.0237548 (2020).

149   den Hartog, G. *et al.* SARS-CoV-2–Specific Antibody Detection for Seroepidemiology: A Multiplex Analysis Approach Accounting for Accurate Seroprevalence. *The Journal of Infectious Diseases* **222**, 1452-1461, doi:10.1093/infdis/jiaa479 (2020).

150   Roxhed, N. *et al.* Multianalyte serology in home-sampled blood enables an unbiased assessment of the immune response against SARS-CoV-2. *Nature Communications* **12**, 3695, doi:10.1038/s41467-021-23893-4 (2021).

151   Mariën, J. *et al.* Evaluating SARS-CoV-2 spike and nucleocapsid proteins as targets for antibody detection in severe and mild COVID-19 cases using a Luminex bead-based assay. *Journal of Virological Methods* **288**, 114025, doi:10.1016/j.jviromet.2020.114025 (2021).

152   Munitz, A. *et al.* Rapid seroconversion and persistent functional IgG antibodies in severe COVID-19 patients correlates with an IL-12p70 and IL-33 signature. *Scientific Reports* **11**, 3461, doi:10.1038/s41598-021-83019-0 (2021).

153   Wang, H. *et al.* SARS-CoV-2 Proteome Microarray for Mapping COVID-19 Antibody Interactions at Amino Acid Resolution. *ACS Central Science* **6**, 2238-2249, doi:10.1021/acscentsci.0c00742 (2020).

154   Amanat, F. *et al.* A serological assay to detect SARS-CoV-2 seroconversion in humans. *Nature Medicine* **26**, 1033-1036, doi:10.1038/s41591-020-0913-5 (2020).

155   Gudbjartsson, D. F. *et al.* Humoral Immune Response to SARS-CoV-2 in Iceland. *New England Journal of Medicine* **383**, 1724-1734, doi:10.1056/NEJMoa2026116 (2020).

156   Havervall, S. *et al.* SARS-CoV-2 induces a durable and antigen specific humoral immunity after asymptomatic to mild COVID-19 infection. *PLOS ONE* **17**, e0262169, doi:10.1371/journal.pone.0262169 (2022).

157   Burbelo, P. D. *et al.* Sensitivity in Detection of Antibodies to Nucleocapsid and Spike Proteins of Severe Acute Respiratory Syndrome Coronavirus 2 in Patients With Coronavirus Disease 2019. *The Journal of Infectious Diseases* **222**, 206-213, doi:10.1093/infdis/jiaa273 (2020).

158   Muench, P. *et al.* Development and Validation of the Elecsys Anti-SARS-CoV-2 Immunoassay as a Highly Specific Tool for Determining Past Exposure to SARS-CoV-2. *Journal of Clinical Microbiology* **58**, e01694-01620, doi:10.1128/JCM.01694-20 (2020).

159   European Medicines Agency. Guideline on bioanalytical method validation. Document No. EMEA/CHMP/EWP/192217/2009 Rev. 1 Corr. 2**, (2015).

160   U.S. Food and Drug Administration. Bioanalytical Method Validation Guidance for Industry. Document No. FDA-2013-D-1020, (2018).

161   World Health Organization. *COVID-19 weekly epidemiological update, 13 April 2021* (2021), https://apps.who.int/iris/handle/10665/340826, accessed 22.10.2022.

162   Turgeon, C. T. *et al.* Detection of SARS-CoV-2 IgG antibodies in dried blood spots. *Diagnostic Microbiology and Infectious Disease* **101**, 115425, doi:10.1016/j.diagmicrobio.2021.115425 (2021).

163   Rottinghaus, E. *et al.* Comparison of Ahlstrom Grade 226, Munktell TFN, and Whatman 903 Filter Papers for Dried Blood Spot Specimen Collection and Subsequent HIV-1 Load and Drug Resistance Genotyping Analysis. *Journal of Clinical Microbiology* **51**, 55-60, doi:10.1128/JCM.02002-12 (2013).

164   Junker, D. *et al.* COVID-19 patient serum less potently inhibits ACE2-RBD binding for various SARS-CoV-2 RBD mutants. *Scientific Reports* **12**, 7168, doi:10.1038/s41598-022-10987-2 (2022).

165   Oran, D. P. & Topol, E. J. Prevalence of Asymptomatic SARS-CoV-2 Infection. *Annals of Internal Medicine* **173**, 362-367, doi:10.7326/M20-3012 (2020).

166   Pollán, M. *et al.* Prevalence of SARS-CoV-2 in Spain (ENE-COVID): a nationwide, population-based seroepidemiological study. *The Lancet* **396**, 535-544, doi:10.1016/S0140-6736(20)31483-5 (2020).

167   CDC. COVID-19 Science Update. Edition 2021-07-30 (100) (2021), https://www.cdc.gov/library/covid19/07302021_covidupdate.html, accessed 23.09.2022.

168   Vygen-Bonnet, S. *et al.* Beschluss der STIKO zur 9. Aktualisierung der COVID-19-Impfempfehlung und die dazugehörige wissenschaftliche Begründung. *Epidemiologisches Bulletin*, 3-46, doi:10.25646/8942.2 (2021).

169   Dowell, A. C. *et al.* Children develop robust and sustained cross-reactive spike-specific immune responses to SARS-CoV-2 infection. *Nature Immunology* **23**, 40-49, doi:10.1038/s41590-021-01089-8 (2022).

170   Yang, H. S. *et al.* Association of Age With SARS-CoV-2 Antibody Response. *JAMA Network Open* **4**, e214302-e214302, doi:10.1001/jamanetworkopen.2021.4302 (2021).

171   Ständige Impfkommission. Beschluss der STIKO zur 20. Aktualisierung der COVID-19-Impfempfehlung. *Epidemiologisches Bulletin*, 3-19 (2022).

172   Earle, K. A. *et al.* Evidence for antibody as a protective correlate for COVID-19 vaccines. *Vaccine* **39**, 4423-4428, doi:10.1016/j.vaccine.2021.05.063 (2021).

173   Khoury, D. S. *et al.* Neutralizing antibody levels are highly predictive of immune protection from symptomatic SARS-CoV-2 infection. *Nature Medicine* **27**, 1205-1211, doi:10.1038/s41591-021-01377-8 (2021).

174   Gornyk, D. *et al.* SARS-CoV-2 Seroprevalence in Germany. *Dtsch Arztebl International* **118**, 824 (2021).

175   Liu, X. *et al.* Safety and immunogenicity of heterologous versus homologous prime-boost schedules with an adenoviral vectored and mRNA COVID-19 vaccine (Com-COV): a single-blind, randomised, non-inferiority trial. *The Lancet* **398**, 856-869, doi:10.1016/S0140-6736(21)01694-9 (2021).

176   Schmidt, T. *et al.* Immunogenicity and reactogenicity of heterologous ChAdOx1 nCoV-19/mRNA vaccination. *Nature Medicine* **27**, 1530-1535, doi:10.1038/s41591-021-01464-w (2021).

177   Vygen-Bonnet, S. *et al.* Beschluss der STIKO zur 8. Aktualisierung der COVID-19-Impfempfehlung und die dazugehörige wissenschaftliche Begründung. *Epidemiologisches Bulletin*, 14-31 (2021).

178   van Gils, M. J. *et al.* Antibody responses against SARS-CoV-2 variants induced by four different SARS-CoV-2 vaccines in health care workers in the Netherlands: A prospective cohort study. *PLOS Medicine* **19**, e1003991, doi:10.1371/journal.pmed.1003991 (2022).

179   Lin, D.-Y. *et al.* Effectiveness of Covid-19 Vaccines over a 9-Month Period in North Carolina. *New England Journal of Medicine* **386**, 933-941, doi:10.1056/NEJMoa2117128 (2022).

180   Ständige Impfkommission. Beschluss der STIKO zur 12. Aktualisierung der COVID-19-Impfempfehlung. *Epidemiologisches Bulletin*, 3-11, doi:10.25646/9156 (2021).

181   Meo, S. A., Bukhari, I. A., Akram, J., Meo, A. S. & Klonoff, D. C. COVID-19 vaccines: comparison of biological, pharmacological characteristics and adverse effects of Pfizer/BioNTech and Moderna Vaccines. *Eur Rev Med Pharmacol Sci* **25**, 1663-1669, doi:10.26355/eurrev_202102_24877 (2021).

182   Ständige Impfkommission. Beschluss der STIKO zur 13. Aktualisierung der COVID-19-Impfempfehlung. 10-19, doi:10.25646/9281 (2021).

183   Ioannou, G. N., Locke, E. R., Green, P. K. & Berry, K. Comparison of Moderna versus Pfizer-BioNTech COVID-19 vaccine outcomes: A target trial emulation study in the U.S. Veterans Affairs healthcare system. *eClinicalMedicine* **45**, doi:10.1016/j.eclinm.2022.101326 (2022).

184   Azzi, L. *et al.* Mucosal immune response in BNT162b2 COVID-19 vaccine recipients. *eBioMedicine* **75**, doi:10.1016/j.ebiom.2021.103788 (2022).

185   Spiekermann, G. M. *et al.* Receptor-mediated Immunoglobulin G Transport Across Mucosal Barriers in Adult Life : Functional Expression of FcRn in the Mammalian Lung. *Journal of Experimental Medicine* **196**, 303-310, doi:10.1084/jem.20020400 (2002).

186   Afkhami, S. *et al.* Respiratory mucosal delivery of next-generation COVID-19 vaccine provides robust protection against both ancestral and variant strains of SARS-CoV-2. *Cell* **185**, 896-915.e819, doi:10.1016/j.cell.2022.02.005 (2022).

187   Shrotri, M. *et al.* Spike-antibody waning after second dose of BNT162b2 or ChAdOx1. *The Lancet* **398**, 385-387, doi:10.1016/S0140-6736(21)01642-1 (2021).

188   Mizrahi, B. *et al.* Correlation of SARS-CoV-2-breakthrough infections to time-from-vaccine. *Nature Communications* **12**, 6379, doi:10.1038/s41467-021-26672-3 (2021).

189   Goldberg, Y. *et al.* Waning Immunity after the BNT162b2 Vaccine in Israel. *New England Journal of Medicine* **385**, e85, doi:10.1056/NEJMoa2114228 (2021).

190   Lau, C. S., Phua, S. K., Liang, Y. L., Oh, M. L. & Aw, T. C. SARS-CoV-2 Spike and Neutralizing Antibody Kinetics 90 Days after Three Doses of BNT162b2 mRNA COVID-19 Vaccine in Singapore. *Vaccines* **10**, doi:10.3390/vaccines10020331 (2022).

191   Hall, V. G. *et al.* Delayed-interval BNT162b2 mRNA COVID-19 vaccination enhances humoral immunity and induces robust T cell responses. *Nature Immunology* **23**, 380-385, doi:10.1038/s41590-021-01126-6 (2022).

192   Turner, J. S. *et al.* SARS-CoV-2 mRNA vaccines induce persistent human germinal centre responses. *Nature* **596**, 109-113, doi:10.1038/s41586-021-03738-2 (2021).

193   Gazit, S. *et al.* Severe Acute Respiratory Syndrome Coronavirus 2 (SARS-CoV-2) Naturally Acquired Immunity versus Vaccine-induced Immunity, Reinfections versus Breakthrough Infections: A Retrospective Cohort Study. *Clinical Infectious Diseases*, ciac262, doi:10.1093/cid/ciac262 (2022).

194   Murugesan, M. *et al.* Protective effect conferred by prior infection and vaccination on COVID-19 in a healthcare worker cohort in South India. *PLOS ONE* **17**, e0268797, doi:10.1371/journal.pone.0268797 (2022).

195   Pozzetto, B. *et al.* Immunogenicity and efficacy of heterologous ChAdOx1–BNT162b2 vaccination. *Nature* **600**, 701-706, doi:10.1038/s41586-021-04120-y (2021).

196   Li, R. *et al.* Differential efficiencies to neutralize the novel mutants B.1.1.7 and 501Y.V2 by collected sera from convalescent COVID-19 patients and RBD nanoparticle-vaccinated rhesus macaques. *Cellular & Molecular Immunology* **18**, 1058-1060, doi:10.1038/s41423-021-00641-8 (2021).

197   Cele, S. *et al.* Escape of SARS-CoV-2 501Y.V2 from neutralization by convalescent plasma. *Nature* **593**, 142-146, doi:10.1038/s41586-021-03471-w (2021).

198   Caniels, T. G. *et al.* Emerging SARS-CoV-2 variants of concern evade humoral immune responses from infection and vaccination. *Science Advances* **7**, eabj5365, doi:doi:10.1126/sciadv.abj5365 (2021).

199   Wang, Z. *et al.* mRNA vaccine-elicited antibodies to SARS-CoV-2 and circulating variants. *Nature* **592**, 616-622, doi:10.1038/s41586-021-03324-6 (2021).

200   Planas, D. *et al.* Reduced sensitivity of SARS-CoV-2 variant Delta to antibody neutralization. *Nature* **596**, 276-280, doi:10.1038/s41586-021-03777-9 (2021).

201   Lopez Bernal, J. *et al.* Effectiveness of Covid-19 Vaccines against the B.1.617.2 (Delta) Variant. *New England Journal of Medicine* **385**, 585-594, doi:10.1056/NEJMoa2108891 (2021).

202   Wall, E. C. *et al.* Neutralising antibody activity against SARS-CoV-2 VOCs B.1.617.2 and B.1.351 by BNT162b2 vaccination. *The Lancet* **397**, 2331-2333, doi:10.1016/S0140-6736(21)01290-3 (2021).

203   Dejnirattisai, W. *et al.* The antigenic anatomy of SARS-CoV-2 receptor binding domain. *Cell* **184**, 2183-2200.e2122, doi:10.1016/j.cell.2021.02.032 (2021).

204   Rey, F. Structure-function relations of the SARS-CoV-2 spike protein and impact of mutations in the variants of concern. *Comptes Rendus. Biologies* **344**, 77-110, doi:10.5802/crbiol.53 (2021).

205   Bar-On, Y. M. *et al.* Protection of BNT162b2 Vaccine Booster against Covid-19 in Israel. *New England Journal of Medicine* **385**, 1393-1400, doi:10.1056/NEJMoa2114255 (2021).

206   Zeng, B., Gao, L., Zhou, Q., Yu, K. & Sun, F. Effectiveness of COVID-19 vaccines against SARS-CoV-2 variants of concern: a systematic review and meta-analysis. *BMC Medicine* **20**, 200, doi:10.1186/s12916-022-02397-y (2022).

207   Danza, P. *et al.* SARS-CoV-2 Infection and Hospitalization Among Adults Aged ≥18 Years, by Vaccination Status, Before and During SARS-CoV-2 B.1.1.529 (Omicron) Variant Predominance - Los Angeles County, California, November 7, 2021-January 8, 2022. *MMWR Morb Mortal Wkly Rep* **71**, 177-181, doi:10.15585/mmwr.mm7105e1 (2022).

208   Bellusci, L. *et al.* Antibody affinity and cross-variant neutralization of SARS-CoV-2 Omicron BA.1, BA.2 and BA.3 following third mRNA vaccination. *Nature Communications* **13**, 4617, doi:10.1038/s41467-022-32298-w (2022).

209   Gruell, H. *et al.* SARS-CoV-2 Omicron sublineages exhibit distinct antibody escape patterns. *Cell Host & Microbe* **30**, 1231-1241.e1236, doi:10.1016/j.chom.2022.07.002 (2022).

210   Andrews, N. *et al.* Covid-19 Vaccine Effectiveness against the Omicron (B.1.1.529) Variant. *New England Journal of Medicine* **386**, 1532-1546, doi:10.1056/NEJMoa2119451 (2022).

211   Iketani, S. *et al.* Antibody evasion properties of SARS-CoV-2 Omicron sublineages. *Nature* **604**, 553-556, doi:10.1038/s41586-022-04594-4 (2022).

212   Zhang, X. *et al.* SARS-CoV-2 Omicron strain exhibits potent capabilities for immune evasion and viral entrance. *Signal Transduction and Targeted Therapy* **6**, 430, doi:10.1038/s41392-021-00852-5 (2021).

213   Kared, H. *et al.* Immune responses in Omicron SARS-CoV-2 breakthrough infection in vaccinated adults. *Nature Communications* **13**, 4165, doi:10.1038/s41467-022-31888-y (2022).

214   Simon-Loriere, E. & Schwartz, O. Towards SARS-CoV-2 serotypes? *Nature Reviews Microbiology* **20**, 187-188, doi:10.1038/s41579-022-00708-x (2022).

215   Suryawanshi, R. K. *et al.* Limited cross-variant immunity from SARS-CoV-2 Omicron without vaccination. *Nature* **607**, 351-355, doi:10.1038/s41586-022-04865-0 (2022).

216   Lee, I. J. *et al.* A booster dose of Delta × Omicron hybrid mRNA vaccine produced broadly neutralizing antibody against Omicron and other SARS-CoV-2 variants. *Journal of Biomedical Science* **29**, 49, doi:10.1186/s12929-022-00830-1 (2022).

217   van der Straten, K. *et al.* Mapping the antigenic diversification of SARS-CoV-2. *Preprint at medRxiv*, doi:10.1101/2022.01.03.21268582 (2022).

218   Schmidt, T. *et al.* Cellular immunity predominates over humoral immunity after homologous and heterologous mRNA and vector-based COVID-19 vaccine regimens in solid organ transplant recipients. *American Journal of Transplantation* **21**, 3990-4002, doi:10.1111/ajt.16818 (2021).

219   Syversen, S. W. *et al.* Immunogenicity and Safety of Standard and Third-Dose SARS–CoV-2 Vaccination in Patients Receiving Immunosuppressive Therapy. *Arthritis & Rheumatology* **74**, 1321-1332, doi:10.1002/art.42153 (2022).

220   Oosting, S. F. *et al.* Immunogenicity after second and third mRNA-1273 vaccination doses in patients receiving chemotherapy, immunotherapy, or both for solid tumours. *The Lancet Oncology* **23**, 833-835, doi:10.1016/S1470-2045(22)00203-0 (2022).

221   Carr, E. J. *et al.* Omicron neutralising antibodies after COVID-19 vaccination in haemodialysis patients. *The Lancet* **399**, 800-802, doi:10.1016/S0140-6736(22)00104-0 (2022).

222   Cinkilic, O. *et al.* Inferior humoral and sustained cellular immunity against wild-type and omicron variant of concern in hemodialysis patients immunized with 3 SARS-CoV-2 vaccine doses compared with 4 doses. *Kidney International* **101**, 1287-1289, doi:doi.org/10.1016/j.kint.2022.03.005 (2022).

223   Anft, M. *et al.* Inferior cellular and humoral immunity against Omicron and Delta variants of concern compared with SARS-CoV-2 wild type in hemodialysis patients immunized with 4 SARS-CoV-2 vaccine doses. *Kidney International* **102**, 207-208, doi:10.1016/j.kint.2022.05.004 (2022).

224   Midtvedt, K. *et al.* Fourth dose of the SARS-CoV-2 vaccine in kidney transplant recipients with previously impaired humoral antibody response. *American Journal of Transplantation* **online before print**, doi:10.1111/ajt.17091 (2022).

225   Chalkias, S. *et al.* A Bivalent Omicron-Containing Booster Vaccine against Covid-19. *New England Journal of Medicine* **387**, 1279-1291, doi:10.1056/NEJMoa2208343 (2022).

226   Hicks, J. *et al.* Serologic Cross-Reactivity of SARS-CoV-2 with Endemic and Seasonal Betacoronaviruses. *Journal of Clinical Immunology* **41**, 906-913, doi:10.1007/s10875-021-00997-6 (2021).

227   Fink, S. *et al.* Multiplexed Serum Antibody Screening Platform Using Virus Extracts from Endemic Coronaviridae and SARS-CoV-2. *ACS Infectious Diseases* **7**, 1596-1606, doi:10.1021/acsinfecdis.0c00725 (2021).

228   Ng, K. W. *et al.* Preexisting and de novo humoral immunity to SARS-CoV-2 in humans. *Science* **370**, 1339-1343, doi:10.1126/science.abe1107 (2020).

229   Aydillo, T. *et al.* Immunological imprinting of the antibody response in COVID-19 patients. *Nature Communications* **12**, 3781, doi:10.1038/s41467-021-23977-1 (2021).

230   Nelde, A. *et al.* SARS-CoV-2-derived peptides define heterologous and COVID-19-induced T cell recognition. *Nature Immunology* **22**, 74-85, doi:10.1038/s41590-020-00808-x (2021).

231   Weiskopf, D. *et al.* Phenotype and kinetics of SARS-CoV-2–specific T cells in COVID-19 patients with acute respiratory distress syndrome. *Science Immunology* **5**, eabd2071, doi:10.1126/sciimmunol.abd2071 (2020).

232   Le Bert, N. *et al.* SARS-CoV-2-specific T cell immunity in cases of COVID-19 and SARS, and uninfected controls. *Nature* **584**, 457-462, doi:10.1038/s41586-020-2550-z (2020).

Acknowledgements

My sincere thanks to all who have supported me along the way, not only during my doctoral studies, but also throughout my scientific career that has led me to this point.

I appreciate every one of you!

I would like to thank Dr. Nicole Schneiderhan-Marra for her excellent supervision, for being open to new ideas and for keeping hierarchies flat and thereby enabling a productive working environment. The latter is extremely valuable in a leader and is by no means guaranteed in the scientific world.

I want to thank Prof. Dr. Ulrich Rothbauer and Prof. Dr. Katja Schenke-Layland for being very supportive during my time at the NMI and for supervising my doctoral studies.

I want to extend special thanks to Daniel Junker, in whom I found a likeminded friend and a great and reliable lab partner. Furthermore, to Dr. Alex Dulovic, with whom it has been a pleasure to work with on many projects. I want to thank all my colleagues from the Multiplex Immunoassays group. You were responsible for creating an environment that allowed me to enjoy almost every day at work. Further, I want to thank everyone at the NMI with whom I have had the privilege to work with and learn from.

I would like to thank all of our cooperation partners, with whom I was able to partake in great research projects. I want to explicitly mention Prof. Dr. Gerard Krause and Dr. Monika Strengert of the Epidemiology Department at the HZI in Braunschweig, but also the groups of Prof. Dr. Georg Behrens in Hannover and Prof. Dr. Tamam Bakchoul in Tübingen.

And finally, I would like to thank my family, who taught and supported me, and who provided me with a loving home to which I could always return and draw strength.

Appendix

Appendix I: Exploring beyond clinical routine SARS-CoV-2 serology using MultiCoV-Ab to evaluate endemic coronavirus cross-reactivity

Matthias Becker*, Monika Strengert*, Daniel Junker, Philipp D. Kaiser, Tobias Kerrinnes, Bjoern Traenkle, Heiko Dinter, Julia Häring, Stéphane Ghozzi, Anne Zeck, Frank Weise, Andreas Peter, Sebastian Hörber, Simon Fink, Felix Ruoff, Alex Dulovic, Tamam Bakchoul, Armin Baillot, Stefan Lohse, Markus Cornberg, Thomas Illig, Jens Gottlieb, Sigrun Smola, André Karch, Klaus Berger, Hans-Georg Rammensee, Katja Schenke-Layland, Annika Nelde, Melanie Märklin, Jonas S. Heitmann, Juliane S. Walz, Markus Templin, Thomas O. Joos, Ulrich Rothbauer, Gérard Krause & Nicole Schneiderhan-Marra

    * = Authors contributed equally

nature COMMUNICATIONS

ARTICLE

Check for updates

Exploring beyond clinical routine SARS-CoV-2 serology using MultiCoV-Ab to evaluate endemic coronavirus cross-reactivity

Matthias Becker [1,24], Monika Strengert[2,3,24], Daniel Junker[1], Philipp D. Kaiser[1], Tobias Kerrinnes[4], Bjoern Traenkle[1,5], Heiko Dinter[1,5], Julia Häring[1], Stéphane Ghozzi[2], Anne Zeck[1], Frank Weise[1], Andreas Peter[6,7,8], Sebastian Hörber [6,7,8], Simon Fink [1], Felix Ruoff[1], Alex Dulovic [1], Tamam Bakchoul [9], Armin Baillot[10], Stefan Lohse [11], Markus Cornberg[12], Thomas Illig[13], Jens Gottlieb[14,15], Sigrun Smola[11], André Karch[16], Klaus Berger[16], Hans-Georg Rammensee[17,18,19], Katja Schenke-Layland [1,19,20,21], Annika Nelde [17,19,22], Melanie Märklin [19,21], Jonas S. Heitmann[19,21], Juliane S. Walz [17,19,23,22], Markus Templin[1], Thomas O. Joos[1], Ulrich Rothbauer[1,5,24], Gérard Krause [2,3] & Nicole Schneiderhan-Marra [1✉]

The humoral immune response to SARS-CoV-2 is a benchmark for immunity and detailed analysis is required to understand the manifestation and progression of COVID-19, monitor seroconversion within the general population, and support vaccine development. The majority of currently available commercial serological assays only quantify the SARS-CoV-2 antibody response against individual antigens, limiting our understanding of the immune response. To overcome this, we have developed a multiplex immunoassay (MultiCoV-Ab) including spike and nucleocapsid proteins of SARS-CoV-2 and the endemic human coronaviruses. Compared to three broadly used commercial in vitro diagnostic tests, our MultiCoV-Ab achieves a higher sensitivity and specificity when analyzing a well-characterized sample set of SARS-CoV-2 infected and uninfected individuals. We find a high response against endemic coronaviruses in our sample set, but no consistent cross-reactive IgG response patterns against SARS-CoV-2. Here we show a robust, high-content-enabled, antigen-saving multiplex assay suited to both monitoring vaccination studies and facilitating epidemiologic screenings for humoral immunity towards pandemic and endemic coronaviruses.

A full list of author affiliations appears at the end of the paper.

ARTICLE

Since its first characterization in late 2019, SARS-CoV-2, the seventh known coronavirus to infect humans, has developed into a worldwide pandemic with dramatic socioeconomic consequences[1–3]. While the majority of individuals suffer only from mild symptoms, approximately 14% of infected adults experience particularly severe disease outcomes (i.e., pneumonia) of COVID-19[4]. Of these 14%, 5% will progress into a critical condition characterized by hypoxaemic respiratory failure, acute respiratory distress syndrome and multiorgan failure[4]. To date, the large number of infected individuals and of those requiring urgent intensive care has put a high burden on public healthcare infrastructures[3].

In contrast to the recently emerged SARS-CoV-2, the four endemic human coronaviruses (hCoVs) NL63 and 229E (α-hCoVs) as well as OC43 and HKU1 (β-hCoVs), regularly circulate in the population[5] (one study reported a 91% prevalence for OC43 in the adult population[6]) and are thought to cause up to 20% of mild colds[7]. As humoral immune responses are in general seen as protective by production of neutralizing antibodies to viral surface proteins[8], it would be tempting to speculate that a previous infection with an endemic strain offers protection against infection with the β-coronavirus SARS-CoV-2, as already seen in in vitro studies[9]. However, it has also been reported that for both SARS coronaviruses and MERS-CoV, disease severity and fatal outcome correlates with early seroconversion and/or increased antibody titers by a yet undefined mechanism[10–13]. Consequentially, a detailed understanding of the humoral SARS-CoV-2 immune response is of importance to provide insights into COVID-19 disease biology[12,14].

Serological tests are essential tools in cohort-based epidemiological studies to determine seroprevalence and precisely assess mortality rates, the extent of asymptomatic or mild infections not currently detectable by molecular testing, and ultimately determine the effectiveness of population-based interventions and direct future preventive strategies. Furthermore, serological testing is a companion diagnostic to monitor vaccination efficacy and mode of action in vaccine trials[15,16]. As a result, there is a need for robust serological tests to quantify antibody production against SARS-CoV-2 in detail. Currently, most commercially available serological assays utilize single analyte technologies (i.e., ELISA) to measure antibodies against SARS-CoV-2 spike (S) or nucleocapsid (N) antigens[16–19]. Few tests combine and correlate N- and S-antigen-based detection[20–22] or attempt global profiling of antibody responses against the entire SARS-CoV-2 genome[23]. To this end, we developed a multiplexed SARS-CoV-2 immunoassay (MultiCoV-Ab) which included not only S and N protein-based antigens of SARS-CoV-2, but also from endemic hCoVs (NL63, 229E, OC43, HKU1) based on findings of numerous SARS-CoV-1 serological studies, which reported on cross-reactive antibodies to antigens from circulating hCoVs[24]. Such an expanded antigen panel allows to both resolve the SARS-CoV-2 antibody response in detail and to assess and correlate potential cross-protection mechanisms between coronaviruses. We measured both IgA and IgG responses, as these isotypes in contrast to IgM can persist for extended periods in the serum and in nasal fluids[25]. Further, SARS-CoV-2 is a mucosal-targeted virus, and reports indicate that IgA, as the dominant antibody isotype in the mucosal defense is a good indicator for early immune defense mechanisms in this case[26].

In this study, to determine how well MultiCoV-Ab performs, we compare our assay to broadly applied commercial in vitro diagnostic (IVD) tests with well-characterized sample sets for clinical validation and further analyze potential sources of cross-reactivity with hCoVs. For the sample set examined, we were able to reach a specificity of 100% with MultiCoV-Ab and achieved an improved sensitivity compared to commercial tests, confirming its value as a serological screening assay.

Results

MultiCoV-Ab: a highly sensitive test for SARS-CoV-2 seroconversion. To investigate the antibody response of SARS-CoV-2-infected individuals, we developed and established a high-throughput and automatable bead-based multiplex assay, termed MultiCoV-Ab. We expressed and immobilized six different SARS-CoV-2-specific antigens on Luminex MAGPLEX beads with distinct color codes, specifically the trimeric full-length spike protein (Spike Trimer), receptor-binding domain (RBD), S1 domain (S1), S2 domain (S2), full-length nucleocapsid (N), and the N-terminal domain of nucleocapsid (N-NTD) (Supplementary Fig. 1). Immunoglobulins from serum and plasma samples were detected using phycoerythrin-labeled anti-human IgG or IgA antibodies. To ensure assay stability and comparability, quality control samples were processed in parallel within every assay run. Quality control and assay performance data sets are provided in Supplementary Fig. 2 and Supplementary Table 1.

To analyze SARS-CoV-2-induced seroconversion, we used the Spike Trimer and RBD (previously described by Amanat et al.[27]) as key antigens for classification, and initially screened a sample set of 205 reconvalescent SARS-CoV-2-infected and 72 uninfected individuals with the MultiCoV-Ab. To critically assess assay performance, we compared our results with three commercially available IVD tests widely used in clinical routine SARS-CoV-2 antibody testing namely: Elecsys Anti-SARS-CoV-2 (antibodies including IgG; Roche[28]), SARS-CoV-2 Total (total antibodies IgM and IgG; Siemens Healthineers[29]) and Anti-SARS-CoV-2 ELISA (IgG/IgA; Euroimmun[30]). Using a combined cut-off of both antigens, we identified all uninfected samples as negative (Fig. 1a). In accordance with our MultiCoV-Ab, none of the uninfected samples was classified as false positive by the Roche and Siemens tests, while one sample was classified as false positive and one as "borderline" by the Euroimmun IgG test. Of the 205 infected samples, both MultiCoV-Ab and commercial IVD tests for total Ig or IgG identified 24 (11.7%) as IgG antibody-negative. However, the IVD tests missed an additional 8 (Roche), 11 (Siemens Healthineers), and 9 (Euroimmun IgG) samples of SARS-CoV-2-infected individuals. Furthermore, the Euroimmun IgG test classified 8 additional samples as "borderline" (Fig. 1b, Supplementary Fig. 3a–c). When testing for IgA antibodies in serum/plasma of SARS-CoV-2-infected individuals, our MultiCoV-Ab classified 47 (22.9%) as IgA-negative, whereas the Euroimmun test classified 32 (15.6%) as IgA-negative, and 16 (7.8%) as borderline (Fig. 1b and Supplementary Fig. 3d). For the uninfected samples, the Euroimmun IgA test identified 7 (9.7%) as false positives and 3 (4.2%) as "borderline", whereas no samples were classified as false positives by the MultiCoV-Ab. Overall, the MultiCoV-Ab achieved a sensitivity of 88.3% and a specificity of 100% in this initial set of samples using IgG detection (Table 1). When comparing the results of the commercial IVD tests to the respective manufacturers' specifications, all tests were unable to reach their stated sensitivity of 100%. In contrast, for all commercial tests, the found specificities were close to the manufacturers' stated specificity in our sample set (Table 1). This demonstrates that antigen selection and assay setup are crucial in achieving optimal performance and must be considered when screening for SARS-CoV-2, particularly in low prevalence scenarios.

Multiplex serology improves assay specificity. Next, to perform a more detailed clinical validation of our MultiCoV-Ab, we expanded our sample set to a total of 310 SARS-CoV-2-infected and 866 uninfected donors (a simplified overview of this set is shown in Table 2; a complete breakdown is displayed in Supplementary Table 2). We performed a ROC analysis[31,32] per
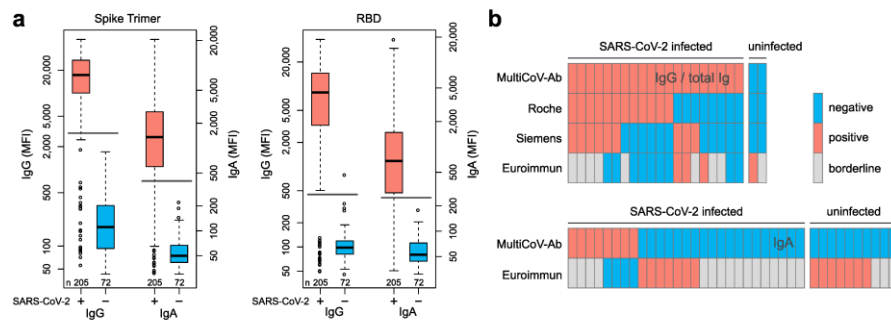
ARTICLE

Fig. 1 MultiCoV-Ab, a sensitive and specific tool to monitor SARS-CoV-2 antibody responses. a Control sera (blue, $n = 72$) and sera from individuals with PCR-confirmed SARS-CoV-2 infection (red, $n = 205$) were screened in a multiplex bead-based assay using Luminex technology (MultiCoV-Ab) to quantify IgG or IgA responses to various antigens. Reactivity towards trimeric SARS-CoV-2 spike protein (Spike Trimer) or SARS-CoV-2 receptor binding domain of spike (RBD) was found to be the best predictor of SARS-CoV-2 infection. Data are presented as Box-Whisker plots of a sample's median fluorescence intensity (MFI) on a logarithmic scale. Box represents the median and the 25th and 75th percentiles, whiskers show the largest and smallest values. Outliers determined by 1.5 times IQR of log-transformed data are depicted as circles. Cut-off values for classification for single antigens are displayed as horizontal lines (Spike Trimer IgG: 3,000 MFI, IgA: 400 MFI; RBD IgG: 450 MFI, IgA: 250 MFI). **b** Sample set from **a**, was used to compare assay performance of the MultiCoV-Ab using Spike Trimer and RBD antigens with commercially available single analyte SARS-CoV-2 IVD assays which detect total Ig (Elecsys Anti-SARS-CoV-2 (Roche); ADVIA Centaur SARS-CoV-2 Total (COV2T) (Siemens Healthineers)) or IgG (Anti-SARS-CoV-2-ELISA - IgG (Euroimmun)) or IgA (Anti-SARS-CoV-2-ELISA - IgA (Euroimmun)). SARS-CoV-2 infection status of samples based on PCR diagnostic is indicated as SARS-CoV-2 positive or negative. Antibody test results were classified as negative (blue), positive (red), or borderline (gray) as per the manufacturer's definition. Only samples with divergent antibody test results are shown. **c** Performance and specifications as stated in the manufacturer's IVD assay manual. For the manufacturer sensitivity specification, information for samples >14 days post-infection are presented. Respective sensitivity and specificity values calculated in this study are given with 95% Clopper-Pearson confidence intervals[52]. Positive and negative predictive values (PPV/NPV) were calculated based on a seropositivity of 3%. Source data are provided as a Source Data file.

SARS-CoV-2 antigen and detection system (Supplementary Fig. 4), which confirmed that Spike Trimer and RBD were the best predictors of SARS-CoV-2 infection. We, therefore, decided to use a combination of both antigens (IgG or IgA overall cut-off) to define overall SARS-CoV-2 reactivity for IgG or IgA, for which the two independent cut-offs for Spike Trimer and RBD had to be met (Table 3). Cut-offs were chosen with focus on maximum specificity for the overall classification (Spike Trimer$^+$/RBD$^+$) to prevent false positive results (Fig. 2a). With the overall IgG cut-off, we reached a specificity of 100%, which would not have been possible for either of the antigens individually, while still retaining acceptable sensitivity (88.7%). IgG detection was shown to be more specific and sensitive than IgA for determination of SARS-CoV-2 infection within our sample set. Only 8 samples which were IgA-positive showed no IgG response (Fig. 2b, dashed lines), 2 of which were uninfected and falsely classified as positive. Of the 6 remaining samples, metadata (including the time between the onset of symptoms and sample collection) was available for 4 (2, 6, 7, and 15 days). As a result, we hypothesized that IgA in these samples can be used to measure an early onset of antibody response as has been proposed by several groups[26,33,34]. Therefore, to give an overall measure of SARS-CoV-2 infection, we used the IgG classification as a basis and included samples with strong IgA positivity–signal to cut-off (S/CO) > 2 for Spike Trimer and RBD–as positive, irrespective of their detected IgG response (Fig. 2b, straight lines). With this combined IgG + IgA classification, we reached an optimal sensitivity of 90% while retaining a specificity of 100%.

Antigen selection affects SARS-CoV-2 serology test performance. While further analyzing the immune response detected

towards our 4 additional SARS-CoV-2 antigens in our Multiplex panel, we assessed the IgG response towards the S1 and S2 subdomains of the spike, which both did not improve sample classification (Fig. 2c). Interestingly, RBD, which is a part of S1, showed fewer uninfected samples with increased IgG response compared to S1. For S2, even more, uninfected samples had increased signals, suggesting the presence of potential cross-reactive antibodies for this domain of the spike protein (Fig. 2c). These findings suggest that the RBD response is highly characteristic of the overall SARS-CoV-2 immune response. To further complement our assay, we included the N and N-NTD proteins. Although these antigens have been successfully used in single-analyte assays[35], we observed a high cross-reactivity in uninfected samples for both (Fig. 2d). Across the entire data set, only one sample showed a distinct immune response to N and N-NTD, but not to all spike-derived antigens. This confirms that the performance of an antigen is specific to the assay setup and cannot be easily generalized, as commercial IVD tests (i.e., Roche) are able to use the N protein to great effect in a different assay setup.

Dynamics of antibody response in COVID-19 patients. Longitudinal samples from 5 hospitalized patients were used to perform a small-scale time-course analysis of IgG and IgA immune responses (Fig. 3a). Levels of both Ig classes strongly increased within the first ten days after the onset of symptoms. While IgG levels appeared constant over roughly two months, IgA levels started to decline between day 10 and 20 after the onset of symptoms. This reduction in IgA antibody levels was also observed with increased time post-infection in samples without longitudinal follow-up (Supplementary Figure 5). These effects were consistent for the majority of SARS-CoV-2 antigens.

ARTICLE

Table 1 Comparison of MultiCoV-Ab and commercial IVD tests in screening results and manufacturer specifications as stated in the assay manuals.

			Manufacturer specification >14 days post infection		Correctly classified		Found sensitivity	Found specificity	PPV at 3%	NPV at 3%
		Antigen							Prevalence	Prevalence
Assay	Detection	used	Sensitivity	Specificity	Infected (of 205)	Uninfected (of 72)	(95% CI)	(95% CI)		
MultiCoV-Ab	IgG	S Trimer + RBD	—	—	181	72	88.3% (83.1-92.4%)	100% (95.0-100%)	100%	99.6%
Roche	Total Ig	N	100% n = 29	99.8% n = 5272	173	72	84.4% (78.7-89.1%)	100% (95.0-100%)	100%	99.5%
Siemens	Total Ig	S1 RBD	100% n = 47	99.8% n = 1589	170	72	82.9% (77.1-87.8%)	100% (95.0-100%)	100%	99.5%
Euroimmun	IgG	S1	100% n = 13	99.0% n = 1261	164	70	80.0% (73.9-85.2%)	97.2% (90.3-99.7%)	46.9%	99.4%
MultiCoV-Ab	IgA	S Trimer + RBD	—	—	158	72	77.1% (70.7-82.6%)	100% (95.0-100%)	100%	99.3%
Euroimmun	IgA	S1	100% n = 13	90.4% n = 1261	157	62	76.6% (70.2-82.2%)	86.1% (75.9-93.1%)	14.6%	99.2%

Table 2 Extended Sample set used to further validate MultiCoV-Ab performance.

Age group	≤39		40-59		≥60		Not available		Σ
n	299 (25.4%)		241 (20.5%)		475 (40.4%)		161 (13.7%)		1176
Sex	Male	Female	Male	Female	Male	Female	Male	Female	
n	139 (11.8%)	160 (13.6%)	144 (12.2%)	97 (8.2%)	271 (23.0%)	204 (17.3%)	5 (0.4%)	3 (0.3%)	1176
SARS-CoV-2 infected	60 (19.4%)	51 (16.5%)	71 (22.9%)	63 (20.3%)	42 (13.5%)	17 (5.5%)	3 (1.0%)	3 (1.0%)	310
hospitalized	6 (10.9%)	2 (3.6%)	14 (25.5%)	6 (10.9%)	23 (41.8%)	4 (7.3%)	0 (0.0%)	0 (0.0%)	55
non-hospitalized	52 (25.0%)	43 (20.7%)	49 (23.6%)	43 (20.7%)	13 (6.3%)	8 (3.8%)	0 (0.0%)	0 (0.0%)	208
hospitalization NA	2 (4.3%)	6 (12.8%)	8 (17.0%)	14 (29.8%)	6 (12.8%)	5 (10.6%)	3 (6.4%)	3 (6.4%)	47
SARS-CoV-2 uninfected	79 (9.1%)	109 (12.6%)	73 (8.4%)	34 (3.9%)	229 (26.4%)	187 (21.6%)	2 (0.2%)	0 (0.0%)	866

82

ARTICLE

Table 3 MultiCoV-Ab sensitivity and specificity of extended sample set for IgA and IgG based on a single analyte or a combined cut-off of Spike Trimer and RBD (IgG or IgA overall) or combined isotype cut-off (IgG and IgA).

|	Correctly classified		Sensitivity	Specificity	PPV at 3%	NPV at 3%
	Infected	Uninfected	(95% CI)	(95% CI)	Prevalence	Prevalence
IgG Spike Trimer	277	849	89.4% (85.4–92.6%)	98.0% (96.9–98.9%)	58.5%	99.7%
IgG RBD	276	862	89.0% (85–92.3%)	99.5% (98.8–99.9%)	85.7%	99.7%
IgG overall	275	866	88.7% (84.6–92%)	100% (99.6–100%)	100%	99.7%
IgA Spike Trimer	272	850	87.7% (83.6–91.2%)	98.2% (97–98.9%)	59.5%	99.6%
IgA RBD	255	855	82.3% (77.5–86.3%)	98.7% (97.7–99.4%)	66.7%	99.4%
IgA overall	254	864	81.9% (77.2–86.1%)	99.8% (99.2–100%)	91.7%	99.4%
Combined IgA & IgG	279	866	90.0% (86.1–93.1%)	100% (99.6–100%)	100%	99.7%
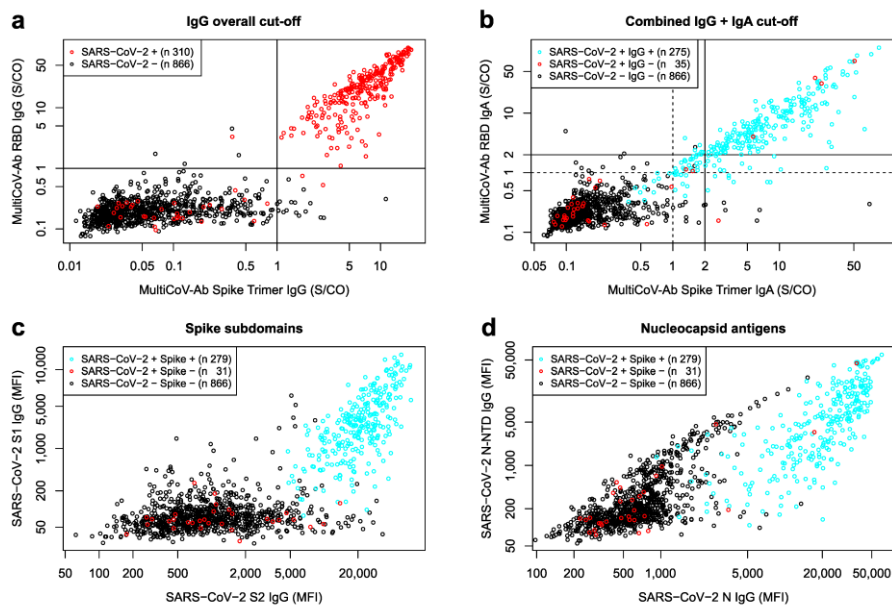
Fig. 2 Combination of 2 spike protein variants and isotype profiling by multiplex assay increases accuracy to identify SARS-CoV-2 antibody-positive individuals. a, b Scatterplot detailing MultiCoV-Ab cut-offs. Signal to cut-off (S/CO) values are displayed for Spike Trimer against RBD on a logarithmic scale. For IgG (**a**), cut-offs are visualized by straight lines and SARS-CoV-2-infected and uninfected samples are separated by color (black circles – SARS-CoV-2-uninfected; red circles – SARS-CoV-2-infected). For IgA (**b**) cut-offs are visualized as dashed lines and S/CO of 2 used for the combined cut-off is shown as straight lines. SARS-CoV-2-infected samples are split into IgG-positives and -negatives by color as indicated in the plot. **c, d** Scatterplots display IgG response to additional SARS-CoV-2 antigens contained in the MultiCoV-Ab panel: MFI for spike subdomains S1 vs S2 (**c**) or nucleocapsid antigens N vs N-NTD (**d**) are displayed on a logarithmic scale. SARS-CoV-2-uninfected samples are distinguished from SARS-CoV-2-infected and MultiCoV-Ab classification into positives or negatives as indicated by color. Source data are provided as a Source Data file.

Furthermore, we found that patients' hospitalization, as a measure of disease severity (Fig. 3b), seemed to correlate with an increased humoral immune response, particularly for IgA. Lastly, we identified a trend for increasing age (Fig. 3c). While we overall see correlation of the immune response with patient hospitalization, age, and time post-infection, our sample set was not designed to single out the leading cause amongst these effects. Patients of higher age also had a higher rate of hospitalization in our study population (see Table 2) and samples with increased

time post-infection were also less often hospitalized. It should also be noted that our samples from infected donors had different origins and thus different determinants of time post-infection, as some were based upon PCR results and others on symptom onset.

Previous endemic hCoV infection indicates higher immune response to SARS-CoV-2. In order to explore cross-reactivity of hCoVs with SARS-CoV-2, we included S1, N, and N-NTD
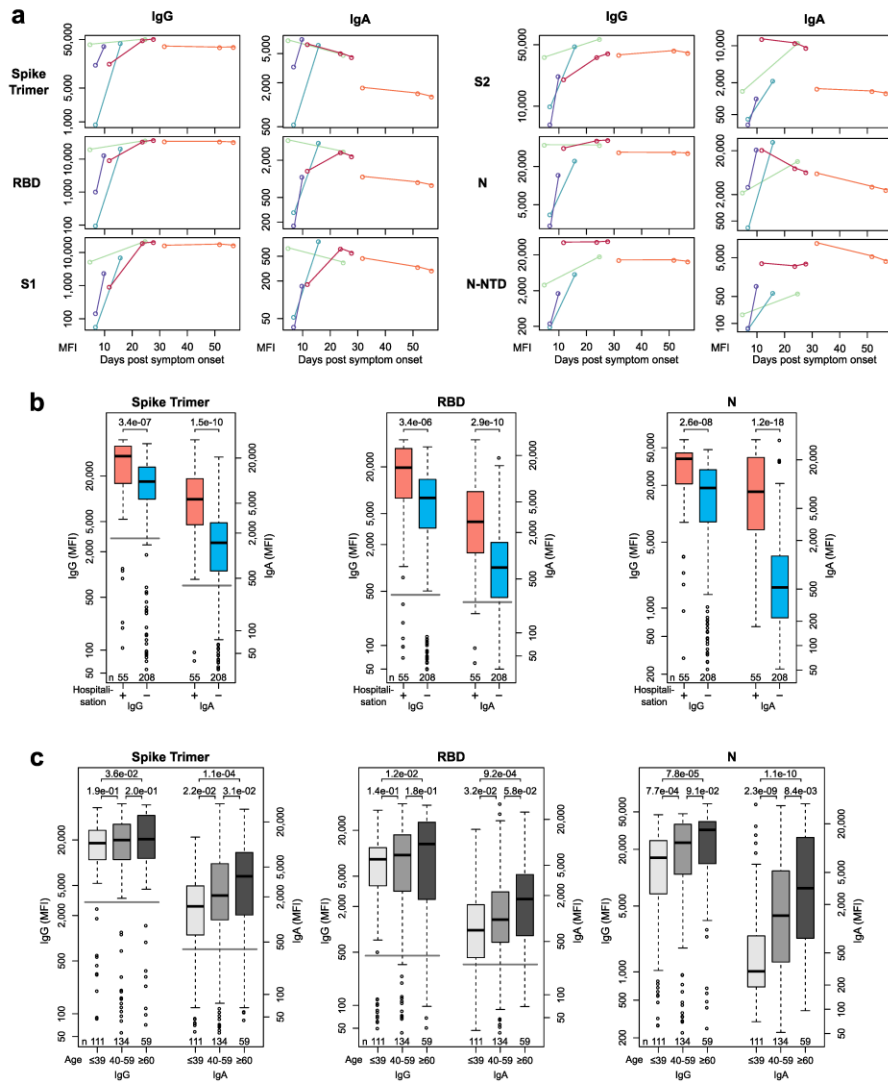
Fig. 3 Multiplex-based seroprofiling allows in-depth characterization of SARS-CoV-2 antibody responses. a Kinetic of SARS-CoV-2 antigen-specific IgA and IgG responses is shown for indicated days after symptom onset for six SARS-CoV-2-specific antigens for five different patients. Patients are indicated by color. **b, c** Samples of SARS-CoV-2-infected individuals were analyzed to identify antigen- and isotype-specific antibody responses based on hospitalization indicating disease severity (**b**) or age (**c**). Data is presented as Box-Whisker plots of sample MFI on a logarithmic scale. Box represents the median and the 25th and 75th percentiles, whiskers show the largest and smallest values. Outliers determined by 1.5 times IQR of log-transformed data are depicted as circles. *p*-value (Mann–Whitney U test, two-sided) is displayed at the top of the boxes, indicating differences between signal distribution for respective groups. Cut-off values for MultiCoV-Ab classification are displayed as horizontal lines (Spike Trimer IgG: 3,000 MFI, IgA: 400 MFI; RBD IgG: 450 MFI, IgA: 250 MFI). Source data are provided as a Source Data file.

ARTICLE
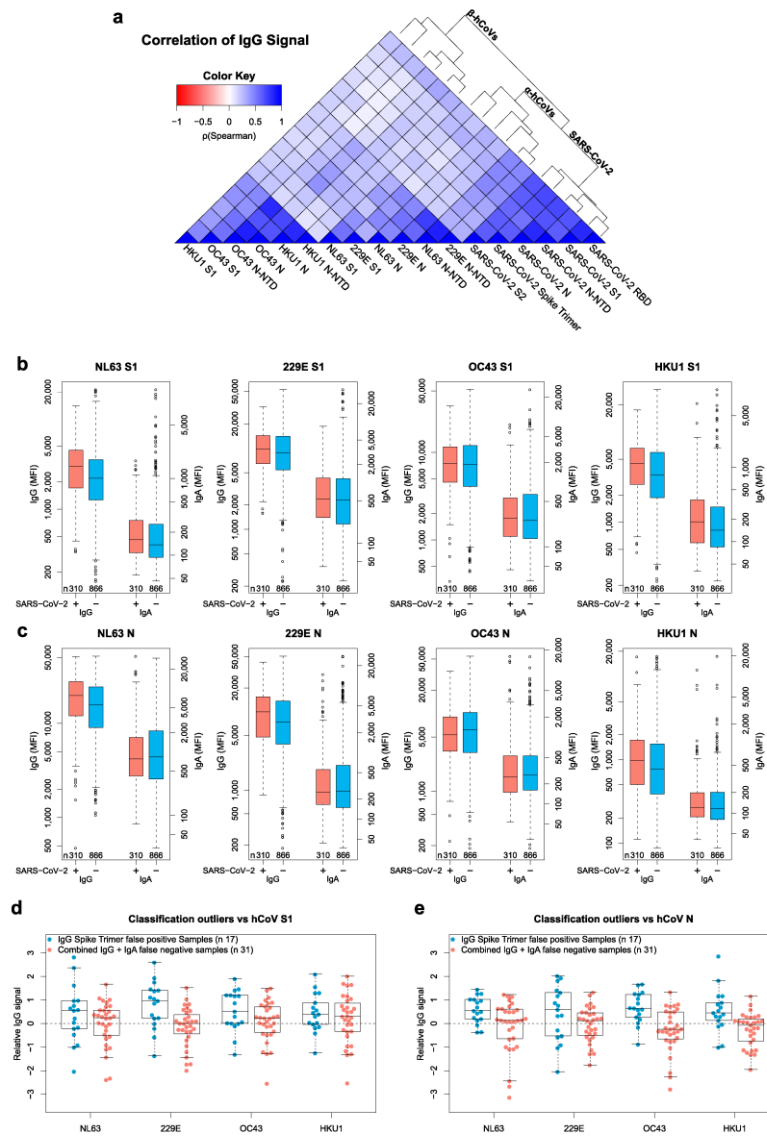
antigens from human α- (NL63 and 229E) and β-hCoVs (OC43 and HKU1) in our MultiCoV-Ab panel (Supplementary Fig. 1). The immune response towards all hCoV antigens was more dependent on coronavirus clade than on antigen choice. However, within the clades of α-hCoVs and β-hCoVs, types of antigens were more dominant than the virus subtype, as demonstrated by rank correlation analysis and hierarchical clustering (Fig. 4a, Supplementary Fig. 6a), suggesting there is potential cross-reactivity within the hCoV clades. Interestingly, IgG response against α-hCoVs clustered more closely to SARS-CoV-2 than to β-hCoVs. This is unexpected, since SARS-CoV-2 has been assigned to the clade of β-CoVs and is also more similar

85

Fig. 4 Correlation of seasonal hCoV and SARS CoV-2 antibody responses. a Correlation of IgG response for the entire sample set ($n = 1176$) is visualized as heatmap based on Spearman's ρ coefficient; dendrogram on the right side displays antigens after hierarchical clustering was performed. b-c, Immune responses (IgG and IgA) towards hCoV S1 (**b**) and N (**c**) proteins are presented as Box-Whisker plots of sample MFI on a logarithmic scale for SARS-CoV-2-infected (red, $n = 310$) and uninfected (blue, $n = 866$) individuals. Box represents the median and the 25th and 75th percentiles, whiskers show the largest and smallest values. Outliers determined by 1.5 times IQR of log-transformed data are depicted as circles. d-e, Relative levels of IgG-specific immune response towards hCoV S1 (**d**) and N (**e**) proteins are presented as Box-Whisker plots/strip chart overlays of log-transformed and per-antigen scaled and centered MFI for the sample subsets of Spike Trimer false positives (blue, $n = 17$) and combined IgG + IgA false negatives (red, $n = 31$). Box represents the median and the 25th and 75th percentiles, whiskers show the largest and smallest values, excluding outliers as determined by 1.5 times IQR. Source data are provided as a Source Data file.
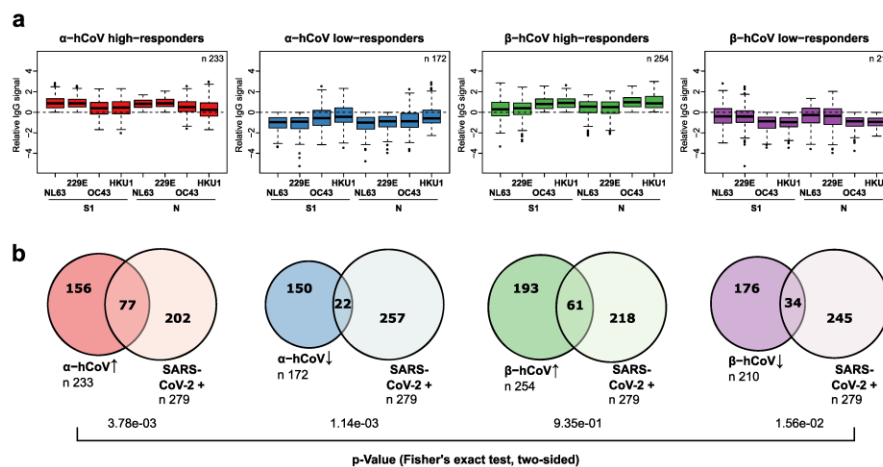

Fig. 5 Analysis of seasonal hCoV high and low responders. a From the entire study population, groups of α- or β-hCoV high and low responders were built as indicated. High responder were defined as samples with above average MFI values for S1 and N-specific IgGs of the respective hCoV clade. Low responders were defined with below MFI values, correspondingly. Responder groups (i) α-hCoV ↑, red, $n = 233$, (ii) β-hCoV ↑, green, $n = 254$, (iii) α-hCoV ↓, blue, $n = 172$ (iv) β-hCoV ↓, purple, $n = 210$ are shown as Box-Whisker plots of log-transformed and per-antigen scaled and centered MFI values across hCoV N and S1 antigens. Box represents the median and the 25th and 75th percentiles, whiskers show the largest and smallest values. Outliers determined by 1.5 times IQR are depicted as circles. **b** The over- or under-representation of SARS-CoV-2 responders (SARS-CoV-2 +, $n = 279$, as determined by positive MultiCoV-Ab classification) within the four sample groups is visualized in Venn diagrams, stochastic significance was calculated using Fisher's exact test (two-sided). Source data are provided as a Source Data file.

in sequence to the β-hCoVs (Supplementary Table 3). Overall, we identified a considerable immune response to hCoV antigens throughout the whole sample set with no notable differences between samples from SARS-CoV-2-infected and uninfected donors in IgG or IgA for S1 (Fig. 4b), N (Fig. 4c), or N-NTD (Supplementary Fig. 6b). We, therefore, used the IgG signal relative to the average response per antigen for further analyses, which allowed comparison among all hCoV antigens on one scale. For those uninfected samples which showed an IgG cross-reactivity towards Spike Trimer (Spike Trimer false positives), we partially observed increased responses towards hCoV antigens. Those samples, which did not show an immune response after SARS-CoV-2 infection (false negatives, as determined by Multi-CoV-Ab, combined IgG + IgA) were closer to the baseline (Fig. 4d, e, Supplementary Fig. 6c). This indicates that cross-reactivity with hCoVs causes some of the observed SARS-CoV-2 immune response in samples taken from individuals not exposed to SARS-CoV-2. To investigate the correlation of hCoV and SARS-CoV-2 immune response further, we grouped samples into high and low responders for α-hCoVs and β-hCoVs, as the

antigens were shown to correlate closely within a single hCoV clade. High responders were defined as having relative IgG signals > 0 for N and S1 antigens of both hCoV subtypes within the clade, while low-responders had signals < 0, respectively (Fig. 5a). Samples with SARS-CoV-2 immune response (as determined by MultiCoV-Ab, combined IgG + IgA classification) were significantly overrepresented within the group of α-hCoV high responders ($p = 3.78e\text{-}03$, Fisher's exact test, two-sided), while being significantly underrepresented within the group of α-hCoV and β-hCoV low responders ($p = 1.14e\text{-}03$ and $p = 1.56e\text{-}02$, respectively, Fisher's exact test, two-sided) (Fig. 5b). These results showed that while there were no discernible global effects for single antigens, there is a correlation between the SARS-CoV-2 immune response with high hCoV responses, especially towards α-hCoVs. This effect, and the clustering of α-hCoVs and SARS-CoV-2 in Fig. 4a may be a result of similar host-pathogen interaction (such as use of the same entry receptor as NL63, an α-hCoV) or similarities in the mode of action of host suppressive viral proteins. Interestingly, some longitudinal samples from Fig. 3a, showed increased hCoV response post SARS-CoV-2

ARTICLE

exposure (Supplementary Fig. 7). However, to further explore cross-reactivity and correlation between CoV-induced immune responses, additional longitudinal samples from donors after SARS-CoV-2 infection are needed to generate meaningful conclusions.

Discussion

We demonstrated that our MultiCoV-Ab, a multiplex immunoassay, is highly suitable to classify seroconversion in SARS-CoV-2-infected individuals. With a combined cut-off using SARS-CoV-2 trimeric full-length spike protein and RBD, we were able to eliminate false positive responses and achieved a sensitivity of 90% with a specificity of 100% for 310 samples from SARS-CoV-2-infected and for 866 samples from uninfected individuals. We found that detection of IgG more accurately reflected infection compared to IgA, although both were highly specific. However, by simultaneously monitoring IgA, we additionally were able to detect an early immune response in some patients. Interestingly, Yu, et al.[26] found that enhanced IgA responses might confer damaging effects in severe COVID-19. This is consistent with the observed significant increase in N protein directed IgA in hospitalized COVID19-cases, and confirms that careful monitoring of serum IgA warrants further attention.

The MultiCoV-Ab approach allows the easy addition of SARS-CoV-2-specific antigens, here 6 in total, which provides an additional level of confidence in patient classification. Thus, for example, we noticed that the spike S1 domain showed fewer false-positive responses compared to the S2 domain. Interestingly, Ng et al.[9] reported reactivity towards SARS-CoV-2 S2 from sera of patients with recent seasonal hCoV infection. These sera prevented infection with SARS-CoV-2 pseudotypes in a neutralization assay. Additionally, we found that spike non-responders also did not show a response to nucleocapsid but not vice versa, where nucleocapsid has been described as the strongest inducer of antibody responses[35,36]. Interestingly, nucleocapsid showed significant unspecific Ig binding in our assay. It has been previously reported, that the SARS-CoV-2 N protein is highly positively charged which may facilitate binding of viral nucleic acid but also result in unspecific binding of negatively charged molecules[37]. In addition, N protein oligomerization which is required to form the capsid[38] could further contribute to non-specific protein-protein interactions Therefore, our results highlight that the performance of an antigen is highly specific to the assay setup and cannot be easily generalized.

Another study measuring comparable numbers of serum/plasma samples using multiplex Luminex technology reports similar sensitivities and specificities for SARS-CoV-2 classification[20]. In our comparison to commercially available IVD tests, the MultiCoV-Ab classified fewer samples from SARS-CoV-2 infected donors as negative. However, for 10% of all infected samples, we could not detect a SARS-CoV-2 specific immune response, both in our measurement with MultiCoV-Ab and the commercial IVD kits. Intriguingly, others have already reported that up to 10% of SARS-CoV-2 patients do not develop detectable Ig levels[12,20,39]. Whether those non-responders are able to limit viral replication by innate immune mechanisms[40], forms of pre-existing immunity[41], or cellular immunity[42–44] is dominant in mediating viral clearance remains however to be determined.

One of the strengths of our study, compared to earlier studies[17,20,27], is the relatively large number of control and SARS-CoV-2 infected sera. However, a limitation is the potential bias introduced by an uneven age distribution across the study population. The uninfected control cohort was heavily skewed towards the age group of >60, whereas non-hospitalized COVID-

19 cases were over-represented in the age groups below 60. Despite this, MultiCoV-Ab specificity will still be accurate as all uninfected samples were identified correctly and all age groups were well represented with >100 samples per group.

Expanding our MultiCoV-Ab to the endemic hCoVs NL63, 229E, OC43, and HKU1 revealed a clear IgG immune response for all tested samples. Furthermore, we did not observe a difference for the samples from PCR-confirmed hCoV-infected individuals, compared to all others, suggesting that there is a significant degree of pre-exposure in the general population for all endemic hCoVs. Due to the general lack of availability of samples from hCoV-naive individuals, it was difficult to analyze hCoV-mediated cross-reactivity, set a cut-off and subsequently calculate specificities and sensitives for the hCoV S1, N-NTD, N antigens used here. Nevertheless, our multiplexed readout indicates a correlation between the SARS-CoV-2 immune response and high hCoV responses. Currently, we are identifying population groups which were highly exposed and showed different susceptibility to SARS-CoV-2 infection, e.g., the "Ischgl-study group" (unpublished data)[45], in order to elucidate potential cross-protection derived from immune responses towards endemic hCoVs in more detail. Alternatively, studies analyzing hCoV signatures in samples from individuals before and after SARS-CoV-2 infection using the MultiCoV-Ab would help to gain insight into a potential cross-protection.

A multiplex setup such as in MultiCoV-Ab is especially suited to vaccination studies, since the flexibility and broad antigen coverage allows to efficiently map vaccine immune responses to an immunoglobulin isotype and subtype level for the target pathogen and related species[17]. Interestingly, previous SARS-CoV-1 vaccine studies clearly indicated that a detailed characterization of vaccine-induced antibody responses is mandatory for efficient coronavirus vaccine development[46,47]. For instance, Yasui et al.[46] reported that although vector vaccines encoding SARS-CoV-1 S or N protein lead to comparable levels of anti-S and anti-N IgG in the respective study groups, N protein-immunized mice showed vaccine-induced pathology characterized by more severe lung damage, increased pulmonary neutrophil and eosinophil infiltration, and a significant upregulation of pro-inflammatory cytokine secretion upon challenge[43].

In summary, we have established and clinically validated the MultiCoV-Ab, a robust, high-content-enabled, and antigen-saving multiplex assay. This assay is suitable for comprehensive characterization of SARS-CoV-2 infection on the humoral immune response and for epidemiological screenings to accurately measure SARS-CoV-2 seroprevalence in large cohort studies. It could also provide the unique opportunity to assess and correlate immunity for both endemic and pathogenic coronaviruses. Finally, a broad and flexible antigen range through the multiplex nature of the MultiCoV-Ab can deliver urgently needed data to help guide decisions for SARS-CoV-2 vaccination strategies.

Methods

Generation of expression constructs for viral antigen production. The sequence optimized cDNAs encoding the full-length nucleocasid proteins of SARS-CoV-2, hCoV-OC43, hCoV-NL63, hCoV-229E, and hCoV-HKU1 (GenBank accession numbers "QHD43423.2"; "YP_009555245.1"; "YP_003771.1"; "NP_073556.1"; "YP_173242.1") were produced with an N-terminal hexahistidine (His$_6$)-tag by DNA synthesis (ThermoFisher Scientific). The cDNAs were cloned by standard techniques into NdeI/HindIII sites of the bacterial expression vector pRSET2b (ThermoFisher Scientific). The N-terminal domains (NTDs) of all nucleocapsid proteins were designed based upon previously published structural data[48]. Through this we were able to monitor the immune response against a rigid folded domain and exclude potential unspecific interactions with the largely unstructured region located between N-NTD and N-CTD of the nucleocapsid proteins. Furthermore, by depleting the N-CTD which is responsible for oligomerization of the nucleocapsid, we aimed to monitor antibody binding of a monomeric version of the

ARTICLE

nucleocapsid. To generate NTDs of the respective nucleocapsid proteins (SARS-CoV-2 NTD aa 1-189; hCoV-OC43 NTD aa 1-204; hCoV-NL63 NTD aa 1 - 154; hCoV-229E NTD aa 1-156; hCoV-HKU1 NTD aa 1- 203), a stop codon located N-terminally to the Serine-Arginine (SR)-rich linker site[49] was introduced via PCR mutagenesis of the nucleocapsid encoding plasmids using the forward primer pRSET2b down-for and respective reverse primers: SARS-CoV2_NTD-rev, OC43_NTD-rev, NL63_NTD-rev, and 229E_NTD-rev, and HKU1_NTD-rev.

Primer sequences are shown in Supplementary Table 4.

The pCAGGS plasmids encoding the stabilized trimeric Spike protein and the receptor binding domain (RBD) of SARS-CoV-2 were kindly provided by F. Krammer[27].

The cDNA encoding the S1 domain (aa 1–681) of the SARS-CoV-2 spike protein was produced by PCR amplification using the forward primer S1_CoV2-for and reverse primer S1_CoV2-rev and the full length SARS-CoV-2 spike cDNA as template and cloned into the XbaI/NotI-digested backbone of the pCAGGS vector, thereby adding a C-terminal His$_6$-Tag.

The cDNAs encoding the S1 domains of hCoV-OC43 (aa 1–760), hCoV-NL63 (aa 1–744), hCoV-229E (aa 1–561) and hCoV-HKU1 (aa 1–755) (GenBank accession numbers "AVR40344.1"; "APF29071.1"; "APT69883.1"; "AGW27881.1") were produced by DNA synthesis (ThermoFisher Scientific), digested using XbaI/NotI and ligated into the pCAGGS vector. All expression constructs were verified by sequence analysis. An overview of all expressed constructs can be found in Supplementary Table 5.

Protein expression and purification. For the expression of the viral nucleocapsid proteins (full-length nucleocapsid and N-NTDs), the respective expression constructs were used to transform *E.coli* BL21 (DE3) cells. Protein expression was induced in 1 L TB medium at an optical density (OD$_{600}$) of 2.5–3 by addition of 0.2 mM isopropyl-β-D-thiogalactopyranoside (IPTG) for 16 h at 20 °C. Cells were harvested by centrifugation (10 min at 6,000 × g) and the pellets were then suspended in binding buffer (1x PBS, at 0.5 M NaCl, 50 mM imidazole, 2 mM phenylmethylsulfonyl fluoride, 2 mM MgCl$_2$, 150 μg/mL lysozyme (Merck) and 625 μg/mL DNaseI (Applichem)). Cell suspensions were sonified for 15 min (Bandelin Sonopuls HD70 - power MS72/D, cycle 50%) on ice, incubated for 1 h at 4 °C in a rotary shaker followed by a second sonification step for 15 min. After centrifugation (30 min at 20,000 × g), urea was added to a final concentration of 6 M to the soluble protein extract. The extract was filtered through a 0.45 μm filter and loaded on a pre-equilibrated 1-mL HisTrap^{FF} column (GE Healthcare). The bound His-tagged nucleocapsid proteins were eluted by a linear gradient (30 mL) ranging from 50 to 500 mM imidazole in elution buffer (1x PBS, pH 7.4, 0.5 M NaCl, 6 M urea). Elution fractions (0.5 mL) containing the His-tagged nucleocapsid proteins were pooled and dialyzed (D-Tube Dialyzer Mega, Novagen) against PBS.

The viral S1-domains, SARS-CoV-2 RBD, and the stabilized trimeric SARS-CoV-2 spike protein were expressed in Expi293 cells following the protocol as described in Stadlbauer et al.[19]. In brief, Expi293F-cells were cultivated (37 °C, 125 rpm, 8% (v/v) CO$_2$) to a density of 5.5×10^6 cells/mL. The cells were diluted with Expi293F expression medium to a density of 3.0×10^6 cells/mL, followed by transfection of the corresponding expression plasmids (1 μg per mL cell culture) with Expifectamine dissolved in Opti-MEM medium, according to the manufacturer's instructions. After 20 h post-transfection, transfection enhancers were added as documented in the Expi293F-cells manufacturer's instructions. The cell suspensions were cultivated for 2–5 days (37 °C, 125 rpm, 8% (v/v) CO$_2$) and centrifuged (4 °C, 23,900 × g, 20 min) to clarify the supernatant. The supernatants were filtered using a 0.22 μm membrane filter (Millipore, Darmstadt, Germany) and supplemented with His-A buffer stock solution (final concentration in the medium: 20 mM Na$_2$HPO$_4$, 300 mM NaCl, 20 mM imidazole, pH 7.4), before the solution was applied to a HisTrap FF crude column on a Äkta pure system (GE Healthcare, Freiburg, Germany). The columns were extensively washed with His-buffer-A (20 mM Na$_2$HPO$_4$, 300 mM NaCl, 20 mM imidazole, pH 7.4) before bound proteins were eluted with a imidazole gradient ranging from 50 mM – 400 mM. Eluted proteins were dialyzed against PBS and concentrated to 1 mg/mL.

All purified proteins were analyzed via standard SDS-PAGE followed by staining with InstantBlue Coomassie stain (Expedeon) and immunoblotting using an anti-His antibody (Penta-His Antibody, #34660, Qiagen, used at 1:1,000 dilution) in combination with a donkey-anti-mouse antibody labeled with AlexaFluor647 (#A31571, Invitrogen, used at 1:1,000 dilution) on a Typhoon Trio (GE-Healthcare, Freiburg, Germany; excitation 633 nm, emission filter settings 670 nm BP 30) to confirm protein integrity. To further confirm correct expression, integrity, and purity, proteins were analyzed by mass spectrometry. To control the production reproducibility of the antigens, potential aggregation and melting temperatures of the proteins were investigated by nano differential scanning fluorimetry (nanoDSF) using a Prometheus (Nanotemper, Munich, Germany).

Commercial antigens. Two commercial antigens were used to complement the in-house-produced antigen panel.

The S2 ectodomain of the SARS-CoV-2 spike protein (aa 686–1213) was purchased from Sino Biological, Eschborn, Germany (cat # 40590, lot # LC14MC3007). A full-length nucleocapsid protein of SARS-CoV-2 was purchased from Aalto Bioreagents, Dublin, Ireland (cat # 6404-b, lot # 4629).

Bead-based serological multiplex assay. All antigens were covalently immobilized on spectrally distinct populations of carboxylated paramagnetic beads (MagPlex Microspheres, Luminex Corporation, Austin, TX) using 1-ethyl-3-(3-dimethylaminopropyl)carbodiimide (EDC)/sulfo-N-hydroxysuccinimide (sNHS) chemistry. For immobilization, a magnetic particle processor (KingFisher 96, Thermo Scientific, Schwerte, Germany) was used.

Bead stocks were vortexed thoroughly and sonicated for 15 s. Subsequently, 83 μL of 0.065% (v/v) Triton X-100 and 1 mL of bead stock containing 12.5×10^7 beads of one single bead population were pipetted into each well. The beads were then washed twice with 500 μL of activation buffer (100 mM Na$_2$HPO$_4$, pH 6.2, 0.005% (v/v) Triton X-100) and beads were activated for 20 min in 300 μL of activation mix containing 5 mg/mL EDC and 5 mg/mL sNHS in activation buffer. Following activation, the beads were washed twice with 500 μL of coupling buffer (500 mM MES, pH 5.0, 0.005% (v/v) Triton X-100) and the antigens were added to the activated beads and incubated for 2 h at 21 °C to immobilize the antigens on the surface.

Antigen-coupled beads were washed twice with wash buffer (1x PBS, 0.005% (v/v) Triton X-100) and were finally resuspended in 1000 μL of storage buffer (1x PBS, 1% (w/v) BSA, 0.05% (v/v) ProClin). The beads were stored at 4°C until further use.

To detect human IgG and IgA responses against SARS-CoV-2 and the endemic human coronaviruses (hCoV-NL63, hCoV-229E, hCoV-OC43 and hCoV-HKU1), the purified trimeric spike protein (S), S1-domain, S2-domain (Sino Biological GmbH, Europe), RBD, nucleocapsid (N) and the N-terminal domain of nucleocapsid (N-NTD) of SARS-CoV-2 as well as the S1-domain, N, and N-NTD of the endemic hCoVs were immobilized on different bead populations as described above. The individual bead populations were combined into a bead mix. A bead-based multiplex assay was performed. Briefly, samples were incubated at a 1:400 dilution for 2 hours at 21 °C. Unbound antibodies were removed and the beads were washed three times with 100 μL of wash buffer (1x PBS, 0.05% (v/v) Tween20) per well using a microplate washer (Biotek 405TS, Biotek Instruments GmbH). Bound antibodies were detected with R-phycoerythrin labeled goat-anti-human IgG (Dianova, Cat# 109-116-098, Lot#148837, used at 3 μg/mL) or IgA (Dianova, Cat# 109-115-011, Lot#143454, used at 5 μg/mL) antibodies (incubation for 45 min at 21 °C). For each sample, a single measurement was performed. Readout was done using a Luminex FLEXMAP 3D instrument and the Luminex xPONENT Software 4.3 (settings: sample size: 80 μL, 50 events, Gate: 7,500–15,000, Reporter Gain: Standard PMT).

Quality control and technical assay validation steps. In order to test the repeatability of the MultiCoV-Ab three quality control samples (QCs) were processed in duplicate on each test plate ($n = 17$) during the sample screening and inter-assay variance was assessed for each antigen in the multiplex. For intra-assay variance, 24 replicates of each of the three QC samples were analyzed on one plate. Results from this are presented in Supplementary Table 1 and Supplementary Fig. 2. A limit of detection (LOD) for each antigen was determined by processing a blank in 24 replicates and the LOD was set as mean MFI + 3 standard deviations. Sample parallelism and comparability of paired serum and plasma samples were assessed over eight dilution steps ranging from 1:100 to 1:12,800 (Supplementary Fig. 2). A set of samples derived from 205 SARS-CoV-2-infected and 72 uninfected individuals was tested repeatedly with two different kit batches. The samples classification in both runs matched 100%. Furthermore, as part of our negative sample panel, we have analyzed samples with potentially interfering characteristics (i.e., samples from patients with PCR-confirmed hCoV infection, presences of HAMA (human anti-mouse antibodies) and rheumatoid factor (RF), with high procalcitonin values (> 3 ng/mL), as well as from pregnant women and patients with neuroinflammatory diseases) (Supplementary Table 2).

Samples. A total of 1176 sera and plasma samples were used for the MultiCoV-Ab assay development. Ethical approval was granted from the Ethics Committee of Hannover Medical School (#9122_BO_K2020). Only de-identified samples were used for the MultiCoV-Ab assay development. All samples were pre-existing. Cohort age was 5-88 years; age was not known for 161 samples.

310 samples were from COVID-19 patients or convalescents. Samples were classified as SARS-CoV-2 infected, if a positive SARS-CoV-2 RT-PCR was reported and/or if hospitalization/quarantine for COVID-19 was indicated as part of the samples metadata. dT defined as time between PCR test or symptom onset and blood draw was 0–73 days (median= 38 d; $n = 258$). dT was not provided for 52 samples. SARS-CoV-2 infected samples used in this study were collected after ethical review (9001_BO_K, Hannover Medical School; 179/2020/BO2, University Hospital Tübingen; 85/20, Ärztekammer des Saarlandes).

866 control samples were from non-SARS-CoV-2 infected individuals and were classified as non-infected as they were obtained prior to the emergence of SARS-CoV-2 in December 2019 or because they were taken from individuals who had not reported cold symptoms since the beginning of 2020.

The majority of non-SARS-COV-2 infected samples were randomly selected and consisted of pre-pandemic blood donors, commercially available (Central BioHub GmbH, Berlin, Germany and BBI Solutions, Crumlin, UK) or bio-banked specimens. 365 samples were from the Memory and Morbidity in Augsburg Elderly (MEMO) study (a sub-cohort of the MONICA S2 cohort (WHO 1988)) and were included based on available serological titers for HSV-1, HSV-2, HHV-6, and

88

ARTICLE

EBV[50]. 88 samples were obtained from transplanted patients with chronic respiratory conditions.

Collection of non-SARS-CoV-2 infected control samples had been approved by several ethic committees: 3232-2016 (Ethics Committee of Hannover Medical School); 62/20 (Ethics Committees of the Medical Faculty of the Saarland University at the Saarland Ärztekammer); WUM 17.02.1997 (Joint ethics committee of the University of Münster and the Westphalian Chamber of Physicians).

All necessary patient/participant consent has been obtained and the appropriate institutional forms have been archived. Additional sample details can be found in Supplementary Table 2. Serum and plasma samples were handled in Class II-laminar flow benches in L2 laboratories[51]. Samples were not heat-inactivated. All incubation steps took place in fully sealed assay plates.

Data analysis. Data analysis and visualization were performed with R Studio (Version 1.2.5001, using R version 3.6.1) using the Median Fluorescent Intensity (MFI). Statistical analysis was performed using R package "stats" from the base repository. Mann-Whitney U test was used to determine the difference between signal distributions from different sample groups. Spearman's ρ coefficient was calculated in order to correlate antigens by response from the entire sample set, followed by hierarchical clustering to group antigens. Fishers' exact test was used to calculate the significance of overlap between sample groups. 95% Confidence intervals for sensitivity and specificity values calculated in this study were calculated after Clopper-Pearson[52] and associated positive and negative predictive values (PPV/NPV) were calculated based on a seropositivity of 3%. Sequence alignments and sequence identity scores were calculated with version 1.2.4. of Clustal Omega[53].

Reporting summary. Further information on research design is available in the Nature Research Reporting Summary linked to this article.

Data availability
Data relating to the findings of this study are available from the corresponding author upon request. Source data have been deposited on GitHub alongside the analysis code: https://github.com/BeckerMatthias/MULTICOV-AB_Publication/. Source data are provided with this paper.

Code availability
Analysis code and required input files have been deposited on GitHub: https://github.com/BeckerMatthias/MULTICOV-AB_Publication/

References
1. Gorbalenya, A. E. et al. The species Severe acute respiratory syndrome-related coronavirus: classifying 2019-nCoV and naming it SARS-CoV-2. *Nat. Microbiol.* **5**, 536–544 (2020).
2. Mofijur, M. et al. Impact of COVID-19 on the social, economic, environmental and energy domains: Lessons learnt from a global pandemic. *Sustain. Prod. Consum.* **26**, 343–359 (2021).
3. Hu, B., Guo, H., Zhou, P. & Shi, Z.-L. Characteristics of SARS-CoV-2 and COVID-19. *Nat. Rev. Microbiol.* https://doi.org/10.1038/s41579-020-00459-7 (2020).
4. Wu, Z. & McGoogan, J. M. Characteristics of and important lessons from the coronavirus disease 2019 (COVID-19) outbreak in China: summary of a report of 72 314 cases from the Chinese Center for Disease Control and Prevention. *Jama* **323**, 1239–1242 (2020).
5. Huang, A. T. et al. A systematic review of antibody mediated immunity to coronaviruses: kinetics, correlates of protection, and association with severity. *Nat. Commun.* **11**, 4704 (2020).
6. Severance, E. G. et al. Development of a nucleocapsid-based human coronavirus immunoassay and estimates of individuals exposed to coronavirus in a US metropolitan population. *Clin. Vaccin. Immunol.* **15**, 1805–1810 (2008).
7. Corman, V. M., Muth, D., Niemeyer, D. & Drosten, C. in *Advances in virus research* Vol. 100 163–188 (Elsevier, 2018).
8. Murin, C. D., Wilson, I. A. & Ward, A. B. Antibody responses to viral infections: a structural perspective across three different enveloped viruses. *Nat. Microbiol.* **4**, 734–747 (2019).
9. Ng, K. W. et al. Preexisting and de novo humoral immunity to SARS-CoV-2 in humans. *Science*, eabe1107, https://doi.org/10.1126/science.abe1107 (2020).
10. Lee, N. et al. Anti-SARS-CoV IgG response in relation to disease severity of severe acute respiratory syndrome. *J. Clin. Virol.* **35**, 179–184 (2006).
11. Ho, M.-S. et al. Neutralizing antibody response and SARS severity. *Emerg. Infect. Dis.* **11**, 1730 (2005).
12. Tan, W. et al. Viral Kinetics and Antibody Responses in Patients with COVID-19. Preprint at: https://www.medrxiv.org/content/10.1101/2020.03.24.20042382v1. (2020).
13. Ko, J.-H. et al. Serologic responses of 42 MERS-coronavirus-infected patients according to the disease severity. *Diagnostic Microbiol. Infect. Dis.* **89**, 106–111 (2017).
14. Long, Q. X. et al. Antibody responses to SARS-CoV-2 in patients with COVID-19. *Nat. Med.* **26**, 845–848 (2020).
15. Amanat, F. & Krammer, F. SARS-CoV-2 vaccines: status report. *Immunity* **52**, 583–589 (2020).
16. Robbiani, D. F. et al. Convergent antibody responses to SARS-CoV-2 in convalescent individuals. *Nature* **584**, 437–442 (2020).
17. Okba, N. M. A. et al. Severe acute respiratory syndrome coronavirus 2-specific antibody responses in coronavirus disease patients. *Emerg. Infect. Dis.* **26**, 1478–1488 (2020).
18. Lassaunière, R. et al. Evaluation of nine commercial SARS-CoV-2 immunoassays. Preprint at: https://www.medrxiv.org/content/10.1101/2020.04.09.20056325v1. (2020).
19. Stadlbauer, D. et al. SARS-CoV-2 seroconversion in humans: a detailed protocol for a serological assay, antigen production, and test setup. *Curr. Protoc. Microbiol* **57**, e100 (2020).
20. den Hartog, G. et al. SARS-CoV-2–specific antibody detection for seroepidemiology: a multiplex analysis approach accounting for accurate seroprevalence. *J. Infect. Dis.* **222**, 1452–1461 (2020).
21. Norman, M. et al. Ultra-sensitive high-resolution profiling of anti-SARS-CoV-2 antibodies for detecting early seroconversion in COVID-19 patients. Preprint at https://www.medrxiv.org/content/10.1101/2020.04.28.20083691v1. (2020).
22. Rudberg, A.-S. et al. SARS-CoV-2 exposure, symptoms and seroprevalence in healthcare workers in Sweden. *Nat. Commun.* **11**, 5064 (2020).
23. Jiang, H.-w et al. SARS-CoV-2 proteome microarray for global profiling of COVID-19 specific IgG and IgM responses. *Nat. Commun.* **11**, 3581 (2020).
24. Meyer, B., Drosten, C. & Müller, M. A. Serological assays for emerging coronaviruses: challenges and pitfalls. *Virus Res.* **194**, 175–183 (2014).
25. Callow, K., Parry, H., Sergeant, M. & Tyrrell, D. The time course of the immune response to experimental coronavirus infection of man. *Epidemiol. Infect.* **105**, 435–446 (1990).
26. Yu, H.-q. et al. Distinct features of SARS-CoV-2-specific IgA response in COVID-19 patients. *Eur. Resp. J.* 2001526, https://doi.org/10.1183/13993003.01526-2020 (2020).
27. Amanat, F. et al. A serological assay to detect SARS-CoV-2 seroconversion in humans. *Nat. Med.* **26**, 1033–1036 (2020).
28. Elecsys® Anti-SARS-CoV-2, https://diagnostics.roche.com/global/en/products/params/elecsys-anti-sars-cov-2.html (2020).
29. SARS-CoV-2-Gesamtantikörpertest, https://www.siemens-healthineers.com/de/laboratory-diagnostics/assays/assays-by-diseases-conditions/infectious-disease-assays/cov2t-assay (2020).
30. SARS-CoV-2, https://www.coronavirus-diagnostik.de/antikoerpertestsysteme-fuer-covid-19.html (2020).
31. Fawcett, T. An introduction to ROC analysis. *Pattern Recognit. Lett.* **27**, 861–874 (2006).
32. Zou, K. H., O'Malley, A. J. & Mauri, L. Receiver-operating characteristic analysis for evaluating diagnostic tests and predictive models. *Circulation* **115**, 654–657 (2007).
33. Guo, L. et al. Profiling early humoral response to diagnose novel coronavirus disease (COVID-19). *Clin. Infect. Dis.* **71**, 778–785 (2020).
34. Iyer, A. S. et al. Persistence and decay of human antibody responses to the receptor binding domain of SARS-CoV-2 spike protein in COVID-19 patients. *Sci Immunol.* **5**, eabe0367 (2020).
35. Burbelo, P. D. et al. Sensitivity in Detection of Antibodies to Nucleocapsid and Spike Proteins of Severe Acute Respiratory Syndrome Coronavirus 2 in Patients With Coronavirus Disease 2019. *J Infect Dis.* **222**, 206–213 (2020).
36. Sun, B. et al. Kinetics of SARS-CoV-2 specific IgM and IgG responses in COVID-19 patients. *Emerg. Microbes Infect.* **9**, 940–948 (2020).
37. Zeng, W. et al. Biochemical characterization of SARS-CoV-2 nucleocapsid protein. *Biochem. Biophys. Res Commun.* **527**, 618–623 (2020).
38. McBride, R., Van Zyl, M. & Fielding, B. C. The coronavirus nucleocapsid is a multifunctional protein. *Viruses* **6**, 2991–3018 (2014).
39. Wang, H. et al. SARS-CoV-2 Proteome microarray for mapping COVID-19 antibody interactions at amino acid resolution. *ACS Central Science*, https://doi.org/10.1021/acscentsci.0c00742 (2020).
40. Angka, L., Market, M., Ardolino, M. & Auer, R. C. Is innate immunity our best weapon for flattening the curve? *J. Clin. Investig.* **130**, 3954–3956 (2020).
41. Sette, A. & Crotty, S. Pre-existing immunity to SARS-CoV-2: the knowns and unknowns. *Nat. Rev. Immunol.* **20**, 457–458 (2020).
42. Nelde, A. et al. SARS-CoV-2-derived peptides define heterologous and COVID-19-induced T cell recognition. *Nat. Immunol.* https://doi.org/10.1038/s41590-020-00808-x (2020).

ARTICLE

43. Liu, L. et al. Anti-spike IgG causes severe acute lung injury by skewing macrophage responses during acute SARS-CoV infection. *JCI Insight* **4**, e123158 (2019).

44. Gallais, F. *et al.* Intrafamilial exposure to SARS-CoV-2 induces cellular immune response without seroconversion. Preprint at https://www.medrxiv.org/content/10.1101/2020.06.21.20132449v1. (2020).

45. Ischgl: 42,4 Prozent sind Antikörper-positiv, https://www.deutsche-apotheker-zeitung.de/news/artikel/2020/06/26/viele-buerger-ischgls-waren-infiziert (2020).

46. Yasui, F. et al. Prior immunization with severe acute respiratory syndrome (SARS)-associated coronavirus (SARS-CoV) nucleocapsid protein causes severe pneumonia in mice infected with SARS-CoV. *J. Immunol.* **181**, 6337–6348 (2008).

47. Bolles, M. et al. A double-inactivated severe acute respiratory syndrome coronavirus vaccine provides incomplete protection in mice and induces increased eosinophilic proinflammatory pulmonary response upon challenge. *J. Virol.* **85**, 12201–12215 (2011).

48. Chen, I.-J. et al. Crystallization and preliminary X-ray diffraction analysis of the N-terminal domain of human coronavirus OC43 nucleocapsid protein. *Acta Crystallogr. Sect. F: Struct. Biol. Crystallization Commun.* **66**, 815–818 (2010).

49. Kang, S. *et al.* Crystal structure of SARS-CoV-2 nucleocapsid protein RNA binding domain reveals potential unique drug targeting sites. *Acta Pharm Sin B*, https://doi.org/10.1016/j.apsb.2020.04.009 (2020).

50. Zeeb, M. *et al.* Seropositivity for pathogens associated with chronic infections is a risk factor for all-cause mortality in the elderly: findings from the Memory and Morbidity in Augsburg Elderly (MEMO) Study. *GeroScience*, https://doi.org/10.1007/s11357-020-00216-x (2020).

51. Offergeld, R. *Stellungnahme des AK Blut (S20) zu SARS-Coronavirus-2 (17.3.2020)*, https://www.rki.de/DE/Content/Kommissionen/AK_Blut/Stellungnahmen/download/COVID.pdf?__blob=publicationFile (2020).

52. Clopper, C. J. & Pearson, E. S. The use of confidence or fiducial limits illustrated in the case of the binomial. *Biometrika* **26**, 404–413 (1934).

53. Madeira, F. et al. The EMBL-EBI search and sequence analysis tools APIs in 2019. *Nucleic acids Res.* **47**, W636–W641 (2019).

Acknowledgements

Author contributions

M.B. designed and performed experiments and data analysis; M.S. designed experiments; D.J., J.H., S.F., F.R., planned and performed experiments; A.Z. performed mass spectrometry analysis; J.H. performed nanoDSF analyses; H.D., B.T., P.D.K., F.W., U.R. designed, cloned, expressed and purified the antigens; S.H. and A.P. performed sample analysis; T.B., A.B., S.L., S.S., M.C., T.I., J.G., A.K., K.B., H-G.R., A.N., M.M., J.S.H., J.S.W., M.T., T.O.J. arranged sample and data collection; K.S-L., M.T., T.O.J, T.K., G.K. supported the study planning; S.G. reviewed the analysis code; N.S-M. planned the study, assay development, and validation and designed experiments; M.B., M.S., A.D., U.R., and N.S-M. wrote the manuscript. All authors reviewed the manuscript.

Competing interests

The authors declare the following competing interests: T.O.J. is a scientific advisor for Luminex. N.S-M. was a speaker at Luminex user meetings in the past. The Natural and Medical Sciences Institute at the University of Tübingen is involved in applied research projects as a fee for services with Luminex. The remaining authors declare no competing interests.

Additional information

Supplementary information The online version contains supplementary material available at https://doi.org/10.1038/s41467-021-20973-3.

Correspondence and requests for materials should be addressed to N.S.-M.

Peer review information *Nature Communications* thanks the anonymous reviewers for their contribution to the peer review of this work. Peer reviewer reports are available.

Reprints and permission information is available at http://www.nature.com/reprints

Publisher's note Springer Nature remains neutral with regard to jurisdictional claims in published maps and institutional affiliations.

[1]NMI Natural and Medical Sciences Institute at the University of Tübingen, Reutlingen, Germany. [2]Department of Epidemiology, Helmholtz Centre for Infection Research, Braunschweig, Germany. [3]TWINCORE GmbH, Centre for Experimental and Clinical Infection Research, a joint venture of the Hannover Medical School and the Helmholtz Centre for Infection Research, Hannover, Germany. [4]Helmholtz-Institute for RNA-based Infection Research (HIRI), Würzburg, Germany. [5]Pharmaceutical Biotechnology, University of Tübingen, Tübingen, Germany. [6]Institute for Clinical Chemistry and Pathobiochemistry, Department for Diagnostic Laboratory Medicine, University Hospital Tübingen, Tübingen, Germany. [7]Institute for Diabetes Research and Metabolic Diseases of the Helmholtz Center Munich at the University of Tübingen, Tübingen, Germany. [8]German Center for Diabetes Research (DZD), München-Neuherberg, Germany. [9]Institute for Clinical and Experimental Transfusion Medicine, University Hospital Tübingen, Tübingen, Germany. [10]Niedersächsisches Landesgesundheitsamt, Department of Virology/Serology, Hannover, Germany. [11]Institute of Virology, Saarland University Medical Center, Homburg/Saar, Germany. [12]Department of Gastroenterology, Hepatology, Endocrinology, Hannover Medical School, Hannover, Germany; Centre for Individualized Infection Medicine (CiiM), Hannover, Germany. [13]Hannover Unified Biobank (HUB), Hannover Medical School, Hannover, Germany. [14]Department of Respiratory Medicine, Hannover Medical School, Hannover, Germany. [15]Biomedical Research in End-stage and obstructive Lung Disease Hannover (BREATH), Member of the German Center for Lung Research (DZL), Hannover, Germany. [16]Institute of Epidemiology and Social Medicine, University of Münster, Münster, Germany. [17]Institute for Cell Biology, Department of Immunology, University of Tübingen, Tübingen, Germany. [18]German Cancer Consortium (DKTK) and German Cancer Research Center (DKFZ), partner site Tübingen, Tübingen, Germany. [19]Cluster of Excellence iFIT (EXC2180) "Image-Guided and Functionally Instructed Tumor Therapies", University of Tübingen, Tübingen, Germany. [20]Department of Women's Health, Research Institute for Women's Health, Eberhard-Karls-University, Tübingen, Germany. [21]Department of Medicine/Cardiology, Cardiovascular Research Laboratories, David Geffen School of Medicine at UCLA, Los Angeles, CA, USA. [22]Clinical Collaboration Unit Translational Immunology, German Cancer Consortium (DKTK), Department of Internal Medicine, University Hospital Tübingen, Tübingen, Germany. [23]Dr. Margarete Fischer-Bosch Institute of Clinical Pharmacology (IKP) and Robert Bosch Center for Tumor Diseases (RBCT), both Stuttgart, Germany. [24]These authors contributed equally: Matthias Becker, Monika Strengert, Ulrich Rothbauer. ✉email: Nicole.Schneiderhan@nmi.de

Supplementary Information

Exploring beyond clinical routine SARS-CoV-2 serology using MultiCoV-Ab to evaluate endemic coronavirus cross-reactivity

Matthias Becker[1,#], Monika Strengert[2,3,#], Daniel Junker[1], Philipp D. Kaiser[1], Tobias Kerrinnes[4], Bjoern Traenkle[1,5], Heiko Dinter[1,5], Julia Häring[1], Stéphane Ghozzi[2], Anne Zeck[1], Frank Weise[1], Andreas Peter[6,7,8], Sebastian Hörber[6,7,8], Simon Fink[1], Felix Ruoff[1], Alex Dulovic[1], Tamam Bakchoul[9], Armin Baillot[10], Stefan Lohse[11], Markus Cornberg[12], Thomas Illig[13], Jens Gottlieb[14,15], Sigrun Smola[11], André Karch[16], Klaus Berger[16], Hans-Georg Rammensee[17,18,19], Katja Schenke-Layland[1,19,20,21], Annika Nelde[17,19,22], Melanie Märklin[19,21], Jonas S. Heitmann[19,21], Juliane S. Walz[17,19,23,22], Markus Templin[1], Thomas O. Joos[1], Ulrich Rothbauer[1,5,#], Gérard Krause[2,3], Nicole Schneiderhan-Marra[1,*]

Affiliations

[1] NMI Natural and Medical Sciences Institute at the University of Tübingen, Reutlingen, Germany

[2] Department of Epidemiology, Helmholtz Centre for Infection Research, Braunschweig, Germany

[3] TWINCORE GmbH, Centre for Experimental and Clinical Infection Research, a joint venture of the Hannover Medical School and the Helmholtz Centre for Infection Research, Hannover, Germany

[4] Helmholtz-Institute for RNA-based Infection Research (HIRI), Würzburg, Germany

[5] Pharmaceutical Biotechnology, University of Tübingen, Germany

[6] Institute for Clinical Chemistry and Pathobiochemistry, Department for Diagnostic Laboratory Medicine, University Hospital Tübingen, Tübingen, Germany

[7] Institute for Diabetes Research and Metabolic Diseases of the Helmholtz Center Munich at the University of Tübingen, Tübingen, Germany

1

[8] German Center for Diabetes Research (DZD), München-Neuherberg, Germany

[9] Institute for Clinical and Experimental Transfusion Medicine, University Hospital Tübingen, Tübingen, Germany

[10] Niedersächsisches Landesgesundheitsamt, Department of Virology/Serology, Hannover, Germany

[11] Institute of Virology, Saarland University Medical Center, Homburg/Saar, Germany

[12] Department of Gastroenterology, Hepatology, Endocrinology, Hannover Medical School, Hannover, Germany; Centre for Individualized Infection Medicine (CiiM), Hannover, Germany

[13] Hannover Unified Biobank (HUB), Hannover Medical School, Hannover, Germany

[14] Department of Respiratory Medicine, Hannover Medical School, Hannover Germany

[15] Biomedical Research in End-stage and obstructive Lung Disease Hannover (BREATH), member of the German Center for Lung Research (DZL), Hannover, Germany

[16] Institute of Epidemiology and Social Medicine, University of Münster, Münster, Germany

[17] Institute for Cell Biology, Department of Immunology, University of Tübingen, Tübingen, Germany

[18] German Cancer Consortium (DKTK) and German Cancer Research Center (DKFZ), partner site Tübingen, Tübingen, Germany.

[19] Cluster of Excellence iFIT (EXC2180) "Image-Guided and Functionally Instructed Tumor Therapies", University of Tübingen, Tübingen, Germany

[20] Department of Women's Health, Research Institute for Women's Health, Eberhard-Karls-University, Tübingen, Germany

[21] Department of Medicine/Cardiology, Cardiovascular Research Laboratories, David Geffen School of Medicine at UCLA, Los Angeles, CA, USA

[22] Clinical Collaboration Unit Translational Immunology, German Cancer Consortium (DKTK), Department of Internal Medicine, University Hospital Tübingen, Tübingen, Germany

[23] Dr. Margarete Fischer-Bosch Institute of Clinical Pharmacology (IKP) and Robert Bosch Center for Tumor Diseases (RBCT), both Stuttgart, Germany

[#] These authors contributed equally to this work.

2

92

* Corresponding author:

Dr. Nicole Schneiderhan-Marra

Markwiesenstrasse 55, 72770 Reutlingen, Germany

Phone: 0049 7121 51530 815

Fax: 0049 7121 51530 16

E-Mail: Nicole.Schneiderhan@nmi.de

3
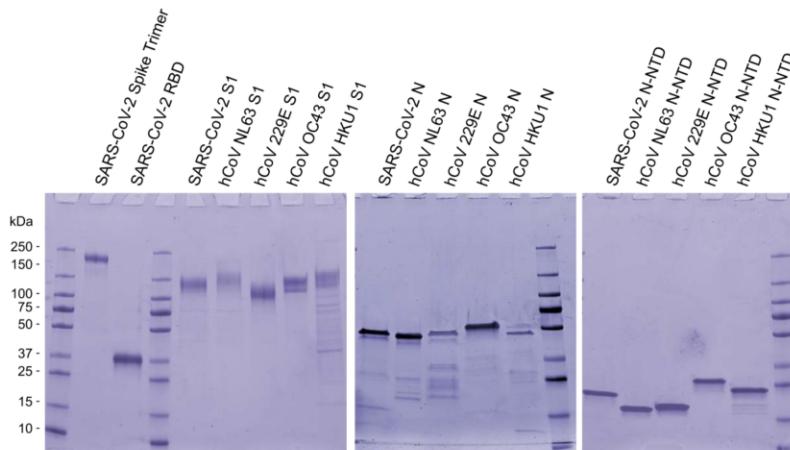
Supplementary Figure 1

SDS-PAGE analysis of the recombinant viral antigens used in this study. To test for purity and integrity 1 - 2 µg of indicated recombinant proteins were boiled in reducing SDS-sample buffer and subjected to a gradient (4 – 20 %) SDS-PAGE followed by Coomassie staining. SARS-CoV-2 Spike Trimer, SARS-CoV-2 RBD and the S1-domains of SARS-CoV-2, hCoV-NL63, hCoV-229E, hCoV-OC43 and hCoV-HKU1 were produced in ExpiHEK™ cells. Nucleocapsid (N) and N-terminal domain of nucleocapsid (N-NTD) of SARS-CoV-2, hCoV-NL63, hCoV-229E, hCoV-OC43 and hCoV-HKU1 were produced in *E.coli*. The image is an assembly of all expressed proteins and is representative for single protein purity after purification. Source data are provided as a Source Data file.

4
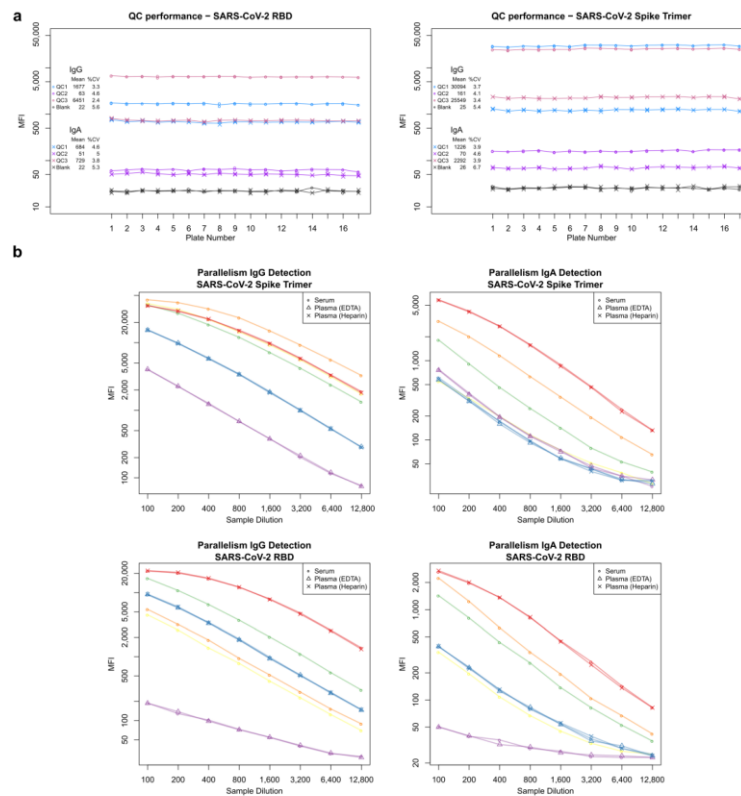
Supplementary Figure 2

a, Three quality control (QC) samples, as well as a sample of assay buffer (blank sample) were processed in duplicates on every plate. Performance across 17 assay runs is depicted and mean and %CVs are shown on the left side (n=34). For plate 14, a processing error lead to exclusion of one blank sample from this evaluation. **b,** To assess parallelism of signals from different samples, 6 unique serum samples were processed over a dilution series of 8 steps from 1:100 to 1:12,800. For 3 samples, paired plasma (EDTA and/or Heparin) were available and processed together. For IgG and IgA detection of Spike Trimer and RBD, MFI are plotted against sample dilution. Color indicates unique sample and shapes indicate sample type. The data represent a single measurement per sample and dilution (n=1). Source data are provided as a Source Data file.

5
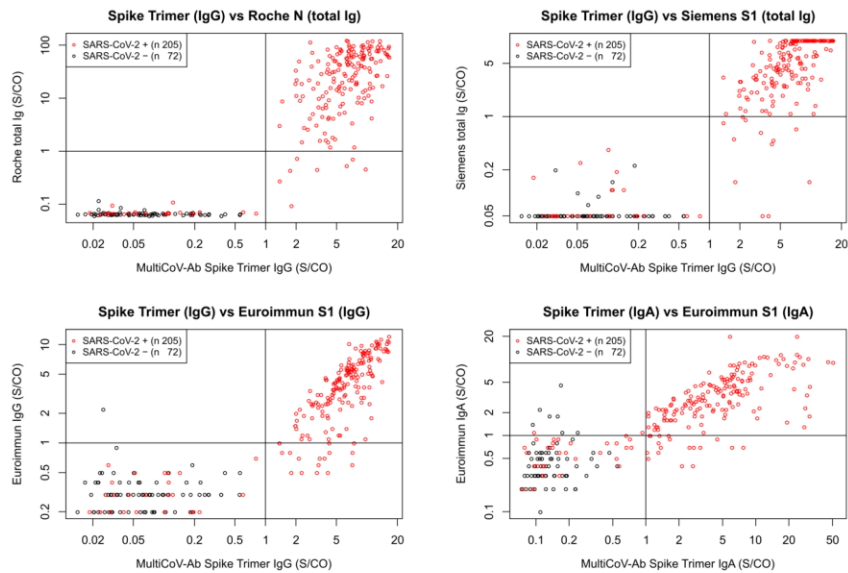
Supplementary Figure 3

Scatterplots of sample set with defined SARS-CoV-2 infection status (infected: red, n=205; uninfected: black, n=72) to compare performance of the MultiCoV-Ab Spike Trimer vs indicated antigens of commercial SARS-CoV-2 test kits. Signals are depicted as Signal to cut-off ratios (S/CO) on a logarithmic scale. Lines indicate the respective cut-off values as defined by the manufacturer to determine positive and negative test results. Source data are provided as a Source Data file.

6
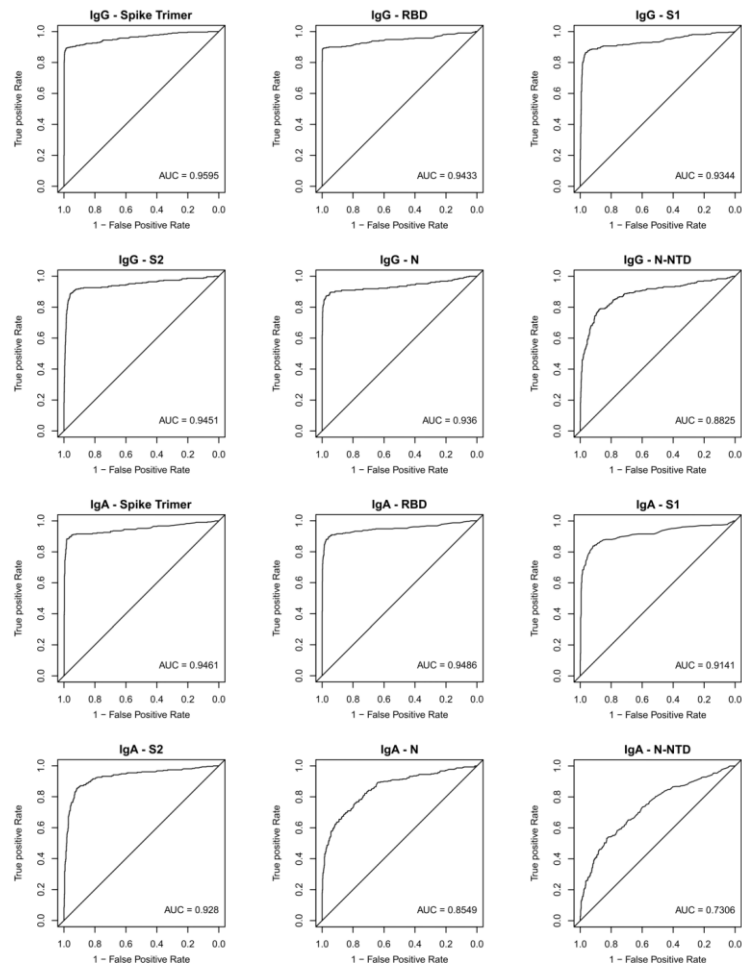
Supplementary Figure 4

ROC analysis[1,2] for IgG and IgA detection of SARS-CoV-2 antigens based on the extended sample set of 866 uninfected and 310 infected samples used for clinical validation for MultiCoV-Ab. True positive rate is displayed against 1 - false positive rate, corresponding to sensitivity and specificity at a given cut-off. AUC-values indicating individual antigen performance are shown. Source data are provided as a Source Data file.

7
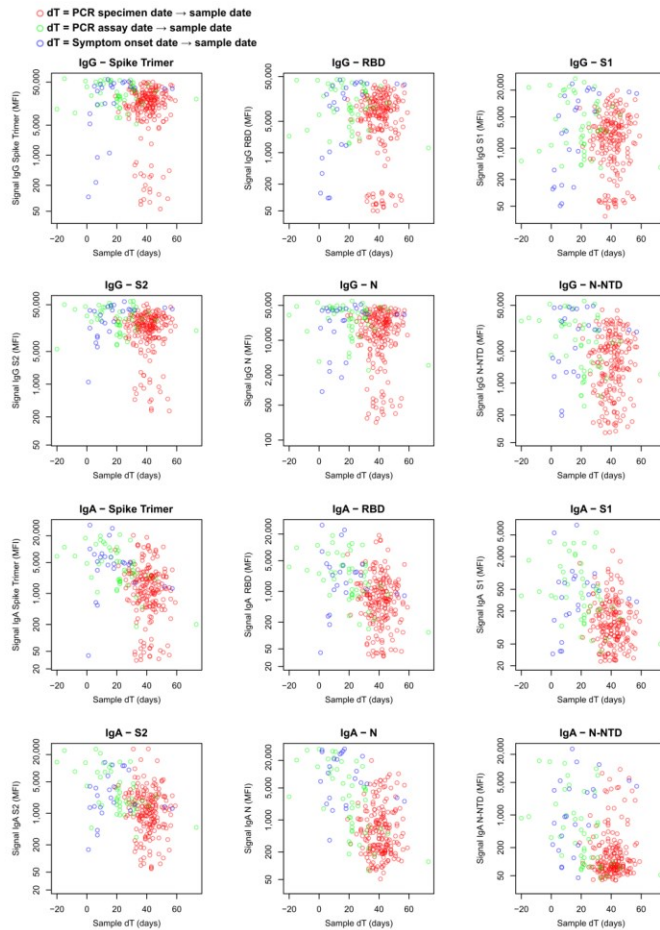
Supplementary Figure 5

Impact of sample time on antibody response is visualized by scatter plots. Sample dT in days is displayed against the observed MFI signal per antigen. Definition of dT is not consistent as samples measured in this study were taken from various sources. dT was calculated from the day of a positive PCR result (red circles), from the day of the PCR test itself (green circles) or from the day of symptom onset (blue circles). Source data are provided as a Source Data file.

8
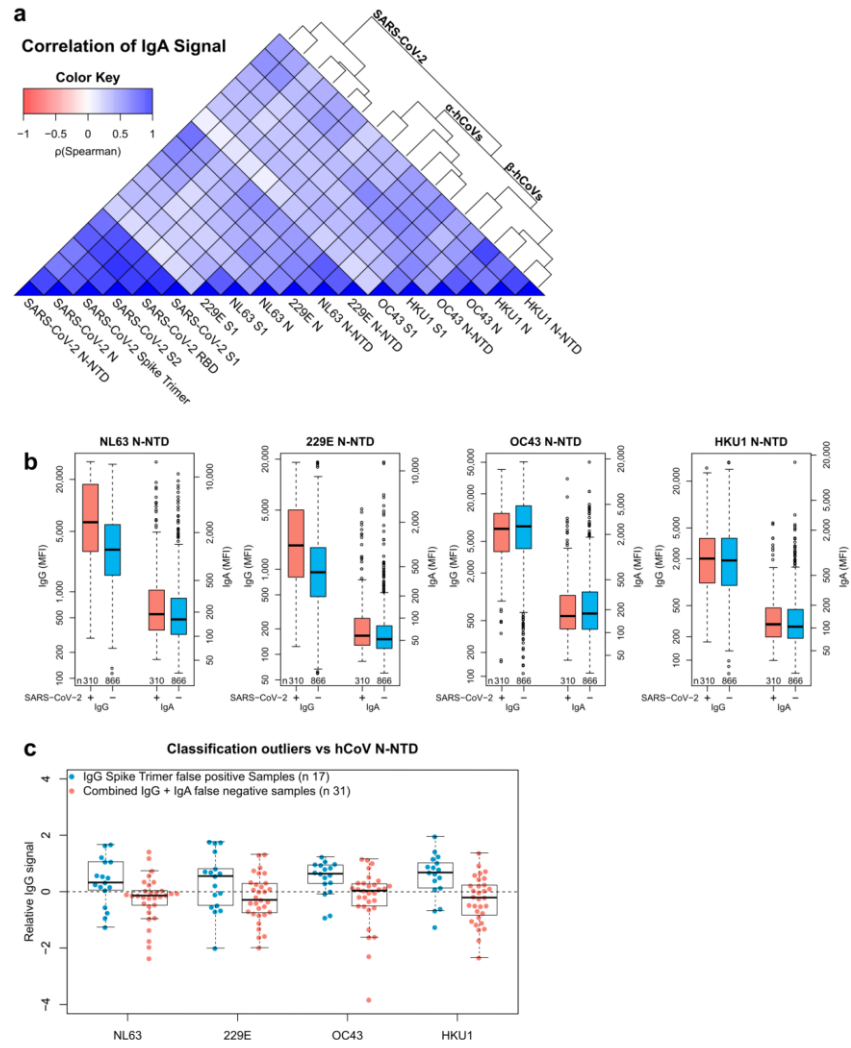
Supplementary Figure 6

a, Correlation of IgA response for the entire sample set (n=1176) is visualized as heatmap based on Spearman's ρ coefficient; dendrogram on the right side displays antigens after hierarchical clustering was performed. **b,** Immune response (IgG and IgA) towards hCoV N-NTD proteins are presented as Box-Whisker plots of sample MFI on a logarithmic scale for SARS-CoV-2-infected (red, n=310) and uninfected (blue, n=866) individuals. Box represents the median and the 25th and 75th percentiles, whiskers show the largest and smallest values. Outliers determined by 1.5 times IQR of log-transformed data are depicted as circles. **c,** Relative levels of IgG-specific immune response towards hCoV N-NTD proteins are presented as Box-Whisker plots / stripchart overlays of log-transformed and per-antigen scaled and centred MFI for the sample subsets of Spike Trimer false positives (blue, n=17) and combined IgG + IgA false negatives (red, n=31). Box represents the median and the 25th and 75th percentiles, whiskers show the largest and smallest values, excluding outliers as determined by 1.5 times IQR. Source data are provided as a Source Data file.

10
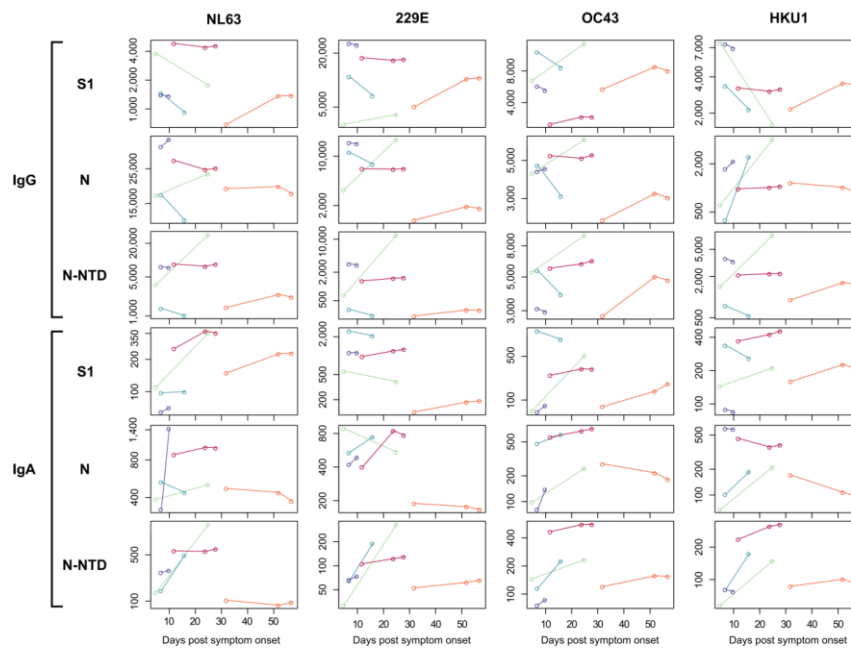
Supplementary Figure 7

Kinetic of hCoV antigen-specific IgA and IgG responses is shown for indicated days after symptom onset for the three used hCoV antigens across five different patients. Colored lines indicated kinetic of respective SARS-CoV-2 antigen per patient. Source data are provided as a Source Data file.

11

101

Supplementary Table 1 | Assay Variance and LOD

Intra- and inter-assay variance were determined by repeated measurement of QC samples and blank sample as replicates on one plate and in duplicates over 17 plates, respectively. Standard deviation relative to mean (%CV) is given for each antigen. A limit of detection (LOD) was calculated from 24 blank sample replicates on the same plate as the mean MFI + 3 times standard deviation.

			SARS-CoV-2						hCoV NL63			hCoV 229E			hCoV OC43			hCoV HKU1		
			Spike Trimer	RBD	S1	S2	N	N-NTD	S1	N	N-NTD	S1	N	N-NTD	S1	N	N-NTD	S1	N	N-NTD
Inter-assay variance (%CV) n = 34, duplicates, 17 plates	IgG	QC1	3.7	3.3	3.4	3.7	2.8	7.4	3.5	3.2	4.4	3.3	2.8	5.2	3.1	6.0	4.4	3.4	4.7	5.4
		QC2	4.1	4.6	6.9	3.4	5.3	4.8	3.0	2.2	6.3	2.4	2.1	6.7	2.7	4.5	2.3	2.7	5.1	2.8
		QC3	3.4	2.4	2.3	3.6	2.1	4.6	3.1	2.5	3.5	2.9	2.0	4.7	2.9	6.4	4.6	3.2	3.2	3.5
		Blank	5.4	5.6	6.7	6.4	5.6	6.1	6.3	7.1	5.7	9.1	6.1	6.1	5.6	7.3	4.1	4.9	6.1	8.3
	IgA	QC1	3.9	4.6	4.9	4.0	5.1	5.0	4.2	3.6	3.9	4.0	5.3	7.4	4.3	7.4	5.0	4.2	6.0	5.0
		QC2	4.6	5.0	5.1	3.9	3.9	4.2	3.7	2.4	7.6	2.9	2.2	6.0	4.1	16.4	4.2	4.3	5.5	3.9
		QC3	3.9	3.8	4.5	3.4	3.4	4.8	3.9	2.8	4.0	3.0	5.1	4.5	3.6	6.1	4.1	3.7	4.5	5.1
		Blank	6.7	5.3	8.2	6.3	5.3	5.3	3.3	5.0	5.0	6.7	7.0	6.1	5.3	7.1	4.7	6.0	6.8	6.3
Intra-assay variance (%CV) n = 24	IgG	QC1	2.5	1.9	2.0	2.1	1.8	2.1	2.4	1.7	2.8	2.0	2.7	3.2	1.9	2.0	2.2	2.7	2.4	2.2
		QC2	5.9	4.3	4.1	2.8	2.7	3.2	1.9	1.9	2.6	2.0	2.2	2.7	2.2	1.6	2.1	2.5	3.1	2.5
		QC3	1.6	4.3	5.1	1.9	1.9	4.5	4.2	1.7	3.2	3.3	4.1	5.7	3.2	3.1	5.5	5.6	6.0	8.4
		Blank	6.0	5.6	5.2	5.8	5.2	4.2	5.0	4.8	4.8	7.3	6.2	6.3	6.5	6.2	4.4	6.1	6.0	6.2
	IgA	QC1	2.5	3.3	5.2	3.8	3.7	4.2	3.2	2.3	2.2	2.0	4.8	4.7	2.9	4.7	3.4	3.3	4.5	4.3
		QC2	4.8	5.7	5.7	3.2	4.1	4.3	3.4	2.0	5.7	2.1	2.1	6.1	3.0	3.1	1.9	3.9	6.4	3.8
		QC3	3.1	4.7	5.5	3.0	4.1	4.4	3.7	2.7	3.7	2.7	5.4	5.8	2.6	4.1	3.1	2.4	4.5	4.3
		Blank	5.8	5.3	6.3	5.0	5.4	5.5	4.5	5.6	5.3	7.2	6.3	7.0	6.7	9.5	7.3	5.2	8.8	7.0
LOD (MFI) n = 24	IgG		32	26	23	29	38	33	29	28	26	65	35	24	33	30	33	37	33	25
	IgA		31	26	26	27	37	32	57	28	40	28	36	22	35	28	32	33	39	28

12

Supplementary Table 2 | Complete overview of study sample set divided into columns by age groups and sex.
Samples from SARS-CoV-2-infected donors are further split up by hospitalization status. Age and gender of patients from which multiple samples were available for time course analyses are indicated. SARS-CoV-2-uninfected samples are further divided into samples drawn during the pandemic, which was defined as all samples taken on 01.01.2020 or later, and pre-pandemic samples. 147 samples with previous hCoV infection were included in the SARS-CoV-2-uninfected group. Detailed diagnosis of hCoV subspecies is indicated where available. Other sample conditions for special groups of uninfected samples are listed. NA: Information was not available.

Age	≤39 (25.4 %)		40-59 (20.5 %)		≥60 (40.4 %)		NA (13.7 %)			Σ
n	299 (25.4 %)		241 (20.5 %)		475 (40.4 %)		161 (13.7 %)			1176
Sex	male	female	male	female	male	female	male	female	NA	
n	139 (11.8 %)	160 (13.6 %)	144 (12.2 %)	97 (8.2 %)	271 (23.0 %)	204 (17.3 %)	5 (0.4 %)	3 (0.3 %)	153 (13.0 %)	1176
SARS-CoV-2-infected (total)	60 (19.4 %)	51 (16.5 %)	71 (22.9 %)	63 (20.3 %)	42 (13.5 %)	17 (5.5 %)	3 (1.0 %)	3 (1.0 %)	0 (0.0 %)	310
Hospitalized (for COVID19)	6 (10.9 %)	2 (3.6 %)	14 (25.5 %)	6 (10.9 %)	23 (41.8 %)	4 (7.3 %)	0 (0.0 %)	0 (0.0 %)	0 (0.0 %)	55
Non-Hospitalized	52 (25.0 %)	43 (20.7 %)	49 (23.6 %)	43 (20.7 %)	13 (6.3 %)	8 (3.8 %)	0 (0.0 %)	0 (0.0 %)	0 (0.0 %)	208
Hospitalisation NA	2 (4.3 %)	6 (12.8 %)	8 (17.0 %)	14 (29.8 %)	6 (12.8 %)	5 (10.6 %)	3 (6.4 %)	3 (6.4 %)	0 (0.0 %)	47
Patients with time series	2 (40.0 %)	0 (0.0 %)	0 (0.0 %)	0 (0.0 %)	2 (40.0 %)	1 (20.0 %)	0 (0.0 %)	0 (0.0 %)	0 (0.0 %)	5
SARS-CoV-2-uninfected (total)	79 (9.1 %)	109 (12.6 %)	73 (8.4 %)	34 (3.9 %)	229 (26.4 %)	187 (21.6 %)	2 (0.2 %)	0 (0.0 %)	153 (17.7 %)	866
Sample during pandemic	10 (15.4 %)	10 (15.4 %)	12 (18.5 %)	14 (21.5 %)	7 (10.8 %)	5 (7.7 %)	1 (1.5 %)	0 (0.0 %)	6 (9.2 %)	65
Sample pre-pandemic	69 (8.6 %)	99 (12.4 %)	61 (7.6 %)	20 (2.5 %)	222 (27.7 %)	182 (22.7 %)	1 (0.1 %)	0 (0.0 %)	147 (18.4 %)	801
Previous hCoV Infection	19 (12.9 %)	18 (12.2 %)	45 (30.6 %)	20 (13.6 %)	29 (19.7 %)	16 (10.9 %)	0 (0.0 %)	0 (0.0 %)	0 (0.0 %)	147
confirmed NL63	2 (20.0 %)	0 (0.0 %)	3 (30.0 %)	1 (10.0 %)	2 (20.0 %)	2 (20.0 %)	0 (0.0 %)	0 (0.0 %)	0 (0.0 %)	10
confirmed 229	5 (25.0 %)	1 (5.0 %)	4 (20.0 %)	1 (5.0 %)	5 (25.0 %)	4 (20.0 %)	0 (0.0 %)	0 (0.0 %)	0 (0.0 %)	20
confirmed OC43	0 (0.0 %)	1 (3.7 %)	14 (51.9 %)	1 (3.7 %)	6 (22.2 %)	5 (18.5 %)	0 (0.0 %)	0 (0.0 %)	0 (0.0 %)	27
confirmed HKU1	3 (20 %)	1 (6.7 %)	4 (26.7 %)	2 (13.3 %)	5 (33.3 %)	0 (0.0 %)	0 (0.0 %)	0 (0.0 %)	0 (0.0 %)	15
unknown hCoV	9 (12 %)	15 (20.0 %)	20 (26.7 %)	15 (20.0 %)	11 (14.7 %)	5 (6.7 %)	0 (0.0 %)	0 (0.0 %)	0 (0.0 %)	75
Pregnant	0 (0.0 %)	9 (90.0 %)	0 (0.0 %)	1 (10.0 %)	0 (0.0 %)	0 (0.0 %)	0 (0.0 %)	0 (0.0 %)	0 (0.0 %)	10
RF/HAMA samples	0 (0.0 %)	0 (0.0 %)	0 (0.0 %)	0 (0.0 %)	0 (0.0 %)	0 (0.0 %)	0 (0.0 %)	0 (0.0 %)	6 (100 %)	6
PCT > 3 ng/mL	0 (0.0 %)	0 (0.0 %)	0 (0.0 %)	0 (0.0 %)	0 (0.0 %)	0 (0.0 %)	0 (0.0 %)	0 (0.0 %)	21 (100 %)	21
Neuroinflammatory disease	6 (40.0 %)	6 (40.0 %)	1 (6.7 %)	0 (0.0 %)	1 (6.7 %)	1 (6.7 %)	0 (0.0 %)	0 (0.0 %)	0 (0.0 %)	15

13

Supplementary Table 3 - Percentage Identity of sequence alignments of used hCoV and corresponding SARS-CoV-2.
Alignments were calculated using version 1.2.4. of Clustal Omega[3]. Sequences of constructs used in alignment are provided as a Source Data file.

Protein	Identifier	% of sequence identity of corresponding antigen				
		hCoV-NL63	hCoV-229E	SARS-CoV-2	hCoV-OC43	hCoV-HKU1
hCoV-NL63 S1	APF29071.1	100.0	50.2	17.8	19.7	18.1
hCoV-229E S1	APT69883.1	50.2	100.0	18.5	20.2	18.7
SARS-CoV-2 S1	QHD43416.1	17.8	18.5	100.0	24.2	24.2
hCoV-OC43 S1	AVR40344.1	19.7	20.2	24.2	100.0	58.0
hCoV-HKU1 S1	AGW27881.1	18.1	18.7	24.2	58.0	100.0
hCoV-NL63 N	YP_003771.1	100.0	47.5	30.9	29.0	29.7
hCoV-229E N	NP_073556.1	47.5	100.0	30.4	30.1	32.2
SARS-CoV-2 N	QHD43423.2	30.9	30.4	100.0	37.1	36.7
hCoV-OC43 N	YP_009555245.1	29.0	30.1	37.1	100.0	65.5
hCoV-HKU1 N	YP_173242.1	29.7	32.2	36.7	65.5	100.0
hCoV-NL63 N-NTD	YP_003771.1	100.0	63.4	35.3	34.4	35.8
hCoV-229E N-NTD	NP_073556.1	63.4	100.0	38.2	37.9	39.2
SARS-CoV-2 N-NTD	QHD43423.2	35.3	38.2	100.0	42.0	42.8
hCoV-OC43 N-NTD	YP_009555245.1	34.4	37.9	42.0	100.0	68.3
hCoV-HKU1 N-NTD	YP_173242.1	35.8	39.2	42.8	68.3	100.0

14

Supplementary Table 4 | Overview of primers used in this study with respective sequence.

Primer	Sequence
pRSET2b down-for	GGTAAGCTTGATCCGGCTGCTAA
SARS-CoV2_NTD-rev	GGGAAGCTTACTCAGCATAGAAGCCCTTTGG
OC43_NTD-rev	GGGAAGCTTATTCGATATAATAGCCCTGCGG
NL63_NTD-rev	GGGAAGCTTATTCAACAACGCTCAGTTCCG
229E_NTD-rev	GGGAAGCTTATTCAACAACGGTAACACCATTC
HKU1_NTD-rev	GGGAAGCTTATTCCACATAGTAGCCCTGAGGC
S1 CoV2-for	CTTCTGGCGTGTGACCGG
S1 CoV2-rev	GTTGCGGCGCCGCTTAGTGGTGGTGGTGGTGGGGGGCTGTTTGTCTGTGTCTG

15

Supplementary Table 5 | Overview of antigens used in this study.

Construct	Manufacturer	Sequence Identifier	Fragment	Mutations	Expression system	Tag	Tag position
SARS-CoV-2 Spike Trimer	In-house expressed	QHD43416.1	1-1213	[682]RRAR to A, K986P and V987P	Expi293	Thrombin cleavage-site/ T4 foldon/ His$_6$	C-terminus
SARS-CoV-2 RBD	In-house expressed	QHD43416.1	1-14 + 319-541		Expi293	His$_6$	C-terminus
SARS-CoV-2 S2	Sino Biological #40590-V08B	YP_009724390.1	686-1213		Baculovirus-Insect cells	His$_6$	C-terminus
SARS-CoV-2 S1	In-house expressed	QHD43416.1	1-681		Expi293	His$_6$	C-terminus
hCoV-OC43 S1	In-house expressed	AVR40344.1	1-760		Expi293	His$_6$	C-terminus
hCoV-NL63 S1	In-house expressed	APF29071.1	1-744		Expi293	His$_6$	C-terminus
hCoV-229E S1	In-house expressed	APT69883.1	1-561		Expi293	His$_6$	C-terminus
hCoV-HKU1 S1	In-house expressed	AGW27881.1	1-755		Expi293	His$_6$	C-terminus
SARS-CoV-2 N	Aalto Bioreagents #CK 6406-b	NA	full length		E. coli	His$_6$	C-terminus
SARS-CoV-2 N-NTD	In-house expressed	QHD43423.2	1-174		E.coli BL21	His$_6$	N-terminus
hCoV-OC43 N	In-house expressed	YP_009555245.1	1-448		E.coli BL21	His$_6$	N-terminus
hCoV-OC43 N-NTD	In-house expressed	YP_009555245.1	1-189		E.coli BL21	His$_6$	N-terminus
hCoV-NL63 N	In-house expressed	YP_003771.1	1-377		E.coli BL21	His$_6$	N-terminus
hCoV-NL63 N-NTD	In-house expressed	YP_003771.1	1-139		E.coli BL21	His$_6$	N-terminus
hCoV-229E N	In-house expressed	NP_073556.1	1-389		E.coli BL21	His$_6$	N-terminus
hCoV-229E N-NTD	In-house expressed	NP_073556.1	1-141		E.coli BL21	His$_6$	N-terminus
hCoV-HKU1 N	In-house expressed	YP_173242.1	1-441		E.coli BL21	His$_6$	N-terminus
hCoV-HKU1 N-NTD	In-house expressed	YP_173242.1	1-188		E.coli BL21	His$_6$	N-terminus

For commercial antigens, catalogue number is given and information is provided as available from the data sheets. NA: Information was not available.

16

Supplementary References

1   Fawcett, T. An introduction to ROC analysis. *Pattern recognition letters* **27**, 861-874 (2006).

2   Zou, K. H., O'Malley, A. J. & Mauri, L. Receiver-operating characteristic analysis for evaluating diagnostic tests and predictive models. *Circulation* **115**, 654-657 (2007).

3   Madeira, F. *et al.* The EMBL-EBI search and sequence analysis tools APIs in 2019. *Nucleic acids research* **47**, W636-W641 (2019).

17

Appendix II: Immune response to SARS-CoV-2 variants of concern in vaccinated individuals

Matthias Becker*, Alex Dulovic*, Daniel Junker, Natalia Ruetalo, Philipp D. Kaiser, Yudi T. Pinilla, Constanze Heinzel, Julia Haering, Bjoern Traenkle, Teresa R. Wagner, Mirjam Layer, Martin Mehrlaender, Valbona Mirakaj, Jana Held, Hannes Planatscher, Katja Schenke-Layland, Gérard Krause, Monika Strengert, Tamam Bakchoul, Karina Althaus, Rolf Fendel, Andrea Kreidenweiss, Michael Koeppen, Ulrich Rothbauer, Michael Schindler & Nicole Schneiderhan-Marra

* = Authors contributed equally

ARTICLE

Immune response to SARS-CoV-2 variants of concern in vaccinated individuals

Matthias Becker [1,14], Alex Dulovic [1,14], Daniel Junker[1], Natalia Ruetalo[2], Philipp D. Kaiser[1], Yudi T. Pinilla[3], Constanze Heinzel[3], Julia Haering[1], Bjoern Traenkle[1], Teresa R. Wagner [1,4], Mirjam Layer[2], Martin Mehrlaender[5], Valbona Mirakaj[5], Jana Held[3,6], Hannes Planatscher[7], Katja Schenke-Layland [1,8,9,10], Gérard Krause [11,12], Monika Strengert[11,12], Tamam Bakchoul [13], Karina Althaus[13], Rolf Fendel [3,6], Andrea Kreidenweiss [3,6], Michael Koeppen[5], Ulrich Rothbauer [1,4 ✉], Michael Schindler [2 ✉] & Nicole Schneiderhan-Marra [1 ✉]

SARS-CoV-2 is evolving with mutations in the receptor binding domain (RBD) being of particular concern. It is important to know how much cross-protection is offered between strains following vaccination or infection. Here, we obtain serum and saliva samples from groups of vaccinated (Pfizer BNT-162b2), infected and uninfected individuals and characterize the antibody response to RBD mutant strains. Vaccinated individuals have a robust humoral response after the second dose and have high IgG antibody titers in the saliva. Antibody responses however show considerable differences in binding to RBD mutants of emerging variants of concern and substantial reduction in RBD binding and neutralization is observed against a patient-isolated South African variant. Taken together our data reinforce the importance of the second dose of Pfizer BNT-162b2 to acquire high levels of neutralizing antibodies and high antibody titers in saliva suggest that vaccinated individuals may have reduced transmission potential. Substantially reduced neutralization for the South African variant further highlights the importance of surveillance strategies to detect new variants and targeting these in future vaccines.

[1] NMI Natural and Medical Sciences Institute at the University of Tübingen, Reutlingen, Germany. [2] Institute for Medical Virology and Epidemiology, University Hospital Tübingen, Tübingen, Germany. [3] Institute of Tropical Medicine, University of Tübingen, Tübingen, Germany. [4] Pharmaceutical Biotechnology, University of Tübingen, Tübingen, Germany. [5] Department of Anaesthesiology and Intensive Care Medicine, University Hospital Tübingen, Tübingen, Germany. [6] German Center for Infection Research (DZIF), partner site Tübingen, Tübingen, Germany. [7] Signatope GmbH, Reutlingen, Germany. [8] Cluster of Excellence iFIT (EXC2180) "Image-Guided and Functionally Instructed Tumor Therapies", University of Tübingen, Tübingen, Germany. [9] Department of Women's Health, Research Institute for Women's Health, University of Tübingen, Tübingen, Germany. [10] Department of Medicine/ Cardiology, Cardiovascular Research Laboratories, David Geffen School of Medicine at UCLA, Los Angeles, USA. [11] Helmholtz Centre for Infection Research, Braunschweig, Germany. [12] TWINCORE GmbH, Centre for Experimental and Clinical Infection Research, a joint venture of the Hannover Medical School and the Helmholtz Centre for Infection Research, Hannover, Germany. [13] Institute for Clinical and Experimental Transfusion Medicine, University Hospital Tübingen, Tübingen, Germany. [14] These authors contributed equally: Matthias Becker, Alex Dulovic. ✉email: Ulrich.rothbauer@nmi.de; Michael. Schindler@med.uni-tuebingen.de; Nicole.schneiderhan@nmi.de

111

ARTICLE

Since the initial outbreak in Wuhan, China in late 2019[1,2], SARS-CoV-2 has evolved into a global pandemic, with more than 138 million infections and nearly 3 million deaths (as per WHO, https://covid19.who.int/, accessed April 15, 2021), impacting severely on mental health[3,4] and global economics[5]. In response, the scientific community has made unprecedented progress, resulting in the generation of multiple vaccines, using a variety of different approaches[6–8], such as the Pfizer BNT-162b2 vaccine, which encodes a full-length trimerized spike protein[9]. In parallel, SARS-CoV-2 is continually evolving impacting its infectivity[10], transmission[11–13], and viral immune evasion[14,15]. To date, advanced genomic approaches have identified thousands of variants of SARS-CoV-2 with multiple RBD mutations circulating due to natural selection[16,17]. The variability of RBD epitopes is of specific concern as such mutations might reduce vaccine efficacy, increase viral transmission, or impair acquired immunity by neutralizing antibodies[10,18,19]. For the pandemic to be brought under control, herd immunity must be achieved through vaccination. However, there is a discourse about how long antibodies generated during the first wave persist, with some studies suggesting seroreversion between 2 and 3 months[20], while others find antibodies present for up to 7 or 8 months post infection[21–23]. Alarmingly, antibodies generated during the first wave also appear to have reduced immunoreactivity and neutralization potency toward emerging variants[22].

As the virus is known to continually mutate, particularly the emerging UK (B.1.1.7)[12], South African (B.1.351)[24], Brazil (P1)[25], Mink (Cluster 5)[26], and Southern California (hereon referred to as "LA" (B1.429)[27] variants are of concern. The UK variant has an increased risk of transmission[13] and mortality[13,28]. It further exhibits reduced neutralization susceptibility[29], which is most substantially related to a subset of RBD-specific monoclonal antibodies[14,29]. The N501Y mutation appears to mediate increased ACE2–RBD interaction[30] and is known to be critical for SARS-CoV-2 infection in vivo in mice[31]. Similarly, the South African variant, which is now spreading globally, has two escape mutations within the RBD (K417N and E484K)[24] in addition to the N501Y mutation. The combination of these three point mutations results in both a higher infection rate and reduced capacity of neutralizing antibodies produced against variants without RBD mutations of concern (hereon referred to as "wild-type")[32]. In light of these developments, and in spite of increasing data provided by vaccine companies, it remains unclear whether vaccines formulated against the original Wuhan strain of the virus will remain effective against new and emerging variants such as UK or South Africa. To understand this, we characterized the antibody response post vaccination with the Pfizer BNT-162b2 vaccine in both serum and saliva and then investigated the presence and efficacy of neutralizing antibodies against emerging variants of concern (UK, South Africa, Mink, and LA).

Results

To analyze the humoral response generated by vaccination, SARS-CoV-2 reactive antibody titers in serum samples from vaccinated, convalescent (hereon referred to as "infected"), and uninfected (hereon referred to as "negative") individuals were measured using MULTICOV-AB[33] (Fig. 1). Descriptions of all groups of donors can be found in Supplementary Table 1. Vaccinated individuals had not been previously infected with SARS-CoV-2 as demonstrated by the absence of anti-nucleocapsid IgG and IgA (Fig. 1a). As expected, there was a typical variation in antibody titers reflecting individual immune responses (Fig. 1a, b). When comparing between vaccine doses (Fig. 1c, d), all vaccinated subjects showed an enhanced antibody response with increasing time after the first dose and a further significant boost after the second dose.

This boosting effect was so pronounced that it reached the upper limit of detection for MULTICOV-AB, as confirmed by a dilution series (Supplementary Fig. 1).

To expand our understanding of the immune response of vaccinated individuals, we analyzed their saliva for IgA and IgG antibodies. The saliva of infected and negative individuals served as controls. Infected individuals had significantly higher levels of IgA than negative (P value = 0.0008) or vaccinated individuals (P value = 0.03), with no significant difference seen between vaccinated and negative individuals (P value = 0.23) (Fig. 2a). Conversely, the IgG response in the saliva of vaccinated individuals was significantly higher than either infected (P value <0.0001) or negative individuals (P value <0.0001) (Fig. 2b). These results were verified using a second antibody test measuring IgG in saliva (Supplementary Fig. 2). We also identified that vaccination with Pfizer BNT-162b2 does not appear to offer any cross-protection against other endemic coronaviruses (Supplementary Fig. 3), as seen by the absence of change in antibody titers following vaccination.

Having determined the humoral response induced by Pfizer BNT-162b2, we then examined how emerging RBD mutations present in different variants of concern impact antibody binding. For this, we included RBD mutants for the UK (501Y), South African (417N, 484K, and 510Y), Mink (453F), and LA (452R) variants in MULTICOV-AB. For the UK variant, nearly identical antibody response was observed for vaccinated and infected individuals compared with wild-type variant (Kendall's tau 0.965) (Fig. 3a). In contrast, a varied and reduced immune response was visible for the South African variant in both groups (Kendall's tau 0.844) (Fig. 3b). Both the Mink and LA variants had a similar response as the wild-type variant (Supplementary Fig. 4). Having seen that antibody-binding responses were reduced in the context of RBD mutants in the South African variant, we examined its neutralizing potential on samples from vaccinated individuals using a virus neutralization test (VNT)[34], employing a patient-derived South African variant of SARS-CoV-2. Despite the detectable variation, the VNT revealed substantially reduced neutralization for the South African variant for sera obtained from vaccinated and infected individuals (Fig. 4a). We further confirmed these findings using an ACE2 inhibition assay (Fig. 4b). Here, we additionally observed increased neutralization capacities for both wild-type (Fig. 4c) and the South African variant (Fig. 4d), in all samples derived from vaccinated individuals following the second dose, which was further confirmed by the NeutrobodyPlex[35] (Supplementary Fig. 5). Overall, our results showed individual differences in neutralization capacity for RBD mutations found in variants (Supplementary Fig. 6), with minimal to no change in neutralization for the UK, Mink, or LA variants. Conversely, neutralization capacity versus the South African variant was severely compromised.

Discussion

RBD mutants are particularly important to track and study due to the role of the RBD:ACE2 interaction site in virus transmission and neutralization[13,30] and their potentially increased infectivity[12] or lethality[28]. This tracking has led to the identification of several variants of concern, notably the UK[12], South African[24], Mink[26], and LA[27] variants. We initiated this study to reveal the vaccine-induced immune response and most importantly to shed light on the still controversial question of how efficiently antibodies can bind and neutralize SARS-CoV-2 variants of concern. The presence of large titers of IgG antibodies within the saliva of vaccinated individuals far exceeded those seen in convalescent individuals. This was both surprising and welcome as it could indicate that vaccination might confer a
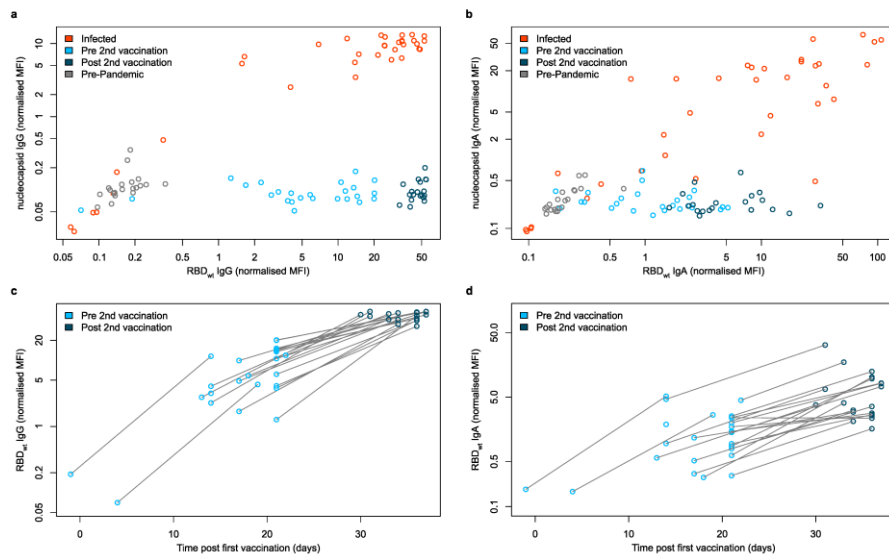
ARTICLE

Fig. 1 IgG and IgA response in serum samples of vaccinated, infected, and negative individuals. IgG (**a**, **c**) and IgA (**b**, **d**) response in sera from vaccinated (pre second vaccination (light blue, $n = 25$), post second vaccination (dark blue, $n = 20$)), infected (red) ($n = 35$), and negative (gray) ($n = 20$) individuals were measured with MULTICOV-AB. IgG (**a**) and IgA (**b**) response is shown as normalized RBD wild-type (wt) versus normalized nucleocapsid MFI values allowing for visualization of separation between the different groups. Increasing antibody titers in vaccinated individuals for IgG (**c**) and IgA (**d**) is shown with increasing days post vaccination, with samples colored based on whether they are before (light blue) or after (dark blue) the second dose. Lines indicate paired samples from the same donor. Source data are provided as a Source Data file.
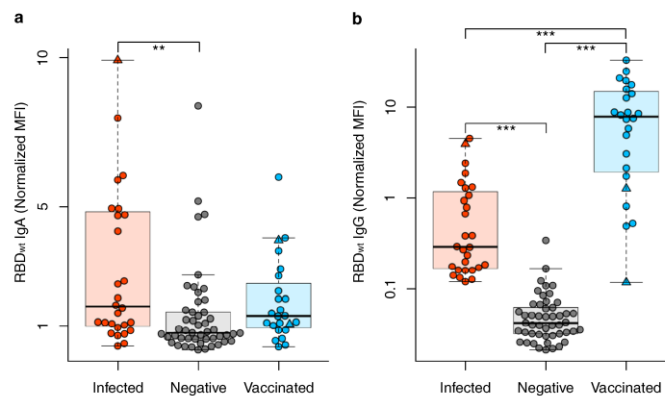

Fig. 2 IgA and IgG response in saliva samples of vaccinated, infected, and negative individuals. Box and whisker plots for the IgA (**a**) and IgG (**b**) response in the saliva of vaccinated (blue, $n = 22$), infected (red, $n = 26$), and negative (gray, $n = 45$) individuals. All samples were measured three times using MULTICOV-AB, normalized against QC values to remove confounding effects, and the mean calculated and displayed. Panel **b** is presented using a logarithmic scale for clarity. As additional controls, one infected and then vaccinated sample and two vaccinated samples from individuals not in contact with active COVID-19 infections are displayed as triangles. Boxes represent the median, 25th and 75th percentiles, whiskers show the largest and smallest non-outlier values. Outliers were determined by 1.5 times IQR. Statistical significance was calculated by Mann–Whitney U (two-sided) with significance determined as being < 0.01. **< 0.001; ***< 0.0001. Source data are provided as a Source Data file.
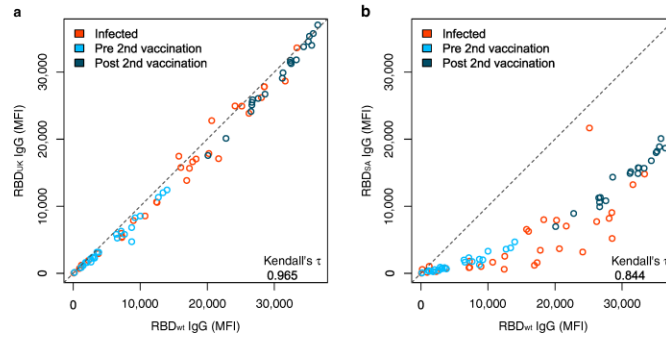
3

Fig. 3 South African RBD mutant has a reduced response compared to UK RBD mutant. UK (**a**) and South African (SA) RBD mutants (**b**) have differing effects upon antibody binding. RBD mutant antigens were generated and added to MULTICOV-AB to measure the immune response towards them in sera from vaccinated pre-second dose (light blue, $n = 25$), post second dose (dark blue, $n = 20$), and infected (red, $n = 35$) individuals, compared to the wild-type (wt) RBD. A linear curve ($y = x$) is shown as a dashed gray line to indicate an identical response between wild-type and mutant. Kendall's tau was calculated to measure the ordinal association between the mutant and wild-type. Source data are provided as a Source Data file.
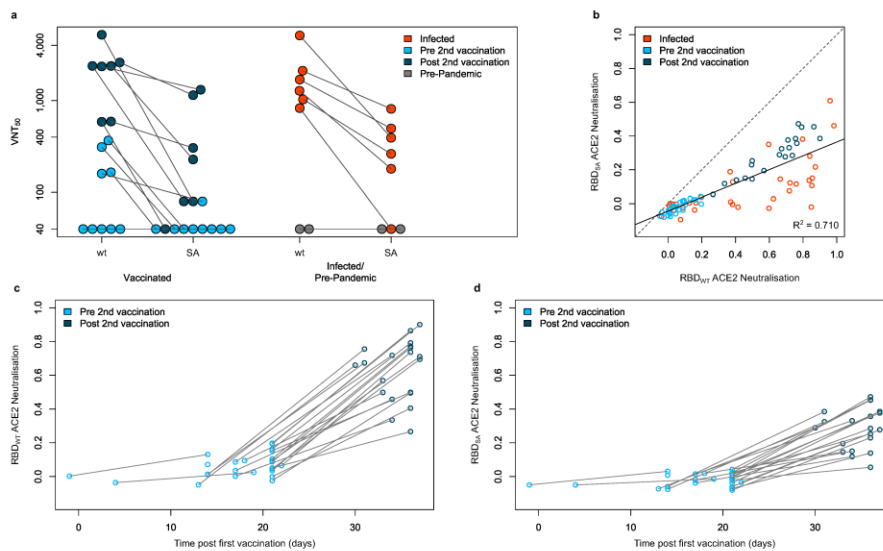

Fig. 4 South African RBD variant has decreased neutralization compared to wild-type in vaccinated and infected samples. Neutralization for the South African variant (SA) displayed as virus neutralizing titers (VNT_{50}) was measured in a virus neutralization assay compared to a wild-type variant (wt) (**a**) with sera from vaccinated (pre second vaccination (light blue, $n = 9$), post second vaccination (dark blue, $n = 7$), infected (red, $n = 6$), and negative (pre-pandemic) (gray, $n = 2$) individuals. To confirm the reduction in neutralization seen, an ACE2 competition assay was developed and used to measure neutralization capacity for wild-type RBD (wt) and the South African RBD mutant (SA) (**b**) on sera from vaccinated (pre second vaccination (light blue, $n = 25$), post second vaccination (dark blue, $n = 20$)), infected (red, $n = 35$) and negative (pre-pandemic, gray, $n = 20$) individuals. 0 indicates that no neutralization is present while 1 indicates maximum neutralization. A linear regression ($y = -0.044 + 0.408x$) for all samples is shown in gray with the R^2 included. When examining vaccinated samples only, wild-type neutralization (**c**) is significantly increased following the second vaccine dose. For South African neutralization (**d**), while it is increased following the second dose, there is a significant reduction when compared to wild-type. Lines in (**a**), (**c**), and (**d**) indicate paired samples from the same donor. Source data are provided as a Source Data file.

114

ARTICLE

sterilizing immune response in the oral cavity and thereby lower virus transmission. Focusing on antibody response, we examined in detail the effects of RBD mutations observed in emerging variants of concern. While only minor differences were detectable for the UK, Mink, and LA variants, a substantial reduction in RBD-binding antibodies was observed for the South African variant. These findings were confirmed at the functional level by a VNT using patient-derived viral isolates, showing a significant decrease in the neutralizing capacity of sera from vaccinated or infected individuals for the South African variant, in accordance with other recently published studies[36–39]. This could provide a reasonable explanation for infection in vaccinated or convalescent individuals with the South African variant and suggests a potential reduction in the efficacy of the Pfizer BNT-162b2 vaccine from a B-cell perspective.

This study is limited by the sample size, the restriction to only two time points after vaccination for data analysis, and the lack of paired saliva and serum samples for our infected and negative groups. However, we want to note that our sample size examined is similar to or larger than most other sample sets used to examine immune response to mutants in detail[40] and that we examined paired serum and saliva samples for all of our vaccinated subjects. Furthermore, we performed VNT assays comparing wild-type to the South African variant with authentic virus isolates on human cells, in contrast to utilizing a pseudotype neutralization assay[40] or genetically engineered wild-type variant[37]. Notably, we focused our study on a detailed characterization of the humoral immune response, as a proxy of an individual's immune response, as T-cell immunity has already been extensively studied[21,41]. Future work should investigate the antibody response and their persistence from different vaccines (i.e., AstraZeneca-Oxford, Moderna) against similar or newly emerging RBD mutants over a longer timeframe with increased sample size.

Viewed in a larger context, the impaired RBD-binding capacity to mutations in emerging variants of concern highlights the importance of updating current vaccines accordingly. Particular attention should be paid to the South African variant, because of the reduced neutralizing potency identified, while spontaneous independent enrichments of the E484K mutation have been observed in several countries[42].

Methods

Data reporting. No statistical analysis was used to determine the sample size. The experiments were not randomized, and the investigators were not blinded during either experimentation or data analysis.

Study recruitment, sample collection, and ethics statement. Serum and saliva samples were collected from healthcare workers, vaccinated with the Pfizer BNT-162b2 vaccine. Two serum samples were collected from each individual. The first collection took place on average 17 days following administration of the first dose, while the second collection took place on average 12 days following administration of the second dose. Saliva samples were collected 7–10 days following the second serum sampling. Infected serum and saliva samples were collected from different groups of individuals. Serum samples were collected from individuals hospitalized at Universität Klinikum Tübingen between March 25, 2020 and January 22, 2021. All individuals tested positive for SARS-CoV-2 by PCR. Saliva samples were collected from individuals who had previously been infected with SARS-CoV-2 between March 7, 2020 and June 19, 2020. All individuals had previously tested positive by PCR, or were confirmed as being previously infected by ELISA measurements plus the presence of at least one key symptom (i.e., coughing, fever). Negative serum and saliva samples were also from different groups of individuals. Negative serum samples were purchased from Central Biohub. All of these samples were collected pre-pandemic. Negative saliva samples were collected at the Institute of Tropical Medicine, Universität Tübingen from negative individuals and were confirmed to be anti-SARS-CoV-2 negative by serum ELISA. As additional controls, serum and saliva samples were collected from two individuals vaccinated with Pfizer BNT-162b2, who do not have contact with active SARS-CoV-2 infected patients, and one individual who had been previously infected with SARS-CoV-2 and was later vaccinated.

For serum collection, blood was taken by venipuncture, the serum extracted, and then frozen at −80 °C until use. For saliva collection, all individuals spat directly into a collecting tube. To inactive the samples, TnBP and Triton X-100 were added to final concentrations of 0.3% and 1×, respectively. Saliva samples were then frozen at −80 °C until further use.

This study was approved by the Ethics Committee of Eberhard Karls University Tübingen and the University Hospital Tübingen under the approval number 222/2020BO2 to Dr. Karina Althaus, Institute for Clinical and Experimental Transfusion Medicine, University Hospital Tübingen, and 312/2020BO1 (Coro-Buddy) to Dr. Andrea Kreidenweiss, Institute of Tropical Medicine, University Hospital Tübingen and Eberhard Karls University Tübingen. All participants gave written informed consent. Characteristics of vaccinated and infected serum donors can be found in Supplementary Table 1. Characteristics of vaccinated, infected, and negative saliva donors can be found in Supplementary Table 2.

Expression of RBD mutants. The pCAGGS plasmid encoding the receptor-binding domain (RBD) of SARS-CoV-2 was kindly provided by F. Krammer[43]. RBDs of SARS-CoV-2 variants of concern were generated by PCR amplification of fragments from wild-type DNA template followed by fusion PCRs to introduce described mutation N501Y for the UK variant and additional mutations K417N and E484K for the South African variant[28,44]. Forward primer RBDfor and reverse primer N501Yrev were used for amplification of fragment 1, forward primer N501Yfor and reverse primer RBDrev were used for amplification of fragment 2. Both fragments containing an overlap sequence at the 3' and 5' end were fused by an additional PCR using forward primer RBDfor and RBDrev. Based on cDNA for the UK variant, additional mutations of the South African Variant were introduced by PCR amplification of three fragments using forward primer RBD-for and reverse primer K417Nrev, forward primer K417Nfor and reverse primer E484Krev, forward primer E484Kfor and reverse primer RBDrev. Amplified fragments were assembled by subsequent fusion PCR using forward primer RBDfor and RBDrev. RBD mutation L452R as recently reported for the SARS-CoV-2 variant of concern identified in Southern California (referred to in this manuscript as "LA"), was introduced using primer RBD-for and reverse primer L452Rrev for amplification of fragment 1 and forward primer L452Rfor for fragment 2. Both fragments were subsequently fused using primers RBDfor and RBDrev. DNA coding for mutant RBDs (amino acids 319–541 of respective spike proteins) was cloned into Esp3I and EcoRI site of pCDNA3.4 expression vector with the N-terminal signal peptide (MGWTLVFLFLLSVTAGVHS) for the secretory pathway that comprises Esp3I site. All expression constructs were verified by sequence analysis. A full list of primers used in this study can be found in Supplementary Table 3. Confirmed constructs were expressed in Expi293 cells[33]. Briefly, cells were cultivated (37 °C, 125 rpm, 8% (v/v) CO_2) to a density of 5.5×10^6 cells/mL, diluted with Expi293F expression medium and transfection of the corresponding plasmids (1 μg/mL) with expifectamine as per the manufacturer's instructions. 20 h post transfection enhancers were added as per the manufacturer's instructions. Cell suspensions were then cultivated for 2–5 days (37 °C, 125 rpm, 8 % (v/v) CO_2) and then centrifuged (4 °C, 23,900×g, 20 min) to clarify the supernatant. Supernatants were then filtered with a 0.22-μm membrane (Millipore, Darmstadt, Germany) and supplemented with His-A buffer stock solution (20 mM Na_2HPO_4, 300 mM NaCl, 20 mM imidazole, pH 7.4). The solution was then applied to a HisTrap FF crude column on an Äkta pure system (GE Healthcare, Freiburg, Germany), extensively washed with His-A buffer, and eluted with an imidazole gradient (50–400 mM). Eluted proteins were dialyzed against PBS.

Bead coupling. Coupling of RBD mutant antigens was done by Anteo coupling (#A-LMPAKMM-10, Anteo Tech Reagents) following the manufacturer's instructions. Briefly, 100 μL of spectrally distinct populations of MagPlex beads (1.25×10^6) (Luminex) were activated in 100 μL of AnteoBind Activation Reagent for 1 h at room temperature. The activated beads were washed twice with 100 μL of Coupling Buffer using a magnetic separator. Following this, 50 μg/mL of antigen (diluted in Coupling buffer) was added to the beads and incubated for 1 h at room temperature. The beads were then washed twice with 100 μL Coupling buffer and blocked for 1 h at room temperature in 0.1% BSA in Coupling Buffer. After washing twice in storage buffer, the beads were stored at 4 °C until further use.

MULTICOV-AB. MULTICOV-AB[33], a multiplex immunoassay that simultaneously analyses 20 antigens was performed on all samples. In addition to the antigens presently included in MULTICOV-AB (Supplementary Table 4), RBD mutants from variants of concern were also included for measurements of all serum samples. All RBD mutants except the Mink variant (#40592-V08H80, Sino Biological) were produced in-house. Both IgG and IgA were measured for all serum samples. To adapt MULTICOV-AB to analyze antibodies in saliva, the dilution factor was changed from 1:400 for the serum to 1:12 for saliva. Samples were diluted into assay buffer (1:4 Low Cross Buffer (Candor Bioscience GmbH) in CBS (1× PBS + 1% BSA) + 0.05% Tween20) inside a sterile workbench. In total, 25 μL of diluted sample was then added to 25 μL of 1× Bead Mix[33] using a 96-well plate (#3600, Corning). Samples were incubated for 2 h at 20 °C, 750 rpm on a Thermomixer (Eppendorf), after which the unbound antibodies were removed by washing three times with Wash Buffer (1× PBS, 0.05% Tween20) using a

115

ARTICLE

microplate washer (Biotek 405TS, Biotek Instruments GmBH). Bound antibodies were detected using either 3 µg/mL RPE-huIgG (#109-116-098, Dianova) or 5 µg/mL RPE-huIgA (#109-115-011, Dianova) by incubation for 45 min at 20 °C, 750 rpm on a thermomixer. Following another washing step, beads were re-suspended in 100 µL of Wash Buffer and re-shaken for 3 mins at 20 °C, 1000 rpm. Plates were then measured using a FLEXMAP3D instrument (Luminex) using the following settings: 80 µL (no timeout), 50 events, Gate:7500–15000 and Report Gain:Standard PMT. Each sample was measured in three independent experiments. Three cut-off (CO) samples with a known MFI value were generated as in ref. [45] and included on each plate as a quality control. CO2 was used to generate the plate-by-plate CO value for the IgG Spike and wtRBD of SARS-CoV-2, with CO3 being used for the same purpose but for IgA. Raw median fluorescence intensity (MFI) values were divided by the mean MFI of CO2 (for IgG) or CO3 (for IgA), included on each plate to produce a normalization value. For serum measurements of the Spike and wtRBD of SARS-CoV-2, a normalized MFI value > 1 indicates positivity.

Saliva IgG ELISA. To validate saliva measurements by MULTICOV-AB, samples were re-measured using an in-house ELISA established by the Institute of Tropical Medicine, Universität Tübingen. Saliva samples were analyzed for SARS-CoV-2 wild-type RBD reactive IgG antibodies by an in-house ELISA developed at the Institute of Tropical Medicine, University of Tübingen. SARS-CoV-2 RBD recombinant protein was dissolved in PBS to a final concentration of 2 µg/mL. In all, 50 µL was then coated into 96-well Costar microtiter high binding plates (#3590, Corning) and blocked at 4 °C overnight with The Blocking Solution (Candor Bioscience GmbH), at room temperature on a microplate shaker set to 700 rpm. Before each of the following steps, wells were washed with PBS/0.1% Tween20. Saliva samples were diluted using The Blocking Solution (1:3–1:729) and 100 µL added to each well. Plates were then incubated at room temperature for 1 h. For detection, 1:20,000 biotinylated anti-human IgG (#109-065-008, Jackson Immuno Research Laboratories) and 1:20,000 Streptavidin-HRP (#109-035-098) were added and incubated for 1 h and 30 min, respectively. For visualization, TMB was added and the reaction was stopped using 1 M HCl. The plate was read at 450 nm and 620 nm using a microplate reader (CLARIOstar, BMG LABTECH, running Software Version 5.40 R2). To estimate the concentration of the IgG antibodies in the saliva, a dilution series of highly pure human IgG (#31154, ThermoFisher) was in parallel coated on the ELISA plates and quantified using the secondary antibodies. A four-parameter logistic curve using MARS Data Analysis Software Version 3.31 was fitted to the respective OD values and the antibody concentrations in the sample specimen calculated[46].

Neutralization assays. Viral neutralization assays[34] for the wild-type (Tü1) variant and the South African variant were performed on 16 vaccinated, 6 infected, and 2 negative serum samples. Briefly, Caco-2 cells were cultured at 37 °C with 5% CO2 in Dulbecco's modified Eagle medium (DMEM), supplemented with 10% fetal calf serum (FCS), 2 mM L-glutamine, 100 mg/mL penicillin–streptomycin, and 1% non-essential amino acids (NEAA). The clinical isolate (200325_Tü1)[34] which belongs to the lineage B.1.126 is referred to as "wild-type" in this manuscript. The South African variant (210211_SaV) was isolated from a throat swab collected in January 2021 at the Institute for Medical Virology and Epidemiology of Viral Diseases, University Hospital Tübingen, from a PCR-positive patient. In total, 100 µL of patient material was diluted in medium and used to freshly inoculate 150,000 Caco-2 cells in a six-well plate. At 48 h post infection, the supernatant was collected, centrifuged, and stored at −80 °C. After two consecutive passages, the supernatant was tested by qRT-PCR confirming the presence of three point mutations (N501Y, K417N, and E484K). NGS confirmed that the clinical isolate belongs to the lineage B.1.351. Sequence comparison of the Spike protein of 200325_Tü1 and 210211_SaV can be found as Supplementary Data 1. Caco-2 cell infection with 210211_SAv was detected by western blotting, using sera from a convalescent patient. The multiplicity of infection determination (MOI) was conducted by titration using serial dilutions of both virus stocks. The number of infectious virus particles per millimeter was calculated as (MOI x cell number)/(infection volume), where MOI = -ln (1 – infection rate). For neutralization experiments, 1 × 10^4 Caco-2 cells/well were seeded in 96-well plates the day before infection in a medium containing 5% FCS. Cells were co-incubated with SARS-CoV-2 clinical isolate 200325_Tü1 or SARS-CoV-2 clinical isolate 210211_SAv at an MOI of 0.7. Patient sera were added in serial twofold dilutions from 1:40 to 1:5120. At 48 h post infection, cells were fixed with 80% acetone for 5 min, washed with PBS, and blocked for 1 h at room temperature (RT) with 10% normal goat serum (NGS). Cells were incubated for 1 h at RT with 100 µL of serum from a hospitalized convalescent donor in a 1:10,000 dilution and washed three times with PBS. In total, 100 µL of goat anti-human Alexa594 (1:2000) in PBS was used as a secondary antibody for 1 h at RT. Cells were then washed three times with PBS and counterstained with 1:20,000 DAPI solution (2 mg/mL) for 10 min at RT. For quantification of infection rates, images were taken with the Cytation3 (BioTek) and DAPI-positive and Alexa594-positive cells were automatically counted by the Gen5 software (BioTek). Virus neutralizing titers (VNT50S) were calculated as the half-maximal inhibitory dose (ID50) using 4-parameter nonlinear regression (GraphPad Prism). An overview of the VNT assay and examples of cells treated with both variants from one vaccinated and one infected individual's serum can be found in Supplementary Fig. 7.

ACE2 competition assay. Biotinylated recombinant human ACE2 (#10108-H08H-B, Sino Biological) was diluted to a final concentration of 571.4 ng/mL in assay buffer (1:4 Low Cross Buffer (Candor Bioscience GmBH) in CBS (1× PBS + 1% BSA) + 0.05% Tween20) to create ACE2 buffer. Plasma samples were diluted 1:50 in assay buffer and then to a final concentration of 1:400 in ACE2 buffer under a sterile workbench, resulting in a final ACE2 concentration of 500 ng/mL in all samples. In all, 25 µL of diluted plasma samples were then added to 25 µL of 1× BeadMix[33] per well of a 96-well plate (#3642, Corning). In addition to the standard bead mix used in MULTICOV-AB, all bead coupled RBD mutants were included. As a control, 500 ng/mL ACE2 was also used. Samples were incubated at 21 °C, 750 rpm for 2 h on a thermomixer. Samples were then washed using a microplate washer with Wash Buffer (1× PBS + 0.05% Tween20). 30 µL of 2 µg/mL Streptavidin-PE (#SAPE-001, Moss) was added to each well and incubated for 45 min, 21 °C, 750 rpm in darkness on a thermomixer. Following incubation, samples were washed again and then resuspended in 100 µL of Wash Buffer, before being shaken again for 3 min at 1000 rpm. Samples were read individually on a FLEXMAP3D instrument under the following settings: 80 µL (no timeout), 50 events, Gate: 7500–15,000, Reporter Gain: Standard PMT. MFI values were then normalized against the control wells. All samples were measured in duplicates and the mean is reported.

Neutrobody Plex. For further validation of the neutralization response, all samples were analyzed using the NeutrobodyPlex[35] using a final Nanobody (NMI1267) concentration of 2 nM. Samples were diluted 1:25 into assay buffer (same as MULTICOV-AB) and then a further 1:8 in neutrobody buffer (MULTICOV-AB assay buffer + 4.56 nM nanobody). In total, 25 µL of diluted sample was then added to 25 µL of 1× MULTICOV-AB Bead Mix[33] using a 96-well plate (#3600, Corning). Samples were incubated for 2 h at 21 °C, 750 rpm on a thermomixer (Eppendorf), after which the unbound antibodies were removed by washing three times with Wash Buffer (1× PBS, 0.05% Tween20) using a microplate washer (Biotek 405TS, Biotek Instruments GmBH). Bound antibodies were detected using 3 µg/mL RPE-huIgG (#109-116-098, Dianova) by incubation for 45 mins at 21 °C, 750 rpm on a thermomixer. Following another washing step, beads were re-suspended in 100 µL of Wash Buffer and re-shaken for 3 min at 21 °C, 1000 rpm. Plates were then measured using a FLEXMAP3D instrument (Luminex) using the same settings as in MULTICOV-AB above. Samples were measured on the same plate with their respective MULTICOV-AB IgG measurement. In addition to MULTICOV-AB controls, for plate-to-plate qualification one control sample was processed on all plates.

Data analysis. Data analysis and figure generation were performed in RStudio (Version 1.2.5001), running R (version 3.6.1) with the additional packages "beeswarm" and "RcolorBrewer" for data depiction purposes only. The type of statistical analysis performed (when appropriate) is listed in the figure legends. Figures were generated in Rstudio and then edited for clarity in Inkscape (Inkscape 0.92.4). Mann–Whitney U test was used to determine the difference between signal distributions from different sample groups using the "wilcox.test" function from R's "stats" library. Kendall's τ coefficient was calculated in order to determine the ordinal association between the observed antibody responses towards RBD mutant and wild-type proteins using the "cor" function from R's "stats" library. Linear regression was performed to assess the reduction in ACE2 neutralization observed for RBD mutants compared to wild-type proteins using the "lm" function from R's "stats" library. Pre-processing of data such as matching sample metadata and collecting results from multiple assay runs was performed in Excel 2016. GraphPad Prism version 8.4.0 was used to process VNT data.

Data availability
Source data are provided with this paper.

Code availability
Custom analysis code in R and required input files have been deposited on GitHub: https://github.com/BeckerMatthias/Vaccination_VoC_Publication.

References
1. Zhou, P. et al. A pneumonia outbreak associated with a new coronavirus of probable bat origin. *Nature* **579**, 270–273 (2020).
2. Zhu, N. et al. A novel coronavirus from patients with pneumonia in China, 2019. *N. Engl. J. Med.* **382**, 727–733 (2020).

ARTICLE

3. Pan, K.-Y. et al. The mental health impact of the COVID-19 pandemic on people with and without depressive, anxiety, or obsessive-compulsive disorders: a longitudinal study of three Dutch case-control cohorts. *Lancet Psychiatry* **8**, 121–129 (2021).

4. Pierce, M. et al. Mental health before and during the COVID-19 pandemic: a longitudinal probability sample survey of the UK population. *Lancet Psychiatry* **7**, 883–892 (2020).

5. Mofijur, M. et al. Impact of COVID-19 on the social, economic, environmental and energy domains: lessons learnt from a global pandemic. *Sustain. Prod. Consum.* **26**, 343–359 (2021).

6. Baden, L. R. et al. Efficacy and safety of the mRNA-1273 SARS-CoV-2 Vaccine. *N. Engl. J. Med.* **384**, 403–416 (2021).

7. Voysey, M. et al. Safety and efficacy of the ChAdOx1 nCoV-19 vaccine (AZD1222) against SARS-CoV-2: an interim analysis of four randomised controlled trials in Brazil, South Africa, and the UK. *Lancet* **397**, 99–111 (2021).

8. Polack, F. P. et al. Safety and efficacy of the BNT162b2 mRNA Covid-19 vaccine. *N. Engl. J. Med.* **383**, 2603–2615 (2020).

9. Mulligan, M. J. et al. Phase I/II study of COVID-19 RNA vaccine BNT162b1 in adults. *Nature* **586**, 589–593 (2020).

10. Korber, B. et al. Tracking changes in SARS-CoV-2 spike: evidence that D614G increases infectivity of the COVID-19 virus. *Cell* **182**, 812–827.e819 (2020).

11. Volz, E. et al. Assessing transmissibility of SARS-CoV-2 lineage B.1.1.7 in England. *Nature* https://doi.org/10.1038/s41586-021-03470-x (2021).

12. Graham, M. S. et al. Changes in symptomatology, reinfection, and transmissibility associated with the SARS-CoV-2 variant B.1.1.7: an ecological study. *Lancet Public Health* https://doi.org/10.1016/S2468-2667(21)00055-4 (2021).

13. Davies, N. G. et al. Estimated transmissibility and impact of SARS-CoV-2 lineage B.1.1.7 in England. *Science* **372**, eabg3055 (2021).

14. Collier, D. A. et al. Sensitivity of SARS-CoV-2 B.1.1.7 to mRNA vaccine-elicited antibodies. *Nature* https://doi.org/10.1038/s41586-021-03412-7 (2021).

15. Kemp, S. A. et al. SARS-CoV-2 evolution during treatment of chronic infection. *Nature* **592**, 277–282 (2021).

16. Schrörs, B. et al. Large-scale analysis of SARS-CoV-2 spike-glycoprotein mutants demonstrates the need for continuous screening of virus isolates. Preprint at *bioRxiv* https://doi.org/10.1101/2021.02.04.429765 (2021).

17. Ou, J. et al. Emergence of SARS-CoV-2 spike RBD mutants that enhance viral infectivity through increased human ACE2 receptor binding affinity. Preprint at *bioRxiv* https://doi.org/10.1101/2020.03.15.991844 (2020).

18. Sun, C. et al. SARS-CoV-2 and SARS-CoV spike-RBD structure and receptor binding comparison and potential implications on neutralizing antibody and vaccine development. Preprint at *bioRxiv* https://doi.org/10.1101/2020.02.16.951723 (2020).

19. Cerutti, G. et al. Potent SARS-CoV-2 neutralizing antibodies directed against spike N-terminal domain target a single supersite. *Cell Host Microbe* https://doi.org/10.1016/j.chom.2021.03.005 (2021).

20. Ibarrondo, F. J. et al. Rapid decay of anti-SARS-CoV-2 antibodies in persons with mild Covid-19. *N. Engl. J. Med.* **383**, 1085–1087 (2020).

21. Dan, J. M. et al. Immunological memory to SARS-CoV-2 assessed for up to 8 months after infection. *Science* **371**, eabf4063 (2021).

22. Tea, F. et al. SARS-CoV-2 neutralizing antibodies; longevity, breadth, and evasion by emerging viral variants. Preprint at *medRxiv* https://doi.org/10.1101/2020.12.19.20248567 (2020).

23. Flehmig, B. et al. Persisting neutralizing activity to SARS-CoV-2 over months in sera of COVID-19 patients. *Viruses* **12**, https://doi.org/10.3390/v12121357 (2020).

24. Tegally, H. et al. Detection of a SARS-CoV-2 variant of concern in South Africa. *Nature* https://doi.org/10.1038/s41586-021-03402-9 (2021).

25. Sabino, E. C. et al. Resurgence of COVID-19 in Manaus, Brazil, despite high seroprevalence. *Lancet* **397**, 452–455 (2021).

26. Larsen, H. D. et al. Preliminary report of an outbreak of SARS-CoV-2 in mink and mink farmers associated with community spread, Denmark, June to November 2020. *Eurosurveillance* **26**, 2100009 (2021).

27. Zhang, W. et al. Emergence of a novel SARS-CoV-2 variant in Southern California. *J. Am. Med. Assoc.* https://doi.org/10.1001/jama.2021.1612 (2021).

28. Davies, N. G. et al. Increased mortality in community-tested cases of SARS-CoV-2 lineage B.1.1.7. *Nature* https://doi.org/10.1038/s41586-021-03426-1 (2021).

29. Shen, X. et al. SARS-CoV-2 variant B.1.1.7 is susceptible to neutralizing antibodies elicited by ancestral spike vaccines. *Cell Host Microbe* https://doi.org/10.1016/j.chom.2021.03.002 (2021).

30. Yan, R. et al. Structural basis for the recognition of SARS-CoV-2 by full-length human ACE2. *Science* **367**, 1444 (2020).

31. Gu, H. et al. Adaptation of SARS-CoV-2 in BALB/c mice for testing vaccine efficacy. *Science* **369**, 1603 (2020).

32. Planas, D. et al. Sensitivity of infectious SARS-CoV-2 B.1.1.7 and B.1.351 variants to neutralizing antibodies. *Nat. Med.* https://doi.org/10.1038/s41591-021-01318-5 (2021).

33. Becker, M. et al. Exploring beyond clinical routine SARS-CoV-2 serology using MultiCoV-Ab to evaluate endemic coronavirus cross-reactivity. *Nat. Commun.* **12**, 1152 (2021).

34. Ruetalo, N. et al. Antibody response against SARS-CoV-2 and seasonal coronaviruses in nonhospitalized COVID-19 patients. *mSphere* **6**, https://doi.org/10.1128/mSphere.01145-20 (2021).

35. Wagner, T. R. et al. NeutrobodyPlex—nanobodies to monitor a SARS-CoV-2 neutralizing immune response. *EMBO Rep.* **22**, e52325 https://doi.org/10.15252/embr.202052325 (2021).

36. Zhou, D. et al. Evidence of escape of SARS-CoV-2 variant B.1.351 from natural and vaccine-induced sera. *Cell* https://doi.org/10.1016/j.cell.2021.02.037.

37. Liu, Y. et al. Neutralizing activity of BNT162b2-elicited serum—preliminary report. *N. Engl. J. Med.* https://doi.org/10.1056/NEJMc2102017 (2021).

38. Wang, P. et al. Antibody resistance of SARS-CoV-2 variants B.1.351 and B.1.1.7. *Nature* https://doi.org/10.1038/s41586-021-03398-2 (2021).

39. Kuzmina, A. et al. SARS-CoV-2 spike variants exhibit differential infectivity and neutralization resistance to convalescent or post-vaccination sera. *Cell Host Microbe* https://doi.org/10.1016/j.chom.2021.03.008 (2021).

40. Wang, Z. et al. mRNA vaccine-elicited antibodies to SARS-CoV-2 and circulating variants. *Nature* https://doi.org/10.1038/s41586-021-03324-6 (2021).

41. Nelde, A. et al. SARS-CoV-2-derived peptides define heterologous and COVID-19-induced T cell recognition. *Nat. Immunol.* **22**, 74–85 (2021).

42. Rambaut, A. et al. A dynamic nomenclature proposal for SARS-CoV-2 lineages to assist genomic epidemiology. *Nat. Microbiol.* **5**, 1403–1407 (2020).

43. Amanat, F. et al. A serological assay to detect SARS-CoV-2 seroconversion in humans. *Nat. Med.* **26**, 1033–1036 (2020).

44. Lauring, A. S. & Hodcroft, E. B. Genetic variants of SARS-CoV-2—what do they mean? *J. Am. Med. Assoc.* **325**, 529–531 (2021).

45. Planatscher, H. et al. Systematic reference sample generation for multiplexed serological assays. *Sci. Rep.* **3**, 1–5 (2013).

46. Sulyok, Z. et al. Heterologous protection against malaria by a simple chemoattenuated PfSPZ vaccine regimen in a randomizedtrial. *Nat. Commun.* **12**, 2518, https://doi.org/10.1038/s41467-021-22740-w (2021).

Author contributions

U.R., M.K., M.B., A.D., and N.S.M. conceived the study. M.B., A.D., Ja.H., R.F., A.K., Mi.S., U.R., and N.S.M. designed the experiments. K.S.L., Mo.S., G.K., Mi.S., M.K., and N.S.M. procured funding. M.B., A.D., D.J., N.R., C.H., Ju.H., and M.L. performed experiments. Y.T.P., M.M., V.M., T.B., K.A., R.F., A.K., M.K., U.R., and N.S.M. collected samples or organized their collection. P.D.K., B.T., and T.W. produced the RBD mutants. H.P., M.B., and D.J. produced and analyzed the QC samples in MULTICOV-AB. M.B., A.D., N.R., and Mi.S. performed the data analysis. M.B., A.D., D.J., and N.S.M. generated the figures. A.D. wrote the first draft of the manuscript with input from M.B., D.J., Ja.H., K.S.L., Mo.S., R.F., A.K., Mi.S., U.R., and N.S.M. A.D., M.B., R.F., Mi.S., U.R., and N.S.M. revised the manuscript. All authors approved the final version of the manuscript.

117

ARTICLE

Additional information

Supplementary information The online version contains supplementary material available at https://doi.org/10.1038/s41467-021-23473-6.

Correspondence and requests for materials should be addressed to U.R., M.S. or N.S-M.

Peer review information *Nature Communications* thanks Fridtjof Lund-Johansen and the other, anonymous, reviewer(s) for their contribution to the peer review of this work. Peer reviewer reports are available.

Reprints and permission information is available at http://www.nature.com/reprints

Publisher's note Springer Nature remains neutral with regard to jurisdictional claims in published maps and institutional affiliations.

118

Supplementary Information – Immune response to SARS-CoV-2 variants of concern in vaccinated individuals

Matthias Becker[1#], Alex Dulovic[1#], Daniel Junker[1], Natalia Ruetalo[2], Philipp D. Kaiser[1], Yudi T. Pinilla[3], Constanze Heinzel[3], Julia Haering[1], Bjoern Traenkle[1], Teresa R. Wagner[1,4], Mirjam Layer[2], Martin Mehrlaender[5], Valbona Mirakaj[5], Jana Held[3,6], Hannes Planatscher[7], Katja Schenke-Layland[1,8,9,10], Gérard Krause[11,12], Monika Strengert[11,12], Tamam Bakchoul[13], Karina Althaus[13], Rolf Fendel[3,6], Andrea Kreidenweiss[3,6], Michael Koeppen[5], Ulrich Rothbauer[1,4*], Michael Schindler[2*], Nicole Schneiderhan-Marra[1*]

Author Affiliations

1 NMI Natural and Medical Sciences Institute at the University of Tübingen, Reutlingen, Germany

2 Institute for Medical Virology and Epidemiology, University Hospital Tübingen, Tübingen, Germany

3 Institute of Tropical Medicine, University of Tübingen, Germany

4 Pharmaceutical Biotechnology, University of Tübingen, Germany

5 Department of Anaesthesiology and Intensive Care Medicine, University Hospital Tübingen, Tübingen, Germany

6 German Center for Infection Research (DZIF), partner site Tübingen, Germany

7 Signatope GmbH, Reutlingen, Germany

8 Cluster of Excellence iFIT (EXC2180) "Image-Guided and Functionally Instructed Tumor Therapies", University of Tübingen, Tübingen, Germany

9 Department of Women's Health, Research Institute for Women's Health, University of Tübingen, Tübingen, Germany

10 Department of Medicine/Cardiology, Cardiovascular Research Laboratories, David Geffen School of Medicine at UCLA, Los Angeles, USA

11 Helmholtz Centre for Infection Research, Braunschweig, Germany

1

12 TWINCORE GmbH, Centre for Experimental and Clinical Infection Research, a joint venture of the Hannover Medical School and the Helmholtz Centre for Infection Research, Hannover, Germany

13 Institute for Clinical and Experimental Transfusion Medicine, University Hospital Tübingen, Tübingen, Germany

# these authors contributed equally to this work

* corresponding authors.

Contact Information

Nicole Schneiderhan-Marra – Phone number +49 (0)7121 51530 815. Email Address Nicole.schneiderhan@nmi.de Postal Address – Markwiesenstrasse 55, 72770 Reutlingen, Germany.

Michael Schindler – Phone number +49 (0)7071 2987459. Email Address Michael.Schindler@med.uni-tuebingen.de Postal Address – Elfriede-Aulhorn-Strasse 6, 72076 Tübingen, Germany

Ulrich Rothbauer – Phone number +49 (0)7121 51530 415. Email Address Ulrich.rothbauer@nmi.de Postal Address – Markwiesenstrasse 55, 72770 Reutlingen, Germany

Competing Interests

T.R.W., P.K., N.S.M. and U.R. are named as inventors on a patent application (EP 20 197 031.6) claiming the use of the described Nanobodies used in the NeutrobodyPlex for diagnosis and therapeutics filed by the Natural and Medical Sciences Institute. The other authors declare no competing interest.

2

Supplementary Table 1 – Characteristics of Vaccinated and Infected sera

Characteristic	Vaccinated	Infected
Number of donors	23	35
Median age (IQR) – years	42 (16)	59 (19)
Female sex (%)	5 (21.7)	10 (28.6)
1st sample collection – median ΔT post first vaccination (range)	21 days (-1 to 22 days)	Not applicable
2nd sample collection – median ΔT post second vaccination (range)	15 days (-7 to 16 days)	Not applicable
Median ΔT post positive PCR test (range)	Not applicable	14 days (2 – 85 days)

For both vaccinated and infected groups, the number of donors, median age in years (including inter-quartile range) and number of females are provided. For vaccinated groups, the median time post-first vaccination is provided for the first sample, and the median time post-second vaccination is provided for the second sample. The full range is included for both samples. A total of 45 samples from 23 vaccinated donors were included in this study. For one individual a second sample was not taken. One individual had their first sample collected before they received a vaccination and so they have a negative ΔT for the first sample. Similarly, two individuals had their second sample collected before they received their second vaccination and so they have a negative ΔT for the second sample. For the infected group, the median ΔT for time between positive PCR test and sample collection is given including the full range.

3

**Supplementary Table 2 – Characteristics of Vaccinated, Infected and Negative saliva
samples**

Characteristic	Vaccinated	Infected	Negative
Number of donors	22	27	49
Median age (IQR) – years	43 (16)	38 (25 – 58)	29 (25 – 38)
Female sex (%)	5 (22.7)	17 (63)	27 (55)

For all three groups, the total number of samples, median age in years (including inter-quartile
range) and number of females are provided. The vaccinated samples are from the same
sample group as the serum samples. Infected samples were confirmed by either PCR test or
ELISA (EuroImmun) plus the presence of at least one identifying COVID-19 symptom.
Negative samples were confirmed to be negative by ELISA (EuroImmun).

4

Supplementary Table 3 – Full list of primers used in this study

Primer Name	Sequence (5' to 3')
RBDfor	ATATCTAGAGCCACCATGTTCGTGTTTCTGG
N501Yrev	CCACGCCATATGTGGGCTGAAAGCCGTAG
N501Yfor	GGCTTTCAGCCCACATATGGCGTGGGCTATCAGC
RBDrev	AAGATCTGCTAGCTCGAGTCGC
K417Nrev	GTTGTAGTCGGCGATGTTGCCTGTCTGTCCAGGG
K417Nfor	GACAGACAGGCAACATCGCCGACTACAACTACAAGC
E484Krev	GCAGTTGAAGCCTTTCACGCCGTTACAAGGGGT
E484Kfor	GTAACGGCGTGAAAGGCTTCAACTGCTACTTCCC
L452Rrev	CGGTACCGGTAATTGTAGTTGCCGCCG
L452Rfor	GGCAACTACAATTACCGGTACCGGCTGTTCCGGAAG

Full List of primers used in this study for the production of RBD Mutants

5

123

Supplementary Table 4 – Antigens included in MULTICOV-AB

Disease	Antigen	Manufacturer	Category number
SARS-CoV-2	Spike Trimer	NMI	-
SARS-CoV-2	RBD	NMI	-
SARS-CoV-2	S1 domain	NMI	-
SARS-CoV-2	S2 domain	Sino	40590
SARS-CoV-2	Nucleocapsid	Aalto	6404-b
SARS-CoV-2	Nucleocapsid N-terminal domain	NMI	-
hCoV-OC43	Spike	Sino	40607-V08B
hCoV-OC43	S1 domain	NMI	-
hCoV-OC43	Nucleocapsid	NMI	-
hCoV-OC43	Nucleocapsid N-terminal domain	NMI	-
hCoV-HKU1	S1 domain	NMI	-
hCoV-HKU1	Nucleocapsid	NMI	-
hCoV-HKU1	Nucleocapsid N-terminal domain	NMI	-
hCoV-NL63	Spike Trimer	NMI	-
hCoV-NL63	S1 domain	NMI	-
hCoV-NL63	Nucleocapsid	NMI	-
hCoV-NL63	Nucleocapsid N-terminal domain	NMI	-
hCoV-229E	S1 domain	NMI	-
hCoV-229E	Nucleocapsid	NMI	-
hCoV-229E	Nucleocapsid N-terminal domain	NMI	-

Full list of antigens included as standard in MULTICOV-AB (minus controls), their manufacturer, and if available, their category number. Full details on all NMI produced antigens can be found in [1].

6

124

Supplementary Figure 1 – High serum antibody titers after the second vaccination dose
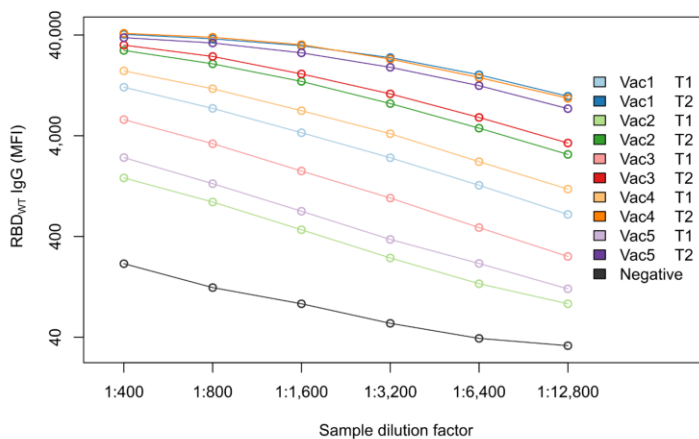
The second vaccination appears to plateau the serum antibody response at the Upper Limit of Detection for MULTICOV-AB. To confirm this, 11 samples consisting of 10 paired samples from five vaccinated individuals (shown in paired colours) and one negative individual (shown in black) were examined in a dilution series. Due to the wide range of samples, a log curve is used for the y axis. The three sera with the highest response maintained a similarly high response for the initial dilution, indicating a plateau in the range of >40,000 MFI, therefore suggesting that even for donors with high responses in the first sample, the second vaccination strongly increased the antibody response. A uniform curve shape for all samples (including the negative control) confirmed reliability of the generated data. Source data are provided as a Source Data file.

7

Supplementary Figure 2 – RBD reactive IgG detected by ELISA.
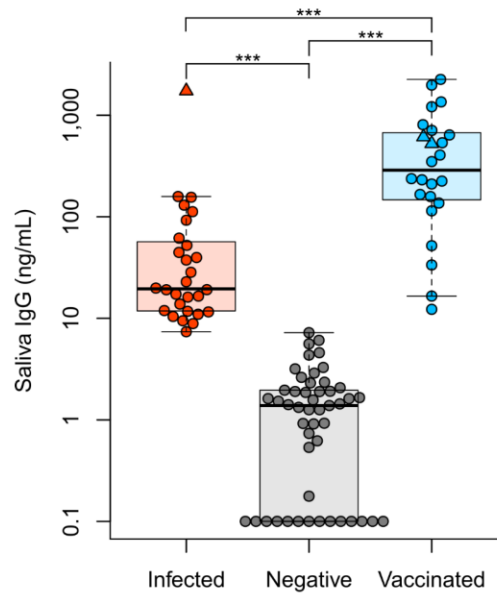
To confirm results for MULTICOV-AB, anti-RBD IgG antibodies in saliva were measured by an in-house ELISA. As in Fig 2, saliva IgG response was highest in vaccinated individuals. Results for vaccinated (blue, n=22), infected (red, n=26) and negative (grey, n=45) individuals are displayed as a Box and whisker plot. Two vaccinated sera samples from individuals not in contact with active SARS-CoV-2 infected individuals and one sera sample from an individual who was previously infected with SARS-CoV-2 and then later vaccinated are included as triangles. Boxes represent the median, 25th and 75th percentiles, whiskers show the largest and smallest non-outlier values. Outliers were determined by 1.5 times IQR. Negative samples that measured 0 were raised to 0.1 for display purposes only. For statistical analysis, their true value was used. Mann-Whitney U (two-sided) was used to determine statistical significance between the groups. *** indicates p-values lower than 0.0001. Source data are provided as a Source Data file.

8

Supplementary Figure 3 – Cross-reactivity of antibodies to endemic coronaviruses in vaccinated individuals
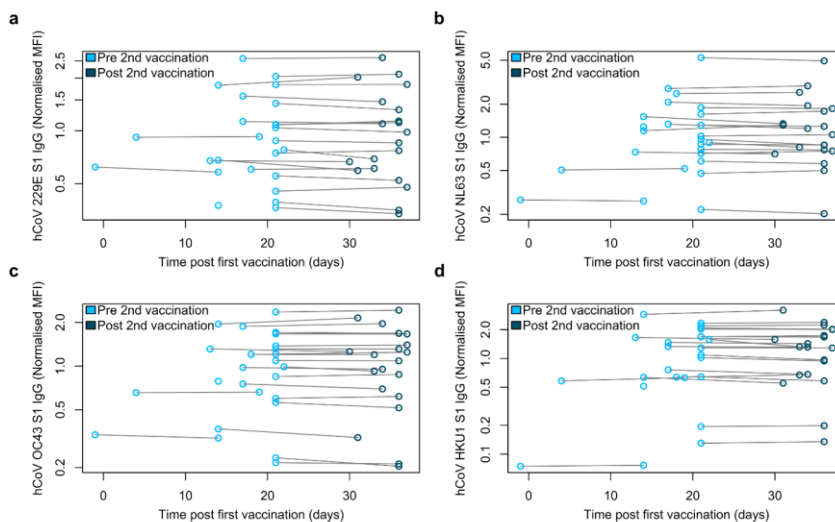
Vaccinated individuals did not have an increased antibody response towards S1 proteins of the endemic coronaviruses 229E (**a**), NL63 (**b**), OC43 (**c**) and HKU1 (**d**). All samples were measured using MULTICOV-AB. Light blue (n=25) indicates samples are pre second vaccination, while dark blue (n=20) indicates samples are post second vaccination. Lines indicated paired samples from the same donor. Source data are provided as a Source Data file.

9

Supplementary Figure 4 – RBD mutants for the LA and Mink variants have similar antibody binding compared to the wild-type variant.
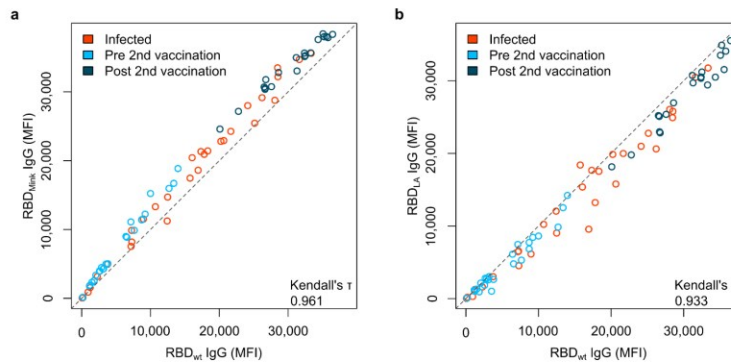
When compared to wild-type (wt), RBD mutants for both the Mink (**a**) and LA (**b**) variants of concern resulted in similar response. RBD mutant antigens were generated (LA) or purchased (Mink) and added to MULTICOV-AB to measure the immune response towards them from vaccinated (blue, n=45) and infected (red, n=35) sera, compared to the wild-type RBD. A linear curve (y=x) is shown as a dashed grey-line to indicate identical response between wild-type and mutant. Kendall's tau was calculated to measure ordinal association between the mutant and wild-type. Source data are provided as a Source Data file.

10

Supplementary Figure 5 – NeutrobodyPlex confirms reduced neutralization potential of vaccinated and infected sera for the wild-type variant
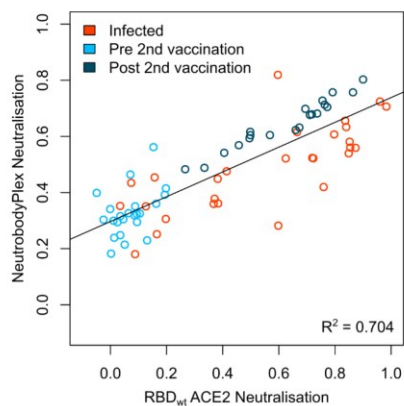
To further validate the results of the VNT and ACE2 competition assay, NeutrobodyPlex was used to examine neutralization potential of sera from vaccinated (pre-second dose (light blue, n=23), post-second dose (dark blue, n=20)) and infected individuals (red, n=28) for wild-type (wt) RBD. The correlation between NeutrobodyPlex and ACE2 competition assay results is shown. A linear regression (y=x) was calculated with the R^2 value shown. Source data are provided as a Source Data file.

11

Supplementary Figure 6 – Neutralization as measured by ACE2 inhibition assay for the UK, Mink and LA RBD mutants compared to wild-type RBD
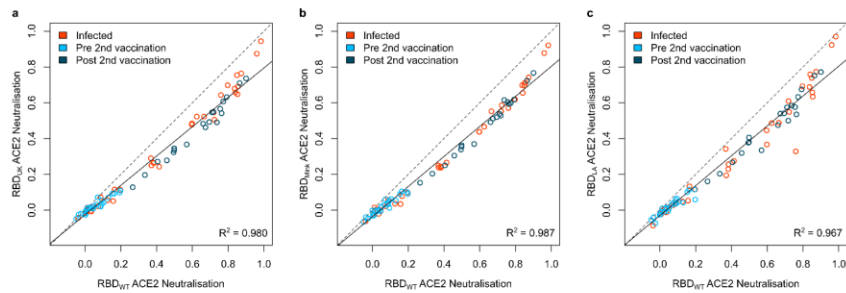
To determine the effect variants of concern had upon neutralization potential, an ACE2 competition assay was developed. RBD mutants for all variants of concern included within this manuscript (UK (**a**), Mink (**b**), LA (**c**)) were examined as well as the wild-type (wt) variant on sera from infected (red, n=35) and vaccinated (pre second vaccination (light blue, n=25), post second vaccination (dark blue, n=20)) individuals. Linear regression (y=x) was calculated for each panel, with the R^2 value shown. Linear regressions had the following equations for the different figure panels: (**a**) y = -0.026 + 0.820x (**b**) y = -0.036 + 0.840x (**c**) y = -0.03 + 0.835x. Source data are provided as a Source Data file.

12

Supplementary Figure 7 – Overview of VNT
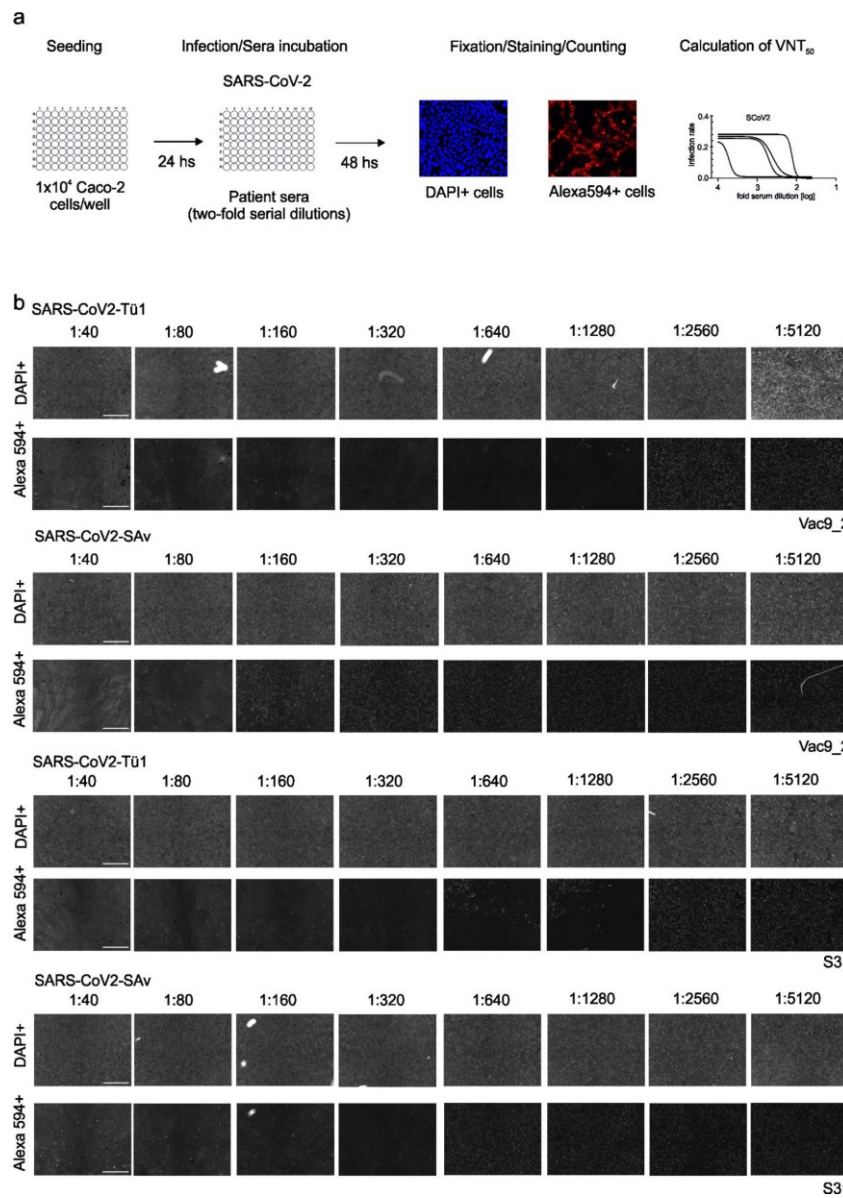
Simple overview of the VNT protocol (**a**) with examples (**b**) for cells treated with the wild-type (SARS-CoV-2-Tü1) and South African (SARS-CoV-2-SAv) for sera from one vaccinated (Vac9_2) and one infected (S31) individual. A dilution series (1:40 – 1:5120) is shown with the corresponding images for DAPI-positive and Alexa 594-positive cells. Scale bar = 1000 μm.

14

133

References

1   Becker, M. *et al.* Exploring beyond clinical routine SARS-CoV-2 serology using MultiCoV-Ab to evaluate endemic coronavirus cross-reactivity. *Nature Communications* **12**, 1152, doi:10.1038/s41467-021-20973-3 (2021).

15

Appendix III: Robust and durable serological response following pediatric SARS-CoV-2 infection

Hanna Renk*, Alex Dulovic*, Alina Seidel*, **Matthias Becker**, Dorit Fabricius, Maria Zernickel, Daniel Junker, Rüdiger Groß, Janis Müller, Alexander Hilger, Sebastian F. N. Bode, Linus Fritsch, Pauline Frieh, Anneke Haddad, Tessa Görne, Jonathan Remppis, Tina Ganzemueller, Andrea Dietz, Daniela Huzly, Hartmut Hengel, Klaus Kaier, Susanne Weber, Eva-Maria Jacobsen, Philipp D. Kaiser, Bjoern Traenkle, Ulrich Rothbauer, Maximilian Stich, Burkhard Tönshoff, Georg F. Hoffmann, Barbara Müller, Carolin Ludwig, Bernd Jahrsdörfer, Hubert Schrezenmeier, Andreas Peter, Sebastian Hörber, Thomas Iftner, Jan Münch, Thomas Stamminger, Hans-Jürgen Groß, Martin Wolkewitz, Corinna Engel, Weimin Liu, Marta Rizzi, Beatrice H. Hahn, Philipp Henneke, Axel R. Franz, Klaus-Michael Debatin, Nicole Schneiderhan-Marra, Ales Janda & Roland Elling

* = Authors contributed equally

Robust and durable serological response following pediatric SARS-CoV-2 infection

Hanna Renk [1,21], Alex Dulovic [2,21], Alina Seidel[3,21], Matthias Becker [2], Dorit Fabricius[4], Maria Zernickel[4], Daniel Junker[2], Rüdiger Groß [3], Janis Müller [3], Alexander Hilger[5], Sebastian F. N. Bode [4], Linus Fritsch [5], Pauline Frieh[5], Anneke Haddad [5], Tessa Görne[5], Jonathan Remppis[1], Tina Ganzemueller[6], Andrea Dietz [7], Daniela Huzly[8], Hartmut Hengel[8], Klaus Kaier[9], Susanne Weber[9], Eva-Maria Jacobsen[4], Philipp D. Kaiser[2], Bjoern Traenkle[2], Ulrich Rothbauer [2], Maximilian Stich [10], Burkhard Tönshoff[10], Georg F. Hoffmann[10], Barbara Müller[11], Carolin Ludwig[12,13,14], Bernd Jahrsdörfer[12,13,14], Hubert Schrezenmeier[12,13,14], Andreas Peter[15], Sebastian Hörber [15], Thomas Iftner[6], Jan Münch [3], Thomas Stamminger[7], Hans-Jürgen Groß[16], Martin Wolkewitz[9], Corinna Engel[1,17], Weimin Liu[18], Marta Rizzi[19], Beatrice H. Hahn [18], Philipp Henneke [5,20], Axel R. Franz [1,17], Klaus-Michael Debatin[4], Nicole Schneiderhan-Marra [2], Ales Janda[4,22] & Roland Elling [5,20,22✉]

The quality and persistence of children's humoral immune response following SARS-CoV-2 infection remains largely unknown but will be crucial to guide pediatric SARS-CoV-2 vaccination programs. Here, we examine 548 children and 717 adults within 328 households with at least one member with a previous laboratory-confirmed SARS-CoV-2 infection. We assess serological response at 3–4 months and 11–12 months after infection using a bead-based multiplex immunoassay for 23 human coronavirus antigens including SARS-CoV-2 and its Variants of Concern (VOC) and endemic human coronaviruses (HCoVs), and additionally by three commercial SARS-CoV-2 antibody assays. Neutralization against wild type SARS-CoV-2 and the Delta VOC are analysed in a pseudotyped virus assay. Children, compared to adults, are five times more likely to be asymptomatic, and have higher specific antibody levels which persist longer (96.2% versus 82.9% still seropositive 11–12 months post infection). Of note, symptomatic and asymptomatic infections induce similar humoral responses in all age groups. SARS-CoV-2 infection occurs independent of HCoV serostatus. Neutralization responses of children and adults are similar, although neutralization is reduced for both against the Delta VOC. Overall, the long-term humoral immune response to SARS-CoV-2 infection in children is of longer duration than in adults even after asymptomatic infection.

A full list of author affiliations appears at the end of the paper.

137

ARTICLE

To date, our knowledge of children's immune response to infection with severe acute respiratory syndrome coronavirus type 2 (SARS-CoV-2) remains incomplete. In light of current debates on vaccination strategies and non-pharmaceutical preventative measures (e.g. school closures), a comprehensive understanding of protective immunity after natural infection in children is required. As with other viral infections, immune control of SARS-CoV-2 is achieved through a concerted interplay of humoral and cellular immunity[1]. Neutralizing antibodies in children are of particular interest in this context, given their role in blocking virus entry into cells by inhibiting the interaction between the viral receptor binding domain (RBD) within the S-glycoprotein and the angiotensin-converting enzyme 2 (ACE2) receptor[2].

Previous longitudinal studies of the humoral response have found that neutralizing antibodies peak within 3–5 weeks post-infection with a calculated half-life of up to 8 months, suggesting long-term protection in convalescent individuals[1,3–5]. However, most studies only included adults, and longitudinal studies on SARS-CoV-2 infections in children had limited sample size and duration of follow-up post-infection[6–15]. Furthermore, it remains unclear as to whether any form of cross-protection is offered by endemic human coronaviruses (HCoVs) that regularly circulate in the pediatric population, with some studies identifying cross-protection and others not[16,17].

To provide an in-depth characterization of the humoral response in children, we initiated a multi-center longitudinal study, encompassing 328 households each with at least one SARS-CoV-2-infected member, which were followed for up to 12 months after the first infection in each household. This cohort is unique as the subjects exhibited mainly asymptomatic or mild disease with uninfected family members serving as environmental and age-matched controls. We performed an extensive serological evaluation of SARS-CoV-2 infection in all household members, comprising analyses of production of antibodies against various SARS-CoV-2 antigens, including Variants of Concern (VOCs), production of neutralizing antibodies and the role of HCoVs.

Results

A total of 548 children and 717 adults from 328 households were examined at T1 and 279 households including 402 children and 569 adults were followed to T2 (see Methods and Appendix for full details, Table 1 for a description of the study population, Fig. S2 in the Supplementary Appendix for details on the age structure of the study population). Children were substantially less often seropositive (33.0% at T1, 37.3% at T2) than adults (57.7% at T1, 49.4% at T2) (Table 1). Seropositive participants were almost exclusively mildly or asymptomatically infected. In seropositive individuals, asymptomatic infections were five times more common in children (44.8% T1, 46.0% T2) than in adults (8.7% T1, 11.0% T2) (Table 1), with the proportion of asymptomatic infections decreasing with increasing age (Fig. S3). Overall, hospitalization was rare (3·6% of adults, 0% of children, Table 1). The performance of the four serological assays for children and adults at T1 and T2 is shown in Table S1 and Fig. S4.

The detailed humoral immune response against different SARS-CoV-2 antigens, assessed by MULTICOV-AB is shown in Fig. 1. Children had significantly higher antibody titers against spike ($p < 0.001$), RBD ($p < 0.001$), S1 domain ($p < 0.001$) and nucleocapsid ($p = 0.01$) compared to adults at T1. This increased response was confirmed by the three commercial assays (Fig. S5). In addition, we observed a large difference in seroreversion, with only 3.8% of children, but 17.1% of adults seroreverting between T1 and T2 (Table 1). Seroreversion was not associated with the

response to particular antigens, although the largest and smallest decay in antibody concentrations were observed for antibodies against the S2 domain and nucleocapsid, respectively, regardless of age (Fig. S6).

For both children and adults, there was no significant difference in antibody response between symptomatic and asymptomatic infections (Figs. 2a, b, S7). The frequency of reported symptoms differed between adults and children and the predictive value of each symptom varied between both groups (Fig. 2c, d). While any of the symptoms fever, cough, diarrhea or dysgeusia proved to be a good indicator of infection in adults, dysgeusia was by far the best predictive symptom in children (87.50% of children with dysgeusia were seropositive; 95% CI 71.4–95.2%, 30.5% of children without dysgeusia were seropositive for SARS-CoV-2, 95% CI 29.7–31.3% Fig. 2d). Conversely, cough was a poor predictor of SARS-CoV-2 infection in children (37.4% of children with a cough were seropositive; 95% CI 29.3–46.3%, 33.0% of children without a cough were seropositive; 95% CI 31.0–35.2%, Fig. 2d). Further examination of predictive symptoms among children showed that in contrast to dysgeusia, cough only gained predictive value in children above the age of 12 and the predictive value of fever increased with age (Table S2). There was no difference in the humoral response associated with the presence of particular symptoms in either adults or children (Fig. S8).

To further explore differences in the antibodies produced by children and adults, we analyzed their neutralization potential as well as their binding towards VOCs. The neutralizing potential of a subset of children's sera exceeded that of a subset of adults' at T1 ($p < 0.001$) and T2 ($p = 0.02$) (Fig. 3a). However, this could be attributed to antibody titers, as neutralization in children correlated with the S1-directed antibody response (Spearman's rank 0.86, Fig. 3b). There was no difference in antibody binding responses to the RBD of Alpha and Beta VOCs between adults and children, with an identical binding for the Alpha variant compared to wild-type (Spearman's rank 0.95, Fig. 3c) and a reduction in binding for the Beta variant (Spearman's rank 0.69, Fig. 3d). Neutralization capacity in the pseudotyped virus assay was significantly reduced against the Delta VOC compared to wild-type in both children and adults ($p < 0.01$, Fig. 3e, f). However, neutralization was present in the majority of the seropositive participants–both adults (77.5%) and children (82.0%).

Seroprevalence against endemic coronaviruses rose sharply with age in early childhood, and was stable in older children, adolescents and adults independent of age (Figs. 4a and S9). In contrast to SARS-CoV-2 seroreversion, HCoV antibody titers decreased faster in younger children than in adults (Fig. S10). There were HCoV naïve samples in this cohort and some individuals showed a substantial increase in HCoV antibody response indicating exposure towards endemic HCoVs between the two time points (Fig. 4b in red, Fig. S11). Amongst SARS-CoV-2 exposed individuals in households with a defined index case (index cases excluded from the analysis, see Methods), there was no difference in HCoV antibody titers between SARS-CoV-2 seropositive and seronegative children or adults ($p = 0.21$, Figs. 4c and S12). In addition, we assessed whether SARS-CoV-2 infection boosted HCoV antibody responses, however there was no evidence for an association between HCoV antibody responses and SARS-CoV-2 antibody responses in exposed children or adults (Spearman's rank 0.03, Fig. 4d).

Discussion

To our knowledge, this is the largest prospective multi-center study comprehensively comparing the adult and pediatric longitudinal humoral immune response following SARS-CoV-2

138

ARTICLE

Table 1 Demographics and key information for the study cohort.

	Time point T1	Time point T1	Time point T2	Time point T2
Number of participants by age group (n)	Adult (717)	Children (548)	Adult (569)	Children (402)
Median Age – years (IQR)	44 (37-49)	10 (6-13)	45 (38-50)	10 (6-14)
Number of females (%)	362 (50.5)	277 (50.6)	297 (52.2)	202 (50.3)
BMI (IQR)	25.4 (22.2-27.7)	17.4 (14.9-19.5)	24.7 (22.3-28.1)	17.0 (15.0-19.7)
Number of seropositive participants	414 (57.7)	181 (33.0)	281 (49.4)	150 (37.3)
• Asymptomatic (%)	36 (8.7)	81 (44.8)	31 (11.0)	69 (46.0)
• Symptomatic (%)	378 (91.3)	100 (55.2)	250 (89.0)	81 (54.0)
Seroreverted at T2 (%)	NA	NA	71 (17.1)	7 (3.8)
Symptoms at disease onset (of seropositive)	..	..	..	..
• Fever (%)	217 (52.4)	66 (36.5)	151 (53.7)	49 (32.7)
• Cough (%)	221 (53.4)	37 (20.4)	154 (54.8)	33 (22.0)
• Dysgeusia (%)	266 (64.3)	28 (15.5)	176 (62.6)	24 (16.0)
• Diarrhea (%)	75 (18.1)	18 (9.9)	55 (19.6)	16 (10.7)
Median (IQR) days from positive PCR test result to timepoint	96 (63-120)	96 (63-120)	333 (319-353)	333 (319-353)
Median (IQR) days from symptoms onset to timepoint (of seropositive)	109 (67-122)	109 (67-122)	340 (322-356)	340 (322-356)
Hospitalized (of seropositive) (%)	15 (3.6)	0 (0.0)	NA	NA
Vaccinated (%)	NA	NA	24 (4.2)	1 (0.3)
Number of households	328	328	279	279
Median (IQR) number of household members	4 (3-4)	4 (3-4)	4 (3-4)	4 (3-4)

See methods for definition of how samples were defined as being seropositive, asymptomatic or symptomatic. Median time from positive PCR test to time point (n = 368 at T1, n = 310 at T2) and median time from symptoms onset to time point (n = 349 at T1, n = 243 at T2) are calculated using adult samples for which this data was available. Percentages of seropositive participants refer to the sample size at Time point 1 and Time point 2, respectively.
BMI Body Mass Index, IQR Interquartile Range, NA not applicable, PCR Polymerase Chain Reaction.
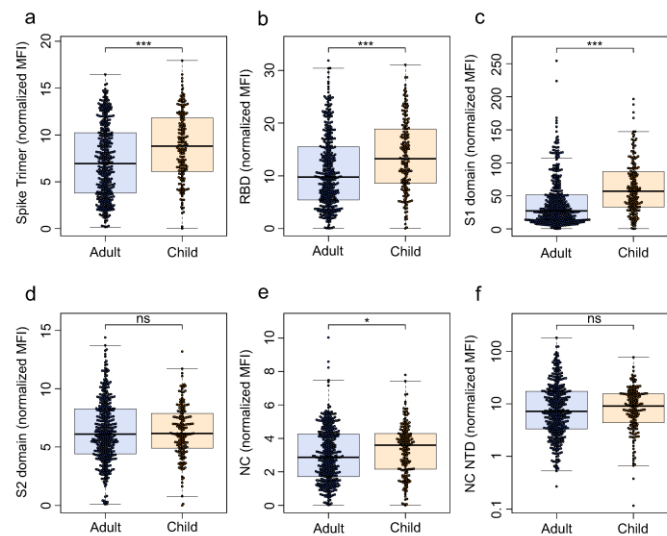
Fig. 1 Children have a significantly higher humoral response to SARS-CoV-2 than adults. The humoral response generated following SARS-CoV-2 household exposure with seroconversion was examined using MULTICOV-AB. Children (orange, $n = 181$) produced significantly more antibodies against the Spike (**a** $p = 6.00 \times 10^{-6}$), Receptor Binding Domain (RBD) (**b** $p = 2.86 \times 10^{-6}$), S1 domain (**c** $p = 3.00 \times 10^{-14}$) and nucleocapsid (NC) (**e** $p = 1.76 \times 10^{-2}$) than adults (blue, $n = 414$). There was no significant difference for either the S2 domain (**d** $p = 0.66$) or the N-terminal domain of the nucleocapsid (NC NTD) (**f** $p = 0.40$). Only samples from T1 with a seropositive status (see Methods) are shown. Box and whisker plots with the box representing the median, 25th and 75th percentiles, while whiskers show the largest and smallest non-outlier values. Outliers were identified using upper/lower quartile ±1.5 times IQR. Statistical significance was calculated using Mann–Whitney-U (two-sided) with significance defined as being *<0.05, ***<0.001. Values >0.05 were defined as non-significant (ns). MFI Median Fluorescence Intensity.

139
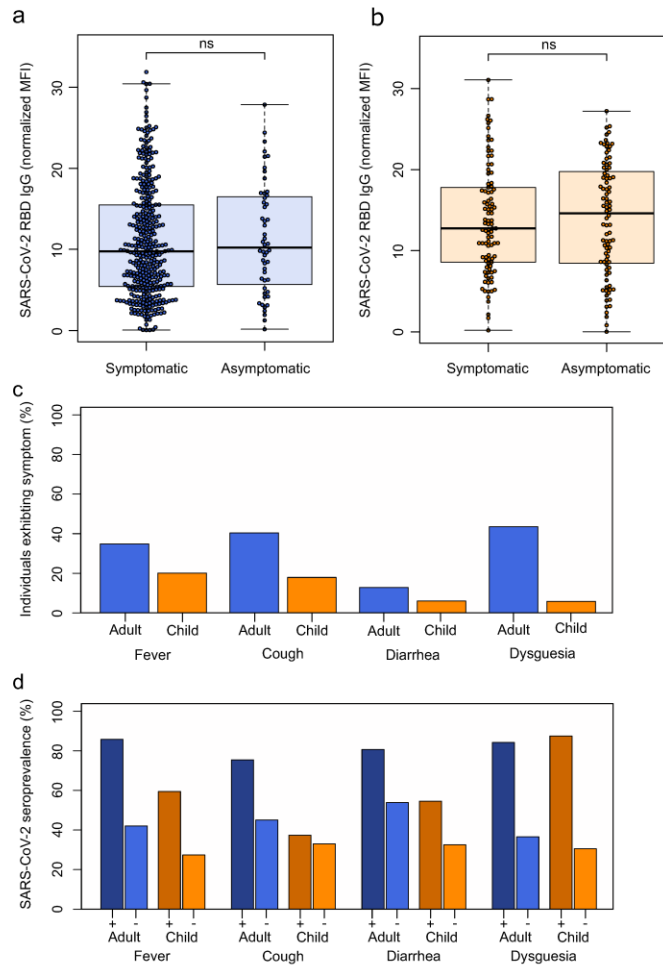
Fig. 2 SARS-CoV-2 infections in children are more often asymptomatic than in adults, although dysgeusia is a good indicator of SARS-CoV-2 infection in both adults and children. Box and whisker plots showing that there is no difference in antibody response between asymptomatic and symptomatic SARS-CoV-2 infections in adults (**a** in blue, $p = 0.684$, $n = 414$) or children (**b** in orange, $p = 0.712$, $n = 181$), as assessed by MULTICOV-AB. The receptor binding domain (RBD) is shown as an example, all other SARS-CoV-2 antigens are shown in Fig. S7. Boxes represent the median, 25th and 75th percentiles, while whiskers show the largest and smallest non-outlier values. Outliers were identified using upper/lower quartile ±1.5 times IQR. Statistical significance was calculated using Mann–Whitney-U (two-sided). ns indicates a non-significant p value >0.05. The four symptoms reported in this study were then examined for their frequency within the study population (**c**), with all symptoms more commonly reported in seropositive adults (in blue) than seropositive children (in orange). Each symptom was then examined for its predictive ability to indicate SARS-CoV-2 infection (**d**), with dysgeusia a strong predictor in both adults (dark blue, 84.2%) and children (dark orange, 87·5%). All other symptoms were poor predictors in children (fever 59.5%, cough 37.4%, diarrhea 54.6%) compared to adults (fever 85.8%, cough 75.0%, diarrhea 80.7%). Only samples from T1 were analyzed for this figure ($n = 717$ adults, 548 children). "+" indicates presence of the symptom "−" indicates absence of the symptom. MFI Median Fluorescence Intensity.

ARTICLE
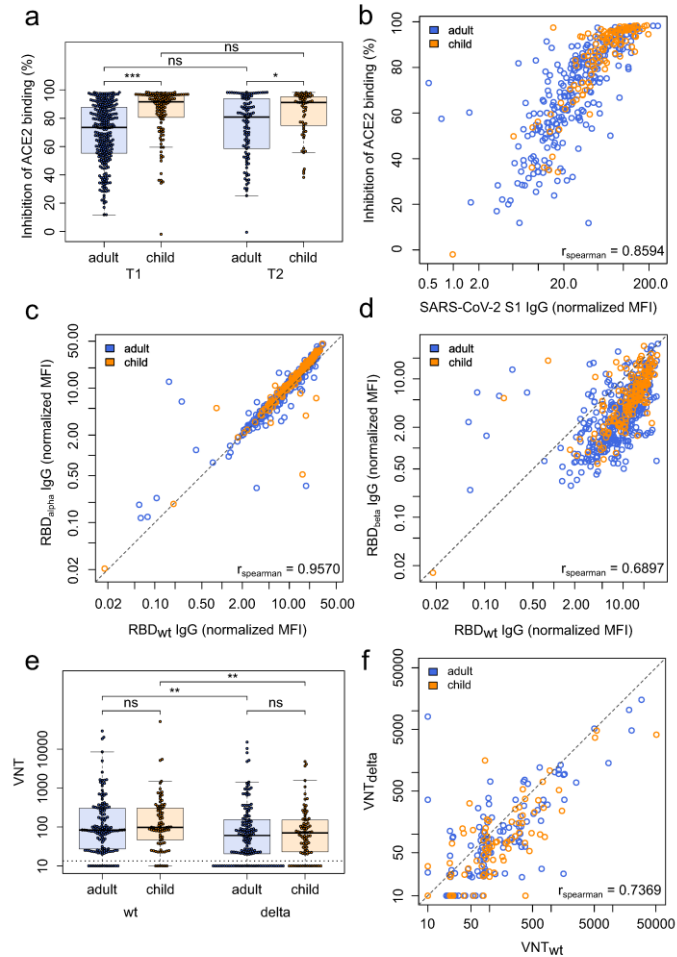
household exposure. As the humoral immunity against SARS-CoV-2 is now increasingly accepted as the central correlate of protection[18–20], improving our incomplete understanding in children[21,22] is of considerable value for public health and vaccination strategies. Importantly, our outpatient cohort has high epidemiological relevance, as a mild course is the most frequent outcome of SARS-CoV-2 infection overall[23]. Our findings identify several unique features of the pediatric serological immune response against SARS-CoV-2.

Children had a lower seroprevalence after household exposure and seropositivity followed asymptomatic infection more frequently than in adults. This is in agreement with our previous report of a different cohort consisting of parent–child pairs[24]. In light of potential pediatric vaccination campaigns, children's

humoral response to SARS-CoV-2 is markedly increased in both quantity and longevity, with children seroreverting at a significantly lower pace than adults. Children generated higher titers of SARS-CoV-2 antibodies than their parents after being exposed to likely same viral strain, and antibody titers negatively correlated with age. Of particular interest are the increase in antibodies produced against the S1 domain and RBD, both of which are associated with higher neutralization capacity, indicating that children produce a high quality humoral response against SARS-CoV-2[2,18,25]. The quality of the pediatric humoral response is further illustrated by the similar binding capacity against the SARS-CoV-2 Alpha and Beta VOCs and a similar neutralization capacity towards the Delta VOC compared to adults. These data argue for the generation of a protective long-term humoral

141

ARTICLE

Fig. 3 Children and adults produce antibodies with equal neutralizing potential and their antibodies offer the same protection against Variants of Concern. a Box and whisker plot showing that antibodies produced by children (orange, $n = 118$) have a significantly higher inhibition of ACE2 binding than those produced by adults (blue, $n = 267$, $p = 4.37 \times 10^{-13}$) at T1 and T2 ($p = 0.02$, child $n = 59$, adult $n = 106$) as determined by the sVNT assay. Boxes represent the median, 25th and 75th percentiles, while whiskers show the largest and smallest non-outlier values. Outliers were identified using upper/lower quartile ±1.5 times IQR. Statistical significance was calculated using Mann–Whitney-U (two-sided) with *** indicating a p value < 0.001, * indicating a p value < 0.05, and ns indicating a non-significant p value > 0.05. To determine whether this was due to the higher titers in children, SARS-CoV-2 S1 humoral response was determined using MULTICOV-AB for T1 and plotted against the results of the sVNT assay (**b**). Spearman's rank was calculated to measure the ordinal association between them, confirming that the increase in neutralization is due to higher titers. Protection against the Alpha (**c**) and Beta (**d**) VOCs was determined by MULTICOV-AB and plotted as a linear regression against the antibody binding response to the wild-type (wt) receptor binding domain (RBD), with Spearman's rank calculated to measure the ordinal association. There was no difference in antibody response between children ($n = 166$, T1 samples only) and adults ($n = 381$, T1 samples only) for either variant. (**e**) Box and whisker plot showing reduced neutralization responses in both adults (blue, $n = 142$, $p = 4.38 \times 10^{-3}$) and children (orange, $n = 83$, $p = 6.36 \times 10^{-3}$) against Delta VOC as compared to WT as determined by a pseudotype virus assay (VNT). Boxes represent the median, 25th and 75th percentiles, while whiskers show the largest and smallest non-outlier values. Outliers were identified using upper/lower quartile ±1.5 times IQR. Statistical significance was calculated using Mann–Whitney-U (two-sided) with ** indicating a p value < 0·01 and ns indicating a non-significant value >0.05. Titers are given as serum dilution factor resulting in 50% pseudovirus neutralization (PVNT50). The dashed line represents the lower limit of detection. **f** Linear regression comparing wild-type (VNTwt) and delta (VNTdelta) neutralization responses with Spearman's rank calculated to measure the ordinal association. ACE2 angiotensin-converting enzyme 2, MFI Median Fluorescence Intensity, (s)VNT (surrogate) Virus Neutralization Test, wt wild type.

immune response also against VOCs after wild-type SARS-CoV-2 infection, but the quality and duration of this protection can only be estimated following known exposure to VOCs. Children also had significantly higher neutralizing antibody titers than adults, indicating increased protection. This increase in neutralization was directly correlated with higher antibody titers in the other assays, and therefore may not be due to substantial qualitative changes of the pediatric antibody profiles. These findings are in line with one preprinted study[26] but in contrast to two previous studies, which found that children generated a lower humoral response to SARS-CoV-2 than adults, with a corresponding reduction in neutralization activity[10,12]. However, compared to our cohort, all three studies were substantially smaller in sample size and the latter two investigated a different disease spectrum comprising mostly hospitalized children or those diagnosed with hyperinflammatory MIS-C syndrome, and sampled blood at earlier time points after presumed infection.

It is striking that antibody levels in seropositive individuals were independent of fever, cough or diarrhea, as clinical proxies for systemic or localized inflammation of the respiratory or gastrointestinal tract, respectively. Previous studies have reported a clear correlation between disease severity and neutralizing antibody titers in adults[5,27]. At the other end of the disease spectrum with mildly affected younger adults and children as in our cohort, this association was not detectable irrespective of age. This diverges from the classical infection immunology dogma that systemic pathogen–host interaction is required for the generation of robust immune memory. While titers themselves did not differ between asymptomatic and symptomatic infections, we found substantial differences in titers between adults and children. Presence of any symptom was predictive of seropositivity in adults, whereas children showed substantial differences in both the prevalence of symptoms in seropositive individuals and the predictive values of symptoms with respect to SARS-CoV-2 seropositivity. Since cough was a relatively common symptom in children irrespective of seroconversion, it was not useful in predicting SARS-CoV-2 infection. In contrast, dysgeusia, an infrequent symptom among children, was highly accurate in predicting infection. These findings suggest that symptom criteria used for subsequent PCR testing need to be different for children and adults.

Similarly to other authors[28], we identified that exposure to HCoVs, as measured by seropositivity typically happens within the first five years of life. The relatively small decline of HCoV antibody levels during the study period, especially in the adult population, in comparison to the decline in SARS-CoV-2 antibody levels after a single infection suggests that long-term serological immunity against HCoVs may be driven by recurrent exposure. We observed HCoV infections in previously naïve individuals, indicating that endemic HCoVs still circulated between T1 and T2 despite SARS-CoV-2 related distancing and hygiene measures. Although cross-reactivity and/or cross-protection between SARS-CoV-2 and HCoVs have been hypothesized, our analyses did not find evidence for such effects. For both Alpha- and Beta-coronaviruses, HCoV antibody responses were not associated with a lower likelihood of seroconversion following SARS-CoV-2 exposure. Along with frequent HCoV seronegativity in younger childhood, this strongly argues that the lower incidence of SARS-CoV-2 infection in children is not due to HCoV cross-protection. Moreover, there was no evidence for boosting of HCoV titers following SARS-CoV-2 infection. In contrast to other studies which did identify an effect for endemic HCoV infection, our cohort is composed of intensely exposed individuals from within the same households, which is a substantial strength compared to previous studies that have used pre-pandemic sera or indirect control groups[16,26,29].

Limitations of our study include the potential recall-bias inherent to retrospective self- or parent-reporting of symptoms via questionnaires and physician-interviews. Additionally, PCR tests for SARS-CoV-2 during the first wave in Germany were mostly limited to the household index case, meaning it is possible that infected individuals were not identified as such, despite the multi-assay serological approach. However, the in-depth characterization of the humoral response provides valuable data for clinicians, public health officials and the public, at a time when children are increasingly viewed as a potential viral reservoir due to exclusion of pediatric populations from current vaccination strategies. Moreover, the limited PCR capacities make it also possible that non-index study participants were additionally exposed to unknown infection sources outside of their household. Given the relatively low incidence in Germany during the first wave (peak incidence spring 2020 45 cases/100.000/7 days) and the strict lockdown measures including school closures, this scenario can be assumed to be a rare event. Similarly, while PCR testing was not available for all individuals, the strength of this cohort comes from the comparatively large number of children, inclusion of children and adults from the same household, inclusion of seronegative household members as well-matched controls, and the prospective longitudinal analysis of the humoral response in children for up to one year post-infection. The

142

ARTICLE

a

b

c

d
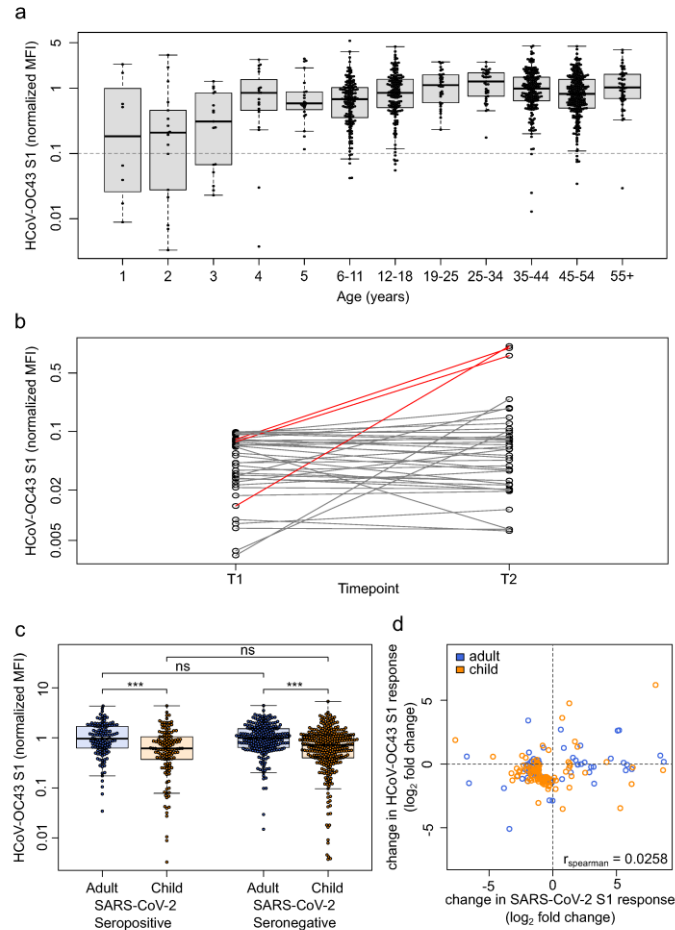
seropositive cohort also comprises almost exclusively individuals with mild or asymptomatic infections and so provides real-world data representative for the majority of SARS-CoV-2 infections in the community. It should be also stated that while all samples were analysed using a range of serological assays, only a subset of samples were analysed for their neutralizing capabilities, and as such, caution should be applied in extrapolating the implications regarding the neutralizing response to all study participants.

In summary, although children mostly show mild or even asymptomatic clinical courses following SARS-CoV-2 infection, they mount a strong and enduring humoral immune response. This strongly argues for sustained protection after infection, and might inform the design of vaccination strategies for SARS-CoV-2 convalescent children.

Methods

Cohort. This study forms part of a non-interventional, prospective observational national multi-center cohort study[30], including 548 children and 717 adults from 328 households each with at least one individual with a SARS-CoV-2 reverse-transcriptase polymerase chain reaction (RT-PCR) proven infection and/or a symptomatic and later serologically proven infection. Participants were recruited during the first wave of the pandemic (May to August 2020) via local health authorities and an in-hospital database of households with at least one laboratory-confirmed SARS-CoV-2 infection. Due to restrictions in obtaining a SARS-CoV-2 RT-PCR test during the first wave (children and asymptomatic contacts of an index case were not tested routinely), serological assays were the only means to identify previous infection. This study was initiated by the four University Children's Hospitals of Freiburg, Heidelberg, Tübingen and Ulm and approved by the independent ethics committees of each center. Sera and data for this substudy were collected at the study sites in Freiburg, Tübingen and Ulm. Participants were asked to fill a questionnaire at time point 1 (May– August 2020) and follow-up time point 2 (February–March 2021).

ARTICLE

Fig. 4 HCoVs offer no protection against SARS-CoV-2, nor do they show a boost-back antibody response following SARS-CoV-2 infection. Samples from households with a known index case ($n = 971$) were examined with MULTICOV-AB to determine whether the antibody response to endemic coronaviruses (HCoV) provides any protection against infection with SARS-CoV-2. Initial screening of the population showed that seroprevalence increases with age, although several samples were within the blank range of the HCoV assays, indicating the presence of naïve samples (**a**). Naïve samples were defined as those having less than one-tenth the mean antibody response (indicated by dotted line), with the majority of these samples occurring in children under the age of five. HCoV-OC43 is shown as an example, all other HCoVs can be found as Fig. S9. Boxes represent the median, 25th and 75th percentiles, while whiskers show the largest and smallest non-outlier values. Outliers were identified using upper/lower quartile ±1·5 times IQR. **b** Line graph showing the longitudinal response of these naïve samples from T1 to T2, with new infections in HCoV-OC43 shown in red. **c** Box and whisker plot showing there is no significant difference in HCoV-OC43 antibody response between SARS-CoV-2 seropositive and seronegative individuals, among either adults (blue, $n = 440$, $p = 0·974$) or children (orange, $n = 436$, $p = 0·214$). Boxes represent the median, 25th and 75th percentiles, while whiskers show the largest and smallest non-outlier values. Outliers were identified using upper/lower quartile ±1·5 times IQR. Statistical significance was calculated by Mann–Whitney-U (two-sided) with *** indicating a p value < 0·001 and ns indicating a p value > 0·05. **d** When comparing paired samples longitudinally within the SARS-CoV-2 seropositive subgroup, there was no increase in HCoV-OC43 S1 response in either adults (blue, $n = 76$) or children (orange, $n = 103$) following SARS-CoV-2 infection. Change in response is presented as log2-fold change from T1 to T2 and only samples with either log2-fold change greater than 1 or smaller than −1 are shown. Spearman's rank was used to calculate the ordinal association between the change in response for HCoV-OC43 and SARS-CoV-2. The same figures for the endemic coronaviruses HCoV-NL63, HCoV-HKU1 and HCoV-229E can be found as Figs. S9, S11 and S12. HCoV human Coronavirus, MFI Median Fluorescence Intensity, S1 Spike S1 domain., S1 Spike S1.

Study participants and eligibility criteria. Families were identified during the first wave of the pandemic between May and August 2020 in the region of Baden–Württemberg, Germany.

Inclusion criteria:

(i) Children (male or female) aged 1–18 years.
(ii) Parents and other adults (male or female) living in the same household with the investigated children (without age limit).
(iii) Residency in the state of Baden-Württemberg.
(iv) Written consent to the study.

Key exclusion criteria:

(i) Severe congenital diseases (e.g. infantile cerebral palsy, severe congenital malformations).
(ii) Congenital or acquired immunodeficiencies.
(iii) Insufficient comprehension of German language.

Data collection. Children and adults within eligible households completed a questionnaire containing demographic information (date of birth, gender, height, weight, smoking), the presence of symptoms (fever, cough, dysgeusia or diarrhea) in plausible temporal association (max. two weeks prior or later) with the onset of the SARS-CoV-2 infection within the household or around the time of a positive SARS-CoV-2 RT-PCR, and symptom duration. For younger children, parents provided symptom information. They additionally provided serum samples for immunological analysis at time point 1 and at follow-up time point 2 after the SARS-CoV-2 infection within the household. Data on vaccination and potential re-infection within the household were collected at time point 2. We investigated all invited households with at least one child to avoid selection bias. Questionnaires were checked for missing or inadequate data and inconsistencies; where possible, these points were clarified retrospectively with the families. To predetermine the sample size, we used a one-factor variance analysis design. Assuming 1.5 children per household participating in the study and three different age ranges, we aimed at a sample size of ≈200 households to reveal small effect sizes of about 0.1 at a significance level of 5% and a test strength of 80%.

Data variables. Samples were defined as being "symptomatic" on the basis of having at least one of four (fever, cough, diarrhea and dysguesia) symptoms, in addition to a positive serology result. "Asymptomatic" samples were defined as those without any of the above symptoms and a positive serology result. For some households ($n = 272$) an "index case" was defined. This is the first household member to test positive for SARS-CoV-2 by RT-PCR. The majority of index cases in this study were adults (249 of 272). No index was defined for households where additional household members tested positive by RT-PCR within 48 hours of the first positive test or where infection was identified by the combination of positive serology and symptoms only. If a household had a defined index case, then all other household members were considered "exposed". "Time post symptom onset" within a household was calculated as the number of days between the first date of symptom onset in any seropositive individual within a household and the sampling date at T1 and T2 respectively.

Study oversight. This part of the study was conducted by the University Children's Hospitals in Freiburg, Tübingen and Ulm, Germany. Ethics approval was obtained from the respective Medical Faculties' independent ethics committees (University of Freiburg: 256/20_201553; University of Tübingen: 293/2020BO2;

University of Ulm: 152/20). Written informed consent was obtained from adult participants and from parents or legal guardians on behalf of their children at both sampling time points. Children's preferences on whether or not to provide a blood sample were respected throughout. This study was registered at the German Clinical Trials Register (DRKS), study ID 00021521, conducted according to the Declaration of Helsinki, and designed, analyzed and reported according to the Strengthening the Reporting of Observational Studies in Epidemiology (STROBE) reporting guidelines. The full study protocol can be found at (https://www.drks.de/drks_web/navigate.do?navigationId=trial.HTML&TRIAL_ID=DRKS00021521).

Blood sample collection. Samples were collected at two separate time points, an early time point (T1) at a median of 109 days (IQR 67–122 days) after earliest symptom onset in household and a late time point (T2) at 340 days (IQR 322–356 days) post-symptom onset (Table 1, Fig. S1 in Supplementary Appendix). Blood samples were collected by venipuncture from all consenting adults and children within the study. Serum was separated on the same day by centrifugation, aliquoted and frozen at −80 °C until used.

Serological assays. Antibodies against SARS-CoV-2 in 2236 samples were detected using the following four assays: (1) EuroImmun-Anti-SARS-CoV-2 ELISA IgG (S1), (2) Siemens Healthineers SARS-CoV-2 IgG (RBD), (3) Roche Elecsys Ig (Nucleocapsid Pan Ig) and (4) MULTICOV-AB, a previously published bead-based multiplex immunoassay that simultaneously analyses antibody binding to 23 antigens from SARS-CoV-2 (including VOCs)[31,32]. Seropositivity was defined as any three of the four SARS-CoV-2 assays being positive. The MULTICOV-AB assay also analyses antibody binding to endemic coronavirus antigens (i.e. HCoV-OC43, -NL63, -HKU1 and −229E)[31,32].

EuroImmun Anti-SARS-CoV-2 ELISA. The EuroImmun Anti-SARS-CoV-2 ELISA (IgG) was performed as the manufacturer's instructions to detect IgG antibodies against the S1 domain of the SARS-CoV-2 spike protein. All 2236 samples used in the final analysis were measured with this assay. All samples were processed with the specified controls and calibrators. Serological analysis was performed blinded for all clinical covariables.

Siemens Healthineers SARS-CoV-2 IgG (sCOVG). The Siemens sCOVG assay was performed as per the manufacturer's instructions on an Advia Centaur XPT platform to detect IgG antibodies against the receptor-binding-domain (RBD) of the SARS-CoV-2 spike protein. All 2,236 samples used in the final analysis were measured with this assay. All samples were processed with the specified controls and calibrators. Serological analysis was performed blinded for all clinical covariables.

Roche Elecsys Electrochemiluminescence immunoassay (ECLIA). The Roche Elecsys ECLIA was performed as per the manufacturer's instruction on a Cobas e411 or e811 platform to detect IgG, IgA and IgM antibodies against the nucleocapsid of SARS-CoV-2. All 2236 samples used in the final analysis were measured with this assay. All samples were processed with the specified controls and calibrators. Serological analysis was performed blinded for all clinical covariables.

MULTICOV-AB™. All 2236 samples used in the final analysis were analyzed using MULTICOV-AB[1], a bead-based multiplex immunoassay that simultaneously analyzes 23 antigens from SARS-CoV-2 (including RBDs from variants of concern and endemic human coronaviruses)[31]. A full list of antigens used in this study can

ARTICLE

be found in Table S3. Samples were measured in 384-well plates, with all pipetting steps performed using a Beckmann Coulter i7 pipetting robot. Antigens were coupled by EDC/s-NHS or Anteo coupling to spectrally distinct populations of MagPlex beads (Luminex Technology). Samples were diluted in assay buffer (1:4 Low Cross Buffer (Candor Bioscience GmBH) in CBS (1x PBS + 1% BSA) + 0.05% Tween20) and added to bead mix to a final dilution factor of 1:400, before being incubated for 2 hours at 21 °C on a thermomixer (1500rpm). Unbound antibodies were then removed by washing with Wash buffer (1x PBS, 0.05% Tween20). Bound antibodies were detected using RPE-conjugated human IgG (3 µg/mL) and IgA (5 µg/mL) (both Biozol) by incubation for 45 mins at 21 °C, 1800 rpm on a thermomixer. Following a further washing step, beads were resuspended in 80 µL of washing buffer and shaken briefly for 3 mins at 1500 rpm. Plates were then measured using a FLEXMAP-3D (Luminex Technology) instrument running xPONENT Software (version 4.3) with the following settings: 60 µL, 80 s timeout, 35 events, Gate 7500-15000 and Reporter Gain: Standard PMT. For quality control, eight wells for each QC sample plus eight blank wells (negative control) were included on each 384-well plate[31–33]. Additionally, control beads coupled with human IgG, goat-anti-human IgG, human IgA and goat-anti-human IgA were included in each well to act as controls for both sample addition and signal system addition. To pass QC, each sample had to meet the minimum threshold for number of beads per ID (35), have a sample and signal system control bead value within normal range and pass plate-by-plate QC sample controls. Any plate or sample that failed QC was re-measured (83/2,390). Normalization values for each antigen were generated by dividing the raw median fluorescence intensity (MFI) value by the mean plate-by-plate MFI of QC2 (IgG) or QC3 (IgA). For SARS-CoV-2, normalization values >1 for the trimeric spike and wild-type RBD indicate positivity. To reduce analytical variations, all samples were analyzed in the same run. Serological analysis was performed blinded for all clinical covariables. Technical questions regarding the MULTICOV-AB™assay should be directed to nicole.schneiderhan@nmi.de.

Surrogate SARS-CoV-2 Neutralization Test. A subset of 385 samples were analyzed for neutralization with the surrogate SARS-CoV-2 neutralization test (GenScript) as per the manufacturer's instructions and as published previously[34]. Briefly, samples and controls were incubated with an HRP-conjugated RBD fragment. Following this, the mixture was added to wells of a capture plate coated with human ACE2 protein. The plate was then washed three times to remove any complexes or non-bound antibodies. TMB was added and then stopped with the addition of a stop reagent. The plate was then read by a microtiter plate reader (POLARstar Omega) at 450 nm. The absorbance of the sample is inversely correlated with the amount of SARS-CoV-2 neutralizing antibodies. Positive and negative controls served as internal assay quality controls. The test was considered valid only if the OD450 for each control fell within the respective range (OD450negative control >1.0, OD450positive control <0.3). For final interpretation, inhibition rates were calculated as follows: Inhibition score (%) = (1 − (OD valuesample/OD valuenegative control) × 100%). Scores <30% were considered negative, scores ≥30% were considered positive.

Cell culture. Vero E6 (African green monkey, female, kidney; CRL-1586, ATCC, RRID:CVCL_0574) cells were grown in Dulbecco's modified Eagle's medium (DMEM, Gibco) supplemented with 2.5% heat-inactivated fetal calf serum (FCS), 100 units/ml penicillin, 100 µg/ml streptomycin, 2 mM L-glutamine, 1 mM sodium pyruvate, and 1x non-essential amino acids. HEK293T (human, female, kidney; ACC-635, DSMZ, RRID: CVCL_0063) cells were grown in DMEM supplemented with 10% FCS, 100 units/ml penicillin, 100 µg/ml streptomycin, and 2 mM L-glutamine. All cells were grown at 37 °C in a 5% CO2 humidified incubator.

Preparation of pseudotyped particles. Rhabdoviral pseudotype particles were prepared as previously described[34]. A replication-deficient VSV vector in which the genetic information for VSV-G is replaced by genes encoding enhanced green fluorescent protein and firefly luciferase 3 (kindly provided by Gert Zimmer, Institute of Virology and Immunology, Mittelhäusern, Switzerland) was used for pseudotyping. HEK293T cells were transfected with expression plasmids encoding SARS-CoV-2 spike variants D614G 4 (pCG1_SARS-2-Sdel18_D614G, kindly provided by Stefan Pöhlmann) or B.1.617.2/Delta[35], containing the spike mutations T19R, G142D, E156-, F157-, R158G, L452R, T478K, D614G, P681R, D950N and a 19AA C-terminal deletion (pcDNA3.1-S2S-IN2(B.1.617.2)Δ19. 24 h post transfection, cells were inoculated with VSV vector. After 2 h incubation at 37 °C, the inoculum was removed, cells were washed with PBS and fresh medium added. After 16–18 h, the supernatant was collected and centrifuged (2,000 × g, 5 min, room temperature) to remove cellular debris. Cell culture medium containing anti-VSV-G antibody (I1-hybridoma cells; ATCC no. CRL-2700) was added to block residual VSV-G-containing particles. Samples were then aliquoted and stored at −80 °C.

Pseudovirus neutralization assay. A subset of 225 samples were examined by Pseudovirus neutralization assay against Wild-type (B1 isolate) and the delta VOC (B.1.617.2). For pseudovirus neutralization experiments, Vero E6 cells were seeded in 96-well plates one day prior. Heat-inactivated (56 °C, 30 min) sera were serially diluted in PBS, mixed with pseudovirus stocks (1:1, v/v) and incubated for 30 min at 37 °C before being added to cells. After 16-18 h, firefly luciferase activity was quantified as a readout for transduction efficiency. For this, cells were lysed by incubation with Cell Culture Lysis Reagent (Promega) at room temperature. Lysates were then transferred into white 96-well plates and luciferase activity was measured using a commercially available substrate (Luciferase Assay System, Promega) and a plate luminometer (Orion II Microplate Luminometer running Simplicity Software v4.2, Berthold). For analysis, background signal of untreated cells was subtracted and values normalized to pseudovirus mixed with PBS only. Results are given as serum dilution resulting in 50% pseudovirus neutralization (PVNT50) on cells, calculated by nonlinear regression ([Inhibitor] vs. normalized response–Variable slope) in GraphPad Prism Version 9.1.1. The upper and lower cutoff values of this assay were set at PVNT50 >81,920 and PVNT50 <20, respectively.

Data analysis. Initial data collection was done using Microsoft Excel and Access. Formal data analysis was performed on RStudio (Version 1.2.5001, running R 3.6.1) with the following additional packages: "RColorBrewer", "beeswarm", "gplots", "VennDiagram", all of which were used solely for data depiction and not statistical analysis. Figures were generated in RStudio and then edited for clarity in Inkscape (Inkscape 0.92.4). Only samples for which full data for MULTICOV-AB was available were included in the analysis. Furthermore, only samples from time point 1 were used for all non-longitudinal analyses. For longitudinal analyses, only those participants for whom both T1 and T2 samples were available were included and all participants who were vaccinated prior to T2 were excluded. For analysis of potential cross-protection though endemic coronaviruses, only households with a known index case were used and the index case itself was excluded. Statistical analyses performed are described in the figure legends. For comparison of signal distribution between sample groups, Mann–Whitney-U tests were performed using the "wilcox.test" function from R's "stats" library. For correlation analysis, Spearman's rank was calculated using the "cor" function from R's "stats" library. p values < 0.05 were considered to be significant.

Reporting summary. Further information on research design is available in the Nature Research Reporting Summary linked to this article.

Data availability
A short version of the study protocol is available at the German Clinical Trials Register (DRKS, www.drks.de), study ID 00021521. The full study protocol is available from https://www.drks.de/drks_web/navigate.do?navigationId=trial.HTML&TRIAL_ID=DRKS00021521. Individual participant data, including data dictionaries will not be available, since we did not seek parental consent for data sharing.

Code availability
Code will be available upon reasonable request.

References
1. Sette, A. & Crotty, S. Adaptive immunity to SARS-CoV-2 and COVID-19. *Cell* **184**, 861–880 (2021).
2. Robbiani, D. F. et al. Convergent antibody responses to SARS-CoV-2 in convalescent individuals. *Nature* **584**, 437–442 (2020).
3. Dan, J. M. et al. Immunological memory to SARS-CoV-2 assessed for up to 8 months after infection. *Science* **371**, eabf4063 (2021).
4. Wheatley, A. K. et al. Evolution of immune responses to SARS-CoV-2 in mild-moderate COVID-19. *Nat. Commun.* **12**, 1162 (2021).
5. Seow, J. et al. Longitudinal observation and decline of neutralizing antibody responses in the three months following SARS-CoV-2 infection in humans. *Nat. Microbiol.* **5**, 1598–1607 (2020).
6. Bartsch, Y. C. et al. Humoral signatures of protective and pathological SARS-CoV-2 infection in children. *Nat. Med.* **27**, 454–462 (2021).
7. Bloise S. et al. Serum IgG levels in children 6 months after SARS-CoV-2 infection and comparison with adults. *Eur. J. Pediatr.* **180**, 1–8 (2021).
8. Bavaro, D. F. et al. Anti-spike S1 receptor-binding domain antibodies against SARS-CoV-2 persist several months after infection regardless of disease severity. *J. Med. Virol.* **93**, 3158–3164 (2021).
9. Cotugno, N. et al. Virological and immunological features of SARS-CoV-2-infected children who develop neutralizing antibodies. *Cell Rep.* **34**, 108852 (2021).
10. Pierce, C. A. et al. Immune responses to SARS-CoV-2 infection in hospitalized pediatric and adult patients. *Sci. Transl. Med.* **12**, 5487 (2020).
11. Selva, K. J. et al. Systems serology detects functionally distinct coronavirus antibody features in children and elderly. *Nat. Commun.* **12**, 2037 (2021).

9

145

ARTICLE

12. Weisberg, S. P. et al. Distinct antibody responses to SARS-CoV-2 in children and adults across the COVID-19 clinical spectrum. *Nat. Immunol.* **22**, 25–31 (2021).
13. Yang, H. S. et al. Association of age with SARS-CoV-2 antibody response. *JAMA Netw. Open* **4**, e214302 (2021).
14. Waterfield, T. et al. Seroprevalence of SARS-CoV-2 antibodies in children: a prospective multicentre cohort study. *Arch. Dis. Child* **106**, 680–686 (2021).
15. Gudbjartsson, D. F. et al. Humoral immune response to SARS-CoV-2 in Iceland. *N. Engl. J. Med.* **383**, 1724–1734 (2020).
16. Anderson, E. M. et al. Seasonal human coronavirus antibodies are boosted upon SARS-CoV-2 infection but not associated with protection. *Cell* **184**, 1858–1864.e10 (2021).
17. Sagar, M. et al. Recent endemic coronavirus infection is associated with less-severe COVID-19. *J. Clin. Invest* **131**, e143380 (2021).
18. Khoury D. S. et al. Neutralizing antibody levels are highly predictive of immune protection from symptomatic SARS-CoV-2 infection. *Nat. Med.* **27**, 1205–1211 (2021).
19. Hall, V. J. et al. SARS-CoV-2 infection rates of antibody-positive compared with antibody-negative health-care workers in England: a large, multicentre, prospective cohort study (SIREN). *Lancet* **397**, 1459–1469 (2021).
20. Earle, K. A. et al. Evidence for antibody as a protective correlate for COVID-19 vaccines. *Vaccine* **39**, 4423–4428 (2021).
21. Zimmermann, P. & Curtis, N. Why is COVID-19 less severe in children? A review of the proposed mechanisms underlying the age-related difference in severity of SARS-CoV-2 infections. *Arch. Dis. Child* **106**, 429–439 (2021).
22. Viner, R. M. et al. Susceptibility to SARS-CoV-2 infection among children and adolescents compared with adults: a systematic review and meta-analysis. *JAMA Pediatr.* **175**, 143–156 (2021).
23. Götzinger, F. et al. COVID-19 in children and adolescents in Europe: a multinational, multicentre cohort study. *Lancet Child Adolesc. Heal* **4**, 653–661 (2020).
24. Tönshoff, B. et al. Prevalence of SARS-CoV-2 infection in children and their parents in Southwest Germany. *JAMA Pediatr.* **175**, 586–593 (2021).
25. Feng S. et al. Correlates of protection against symptomatic and asymptomatic SARS-CoV-2 infection. *Nat Med.* 2021. Epub ahead of print.
26. Dowell A. C. et al. Children develop strong and sustained cross-reactive immune responses against Spike protein following SARS-CoV-2 infection, with enhanced recognition of variants of concern. April 29, 2021. medRxiv. (https://doi.org/10.1101/2021.04.12.21255275). Preprint.
27. Hansen, C. B. et al. SARS-CoV-2 antibody responses are correlated to disease severity in COVID-19 convalescent individuals. *J. Immunol.* **206**, 109–117 (2021).
28. Huang, A. T. et al. A systematic review of antibody mediated immunity to coronaviruses: kinetics, correlates of protection, and association with severity. *Nat. Commun.* **11**, 4704 (2020).
29. Guo, L. et al. Cross-reactive antibody against human coronavirus OC43 spike protein correlates with disease severity in COVID-19 patients: a retrospective study. *Emerg. Microbes Infect.* **10**, 664–676 (2021).
30. Stich M. et al. Transmission of severe acute respiratory syndrome coronavirus 2 in households with children, Southwest Germany, May-August 2020. *Emerg Infect Dis.* 2021 25;27. Epub ahead of print.
31. Becker, M. et al. Immune response to SARS-CoV-2 variants of concern in vaccinated individuals. *Nat. Commun.* **12**, 3109 (2021).
32. Becker, M. et al. Exploring beyond clinical routine SARS-CoV-2 serology using MultiCoV-Ab to evaluate endemic coronavirus cross-reactivity. *Nat. Commun.* **12**, 1152 (2021).
33. Planatscher, H. et al. Systematic reference sample generation for multiplexed serological assays. *Sci. Rep.* **3**, 3259 (2013).
34. Jahrsdörfer, B. et al. Characterization of the SARS-CoV-2 neutralization potential of COVID-19-convalescent donors. *J. Immunol.* **206**, 2614–2622 (2021).
35. Wang, L. et al. Ultrapotent antibodies against diverse and highly transmissible SARS-CoV-2 variants. *Science* **373**, eabh1766 (2021). Aug 13.

Acknowledgements

Author contributions

R.E., H.R., A.J., D.F., P.H., A.R.F. and K.M.D. conceived the study. H.R., A.D., R.E., A.J., P.H., A.R.F., K.M.D. and N.S.M. designed the experiments. R.E., H.R., A.J., B.H.H., P.H., A.R.F., K.M.D. and N.S.M. procured funding. A.D., M.B., D.J., A.S., R.G., J.M., J.M., A.H., C.L., T.G., A.D., D.H., H.H., A.P., S.H., T.I., T.S., W.L. and H.-J.G. performed experiments. R.E., H.R., A.J., D.F., M.Z., S.B., L.F., P.F., A.H., J.R., E.-M.J., C.E., M.W., T.G. and M.R. collected samples or organized their collection. B.J., H.S., M.S., B.T., G.F.H. and B.M. supported the sample collection and provided key resources. P.K., B.T. and U.R. produced the R.B.D. mutants. H.R., A.J., A.D., M.B., D.F., A.H., A.D., K.K., S.W., E.-M.J., A.P., T.I., T.S., H.-J.G., M.W., C.E., K.M.D. and M.R. curated the data. M.B. and A.D. performed the data analysis. A.D. and M.B. generated the figures. A.D., H.R., A.J. and R.E. wrote the first draft of the manuscript. All authors approved the final version of the manuscript. All authors confirm that they had full access to all the data in the study and accept responsibility to submit for publication.

Funding

Competing interests

Additional information

Supplementary information The online version contains supplementary material available at https://doi.org/10.1038/s41467-021-27595-9.

Correspondence and requests for materials should be addressed to Roland Elling.

Peer review information *Nature Communications* thanks Karin Nielsen and the other, anonymous, reviewer(s) for their contribution to the peer review of this work. Peer reviewer reports are available.

Reprints and permission information is available at http://www.nature.com/reprints

Publisher's note Springer Nature remains neutral with regard to jurisdictional claims in published maps and institutional affiliations.

146

ARTICLE

[1]University Children's Hospital Tübingen, Tübingen, Germany. [2]NMI Natural and Medical Sciences Institute at the University of Tübingen, Reutlingen, Germany. [3]Institute of Molecular Virology, Ulm University Medical Center, Ulm, Germany. [4]Department of Pediatrics and Adolescent Medicine, Ulm University Medical Center, Ulm University, Ulm, Germany. [5]Center for Pediatrics and Adolescent Medicine, Medical Center Freiburg, Germany and Faculty of Medicine, University of Freiburg, Freiburg, Germany. [6]Institute for Medical Virology and Epidemiology of Viral Diseases, University Hospital Tübingen, Tübingen, Germany. [7]Institute of Virology, Ulm University Medical Center, Ulm, Germany. [8]Institute of Virology, Medical Center Freiburg, Germany and Faculty of Medicine, University of Freiburg, Freiburg, Germany. [9]Institute of Medical Biometry and Statistics, Medical Center Freiburg, Germany and Faculty of Medicine, University of Freiburg, Freiburg, Germany. [10]Department of Pediatrics I, University Children's Hospital Heidelberg, Heidelberg, Germany. [11]Department of Infectious Diseases, Virology, Heidelberg University Hospital, Heidelberg, Germany. [12]Institute of Transfusion Medicine, Ulm University, Ulm, Germany. [13]Institute for Clinical Transfusion Medicine and Immunogenetics, Ulm, Germany. [14]German Red Cross Blood Transfusion Service, Baden-Württemberg-Hessen, Germany. [15]Institute for Clinical Chemistry and Pathobiochemistry, University Hospital Tübingen, Tübingen, Germany. [16]Institute of Clinical Chemistry, Ulm University, Ulm, Germany. [17]Center for Pediatric Clinical Studies, University Hospital Tübingen, Tübingen, Germany. [18]Department of Microbiology and Department of Medicine, University of Pennsylvania, Philadelphia, USA. [19]Department of Rheumatology and Clinical Immunology, Medical Center Freiburg, Germany and Faculty of Medicine, University of Freiburg, Freiburg, Germany. [20]Institute for Immunodeficiency, Medical Center Freiburg, Germany and Faculty of Medicine, University of Freiburg, Freiburg, Germany. [21]These authors contributed equally: Hanna Renk, Alex Dulovic, Alina Seidel. [22]These authors jointly supervised this work: Ales Janda, Roland Elling. ✉email: roland.elling@uniklinik-freiburg.de

147

Supplementary Information – Robust and durable serological response following pediatric SARS-CoV-2 infection

Hanna Renk MD[1*], Alex Dulovic Dr.rer.nat[2*], Alina Seidel M.Sc[3*], Matthias Becker M.Sc[2], Dorit Fabricius MD[4], Maria Zernickel M.Sc[4], Daniel Junker M.Sc[2], Rüdiger Groß M.Sc[3], Janis A. Müller Dr.rer.nat[4], Alexander Hilger M.Sc[5], Sebastian F.N. Bode MD[4], Linus Fritsch[5], Pauline Frieh[5], Anneke Haddad DPhil[5], Tessa Görne[5], Jonathan Remppis MD[1], Tina Ganzemueller MD[7], Andrea Dietz Dr.biol.hum[6], Daniela Huzly MD[8], Hartmut Hengel MD[8], Klaus Kaier PhD[9], Susanne Weber Dipl.Math[9], Eva-Maria Jacobsen Dr.rer.physiol[4], Philipp D. Kaiser Dr.rer.nat[2], Bjoern Traenkle Dr.rer.nat[2], Ulrich Rothbauer Dr.rer.nat[2], Maximilian Stich MD[10], Burkhard Tönshoff MD[10], Georg F. Hoffmann MD[10], Barbara Müller PhD[11], Carolin Ludwig[12,13,14], Bernd Jahrsdörfer MD[12,13,14], Hubert Schrezenmeier MD[12,13,14], Andreas Peter MD[15], Sebastian Hörber MD[15], Thomas Iftner PhD[7], Jan Münch PhD[3], Thomas Stamminger MD[6], Hans-Jürgen Groß MD[16], Martin Wolkewitz PhD[9], Corinna Engel Dr.biol.hum[1,17], Marta Rizzi MD[18], Weimin Liu MD[19], Beatrice H. Hahn MD[19], Philipp Henneke MD[5,20], Axel R. Franz MD[1,17], Klaus-Michael Debatin MD[4], Nicole Schneiderhan-Marra Dr.rer.nat[2], Ales Janda MD[4,#] and Roland Elling MD[5,20,#,†]

1 – University Children's Hospital Tübingen, Tübingen, Germany

2 – NMI Natural and Medical Sciences Institute at the University of Tübingen, Reutlingen, Germany

3 – Institute of Molecular Virology, Ulm University Medical Center, Ulm University, Ulm, Germany

4 – Department of Pediatrics and Adolescent Medicine, Ulm University Medical Center, Ulm University, Ulm, Germany

1

5 – Center for Pediatrics and Adolescent Medicine, Medical Center Freiburg, Germany and Faculty of Medicine, University of Freiburg, Freiburg, Germany

6 – Institute of Virology, Ulm University Medical Center, Ulm, Germany

7 – Institute for Medical Virology and Epidemiology of Viral Diseases, University Hospital Tübingen, Tübingen, Germany

8 – Institute of Virology, Medical Center Freiburg, Germany and Faculty of Medicine, University of Freiburg, Freiburg, Germany

9 – Institute of Medical Biometry and Statistics, Medical Center Freiburg, Germany and Faculty of Medicine, University of Freiburg, Freiburg, Germany

10 – Department of Pediatrics I, University Children's Hospital Heidelberg, Heidelberg, Germany

11 - Department of Infectious Diseases, Virology, Heidelberg University Hospital, Heidelberg, Germany

12 – Department of Transfusion Medicine, Ulm University, Ulm, Germany

13 – Institute for Clinical Transfusion Medicine and Immunogenetics, Ulm, Germany

14– German Red Cross Blood Transfusion Service, Baden-Württemberg-Hessen, Germany

15 – Institute for Clinical Chemistry and Pathobiochemistry, University Hospital Tübingen, Tübingen, Germany

16 – Institute of Clinical Chemistry, Ulm University, Ulm, Germany

17 – Center for Pediatric Clinical Studies, University Hospital Tübingen, Tübingen, Germany

2

149

18 - Department of Rheumatology and Clinical Immunology, Medical Center Freiburg, Germany and Faculty of Medicine, University of Freiburg, Freiburg, Germany

19 - Department of Microbiology and Department of Medicine, University of Pennsylvania, Philadelphia, USA

20 – Institute for Immunodeficiency, Medical Center Freiburg, Germany and Faculty of Medicine, University of Freiburg, Freiburg, Germany

*These authors contributed equally

#These authors jointly supervised this work

†indicates corresponding author

3

150

Supplementary Figures
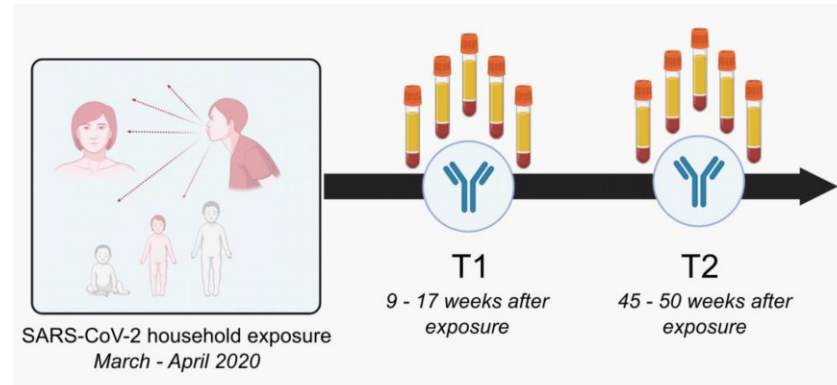
Figure S1: **Overview of the time points within the study population.** Illustration of study design, from exposure to study participation time points. Times shown are the IQR for each time point. T1 – Time point 1, T2 – Time point 2.

4
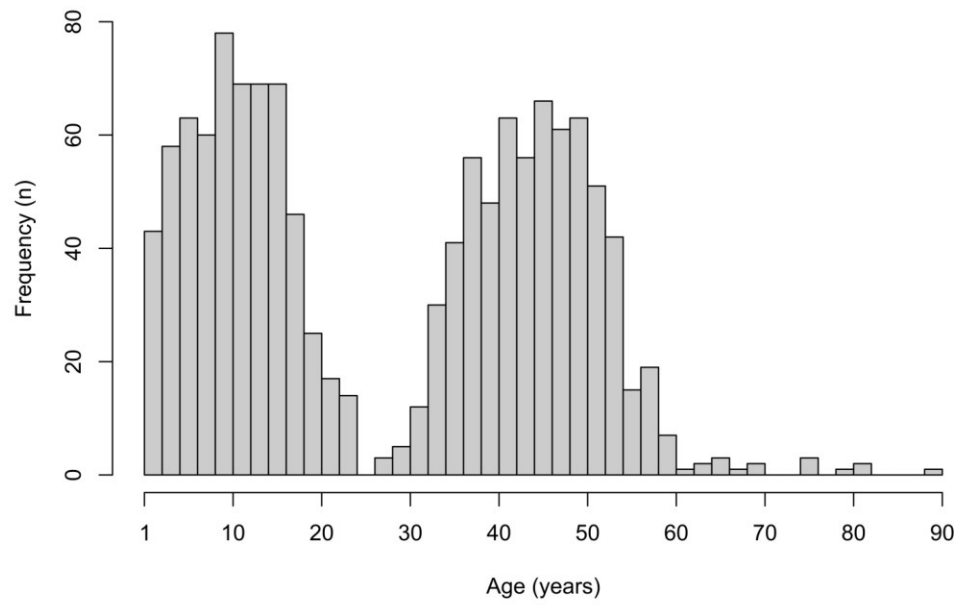
Figure S2 – **Study population age distribution**. Histogram showing age distribution within the study population at T1 (n=1265).

5

152
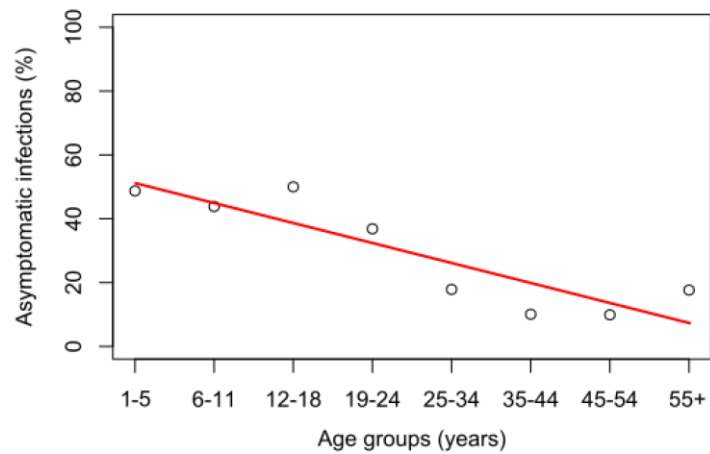
Figure S3 – **Proportion of asymptomatic infections decreases with age**. Line graph demonstrating the decrease in the proportion of asymptomatic infections with increasing age across age-group. Red line indicates line of best fit. Only samples at T1 were included in this analysis (n=1265).

6
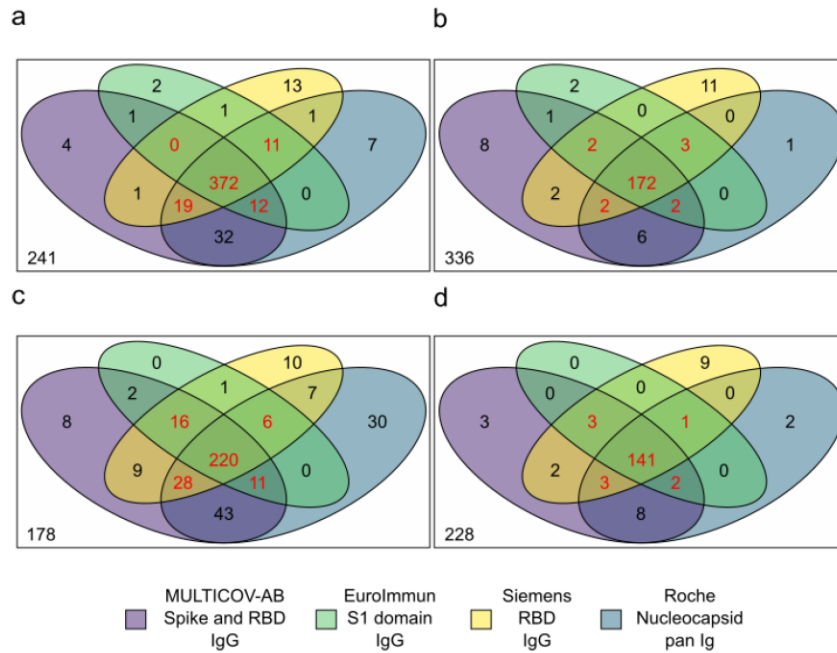
Figure S4 – **Comparative performance of the different serology assays used in this study**. 4-way Venn diagrams showing how each assay classified samples as being seropositive for T1 (a and b) and T2 (c and d) for adults (a and c) and children (b and d). Samples were classified as being positive if three or more assays classified them as being positive (shown in red). Negative samples for all assays are indicated in the bottom left corner of the boxes. Assays are color-coded as defined by the key including the manufacturer or name of the assay, which antigen it uses as a target and which Ig-isotype it measures. RBD – receptor binding domain.

7
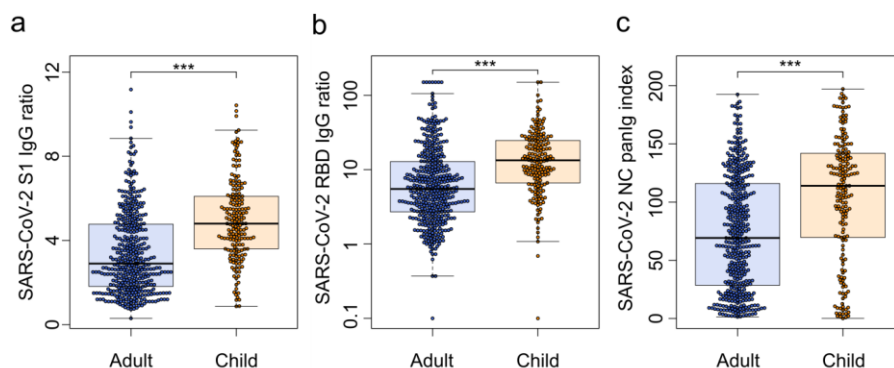
Figure S5 – **Children have higher antibody responses than adults**. Seropositive children (orange, n=181) had significantly higher IgG antibody titres against S1 (a, $p=1.52 \times 10^{-18}$), receptor binding domain (RBD) (b, $p=7.05 \times 10^{-14}$) and nucleocapsid (NC) (c, $p=7.55 \times 10^{-10}$) than seropositive adults (blue, n=414) as determined using the commercial EuroImmun (a), Siemens (b) and Roche (c) assays at T1. The Ig isotype measured with each assay is indicated on the axis. Seropositive adults and children were identified using the multi-assay definition of seropositivity explained in the Method section. Box and whisker plots with the box representing the median, 25th and 75th percentiles, while whiskers show the largest and smallest non-outlier values. Outliers were identified using upper/lower quartile ± 1·5 times IQR. Statistical significance was calculated by Mann-Whitney-U (two-sided) with *** indicating a p-value <0·001.

8

155
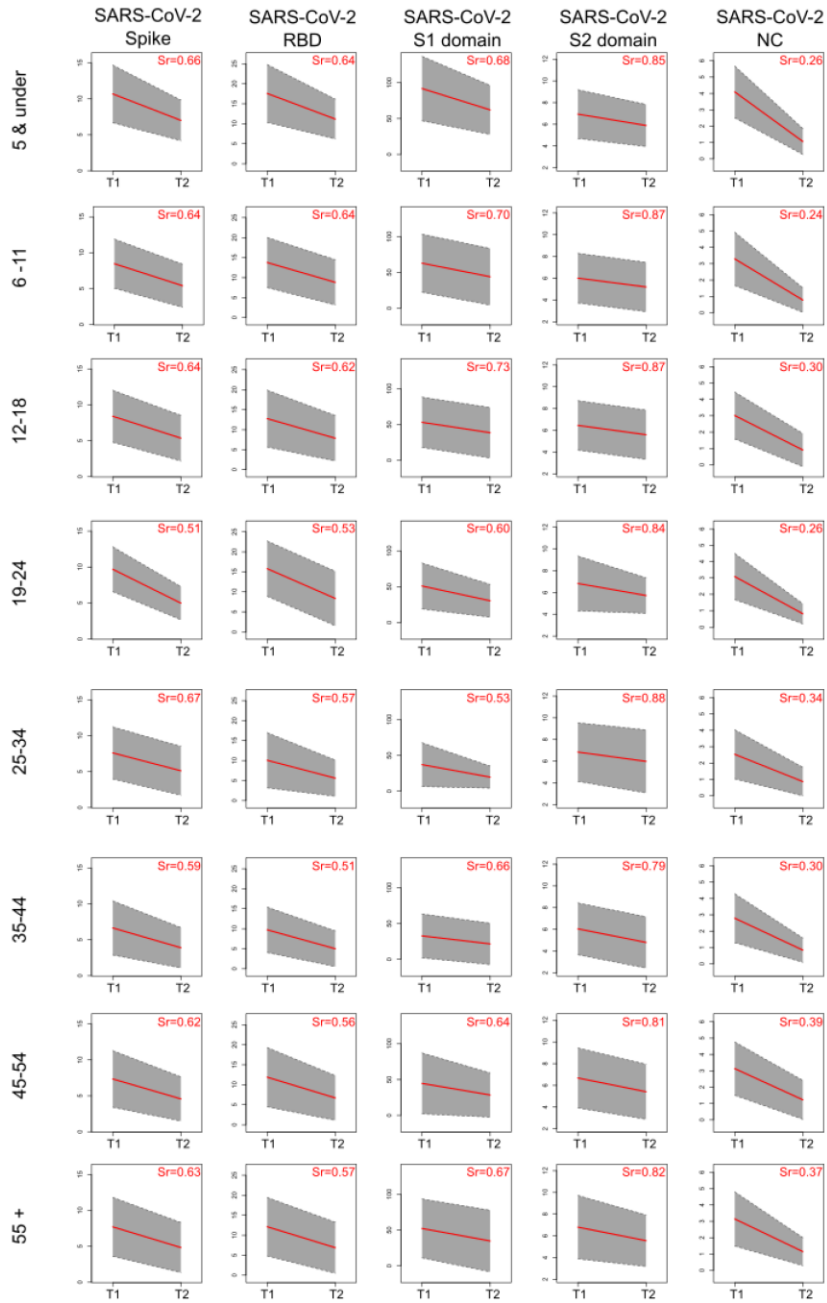
Figure S6 – **Antibody decay occurs at the same rate in adults and children.**
Longitudinal comparison of T1 and T2 samples using MULTICOV-AB to determine
the rate of antibody decay. The IgG antibodies against spike trimer, receptor binding
domain (RBD), S1 domain, S2 domain and nucleocapsid (NC) of SARS-CoV-2 are
shown. Samples are separated into distinct age groups: under 5 years old (n=28), 6-
11 (n=61), 12-18 (n=68), 19-24 (n=14), 25-34 (n=21), 35-44 (n=117), 45-54 (n=148)
and over 55 years old (n=31). All y-axis show the normalized MFI. Red lines indicate
mean rates of decrease; grey boxes indicate ±1 standard deviation. Sr indicates
proportion of signal remaining, calculated as the ratio of the mean MFI at T2
compared to the mean MFI at T1. MFI – median fluorescence intensity.

10
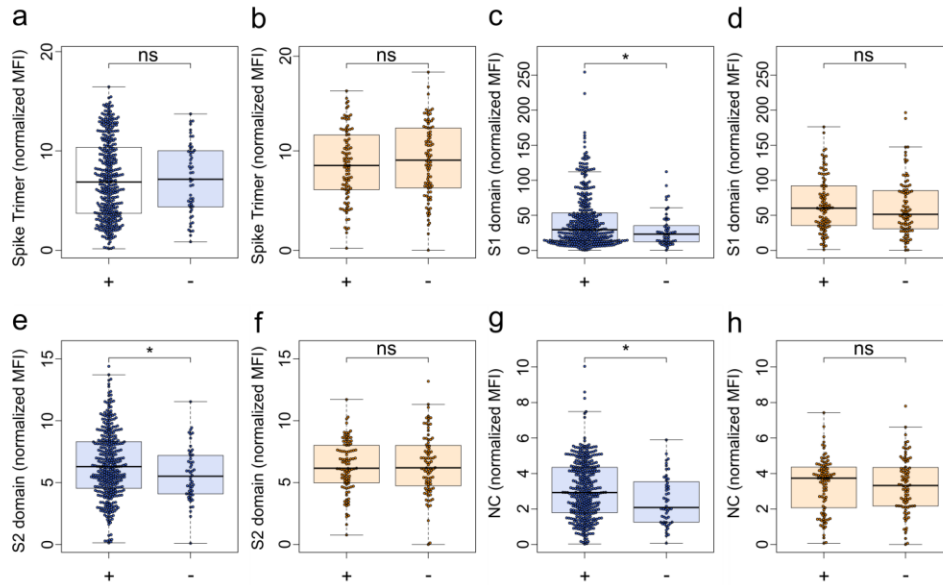
Figure S7 – **There is no difference in antibody response between asymptomatic and symptomatic infections in children**. Box and whisker plots with the box representing the median, 25th and 75th percentiles, while whiskers show the largest and smallest non-outlier values. Outliers were identified using upper/lower quartile ±1·5 times IQR. Statistical significance was calculated by Mann-Whitney-U (two-sided) with * indicating a p-value <0·05. and ns indicating a non-significant p-value >0·05. "+" indicates a symptomatic infection while "-" indicates an asymptomatic infection. There were no significant differences between symptomatic and asymptomatic seropositive children (orange, n=185) in terms of antibody response for the spike trimer (b, p=0·43), S1 domain (d, p=0·34), S2 domain (f, p=0·87) or Nucleocapsid (NC) (h, p=0·78). Symptomatic and asymptomatic seropositive adults (blue, n=414) showed no significant difference for the spike trimer (a, p=0·94), although there were small significant differences in the S1 domain (c, p=0·03) and S2 domain (e, p=0·05) and NC (g, p=0·01). MFI – median fluorescence intensity.

11

158
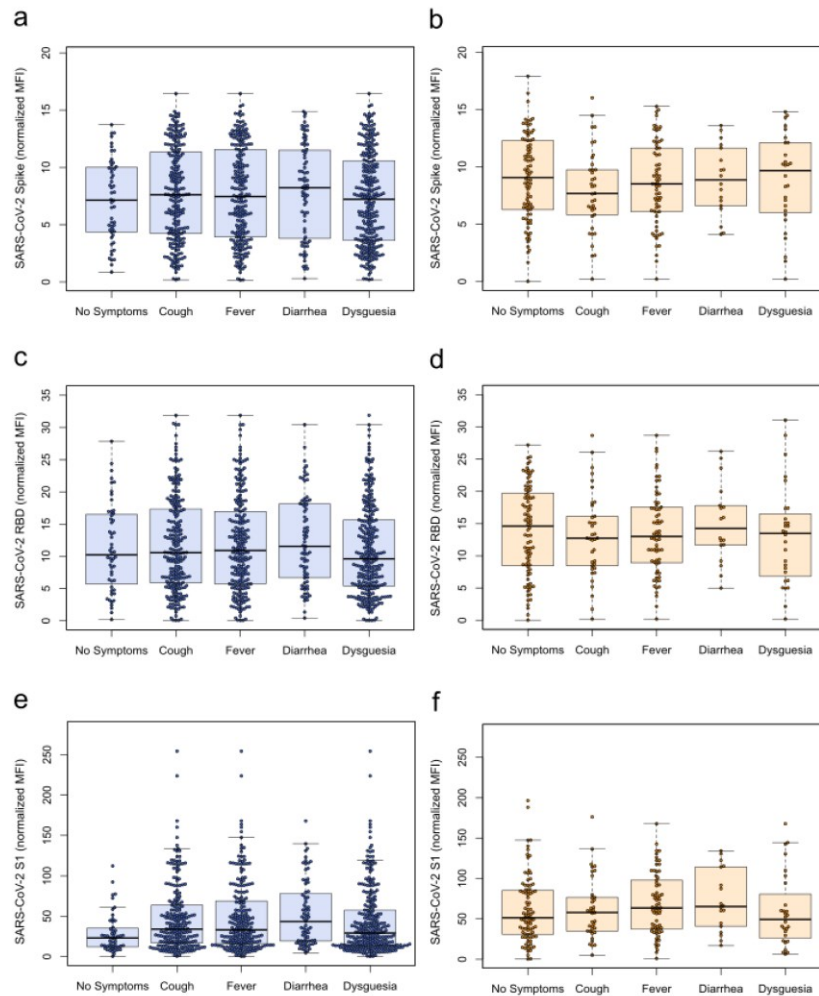
Figure S8 – **Symptoms do not moderate antibody response amongst seropositive individuals after mild COVID-19**. Box and whisker plots with the box representing the median, 25th and 75th percentiles, while whiskers show the largest and smallest non-outlier values. Outliers were identified using upper/lower quartile ±1·5 times IQR. Within the seropositive subgroups, neither adults (blue, a, c, e) nor children (orange, b, d, f) showed any difference in response based on presence of

12

symptoms for either the spike trimer (a and b), receptor binding domain (RBD) (c and

d) or S1 domain (e and f) of SARS-CoV-2. Symptom group sizes: no symptoms –

adults n=36, children n=83, cough – adults n=221, children n=37, fever – adults

n=217, children n=66, diarrhea – adults n=75, children n=18, dysgeusia – adults

n=266, children n=28. MFI – median fluorescence intensity.

13

a

b

c

14
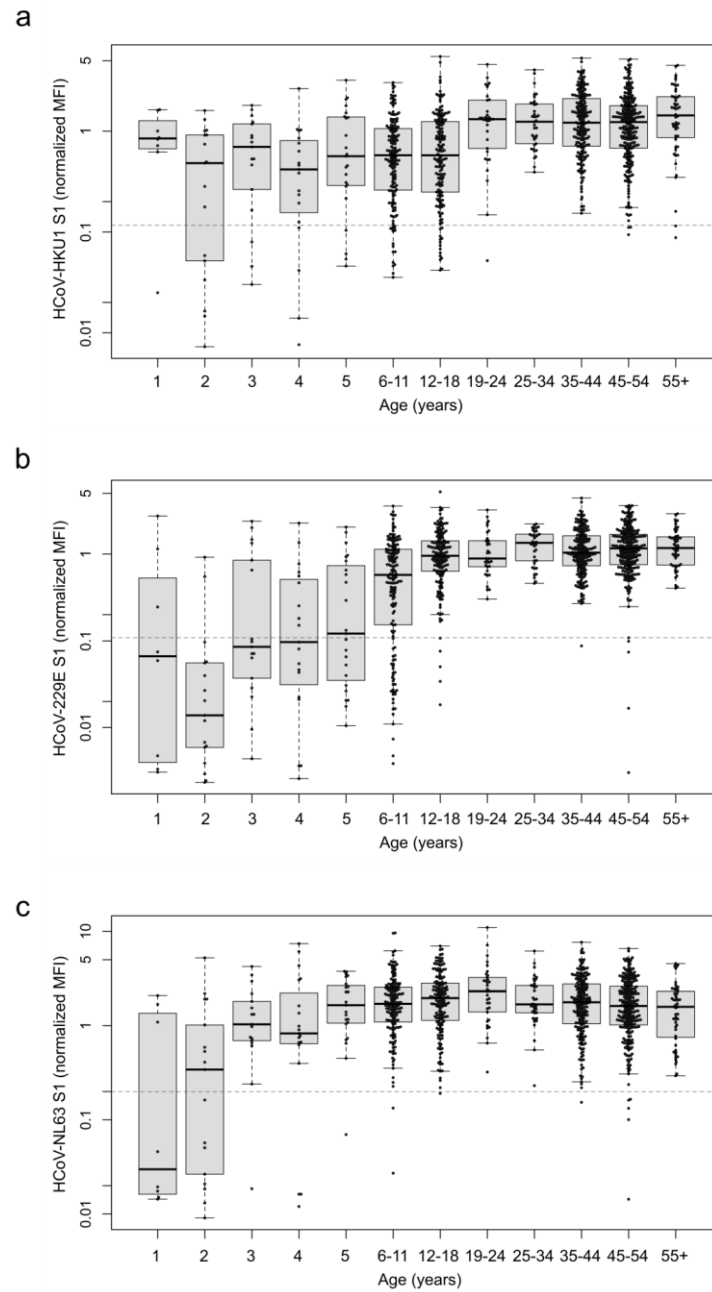
Figure S9 – **Initial HCoV infection often occurs during the first five years of life**.

Box and whisker plots with the box representing the median, 25th and 75th

percentiles, while whiskers show the largest and smallest non-outlier values. Outliers

were identified using upper/lower quartile ±1·5 times IQR. Single ages from 1 to 5 are

shown (1 – n=8, 2 – n=17, 3 – n=17, 4 – n=19, 5 – n=23) with age then grouped into:

6-11 (n=160), 12-18 (n=163), 19-24 (n=34), 25-34 (n=37), 35-44 (n=195), 45-54

(n=346) and over 55 years olds (n=52). For all HCoVs (a – HKU1, b – 229E, c –

NL63), the majority of naïve samples are children. Dashed line indicates one-tenth of

the mean response of all samples. All samples below the dashed line are considered

to be naïve. HCoV – human endemic Coronavirus, MFI – median fluorescence

intensity.

15
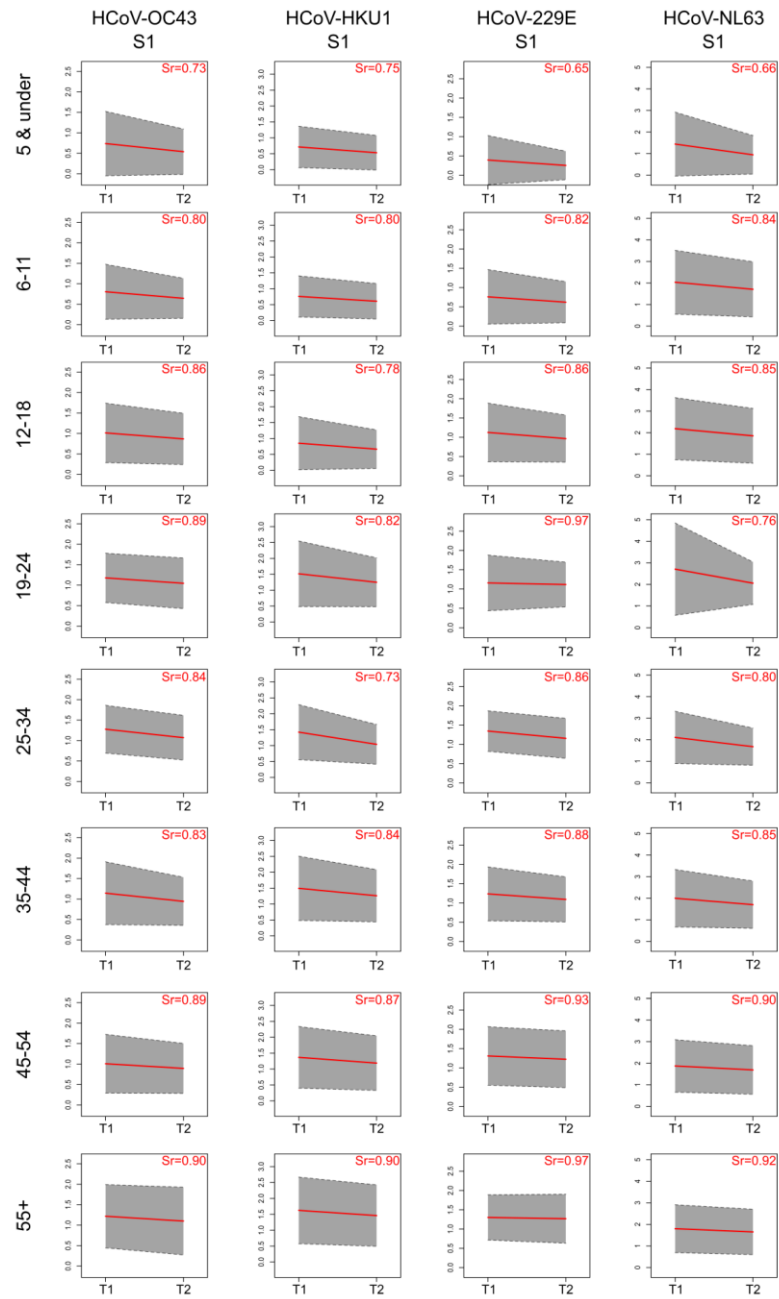
Figure S10 – **Children serorevert faster for HCoVs than adults**. Longitudinal comparison of T1 and T2 samples using MULTICOV-AB to determine the rate of seroreversion. The S1 domain of HCoV-OC43, HCoV-HKU1, HCoV-229E and HCoV-NL63 are shown. Samples are separated into distinct age groups: five years old and under (n=84), 6-11 (n=160), 12-18 (n=162), 19-24 (n=32), 25-34 (n=36), 35-44 (n=182), 45-54 (n=228) and over 55 years old (n=48). Red lines indicate mean rate of decrease; grey boxes indicate ±1 standard deviation. Sr indicates the proportion of signal remaining, calculated as the ratio of the mean MFI at T2 compared to the mean MFI at T1. HCoV – human endemic Coronavirus, MFI – median fluorescence intensity.

17

a

b

c

18
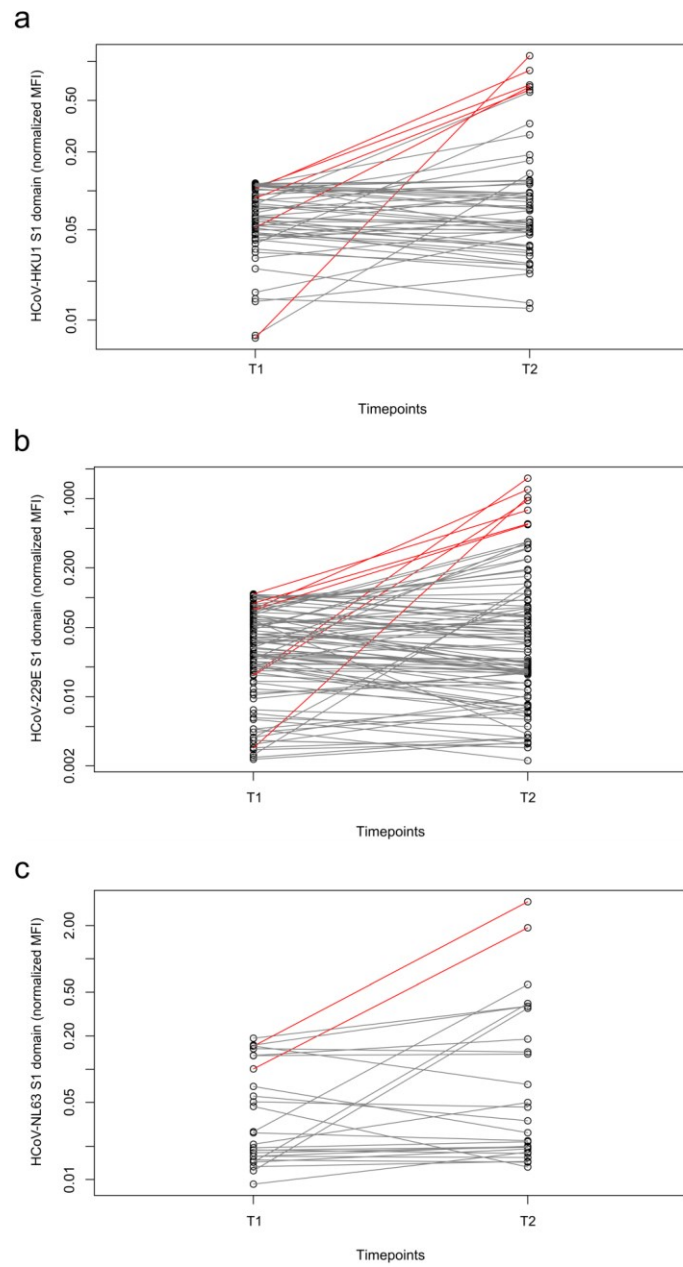
Figure S11 – **Naïve samples are present within the study, although endemic coronavirus infections persisted during the SARS-CoV-2 pandemic**. Line graphs showing longitudinal antibody response from T1 to T2 for samples defined as naïve at T1. Individuals who remain naïve are shown in grey, individuals who seroconvert between T1 and by T2 are shown in red. Not all individuals who show increased HCoV antibody levels at T2 compared to T1 are considered to have been infected, as some remain within the negative range for the assay at T2. Normalized MFI is shown on a logscale for clarity. Although there is variation in the number of naïve samples between the different HCoVs (a – HKU1, b – 229E, c – NL63), new HCoV infections are seen across all HCoVs. HCoV – human endemic Coronavirus, MFI – median fluorescence intensity.

19
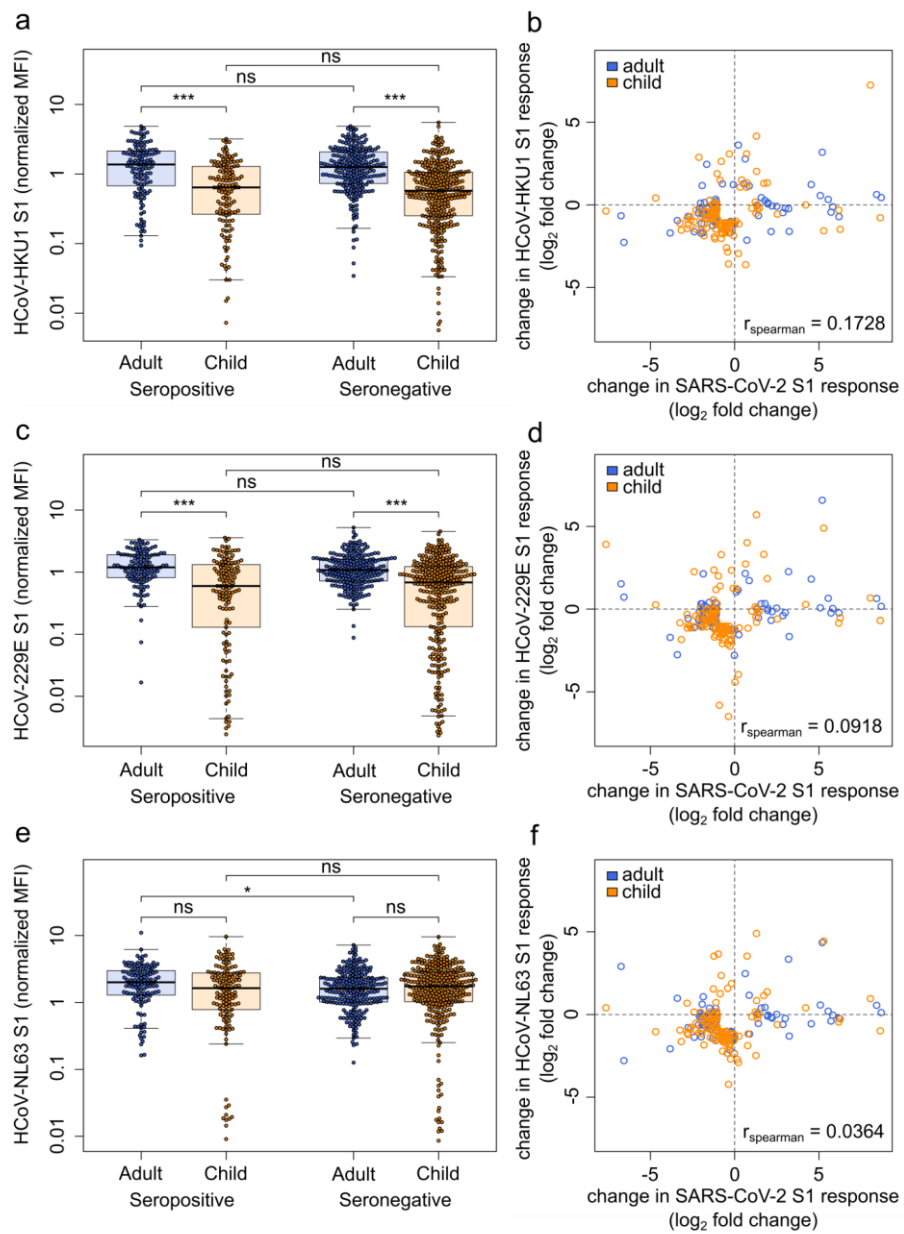
Figure S12 – **HCoVs offer no cross protection towards SARS-CoV-2, nor do they show a boost-back antibody response following SARS-CoV-2 infection**. Samples from households with a known index case were examined with MULTICOV-AB to determine whether the antibody response to endemic coronaviruses (HCoV) provides any protection against SARS-CoV-2. (a, c and e) Box and whisker plots demonstrating no significant difference between SARS-CoV-2 seropositive and seronegative adults (blue, n=440) or children (orange, n=436) in terms of HCoV-HKU1 (a, adult p=0·67, child p=0·47) or HCoV-229E (c, adult p=0·14, child p=0·99). For HCoV-NL63, there was a small significant difference for adults only (e, adults p=0·01, children p=0·35). Boxes represent the median, 25th and 75th percentiles, and whiskers show the largest and smallest non-outlier values. Outliers were identified using upper/lower quartile ± 1·5 times IQR. Statistical significance was calculated by Mann-Whitney-U (two-sided) with *** indicating a p-value <0·001, * indicating a p-value <0·05 and ns indicating a p-value >0·05 (b, d and f). When comparing paired samples longitudinally within the SARS-CoV-2 seropositive subgroup, there was no association between change in SARS-CoV-2 antibody level and change in HCoV antibody level for HCoV-HKU1 (b), HCoV-229E (d) or HCoV-NL63 (f) and in either adults (b - n=79, d – n=74, f – n=80) or children (b - n=117, d – n=114, f – n=118). Change in response is presented as log2-fold change from T1 to T2 and only samples with a log2-fold change > 1 or < -1 are shown. Spearman's rank was used to calculate ordinal associations between the changes in HCoV antibody level and change in SARS-CoV-2 antibody level. MFI – median fluorescence intensity.

21

Supplementary Tables

Table S1 – **Comparative seroprevalence between different assays used in the study**

Assay	Seropositive	Seronegative	Total	% of Seropositive
EuroImmun S1 IgG	991	1245	2236	44.3
Roche Elecsys N pan Ig	1149	1087	2236	51·4
Siemens RBD IgG	1067	1169	2236	47·7
MULTICOV S and RBD IgG	1142	1094	2236	51·1

Only samples that were measured with all four assays are considered. For each assay, the manufacturer or name of the assay is stated, as well as the target antigen and Ig-isotype detected. N – Nucleocapsid, RBD – receptor binding domain, S – spike protein.

22

Table S2 – **Symptom frequency and diagnostic performance in children under 18**

Symptom	Present or Absent	Age group								All children	
		Under 5		6 to 11		12 to 18					
		n (%)	Seropositive (PPV, 95% CI)	n (%)	Seropositive (PPV, 95% CI)	n (%)	Seropositive (PPV, 95% CI)			n (%)	Seropositive (PPV, 95% CI)
Fever	Present	37 (28·03)	17 (0·46, 0·33-0·59)	46 (21·70)	28 (0·61, 0·48-0·72)	28 (13·40)	21 (0·75, 0·57-0·87)			111 (20·07)	66 (0·59, 0·51-0·67)
	Absent	95 (71·97)	23 (0·24, 0·19-0·30)	166 (78·30)	45 (0·27, 0·24-0·31)	181 (86·60)	53 (0·29, 0·27-0·32)			442 (79·93)	121 (0·27, 0·25-0·29)
Cough	Present	28 (21·21)	9 (0·32, 0·19-0·48)	43 (20·28)	14 (0·33, 0·21-0·46)	28 (13·40)	14 (0·50, 0·34-0·66)			99 (17·90)	37 (0·37, 0·29-0·46)
	Absent	104 (78·79)	31 (0·30, 0·25-0·35)	169 (79·72)	59 (0·35, 0·31-0·38)	181 (86·60)	60 (0·33, 0·30-0·36)			454 (82·10)	150 (0·33, 0·31-0·35)
Diarrhea	Present	8 (6·06)	3 (0·38, 0·13-0·71)	17 (8·02)	11 (0·65, 0·41-0·83)	8 (3·83)	4 (0·50, 0·20-0·80)			33 (5·97)	18 (0·55, 0·38-0·70)
	Absent	124 (93·94)	37 (0·30, 0·27-0·32)	195 (91·98)	62 (0·32, 0·30-0·34)	201 (96·17)	70 (0·35, 0·33-0·36)			520 (94·03)	169 (0·33, 0·31-0·34)
Dysguesia	Present	1 (0·76)	1 (1·00, n/a)	7 (3·30)	6 (0·86, 0·42-0·98)	24 (11·48)	21 (0·88, 0·68-0·96)			32 (5·79)	28 (0·88, 0·71-0·95)
	Absent	131 (99·24)	39 (0·30, 0·29-0·30)	205 (69·70)	67 (0·33, 0·32-0·34)	185 (88·52)	53 (0·29, 0·27-0·31)			521 (94·21)	159 (0·31, 0·30-0·31)

The frequency of each symptom within the study population, shown number of individuals (n, also as %) either with (present) or without (absent) this symptom, and the number of individuals (n, also as %) within these groups who were seropositive for SARS-CoV-

23

170

2. Children are split into three groups: under 5-year olds (n=132), 6- to 11-year olds (n=212) and 12- to 18-year olds (n=209). Positive

Predictive Value (PPV) for seropositivity in the presence or absence of each symptom, 95% Confidence Intervals (CI) are standard

logit confidence intervals[1].

24

Table S3 – **List of antigens used in MULTICOV-AB**

Disease	Antigen	Manufacturer	Cat. No.
SARS-CoV-2	Spike Trimer	NMI	-
SARS-CoV-2	RBD	NMI	-
SARS-CoV-2	S1 domain	NMI	-
SARS-CoV-2	S2 domain	Sino	40590
SARS-CoV-2	Nucleocapsid	Aalto	6404-b
SARS-CoV-2	Nucleocapsid N-terminal domain	NMI	-
SARS-CoV-2	RBD alpha variant	NMI	-
SARS-CoV-2	RBD beta variant	NMI	-
HCoV-OC43	S1 domain	NMI	-
HCoV-OC43	Nucleocapsid	NMI	-
HCoV-OC43	Nucleocapsid N-terminal domain	NMI	-
HCoV-HKU1	S1 domain	NMI	-
HCoV-HKU1	Nucleocapsid	NMI	-
HCoV-HKU1	Nucleocapsid N-terminal domain	NMI	-
HCoV-NL63	S1 domain	NMI	-
HCoV-NL63	Nucleocapsid	NMI	-
HCoV-NL63	Nucleocapsid N-terminal domain	NMI	-
HCoV-229E	S1 domain	NMI	-
HCoV-229E	Nucleocapsid	NMI	-
HCoV-229E	Nucleocapsid N-terminal domain	NMI	-

List of antigens included in MULTICOV-AB in this study, including information about their manufacturer, and if available, their category number. Full information on the NMI produced antigens can be found at[2,3].

25

172

Supplementary References

1.   Mercaldo N.D, Lau K.F and Zhou X.H. Confidence intervals for predictive values with an emphasis to case-control studies. Statist Med 2007;26:2170-2183.

2.   Becker M, Dulovic A, Junker D, et al. Immune response to SARS-CoV-2 variants of concern in vaccinated individuals. Nat Commun 2021;12(1):3109.

3.   Becker M, Strengert M, Junker D, et al. Exploring beyond clinical routine SARS-CoV-2 serology using MultiCoV-Ab to evaluate endemic coronavirus cross-reactivity. Nat Commun 2021;12(1):1152.

26

Appendix IV: Comparative Magnitude and Persistence of Humoral SARS-CoV-2 Vaccination Responses in the Adult Population in Germany

Alex Dulovic*, Barbora Kessel*, Manuela Harries*, **Matthias Becker**, Julia Ortmann, Johanna Griesbaum, Jennifer Jüngling, Daniel Junker, Pilar Hernandez, Daniela Gornyk, Stephan Glöckner, Vanessa Melhorn, Stefanie Castell, Jana-Kristin Heise, Yvonne Kemmling, Torsten Tonn, Kerstin Frank, Thomas Illig, Norman Klopp, Neha Warikoo, Angelika Rath, Christina Suckel, Anne Ulrike Marzian, Nicole Grupe, Philipp D. Kaiser, Bjoern Traenkle, Ulrich Rothbauer, Tobias Kerrinnes, Gérard Krause, Berit Lange, Nicole Schneiderhan-Marra & Monika Strengert

    * = Authors contributed equally

Comparative Magnitude and Persistence of Humoral SARS-CoV-2 Vaccination Responses in the Adult Population in Germany

Alex Dulovic[1†], Barbora Kessel[2†], Manuela Harries[2†], Matthias Becker[1], Julia Ortmann[2], Johanna Griesbaum[1], Jennifer Jüngling[1], Daniel Junker[1], Pilar Hernandez[2], Daniela Gornyk[2], Stephan Glöckner[2], Vanessa Melhorn[2], Stefanie Castell[2], Jana-Kristin Heise[2], Yvonne Kemmling[2], Torsten Tonn[3], Kerstin Frank[3], Thomas Illig[4], Norman Klopp[4], Neha Warikoo[2], Angelika Rath[2], Christina Suckel[2], Anne Ulrike Marzian[2], Nicole Grupe[2], Philipp D. Kaiser[1], Bjoern Traenkle[1], Ulrich Rothbauer[1,5], Tobias Kerrinnes[6], Gérard Krause[2,7,8], Berit Lange[2,8*‡], Nicole Schneiderhan-Marra[1*‡] and Monika Strengert[2,7*‡]

[1] NMI Natural and Medical Sciences Institute at the University of Tübingen, Reutlingen, Germany, [2] Department of Epidemiology, Helmholtz Centre for Infection Research, Braunschweig, Germany, [3] German Red Cross Blood Donation Service North East, Dresden, Germany, [4] Hannover Unified Biobank, Hannover Medical School, Hannover, Germany, [5] Pharmaceutical Biotechnology, Department of Pharmacy and Biochemistry, University of Tübingen, Tübingen, Germany, [6] Department of RNA-Biology of Bacterial Infections, Helmholtz Institute for RNA-Based Infection Research, Würzburg, Germany, [7] TWINCORE, Centre for Experimental and Clinical Infection Research, a Joint Venture of the Hannover Medical School and the Helmholtz Centre for Infection Research, Hannover, Germany, [8] German Centre for Infection Research (DZIF), Partner Site Hannover-Braunschweig, Braunschweig, Germany

Recent increases in SARS-CoV-2 infections have led to questions about duration and quality of vaccine-induced immune protection. While numerous studies have been published on immune responses triggered by vaccination, these often focus on studying the impact of one or two immunisation schemes within subpopulations such as immunocompromised individuals or healthcare workers. To provide information on the duration and quality of vaccine-induced immune responses against SARS-CoV-2, we analyzed antibody titres against various SARS-CoV-2 antigens and ACE2 binding inhibition against SARS-CoV-2 wild-type and variants of concern in samples from a large German population-based seroprevalence study (MuSPAD) who had received all currently available immunisation schemes. We found that homologous mRNA-based or heterologous prime-boost vaccination produced significantly higher antibody responses than vector-based homologous vaccination. Ad26.CoV2S.2 performance was particularly concerning with reduced titres and 91.7% of samples classified as non-responsive for ACE2 binding inhibition, suggesting that recipients require a booster mRNA vaccination. While mRNA vaccination induced a higher ratio of RBD- and S1-targeting antibodies, vector-based vaccines resulted in an increased proportion of S2-targeting antibodies. Given the role of RBD- and S1-specific antibodies in neutralizing SARS-CoV-2, their relative over-representation after mRNA vaccination may explain why these vaccines have increased efficacy compared to vector-based formulations. Previously infected individuals

177

had a robust immune response once vaccinated, regardless of which vaccine they received, which could aid future dose allocation should shortages arise for certain manufacturers. Overall, both titres and ACE2 binding inhibition peaked approximately 28 days post-second vaccination and then decreased.

Keywords: SARS-CoV-2, mRNA vaccines, vector-based vaccines, variants of concern, protective immunity, population-based study, longitudinal study, antibody persistence

INTRODUCTION

In response to the global SARS-CoV-2 pandemic, multiple vaccines have been developed, tested and licensed for use within record time (1–4). As vaccination coverage became more widespread at the beginning of 2021, countries experienced a reduction in SARS-CoV-2 infections (5, 6), although case numbers have again begun to increase in recent months due to spread among and by unvaccinated individuals (7) as well as longevity-related reductions in vaccine protection (8–11). Although a measurable correlate of protection that either prevents SARS-CoV-2 infection or limits COVID-19 disease progression is not yet defined, sufficient levels of neutralizing antibodies are assumed to be a key element (12, 13). As in most other countries, the German national vaccination strategy (until June 7th 2021) was based on prioritisation by occupation, underlying medical conditions or advanced age. Currently, 56.8 million German residents are reported to be completely vaccinated (68.3% coverage), with a further 2.4 million having so far received one dose. The majority of doses administered based on delivery numbers in Germany are BNT162b2 from Pfizer (77.0%), followed by Astra Zeneca´s AZD1222 (11.3%), Moderna's mRNA-1273 (8.7%) and Janssen's single-shot Ad26.CoV2.S (3.0%; impfdashboard.de and rki.de as of November 25th 2021). However, based on a lack of efficacy data from phase III clinical trials, the German Standing Committee on Vaccination (STIKO) recommended AZD1222 only for use in those below the age of 60. Following reports of moderate to severe thrombocytopenia and atypical thrombosis cases after AZD1222 vaccination in spring 2021 (14–16), temporary suspensions and eligibility restrictions were not only enacted in Germany (on March 15th 2021) but in 12 other EU member states (17). Administration of AZD1222 was resumed by the 1st of April 2021 in Germany, however only for those above the age of 60 or after an individual risk analysis. Individuals who had received a first dose of AZD1222 and were below the age of 60 were instead offered a mRNA-based vaccine as second dose which resulted in a heterologous prime-boost vaccination scheme (18). Although these "mix and match" approaches were not covered by the initial licensing terms, it has by now been shown that they result in a more robust humoral and cell-mediated immune response compared to the homologous AZD1222 immunisation (19, 20). While multiple studies have so far investigated vaccine-induced responses, predominantly in at-risk groups such as dialysis or transplant recipients (21, 22), groups with increased exposure risk such as

health care workers (23–25) or as part of the initial clinical efficacy trials which in general enroll healthier than average populations (26), we report immunological vaccination response data from the general adult population. By using samples from a population-based seroprevalence study (MuSPAD), which assessed SARS-CoV-2 seroprevalence from July 2020 to August 2021 in eight regions in Germany (27), we examined the dynamics of vaccine-induced humoral responses using MULTICOV-AB (28) and an ACE2-RBD competition assay (29) to analyze ACE2 binding inhibition.

MATERIAL AND METHODS

MuSPAD Study Recruitment

Vaccination responses were analyzed in participants of the multi-local and serial cross-sectional prevalence study on antibodies against SARS-CoV-2 in Germany (MuSPAD) study, a nationwide population-based SARS-CoV-2 seroprevalence study (27) from July 2020 to August 2021. The study was approved by the Ethics Committee of the Hannover Medical School (9086_BO_S_2020). MuSPAD participants were recruited by age- and gender-stratified random sampling based on records from the respective local residents' registration offices. Study locations in eight regions across Germany were selected in spring 2020 based on differing epidemic activity at that time. In addition to the successive cross-sectional study design, certain study locations were sampled longitudinally within a 3-4 month interval. At the study center, following written informed consent, all eligible participants (>18 years) were subject to a standardised computer-based interview using the digital eResearch system PIA (Prospective Monitoring and Management-App) to gather basic sociodemographic data, information on pre-existing medical conditions including a previously confirmed SARS-CoV-2 infection or a SARS-CoV-2 vaccination, once it became available in Germany in late December 2020. Information about SARS-CoV-2 infections or vaccinations are self-reported. After serum was obtained by venipuncture from a serum gel S-Monovette (Sarstedt), samples were aliquoted in Matrix 2D Barcoded Screw Top Tubes (Thermo Scientific) at the Institute of Transfusion Medicine and Immunohematology and frozen at -20°C before being transported on dry ice to the Hannover Unified Biobank (Germany). After registration and quality control, one serum aliquot was shipped to the Natural and Medical Sciences Institute (Reutlingen, Germany) where they were stored at -80°C until analysis.

178

Study Design and Eligibility

Our study contains a total of 1821 samples from 1731 MuSPAD participants which were divided into three subgroups to examine different aspects of the vaccine-induced humoral response. Based on our inclusion criteria, individual samples can be part of several subgroups.

1. Individuals who received a homologous or heterologous complete two-dose vaccination with AZD1222, BNT162b2 and mRNA-1273 or the one-dose vaccine Ad26.CoV2.S with a blood sample taken at least 7 days but no more than 65 days post the last vaccination (hereon referred to as "mix and match sample cohort").
2. Individuals who donated one blood sample following a two-dose homologous vaccination with BNT162b2 or mRNA-1273 within the defined time frames of day 5 to 12, day 26 to 30, day 54 to 58, day 94 to 103, day 129 to 146 or day 176 to 203 after the second dose to monitor antibody kinetics (hereon referred to as "time point sample cohort").
3. Individuals with paired blood samples taken at two separate successive time points where the first sample had to be taken a minimum of seven days after the second homologous dose of BNT162b2 (hereon referred to as "longitudinal sample cohort").

All samples originated from the following locations where the MuSPAD study had previously been scheduled to take place and were collected from January to August 2021: Aachen (Städteregion), Magdeburg (Stadtkreis), Osnabrück (Stadt- und Landkreis), Chemnitz (Stadtkreis) or Landkreis Vorpommern-Greifswald. A flow chart to illustrate sample selection form the entire MuSPAD cohort can be found in **Supplementary Figure 1**. Basic sociodemographic information and details of comorbidities (hypertension, cardiovascular disease, diabetes, lung disease, immunosuppression, cancer) for each group are provided in more detail in **Table 1** and **Supplementary Table 1**. Apart from the homologous BNT162b2 samples which are part of our mix and match sample cohort, the maximum available sample number meeting the specified criteria in groups 1-3 was used. For the homologous BNT162b2 vaccination samples within our mix and match sample cohort, we applied a random selection from the entire available sample pool of BNT162b2 vaccinees who took part in the MuSPAD study to select 771 sera. Individuals with a previous SARS-CoV-2 infection either defined by a positive SARS-CoV-2 PCR or antigen test result, or a MULTICOV-AB nucleocapsid IgG normalisation ratio above 1 are listed separately (hereon referred to as "recovered") within the mix and match sample cohort. Additional sample eligibility criteria were having a complete vaccination record (manufacturer and vaccination dates) and information on age and gender as part of the participant's metadata.

MULTICOV-AB

Vaccine-induced humoral responses were analyzed using MULTICOV-AB (28), a previously published semi-quantitative multiplex immunoassay that includes both antigens of SARS-CoV-2 (e.g. Spike, Receptor Binding Domain (RBD), S1 domain, S2 domain and nucleocapsid) and the endemic coronaviruses (OC43, HKU1, NL63 and 229E). While samples were processed using an automated platform on a Beckman Coulter i7 pipetting robot as previously described (30) with minor modifications, all sample and reagent dilutions were already established and verified as part of the initial MULTICOV-AB technical assay validation process which is detailed in (28). Briefly, samples were thawed at room temperature, vortexed and then centrifuged at 2000 g for 3 mins to pellet any cell debris within the sample. Samples were then opened using a LabElite DeCapper SL (Hamilton Company). Opened sample matrix racks were then loaded into the pipetting robot, where the sample was diluted 1:200 in assay buffer, before being combined in a 384-well plate and mixed 1:1 with 1x bead mix (see **Supplementary Table 2** for antigen panel), resulting in a final dilution of 1:400. Samples were then incubated in a Thermomixer (Eppendorf) for 2 h at 1400 rpm, 20°C, in darkness. Following this initial incubation, samples were washed to remove unbound antibodies using an automated magnetic plate washer (Biotek). Bound IgG was detected by adding R-phycoerythrin labelled goat-anti-human IgG (3 µg/mL; #109-116-098, Jackson Immunoresearch Labs) and incubating for a further 45 mins at 1400 rpm, 20°C, in darkness. Following a further washing step, beads were resuspended in 100 µl of wash buffer, shaken for 1 min at 1400 rpm and then measured once on a FLEXMAP 3D instrument (Luminex Corporation) using the following settings: Timeout 100 sec, Gate 7500-15000, Reporter Gain: Standard PMT, 40 events. To ensure reproducibility, 3 quality control (QC) samples were included in octuplicate per plate. Additionally, each plate had to pass 3 QC criteria to be considered as valid run: first, throughout acquisition each sample had to reach a minimum bead count of 35 per bead ID, second median fluorescence intensity (MFI) values of sample and signal system control beads and third plate-by-plate QC sample controls had to be within normal range. Beads coupled with human IgG and goat-anti-human IgG were utilized to control for sample and signal system addition. Any sample that failed QC was remeasured for MULTICOV-AB and the ACE2-RBD competition assay (30/1821). Raw MFI values were normalised to a QC sample for all antigens as in (24, 31). A Signal to Cutoff ratio (S/CO) of 1 or above for both the trimeric Spike and RBD antigen was defined as reactive for SARS-CoV-2 Spike-specific IgG.

ACE2-RBD Competition Assay

To enable high-throughput screening of ACE2-RBD binding inhibition in the presence of sera, a previously established ACE2-RBD competition assay (29) was automated on a Beckmann Coulter i7 pipetting robot with minor modifications. 1:20 previously diluted samples from MULTICOV-AB were diluted 1:200 in ACE2 buffer (29) containing 150 ng/mL biotinylated ACE2. Samples were then mixed 1:1 with 1x VoC (Variant of Concern) bead mix containing RBDs of SARS-CoV-2 wild-type and the Alpha, Beta, Gamma, Delta VoCs (**Supplementary Table 3**), resulting in a final dilution of 1:400. Samples were then incubated in a Thermomixer for 2 h at 1400 rpm, 20°C, in darkness. Following this initial incubation, samples were washed to remove unbound ACE2 using an automated magnetic plate

179

TABLE 1 | Demographics of study population (n. a., not applicable; NA, not available).

Sample cohort (n)	SARS-CoV-2 infection status* (n)	Vaccine (n)	Mean ΔT (SD) in days post-vaccination	Mean ΔT (SD) in days between doses	Age (y), median (IQR)	Female (n, %)	Comorbidities (min. 1/person) (n, %)	Number of comorbidities (mean, SD)
Mix and match (1470)	+ (70)	M/M (13)	34.7 (16.3)	42.5 (27.9)	59 (11)	8 (61.5)	5 (38.5)	0.5 (0.8)
		P/P (33)	31.5 (13.5)	25.3 (9.6)	66 (29)	25 (75.8)	13 (39.4)	0.6 (0.9)
		A/A (12)	35.3 (13.5)	70.3 (19.8)	69 (7)	7 (58.3)	10 (83.3)	1.3 (0.9)
		A/M (1)**	17.0 (0.0)	66.0 (0.0)	age group 66-79	0 (0.0)	1 (100.0)	1.0 (0.0)
		A/P (6)	47.8 (14.5)	72.0 (11.6)	57 (25)	3 (50.0)	4 (66.7)	0.8 (0.7)
		J (5)	42.2 (18.0)	n. a.	40 (15)	3 (60.0)	3 (60.0)	0.6 (0.5)
	- (1400)	M/M (272)	36.5 (16.5)	31.2 (7.1)	56 (26)	162 (59.6)	108 (39.7)	0.6 (0.8)
		P/P (738)	34.7 (17.1)	27.9 (9.7)	59 (26)	456 (61.8)	438 (4 NA; 46.1)	0.7 (1.0)
		A/A (228)	37.3 (13.8)	73.6 (10.9)	66 (10)	122 (53.5)	114 (50.0)	0.7 (0.9)
		A/M (24)	20.8 (7.8)	69.6 (16.9)	68 (5)	15 (62.5)	14 (58.3)	0.8 (0.8)
		A/P (114)	31.6 (17.4)	72.2 (14.8)	59 (20)	64 (56.1)	55 (48.3)	0.8 (1.0)
		J (24)	49.8 (10.8)	n. a.	62 (14)	15 (62.5)	11 (45.8)	0.8 (1.2)
Time points (597)	–	P/P (107)	6.9 (1.4)	34.7 (13.5)	64 (26)	57 (53.3)	61 (57.0)	0.8 (0.9)
		M/M (40)	6.7 (1.3)	39.7 (11.2)	58 (27)	20 (50.0)	15 (37.5)	0.5 (0.8)
		P/P (103)	27.9 (1.4)	28.2 (9.9)	52 (42)	60 (58.3)	42 (1 NA; 41.2)	0.8 (1.1)
		M/M (8)	28.1 (1.4)	30.3 (4.7)	67 (39)	5 (62.5)	3 (37.5)	0.5 (0.7)
		P/P (92)	55.9 (1.5)	29.1 (9.6)	61 (20)	60 (65.2)	45 (48.9)	0. 8 (1.0)
		M/M (22)	55.5 (1.2)	28.0 (0.3)	57 (15)	17 (77.3)	5 (22.7)	0.3 (0.6)
		P/P (139)	97.7 (2.6)	22.3 (4.0)	60 (22)	87 (62.6)	72 (51.8)	0.8 (1.0)
		M/M (7)	98.1 (2.6)	28.9 (2.3)	64 (8)	5 (71.4)	3 (42.9)	0.9 (1.1)
		P/P (38)	138.0 (3.8)	21.0 (2.2)	80 (24)	25 (68.8)	24 (63.1)	1.2 (1.2)
		M/M (5)	141.0 (5.1)	29.2 (1.6)	83 (4)	2 (40.0)	3 (60.0)	1.2 (1.2)
		P/P (36)	189.0 (5.6)	21.7 (1.4)	50 (13)	30 (83.3)	11 (30.6)	0.4 (0.6)
		M/M (0)	n. a	n. a.	n. a.	n. a.	n. a.	n. a.
Longitudinal (180)	–	P/P T1 (90)	27.9 (14.8)	21.3 (1.2)	58 (34)	65 (72.2)	45 (2 NA; 51.1)	0.8 (1.0)
		P/P T2 (90)	166.4 (19.4)		58 (33)	65 (72.2)	48 (53.3)	0.7 (1.0)

Different vaccines and combinations are abbreviated as follows: M/M (two-dose mRNA-1273), P/P (two-dose BNT162b2), A/A (two-dose AZD1222), A/M (first dose AZD1222, second dose mRNA-1273), A/P (first dose AZD1222, second dose BNT162b2) and J (one-dose Ad26.CoV2.S). The time points sample cohort contains only homologous BNT162b2 and mRNA-1273 samples. The longitudinal sample cohort contains only paired homologous BNT162b2 taken at time 1 (T1) or 2 (T2).
*Based on self-reported positive PCR/antigen test result at study center visit and/or MULTICOV-AB nucleocapsid IgG S/CO ratio above 1; **only age group reported as n=1.

washer. ACE2 was detected using R-phycoerythrin labelled streptavidin (2 μg/mL, #SAPE-001, Moss) by incubating the bead-sample mix for a further 45 mins at 1400 rpm, 20°C, in darkness. Following a further washing step, beads were resuspended in 100 μl of wash buffer, shaken for 1 min at 1400 rpm and then measured once on a FLEXMAP 3D instrument using the following settings: Timeout 100 sec, Gate 7500-15000, Reporter Gain: Standard PMT, 40 events. As controls, 12 blank wells, 10 wells with 150 ng/mL ACE2 alone and 10 wells with an ACE2 QC sample were included. ACE2 binding inhibition was calculated as percentage ACE2 inhibition as in (29) with 100% indicating maximum ACE2 binding inhibition and 0% no ACE2 binding inhibition. Samples with an ACE2 binding inhibition less than 20% are classified as non-responders (29).

Data Analysis and Statistics

Initial results collation and matching to metadata was done in Excel 2016 and R 4.1.0 (32).

For pair-wise comparisons of titres and ACE2 binding inhibition between vaccination schemes within our mix and match sample cohort, we used a two-sided generalized Wilcoxon test also referred to as Brunner-Munzel test (33) with a significance level of 0.05 as part of the lawstat package (34). In each comparison of two vaccination schemes, the test assesses if a titre (or ACE2 binding inhibition) tends to larger (smaller) values under one vaccination scheme in comparison to the other. Where indicated, we adjusted for multiple testing by using the Bonferroni-Holm's procedure (35) to control the family-wise error rate to be at most 0.05.

To investigate the impact of age, sex, comorbidities and time post-vaccination on the ACE2 binding inhibition between the different vaccination schemes, we used a normal linear mixed model for logit-transformed ACE2 binding inhibition. Negative measurement values were replaced by 0.001 to enable the transformation. The model included additive effects of age, sex, time post-vaccination (peak response period: 7-27 days vs plateau response period: 28-65 days) and comorbidities [cardiovascular disease, hypertension, diabetes, lung disease and cancer/immunosuppression (which were combined to a binary indicator based on low sample numbers)]. The model further included a random effect defined by the variable "plate number" to account for dependencies due to the measurement procedure, and allowed for heteroscedastic variances for younger (<=70) and older (>70) ages and vaccination types. REML estimation was implemented using the lme function [nlme library (36)]. Statistical testing was based on the asymptotic normality of the estimates. As part of a sensitivity analysis, we extended the model with interaction terms between each confounder and the time post-vaccination, allowing for possibly differing effects in the peak (7-27 days) and plateau (28-65 days) period after the last vaccination.

180

Since the effects of the considered covariates were allowed to differ between the individual vaccination schemes, we analyzed only four vaccination schemes (BNT162b2-BNT162b2, mRNA-1273-mRNA-1273, AZD1222-BNT162b2, AZD1222-AZD1222) with a reasonable sample size in the mix and match study cohort, while we excluded immunisation with AZD1222-mRNA-1273 and Ad26.CoV2.S due to the low sample number of 24 per scheme. Additionally, four individuals with a BNT162b2-BNT162b2 vaccination with missing comorbidity metadata were excluded from this analysis. The described statistical comparison of vaccination schemes within the mix and match cohort was performed after the exclusion of recovered individuals.

To assess the impact of a previous SARS-CoV-2 infection on RBD antibody titres and wild-type ACE2 binding inhibition among the different vaccination schemes, we also used a two-sided generalized Wilcoxon (Brunner-Munzel) test.

To generate a heat map for comparing antigen-specific antibody formation across different vaccination schemes within the mix and match sample cohort, normalised antibody responses were initially scaled using the function "z-score", before being plotted as a heat map. To evaluate longitudinal changes in antibody response and ACE2 binding inhibition within our longitudinal sample cohort, changes from T1 to T2 were calculated using log2 fold change. Any increase in titre or binding is represented by a positive value, while decreases in titre or binding are represented by negative values.

Data visualization was done in RStudio (Version 1.2.5001 running R version 3.6.1). Additional packages "gplots" (37) and "beeswarm" (38) were used for specific displays (22). Graphs were exported from RStudio and further edited in Inkscape (Version 0.92.4) to generate final figures.

RESULTS

First, we examined differences in humoral responses between individuals who received homologous or heterologous immunisation schemes within our mix and match sample cohort where vaccine dose distribution is similar to the German vaccine coverage. Using MULTICOV-AB, we compared vaccination-induced antibody titres generated against the full-length Spike trimer, RBD, S1 and S2 domains and found that mRNA-based homologous vaccinations induced a greater Spike (median normalised MFI: mRNA-1273 13.78, BNT162b2 12.49, AZD1222 5.68, Ad26.CoV2.S 3.65), RBD (median normalised MFI: mRNA-1273 29.12, BNT162b2 24.89, AZD1222 9.61, Ad26.CoV2.S 5.25) and S1 response (median normalised MFI: mRNA-1273 195.9, BNT162b2 139.8, AZD1222 56.40, Ad26.CoV2.S 10.14) than vector-based ones (**Figure 1**). When comparing between the two vector-based vaccinations, the two-dose immunisation with AZD1222 resulted in higher titres than the one-dose Ad26.CoV2.S from Janssen. For mRNA vaccines, Moderna's mRNA-1273 produced a significantly higher response than Pfizer's BNT162b2 (p-values <0.001, **Supplementary Table 5**). Heterologous dose vaccination schemes resulted in comparable titres (for Spike and RBD) as homologous mRNA vaccine regimens

among our study group independent of the origin of the second dose (Spike normalised MFI: AZD1222-mRNA-1273 13.59, AZD1222-BNT162b2 13.27, RBD normalised MFI: AZD1222-mRNA-1273 28.17, AZD1222-BNT162b2 25.93). Heterologous titres were in addition significantly higher than those after a homologous AZD1222 two-dose immunisation (p-values <0.001, **Supplementary Table 5**). In line with their lower titres, serological non-responder rate (defined as a Signal to Cutoff ratio (S/CO) below 1 for either Spike or RBD antigen) was highest for vector-based homologous vaccination schemes (**Table 2**).

As multiplex-based serology tests such as MULTICOV-AB offer the unique opportunity for in-depth profiling of polyclonal antibody reactivity towards multiple viral antigens, we then assessed differences in antibody specificities between the different vaccines. Within the mix and match sample cohort, we observed that mRNA-based SARS-CoV-2 vaccinations resulted in reduced S2-specific antibody titres compared to vector-based ones (**Figure 1**). To investigate this unequal antibody distribution further, we initially scaled titres for each individual antigen (**Figure 2**), and found that while Spike, RBD, S1 titres were low for both AZD1222 and Ad26.CoV2.S, S2-specific titres were considerably higher than expected. We then calculated proportional ratios between antigens (**Table 3**), confirming that homologous mRNA vaccination resulted in significantly higher proportion of RBD- (mRNA-1273 14.01-fold, BNT162b2 18.63-fold, AZD1222 5.23-fold) and S1-targeted antibodies (mRNA-1273 97.21-fold, BNT162b2 110.10-fold, AZD1222 33.48-fold) compared to S2-targeted immunoglobulins. This over-representation of S1-targeting antibodies following mRNA vaccination, was also present in those who received a heterologous immunisation scheme (AZD1222-mRNA-1273 47.60-fold, AZD1222-BNT162b2 65.06-fold).

Having determined that mRNA vaccines produce a significantly higher proportion of RBD and S1 antibodies, we next investigated their ACE2 binding inhibition as these antigens are predominantly responsible for antibody-mediated virus neutralization (12, 13). For this, we used a previously published ACE2-RBD competition assay (22, 29, 30), which detects neutralizing antibody activity only and is comparable to classical viral neutralization assays (24, 29). As expected, homologous mRNA vaccination resulted in higher ACE2 binding inhibition than homologous vector-based vaccination (median ACE2 binding inhibition mRNA-1273 93.1%, BNT162b2 80.1%, AZD1222 38.5%, Ad26.CoV2.S 3.3%, **Figure 3**). Neutralizing antibodies generated following vaccination with Ad26.CoV2.S resulted in minimal ACE2 binding inhibition, with only 8.3% being classified as responders (29). As variants of concern now comprise the majority of infections globally (39), we also assessed ACE2 binding inhibition against the Alpha, Beta, Gamma and Delta SARS-CoV-2 VoC strains. ACE2 binding inhibition was most similar to wild-type for the Alpha variant, followed by Delta whereas Beta and Gamma variants had the largest reductions in ACE2 binding inhibition (**Supplementary Figure 2**).

Due to the range of responses recorded for each dose combination and likely differences in population characteristics

FIGURE 1 | Different SARS-CoV-2 vaccination schemes result in distinct humoral responses. IgG antibody titres against full-length Spike trimer **(A)**, receptor-binding domain (RBD) **(B)**, S1 domain **(C)** and S2 domain **(D)** were measured with MULTICOV-AB. Individuals received either homologous mRNA-1273 (M/M, blue, n = 272), BNT162b2 (P/P, orange, n = 738) or AZD1222 (A/A, green, n = 228), heterologous AZD1222-mRNA-1273 (A/M, light blue, n = 24), AZD1222-BNT162b2 (A/P, light green, n = 114), or a single dose of Ad26.CoV2.S (J, grey, n = 24). Raw MFI values were normalised against QC samples to generate signal ratios for each antigen. Data is shown as box and whisker plots overlaid with strip charts. Boxes represent medians, 25th and 75th percentiles and whiskers show the largest and smallest non-outlier values based on 1.5 IQR calculation. Time between sampling and full vaccination is displayed as mean and SD for each group. Number of samples per vaccination scheme are stated below.

as a result of changing vaccine recommendations, we examined whether confounders (sampling time post-vaccination (ΔT), age, gender or comorbidities) were instead responsible. To analyze impact of ΔT, we separated samples into 7 to 27 days post-final dose to capture peak response and 28 to 65 days post-final dose to capture plateau response (**Figure 4**). While there was a reduction in median response for samples from individuals collected within the plateau phase, the pattern between the vaccines remained consistent. While increasing age did result in small reductions in ACE2 binding inhibition (only significant for BNT162b2, $p<0.001$), the vaccine dosing scheme received had a substantially larger effect, with the eldest age group (>79) of homologous mRNA vaccine recipients still having increased IgG titres and ACE2 inhibition capacities than the youngest (26 to 45) AZD1222 recipients (**Figure 4**). Regression modelling for ACE2 binding inhibition against wild-type confirmed the decrease of ACE2 binding inhibition with time post-vaccination for all vaccination types except homologous AZD1222 (**Supplementary Table 4A**). While age did not cause a significant decrease for homologous AZD1222, this may have

been due to the low number of samples at both ends of the age range within our cohort. For mRNA-1273, while age did result in a significant decrease during the peak period ($p=0.029$), this was not present within the plateau phase ($p=0.615$). For homologous BNT162b2 vaccination, male sex seemed to be associated with a decreased ACE2 binding inhibition, although the same was not true for mRNA-1273. Similar patterns were observed for the ACE2 binding inhibition against Alpha, Beta, Gamma and Delta VoCs (**Supplementary Tables 4B–E**). As we observed serological non-responders within our mix and match study cohort, we systematically evaluated their distribution among the different immunisation schemes (**Table 2**). Overall, vector-based homologous vaccination (2.8%) resulted in a higher proportion of non-responders than homologous mRNA-based vaccination (0.9%). Neither age nor gender was a determining factor in being a non-responder.

As our population-based cohort also contained individuals who had been previously infected and then vaccinated, we examined what effect this had upon their vaccine-induced response. As previously observed (40), recovered and then

TABLE 2 | Vaccine non-responder rates across study population.

Sample cohort (n)	ΔT range post-vaccination (days)	Vaccine (n)	Non-responders MULTICOV-AB (n, %)	Non-responders ACE2-RBD WT (n, %)
Mix and match (1400)	7-65	M/M (272)	0 (0.0)	0 (0.0)
		P/P (738)	9 (1.2)	18 (2.4)
		A/A (228)	4 (1.8)	26 (11.4)
		A/M (24)	0 (0.0)	0 (0.0)
		A/P (114)	0 (0.0)	0 (0.0)
		J (24)	3 (12.5)	22 (91.7)
Time points (597)	5-12	P/P (107)	6 (5.6)	13 (12.2)
		M/M (40)	1 (2.5)	1 (2.5)
	26-30	P/P (103)	1 (1.0)	2 (1.9)
		M/M (8)	0 (0.0)	0 (0.0)
	54-58	P/P (92)	1 (1.1)	3 (3.3)
		M/M (22)	0 (0.0)	0 (0.0)
	94-103	P/P (139)	2 (1.4)	8 (5.8)
		M/M (7)	0 (0.0)	0 (0.0)
	129-146	P/P (38)	3 (7.9)	2 (5.3)
		M/M (5)	1 (20.0)	1 (20.0)
	176-203	P/P (36)	0 (0.0)	8 (22.2)
		M/M (0)	n. a.	n. a.
Longitudinal (180)	T1: 7-63	P/P T1 (90)	2 (2.2)	3 (3.3)
	T2: 121-203	P/P T2 (90)	2 (2.2)	17 (18.9)

MULTICOV-AB non-responders were determined as in (28), with samples that had a signal to cutoff ratio below 1 for either the Spike or RBD being considered non-responders. ACE2-RBD non-responders were determined as in (29), with samples that had a ACE2 binding inhibition less than 20% being considered non-responders. Different vaccines and combinations are abbreviated as follows: M/M (two-dose mRNA-1273), P/P (two-dose BNT162b2), A/A (two-dose AZD1222), A/M (first dose AZD1222, second dose mRNA-1273), A/P (first dose AZD1222, second dose BNT162b2) and J (one-dose Ad26.CoV2.S). The time points sample cohort contains only homologous BNT162b2 and mRNA-1273 samples. The longitudinal sample cohort contains only paired homologous BNT162b2 taken at time 1 (T1) or 2 (T2).

vaccinated individuals developed high levels of IgG with strong ACE2 binding inhibition (**Figure 5** and **Supplementary Table 6**). While mRNA or heterologous vaccination of recovered individuals still elevated median RBD IgG titres (mRNA-1273 31.81, BNT162b2 32.23, AZD1222-mRNA-1273 35.18, AZD1222-BNT162b2 30.49, **Supplementary Figure 3**) and median ACE2 binding inhibition (mRNA-1273 98.1%, BNT162b2 98.8%, AZD1222-mRNA-1273 99.3%, AZD1222-BNT162b2 97.7%, **Figure 5**), increases were particularly apparent for the vector-based vaccinations where median RBD IgG titres (AZD1222 24.69, Ad26.CoV2.S 36.53, **Supplementary Figure 3**) and median ACE2 binding inhibition (AZD1222 92.9%, Ad26.CoV2.S 70.8%, **Figure 5**) were significantly higher than in SARS-CoV-2 naïve vaccinated individuals (median RBD IgG mRNA-1273 29.12, BNT162b2 24.89, AZD1222-mRNA-1273 28.17, AZD1222-BNT162b2 25.93, AZD1222 9.61, Ad26.CoV2.S 5.25, **Figure 1**) and median ACE2 binding inhibition (mRNA-1273 93.1%, BNT162b2 80.1%, AZD1222-mRNA-1273 94.5%, AZD1222-BNT162b2 88.6%, AZD1222 38.5%, Ad26.CoV2.S 3.3%, **Figure 3**).

Having determined that mRNA-based vaccination resulted in an increased humoral response, we evaluated lifespan and antibody response kinetics using our time point sample cohort which were selected to mimic key response periods for antibody-producing B-cell activity such as expansion, peak and plateau phase after a complete vaccination scheme. Vaccine-induced titres and ACE2 binding inhibition both initially increased, peaked during the second time point (26 to 30 days post-second dose), and then decreased linearly as time increased (**Figure 6** and **Supplementary Table 7**). ACE2 binding inhibition followed the same pattern of decrease as time increased. In contrast to antibody levels, the percentage of

non-responders showed however a trend for increased decline already from time point 94 to 103 days post-second vaccination onwards for BNT162b2, with 22.2% of samples considered as non-responders at 176-203 days post-second vaccination (**Table 2**). As already observed in **Figure 1**, mRNA-1273 (blue line) resulted in higher titres and ACE2 binding inhibition compared to BNT162b2 (yellow line) for all monitored time points. To validate this pattern of decreasing antibody titres and ACE2 inhibition activity, we examined samples from a cohort of longitudinal donors (longitudinal sample cohort). Unlike the time point sample cohort, this cohort contained paired samples from each donor which allows to directly compare changes in titre and neutralization activity from the first sampling to the second sampling. While these samples had a variable initial ΔT post-full vaccination (7-63 days), the sampling intervals between first and second donation were more comparable (114-163 days). Overall, mean reduction in RBD-specific antibody titres were 66.3% between their first and second sampling (**Figure 7**). Among the different SARS-CoV-2 antigens, RBD and S1 antibodies had the largest decrease, while Spike Trimer and S2 had the smallest. This reduction in titre was also reflected in ACE2 binding inhibition from the first to second sampling for both the wild-type RBD which was reduced substantially (mean difference of 42%) and for all the VoC RBDs (mean difference: Alpha 36%, Beta 30%, Gamma 29%, Delta 38%).

DISCUSSION

We report both significant and substantial differences in humoral responses generated by the different vaccines and immunisation schemes currently available in Germany, with homologous

183

FIGURE 2 | Humoral immune response after mRNA vaccination is skewed towards increased RBD and S1 titres, while vector-based vaccination results in increased S2 antibody levels. Antigen-specific antibody titres measured in the mix and match sample cohort were scaled and centered per antigen. Resulting values greater than 2.5 and smaller than -2.5 were set to these extreme values instead. Samples were then clustered within their subgroups based on immunisation scheme and are displayed as a heat map. Negative values represent below average titres and positive values represent positive above average titres per antigen. Colour shades indicate low (grey) to high (red) value distribution. A/A – two-dose AZD1222. A/M – first dose AZD1222, second dose mRNA-1273. A/P – first dose AZD1222, second dose BNT162b2. M/M – two-dose mRNA-1273. P/P – two-dose BNT162b2. J – one-dose Ad26.CoV2.S.

184

TABLE 3 | Antigen-specific ratios for different vaccination schemes.

Vaccine	Antibody target (95% CI)					
	RBD vs S	S1 vs S	S1 vs RBD	S vs S2	RBD vs S2	S1 vs S2
A/A	1.72 (1.66-1.78)	10.09 (9.72-10.47)	5.89 (5.73-6.11)	3.38 (3.04-3.60)	5.23 (4.65-6.07)	33.48 (27.92-37.56)
A/M	1.97 (1.85-2.26)	16.71 (15.04-18.37)	8.15 (7.86-8.68)	2.76 (2.15-3.48)	5.86 (4.58-6.28)	47.60 (41.28-53.66)
A/P	1.97 (1.90-2.04)	14.16 (13.42-14.64)	7.17 (6.95-7.36)	4.76 (4.08-5.46)	8.60 (7.85-10.53)	65.06 (58.95-69.61)
M/M	2.10 (2.06-2.12)	14.19 (13.67-14.47)	6.80 (6.61-6.93)	6.88 (6.24-7.55)	14.01 (12.74-15.09)	97.21 (92.07-100.90)
P/P	2.00 (1.96-2.04)	11.21 (10.95-11.52)	5.72 (5.64-5.78)	9.99 (9.48-10.43)	18.63 (17.82-20.00)	110.10 (104.20-114.10)
J	1.23 (0.97-1.61)	3.30 (2.72-4.18)	2.79 (2.35-4.06)	8.89 (3.71-13.27)	6.83 (4.70-22.35)	31.53 (15.53-38.63)

Ratios were calculated by dividing normalised MFI values for the two targets for all samples. RBD – receptor-binding domain, S – full-length trimeric Spike protein. Median values with 95% CI in brackets are shown. A/A – two-dose AZD1222. A/M – first dose AZD1222, second dose mRNA-1273. A/P – first dose AZD1222, second dose BNT162b2. M/M – two-dose mRNA-1273. P/P – two-dose BNT162b2. J – one-dose Ad26.CoV2.S.
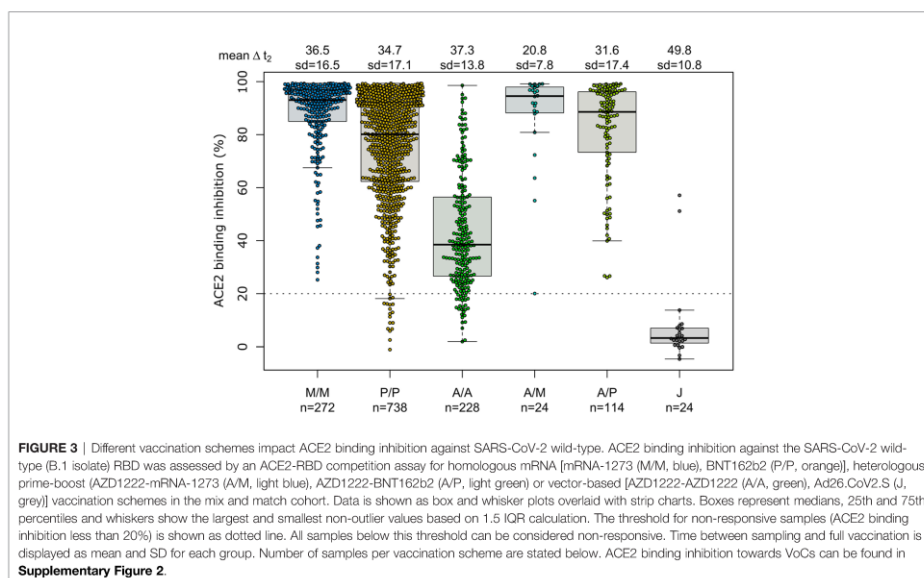
FIGURE 3 | Different vaccination schemes impact ACE2 binding inhibition against SARS-CoV-2 wild-type. ACE2 binding inhibition against the SARS-CoV-2 wild-type (B.1 isolate) RBD was assessed by an ACE2-RBD competition assay for homologous mRNA [mRNA-1273 (M/M, blue), BNT162b2 (P/P, orange)], heterologous prime-boost (AZD1222-mRNA-1273 (A/M, light blue), AZD1222-BNT162b2 (A/P, light green) or vector-based [AZD1222-AZD1222 (A/A, green), Ad26.CoV2.S (J, grey)] vaccination schemes in the mix and match cohort. Data is shown as box and whisker plots overlaid with strip charts. Boxes represent medians, 25th and 75th percentiles and whiskers show the largest and smallest non-outlier values based on 1.5 IQR calculation. The threshold for non-responsive samples (ACE2 binding inhibition less than 20%) is shown as dotted line. All samples below this threshold can be considered non-responsive. Time between sampling and full vaccination is displayed as mean and SD for each group. Number of samples per vaccination scheme are stated below. ACE2 binding inhibition towards VoCs can be found in **Supplementary Figure 2**.

mRNA or combined heterologous vector and mRNA vaccination approaches inducing significantly higher titres and ACE2 binding inhibition compared to homologous vector-based vaccination schemes. This expands on results from on-going randomized and observational trials such as the ComCoV (41) or CoCo (42) study which provided only information on AZD1222-BNT162b2 schemes (20, 43). Further, as expected titres and ACE2 binding inhibition for AZD1222 were reduced compared to mRNA-based vaccination (43). Among homologous mRNA regimens, we identified like others, that mRNA-1273 resulted in higher antibody titres and ACE2 binding inhibition than BNT162b2 (40, 44). Extending time periods between successive doses of mRNA and vector-based vaccinations also positively impacted on serological and cellular response levels or vaccine

efficiency and effectiveness (1, 45–49). The German STIKO recommended at the time of the study dosing intervals of six weeks between mRNA vaccines, 12 weeks for vector vaccines and 9-12 weeks for heterologous vaccination approaches (18). While heterologous and vector vaccination dosing intervals in our mix and match cohort adhere more closely to those extended intervals (1), time periods for mRNA vaccine dosing across our study population mimic 21 or 28 days from clinical trials (3, 4) and licensing agreements (50, 51) making them unlikely contributors to the observed differences in humoral responses. While we have used an ACE2-RBD competition assay to measure ACE2 binding inhibition as opposed to classic virus neutralization assays, this assay analyses neutralizing antibodies as seen by its similar performance to VNT (24, 29). ACE2

185

FIGURE 4 | Effect of time post-vaccination, gender and age on ACE2 binding inhibition for different SARS-CoV-2 vaccination schemes. ACE2 binding inhibition against the SARS-CoV-2 wild-type (B.1 isolate) RBD was assessed by an ACE2-RBD competition assay. Samples were split according to vaccination scheme (homologous mRNA [mRNA-1273 (M/M, blue), BNT162b2 (P/P, orange)], heterologous prime-boost (AZD1222-mRNA-1273 (A/M, light blue), AZD1222-BNT162b2 (A/P, light green) or vector-based [AZD1222-AZD1222 (A/A, green), Ad26.CoV2.S (J, grey)]. To display impact of potential confounders, samples were further split in time post-vaccination up to 27 and above 27 days **(A)**, gender **(B)** and indicated age groups **(C)**. Boxes represent medians, 25th and 75th percentiles and whiskers show the largest and smallest non-outlier values based on 1.5 IQR calculation. The threshold for non-responsive samples (ACE2 binding inhibition less than 20%) is shown as dotted line. All samples below this threshold can be considered non-responsive. Time between sampling and full vaccination is displayed as mean and SD for each group. Number of samples per vaccination scheme are stated below the figure. Statistical significance was calculated by a regression model (**Supplementary Table 4**).

inhibition assays instead of a VNT have also already been used successfully by other groups to determine neutralizing antibody activity (52). Methodically, MULTICOV-AB and the ACE2-RBD competition assay are also complementary and are measured using a single initial sample dilution which further reduces variability between their results. By multiplex-based antibody profiling, we were able to further investigate titre differences and determined that vector- and mRNA-based vaccines induced a distinct pattern of Spike subdomain-targeted antibodies. While vector-based formulations result in a significantly larger proportion of S2-domain antibodies, RBD- and S1-domain antibodies dominated in mRNA vaccines. While these observations require further detailed investigation, the relative over-representation of RBD- and S1-targeting antibodies within mRNA vaccines is particularly intriguing as these two antigens comprise the majority of neutralizing antibody activity (13, 53). Although a series of modelling studies have now linked levels of neutralizing antibodies to vaccine efficacy (12, 54), a clearly defined correlation of vaccine efficacy and neutralizing antibody levels is still lacking. Nevertheless it appears logical that increased

antibody levels specific to virus proteins-mediating cell attachment could result in enhanced levels of protection from infection and contribute to observed differences in vaccine efficacy and effectiveness levels (3, 55, 56). Interestingly, our conclusions are strengthened by studies examining the relative immunogenicity of the different Spike subdomains. By immunising rabbits with SARS-CoV-2 S2, S1 or RBD proteins, Ravichandran et al. were able to show that S2 protein elicited considerable lower neutralizing antibody levels compared to the S1 and RBD antigens (57). Similar results were obtained from isolating immunoglobulins of COVID-19 convalescents where S2 subunit-targeting antibodies showed weaker SARS-CoV-2 neutralization activity compared to the RBD-targeting ones (58). While the Spike protein surface is extensively glycosylated, including the membrane-proximal S2 domain, the RBD completely lacks N-glycans which might explain its immunodominance (59–61).

An additional finding of our study requiring further investigation is the relatively poor performance of Ad26.CoV2.S, particularly for induction of neutralizing antibodies for both SARS-CoV-2 wild-type and VoC RBDs. While some studies have reported

FIGURE 5 | SARS-CoV-2 vaccination boosts ACE2 binding inhibition among recovered individuals independent of vaccination scheme. Differences in vaccination responses of recovered previously SARS-CoV-2 infected individuals from our mix and match cohort were analyzed using an ACE2-RBD competition assay **(A)**. SARS-CoV-2 infection status was based on a previous self-reported positive PCR/antigen test or a MULTICOV-AB nucleocapsid IgG normalisation ratio above 1. Samples were split according to vaccination scheme in homologous mRNA (mRNA-1273 (M/M, blue), BNT162b2 (P/P, orange)), heterologous prime-boost (AZD1222-mRNA-1273 (A/M, light blue), AZD1222-BNT162b2 (A/P, light green) or vector-based (AZD1222-AZD1222 (A/A, green), Ad26.CoV2.S (J, grey)). For clarity and comparison, ACE2 inhibition of SARS-CoV-2 naïve individuals are displayed **(B)**. Boxes represent medians, 25th and 75th percentiles and whiskers show the largest and smallest non-outlier values based on 1.5 IQR calculation. If not enough sample to generate a box were present (minimum 5), then only the median is indicated by a line. The threshold for non-responsive samples (ACE2 binding inhibition less than 20%) is shown as dotted line. All samples below this can be considered non-responsive. Time between sampling and full vaccination is displayed as mean and SD for each group. Number of samples per vaccination scheme are stated below the graph. Results of a formal statistical comparison of recovered-vaccinated and SARS-CoV-2 naïve-vaccinated individuals are shown in **Supplementary Table 6**.
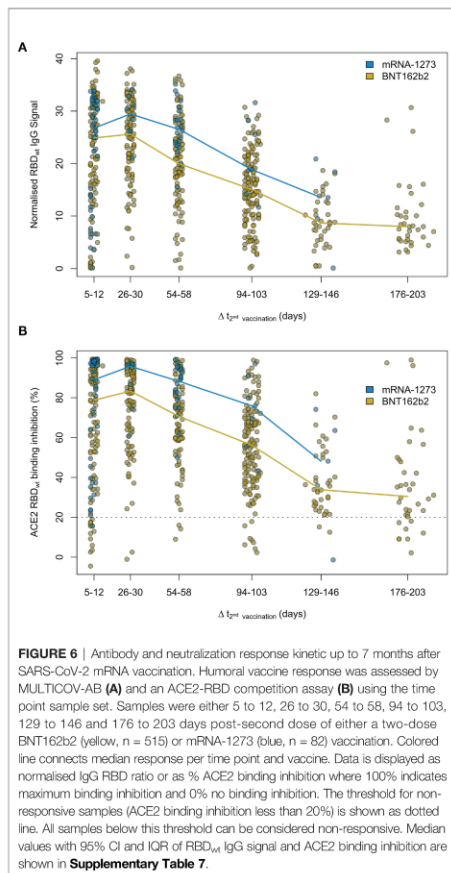
sufficient levels of neutralizing activity after vaccination with Ad26.CoV2.S (2), others identified minimal neutralizing activity, particularly when compared to other COVID-19 vaccines from Pfizer or Moderna (44). The relatively poor performance of Ad26.CoV2.S in inducing an antibody response has also been identified by researchers studying other bodily fluids (e.g. breast milk), who found that Ad26.CoV2.S produced significantly fewer IgA antibodies than BNT162b2 or mRNA-1273 (62). While our Ad26.CoV2.S sample group size is low (n=29), it is three times larger than a recent study from the manufacturer which reported neutralizing activity against Delta and other VoCs [n=8 (63)]. It should be noted that four of the eight individuals within their cohort were reported as being spike seropositive at baseline which is a consistent finding with our cohort, where strong ACE2 binding inhibition was only achieved in those individuals who had been previously infected. Our median time point is however earlier than the reported peak of antibody activity (2, 64). Further independent investigations into the neutralizing activity generated by single-dose Ad26.CoV2.S to clarify those differing results within SARS-CoV-2 naïve individuals are therefore urgently needed.

Among confounding variables, we identified like others that age resulted in a general reduction in titre and ACE2 binding inhibition (11, 40, 65), although the vaccination scheme received had a more significant effect. While recovered individuals developing high titres and ACE2 binding inhibition once vaccinated has been previously reported (40, 43), we found that these responses were similar among all vaccines and immunisation schemes. Given that current German guidelines require a six month post-positive PCR waiting period before receiving a first dose, this suggests that such individuals would be

suitable for all currently licensed vaccines, assuming they meet pre-existing EMA and STIKO criteria. This ability to use all vaccines and generate a substantial response will be of particular public health importance, given the on-going booster dose administration which could impact availability for some vaccine brands, as happened earlier in 2021.

Our results on the longevity of the humoral response post-vaccination is similar to others, in identifying an initial peak from approximately 28 days post-second dose onwards followed by a gradual reduction over time (66). As expected, ACE2 binding inhibition and titre are mostly mirrored in their decline over time. However, the increased numbers of non-responders from BNT162b2-vaccinated individuals from six months after the second vaccine needs further careful monitoring until a precise correlate of protection has been defined. Among the different SARS-CoV-2 antibodies, it is unsurprising that the RBD and S1 underwent the greatest reductions as they had the largest titres to begin with. Between VoCs, we did not identify any apparent differences in ACE2 binding inhibition between the differing immunisation schemes for confounders. Instead, again vaccine type or regimen (homologous vs heterologous) received had the largest effect upon ACE2 binding inhibition. The VoCs themselves followed a previously published pattern (9, 22, 67), with the lowest reduction for the Alpha variant, and the highest for the Beta and Gamma variants. It should be stated that in our analysis of longitudinal samples, there is a wide variety of timeframes post-vaccination, meaning that initial samples are collected both before, during and after the initial peak response at around 28 days. While we have then made the assumption that decreases in responses would be linear to the second sampling, this is not the case as some

FIGURE 6 | Antibody and neutralization response kinetic up to 7 months after SARS-CoV-2 mRNA vaccination. Humoral vaccine response was assessed by MULTICOV-AB **(A)** and an ACE2-RBD competition assay **(B)** using the time point sample set. Samples were either 5 to 12, 26 to 30, 54 to 58, 94 to 103, 129 to 146 and 176 to 203 days post-second dose of either a two-dose BNT162b2 (yellow, n = 515) or mRNA-1273 (blue, n = 82) vaccination. Colored line connects median response per time point and vaccine. Data is displayed as normalised IgG RBD ratio or as % ACE2 binding inhibition where 100% indicates maximum binding inhibition and 0% no binding inhibition. The threshold for non-responsive samples (ACE2 binding inhibition less than 20%) is shown as dotted line. All samples below this threshold can be considered non-responsive. Median values with 95% CI and IQR of RBD_wt IgG signal and ACE2 binding inhibition are shown in **Supplementary Table 7**.
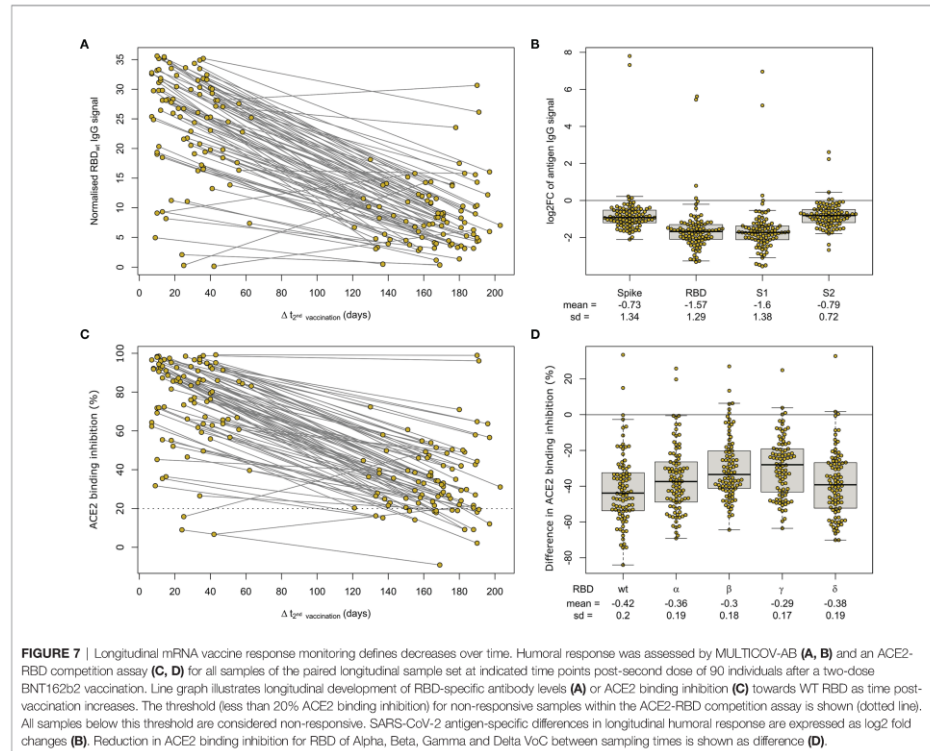
of the early collected samples (e.g. 7 days post-second vaccination) would have initially increased before later decreasing. However, our purpose of this analysis was to measure changes over a larger timeframe (4 months) and the difference in time from first to second sampling, means that all samples should be in the decline phase by their second sampling.

Our manuscript has several limitations, namely that we are only measuring antibodies (including neutralizing antibodies) that are present within serum. As previously stated, we have used an ACE2-RBD competition assay to measure inhibition of ACE2 binding instead of classical virus neutralization assays, although the results of this assay have already been shown to be similar to VNT and are known to be specific to neutralizing antibody responses only. While

neutralizing antibodies themselves are considered a strong correlate for protection (13), other components that are not measured within our assays such as T-cell mediated immunity will also offer protection (68, 69). Our use of serum also means that memory B-cells, which are involved in protection against severe disease progression (70), are equally excluded from our analysis. Our study cohort consists of relatively low sample numbers for both heterologous and Ad26.CoV2.S vaccinations whereas BNT162b2 samples are overrepresented. However, our sample numbers are similar or in case of Ad26.CoV2.S exceed other previously published work making our study one of the largest independent evaluation studies of this vaccine. Our BNT162b2 sample size mimics dose distribution in Germany where approximately 70% of delivered vaccine doses were from Pfizer. Our study population is also relatively similar in regard to age and gender. Last, self-reported information about a previous SARS-CoV-2 infection or vaccination could bias study outcome. However, recent studies have found a good correlation between self-reported and administrative records with 98% consistency for vaccination type and 95% for vaccination date or detection of SARS-CoV-2 antibodies with a positive predictive value of 98.2% and a negative predictive value of 97.3%, respectively (71, 72). Additionally, our data on persistence and magnitude of vaccine-induced humoral responses is consistent with several other cohort-based studies (11, 20, 41, 66) which did not rely on self-reported vaccination records, therefore stressing the validity of our approach.

Next to an increasing number of observational studies including ours which examine vaccine-induced protection by assessing levels of humoral immunity, several large scale test-negative design (TND) studies have by now been conducted to determine vaccine effectiveness against a laboratory-confirmed SARS-CoV-2 infection requiring medical attention outside of randomized clinical trials (45, 73, 74). While readouts between those study types are fundamentally different and both are subject to different limitations (75–79), results are comparable. For instance, our findings of significantly higher titres and ACE2 binding inhibition after mRNA or heterologous immunisation schemes compared vector-based ones also translate to differing levels of vaccine effectiveness against SARS-CoV-2 infection of above 90% with at least one mRNA vaccine dose or of less than 70% with two doses of AZD1222 in a TND study from Canada (45). Equally, our results of decreasing humoral response levels after a full BNT162b2 vaccination correlate with increases in PCR-confirmed SARS-CoV-2 infections up to six month post-vaccination with BNT162b2 in an Israeli TND study (73).

Overall, we provide data on the vaccine-induced humoral response for all currently available mRNA-, vector-based and heterologous immunisation schemes in Germany. Within our population-based cohort, mRNA homologous or heterologous vaccination resulted in increased humoral responses. Our multiplex approach identified differences in quantities and ratios of RBD- and S1-targeting antibodies following mRNA homologous or heterologous vaccination. Further investigation into this targeting will be of particular interest to improve vaccine performance particularly for next generation vector-based vaccines.

FIGURE 7 | Longitudinal mRNA vaccine response monitoring defines decreases over time. Humoral response was assessed by MULTICOV-AB **(A, B)** and an ACE2-RBD competition assay **(C, D)** for all samples of the paired longitudinal sample set at indicated time points post-second dose of 90 individuals after a two-dose BNT162b2 vaccination. Line graph illustrates longitudinal development of RBD-specific antibody levels **(A)** or ACE2 binding inhibition **(C)** towards WT RBD as time post-vaccination increases. The threshold (less than 20% ACE2 binding inhibition) for non-responsive samples within the ACE2-RBD competition assay is shown (dotted line). All samples below this threshold are considered non-responsive. SARS-CoV-2 antigen-specific differences in longitudinal humoral response are expressed as log2 fold changes **(B)**. Reduction in ACE2 binding inhibition for RBD of Alpha, Beta, Gamma and Delta VoC between sampling times is shown as difference **(D)**.

DATA AVAILABILITY STATEMENT

Source data and the analysis code have been deposited on GitHub (https://github.com/BeckerMatthias/MuSPAD_VaccStudy).

ETHICS STATEMENT

The studies involving human participants were reviewed and approved by the Ethics Committee of Hannover Medical School (9086_BO_S_2020). The participants provided their written informed consent to participate in this study.

AUTHOR CONTRIBUTIONS

MS, AD, BL, GK, and NS-M conceived the study. NS-M, MS, BL, VM, SC, and GK procured funding. AD, MS, MB, and NS-M designed the experiments. AD, JG, JJ, and DJ performed the experiments. AD, MS, MB, MH, JO, SC, NW, SG, J-KH, and BK performed data collection and analysis. AD, MB, MH, and BK generated figures and tables. TT, KF, TI, and NK organized sample collection and processing. AD, MS, MH, and BK verified the underlying data. AD, MS, and MB wrote the manuscript. AD, MH, JO, PH, BL, NS-M, MS, YK, DG, VM, DJ, PK, BT, UR, TT, KF, NK, TI, TK, AR, CS, AR, AM, and NG contributed resources or were involved in project administration. All authors critically reviewed and approved the final manuscript.

FUNDING

189

Württemberg for Economic Affairs, Labour and Tourism (grant numbers FKZ 3-4332.62-NMI-67 and FKZ 3-4332.62-NMI-68). The funders had no role in study design, data collection and analysis, decision to publish, or preparation of the manuscript.

ACKNOWLEDGMENTS

First and foremost, we would like to thank the MuSPAD participants for their willingness and commitment to make this study possible. We also want to thank all laboratory members and administrative staff at the Institute of Transfusion Medicine and Immunohematology in Plauen for continued excellent technical and organizational support in sample processing. We

are grateful to the entire team of BOS112 for running of MuSPAD study sites. We sincerely thank all participating counties, cities and local health care authorities for their support. We thank Astrid Hans and Carina Lützow for administrative assistance. We thank members of the Multiplex Immunoassays Group at the NMI for their assistance in sample arrival and storage.

SUPPLEMENTARY MATERIAL

The Supplementary Material for this article can be found online at: https://www.frontiersin.org/articles/10.3389/fimmu.2022.828053/full#supplementary-material

REFERENCES

1. Voysey M, Clemens SAC, Madhi SA, Weckx LY, Folegatti PM, Aley PK, et al. Safety and Efficacy of the ChAdOx1 Ncov-19 Vaccine (AZD1222) Against SARS-CoV-2: An Interim Analysis of Four Randomised Controlled Trials in Brazil, South Africa, and the UK. Lancet (2021) 397(10269):99–111. doi: 10.1016/S0140-6736(20)32661-1
2. Sadoff J, Gray G, Vandebosch A, Cárdenas V, Shukarev G, Grinsztejn B, et al. Safety and Efficacy of Single-Dose Ad26.Cov2.S Vaccine Against Covid-19. New Engl J Med (2021) 384(23):2187–201. doi: 10.1056/NEJMoa2101544
3. Baden LR, El Sahly HM, Essink B, Kotloff K, Frey S, Novak R, et al. Efficacy and Safety of the mRNA-1273 SARS-CoV-2 Vaccine. N Engl J Med (2020) 384 (5):403–16. doi: 10.1056/NEJMoa2035389
4. Polack FP, Thomas SJ, Kitchin N, Absalon J, Gurtman A, Lockhart S, et al. Safety and Efficacy of the BNT162b2 mRNA Covid-19 Vaccine. N Engl J Med (2020) 383(27):2603–15. doi: 10.1056/NEJMoa2034577
5. RKI COVID-19 Dashboard. Available at: https://experience.arcgis.com/experience/478220a4c454480e823b17327b2bf1d4/page/page_1/2021.
6. Statistisches Beratungslabor, Institut für Statistik and LMU München. (2021): Corona.stat.uni-muenchen.de/maps/
7. Scobie HM, Johnson AG, Suthar AB, Severson R, Alden NB, Balter S, et al. Monitoring Incidence of COVID-19 Cases, Hospitalizations, and Deaths, by Vaccination Status - 13 U.S. Jurisdictions, April 4-July 17, 2021. MMWR Morb Mortal Wkly Rep (2021) 70(37):1284–90. doi: 10.15585/mmwr.mm7037e1
8. Israeli Government. (2021) Report available under: https://www.gov.il/BlobFolder/reports/vaccine-efficacy-safety-follow-up-committee/he/files_publications_corona_two-dose-vaccination-data.pdf2021.
9. Dulovic A, Strengert M, Ramos GM, Becker M, Griesbaum J, Junker D, et al. Diminishing Immune Responses Against Variants of Concern in Dialysis Patients Four Months After SARS-CoV-2 mRNA Vaccination. medRxiv (2021) 2021.08.16.21262115. doi: 10.1101/2021.08.16.21262115
10. Kustin T, Harel N, Finkel U, Perchik S, Harari S, Tahor M, et al. Evidence for Increased Breakthrough Rates of SARS-CoV-2 Variants of Concern in BNT162b2-mRNA-Vaccinated Individuals. Nat Med (2021) 27(8):1379–84. doi: 10.1038/s41591-021-01413-7
11. Naaber P, Tserel L, Kangro K, Sepp E, Jürjenson V, Adamson A, et al. Dynamics of Antibody Response to BNT162b2 Vaccine After Six Months: A Longitudinal Prospective Study. Lancet Regional Health - Europe (2021) 10:100208. doi: 10.1016/j.lanepe.2021.100208
12. Earle KA, Ambrosino DM, Fiore-Gartland A, Goldblatt D, Gilbert PB, Siber GR, et al. Evidence for Antibody as a Protective Correlate for COVID-19 Vaccines. Vaccine (2021) 39(32):4423–8. doi: 10.1016/j.vaccine.2021.05.063
13. Khoury DS, Cromer D, Reynaldi A, Schlub TE, Wheatley AK, Juno JA, et al. Neutralizing Antibody Levels Are Highly Predictive of Immune Protection From Symptomatic SARS-CoV-2 Infection. Nat Med (2021) 27(7):1205–11. doi: 10.1038/s41591-021-01377-8
14. Althaus K, Möller P, Uzun G, Singh A, Beck A, Bettag M, et al. Antibody-Mediated Procoagulant Platelets in SARS-CoV-2-Vaccination Associated

Immune Thrombotic Thrombocytopenia. Haematologica (2021) 106 (8):2170–9. doi: 10.3324/haematol.2021.279000
15. Greinacher A, Thiele T, Warkentin TE, Weisser K, Kyrle PA, Eichinger S. Thrombotic Thrombocytopenia After ChAdOx1 Ncov-19 Vaccination. New Engl J Med (2021) 384(22):2092–101. doi: 10.1056/NEJMoa2104840
16. Pottegård A, Lund LC, Karlstad Ø, Dahl J, Andersen M, Hallas J, et al. Arterial Events, Venous Thromboembolism, Thrombocytopenia, and Bleeding After Vaccination With Oxford-AstraZeneca ChAdOx1-S in Denmark and Norway: Population Based Cohort Study. BMJ (2021) 373:n1114. doi: 10.1136/bmj.n1114
17. Wise J. Covid-19: European Countries Suspend Use of Oxford-AstraZeneca Vaccine After Reports of Blood Clots. BMJ (2021) 372:n699. doi: 10.1136/bmj.n699
18. Vygen-Bonnet S, Koch J, Bogdan C, Harder T, Heininger U, Kling K, et al. Beschluss Der STIKO Zur 5. Aktualisierung Der COVID-19-Impfempfehlung Und Die Dazugehörige Wissenschaftliche Begründung. Epid Bull (2021) (19):24–36. doi: 10.25646/8467
19. Schmidt T, Klemis V, Schub D, Mihm J, Hielscher F, Marx S, et al. Immunogenicity and Reactogenicity of Heterologous ChAdOx1 Ncov-19/mRNA Vaccination. Nat Med (2021) 27(9):1530–5. doi: 10.1038/s41591-021-01464-w
20. Barros-Martins J, Hammerschmidt SI, Cossmann A, Odak I, Stankov MV, Morillas Ramos G, et al. Immune Responses Against SARS-CoV-2 Variants After Heterologous and Homologous ChAdOx1 Ncov-19/BNT162b2 Vaccination. Nat Med (2021) 27(9):1525–9. doi: 10.1038/s41591-021-01449-9
21. Carr EJ, Wu M, Harvey R, Wall EC, Kelly G, Hussain S, et al. Neutralising Antibodies After COVID-19 Vaccination in UK Haemodialysis Patients. Lancet (2021) 398(10305):1038–41. doi: 10.1016/S0140-6736(21)01854-7
22. Strengert M, Becker M, Ramos GM, Dulovic A, Gruber J, Juengling J, et al. Cellular and Humoral Immunogenicity of a SARS-CoV-2 mRNA Vaccine in Patients on Haemodialysis. EBioMedicine (2021) 70:103524. doi: 10.1016/j.ebiom.2021.103524
23. Harsch IA, Ortloff A, Reinhöfer M, Epstude J. Symptoms, Antibody Levels and Vaccination Attitude After Asymptomatic to Moderate COVID-19 Infection in 200 Healthcare Workers. GMS Hygiene Infect Control (2021) 16:Doc15. doi: 10.3205/dgkh000386
24. Becker M, Dulovic A, Junker D, Ruetalo N, Kaiser PD, Pinilla YT, et al. Immune Response to SARS-CoV-2 Variants of Concern in Vaccinated Individuals. Nat Commun (2021) 12(1):3109. doi: 10.1038/s41467-021-23473-6
25. Galanis P, Vraka I, Fragkou D, Bilali A, Kaitelidou D. Seroprevalence of SARS-CoV-2 Antibodies and Associated Factors in Healthcare Workers: A Systematic Review and Meta-Analysis. J Hosp Infect (2021) 108:120–34. doi: 10.1016/j.jhin.2020.11.008
26. Tregoning JS, Flight KE, Higham SL, Wang Z, Pierce BF. Progress of the COVID-19 Vaccine Effort: Viruses, Vaccines and Variants Versus Efficacy, Effectiveness and Escape. Nat Rev Immunol (2021) 21(10):626–36. doi: 10.1038/s41577-021-00592-1

190

27. Gornyk D, Harries M, Glöckner S, Strengert M, Kerrinnes T, Heise J-K, et al. SARS-CoV-2 Seroprevalence in Germany. *Dtsch Arztebl Int* (2021) 0 (OnlineFirst):1–. doi: 10.3238/arztebl.m2021.0364

28. Becker M, Strengert M, Junker D, Kaiser PD, Kerrinnes T, Traenkle B, et al. Exploring Beyond Clinical Routine SARS-CoV-2 Serology Using MultiCoV-Ab to Evaluate Endemic Coronavirus Cross-Reactivity. *Nat Commun* (2021) 12(1):1152. doi: 10.1038/s41467-021-20973-3

29. Junker D, Dulovic A, Becker M, Wagner TR, Kaiser PD, Traenkle B, et al. Reduced Serum Neutralization Capacity Against SARS-CoV-2 Variants in a Multiplex ACE2 RBD Competition Assay. *medRxiv* (2021) 2021.08.20.21262328. doi: 10.1101/2021.08.20.21262328

30. Renk H, Dulovic A, Seidel A, Becker M, Fabricius D, Zernickel M, et al. Robust and Durable Serological Response Following Pediatric SARS-CoV-2 Infection. *Nat Commun* (2022) 13(1):128. doi: 10.1038/s41467-021-27595-9

31. Planatscher H, Rimmele S, Michel G, Potz O, Joos T, Schneiderhan-Marra N. Systematic Reference Sample Generation for Multiplexed Serological Assays. *Sci Rep* (2013) 3. doi: 10.1038/srep03259

32. R Core Team. *R: A Language and Environment for Statistical Computing*. Vienna, Austria: R Foundation for Statistical Computing (2021).

33. Brunner E, Munzel U. (2000). The Nonparametric Behrens-Fischer Problem: Asymptotic Theory and A Small-Sample Approximation. *Biometrical J* 42 (1):17-25.

34. Gastwirth JL, Gel YR, Wallace Hui WL, Lyubchich V, Miao W, Noguchi K. (2020). lawstat: Tools for biostatistics, public policy, and law. R-package version 3.4, https://CRAN.R-project.org/package=lawstat

35. Holm S. A Simple Sequentially Rejective Multiple Test Procedure. *Scandinavian J Stat* (1979) 6(2):65–70.

36. Pinheiro J, Bates D, DebRoy S, Sarkar D. R Core Team (2022). nlme: Linear and nonlinear mixed effects models. R-package version 3.1-155, https://Cran.R-project.org/package=nlme

37. Warnes GR, Bolker B, Bonebakker L, Gentleman R, Huber W, Liaw A, et al. *Gplots: Various R Programming Tools for Plotting Data. R package version 3.1.1.* (2021) https://CRAN.R-project.org/package=gplots

38. Eklund A, Trimble J. *Beeswarm: The Bee Swarm Plot, an Alternative to Stripchart. R Package Version 0.4.0.* (2021) https://CRAN.R-project.org/package=beeswarm.

39. CoVariants. *Shared Mutations*. Available at: https://covariants.org/shared-mutations.

40. Steensels D, Pierlet N, Penders J, Mesotten D, Heylen L. Comparison of SARS-CoV-2 Antibody Response Following Vaccination With BNT162b2 and mRNA-1273. *JAMA* (2021) 326(15):1533–35. doi: 10.1001/jama.2021.15125

41. Liu X, Shaw RH, Stuart ASV, Greenland M, Aley PK, Andrews NJ, et al. Safety and Immunogenicity of Heterologous Versus Homologous Prime-Boost Schedules With an Adenoviral Vectored and mRNA COVID-19 Vaccine (Com-COV): A Single-Blind, Randomised, Non-Inferiority Trial. *Lancet (London England)* (2021) 398(10303):856–69. doi: 10.1016/S0140-6736(21)01694-9

42. Behrens GMN, Cossmann A, Stankov MV, Schulte B, Streeck H, Förster R, et al. Strategic Anti-SARS-CoV-2 Serology Testing in a Low Prevalence Setting: The COVID-19 Contact (CoCo) Study in Healthcare Professionals. *Infect Dis Ther* (2020) 9(4):837–49. doi: 10.1007/s40121-020-00334-1

43. Eyre DW, Lumley SF, Wei J, Cox S, James T, Justice A, et al. Quantitative SARS-CoV-2 Anti-Spike Responses to Pfizer-BioNTech and Oxford-AstraZeneca Vaccines by Previous Infection Status. *Clin Microbiol Infect* (2021) 27(10):1516.e7–.14. doi: 10.1016/j.cmi.2021.05.041

44. Tada T, Zhou H, Samanovic MI, Dcosta BM, Cornelius A, Mulligan MJ, et al. Comparison of Neutralizing Antibody Titers Elicited by mRNA and Adenoviral Vector Vaccine Against SARS-CoV-2 Variants. *bioRxiv* (2021) 2021.07.19.452771. doi: 10.1101/2021.07.19.452771

45. Skowronski DM, Setayeshgar S, Febriani Y, Ouakki M, Zou M, Talbot D, et al. Two-Dose SARS-CoV-2 Vaccine Effectiveness With Mixed Schedules and Extended Dosing Intervals: Test-Negative Design Studies From British Columbia and Quebec, Canada. *medRxiv* (2021) 2021.10.26.21265397. doi: 10.1101/2021.10.26.21265397

46. Amirthalingam G, Bernal JL, Andrews NJ, Whitaker H, Gower C, Stowe J, et al. Higher Serological Responses and Increased Vaccine Effectiveness Demonstrate the Value of Extended Vaccine Schedules in Combatting COVID-19 in England. *medRxiv* (2021) 2021.07.26.21261140. doi: 10.1101/2021.07.26.21261140

47. Grunau B, Asamoah-Boaheng M, Lavoie PM, Karim ME, Kirkham TL, Demers PA, et al. A Higher Antibody Response Is Generated With a 6- to 7-Week (vs Standard) Severe Acute Respiratory Syndrome Coronavirus 2 (SARS-CoV-2) Vaccine Dosing Interval. *Clin Infect Dis* (2021) ciab938. doi: 10.1093/cid/ciab938

48. Payne RP, Longet S, Austin JA, Skelly DT, Dejnirattisai W, Adele S, et al. Immunogenicity of Standard and Extended Dosing Intervals of BNT162b2 mRNA Vaccine. *Cell* (2021) 184(23):5699–714.e11. doi: 10.1016/j.cell.2021.10.011

49. Tauzin A, Gong SY, Beaudoin-Bussières G, Vézina D, Gasser R, Nault L, et al. Strong Humoral Immune Responses Against SARS-CoV-2 Spike After BNT162b2 mRNA Vaccination With a 16-Week Interval Between Doses. *Cell Host Microbe* (2021). doi: 10.1016/j.chom.2021.12.004

50. European Medicines Agency, Committee for Medicinal Products for Human Use (CHMP, 2021): Assessment report Comirnaty. EMA/707383/2020 Corr1.

51. European Medicines Agency, Committee for Medicinal Products for Human Use (CHMP, 2021): Assessment report COVID-19 Vaccine Moderna. EMA/702084/2021; EMEA/H/C/005735.

52. Lopez E, Haycroft ER, Adair A, Mordant FL, O'Neill MT, Pymm P, et al. Simultaneous Evaluation of Antibodies That Inhibit SARS-CoV-2 Variants via Multiplex Assay. *JCI Insight* (2021) 6(16). doi: 10.1172/jci.insight.150012

53. Zost SJ, Gilchuk P, Case JB, Binshtein E, Chen RE, Nkolola JP, et al. Potently Neutralizing and Protective Human Antibodies Against SARS-CoV-2. *Nature* (2020) 584(7821):443–9. doi: 10.1038/s41586-020-2548-6

54. Feng S, Phillips DJ, White T, Sayal H, Aley PK, Bibi S, et al. Correlates of Protection Against Symptomatic and Asymptomatic SARS-CoV-2 Infection. *Nat Med* (2021) 27:2032–40. doi: 10.1101/2021.06.21.21258528

55. Madhi SA, Baillie V, Cutland CL, Voysey M, Koen AL, Fairlie L, et al. Efficacy of the ChAdOx1 nCoV-19 Covid-19 Vaccine against the B.1.351 Variant. *New Engl J Med* (2021) 384(20):1885–98.

56. Self WH, Tenforde MW, Rhoads JP, Gaglani M, Ginde AA, Douin DJ, et al. Comparative Effectiveness of Moderna, Pfizer-BioNTech, and Janssen (Johnson & Johnson) Vaccines in Preventing COVID-19 Hospitalizations Among Adults Without Immunocompromising Conditions - United States, March-August 2021. *MMWR Morb Mortal Wkly Rep* (2021) 70(38):1337–43. doi: 10.15585/mmwr.mm7038e1

57. Ravichandran S, Coyle Elizabeth M, Klenow L, Tang J, Grubbs G, Liu S, et al. Antibody Signature Induced by SARS-CoV-2 Spike Protein Immunogens in Rabbits. *Sci Trans Med* (2020) 12(550):eabc3539. doi: 10.1126/scitranslmed.abc3539

58. Wec AZ, Wrapp D, Herbert AS, Maurer DP, Haslwanter D, Sakharkar M, et al. Broad Neutralization of SARS-Related Viruses by Human Monoclonal Antibodies. *Science* (2020) 369(6504):731–6. doi: 10.1126/science.abc7424

59. Watanabe Y, Allen JD, Wrapp D, McLellan JS, Crispin M. Site-Specific Glycan Analysis of the SARS-CoV-2 Spike. *Science* (2020) 369(6501):330–3. doi: 10.1126/science.abb9983

60. Walls AC, Park Y-J, Tortorici MA, Wall A, McGuire AT, Veesler D. Structure, Function, and Antigenicity of the SARS-CoV-2 Spike Glycoprotein. *Cell* (2020) 181(2):281–92.e6. doi: 10.1016/j.cell.2020.02.058

61. Grant OC, Montgomery D, Ito K, Woods RJ. Analysis of the SARS-CoV-2 Spike Protein Glycan Shield Reveals Implications for Immune Recognition. *Sci Rep* (2020) 10(1):14991. doi: 10.1038/s41598-020-71748-7

62. Fox A, DeCarlo C, Yang X, Norris C, Powell RL. Comparative Profiles of SARS-CoV-2 Spike-Specific Milk Antibodies Elicited by COVID-19 Vaccines Currently Authorized in the USA. *medRxiv* (2021) 2021.07.19.21260794. doi: 10.1101/2021.07.19.21260794

63. Jongeneelen M, Kaszas K, Veldman D, Huizingh J, van der Vlugt R, Schouten T, et al. Ad26.COV2.S Elicited Neutralizing Activity Against Delta and Other SARS-CoV-2 Variants of Concern. *bioRxiv* (2021) 2021.07.01.450707. doi: 10.1101/2021.07.01.450707

64. Barouch DH, Stephenson KE, Sadoff J, Yu J, Chang A, Gebre M, et al. Durable Humoral and Cellular Immune Responses 8 Months After Ad26.COV2.S Vaccination. *N Engl J Med* (2021) 385(10):951–3. doi: 10.1056/NEJMc2108829

65. Shrotri M, Fragaszy E, Geismar C, Nguyen V, Beale S, Braithwaite I, et al. Spike-Antibody Responses to ChAdOx1 and BNT162b2 Vaccines by Demographic and Clinical Factors (Virus Watch Study). *medRxiv* (2021) 2021.05.12.21257102. doi: 10.1101/2021.05.12.21257102

66. Doria-Rose N, Suthar MS, Makowski M, O'Connell S, McDermott AB, Flach B, et al. Antibody Persistence Through 6 Months After the Second Dose of

191

mRNA-1273 Vaccine for Covid-19. *N Engl J Med* (2021) 384(23):2259–61. doi: 10.1056/NEJMc2103916

67. van Gils MJ, Lavell AHA, van der Straten K, Appelman B, Bontjer I, Poniman M, et al. Four SARS-CoV-2 Vaccines Induce Quantitatively Different Antibody Responses Against SARS-CoV-2 Variants. *medRxiv* (2021) 2021.09.27.21264163. doi: 10.1101/2021.09.27.21264163

68. Mateus J, Dan Jennifer M, Zhang Z, Rydyznski Moderbacher C, Lammers M, Goodwin B, et al. Low-Dose mRNA-1273 COVID-19 Vaccine Generates Durable Memory Enhanced by Cross-Reactive T Cells. *Science* (2021) eabj9853. doi: 10.1126/science.abj9853

69. Israelow B, Mao T, Klein J, Song E, Menasche B, Omer Saad B, et al. Adaptive Immune Determinants of Viral Clearance and Protection in Mouse Models of SARS-CoV-2. *Sci Immunol* (2021) eabl4509. doi: 10.1126/sciimmunol.abl4509

70. Goel RR, Apostolidis SA, Painter MM, Mathew D, Pattekar A, Kuthuru O, et al. Distinct Antibody and Memory B Cell Responses in SARS-CoV-2 Naïve and Recovered Individuals Following mRNA Vaccination. *Sci Immunol* (2021) 6(58):abm0829. doi: 10.1126/sciimmunol.abi6950

71. Pritchard E, Matthews PC, Stoesser N, Eyre DW, Gethings O, Vihta K-D, et al. Impact of Vaccination on New SARS-CoV-2 Infections in the United Kingdom. *Nat Med* (2021) 27(8):1370–8. doi: 10.1038/s41591-021-01410-w

72. Siegler AJ, Luisi N, Hall EW, Bradley H, Sanchez T, Lopman BA, et al. Trajectory of COVID-19 Vaccine Hesitancy Over Time and Association of Initial Vaccine Hesitancy With Subsequent Vaccination. *JAMA Network Open* (2021) 4(9):e2126882–e. doi: 10.1001/jamanetworkopen.2021.26882

73. Israel A, Merzon E, Schäffer AA, Shenhar Y, Green I, Golan-Cohen A, et al. Elapsed Time Since BNT162b2 Vaccine and Risk of SARS-CoV-2 Infection: Test Negative Design Study. *BMJ* (2021) 375:e067873. doi: 10.1136/bmj-2021-067873

74. Thompson MG, Stenehjem E, Grannis S, Ball SW, Naleway AL, Ong TC, et al. Effectiveness of Covid-19 Vaccines in Ambulatory and Inpatient Care Settings. *N Engl J Med* (2021) 385(15):1355–71. doi: 10.1056/NEJMoa2110362

75. Houlihan CF, Beale R. The Complexities of SARS-CoV-2 Serology. *Lancet Infect Dis* (2020) 20(12):1350–1. doi: 10.1016/S1473-3099(20)30699-X

76. Dean NE, Hogan JW, Schnitzer ME. Covid-19 Vaccine Effectiveness and the Test-Negative Design. *N Engl J Med* (2021) 385(15):1431–3. doi: 10.1056/NEJMe2113151

77. Vandenbroucke JP, Brickley EB, Vandenbroucke-Grauls CMJE, Pearce N. A Test-Negative Design With Additional Population Controls Can Be Used to Rapidly Study Causes of the SARS-CoV-2 Epidemic. *Epidemiology* (2020) 31 (6). doi: 10.1097/EDE.0000000000001251

78. Galipeau Y, Greig M, Liu G, Driedger M, Langlois M-A. Humoral Responses and Serological Assays in SARS-CoV-2 Infections. *Front Immunol* (2020) 11:3382. doi: 10.3389/fimmu.2020.610688

79. Patel MK, Bergeri I, Bresee JS, Cowling BJ, Crowcroft NS, Fahmy K, et al. Evaluation of Post-Introduction COVID-19 Vaccine Effectiveness: Summary of Interim Guidance of the World Health Organization. *Vaccine* (2021) 39 (30):4013–24. doi: 10.1016/j.vaccine.2021.05.099

192

Supplementary Material - Comparative magnitude and persistence of humoral SARS-CoV-2 vaccination responses in the adult population in Germany

Alex Dulovic[1,#], Barbora Kessel[2,#], Manuela Harries[2,#], Matthias Becker[1], Julia Ortmann[2], Johanna Griesbaum[1], Jennifer Jüngling[1], Daniel Junker[1], Pilar Hernandez[2], Daniela Gornyk[2], Stephan Glöckner[2], Vanessa Melhorn[2], Stefanie Castell[2], Jana-Kristin Heise[2], Yvonne Kemmling[2], Torsten Tonn[3], Kerstin Frank[3], Thomas Illig[4], Norman Klopp[4], Neha Warikoo[2], Angelika Rath[2], Christina Suckel[2], Anne Ulrike Marzian[2], Nicole Grupe[2], Philipp D. Kaiser[1], Bjoern Traenkle[1], Ulrich Rothbauer[1,5], Tobias Kerrinnes[6], Gérard Krause[2,7,8], Berit Lange[2,8,§,*], Nicole Schneiderhan-Marra[1,§,*], Monika Strengert [2,7,§,*]

[1] NMI Natural and Medical Sciences Institute at the University of Tübingen, Reutlingen, Germany
[2] Helmholtz Centre for Infection Research, Department of Epidemiology, Braunschweig, Germany
[3] German Red Cross Blood Donation Service North East, Dresden, Germany
[4] Hannover Unified Biobank, Hannover Medical School, Hannover, Germany
[5] Pharmaceutical Biotechnology, Department of Pharmacy and Biochemistry, University of Tübingen, Tübingen, Germany
[6] Helmholtz Institute for RNA-based Infection Research, Department of RNA-Biology of Bacterial Infections, Würzburg, Germany
[7] TWINCORE, Centre for Experimental and Clinical Infection Research, a joint venture of the Hannover Medical School and the Helmholtz Centre for Infection Research, Hannover, Germany
[8] German Centre for Infection Research (DZIF), partner site Hannover-Braunschweig, Braunschweig, Germany

# these authors have contributed equally to this work and share first authorship.
§ these authors have contributed equally to this work and share last authorship.
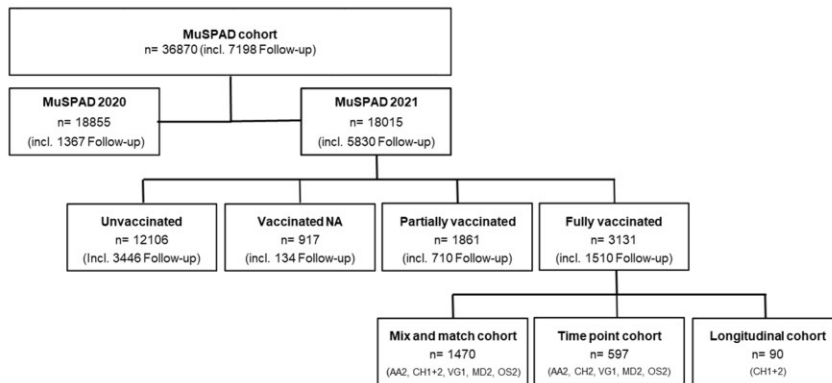* corresponding authors.

* Correspondence:

Monika Strengert
monika.strengert@helmholtz-hzi.de

Berit Lange
berit.lange@helmholtz-hzi.de

Nicole Schneiderhan-Marra
nicole.schneiderhan@nmi.de

Supplementary Figure 1. Flow chart for sample selection from MuSPAD cohort.
Sample selection for our vaccine response study from the entire MuSPAD cohort is displayed in a flow chart. Samples were selected based on selection criteria outlined in method section to examine impact of vaccination scheme, length and persistence of antibody response. Samples originated from the following study locations: Aachen 2 (AA2), Chemnitz 1(CH1), Chemnitz 2 (CH2), Vorpommern-Greifswald 1 (VG1), Osnabrück 2 (OS2), and Magdeburg 2 (MD2). Number of participants is given per group (n), NA: not available.
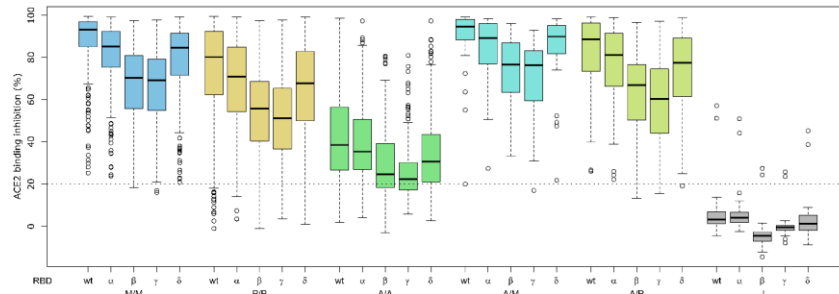
Supplementary Figure 2. Different VoCs reduce antibody ACE2 binding inhibition comparably between SARS-CoV-2 vaccination schemes.
ACE2 binding inhibition against the SARS-CoV-2 VoC Alpha (B.1.1.7), Beta (B.1.351), Gamma (P1) and Delta (B.1.617.2) RBDs was assessed by an ACE2-RBD competition assay for homologous mRNA (mRNA-1273 (M/M, blue), BNT162b2 (P/P, orange)), heterologous prime-boost (AZD1222-mRNA-1273 (A/M, light blue), AZD1222-BNT162b2 (A/P, light green) or vector-based (AZD1222-AZD1222 (A/A, green), Ad26.CoV2.S (J, grey)) vaccination schemes in the mix and match cohort. SARS-CoV-2 RBD WT (Figure 3) is again shown for clarity and comparison. Data is shown as box and whisker plots. Boxes represent medians, 25th and 75th percentiles and whiskers show the largest and smallest non-outlier values based on 1.5 IQR calculation. Outlier values are shown in clear circles. The threshold for non-responsive samples (ACE2 binding inhibition less than 20%) is shown as dotted line. All samples below this can be considered non-responsive. Number of samples per vaccination scheme are stated below the figure.
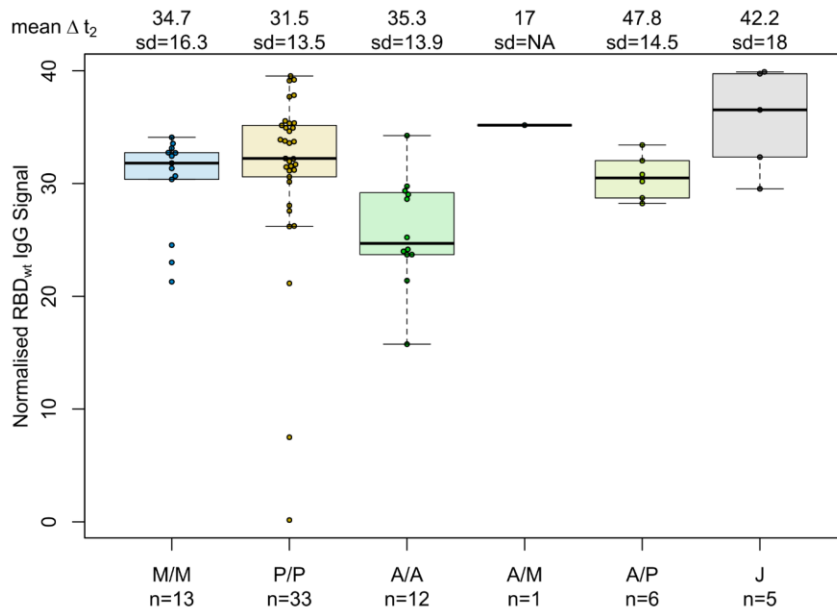
Supplementary Figure 3. SARS-CoV-2 vaccination boosts humoral response among recovered individuals independent of vaccination scheme.

Differences in vaccination responses of recovered previously SARS-CoV-2 infected individuals from our mix and match cohort were analyzed using MULTICOV-AB. SARS-CoV-2 infection status was based on a previous self-reported positive PCR/antigen test or a MULTICOV-AB nucleocapsid IgG normalisation ratio above 1. Samples were split according to vaccination scheme (homologous mRNA (mRNA-1273 (M/M, blue), BNT162b2 (P/P, orange)), heterologous prime-boost (AZD1222-mRNA-1273 (A/M, light blue), AZD1222-BNT162b2 (A/P, light green) or vector-based (AZD1222-AZD1222 (A/A, green), Ad26CoV2.S (J, grey)). Boxes represent medians, 25th and 75th percentiles and whiskers show the largest and smallest non-outlier values based on 1.5 IQR calculation. When less than 5 samples were available per group, only the median is indicated by a line. Time between sampling and full vaccination is displayed as mean and SD for each group. Number of samples per vaccination scheme are stated below the figure. Results of a formal statistical comparison of recovered-vaccinated and SARS-CoV-2 naïve-vaccinated individuals is shown in Table S6.

Supplementary Table 1. Comorbidities in study participants (n. a.: not applicable; NA: not available; CVD: cardiovascular disease).

Sample cohort (n)	SARS-CoV-2 infection status (n) *	ΔT range in days post-vaccination	Vaccine (n)	Hyper-tension (n, %)	CVD (n, %)	Diabetes (n, %)	Lung disease (n, %)	Cancer (n, %)	Immuno-suppression (n, %)
Mix and match (1470)	+ (70)	7-65	M/M (13)	4 (30.8)	1 (7.7)	2 (15.4)	0 (0.0)	0 (0.0)	0 (0.0)
			P/P (33)	12 (36.0)	4 (12.0)	3 (9.1)	0 (0.0)	0 (0.0)	1 (3.0)
			A/A (33)	7 (58.3)	3 (25.0)	2 (16.7)	1 (8.3)	1 (8.3)	2 (16.7)
			A/M (1)	1 (100.0)	0 (0.0)	0 (0.0)	0 (0.0)	0 (0.0)	0 (0.0)
			A/P (6)	3 (50.0)	1 (16.7)	0 (0.0)	1 (16.7)	0 (0.0)	0 (0.0)
			J (5)	2 (40.0)	0 (0.0)	0 (0.0)	0 (0.0)	0 (0.0)	1 (20.0)
	- (1400)		M/M (272)	84 (30.9)	23 (8.5)	13 (4.8)	17 (6.3)	2 (0.7)	11 (4.0)
			P/P (734, 4 NA)	263 (35.8)	101 (13.8)	64 (8.7)	59 (8.1)	20 (2.7)	37 (5.0)
			A/A (228)	91 (39.9)	25 (11.1)	25 (11.0)	12 (5.3)	2 (0.9)	9 (4.0)
			A/M (24)	12 (50.0)	4 (16.7)	2 (8.3)	0 (0.0)	1 (4.2)	0 (0.0)
			A/P (114)	43 (37.7)	16 (14.0)	10 (8.8)	10 (8.8)	4 (3.5)	6 (5.3)
			J (24)	9 (37.5)	2 (8.3)	2 (8.3)	2 (8.3)	1 (4.2)	2 (8.3)
Time points (597)	-	5-12	P/P (107)	50 (46.7)	16 (15.0)	6 (5.6)	3 (2.8)	0 (0.0)	7 (6.5)
			M/M (40)	13 (32.5)	3 (7.5)	3 (7.5)	1 (2.5)	0 (0.0)	1 (2.5)
		26-30	P/P (102; 1 NA)	31 (30.4)	15 (14.7)	11 (10.8)	12 (11.8)	0 (0.0)	0 (0.0)
			M/M (8)	3 (37.5)	1 (12.5)	0 (0.0)	0 (0.0)	0 (0.0)	0 (0.0)
		54-58	P/P (92)	37 (40.2)	14 (15.2)	7 (7.6)	0 (0.0)	2 (2.2)	4 (4.4)
			M/M (22)	2 (9.1)	0 (0.0)	2 (9.1)	2 (9.1)	0 (0.0)	1 (4.6)
		94-103	P/P (139)	59 (42.5)	18 (13.0)	12 (8.6)	1 (0.7)	7 (5.0)	0 (0.0)
			M/M (7)	3 (42.9)	1 (14.3)	1 (14.3)	1 (14.3)	1 (14.3)	0 (0.0)
		129-146	P/P (38)	19 (50.0)	9 (23.7)	7 (18.4)	4 (10.5)	2 (5.3)	4 (10.5)
			M/M (5)	3 (60.0)	2 (40.0)	1 (20.0)	1 (20.0)	0 (0.0)	0 (0.0)
		176-203	P/P (36)	5 (13.9)	2 (5.6)	1 (2.8)	2 (5.6)	0 (0.0)	3 (8.3)
			M/M (0)	n. a.	n. a.	n. a.	n. a.	n. a.	n. a.
Longi-tudinal (180)	-	P/P T1: 7-63	P/P T1 (90; 2 NA)	35 (39.8)	15 (17.1)	11 (12.5)	4 (4.6)	2 (2.2)	3 (3.4)
		P/P T2: 121-203	P/P T2 (90)	33 (36.7)	12 (13.3)	8 (8.9)	3 (3.3)	1 (1.1)	9 (10.0)

Different vaccines and combinations are abbreviated as follows: M/M (two-dose mRNA-1273), P/P (two-dose BNT162b2), A/A (two-dose AZD1222), A/M (first dose AZD1222, second dose mRNA-1273), A/P (first dose AZD1222, second dose BNT162b2) and J (one-dose Ad26.CoV2.S). The time points sample cohort contains only homologous BNT162b2 and mRNA-1273 samples. The longitudinal sample cohort contains only paired homologous BNT162b2 taken at time 1 (T1) or 2 (T2).
* based on self-reported positive PCR/antigen test result at study center visit and/or MULTICOV-AB nucleocapsid IgG S/CO ratio above 1

Supplementary Table 2. MULTICOV-AB antigen panel.

Virus	Antigen	Manufacturer	Product number
SARS-CoV-2	Spike Trimer	NMI	-
SARS-CoV-2	RBD B.1 (wild-type)	NMI	-
SARS-CoV-2	Nucleocapsid	Aalto	6404-b
SARS-CoV-2	RBD B.1.1.7 (Alpha)	NMI	
SARS-CoV-2	RBD B.1.351 (Beta)	NMI	
SARS-CoV-2	RBD P.3 (Gamma)	NMI	
SARS-CoV-2	RBD B.1.617.2 (Delta)	NMI	
hCoV-OC43	S1 domain	NMI	-
hCoV-OC43	Nucleocapsid	NMI	-
hCoV-HKU1	S1 domain	NMI	-
hCoV-HKU1	Nucleocapsid	NMI	-
hCoV-NL63	S1 domain	NMI	-
hCoV-NL63	Nucleocapsid	NMI	-
hCoV-229E	S1 domain	NMI	-
hCoV-229E	Nucleocapsid	NMI	-

List of antigens included in MULTICOV-AB as well as their manufacturer and, if applicable, their product number.

Supplementary Table 3. ACE2-RBD competition antigen panel.

Virus	Antigen	Manufacturer	Amino acid exchanges in RBD
SARS-CoV-2	RBD B.1 (wild-type)	NMI	-
SARS-CoV-2	RBD B.1.1.7 (Alpha)	NMI	N501Y
SARS-CoV-2	RBD B.1.351 (Beta)	NMI	N501Y, E484K, K417N
SARS-CoV-2	RBD P.1 (Gamma)	NMI	N501Y, E484K, K417T
SARS-CoV-2	RBD B.1.617.2 (Delta)	NMI	T478K, L452R

List of antigens included in ACE2-RBD competition assay as well as their manufacturer, and the mutations covered within the RBD.

Supplementary Table 4. Impact of confounders on ACE2 inhibition response towards SARS-CoV-2 wild-type and VoC RBDs.

A. WT ACE2 binding inhibition, logit	P/P, n=734		M/M, n=272		A/P, n=114		A/A, n=228	
scale	Est (sd)	p-value	Est (sd)	p-value	Est (sd)	p-value	Est (sd)	p-value
Intercept	3.50 (0.231)	---	3.39 (0.330)	---	3.07 (0.538)	---	-0.52 (0.496)	---
Male	-0.25 (0.103)	0.014	-0.05 (0.149)	0.752	-0.33(0.267)	0.218	0.30(0.152)	0.050
Age (per 1 year)	-0.03 (0.003)	<0.001	0.00 (0.005)	0.431	-0.01 (0.010)	0.251	0.00(0.008)	0.960
Days post-vaccination (ΔT)								
7-27	Ref.		Ref.		Ref.		Ref.	
28-65	-0.69 (0.104)	<0.001	-0.97 (0.169)	<0.001	-0.74 (0.260)	0.005	-0.10(0.188)	0.584
Comorbidities								
Cardiovascular	-0.12(0.158)	0.454	-0.54 (0.309)	0.083	-0.03(0.424)	0.937	0.02 (0.241)	0.943
Hypertension	0.19(0.119)	0.109	-0.13 (0.180)	0.480	-0.08(0.301)	0.789	0.11(0.161)	0.485
Diabetes	-0.04(0.185)	0.808	0.58(0.386)	0.136	0.84(0.501)	0.095	-0.15(0.242)	0.547
Lung disease*	-0.03(0.187)	0.853	0.53(0.324)	0.104	-0.87(0.513)	0.091	-0.11(0.349)	0.758
Cancer or Immunosuppression*	-0.26(0.192)	0.176	0.29(0.362)	0.418	0.22(0.508)	0.662	-0.61(0.368)	0.099

B. Alpha ACE2 binding inhibition, logit	P/P, n=734		M/M, n=272		A/P, n=114		A/A, n=228	
scale	Est (sd)	p-value	Est (sd)	p-value	Est (sd)	p-value	Est (sd)	p-value
Intercept	2.50(0.211)	---	2.64(0.301)	---	2.26(0.465)	---	-0.77(0.420)	---
Male	-0.22(0.083)	0.008	-0.02(0.130)	0.862	-0.27(0.226)	0.228	0.24(0.126)	0.060
Age (per 1 year)	-0.02(0.003)	<0.001	-0.01(0.004)	0.218	-0.01(0.009)	0.270	0.00(0.006)	0.826
Days post-vaccination (ΔT)								
7-27	Ref.		Ref.		Ref.		Ref.	
28-65	-0.56(0.083)	<0.001	-0.89(0.147)	<0.001	-0.58(0.219)	0.008	-.03(0.155)	0.842
Comorbidities								
Cardiovascular	-0.10(0.125)	0.434	-0.42(0.266)	0.112	-0.02(0.361)	0.961	0.04(0.202)	0.842
Hypertension	0.16(0.095)	0.087	-0.10(0.156)	0.524	-0.06(0.255)	0.800	0.05(0.134)	0.715
Diabetes	-0.03(0.149)	0.828	0.41(0.332)	0.216	0.81(0.425)	0.057	-0.05(0.204)	0.815
Lung disease*	-0.03(0.149)	0.851	0.40(0.281)	0.156	-0.78(0.433)	0.073	-0.08(0.288)	0.789
Cancer or Immunosuppression*	-0.15(0.153)	0.343	0.21(0.314)	0.510	0.15(0.428)	0.724	-0.45(0.302)	0.139

C. Beta ACE2 binding inhibition, logit	P/P, n=734		M/M, n=272		A/P, n=114		A/A, n=228	
scale	Est (sd)	p-value	Est (sd)	p-value	Est (sd)	p-value	Est (sd)	p-value
Intercept	1.27(0.259)	---	1.55(0.309)	---	1.12(0.420)	---	-1.18(0.432)	---
Male	-0.19(0.070)	0.006	-0.08(0.105)	0.448	-0.27(0.180)	0.131	0.11(0.116)	0.337
Age (per 1 year)	-0.02(0.002)	<0.001	0.00(0.004)	0.170	-0.01(0.007)	0.268	0.00(0.006)	0.584
Days post-vaccination (ΔT)								
7-27	Ref.		Ref.		Ref.		Ref.	
28-65	-0.44(0.070)	<0.001	-0.86(0.119)	<0.001	-0.59(0.175)	0.001	0.07(0.144)	0.645
Comorbidities								
Cardiovascular	0.00(0.106)	0.971	-0.37(0.216)	0.088	-0.04(0.294)	0.899	0.06(0.181)	0.741
Hypertension	0.08(0.081)	0.306	-0.12(0.126)	0.323	-0.02(0.205)	0.923	0.01(0.122)	0.940
Diabetes	0.01(0.124)	0.917	0.24(0.270)	0.380	0.48(0.345)	0.165	0.09(0.180)	0.636
Lung disease*	-0.08(0.126)	0.520	0.39(0.227)	0.087	-0.54(0.346)	0.117	0.10(0.268)	0.705
Cancer or Immunosuppression*	-0.19(0.130)	0.155	0.13(0.254)	0.606	0.27(0.340)	0.426	-0.40(0.286)	0.163

D. Gamma ACE2 binding inhibition, logit scale	P/P, n=734		M/M, n=272		A/P, n=114		A/A, n=228	
	Est (sd)	p-value	Est (sd)	p-value	Est (sd)	p-value	Est (sd)	p-value
Intercept	1.31(0.169)	---	1.64(0.250)	---	1.24(0.377)	---	-1.05(0.313)	---
Male	-0.20(0.067)	0.003	-0.06(0.109)	0.612	-0.36(0.183)	0.049	0.13(0.092)	0.165
Age (per 1 year)	-0.02(0.002)	<0.001	0.00(0.004)	0.222	-0.01(0.007)	0.183	0.00(0.005)	0.382
Days post-vaccination (ΔT)								
7-27	Ref.		Ref.		Ref.		Ref.	
28-65	-0.46(0.068)	<0.001	-0.91(0.124)	<0.001	-0.52(0.177)	0.004	-0.03(0.114)	0.769
Comorbidities								
Cardiovascular	-0.06(0.101)	0.556	-0.41(0.225)	0.069	-0.05(0.299)	0.862	0.13(0.145)	0.352
Hypertension	0.14(0.078)	0.063	-0.08(0.132)	0.548	0.04(0.208)	0.862	0.07(0.097)	0.496
Diabetes	-0.01(0.118)	0.960	0.21(0.281)	0.463	0.53(0.351)	0.134	0.03(0.145)	0.821
Lung disease*	-0.04(0.121)	0.770	0.27(0.237)	0.252	-0.62(0.351)	0.076	-0.13(0.212)	0.554
Cancer or Immunosuppression*	-0.17(0.125)	0.178	0.12(0.265)	0.654	0.17(0.344)	0.626	-0.45(0.225)	0.047

E. Delta ACE2 binding inhibition, logit	P/P, n=734		M/M, n=272		A/P, n=114		A/A, n=228	
scale	Est (sd)	p-value	Est (sd)	p-value	Est (sd)	p-value	Est (sd)	p-value
Intercept	2.34(0.218)	---	2.53(0.312)	---	2.16(0.468)	---	-1.10(0.430)	---
Male	-0.21(0.085)	0.013	-0.03(0.135)	0.830	-0.34(0.226)	0.132	0.20(0.128)	0.128
Age (per 1 year)	-0.02(0.003)	<0.001	0.00(0.004)	0.349	-0.01(0.009)	0.203	0.00(0.007)	0.698
Days post-vaccination (ΔT)								
7-27	Ref.		Ref.		Ref.		Ref.	
28-65	-0.55(0.086)	<0.001	-0.99(0.152)	<0.001	-0.70(0.220)	0.001	0.01(0.159)	0.938
Comorbidities								
Cardiovascular	-0.10(0.130)	0.445	-0.52(0.276)	0.058	0.12(0.365)	0.744	0.09(0.203)	0.641
Hypertension	0.15(0.099)	0.125	-0.11(0.162)	0.501	0.01(0.256)	0.957	-0.04(0.136)	0.762
Diabetes	-0.01(0.152)	0.969	0.42(0.345)	0.227	0.68(0.429)	0.116	-0.01(0.204)	0.953
Lung disease*	-0.02(0.155)	0.920	0.39(0.292)	0.182	-0.67(0.434)	0.125	-0.15(0.295)	0.604
Cancer or Immunosuppression*	-0.18(0.159)	0.261	0.17(0.326)	0.603	0.06(0.428)	0.888	-0.50(0.311)	0.111

ACE2 binding inhibition towards SARS-CoV-2 wild-type (A) and Alpha (B), Beta (C), Gamma (D), Delta (E) VoC in the mix and match sample cohort was modelled to assess the role of confounders (see methods for model details). Four samples (P/P) had missing information on comorbidities and were excluded from the analysis. Est=estimate, sd=standard deviation. Categories denoted with * were merged in the sensitivity analysis including interaction terms with time post-vaccination due to limited sample sizes (selected results reported in the main text). Different vaccines and combinations are abbreviated as follows: M/M (two-dose mRNA-1273), P/P (two-dose BNT162b2), A/A (two-dose AZD1222), A/M (first dose AZD1222, second dose mRNA-1273), A/P (first dose AZD1222, second dose BNT162b2) and J (one-dose Ad26.CoV2.S).

.

Supplementary Table 5. Statistical comparison of antibody titres between vaccination schemes.

Comparison X vs. Y		Full-length Spike trimer p'' (p-value)	RBD p'' (p-value)	S1 p'' (p-value)	S2 p'' (p-value)
J	M/M	0.91 (< 0.001) *	0.93 (<0.001) *	0.96 (<0.001) *	0.86 (< 0.001) *
	P/P	0.89 (<0.001) *	0.90 (<0.001) *	0.92 (<0.001) *	0.79 (< 0.001) *
	A/M	0.89 (<0.001) *	0.91 (<0.001) *	0.97 (<0.001) *	0.93 (<0.001) *
	A/P	0.90 (<0.001) *	0.92 (<0.001) *	0.95 (<0.001) *	0.88 (<0.001) *
	A/A	0.63 (<0.080)	0.74 (<0.001) *	0.86 (<0.001) *	0.81 (<0.001) *
A/A	M/M	0.96 (<0.001) *	0.94 (<0.001) *	0.93 (<0.001) *	0.57 (0.013) *
	P/P	0.91 (<0.001) *	0.87 (<0.001) *	0.83 (<0.001) *	0.39 (<0.001) *
	A/M	0.93 (<0.001) *	0.91 (<0.001) *	0.93 (<0.001) *	0.84 (< 0.001) *
	A/P	0.93 (<0.001) *	0.89 (<0.001) *	0.91 (<0.001) *	0.66 (< 0.001) *
A/P	M/M	0.60 (0.002) *	0.64 (<0.001) *	0.55 (0.114)	0.38 (< 0.001) *
	P/P	0.42 (0.012)	0.49 (0.608)	0.34 (<0.001) *	0.21 (< 0.001) *
	A/M	0.59 (0.204)	0.59 (0.155)	0.69 (0.004) *	0.77 (<0.001) *
A/M	M/M	0.50 (0.982)	0.53 (0.623)	0.33 (0.014) *	0.16 (<0.001) *
	P/P	0.33 (0.014)	0.40 (0.085)	0.18 (<0.001)*	0.09 (<0.001) *
P/P	M/M	0.69 (<0.001) *	0.64 (<0.001) *	0.72 (<0.001) *	0.71 (<0.001) *

Estimated probability (p'') that a random individual under one vaccination scheme in the mix and match sample cohort, has a larger titre than a random individual under another vaccination scheme. Two-sided generalized Wilcoxon also referred to as Brunner-Munzel test was used to determine statistical significance with Bonferroni-Holm's adjustment for multiple testing. For a comparison of a scheme X with a scheme Y, a significant p'' larger than ½ means that the vaccination-induced titres under Y tend to be higher and a significant p'' smaller than ½ means that the vaccination-induced titres under X tend to be higher. Different vaccines and combinations are abbreviated as follows: M/M (two-dose mRNA-1273), P/P (two-dose BNT162b2), A/A (two-dose AZD1222), A/M (first dose AZD1222, second dose mRNA-1273), A/P (first dose AZD1222, second dose BNT162b2) and J (one-dose Ad26.CoV2.S).

Supplementary Table 6. Statistical comparison of RBD antibody titres and wild-type ACE2 binding inhibition in recovered-vaccinated and SARS-CoV-2 naïve-vaccinated individuals for different vaccination schemes.

	M/M p" (p-value)	P/P p" (p-value)	A/M p" (p-value)	A/P p" (p-value)	A/A p" (p-value)	J p" (p-value)
RBD	0.66 (0.074)	0.79 (<0.001)	-- (only 1 convalescent)	0.79 (<0.001)	0.94 (<0.001)	0.98 (<0.001)
AC2 binding inhibition against WT	0.74 (0.016)	0.85 (<0.001)	-- (only 1 convalescent)	0.84 (0.004)	0.97 (<0.001)	0.98 (<0.001)

Estimated probability (p'') that a random recovered-vaccinated individual has a larger titre than a random SARS-CoV-2 naïve vaccinated individual under the respective vaccination scheme. Statistical analysis was determined by two-sided generalized Wilcoxon/Brunner-Munzel test. A significant p'' larger than ½ means that the vaccination-induced titres tend to be higher in recovered-vaccinated individuals. Different vaccines and combinations are abbreviated as follows: M/M (two-dose mRNA-1273), P/P (two-dose BNT162b2), A/A (two-dose AZD1222), A/M (first dose AZD1222, second dose mRNA-1273), A/P (first dose AZD1222, second dose BNT162b2) and J (one-dose Ad26.CoV2.S).

Supplementary Table 7. Antibody titres and ACE2 binding inhibition up to 7 months after SARS-CoV-2 mRNA vaccination.

Sample cohort (n)	ΔT range in days post-vaccination	Vaccine (n)	RBD$_{wt}$ IgG signal (95% CI)	(%) ACE2 binding inhibition (95% CI)	RBD$_{wt}$ IgG signal (IQR)	(%) ACE2 binding inhibition (IQR)
Time points (597)	5-12	P/P (107)	24.88 (20.02-27.10)	78.73 (64.37-87.92)	24.88 (15.09-31.17)	78.73 (52.27-94.27)
		M/M (40)	26.76 (21.38-30.47)	89.03 (65.66-97.16)	26.76 (12.24-31.69	89.03 (41.06-97.95)
	26-30	P/P (103)	25.60 (23.15-27.79)	83.34 (78.04-0.86.00)	25.60 (18.76-30.87)	83.34 (63.63-93.37)
		M/M (8)	29.45 (21.01-34.13)	95.75 (60.74-96.97)	29.45 (26.20-32.42)	95.75 (77.52-96.82)
	54-58	P/P (92)	19.96 (18.22-22.73)	70.59 (62.66-75.07)	19.96 (14.00-26.37)	70.59 (58.54-83.18)
		M/M (22)	26.52 (23.56-30.01)	88.22 (78.90-94.10)	26.52 (23.54-30.20)	88.22 (77.92-94.32)
	94-103	P/P (139)	15.07 (13.97-16.77)	56.22 (50.18-61.20)	15.07 (10.20-20.70)	56.22 (39.97-69.67)
		M/M (7)	18.85 (11.67-31.61)	75.94 (43.40-96.95)	18.85 (14.18-28.24)	75.94 (55.40-90.74)
	129-146	P/P (38)	8.67 (7.24-10.27)	33.82 (27.95-39.87)	8.67 (5.48-12.68)	33.82 (25.52-50.97)
		M/M (5)	13.51 (n. a.)	48.16 (n. a.)	13.51 (4.78-19.64)	48.16 (17.95-68.86)
	176-203	P/P (36)	7.97 (5.98-10.03)	30.44 (23.38-42.16)	7.97 (5.51-11.36)	30.44 (20.50-48.77)
		M/M (0)	n. a.	n. a.	n. a.	n. a.

Median values with 95% CI and IQR are shown for normalised RBD$_{wt}$ IgG signal or ACE2 binding inhibition. Data is graphically displayed in Figure 6. Different vaccines are abbreviated as follows: M/M – two-dose mRNA-1273. P/P – two-dose BNT162b2.

Appendix V: Antibody binding and ACE2 binding inhibition is significantly reduced for both the BA1 and BA2 omicron variants

Daniel Junker*, **Matthias Becker***, Teresa R. Wagner*, Philipp D. Kaiser, Sandra Maier, Tanja M. Grimm, Johanna Griesbaum, Patrick Marsall, Jens Gruber, Bjoern Traenkle, Constanze Heinzel, Yudi T. Pinilla, Jana Held, Rolf Fendel, Andrea Kreidenweiss, Annika Nelde, Yacine Maringer, Sarah Schroeder, Juliane S. Walz, Karina Althaus, Gunalp Uzun, Marco Mikus, Tamam Bakchoul, Katja Schenke-Layland, Stefanie Bunk, Helene Haeberle, Siri Göpel, Michael Bitzer, Hanna Renk, Jonathan Remppis, Corinna Engel, Axel R. Franz, Manuela Harries, Barbora Kessel, Berit Lange, Monika Strengert, Gerard Krause, Anne Zeck, Ulrich Rothbauer & Alex Dulovic

* = Authors contributed equally

Antibody Binding and Angiotensin-Converting Enzyme 2 Binding Inhibition Is Significantly Reduced for Both the BA.1 and BA.2 Omicron Variants

Daniel Junker,[1,a] Matthias Becker,[1,a] Teresa R. Wagner,[1,2,a] Philipp D. Kaiser,[1] Sandra Maier,[1] Tanja M. Grimm,[1] Johanna Griesbaum,[1] Patrick Marsall,[1] Jens Gruber,[1] Bjoern Traenkle,[1] Constanze Heinzel,[3] Yudi T. Pinilla,[3] Jana Held,[3] Rolf Fendel,[3,4,5] Andrea Kreidenweiss,[3,4,5] Annika Nelde,[6,7,8,9] Yacine Maringer,[6,7,8,9] Sarah Schroeder,[6,8,10] Juliane S. Walz,[6,7,8,9] Karina Althaus,[11,12] Gunalp Uzun,[11] Marco Mikus,[11] Tamam Bakchoul,[11,12] Katja Schenke-Layland,[1,8,13,14] Stefanie Bunk,[15] Helene Haeberle,[16] Siri Göpel,[4,15] Michael Bitzer,[15,17] Hanna Renk,[18] Jonathan Remppis,[18] Corinna Engel,[18,19] Axel R. Franz,[18,19] Manuela Harries,[20] Barbora Kessel,[20] Berit Lange,[20] Monika Strengert,[20,21] Gerard Krause,[20,21] Anne Zeck,[1] Ulrich Rothbauer,[1,2] Alex Dulovic,[1,b] and Nicole Schneiderhan-Marra[1,b]

[1]NMI Natural and Medical Sciences Institute at the University of Tuebingen, Reutlingen, Germany; [2]Pharmaceutical Biotechnology, University of Tuebingen, Tuebingen, Germany; [3]Institute of Tropical Medicine, University Hospital Tuebingen, Tuebingen, Germany; [4]German Center for Infection Research, partner site Tuebingen, Tuebingen, Germany; [5]Centre de Recherches Médicales de Lambaréné, Lambaréné, Gabon; [6]Department of Peptide-Based Immunotherapy, University of Tuebingen and University Hospital Tuebingen, Tuebingen, Germany; [7]Department of Internal Medicine, Clinical Collaboration Unit Translational Immunology, German Cancer Consortium, University Hospital Tuebingen, Tuebingen, Germany; [8]Department of Immunology, Institute for Cell Biology, University of Tuebingen, Tuebingen, Germany; [9]Cluster of Excellence iFIT (EXC2180) "Image-Guided and Functionally Instructed Tumor Therapies," University of Tuebingen, Tuebingen, Germany; [10]Department of Otorhinolaryngology, Head and Neck Surgery, University of Tuebingen, Tuebingen, Germany; [11]Center for Clinical Transfusion Medicine, Tuebingen, Germany; [12]Institute of Clinical and Experimental Transfusion Medicine, University Hospital Tuebingen, Tuebingen, Germany; [13]Department for Medical Technologies and Regenerative Medicine, Institute of Biomedical Engineering, University of Tuebingen, Tuebingen, Germany; [14]Division of Cardiology, Department of Medicine, University of California, Los Angeles, Los Angeles, California, USA; [15]Infectious Diseases, Department of Internal Medicine I, University Hospital Tuebingen, Tuebingen, Germany; [16]Department of Anaesthesiology and Intensive Care Medicine, University Hospital Tuebingen, Tuebingen, Germany; [17]Center for Personalized Medicine, University of Tuebingen, Tuebingen, Germany; [18]University Children's Hospital, Tuebingen, Germany; [19]Center for Pediatric Clinical Studies, University Hospital Tuebingen, Tuebingen, Germany; [20]Helmholtz Centre for Infection Research, Braunschweig, Germany; and [21]TWINCORE, Centre for Experimental and Clinical Infection Research, a joint venture of Hannover Medical School and the Helmholtz Centre for Infection Research, Hannover, Germany

Background. The rapid emergence of the Omicron variant and its large number of mutations led to its classification as a variant of concern (VOC) by the World Health Organization. Subsequently, Omicron evolved into distinct sublineages (eg, BA.1 and BA.2), which currently represent the majority of global infections. Initial studies of the neutralizing response toward BA.1 in convalescent and vaccinated individuals showed a substantial reduction.

Methods. We assessed antibody (immunoglobulin G [IgG]) binding, ACE2 (angiotensin-converting enzyme 2) binding inhibition, and IgG binding dynamics for the Omicron BA.1 and BA.2 variants compared to a panel of VOCs/variants of interest, in a large cohort (N = 352) of convalescent, vaccinated, and infected and subsequently vaccinated individuals.

Results. While Omicron was capable of efficiently binding to ACE2, antibodies elicited by infection or immunization showed reduced binding capacities and ACE2 binding inhibition compared to wild type. Whereas BA.1 exhibited less IgG binding compared to BA.2, BA.2 showed reduced inhibition of ACE2 binding. Among vaccinated samples, antibody binding to Omicron only improved after administration of a third dose.

Conclusions. Omicron BA.1 and BA.2 can still efficiently bind to ACE2, while vaccine/infection-derived antibodies can bind to Omicron. The extent of the mutations within both variants prevents a strong inhibitory binding response. As a result, both Omicron variants are able to evade control by preexisting antibodies.

Keywords. SARS-CoV-2; Omicron; antibody binding; multiplex; variants of concern.

Since its initial outbreak in late 2019, severe acute respiratory syndrome coronavirus 2 (SARS-CoV-2) has evolved into a global pandemic, characterized by multiple waves of infection within countries and regions. Following the initial global wave, subsequent waves were often triggered by the emergence of variants of concern (VOCs) [1] that outcompeted earlier variants. These emerging VOCs are presumed to have an increased rate of transmission or the ability to escape vaccine and infection-induced immunity [2–7]. Due to concerns that its numerous spike protein mutations would render it able to escape immune control and its rapid spread in South Africa, the World Health Organization classified Omicron as a VOC on 26 November 2021 [8]. Within days of this classification,

211

Omicron had already been reported in multiple other countries and as of 26th April 2022, it is the dominant global variant [9]. The BA.2 lineage has now surpassed BA.1 [9], which is not only genetically distinct in key regions of the spike glycoprotein [10, 11], but has also evolved to give rise to BA.4, BA.5, and BA.2.12.1. Early studies at the end of 2021 of neutralization against BA.1 found a substantial reduction in neutralizing activity, particularly in individuals who did not receive 3 vaccine doses [12–17]. Because of the urgency of these studies to establish real-time data of whether there is an evasion toward vaccine-induced responses or therapeutics, they often included limited sample numbers, diversity of sample types (eg, only those vaccinated with Pfizer BNT162b2), or only directly compared Omicron to wild-type (WT) or a single other VOC. Complementary to these studies, we provide here a comprehensive analysis of the binding capacity, binding dynamics, and angiotensin-converting enzyme 2 (ACE2) binding inhibition of Omicron BA.1 and BA.2 against antibodies generated either by vaccination or natural infection compared to WT, currently recognized VOCs, and the Lambda and Mu variants of interest (VOIs). We also analyzed samples from a range of vaccines and dosing schemes currently available within the European Union, including booster vaccines, as well as convalescent samples from both adults and children from the first, second, and third waves of infection in Germany.

METHODS

Sample Cohort

Serum samples used in this study were originally collected for use in several other studies [18–21]. The sample set was designed to include a broad representation of samples from infected individuals (hereafter referred to as "convalescent") from the different waves of SARS-CoV-2 within Germany, as well as vaccinated samples. We separated our cohort into 4 groups: vaccinated samples, convalescent samples, infected and later vaccinated samples, and prepandemic samples as controls.

Vaccinated study participants received either 2 homologous doses of AZD1222, BNT162b2, or mRNA-1273; 2 heterologous doses of AZD1222 and BNT162b2 or AZD1222 and mRNA-1273; or 3 doses of BNT162b2. To examine how antibody dynamics changed over time, we included samples from both 1–2 months post–second dose and 5–6 months post–second dose. We also included samples from vaccinated individuals who had a previous polymerase chain reaction (PCR)–confirmed infection and then received a single dose of BNT162b2 as per national guidelines. Samples from convalescent study participants were collected approximately 3 months after positive PCR. To assess differences between variants of SARS-CoV-2, we collected samples from those with a WT, Alpha, or Delta infection. WT samples came from both adults and children. To be considered a WT sample, the infection had to occur during the first wave of the SARS-CoV-2 pandemic in Germany (spring–summer 2020). Alpha samples were confirmed by PCR sequencing and were collected between January and May 2021. Delta samples were either confirmed by PCR sequencing, or where collected during a time period when all infections in Germany were considered to be Delta (September–November 2021). To represent naive samples, negative prepandemic samples were obtained from Central BioHub. An overview of the characteristics for each cohort subgroup can be found in Table 1.

Table 1. Overview of Sample Characteristics for the Study Population

Sample Type	Subgroup	No. of Samples	Median dT, Days (IQR)	No. (%) of Females	Median Age, Years (IQR)	History of Immunosuppressive Condition or Medication, No. (%)
Convalescent	WT (adults)	30	104 (94–119)	14 (47)	62 (51–69)	0 (0)
	WT (children)	20	124 (116–129)	7 (35)	11 (7–14)	0 (0)
	Alpha	30	88 (47–104)	12 (40)	56 (42–65)	14 (47)
	Delta	6	18 (10–23)	5 (83)	65 (56–73)	4 (67)
Infected and vaccinated	…	25	54 (23–91)	16 (64)	55 (48–59)	1 (4)
Vaccinated	A/A (1–2 mo)	30	49 (48–52)	20 (67)	64 (60–66)	2 (7)
	A/A (4–6 mo)	30	154 (146–158)	23 (77)	55 (48–60)	0 (0)
	M/M (1–2 mo)	30	51 (48–54)	20 (67)	59 (49–61)	1 (3)
	M/M (4–6 mo)	16	139 (131–145)	9 (56)	70 (51–83)	1 (6)
	P/P (1–2 mo)	30	51 (49–54)	20 (67)	58 (52–66)	1 (3)
	P/P (4–6 mo)	30	152 (141–160)	25 (83)	38 (30–53)	0 (0)
	A/M	20	153 (150–154)	16 (80)	41 (29–56)	0 (0)
	A/P	20	151 (144–157)	19 (95)	48 (42–56)	0 (0)
	P/P/P	20	14 (14–26.5)	13 (65)	33 (29–44)	2 (12)
Negative	…	15	…	8 (53)	37 (29–41)	0 (0)

Abbreviations: A/A, 2-dose AZD1222; A/M, first dose AZD1222, second dose mRNA-1273; A/P, first dose AZD1222, second dose BNT162b2; dT, time post-infection/last vaccination dose; IQR, interquartile range; M/M, 2-dose mRNA-1273; P/P, 2-dose BNT162b2; P/P/P, 3-dose BNT162b2; WT, wild-type (B.1 isolate).

Ethical Oversight

Informed written consent was obtained from all study participants. Ethical approval and oversight for the samples used in this study was provided by the following ethics committees: the Ethics Committee of the University Hospital Tuebingen (293/2020BO2, 764/2020/BO2 [amended 6 December 2021], B312/2020BO1 [amended 2 June 2021], 556/2021BO1), the Ethics Committee of the University of Tuebingen (179/2020/BO2, 188/2020A), and the Ethics Committee of Hannover Medical School (9086_BO_S_2020).

Mass Spectrometry of Omicron Receptor-Binding Domain

Receptor-binding domain (RBD) Omicron protein samples had their structure verified by liquid chromatography–mass spectrometry (LC-MS). In brief, samples were N-deglycosylated using PNGaseF reducing kit (New England Biolabs), diluted 1:3 with His-NaCl buffer and analyzed by liquid chromatography coupled to electrospray ionization quadrupole time-of-flight mass spectrometry. For full details, please consult the Supplementary Methods.

MULTICOV-AB Assay

MULTICOV-AB, a previously published multiplex immunoassay, was performed as described previously [22]. A full list of antigens included within the assay is shown in Table 2. Samples were randomly allocated to plates to ensure that at least 3 samples of every sample group were included on each plate. All samples were measured twice in 2 independent experiments.

No sample failed quality control (QC). Raw median fluorescence intensity values were normalized to a QC sample for all antigens as per Becker et al [23]. Please consult the Supplementary Methods for full details.

RBDCoV-ACE2 Assay

RBDCoV-ACE2, a previously published multiplex ACE2 inhibition assay [19], analyzes neutralizing antibody activity through ACE2 binding inhibition. A full list of antigens included in this assay can be found in Table 2. ACE2 binding inhibition was calculated as a percentage, with 100% indicating maximum ACE2 binding inhibition and 0% indicating no ACE2 binding inhibition. Samples with an ACE2 binding inhibition <20% are classified as nonresponders [19]. Please consult the Supplementary Methods for full details.

Biolayer Interferometry

Analysis of binding kinetics of RBD-specific antibodies in serum samples were performed using the Octet RED96e system (Sartorius) as per the manufacturer's recommendations. Purified RBDs of WT, Delta, and Omicron were biotinylated with Sulfo-NHS-LC-LC-Biotin (Thermo Fisher Scientific) in 5 molar excess at ambient temperature for 30 minutes. Excess of biotin was removed by size exclusion chromatography using Zeba Spin Desalting Columns 7K MWCO 0.5 mL (Thermo Fisher Scientific) according to the manufacturer's protocol. Data were analyzed using the Octet Data Analysis HT 12.0 software applying the 1:1 fitting model for the dissociation step.

Table 2. Overview of Antigens Used in MULTICOV-AB and RBDCoV-ACE2 Assays

Antigen	Manufacturer	Category Number	Mutations Covered
Spike WT (B.1)	NMI	…	…
RBD WT (B.1)	NMI	…	…
S1 domain WT (B.1)	NMI	…	…
S2 domain WT (B.1)	Sino Biological	40590-V08B	…
Nucleocapsid WT (B.1)	Aalto Bioreagents	6404-b	…
RBD Alpha (B.1.1.7)	NMI	…	N501Y
RBD Beta (B.1.351)	NMI	…	K417N, E484K, N501Y
RBD Gamma (P1)	NMI	…	K417T, E484K, N501Y
RBD Delta (B.1.617.2)	NMI	…	L452R, T478K
RBD Omicron (B.1.529/BA.1)	Sino Biological	40592-V08H121	G339D, S371L, S373P, S375F, K417N, N440K, G446S, S477N, T478K, E484A, Q493R, G496S, Q498R, N501Y, Y505H
Spike Omicron (B.1.1.529/BA.1)	Sino Biological	40589-V08H26	A67V, del HV69/70, T95I, G142D, del VYY 143-145, del N211, L212I, ins214EPE, G339D, S371L, S373P, S375F, K417N, N440K, G446S, S477N, T478K, E484A, Q493R, G496S, Q498R, N501Y, Y505H, T547K, H655Y, N679K, P681H, N764K, D796Y, F817P, N856K, A892P, A899P, A942P, Q954H, N969K, L981F, K986P, V987P
RBD Omicron (B.1.1.529/BA.2)	Sino Biological	40592-V08H123	G339D, S371F, S373P, S375F, T376A, D405N, R408S, K417N, N440K, S477N, T478K, E484A, Q493R, Q498R, N501Y, Y505H
Nucleocapsid Omicron (B.1.1.529/BA.2)	Sino Biological	40588-V07E35	P13L, del ERS 31-33, R203K, G204R, S413R
RBD Lambda (C.37)	NMI	…	L452Q, F490S
RBD Mu (B.1.621)	NMI	…	R346K, E484K, N501Y

Mutations present within each antigen are provided. Where appropriate, the manufacturer category number is provided. For details on the NMI antigen production, please see [19, 22, 23].
Abbreviations: NMI, Natural and Medical Sciences Institute; RBD, receptor-binding domain; WT, wild-type.

Omicron BA.1 and BA.2 Binding Dynamics • CID • 3

The binding profile response of each sample is illustrated as the mean wavelength shift in nm. For affinity determination, the 1:1 global fit of the Data Analysis HT 12.0 software was used. Please consult the Supplementary Methods for full details.

Statistical Analysis

Data were collated and matched to metadata in Excel 2016. Data visualization was done in RStudio (version 1.2.5001 running R version 3.6.1). Additional packages gplots and beeswarm were used for specific displays. The "lm" function of R's stats library was used for linear regression analyzes. Correlation analyzes were performed using the "cor" function of R's stats library. The "wilcox.test" function from R's stats library was used to perform either Mann–Whitney U tests (2-sided) to estimate significance of observed differences between different groups, or Wilcoxon signed-rank tests (2-sided) to estimate significance of observed different between antigens. Graphs were exported from RStudio and further edited in Inkscape (version 0.92.4) to generate final figures. Biolayer inferometry graphical representation was prepared using GraphPad Prism Software (version 9.0.0).

RESULTS

Initially, we examined immunoglobulin G (IgG) binding using MULTICOV-AB [22], a previously published SARS-CoV-2 multiplex immunoassay that was adapted to analyze binding
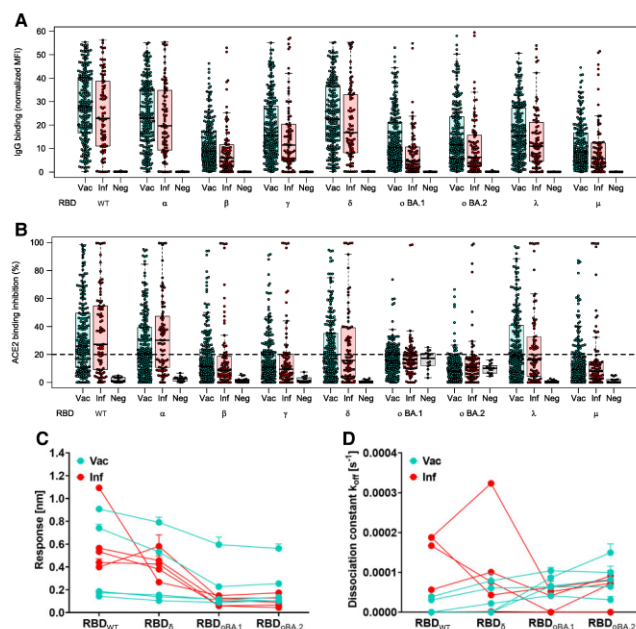
Figure 1. Antibody binding response is significantly reduced for both BA.1 and BA.2. Binding response by preexisting antibodies generated through either infection or vaccination was measured with MULTICOV-AB (*A*) and RBDCoV-ACE2 (*B*) assays and Biolayer interferometry (*C* and *D*). *A*, Boxplot showing that immunoglobulin G binding is significantly reduced for both BA.1 and BA.2 as compared to other variants of concern (VOCs)/variants of interest (VOIs) for convalescent (n = 86) and vaccinated (n = 226) samples. Negative samples are included as controls (n = 15). *B*, Boxplot showing that ACE2 binding inhibition is significantly reduced for both BA.1 and BA.2 as compared to other VOCs/VOIs for both convalescent and vaccinated samples. Boxes represent the median with 25th and 75th percentiles; whiskers show the largest and smallest non-outlier values. Outliers were determined by 1.5 interquartile range. *C* and *D*, Binding kinetics of receptor-binding domain (RBD)–specific antibodies from serum samples of convalescent and vaccinated individuals (both n = 5). Binding response (*C*) and dissociation constant (*D*) were determined by 1:1 fitting model of the individual serum samples between the different RBD variants. Median fold reductions for both (*A*) and (*B*) can be found as Supplementary Tables 1–3 and 5. Statistical differences between all variants was analyzed by Wilcoxon signed-rank test for both (*A*) and (*B*) and is available as Supplementary Tables 4 and 7. The response rate for (*B*) is available as Supplementary Table 6. Abbreviations: ACE2, angiotensin-converting enzyme 2; IgG, immunoglobulin G; Inf, infected; MFI, median fluorescence intensity; Neg, negative; RBD, receptor-binding domain; Vac, vaccinated; WT, wild-type.

toward RBDs from VOC/VOIs (a full list of antigens analyzed and their mutations contained within can be found in Table 2). For both vaccinated and convalescent samples, IgG binding toward both Omicron BA.1 and BA.2 for preexisting antibodies was significantly reduced compared to WT (BA.1: 2.3–4.1 median fold reduction, $P < .001$; BA.2: 2.1–3.0 median fold reduction, $P < .001$) (Figure 1, Supplementary Tables 1–4). This is similar to the statistically significant reduction in binding toward Beta (2.8–3.5 median fold reduction, $P < .001$) and Mu (3.0–3.6 median fold reduction, $P < .001$, Figure 1, Supplementary Tables 1–4). Within Omicron, BA.1 had a significantly increased reduction in IgG binding compared to BA.2 (1.1–1.2 median fold reduction, $P < .001$) (Figure 1, Supplementary Tables 2–4).

Next, we analyzed ACE2 binding inhibition to determine how effective the antibodies were at blocking the RBD-ACE2 interaction, using RBDCoV-ACE2 [19], a multiplex ACE2-RBD inhibition assay. This assay mimics the interaction between ACE2 and the RBD, while the multiplex format allows

for the simultaneous measurement of all VOCs/VOIs in a single well. To evaluate binding against other antigens of SARS-CoV-2, we also include the spike and S1 domain of WT and the spike and nucleocapsid of Omicron. In line with IgG binding, ACE2 binding inhibition against Omicron was significantly reduced compared to WT (Omicron BA.1: median, 15.2%–16.4% and BA.2: median, 8.0%–10.9%; WT: median, 26.1%–27.2%; both $P < .001$) (Figure 1, Supplementary Table 5), with less than half as many samples considered responsive (WT: 62.8%; BA.1: 30.1%–32.6%; BA.2: 8.4%–14.0%) (Figure 1B, Supplementary Table 6). Interestingly, although BA.2 revealed reduced ACE2 binding inhibition and sample response rate compared to BA.1, this was not significant ($P = .08$, Supplementary Table 7). While BA.2 had the lowest response rate of all variants examined, the median ACE2 binding inhibition and response rate for BA.1 was greater than for Beta (median, 8.9–11.4; response, 22.1%–31.0%), Gamma (median, 9.4–10.8; response, 25.5%–30.1%), and Mu (median, 8.1–9.1; response, 19.8%–22.6%).
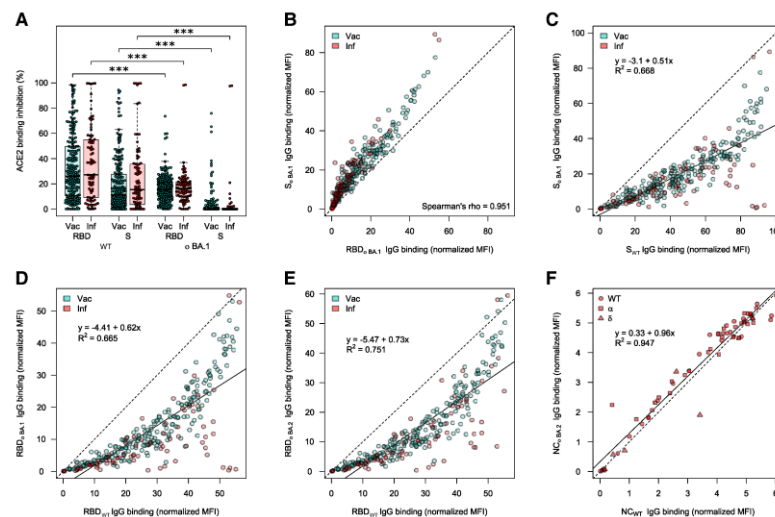
Figure 2. Angiotensin-converting enzyme 2 (ACE2) binding inhibition and correlations of binding capacity between BA.1, BA.2, and wild-type (WT) for different antigens. ACE2 binding inhibition (*A*) and immunoglobulin G (IgG) binding capacity (*B–F*) were compared for the Omicron BA.1 and BA.2 receptor-binding domain (RBD), and spike (S) to the WT RBD and S. *A*, Boxplot showing that ACE2 binding inhibition is significantly reduced toward BA.1 for both RBD and S for both vaccinated (n = 226) and convalescent (n = 86) samples. Boxes represent the median with 25th and 75th percentiles; whiskers show the largest and smallest nonoutlier values. Outliers were determined by 1.5 interquartile range. Statistical significance was calculated by Wilcoxon signed-rank test; ***P < .001. *B*, Correlation analysis of IgG binding capacity for the BA.1 spike compared to the BA.1 RBD. Spearman rank was calculated to assess ordinal association between the variables. *C–F*, Linear regressions of IgG binding capacity for the BA.1 S compared to WT S (*C*), BA.1 RBD compared to wild-type RBD (*D*), BA.2 RBD compared to WT RBD (*E*), and BA.2 nucleocapsid compared to WT nucleocapsid (*F*). R^2 is included to indicate the correlation. Abbreviations: ACE2, angiotensin-converting enzyme 2; IgG, immunoglobulin G; Inf, infected; MFI, median fluorescence intensity; NC, nucleocapsid; RBD, receptor-binding domain; S, spike; Vac, vaccinated; WT, wild-type.

215

To investigate the RBD binding of BA.1 and BA.2 further, we analyzed the binding kinetics of RBD-specific antibodies from vaccinated (2 doses of BNT162b2) and convalescent (WT) study participants by biolayer interferometry analysis (Figure 1C and 1D). Binding response and dissociation constant were measured for each sample as an indicator of amount and binding strength. Binding response toward BA.1 and BA.2 was reduced compared to both WT and Delta (Figure 1C), while most samples showed increased dissociation kinetics for Omicron (Figure 1D). Despite high variation observed for both the vaccinated and convalescent samples, Omicron always showed the lowest binding response (Supplementary Figure 1, Supplementary Table 8). When binding toward ACE2 itself was examined, Omicron BA.1 and BA.2 were still able to bind ACE2 with high affinity (Supplementary Figure 2).

As mutations toward Omicron are not limited to the RBD, we also analyzed ACE2 binding toward the full-length spike protein. Omicron BA.1 ACE2 binding inhibition toward the spike protein was significantly reduced compared to WT ($P <$ .001). Interestingly, the response rate underwent a similar 30% reduction from RBD to S for both WT (62.8% to 34.5%–43.0%) and Omicron (30.1%–32.6% to 3.5%–4.9%) (Figure 2A, Supplementary Table 9). IgG binding capacity toward spike appears to be conserved to a similar degree as the RBD (Figure 2B–D). However, this is substantially reduced compared to the nucleocapsid of BA.2, for which there was no change in binding capacity compared to WT for convalescent samples, regardless with which strain they had been previously infected (Figure 2E, samples highlighted according to strain).

Next, we analyzed whether vaccine type (AZD1222, mRNA-1273, or BNT162b2) and number of doses (homologous or heterologous 2 dose, or homologous 3 dose) received resulted in differences with respect to Omicron binding response. To analyze how this response changed as time postvaccination increased, we also compared the responses at
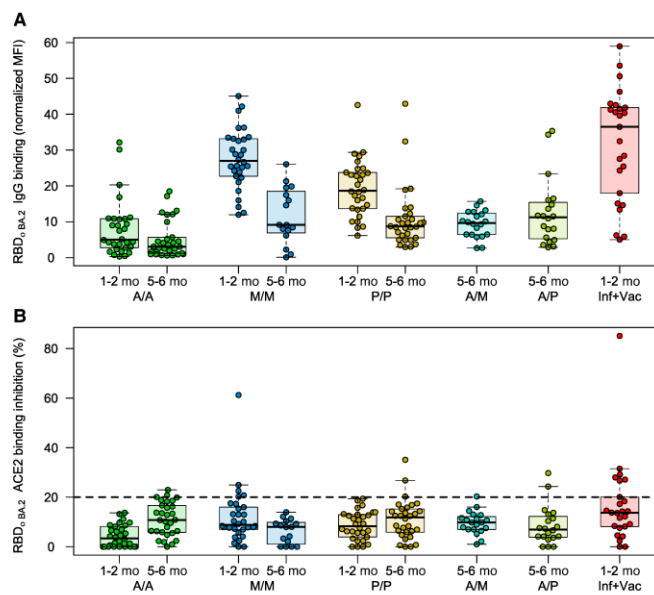
Figure 3. Differences in Omicron binding response among different populations of vaccinated samples. Binding response toward Omicron BA.2 was analyzed by either MULTICOV-AB (A) or RBDCoV-ACE2 (B) assays for samples from different vaccine schemes (n = 30 for all samples, except for mRNA-1273 at 5–6 months (n = 16), heterologous vaccine schemes (both n = 20), and infected and vaccinated (n = 25). To determine the effect of time postvaccination, samples from both 1–2 months and 5–6 months postvaccination were included. Boxes represent the median with 25th and 75th percentiles; whiskers show the largest and smallest nonoutlier values. Outliers were determined by 1.5 interquartile range. The 20% cutoff for nonresponders is indicated by the dashed line on (B). The equivalent data for BA.1 are provided as Supplementary Figure 3. Abbreviations: A/A, AZD1222; ACE2, angiotensin-converting enzyme 2; A/M, first dose AZD1222, second dose mRNA-1273; A/P, first dose AZD1222, second dose BNT162b2; IgG, immunoglobulin G; Inf, infected; MFI, median fluorescence intensity; M/M, mRNA-1273; P/P, BNT162b2; RBD, receptor-binding domain; Vac, vaccinated.

1–2 months post–second dose and 5–6 months post–second dose for the homologous recipients. IgG binding capacity at 5–6 months was low for all recipients regardless of the administered vaccine, although homologous mRNA-based vaccination still had higher binding capacity at this timepoint than 1–2 months post–second dose for vector-based vaccination (median of 9.16, 8.7, and 5.04 for mRNA-1273, BNT-162b2, and AZD1222, respectively; Figure 3A). Among samples from 1–2 months postdosing, infected and then vaccinated had the greatest IgG binding capacity (median, 36.5), followed by 2-dose mRNA-1273 (median, 27.0), BNT162b2 (median, 18.7), and AZD1222 (median, 2.3). This pattern was consistent for both BA.1 (Supplementary Figure 3) and BA.2 (Figure 3). ACE2 binding inhibition was consistently low regardless of type received and timeframe postdose (Figure 3B).

To determine whether a third dose results in increased binding responses against Omicron, we analyzed samples from individuals who had received a third dose of BNT162b2 and compared it to those who had received their second dose in a similar timeframe and individuals 5–6 months post–second dose, who would be eligible to receive a third dose (Figure 4). Further boosting was associated with higher Omicron ACE2 binding inhibition compared to 2 doses (27% and 0% of samples were responders toward BA.1 and BA.2 post–second dose, respectively; 55% and 25% were responders after boosting) suggesting that boosting offers increased protection against Omicron (Figure 4). However, this increase in protection was not limited to Omicron and was present for all VOCs (Figure 4). Compared to the second dose from a similar timepoint (30% and 10% responders to BA.1 and BA.2, respectively), boosting with the third dose increased ACE2 binding inhibition, substantially confirming this effect is generated by the third dose itself, and not by time postvaccination alone (Figure 4C).

Last, we analyzed whether natural infection with different variants resulted in differences in binding responses. There was no difference in ACE2 binding inhibition between convalescent individuals infected with either WT or Alpha, with both having minimal inhibition against Omicron (Figure 5A, Supplementary Figure 3). While some samples with a previous Delta infection showed substantially more activity compared to WT or Alpha, they had been collected much sooner after the infection (median dT, 18 days) than WT (median dT, 104 days) or Alpha (median dT, 88 days). To evaluate whether children's antibodies were more effective at binding toward Omicron than adults, we compared convalescent samples 3–4 months post-PCR from the first wave in children (n = 20), to convalescent samples 3 months post–positive PCR from the same wave in adults (n = 30) (Figure 5B and 5C, Supplementary Figure 4). There was no significant difference between adults and children in ACE2 binding inhibition (P = .48; Figure 5B), although children did have significantly reduced binding capacity toward Omicron (P = .01; Figure 5C).
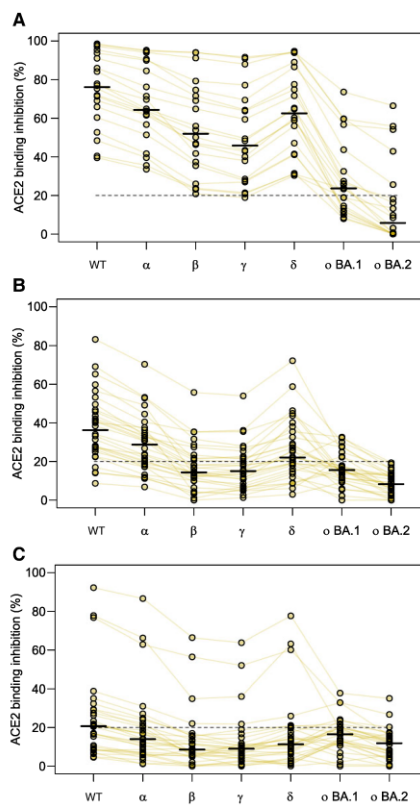

Figure 4. Angiotensin-converting enzyme 2 (ACE2) binding inhibition toward Omicron is boosted by a third vaccine dose. Changes in ACE2 binding response following the third dose of BNT162b2 for all variants within the study. Samples come from either boosted (n = 20, A), 1–2 months post–second dose of BNT162b2 (n = 20, B), or 5–6 months post–second dose of BNT162b2 (n = 20, C). Individual samples are highlighted by connected lines with bars representing medians. The 20% cutoff for nonresponders is indicated by the dashed line. Abbreviations: ACE2, angiotensin-converting enzyme 2; WT, wild-type.

DISCUSSION

In this study, we provide an in-depth characterization of antibody binding to Omicron BA.1 and BA.2 compared to WT and all other VOCs and variants under investigation in a large, diverse sample cohort. The use of an ACE2 inhibition assay enabled the comparison of multiple variants of interest simultaneously, while also producing comparable results to classical virus neutralization assays [19]. Similar to others, we
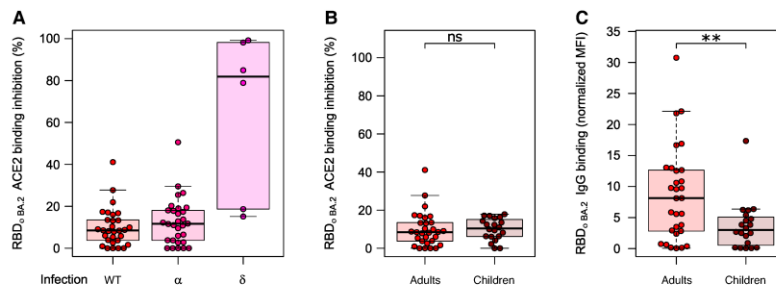
Figure 5. Differences in immunoglobulin G (IgG) binding response and angiotensin-converting enzyme 2 (ACE2) binding inhibition toward BA.2 among different populations of convalescent samples. Comparative ACE2 binding inhibition (*A* and *B*) and IgG binding capacity (*C*) between convalescent samples from different pandemic waves (*A*) and adults and children (*B* and *C*) for BA.2. *A*, There are no differences in ACE2 binding inhibition toward BA.2 for individuals infected with wild-type (WT) (n = 30), Alpha (n = 30), or Delta (n = 6). *B*, Children (n = 20) and adults (n = 30) have similar ACE2 binding inhibition toward BA.2 following WT infection, although they have significantly reduced IgG binding capacity (*P* = .01). *C*, Boxes represent the median with 25th and 75th percentiles; whiskers show the largest and smallest nonoutlier values. Outliers were determined by 1.5 interquartile range. Statistical significance was calculated by Mann–Whitney *U* test: **P < .01; ns, *P* < .05. The equivalent data for BA.1 are provided as Supplementary Figure 4. Abbreviations: ACE2, angiotensin-converting enzyme 2; IgG, immunoglobulin G; MFI, median fluorescence intensity; RBD, receptor-binding domain; WT, wild-type.

identified that antibody binding and ACE2 binding inhibition toward both Omicron BA.1 and BA.2 elicited by either immunization or previous infection were significantly reduced [14, 16, 24–28]. However, we provide here additional information on IgG binding capacity and ACE2 binding inhibition by the inclusion of a large variety of subcohorts representing the present diversity of immunity against SARS-CoV-2, the comparison of the Omicron variant to all other VOCs/VOIs, and the comparison between BA.1 and BA.2.

We found that both IgG binding capacity and ACE2 binding inhibition was significantly reduced for BA.1 and BA.2, similar to reductions for Beta and Mu, with the majority of samples being classified as nonresponsive toward Omicron for ACE2 binding inhibition. Like others researchers [15, 24, 28], we found that antibody binding responses toward Omicron were significantly increased upon administration of a booster dose. Boosting increases were not restricted to just Omicron IgG binding capacity and ACE2 binding inhibition, but were present against all VOCs/VOIs. No significant difference was present between BA.1 and BA.2. However, data regarding the longitudinal response post–third dose remains lacking, with some countries now offering a fourth dose for certain groups (eg, immunocompromised individuals). The increased responses following boosting also appear to apply for convalescent individuals, as seen by the increased IgG binding capacity and ACE2 binding inhibition for previously infected individuals who received a single dose, compared to those who had received any 2 vaccine doses. This increase in responses for individuals who have been both infected and vaccinated is in agreement with Pajon et al [29], who found that infections prior to vaccination resulted in a greater breadth of immune

response, while Lechmere et al [26] found that breakthrough Delta infections among vaccinated individuals acted like a booster dose. Thus, both reinfection and a booster dose leads to appropriate affinity maturation of elicited antibodies. Among those who had received 2 doses, binding responses were consistent with other reports (eg, [16]) in identifying a significant decrease for those who received homologous 2-dose vector vaccination as opposed to homologous mRNA vaccination or heterologous vaccination.

We identified no significant difference in ACE2 binding inhibition toward Omicron for children compared to adults, although IgG binding capacity was significantly reduced. This is in contrast to previous research that has identified that children's antibody titers are higher than adults following infection [21]; however, a limitation of our study is that the children and adult groups were not well-matched in terms of time post–positive PCR (median dT, 104 for adults and 124 for children) or disease severity (majority hospitalized adults vs asymptomatic/mildly symptomatic children). A larger investigation including vaccinated samples from children is needed to investigate any possible protective effect from previous infection and the antibody response toward Omicron itself in children in more detail.

Similar to Carreño et al [27], we identified that IgG binding capacity toward Omicron was not as severely reduced as ACE2 binding inhibition. Interestingly, while BA.2 had significantly increased IgG binding capacity to BA.1, it had reduced ACE2 binding inhibition. While mutations in BA.1 and BA.2 are not limited to the RBD, their reduction in activity was limited to the trimeric spike, with near-identical binding compared to WT for the nucleocapsid. Our analysis of both the spike- and

218

RBD-derived ACE2 binding inhibition suggests that while both epitopes are sufficiently conserved to enable binding, their divergent mutated sequences affect their inhibitory response. Further investigation into this pattern and particularly the role of S1-derived antibodies in neutralization is required to understand the inhibitory protection offered against Omicron.

Overall, our results identify that while Omicron can efficiently bind ACE2 and vaccine/infection-induced antibodies can bind Omicron, the extent of the mutations within the RBD appear too divergent to enable RBD-directed antibodies to mount an inhibitory response. The dramatic reductions in both IgG binding and ACE2 binding inhibition toward Omicron, as opposed to other VOCs/VOIs, confirm that this variant remains capable of immune escape and requires careful sequence monitoring to identify any further sequence evolution. Importantly, booster doses elicit a significant increase in antibody response, which correlates with a significant increase in both IgG binding and ACE2 binding inhibition against Omicron. Our data add weight to a growing body of evidence that the continuous adaptation of vaccines toward novel highly contagious variants needs to be considered in order to control SARS-CoV-2.

Supplementary Data

Supplementary materials are available at *Clinical Infectious Diseases* online. Consisting of data provided by the authors to benefit the reader, the posted materials are not copyedited and are the sole responsibility of the authors, so questions or comments should be addressed to the corresponding author.

Notes

References

1. World Health Organization. Tracking SARS-CoV-2 variants. Available at: https://www.who.int/en/activities/tracking-SARS-CoV-2-variants/. Accessed 1 May 2022.
2. Korber B, Fischer WM, Gnanakaran S, et al. Tracking changes in SARS-CoV-2 spike: evidence that D614G increases infectivity of the COVID-19 virus. Cell 2020; 182:812–27.e19.
3. Graham MS, Sudre CH, May A, et al. Changes in symptomatology, reinfection, and transmissibility associated with the SARS-CoV-2 variant B.1.1.7: an ecological study. Lancet Public Health 2021; 6:E335–45.
4. Davies NG, Abbott S, Barnard RC, et al. Estimated transmissibility and impact of SARS-CoV-2 lineage B.1.1.7 in England. Science 2021; 372:eabg3055.
5. Collier DA, De Marco A, Ferreira IATM, et al. Sensitivity of SARS-CoV-2 B.1.1.7 to mRNA vaccine-elicited antibodies. Nature 2021; 593:136–41.
6. Tao K, Tzou PL, Nouhin J, et al. The biological and clinical significance of emerging SARS-CoV-2 variants. Nat Rev Genet 2021; 22:757–73.
7. Pegu A, O'Connell SE, Schmidt SD, et al. Durability of mRNA-1273 vaccine-induced antibodies against SARS-CoV-2 variants. Science 2021; 373:1372–7.
8. World Health Organization. Classification of Omicron (B.1.1.529): SARS-CoV-2 variant of concern. 2021. Available at: https://www.who.int/news/item/26-11-2021-classification-of-omicron-(b.1.1.529)-sars-cov-2-variant-of-concern. Accessed 1 May 2022.
9. CoVariants. Shared mutations. Available at: https://covariants.org/shared-mutations/. Accessed 1 May 2022.
10. Rambaut A, Holmes EC, O'Toole Á, et al. A dynamic nomenclature proposal for SARS-CoV-2 lineages to assist genomic epidemiology. Nat Microbiol 2020; 5:1403–7.
11. cov-lineages.org. Lineage B.1.1.529. 2022. Available at: https://cov-lineages.org/lineage.html?lineage=B.1.1.529. Accessed 1 May 2022.
12. Cele S, Jackson L, Khoury DS, et al. SARS-CoV-2 Omicron has extensive but incomplete escape of Pfizer BNT162b2 elicited neutralization and requires ACE2 for infection. medRxiv [Preprint]. Posted online 17 December 2021. doi:10.1101/2021.12.08.21267417.
13. Cao Y, Wang J, Jian F, et al. Omicron escapes the majority of existing SARS-CoV-2 neutralizing antibodies. Nature 2022; 602:657–63.
14. Nemet I, Kliker L, Lustig Y, et al. Third BNT162b2 vaccination neutralization of SARS-CoV-2 Omicron infection. N Engl J Med 2022; 386:492–4.
15. Garcia-Beltran WF, StDenis KJ, Hoelzemer A, et al. mRNA-based COVID-19 vaccine boosters induce neutralizing immunity against SARS-CoV-2 Omicron variant. Cell 2022; 185:457–66.e4.

219

16. Schmidt F, Muecksch F, Weisblum Y, et al. Plasma neutralization of the SARS-CoV-2 Omicron variant. N Engl J Med 2022; 386:599–601.

17. Aggarwal A, Stella AO, Walker G, et al. SARS-CoV-2 Omicron: evasion of potent humoral responses and resistance to clinical immunotherapeutics relative to viral variants of concern. medRxiv [Preprint]. Posted online 15 December 2021. doi:10.1101/2021.12.14.21267772.

18. Gornyk D, Harries M, Glöckner S, et al. SARS-CoV-2 seroprevalence in Germany. Dtsch Arztebl Int 2021; 118:824–31.

19. Junker D, Dulovic A, Becker M, et al. COVID-19 patient serum less potently inhibits ACE2-RBD binding for various SARS-CoV-2 RBD mutants. Sci Rep 2021; 12: 7168.

20. Heinzel C, Pinilla YT, Elsner K, et al. Non-invasive antibody assessment in saliva to determine SARS-CoV-2 exposure in young children. Front Immunol 2021; 12: 753435.

21. Renk H, Dulovic A, Seidel A, et al. Robust and durable serological response following pediatric SARS-CoV-2 infection. Na Commun 2022; 13:128.

22. Becker M, Strengert M, Junker D, et al. Exploring beyond clinical routine SARS-CoV-2 serology using MultiCoV-Ab to evaluate endemic coronavirus cross-reactivity. Nat Commun 2021; 12:1152.

23. Becker M, Dulovic A, Junker D, et al. Immune response to SARS-CoV-2 variants of concern in vaccinated individuals. Nat Commun 2021; 12:3109.

24. Gruell H, Vanshylla K, Tober-Lau P, et al. mRNA booster immunization elicits potent neutralizing serum activity against the SARS-CoV-2 Omicron variant. Nat Med 2022; 28:477–80.

25. Wilhelm A, Widera M, Grikscheit K, et al. Reduced neutralization of SARS-CoV-2 Omicron variant by vaccine sera and monoclonal antibodies. medRxiv [Preprint]. Posted online 8 December 2021. doi:10.1101/2021.12.07.21267432.

26. Lechmere T, Snell LB, Graham C, et al. Broad neutralization of SARS–CoV–2 variants, including Omicron, following breakthrough infection with Delta in COVID–19–vaccinated individuals. mBio 2022; 13:e0379821.

27. Carreño JM, Alshammary H, Tcheou J, et al. Activity of convalescent and vaccine serum against SARS-CoV-2 Omicron. Nature 2022; 602:682–8.

28. Pajon R, Doria-Rose NA, Shen X, et al. SARS-CoV-2 Omicron variant neutralization after mRNA-1273 booster vaccination. N Engl J Med 2022; 386:1088–91.

29. Goel RR, Apostolidis SA, Painter MM, et al. Distinct antibody and memory B cell responses in SARS-CoV-2 naive and recovered individuals following mRNA vaccination. Sci Immunol 2021; 6:eabi6950.

220

Supplementary Information - Antibody binding and ACE2 binding inhibition is significantly reduced for both the BA1 and BA2 omicron variants

Daniel Junker[1,*], Matthias Becker[1,*], Teresa R. Wagner[1,2,*], Philipp D. Kaiser[1], Sandra Maier[1], Tanja M. Grimm[1], Johanna Griesbaum[1], Patrick Marsall[1], Jens Gruber[1], Bjoern Traenkle[1], Constanze Heinzel[3], Yudi T. Pinilla[3], Jana Held[3], Rolf Fendel[3,4,5], Andrea Kreidenweiss[3,4,5], Annika Nelde[,6,7,8,9], Yacine Maringer[6,7,8,9], Sarah Schroeder[6,8,10], Juliane S. Walz[6,7,8,9], Karina Althaus[11,12], Gunalp Uzun[11], Marco Mikus[11], Tamam Bakchoul[11,12], Katja Schenke-Layland[1,8,13,14], Stefanie Bunk[15], Helene Haeberle[16], Siri Göpel[4,15], Michael Bitzer[15,17], Hanna Renk[18], Jonathan Remppis[18], Corinna Engel[18,19], Axel R. Franz[18,19], Manuela Harries[20], Barbora Kessel[20], Berit Lange[20], Monika Strengert[20,21], Gerard Krause[20,21], Anne Zeck[1], Ulrich Rothbauer[1,2], Alex Dulovic[1,§,#] and Nicole Schneiderhan-Marra[1,§,#]

Author affiliations

1 – NMI Natural and Medical Sciences Institute at the University of Tuebingen, Reutlingen, Germany

2 – Pharmaceutical Biotechnology, University of Tuebingen, Tuebingen, Germany

3 – Institute of Tropical Medicine, University Hospital Tuebingen, Tuebingen, Germany

4 – German Center for Infection Research (DZIF), Partner Site Tuebingen, Tuebingen, Germany

5 - Centre de Recherches Médicales de Lambaréné (CERMEL), Gabon

6- Department of Peptide-based Immunotherapy, University of Tuebingen and University Hospital Tuebingen, Tuebingen, Germany

7 – Clinical Collaboration Unit Translational Immunology, German Cancer Consortium (DKTK), Department of Internal Medicine, University Hospital Tuebingen, Tuebingen, Germany

8 – Institute for Cell Biology, University of Tuebingen, Tuebingen, Germany

9 – Cluster of Excellence iFIT (EXC2180) "Image-Guided and Functionally Instructed Tumor Therapies", University of Tuebingen, Tuebingen, Germany

10 – Department of Otolaryngology, Head and Neck Surgery, University of Tuebingen, Tuebingen, Germany

11 – Center for Clinical Transfusion Medicine, Tuebingen, Germany

12 – Institute of Clinical and Experimental Transfusion Medicine, University Hospital Tuebingen, Tuebingen, Germany

13 – Institute of Biomedical Engineering, Department for Medical Technologies and Regenerative Medicine, University of Tuebingen, Tuebingen, Germany

14 – Department of Medicine/Cardiology, University of California Los Angeles (UCLA), Los Angeles, USA

15 – Infectious Diseases, Department Internal Medicine I, University Hospital Tuebingen, Tuebingen, Germany

16 – Department of Anaesthesiology and Intensive Care Medicine, University Hospital Tuebingen, Tuebingen, Germany

17 – Center for Personalized Medicine, University of Tuebingen, Tuebingen, Germany

18 – University Children's Hospital, Tuebingen, Germany

19 – Center for Pediatric Clinical Studies, University Hospital Tuebingen, Tuebingen, Germany

20 – Helmholtz Centre for Infection Research, Braunschweig, Germany

21 – TWINCORE, Centre for Experimental and Clinical Infection Research, a joint venture of Hannover Medical School and the Helmholtz Centre for Infection Research, Hannover, Germany

* indicates shared first authorship

§ indicates shared last authorship

# indicates corresponding author

Corresponding author Information

Alex Dulovic – alex.dulovic@nmi.de, +49 (0)7121 51530 580

Nicole Schneiderhan-Marra – nicole.schneiderhan@nmi.de, +49 (0)7121 51530 815

Supplementary Methods

Mass Spectrometry of omicron receptor binding domain (RBD)

The RBD omicron protein samples (5 µg) were N-deglycosylated using a PNGaseF reducing kit (Rapid PNGaseF reducing kit, New England Biolabs, Frankfurt am Main, Germany) by adding ¼ of the volume of reducing buffer included in the kit and denaturation and reduction for 5 minutes at 80 °C. Subsequently, 0.125 µL PNGaseF enzyme preparation, included in the kit, were added and deglycosylation was performed for 10 minutes at 50 °C. Prior to Liquid chromatography-mass spectrometry (LC-MS) analysis, the samples were diluted 1:3 with HisNaCl buffer (20 mmM His 140 mM NaCl, pH 6.0) and analyzed by liquid chromatography (HPLC) coupled to electrospray ionization (ESI) quadrupole time-of-flight (QTOF) MS. Samples (0.4 µg per injection) was desalted using reversed phase chromatography on a Dionex U3000 RSLC system (Thermo Scientific, Dreieich, Germany) using a Acquity BEH300 C4 column (1mm x 50mm, Waters, Eschborn, Germany) at 75°C and 150 µl/min flow rate applying a 11-min linear gradient with varying slopes. In detail, the gradient steps were applied as follows (min/% Eluent B): 0/5, 0.4/5, 2.55/30, 7/50, 7.5/99, 8/5, 8.75/99, 9.5/5, 10/99, 10.25/5 and 11/5. Eluent B was acetonitrile with 0.1% formic acid, and solvent A was water with 0.1% formic acid. To avoid contamination of the mass spectrometer with buffer salts, the HPLC eluate was directed into waste for the first 2 min. Continuous MS analysis was performed using a QTOF mass spectrometer (Maxis UHR-TOF; Bruker, Bremen, Germany) with an ESI source operating in positive ion mode. Spectra were taken in the mass range of 600–2000 m/z. External calibration was applied by infusion of tune mix via a syringe pump during a short time segment at the beginning of the run. Raw MS data were lock-mass corrected (at m/z 1221.9906) and further processed using Data Analysis 5.3 and MaxEnt Deconvolution software tools (Bruker).

Antigen Immobilisation on beads

SARS-CoV-2 wild-type Spike, RBD, S1 domain, S2 domain and Nucleocapsid were immobilised on magnetic MagPlex beads (Luminex) by EDC-sNHS coupling as previously described(1).RBDs from variants of concern and the Omicron Spike protein were immobilised on magnetic MagPlex beads (Luminex) by Anteo coupling (AMG Activation Kit for Multiplex Microspheres, #A-LMPAKMM-400, Anteo Technologies) as previously described(2). Following coupling, beads were stored at 4°C. Prior to experimentation, beads were then combined into a 25x Bead Mix and stored at 4°C until used. The antigens used in these experiments can be found in Table 2.

MULTICOV-AB

MULTICOV-AB, a previously published multiplex immunoassay was performed as described(1). A full list of antigens included within the assay are listed in Table 2. Samples were randomly allocated to plates to ensure that at least three sample of every sample group was included on each plate. Briefly, samples were thawed at room temperature, vortexed and then diluted 1:200 in assay buffer before being mixed 1:1 with 1x Bead Mix in a 96-well plate (final dilution 1:400). Samples were then incubated in darkness on a Thermomixer (20°C, 750 rpm, 2 hours) before being washed three times to remove unbound antibodies. To ensure retention of beads, a magnetic plate washer was used. To detect bound IgG, 3 µg/mL RPE-goat anti-human IgG was added to each well and then incubated for a further 45 mins on a Thermomixer. After another washing step, beads were resuspended in 100 µL of wash buffer, shaken for 3 mins at 1000 rpm, and then measured on a FLEXMAP3D instrument (No Timeout, Gate 7500-15000, Reporter Gain Standard PMT, 50 events). 3 Quality control samples were included in duplicate on each plate. All

samples were measured twice in two independent experiments. No sample failed QC. Raw median fluorescence intensity (MFI) values were normalized to a QC sample for all antigens as per(3) .

RBDCoV-ACE2

RBDCoV-ACE2, a previously published multiplex ACE2 inhibition assay(2), analyzes neutralizing antibody activity through ACE2 binding inhibition. A full list of antigens included in this assay can be found as Table 2. Briefly, 1:25 diluted samples from MULTICOV-AB, were further diluted to 1:200 in ACE2 buffer(2), which contains 300 ng/mL biotinylated ACE2. Samples were then mixed 1:1 with 1x VOC bead mix in 96 well plates and incubated for 2 hours in darkness on a thermomixer (750 rpm, 20°C). Following this initial incubation, samples were washed to remove unbound ACE2 using an automated magnetic plate washer. Bound ACE2 was detected by adding 2 µg/mL RPE-labelled streptavidin and incubating for a further 45 mins. After washing to remove unbound fluorophores, beads were resuspended in 100 µL washing buffer and shaken for 3 mins at 1000 rpm. Plates were measured once on a FLEXMAP3D instrument (No Timeout, Gate 7500-15000, Reporter Gain Standard PMT, 50 events). As controls, 3 wells with 150 ng/mL ACE2, 2 blank wells and 3 wells with a QC sample were included. ACE2 binding inhibition was calculated as a percentage, with 100% indicating maximum ACE2 binding inhibition and 0% indicating no ACE2 binding inhibition. Samples with an ACE2 binding inhibition less than 20% are classified as non-responders(2).

Biolayer Interferometry (BLI)

Purified RBD_{wt}, RBD_{δ}, RBD_{oBA1} and RBD_{oBA2} were biotinylated with Sulfo-NHS-LC-LC-Biotin (Thermo Fisher Scientific) in 5 molar excess at ambient temperature for 30 min. Excess of biotin was removed by size exclusion chromatography using Zeba^{TM}

Spin Desalting Columns 7K MWCO 0.5 ml (Thermo Fisher Scientific) according to the manufacturer's protocol. Analysis of binding kinetics of RBD specific antibodies in serum samples were performed using the Octet RED96e system (Sartorius) as per the manufacturer's recommendations. In brief, 5 µg/ ml of each biotinylated RBD diluted in Octet buffer (PBS, 0.1% BSA, 0.02% Tween20) was immobilized on streptavidin coated biosensor tips (SA, Sartorius) for 20 s. In the association step, serum samples at a 1:100 dilution were reacted for 720 s followed by dissociation in Octet buffer for 1200 s. Every run was normalized to a healthy control sample (pre-pandemic) lacking RBD specific antibodies and for each sample technical duplicates (n = 2) were performed. Data were analyzed using the Octet Data Analysis HT 12.0 software applying the 1:1 fitting model for the dissociation step. The binding profile response of each sample is illustrated as the mean wavelength shift in nm. Binding kinetics for ACE2 were performed by immobilizing 5 µg/ ml of each biotinylated RBD diluted in Octet buffer on streptavidin coated biosensor tips (SA, Sartorius) for 20 s. Dilution series ranging from 50 to 6.25 nM of ACE2 (Sino Biological) were applied for 300 s and one reference was included per run, followed by a dissociation step in Octet buffer (480s). For affinity determination, the 1:1 global fit of the Data Analysis HT 12.0 software was used.

Data Analysis

Data was collated and matched to metadata in Excel 2016. Data visualisation was done in RStudio (Version 1.2.5001 running R version 3.6.1). Additional packages "gplots" and "beeswarm" were used for specific displays. The "lm" function of R's "stats" library was used for linear regression analyzes. Correlation analyzes were performed using the "cor" function of R's "stats" library. The "wilcox.test" function from R's "stats" library was used to perform both Mann-Whitney-U Tests (two-sided) in order to estimate significance of observed differences between different groups, and

Wilcoxon Signed Rank Analysis (two-sided) to estimate the significance of observed

differences between antigens for the same samples. Graphs were exported from

RStudio and further edited in Inkscape (Version 0.92.4) to generate final figures.

Biolayer inferometry graphical representation was prepared using GraphPad Prism

Software (Version 9.0.0).

Supplementary Figures

Supplementary Figure 1: **Binding kinetics of RBD specific antibodies from serum samples of vaccinated and convalescent individuals.**
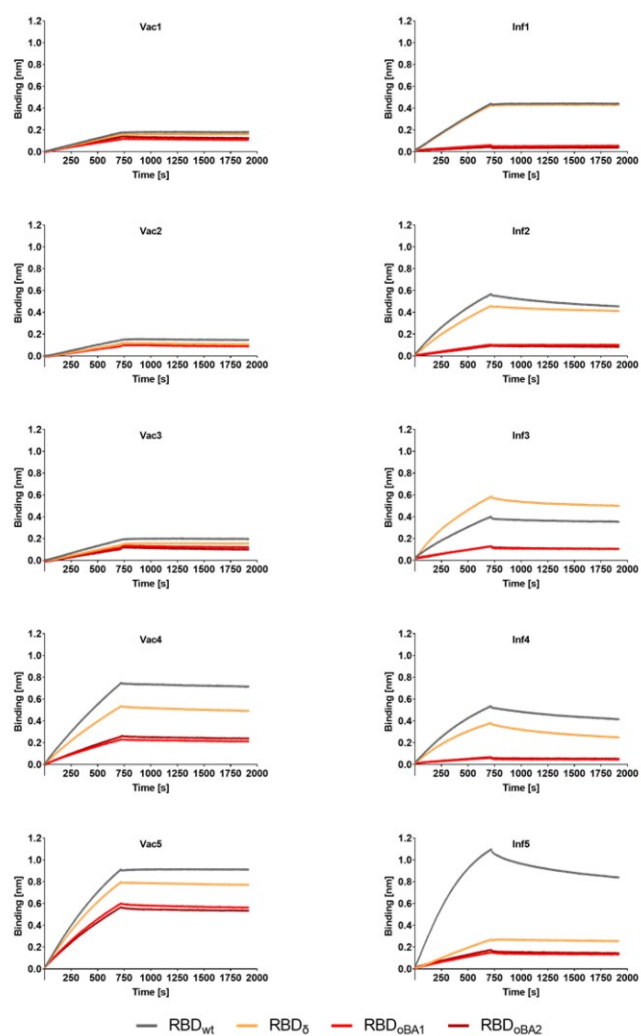
Biotinylated RBD$_{wt}$, RBD$_{\delta}$, RBD$_{oBA1}$, RBD$_{oBA2}$ were immobilized on streptavidin biosensor tips and binding kinetics of serum samples from vaccinated (n = 5, Vac) and convalescent (n =5, Inf) individuals were analyzed using BLI. All sensograms are illustrated as mean of technical duplicates (n = 2).

Supplementary Figure 2: **Binding kinetics of ACE2 to RBD$_{wt}$, RBD$_\delta$, RBD$_{oBA1}$ and RBD$_{oBA2}$ using BLI.**
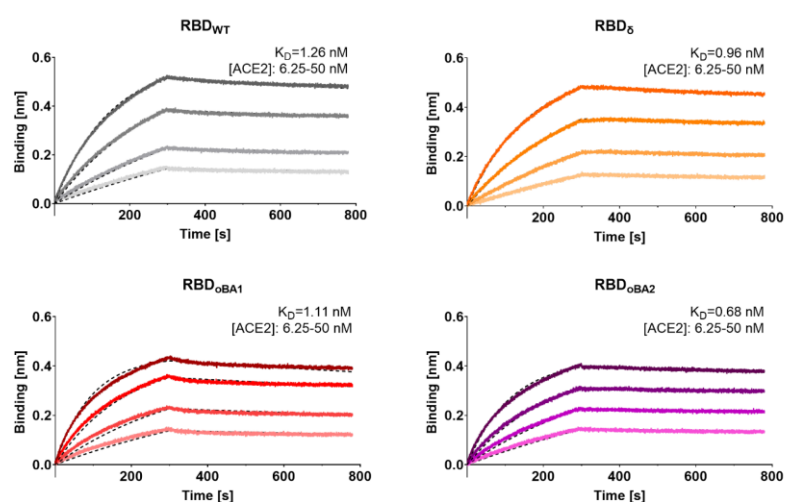
	K$_D$ [nM]	k$_{on}$ [10^5 M^{-1} s^{-1}]	k$_{off}$ [10^{-4} s^{-1}]
RBD$_{wt}$	1.26 ± 0.01	1.37 ± 0.00	1.72 ± 0.01
RBD$_\delta$	0.96 ± 0.01	1.24 ± 0.00	1.19 ± 0.01
RBD$_{oBA1}$	1.11 ± 0.01	2.10 ± 0.01	2.32 ± 0.02
RBD$_{oBA2}$	0.68 ± 0.01	1.75 ± 0.00	1.19 ± 0.02

For biolayer interferometry (BLI)-based affinity measurements, biotinylated RBD$_{wt}$, RBD$_\delta$, RBD$_{oBA1}$ and RBD$_{oBA2}$ were immobilized on streptavidin biosensors. Kinetic measurements were performed using four concentrations of purified ACE2 ranging from 6.25 nM to 50 nM (illustrated with gradually lighter shades). The table summarizes affinities (K$_D$), association (k$_{on}$), and dissociation constants (k$_{off}$) of ACE2 determined for the different RBD variants.

Supplementary Figure 3: **IgG binding capacity and ACE2 binding inhibition for vaccinated samples towards BA1**.

a

b
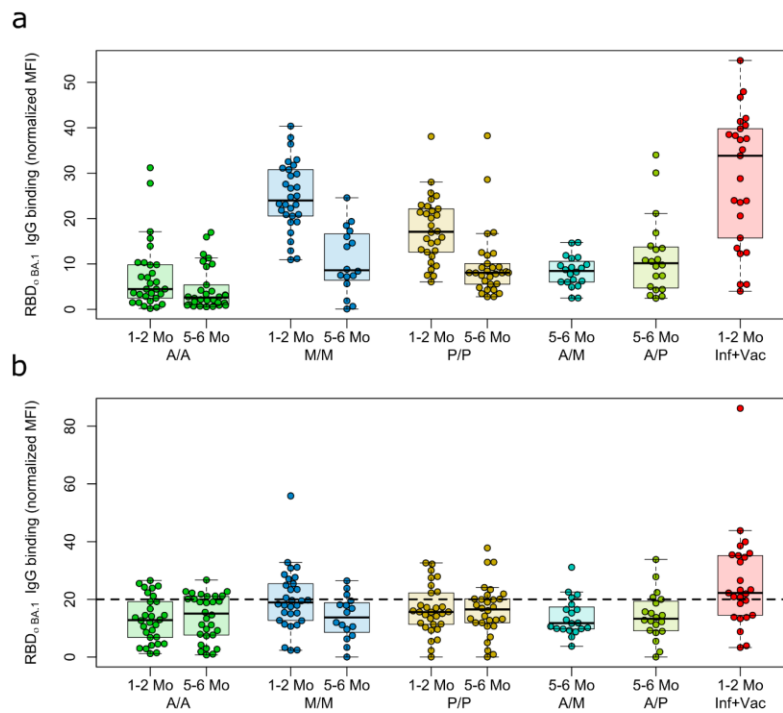
Binding response towards omicron was analyzed by either MULTICOV-AB (a) or RBDCoV-ACE2 (b) for samples from different vaccine schemes (n=30 for all sample groups, except for mRNA-1273 5-6 months (n=16), heterologous vaccine schemes (both n=20) and infected and vaccinated (Inf+vac, n=25). To determine the effect of time post-vaccination, samples from both 1-2 months and 5-6 months post-vaccination were included. A/A = AZD1222. M/M = mRNA-1273. P/P = BNT162b2. A/M = first dose AZD1222, second dose mRNA-1273. A/P = first dose AZD1222, second dose BNT162b2. Boxes represent the median, 25th and 75th percentiles, whiskers show the largest and smallest non-outlier values. Outliers were determined

by 1.5 IQR. The 20% cut off for non-responders is indicated by the dashed line on b.

The equivalent data for BA2 is shown in the main manuscript file as Figure 3.

Supplementary Figure 4: **Differences in IgG binding response and ACE2 binding**

inhibition towards BA1 among different populations of convalescent samples.
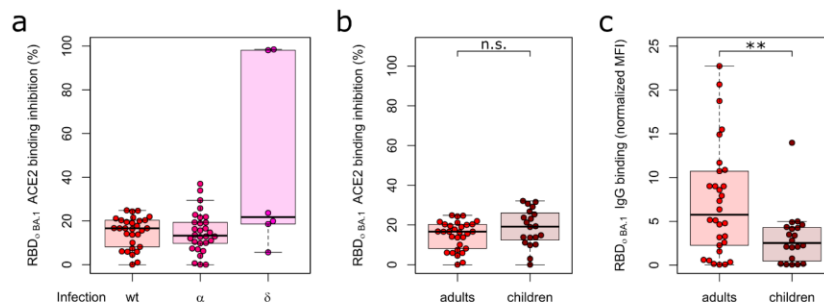
Comparative ACE2 binding inhibition (a and b) and IgG binding capacity (c) between

convalescent samples from different pandemic waves (a) and adults and children (b

and c) for Omicron BA1. (a) ACE2 binding inhibition towards BA1 for individuals

infected with WT (n=30), alpha (n=30) or delta (n=6). (b) There is no significant

difference (p=0.18) in ACE2 binding inhibition between adults (n=30) and children

(n=20). (c) Adults have significantly higher IgG binding capacity (p=0.01) towards

BA1 than children. Boxes represent the median, 25th and 75th percentiles, whiskers

show the largest and smallest non-outlier values. Outliers were determined by 1.5

IQR. Statistical significance was calculated by two-sided Mann-Whitney U.

Supplementary Table 1: **Median fold reduction in IgG binding capacity from wild-**

type to respective variant

Group	Vaccinated	Convalescent
WT	1	1
alpha	1.19 (1.06 – 1.32)	1.17 (0.95 – 1.39)
beta	2.84 (1.80 – 3.88)	3.46 (1.24 – 5.67)
gamma	1.65 (1.17 – 2.13)	1.96 (1.03 – 2.90)
delta	1.21 (1.03 – 1.38)	1.25 (0.95 – 1.55)
omicron BA1	2.32 (0.96 – 3.68)	4.09 (1.31 – 6.87)
omicron BA2	2.14 (0.96 – 3.32)	2.99 (0.93 – 5.05)
lambda	1.73 (1.24 – 2.20)	2.03 (1.29 – 2.76)
mu	3.01 (1.60 – 4.42)	3.62 (1.25 – 5.99)

Median fold change in reduction towards WT for all other variants included within the
MULTICOV-AB assay. The IQR is shown in brackets. Values are shown for both
vaccinated (n=226) and convalescent (n=86) samples. WT – wild-type (B.1. isolate).

Supplementary Table 2: **Median fold reduction in IgG binding capacity from omicron BA1 to respective variant**

Group	Vaccinated	Convalescent
WT	2.32 (0.96 – 3.68)	4.09 (1.31 – 6.87)
alpha	1.91 (0.85 – 2.96)	3.16 (0.40 – 5.91)
beta	0.83 (0.62 – 1.04)	0.99 (0.67 – 1.32)
gamma	1.39 (0.97 – 1.81)	1.76 (1.07 – 2.45)
delta	1.91 (1.03 – 2.80)	3.00 (1.27 – 4.73)
omicron BA1	1	1
omicron BA2	1.10 (1.03 – 1.17)	1.18 (1.02 – 1.34)
lambda	1.31 (0.79 – 1.83)	1.69 (0.73 – 2.66)
mu	0.78 (0.57 – 1.00)	0.94 (0.50 – 1.38)

Median fold change in reduction towards omicron BA1 for all other variants included within the MULTICOV-AB assay. The IQR is shown in brackets. Values are shown for both vaccinated (n=226) and convalescent (n=86) samples. WT – wild-type (B.1. isolate).

Supplementary Table 3: **Median fold reduction in IgG binding capacity from**

omicron BA2 to respective variant

Group	Vaccinated	Convalescent
WT	2.13 (0.95 – 3.32)	2.99 (0.93 – 5.05)
alpha	1.72 (0.86 – 2.58)	2.47 (0.53 – 4.41)
beta	0.76 (0.58 – 0.93)	0.84 (0.63 – 1.04)
gamma	1.26 (0.91 – 1.61)	1.45 (0.90 – 2.00)
delta	1.71 (1.00 – 2.43)	2.30 (0.87 – 3.74)
omicron BA1	0.91 (0.85 – 0.97	0.85 (0.73 – 0.96)
omicron BA2	1	1
lambda	1.18 (0.74 – 1.62)	1.32 (0.62 – 2.01)
mu	0.72 (0.54 – 0.90)	0.80 (0.52 – 1.09)

Median fold change in reduction towards omicron BA2 for all other variants included within the MULTICOV-AB assay. The IQR is shown in brackets. Values are shown for both vaccinated (n=226) and convalescent (n=86) samples. WT – wild-type (B.1. isolate).

Supplementary Table 4: **Statistical significance between variants for IgG binding capacity**

	alpha	beta	gamma	delta	omicron BA1	omicron BA2	lambda	mu
WT	2.37×10^{-50}	2.50×10^{-55}	4.75×10^{-54}	1.76×10^{-49}	4.72×10^{-55}	6.86×10^{-54}	3.06×10^{-55}	2.35×10^{-55}
alpha		7.46×10^{-54}	1.88×10^{-53}	7.87×10^{-4}	1.56×10^{-54}	1.05×10^{-52}	3.75×10^{-55}	2.35×10^{-55}
beta			6.05×10^{-54}	2.35×10^{-55}	8.75×10^{-21}	1.06×10^{-39}	9.28×10^{-53}	6.44×10^{-10}
gamma				2.74×10^{-49}	1.55×10^{-52}	7.59×10^{-45}	4.08×10^{-16}	3.34×10^{-54}
delta					4.46×10^{-55}	1.61×10^{-52}	2.35×10^{-55}	2.35×10^{-55}
omicron BA1						1.26×10^{-50}	6.04×10^{-44}	5.68×10^{-24}
omicron BA2							6.01×10^{-23}	4.47×10^{-39}
lambda								2.14×10^{-53}
mu								

Statistical analysis as determined by Wilcoxon Signed Rank between all variants for IgG binding capacity. WT – wild-type (B.1. isolate).

Supplementary Table 5: **Median ACE2 binding inhibition of the respective variant**

Group	Vaccinated	Convalescent
WT	26.11 (38.7)	27.25 (45.55)
alpha	20.63 (30.37)	30.23 (36.32)
beta	11.38 (18.48)	8.87 (14.52)
gamma	10.81 (17.34)	9.41 (17.19)
delta	16.67 (27.97)	15.72 (34.75)
omicron BA1	15.26 (11.26)	16.44 (11.54)
omicron BA2	8.03 (9.92)	10.88 (12.65)
lambda	18.79 (33.09)	16.13 (27.63)
mu	9.12 (15.08)	8.07 (12.16)

Median ACE2 binding inhibition for all RBD variants included within the RBDCoV-ACE2 assay. The IQR is shown in brackets. Values are shown for both vaccinated (n=226) and convalescent (n=86) samples. WT – wild-type (B.1. isolate).

Supplementary Table 6: **Responder rate for different variants**

	WT	alpha	beta	gamma	delta	BA1	BA2	lambda	mu
Infected	54 (63)	51 (59)	19 (22)	22 (26)	38 (44)	28 (33)	12 (14)	34 (40)	17 (20)
Vaccinated	142 (63)	116 (51)	70 (31)	68 (30)	98 (43)	68 (30)	19 (8)	107 (47)	51 (23)
Negative	0 (0)	0 (0)	0 (0)	0 (0)	0 (0)	0 (0)	0 (0)	0 (0)	0 (0)

Samples were classified as responsive based on having an ACE2 binding inhibition greater than 20% within the RBDCoV-ACE2 assay. Number of samples classified as responsive is shown, with this displayed as a percentage of all samples of this type in brackets. Values are shown for both vaccinated (n=226), convalescent (n=86) and negative (n=15) samples. WT – wild-type (B.1. isolate).

Supplementary Table 7: **Statistical significance between variants for ACE2 binding inhibition**

	WT	alpha	beta	gamma	delta	omicron BA1	omicron BA2	lambda	mu
WT		0.04	8.40×10^{-17}	7.22×10^{-18}	2.12×10^{-6}	3.99×10^{-11}	5.99×10^{-29}	4.00×10^{-5}	2.76×10^{-23}
alpha			2.58×10^{-12}	3.44×10^{-13}	2.24×10^{-3}	6.88×10^{-6}	8.97×10^{-24}	0.02	8.16×10^{-19}
beta				0.77	2.77×10^{-4}	1.20×10^{-6}	0.02	1.70×10^{-5}	0.04
gamma					8.97×10^{-5}	5.61×10^{-7}	0.03	4.61×10^{-6}	0.09
delta						0.53	1.12×10^{-10}	0.50	5.10×10^{-8}
omicron BA1							1.46×10^{-20}	0.15	2.92×10^{-13}
omicron BA2								8.82×10^{-13}	0.95
lambda									1.12×10^{-9}
mu									

Statistical analysis as determined by Wilcoxon Signed Rank between all variants for ACE2 binding inhibition. WT – wild-type (B.1. isolate).

Supplementary Table 8: **Summary of the binding response and dissociation constant (k$_{off}$) of the individual serum samples.**

	Response [nm]				Dissociation constant k$_{off}$ [10^{-5} s^{-1}]			
	RBD$_{wt}$	RBD$_{\delta}$	RBD$_{oBA1}$	RBD$_{oBA2}$	RBD$_{wt}$	RBD$_{\delta}$	RBD$_{oBA1}$	RBD$_{oBA2}$
Vac1	0.175 ± 0.008	0.154 ± 0.018	0.113 ± 0.002	0.134 ± 0.007	0.010 ± 0.000	0.010 ± 0.000	6.565 ± 1.280	8.205 ± 2.326
Vac2	0.143 ± 0.005	0.104 ± 0.005	0.089 ± 0.004	0.105 ± 0.008	3.895 ± 0.148	7.880 ± 1.824	10.405 ± 0.841	9.965 ± 1.605
Vac3	0.186 ± 0.011	0.139 ± 0.002	0.117 ± 0.000	0.101 ± 0.004	0.010 ± 0.000	0.010 ± 0.000	8.660 ± 0.014	14.950 ± 2.192
Vac4	0.741 ± 0.034	0.531 ± 0.020	0.227 ± 0.003	0.254 ± 0.003	3.080 ± 0.170	6.050 ± 0.269	6.325 ± 0.375	6.420 ± 0.141
Vac5	0.908 ± 0.019	0.791 ± 0.045	0.596 ± 0.066	0.562 ± 0.038	0.010 ± 0.000	2.200 ± 0.099	4.165 ± 0.120	3.110 ± 0.863
Inf1	0.439 ± 0.009	0.425 ± 0.072	0.059 ± 0.004	0.044 ± 0.003	0.010 ± 0.000	0.181 ± 0.242	0.010 ± 0.000	0.010 ± 0.000
Inf2	0.565 ± 0.015	0.456 ± 0.011	0.103 ± 0.006	0.092 ± 0.007	16.700 ± 0.141	7.630 ± 0.184	0.010 ± 0.000	7.125 ± 1.167
Inf3	0.399 ± 0.072	0.581 ± 0.099	0.126 ± 0.025	0.128 ± 0.014	5.635 ± 0.502	10.050 ± 0.071	4.105 ± 1.082	9.115 ± 0.092
Inf4	0.534 ± 0.019	0.380 ± 0.039	0.060 ± 0.002	0.067 ± 0.001	18.750 ± 0.212	32.350 ± 0.354	5.185 ± 3.882	7.245 ± 0.926
Inf5	1.094 ± 0.025	0.267 ± 0.010	0.149 ± 0.014	0.174 ± 0.000	18.800 ± 0.283	4.315 ± 0.516	6.240 ± 1.541	8.025 ± 2.157

Binding kinetics of serum samples from (n = 5, Vac) and convalescent (n = 5, Inf) individuals to the different RBD variants were analyzed using BLI. Binding response and dissociation constant (k$_{off}$) determined by the 1:1 fitting model of the individual serum samples were summarized as mean ± SD.

Supplementary Table 9: **Differences in response rate towards the Spike and RBD for BA1 and WT**

	Spike WT	Spike BA1	RBD WT	RBD BA1
Convalescent	37 (43)	3 (3)	54 (63)	28 (33)
Vaccinated	78 (35)	11 (5)	142 (63)	68 (30)
Negative	0 (0)	0 (0)	0 (0)	0 (0)

Samples were classified as responsive based on having an ACE2 binding inhibition greater than 20% within the RBDCoV-ACE2 assay. Number of samples classified as responsive is shown, with this displayed as a percentage of all samples of this type in brackets. Values are shown for both vaccinated (n=226), convalescent (n=86) and negative (n=15) samples. WT – wild-type (B.1. isolate).

References

1.   Becker M, Strengert M, Junker D, Kaiser PD, Kerrinnes T, Traenkle B, et al. Exploring beyond clinical routine SARS-CoV-2 serology using MultiCoV-Ab to evaluate endemic coronavirus cross-reactivity. Nature Communications. 2021;12(1):1152.

2.   Junker D, Dulovic A, Becker M, Wagner TR, Kaiser PD, Traenkle B, et al. COVID-19 patient serum less potently inhibits ACE2-RBD binding for various SARS-CoV-2 RBD mutants. medRxiv. 2021:2021.08.20.21262328.

3.   Becker M, Dulovic A, Junker D, Ruetalo N, Kaiser PD, Pinilla YT, et al. Immune response to SARS-CoV-2 variants of concern in vaccinated individuals. Nature Communications. 2021;12(1):3109.

Appendix VI: Cellular and humoral immunogenicity of a SARS-CoV-2 mRNA vaccine in patients on haemodialysis

Monika Strengert*, **Matthias Becker***, Gema Morillas Ramos*, Alex Dulovic, Jens Gruber, Jennifer Juengling, Karsten Lürken, Andrea Beigel, Eike Wrenger, Gerhard Lonnemann, Anne Cossmann, Metodi V. Stankov, Alexandra Dopfer-Jablonka, Philipp D. Kaiser, Bjoern Traenkle, Ulrich Rothbauer, Gérard Krause, Nicole Schneiderhan-Marra & Georg M.N. Behrens

    * = Authors contributed equally

Contents lists available at ScienceDirect

EBioMedicine

Research paper

Cellular and humoral immunogenicity of a SARS-CoV-2 mRNA vaccine in patients on haemodialysis

Monika Strengert[a,b,1], Matthias Becker[c,1], Gema Morillas Ramos[d,1], Alex Dulovic[c], Jens Gruber[c], Jennifer Juengling[c], Karsten Lürken[e], Andrea Beigel[e], Eike Wrenger[e], Gerhard Lonnemann[e], Anne Cossmann[d], Metodi V. Stankov[d], Alexandra Dopfer-Jablonka[d,f], Philipp D. Kaiser[c], Bjoern Traenkle[c], Ulrich Rothbauer[c,g], Gérard Krause[a,b], Nicole Schneiderhan-Marra[c,1,*], Georg M.N. Behrens[d,f,h,1,*]

a Helmholtz Centre for Infection Research, Braunschweig, Germany
b TWINCORE GmbH, Centre for Experimental and Clinical Infection Research, a joint venture of the Hannover Medical School and the Helmholtz Centre for Infection Research, Hannover, Germany
c NMI Natural and Medical Sciences Institute at the University of Tübingen, Reutlingen, Germany
d Department for Rheumatology and Immunology, Hannover Medical School, Hannover, Germany
e Dialysis Centre Eickenhof, Langenhagen, Germany
f German Centre for Infection Research (DZIF), partner site Hannover-Braunschweig, Germany
g Pharmaceutical Biotechnology, University of Tübingen, Germany
h CiiM - Centre for Individualized Infection Medicine, Hannover, Germany

ARTICLE INFO

ABSTRACT

Background: Patients with chronic renal insufficiency on maintenance haemodialysis face an increased risk of COVID-19 induced mortality and impaired vaccine responses. To date, only a few studies have addressed SARS-CoV-2 vaccine elicited immunity in this immunocompromised population.
Methods: We assessed immunogenicity of the mRNA vaccine BNT162b2 in at-risk dialysis patients and characterised systemic cellular and humoral immune responses in serum and saliva using interferon γ release assay and multiplex-based cytokine and immunoglobulin measurements. We further compared binding capacity and neutralization efficacy of vaccination-induced immunoglobulins against emerging SARS-CoV-2 variants Alpha, Beta, Epsilon and Cluster 5 by ACE2-RBD competition assay.
Findings: Patients on maintenance haemodialysis exhibit detectable but variable cellular and humoral immune responses against SARS-CoV-2 and variants of concern after a two-dose regimen of BNT162b2. Although vaccination-induced immunoglobulins were detectable in saliva and plasma, both anti-SARS-CoV-2 IgG and neutralization efficacy was reduced compared to a vaccinated non-dialysed control population. Similarly, T-cell mediated interferon γ release after stimulation with SARS-CoV-2 spike peptides was significantly diminished.
Interpretation: Quantifiable humoral and cellular immune responses after BNT162b2 vaccination in individuals on maintenance haemodialysis are encouraging, but urge for longitudinal follow-up to assess longevity of immunity. Diminished virus neutralization and interferon γ responses in the face of emerging variants of concern may favour this at-risk population for re-vaccination using modified vaccines at the earliest opportunity.
Funding: Initiative and Networking Fund of the Helmholtz Association of German Research Centres, EU Horizon 2020 research and innovation program, State Ministry of Baden-Württemberg for Economic Affairs, Labour and Tourism.

* Corresponding author at: Nicole Schneiderhan-Marra, Marktwiesenstrasse 55, 72770 Reutlingen; Georg M.N. Behrens, Carl-Neuberg-Strasse 1, 30625 Hannover, Germany.
E-mail addresses: nicole.schneiderhan@nmi.de (N. Schneiderhan-Marra), behrens.georg@mh-hannover.de (G.M.N. Behrens).
1 These authors contributed equally to this work.

1. Introduction

Since its emergence in late 2019, SARS-CoV-2 has become a global pandemic with more than 166 million confirmed cases and 3·46 million deaths (as of 24.05.21) [1]. Vulnerable populations such as the elderly, immunocompromised or those suffering from chronic

Research in context

Evidence before this study

Patients on dialysis tend to have a reduced immune response to both infection and vaccination. We searched PubMed and medRxiv for studies including search terms such as "COVID-19", "vaccine", and "dialysis" but no peer-reviewed studies to date simultaneously assessed both SARS-CoV-2 specific B- and T-cell responses, mucosal immunoglobulins, and considered the impact of SARS-CoV-2 variants of concern in this at-risk population.

Added value of this study

We provide a comprehensive functional characterisation of both T- and B-cell responses following a two-dose regimen of BNT162b2 in at-risk patients on maintenance haemodialysis. More importantly, to the best of our knowledge, we assess for the first time binding and neutralization capacity of vaccination-induced circulation and mucosal antibodies towards emerging SARS-CoV-2 variants of concern in an immunocompromised population.

Implications of all the available evidence

Patients on maintenance haemodialysis develop a substantial cellular and humoral immune response following the BNT162b2 vaccine. These findings should encourage patients on maintenance haemodialysis to receive the vaccine. However, we suggest continuing additional protection measures against variants of concern in this at-risk population until longevity of the vaccine response is fully evaluated.

conditions or requiring continual medical intervention such as dialysis are at-risk of severe COVID-19 disease and associated death [2]. Although a series of vaccines have been developed, tested and approved at unprecedented speed, only one vaccine study for NVX CoV2373 has enrolled patients with chronic diseases such as chronic kidney disease to assess efficacy and safety of SARS-CoV-2 vaccination within this vulnerable population [3]. Patients on maintenance haemodialysis are a particularly high-risk group, as renal disease has been identified as a key risk factor for severe COVID-19 [4-7], while at the same time their regular need for therapy does not allow them to self-isolate and reduce contacts to avoid infection. A recent study also suggested that seroreversion following natural SARS-CoV-2 infection is faster in dialysis patients compared to the general population further increasing the risk of re-infection [8]. Other studies have also demonstrated an impaired humoral immune response in dialysis patients, as seen by the attenuation of antibody titres following vaccination with SARS-CoV-2 vaccines [9-15]. Both, COVID-19 and BNT162b2-induced effective immunity appear to result from

functional T-follicular helper (TfH) cell responses and Th1 cytokines [16,17]. In contrast, end-stage kidney failure is associated with pro-inflammatory markers (including IFNγ, TNFα, IL-8, CCL-2, and others), exhausted T-cell phenotype, and perturbed TfH-cells [18]. Additional data on the efficiency of SARS-CoV-2 vaccination is urgently needed not only for risk mitigation but also to assess whether additional protective measures during therapy must be put in place as seen by the impaired infection and vaccination-induced responses for influenza A and hepatitis B [19-21]. While antibody titres have already been characterised within vaccinated dialysis patients, little is known about the ensuing cellular immune response [22] or about the neutralization potential of vaccine-induced antibodies [23], particularly in light of the increasingly appearing SARS-CoV-2 variants of concern (VoC) which threaten the success of vaccination programs [24].

To assess efficacy of SARS-CoV-2 vaccination in dialysis patients, we characterised cellular and humoral immune responses in serum and saliva of dialysed and non-dialysed individuals after vaccination with the mRNA vaccine BNT162b2. Considering the increasing presence of mutated SARS-CoV-2 strains, we further compared binding capacity and neutralization efficacy of vaccination-induced immunoglobulins against emerging variants of concern such as B.1.1.7 (Alpha), B.1.351 (Beta), B.1.429 (Epsilon) and Cluster 5 (Mink).

2. Methods

2.1. Study design and sample collection

Following written informed consent, heparinized blood samples from haemodialysis patients (n=81) were taken before start of dialysis using a vascular access which was either an arterio-venous fistula or a central venous catheter or by venipuncture from health care workers (n=34), who served as non-dialysed control population. Participants had to be over the age of 18 and able to give written informed consent. All study participants were either patients or worked at the dialysis centre Eickenhof and received the vaccine on the same occasion. 10 of the 81 dialysis patients were on immunosuppressive medication such as prednisolone, tacrolimus, mycophenolatmofetil, hydrocortisone, or a combination. Four of those patients had received a kidney transplant, and one of them additionally a liver transplant. Other reasons for immunosuppressive therapy included polymyositis, polyarthritis, vasculitis and chronic obstructive pulmonary disease. Further details about the study population can be found in Table 1, Table S2 and S3. One haemodialysis patient had previously been tested positive for SARS-CoV-2 by routine PCR screening. As subsequent antibody testing was negative for SARS-CoV-2 IgG, this patient received BNT162b2 and was not excluded from the study. All participants received the standard two-dose regimen of BNT162b2 21 days apart, followed by blood collection for analysis 21 days after the second dose. Plasma was obtained from lithium heparin blood (S-Monovette Plasma, Sarstedt, Germany). Whole blood samples were used immediately for interferon γ release assay (IGRA). For saliva collection, all individuals spat directly into a collection tube. To

Table 1

Characteristics of vaccinated study participants: IQR - Inter Quartile Range. BMI - Body Mass Index. n — absolute numbers per group. NA - Information not available. n. a. - not applicable.

Characteristics	Non-dialysis control group (n=34)	Haemodialysis group (n=81)	p-value for difference between groups
Age (years), median (IQR)	54·5 (15)	69 (18)	$2·91 * 10^{-10}$
Gender (female, n, %)	28 (82·35)	34 (41·98)	$1·71 * 10^{-4}$
Days since start of haemodialysis (median, IQR)	n. a.	1371 (1664)	n. a.
Immunosuppressive medication (n, %)	0 (0)	10 (12·34)	$7·48 * 10^{-2}$
Co-morbidities			
Obesity (BMI, >30)	8 (23·53) (1 NA)	18 (22·22)	$1 * 10^{0}$
Diabetes mellitus (n, %)	1 (2·94)	22 (27·16)	$6·78 * 10^{-3}$
Cardiovascular disease (n, %)	0 (0)	39 (48·15)	$1·92 * 10^{-6}$

inactivate replication-competent SARS-CoV-2 virus particles potentially present in saliva samples, Tri(n-butyl) phosphate (TnBP) and Triton X-100 were added to final concentrations of 0·3% and 1%, respectively [25]. Both plasma and saliva samples were frozen and stored at −80°C until further use.

2.2. Ethics statement

Ethical approval of the study was obtained from the relevant authority - the Internal Review Board of Hannover Medical School (MHH, approval number 8973_BO-K_2020, amendment Dec. 2020). Written informed consent was obtained from all participants prior to starting the study.

2.3. Bead coupling

Coupling of antigens to spectrally distinct MagPlex beads (Cat #MC10XXX-01, Luminex Corporation, USA) was done by EDC/s-NHS coupling for all standard MULTICOV-AB antigens [26]. Receptor-binding domains (RBD)s from VoC were coupled using Anteo coupling (Cat #A-LMPAKMM-10, Anteo Tech Reagents, Australia) following the manufacturer's instructions [27].

2.4. MULTICOV-AB

Antibody titres and binding was analysed using MULTICOV-AB, a multiplex immunoassay which simultaneously analyses 20 antigens, as previously described [26]. The full list of antigens included in this study can be found in Table S1. Plasma samples were diluted 1:400, while saliva samples were diluted 1:12 [27]. Briefly, antigens were immobilised on spectrally distinct populations of MagPlex beads (as above) and combined into a single bead mix. Samples were combined with the bead mix, incubated for 2 h at 21°C and then washed using a microplate washer to remove unbound antibodies. Bound antibodies were detected following a 45 min incubation at 21°C with R-phycoerythrin labeled goat-anti-human IgG (Jackson ImmunoResearch Labs, United Kingdom, Cat #109-116-098, Lot #148837, RRID: AB_2337678, used at 3 μg/mL) or IgA (Jackson ImmunoResearch Labs, Cat #109-115-011, Lot #143454, RRID: AB_2337674, used at 5 μg/mL) as secondary antibodies. Following another washing step, beads were re-suspended and then measured using a FLEXMAP 3D instrument (Luminex Corporation, Texas, USA) using the following settings: Timeout 80 sec, Gate: 7500-15000, Reporter Gain: Standard PMT, 40 events. Each sample was measured once. Three quality control (QC) samples were included on each plate to monitor MULTICOV-AB assay performance. Raw median fluorescence intensity (MFI) values or normalised values (MFI/MFI of QC samples [27]) are reported.

2.5. ACE2-RBD competition assay

To determine neutralization, an ACE2-RBD competition assay was carried out as previously described [27]. Briefly, biotinylated ACE2 was added to the assay buffer to a final concentration of 500 ng/mL for all samples. Samples were then mixed with MULTICOV-AB bead mix (see above) and incubated for 2 h at 21°C, 750 rpm. After washing, ACE2 was detected using Streptavidin-PE (2 μg/mL, Cat #SAPE-001, Moss, Maryland, US) by incubating the sample for 45 min at 750 rpm. After an additional wash step and resuspension, samples were measured on a FLEXMAP 3D instrument (same settings as MULTICOV-AB). As control, 500 ng/mL ACE2 was used. For analysis, MFI values were normalised against the control wells. All samples were measured once.

2.6. SARS-CoV-2 QuantiVac ELISA

To further validate plasma IgG levels measured by MULTICOV-AB, samples were further analysed using the Anti-SARS-CoV-2-Quanti-Vac-ELISA IgG (Cat #EI 2606-9601-10G, Euroimmun, Germany) according to the manufacturer's instructions. Plasma samples were diluted 1:400 to achieve assay linearity.

2.7. Interferon γ release assay

SARS-CoV-2-specific T-cell responses were determined by measuring IFNγ production upon SARS-CoV-2 antigen stimulation using the SARS-CoV-2 Interferon Gamma Release Assay (Cat #ET-2606-3003, Euroimmun, Germany). Briefly, 0·5 mL of full blood was stimulated with peptides of the SARS-CoV-2 S1 domain of the Spike protein for a period of 20-24 h. Negative and positive controls were carried out according to the manufacturer's instruction. Following stimulation, supernatants were isolated through centrifugation and IFNγ measured using ELISA (Cat #EQ-6841-9601, Euroimmun, Germany). The remaining supernatant was stored at -80°C. Background signals from negative controls were subtracted and final results calculated in mIU/mL using standard curves. IFNγ concentrations >200 mIU/mL were considered as reactive. The upper limit of reactivity was 2000 mIU/mL.

2.8. Cytokine measurements

Supernatants of SARS-CoV-2 antigen stimulated blood cells were prepared and isolated as explained for the detection of IFNγ by SARS-CoV-2 Interferon Gamma Release Assay and analysed by LEGENDplex^{TM} using the Human Essential Immune Response Panel (Cat #740930, Bio Legend, California, US) for L-4, IL-2, CXCL-10 (IP-10), IL-1β, TNFα, CCL-2 (MCP-1), IL-17A, IL-6, IL-10, IFNγ, IL-12p70, CXCL-8 (IL-8), TGFβ1) according to manufacturer's instructions. Analysis was performed using an LSR II flow cytometer (Becton Dickinson, Germany) and data analysed using the LEGENDplex^{TM} Data Analysis Software Suite.

2.9. Data analysis and statistics

RStudio (Version 1.2.5001), with R (version 3.6.1) was used for data analysis and figure generation. Additionally, the R add-on package "beeswarm" was utilised to visualise data as stripcharts with overlaying boxplots and to create non-overlaying data points. A second R add-on package "RcolorBrewer" was used to generate specific colours for plots. The type of statistical analysis performed (when appropriate) is listed in the figure legends. Figures were exported from Rstudio and then edited using Inkscape (Inkscape 0.92.4). Spearman's rho coefficient was calculated in order to determine correlation between IGRA results and antibody responses or neutralization using the "cor" function from R's "stats" library. Mann-Whitney-U test was used to determine difference between signal distributions between dialysed and non-dialysed groups using the "wilcox.test" function from R's "stats" library. To assess differences in the study population, Pearson's Chi-squared test with Yates' continuity correction was used for categorical characteristics using the "chisq.test" function from R's "stats" library and Mann-Whitney-U test as above was used for difference in age. Pre-processing of data such as matching sample metadata and collecting results from multiple assay platforms was performed in Excel 2016.

2.10. Role of the funders

3. Results

3.1. Dialysed patients have reduced antibody titres following vaccination

To characterise the vaccination response in patients on maintenance haemodialysis, we measured immunoglobulin levels 21 days after the second dose of Pfizer BNT162b2 using MULTICOV-AB, a multiplex immunoassay containing antigens from Spike and Nucleocapsid proteins of both SARS-CoV-2 and the endemic human coronaviruses (hCoVs) [26]. As a control group, 34 samples from healthcare workers vaccinated at the same time points as the 81 patients on haemodialysis were used. (Detailed information on the study population can be found in Table 1, Table S2 and S3). As indicated by the lack of a significant anti-Nucleocapsid (N) IgG or IgA response at the time of blood draw 21 days after the second vaccination, none of the study participants had been previously infected or seroconverted after a SARS-CoV-2 infection (data not shown). IgG responses towards the original B.1 isolate in vaccinated dialysis patients were significantly reduced ($p < 0.0001$, Mann-Whitney-U

test) and more variable (Fig. 1a) than in the control group, which reached the upper limit of detection of the assay, as seen previously [27]. Interestingly, plasma IgA responses in the dialysis group were comparable to the control group (Fig. 1b, p=0.38, Mann-Whitney-U test). While all participants in the control group seroconverted, within our dialysis population, four from 81 vaccinated individuals (4.92%) were classified as serologic non-responders with antibody titres below the cut-off. As an additional control, S1 IgG titres were measured using a commercial assay (Fig. S2), which identified the same pattern of a significantly diminished antibody response in dialysed patients (272.3 RU/mL) compared to non-dialysed individuals (456.8 RU/mL, $p < 0.0001$, Mann-Whitney-U test). Due to the small sample size, we were unable to confidently identify factors associated with reduced humoral immunity by analysis of variance. Dialysis patients receiving immunosuppressive therapy tended to have lower anti-spike IgG levels (median 65.68 RU/mL, IQR 285.14) compared to the remaining dialysis patients (median 112.3 RU/mL, IQR 323.6, p=0.09, Mann-Whitney-U test), which is consistent with a recent report [28].

As SARS-CoV-2 is a mucosal-targeted virus, we also collected saliva from our vaccination cohort and assessed IgG and IgA levels using MULTICOV-AB. When examining antibody titres found in saliva, dialysed individuals had significantly lower IgG titres (p=0.0007), but similar IgA titres (p=0.70) to the control group (Fig. 1c and d, p-values: Mann-Whitney-U test). To examine responses towards emerging VoC, Spike-RBDs of the B.1.1.7 (Alpha), B.1.351 (Beta), Cluster 5 (Mink) and B.1.429 (Epsilon) strain were included as part of MULTICOV-AB [27]. As expected [24,27], antibody
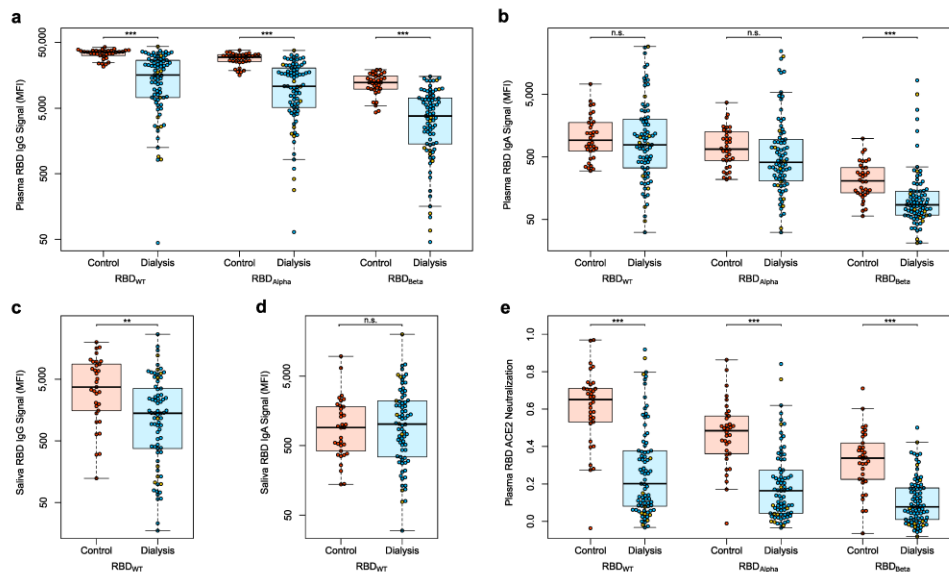

Fig. 1. Humoral immune response in haemodialysed individuals after vaccination with Pfizer BNT162b2.
IgG (a, c), IgA response (b, d) and neutralizing capacity of IgG (e) towards the indicated SARS-CoV-2 WT (B.1), Alpha (B.1.1.7), Beta (B.1.351) in plasma (a, b, e) or saliva (c, d) from controls (red circles, n=34), individuals on maintenance haemodialysis (blue circles, n=71) and haemodialysed individuals on immunosuppressive medication (yellow circles, n=10) 21 days post second vaccination was measured using MULTICOV-AB (a, b, c, d) or an ACE2-RBD competition assay (e). Data is displayed as median fluorescence intensity (MFI) (a-d). Neutralization capacity is displayed as ratio where 1 indicates maximum neutralization and 0 no neutralization (e). Saliva (c, d) was collected from 33 controls (red circles), 65 individuals on maintenance haemodialysis (blue circles) and from 9 individuals on maintenance haemodialysis and immunosuppressive medication (yellow circles). Boxes represent the median, 25th and 75th percentiles, whiskers show the largest and smallest non-outlier values. Outliers were determined by 1.5 times IQR. Statistical significance was calculated by Mann-Whitney-U (two-sided). Significance was defined as *<0.01, **<0.001, ***<0.0001 or n.s.>0.01.

binding towards B.1.1.7 in both dialysed and non-dialysed individuals was comparable to B.1 (original isolate), while binding was clearly reduced for B.1.351 (Fig. 1a). Antibody binding for Cluster 5 and B.1.429 was similar to the B.1 isolate for both groups (Fig. S1). As part of the MULTICOV-AB antigen panel, we also analysed the humoral response towards endemic CoV S1 and N protein, but found no general significant differences between control group and dialysis patients (Fig. S3).

3.2. Neutralization is reduced in dialysis patients after vaccination

To assess neutralizing potency of plasma towards both the original B.1 isolate and VoC RBDs, we used a previously described ACE2-RBD competition assay [27]. Neutralization across both wild-type and all VoCs measured was significantly reduced in dialysed compared to non-dialysed individuals (all p<0·0001, Mann-Whitney-U

test) (Fig. 1e, Fig. S4). As expected, there were differences between the VoCs themselves, with B.1.351 having the lowest neutralization for both control and dialysed individuals. However, responses were comparably low for all VoCs tested for patients on maintenance haemodialysis and additional immunosuppressive medication in the dialysis group further reduced neutralizing potency with the majority of samples located in the 25th quartile (Fig. 1e).

3.3. T-cell response to SARS-CoV-2 vaccination is diminished in dialysed individuals

As clinical studies have suggested that both cellular and humoral response can confer protection from a SARS-CoV-2 infection [29], we also assessed vaccination-induced T-cell responses by IFNγ release assay and characterised cytokine and chemokine responses after stimulation with a Spike S1-derived peptide pool by multiplex
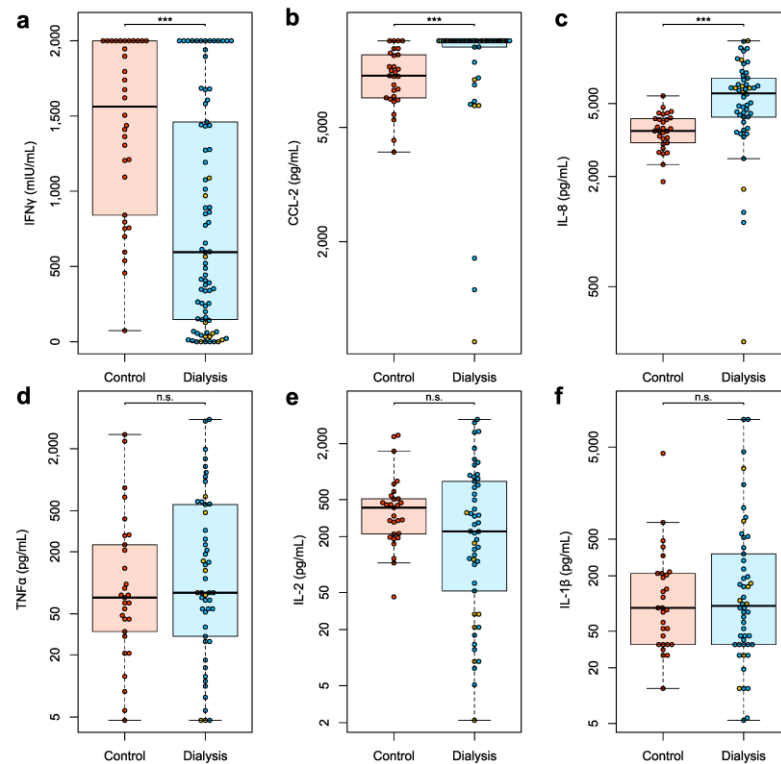

Fig. 2. Cellular immune response in haemodialysed individuals after vaccination with Pfizer BNT162b2.

Whole blood from vaccinated controls (red circles, n=34), individuals on maintenance haemodialysis (blue circles, n=71) and haemodialysed individuals on immunosuppressive medication (yellow circles, n=10) 21 days post second vaccination was *ex vivo* stimulated using a SARS-CoV-2 Spike S1-specific peptide pool. Supernatant fractions were analysed by interferon γ release assay (IGRA, a) or bead-based multiplex-cytokine assay for CCL-2 (b), IL-8 (c), TNFα (d), IL-2 (e) and IL-1β (f). Data is shown in mIU/mL for IGRA or pg/mL for the multiplex-cytokine assay. T-cells were classified as reactive if IFNγ was >200 mIU/mL. IGRA (a) was carried out with samples from all study participants. Bead based-cytokine measurements (b-f) were performed with samples from 29 control, 42 haemodialysed and 8 haemodialysed individuals on immunosuppressive medication. Samples that were classified as above upper or below the lower limit of detection of the cytokine assay or the IGRA are shown at the respective limit. Boxes represent the median, 25th and 75th percentiles, whiskers show the largest and smallest non-outlier values. Outliers were determined by 1·5 times IQR. Statistical significance was calculated by Mann-Whitney-U (two-sided). Significance was defined as *<0·01, **<0·001, ***<0·0001 or n.s.>0·01.
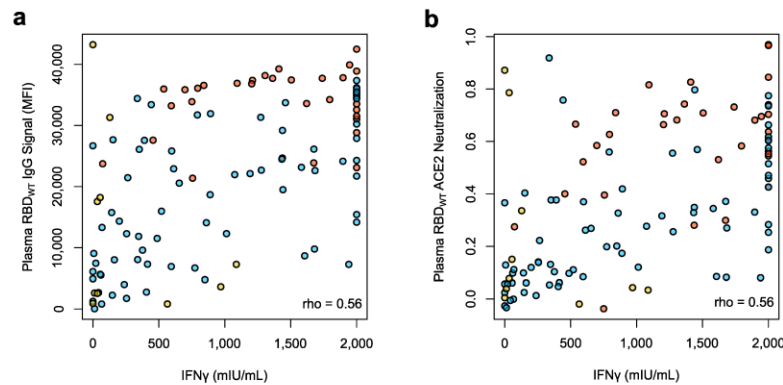
Fig. 3. Relationship of cellular and humoral immune response after vaccination with Pfizer BNT162b2.
T-cell responses assessed by IGRA for IFNγ (mIU/mL) and B-responses assessed by MULTICOV-AB IgG binding to WT (B.1) RBD (a) or ACE2-WT (B.1) RBD competition assay (b) were plotted for correlation analysis in the vaccinated control group (red circles, n=34), in the vaccinated haemodialysed group (blue circles, n=71) and in haemodialysed individuals on additional immunosuppressive medication (yellow circles, n=10). Correlation was calculated using Spearman's coefficient.

cytokine measurements. Consistent with reduced anti-Spike S1 IgG and anti-RBD IgG levels (Fig. 1a, Fig. S2), IGRA showed significantly lower levels of IFNγ released in the supernatants of stimulated T-cells from vaccinated patients on maintenance haemodialysis (p<0·0001, Fig. 2a). In addition, all but one individual within the control group (97·1%) was classified as reactive by IGRA whereas only 71·6 % were within the haemodialysed group. Of the 12 analysed cytokines beyond IFNγ, only IL-8 and CCL-2 (both p<0·0001, Mann-Whitney-U test) were significantly different between the two immunised groups, whereas no other Th1 type cytokines such as TNFα or IL-2 accompanied the IFNγ response (Fig. 2b-f, Fig. S5).

At this moment, there are no defined correlates of protection against a SARS-CoV-2 infection and the relative importance of cellular versus humoral response is equally undefined [30,31]. To shed light on this, we correlated B- and T-cell responses within our vaccination cohort. Comparable to other studies examining vaccination responses of BNT162b2 in a similar setting [32], we observed a moderate correlation between T-cell responses (measured by IGRA) and B-cell responses (determined by RBD B.1-specific IgG levels (Spearman's rho=0·56, Fig. 3a) or RBD B.1 IgG-neutralizing potency (Spearman's rho=0·56, Fig. 3b)). In addition, we observed a skew towards increased B-cell reactivity in both control group and individuals on haemodialysis.

4. Discussion

To control the ongoing COVID-19 pandemic, efficient vaccination to create herd immunity without the infection-induced mortality will be key. We initiated this study to further increase information, including neutralization and response to VoCs, on vaccination-induced immune responses in at-risk immunocompromised populations such as renal dialysis patients. Similar to other groups, we found robust antibody responses following vaccination within dialysed patients [9,13], confirming that our results are comparable to other studies. Overall, 95% of our dialysis patients showed a humoral immune response to vaccination, higher than what other studies with similar time points had found [10-12,14,32]. We can only speculate about potential reasons for those discrepancies such as differences in renal replacement therapies, composition of the patient cohort or co-morbidities. It should be noted that titres were significantly reduced in dialysis patients compared to control individuals, which

could result in reduced vaccine efficacy within this group. We also observed differences in humoral IgG and cellular T-cell response in our dialysis group, with four (4·92%) non-humoral responders and 23 (28·4%) non-T-cell responders, respectively. Overall, it is apparent from our data that in both groups vaccination response was skewed towards secretory immunity. This is in line with exploratory studies using BNT161b1 and other mRNA vaccines, which induce a B-cell response peak around two weeks after the boosting dose to then decline before reaching a memory plateau phase [33, 34]. Future studies will be needed to determine the longevity and relative contribution of both T- and B-cell responses towards vaccination-induced protection. We found no significant differences in vaccination-induced IgA levels in both saliva and plasma between our study groups. Although several studies reported lower protective IgG titres over time following hepatitis B, influenza A or SARS-CoV-2 vaccinations, IgA levels were not analysed to determine if IgA vaccination responses are in general less affected in dialysis patients [9-14,19-21]. Interestingly, a monoclonal IgA antibody capable of recognizing both the SARS-CoV-1 and SARS-CoV-2 spike proteins and blocking ACE2 receptor interaction combined with an increased neutralization ability over its IgG equivalent has been described [35]. Some studies even report a higher neutralizing capacity of purified serum IgA monomers from early convalescent sera compared to IgG and increased saliva IgA titres and neutralization versus IgG in recovered hospitalised COVID-19 patients [36]. We identified a clearly reduced neutralizing capacity towards all VoC RBDs tested in our dialysed individuals compared to controls. Taking into account that SARS-CoV-2 infections were increased in vaccinated dialysis patients compared to vaccinated control individuals [11], further monitoring is urgently needed to determine if vaccine-induced protection prevents infection with increasingly circulating and diverse SARS-CoV-2 mutant strains, or if additional protection measures still need to be put in place throughout therapy session despite a completed vaccination scheme.

Individuals with kidney failure are at increased risk of infections and malignancies, with the uremic milieu potentially triggering a chronic inflammatory state, which promotes T-cell exhaustion and suppression of IFNγ production [37,38]. Indeed, patients with end-stage kidney disease (ESKD) are reported to have elevated serum levels of cytokines such as IFNγ, TNFα, IL-8, and CCL-2 compared to healthy controls. After mitogen stimulation, both CD4$^+$ and CD8$^+$ T-

cells in ESKD group demonstrated a pro-inflammatory phenotype, more exhausted and anergic CD4$^+$ and CD8$^+$ T-cells and a reduced frequency of follicular helper T-cells, which are important for humoral immunity [18]. In light of these immunological changes, our results about diminished SARS-CoV-2 specific T-cell responses and increased proinflammatory cytokine release may account in part for impaired vaccine-induced IgG responses in these patients. Specifically, CCL-2 and IL-8, which both were increased following restimulation with SARS-CoV-2 peptides in dialysis patients, could reflect a more pronounced innate immune response released by monocytes and acting on neutrophils and endothelial cells. We speculate these responses to be secondary to mechanisms triggered by spike-specific T-cells and their cytokines. Which mechanisms critically trigger and facilitate such cytokine patterns in dialysis patients and whether constitutively disturbed cytokine responses in dialysis patients are contributing to hamper humoral or cellular immunity after BNT161b2 vaccination remains to be studied with more careful approaches.

Our study has several limitations. While we have a reasonable sample size (81 dialysis patients), which is similar or even larger compared to several other studies [12,13,32], our control group is not age- and gender-matched. Since others have described that both factors have independent influence on the immunogenicity of COVID-19 vaccines [39−42], our observed differences are likely to be influenced by age and sex to some extent. In addition, we evaluated only one of the currently approved SARS-CoV-2 vaccines with samples from a single dialysis centre and did not perform in-depth immune phenotyping or assessment of SARS-CoV-2 responsive T-cell frequencies. Thus, we cannot extrapolate that other COVID-19 vaccines or vaccine schedules will lead to reduced immune responses in dialysis patients as described here. We also lack paired saliva and plasma samples pre and post first dose to characterise B- and T-cell response kinetics or assess potential cross-reactivity of endemic CoV antibodies in immunocompromised individuals across the dosing scheme. However, all of our samples were collected at the same time with an identical dosing regimen which allows us to make a direct comparison between our two groups of interest (dialysed versus non-dialysed). Additionally, the lack of previously infected samples within our study groups limits us to only study vaccine-induced responses. Several groups independently report high antibody titres and neutralization activity after the first dose of Pfizer or Moderna RNA vaccine in individuals who already had SARS-CoV-2 infections [43]. This effect is likely to be repeated in dialysis patients with a single vaccination post COVID-19.

Taken together, we provide robust evidence that a completed two-dose regimen of BNT162b2 elicits both antibody and T-cell responses in patients on maintenance haemodialysis towards the SARS-CoV-2 B.1 isolate. Future studies are needed to assess the lifespan and long-term kinetics of the vaccination response. As neutralization is reduced in dialysed patients towards all VoCs examined, our data also highlights the need to monitor if infection with SARS-CoV-2 VoC occur more frequently in this vulnerable population compared to vaccinated healthy individuals.

Contributors

AD-J, GMNB, NSM, GL and MS conceived the study. MB, AD, MS, AD-J, GMNB, AC, NSM and MVS designed the experiments. NSM, MS, GMNB, AD-J, and GK procured funding. GMR, JG, JJ and MVS performed experiments. KL, AB, EW, GL, AC, and GMNB collected samples or organised their collection. PDK, BT and UR produced and designed recombinant assay proteins. MB, AD, MS, GMR, MVS and AC performed data collection and analysis. MB generated the figures. MB, MS, AD and GMNB verified the underlying data. MS wrote the first draft of the manuscript with input from MB, NSM, GMNB and AD. All authors critically reviewed and approved the final manuscript.

Declaration of Competing Interest

NSM was a speaker at Luminex user meetings in the past. The Natural and Medical Sciences Institute at the University of Tübingen is involved in applied research projects as a fee for services with the Luminex Corporation. The other authors declare no competing interest.

Data Sharing Statement

Data relating to the findings of this study are available from the corresponding authors upon request.

Supplementary materials

Supplementary material associated with this article can be found in the online version at doi:10.1016/j.ebiom.2021.103524.

References

[1] WHO Coronavirus (COVID-19) Dashboard, Accessed 24th May 2021, https://covid19.who.int/

[2] Williamson EJ, Walker AJ, Bhaskaran K, Bacon S, Bates C, Morton CE, et al. Factors associated with COVID-19-related death using OpenSAFELY. Nature 2020;584 (7821):430–6.

[3] Windpessl M, Bruchfeld A, Anders HJ, Kramer H, Waldman M, Renia L, et al. COVID-19 vaccines and kidney disease. Nat Rev Nephrol 2021;17(5):291–3.

[4] Sim JJ, Huang CW, Selevan DC, Chung J, Rutkowski MP, Zhou H. COVID-19 and survival in maintenance dialysis. Kidney Med 2021;3(1):132–5.

[5] Council E-E, Group EW. Chronic kidney disease is a key risk factor for severe COVID-19: a call to action by the ERA-EDTA. Nephrol Dial Transplant 2021;36 (1):87–94.

[6] Hsu CM, Weiner DE, Aweh G, Miskulin DC, Manley HJ, Stewart C, et al. COVID-19 among US dialysis patients: risk factors and outcomes from a national dialysis provider. Am J Kidney Diseas 2021;77(5):748–56 e1.

[7] Khatri M, Islam S, Dutka P, Carson J, Drakakis J, Imbriano L, et al. COVID-19 antibodies and outcomes among outpatient maintenance hemodialysis patients. Kidney360. 2021;2(2):263–9.

[8] Labriola L, Scohy A, Seghers F, Perlot Q, De Greef J, Desmet C, et al. A longitudinal, 3-Month serologic assessment of SARS-CoV-2 infections in a belgian hemodialysis facility. Clin J Am Soc Nephrol 2021;16(4):613–4.

[9] Anand S, Montez-Rath M, Han J, Garcia P, Cadden L, Hunsader P, et al. Antibody response to COVID-19 vaccination in patients receiving dialysis. J Am Soc Nephrol 2021 ASN.2021050611.

[10] Lacson E, Argyropoulos CP, Manley HJ, Aweh G, Chin AI, Salman LH, et al. Immunogenicity of SARS-CoV-2 vaccine in dialysis. medRxiv 2021.

[11] Yanay NB, Freiman S, Ma Shapira, Wishahi S, Hamze M, Elhaj M, et al. Experience with SARS-CoV-2 BNT162b2 mRNA vaccine in dialysis patients. Kidney Int 2021.

[12] Simon B, Rubey H, Treipl A, Gromann M, Hemedi B, Zehetmayer S, et al. Haemodialysis patients show a highly diminished antibody response after COVID-19 mRNA vaccination compared to healthy controls. Nephrology, dialysis, transplantation: official publication of the European Dialysis and Transplant Association. European Renal Association 2021:gfab179.

[13] Grupper A, Sharon N, Finn T, Cohen R, Israel M, Agbaria A, et al. Humoral response to the Pfizer BNT162b2 vaccine in patients undergoing maintenance hemodialysis. Clin J Am Soc Nephrol 2021.

[14] Agur T, Ben-Dor N, Goldman S, Lichtenberg S, Herman-Edelstein M, Yahav D, et al. Antibody response to mRNA SARS-CoV-2 vaccine among dialysis patients - a prospectivecohort study. Nephrol Dial Transplant 2021.

[15] Longlune N, Nogier MB, Miedougé M, Gabilan C, Cartou C, Seigneuric B, et al. High immunogenicity of a messenger RNA based vaccine against SARS-CoV-2 in chronic dialysis patients. Nephrol Dialysis Transplant 2021.

[16] Dan JM, Mateus J, Kato Y, Hastie KM, Yu ED, Faliti CE, et al. Immunological memory to SARS-CoV-2 assessed for up to 8 months after infection. Science 2021;371 (6529):eabf4063.

[17] Lederer K, Castaño D, Gómez Atria D, Oguin TH, Wang S, Manzoni TB, et al. SARS-CoV-2 mRNA vaccines foster potent antigen-specific germinal center responses associated with neutralizing antibody generation. Immunity 2020;53(6):1281–95 e5.

[18] Hartzell S, Bin S, Cantarelli C, Haverly M, Manrique J, Angeletti A, et al. Kidney failure associates with T cell exhaustion and imbalanced follicular helper T cells. 2020;11(2390).

[19] Crespo M, Collado S, Mir M, Cao H, Barbosa F, Serra C, et al. Efficacy of influenza A H1N1/2009 vaccine in hemodialysis and kidney transplant patients. Clin J Am Soc Nephrol 2011;6(9):2208–14.

[20] Scharpé J, Peetermans WE, Vanwalleghem J, Maes B, Bammens B, Claes K, et al. Immunogenicity of a standard trivalent influenza vaccine in patients on long-term hemodialysis: an open-label trial. Am J Kidney Dis 2009;54(1):77–85.

[21] Udomkarnjananun S, Takkavatakarn K, Praditpornsilpa K, Nader C, Eiam-Ong S, Jaber BL, et al. Hepatitis B virus vaccine immune response and mortality in dialysis patients: a meta-analysis. J Nephrol 2020;33(2):343–54.

[22] Bertrand D, Hamzaoui M, Lemée V, Lamulle J, Hanoy M, Laurent C, et al. Antibody and T cell response to SARS-CoV-2 messenger RNA BNT162b2 vaccine in kidney transplant recipients and hemodialysis patients. J Am Soc Nephrol 2021 ASN.2021040480.

[23] Speer C, Göth D, Benning L, Buylaert M, Schaier M, Grenz J, et al. Early humoral responses of hemodialysis patients after COVID-19 vaccination with BNT162b2. Clin J Am Soc Nephrol 2021 CJN.03700321.

[24] Altmann DM, Boyton RJ, Beale R. Immunity to SARS-CoV-2 variants of concern. Science 2021;371(6534):1103.

[25] Rabenau HF, Biesert L, Schmidt T, Bauer G, Cinatl J, Doerr HW. SARS-coronavirus (SARS-CoV) and the safety of a solvent/detergent (S/D) treated immunoglobulin preparation. Biologicals 2005;33(2):95–9.

[26] Becker M, Strengert M, Junker D, Kaiser PD, Kerrinnes T, Traenkle B, et al. Exploring beyond clinical routine SARS-CoV-2 serology using MultiCoV-Ab to evaluate endemic coronavirus cross-reactivity. Nat Commun 2021;12(1):1152.

[27] Becker M, Dulovic A, Junker D, Ruetalo N, Kaiser PD, Pinilla YT, et al. Immune response to SARS-CoV-2 variants of concern in vaccinated individuals. Nature Commun 2021;12(1):3109.

[28] Deepak P, Kim W, Paley MA, Yang M, Carvidi AB, El-Qunni AA, et al. Glucocorticoids and B cell depleting agents substantially impair immunogenicity of mRNA vaccines to SARS-CoV-2. medRxiv : the preprint server for health sciences 2021 2021.04.05.21254656.

[29] Forni G, Mantovani A, Forni G, Mantovani A, Moretta L, Rappuoli R, et al. COVID-19 vaccines: where we stand and challenges ahead. Cell Death Different 2021;28 (2):626–39.

[30] Krammer F. Correlates of protection from SARS-CoV-2 infection. The Lancet 2021;397(10283):1421–3.

[31] Sui Y, Bekele Y, Berzofsky JA. Potential SARS-CoV-2 immune correlates of protection in infection and vaccine immunization. Pathogens 2021;10(2):138.

[32] Schrezenmeier E, Bergfeld L, Hillus D, Lippert J-D, Weber U, Tober-Lau P, et al. Immunogenicity of COVID-19 Tozinameran vaccination in patients on chronic dialysis. Front Immunol 2021;12:2550.

[33] Feldman RA, Fuhr R, Smolenov I, Mick Ribeiro A, Panther L, Watson M, et al. mRNA vaccines against H10N8 and H7N9 influenza viruses of pandemic potential are immunogenic and well tolerated in healthy adults in phase 1 randomized clinical trials. Vaccine 2019;37(25):3326–34.

[34] Sahin U, Muik A, Derhovanessian E, Vogler I, Kranz LM, Vormehr M, et al. COVID-19 vaccine BNT162b1 elicits human antibody and TH1 T cell responses. Nature 2020;586(7830):594–9.

[35] Wang Z, Lorenzi JCC, Muecksch F, Finkin S, Viant C, Gaebler C, et al. Enhanced SARS-CoV-2 neutralization by dimeric IgA. Sci Translat Med 2021;13(577): eabf1555.

[36] Sterlin D, Mathian A, Miyara M, Mohr A, Anna F, Claër L, et al. IgA dominates the early neutralizing antibody response to SARS-CoV-2. Sci Translat Med 2021;13 (577):eabd2223.

[37] Lonnemann G, Novick D, Rubinstein M, Dinarello CA. Interleukin-18, interleukin-18 binding protein and impaired production of interferon-gamma in chronic renal failure. Clin Nephrol 2003;60(5):327–34.

[38] Lonnemann G, Bahlmann FH, Freise J, Hertel B, Dinarello CA. Low-flux hemodialysis suppresses interferon-gamma production: the possible role of beta2-microglobulin. Clin Nephrol 2009;72(3):170–6.

[39] Collier DA, Ferreira IATM, Kotagiri P, Datir R, Lim E, Touizer E, et al. Age-related immune response heterogeneity to SARS-CoV-2 vaccine BNT162b2. Nature 2021.

[40] Bayart J-L, Morimont L, Closset M, Wieërs G, Roy T, Gerin V, et al. Confounding factors influencing the kinetics and magnitude of serological response following administration of BNT162b2. Microorganisms 2021;9(6).

[41] Abu Jabal K, Ben-Amram H, Beiruti K, Batheesh Y, Sussan C, Zarka S, et al. Impact of age, ethnicity, sex and prior infection status on immunogenicity following a single dose of the BNT162b2 mRNA COVID-19 vaccine: real-world evidence from healthcare workers. Israel 2021;26(6):2100096.

[42] Pellini R, Venuti A, Pimpinelli F, Abril E, Blandino G, Campo F, et al. Initial observations on age, gender, BMI and hypertension in antibody responses to SARS-CoV-2 BNT162b2 vaccine. EClinicalMedicine 2021;36:100928.

[43] Frieman M, Harris AD, Herati RS, Krammer F, Mantovani A, Rescigno M, et al. SARS-CoV-2 vaccines for all but a single dose for COVID-19 survivors. EBioMedicine 2021;68:103401.

Supplementary Material - Cellular and humoral immunogenicity of a SARS-CoV-2 mRNA vaccine in patients on haemodialysis

Monika Strengert[a,b,1], Matthias Becker[c,1], Gema Morillas Ramos[d,1], Alex Dulovic[c], Jens Gruber[c], Jennifer Juengling[c], Karsten Lürken[e], Andrea Beigel[e], Eike Wrenger[e], Gerhard Lonnemann[e], Anne Cossmann[d], Metodi V. Stankov[d], Alexandra Dopfer-Jablonka[d,f], Philipp D. Kaiser[c], Bjoern Traenkle[c], Ulrich Rothbauer[c,g], Gérard Krause[a,b], Nicole Schneiderhan-Marra[c,1,*], Georg M.N. Behrens[d,f,h,1,*]

Author Affiliations
a Helmholtz Centre for Infection Research, Braunschweig, Germany
b TWINCORE GmbH, Centre for Experimental and Clinical Infection Research, a joint venture of the Hannover Medical School and the Helmholtz Centre for Infection Research, Hannover, Germany
c NMI Natural and Medical Sciences Institute at the University of Tübingen, Reutlingen, Germany
d Department for Rheumatology and Immunology, Hannover Medical School, Hannover, Germany
e Dialysis Centre Eickenhof, Langenhagen, Germany
f German Centre for Infection Research (DZIF), partner site Hannover-Braunschweig, Germany
g Pharmaceutical Biotechnology, University of Tübingen, Germany
h CiiM - Centre for Individualized Infection Medicine, Hannover, Germany
1 these authors contributed equally to this work.
* corresponding authors.

Corresponding authors contact details:
Nicole Schneiderhan-Marra, Phone number: +49 (0)7121 51530 815, Email address: nicole.schneiderhan@nmi.de, Postal address: Markwiesenstraße 55, 72770 Reutlingen, Germany.
Georg M.N. Behrens, Phone number: +49 (0)511 532 5337, Email address: behrens.georg@mh-hannover.de, Postal address: Carl-Neuberg-Straße 1, 30625 Hannover, Germany.
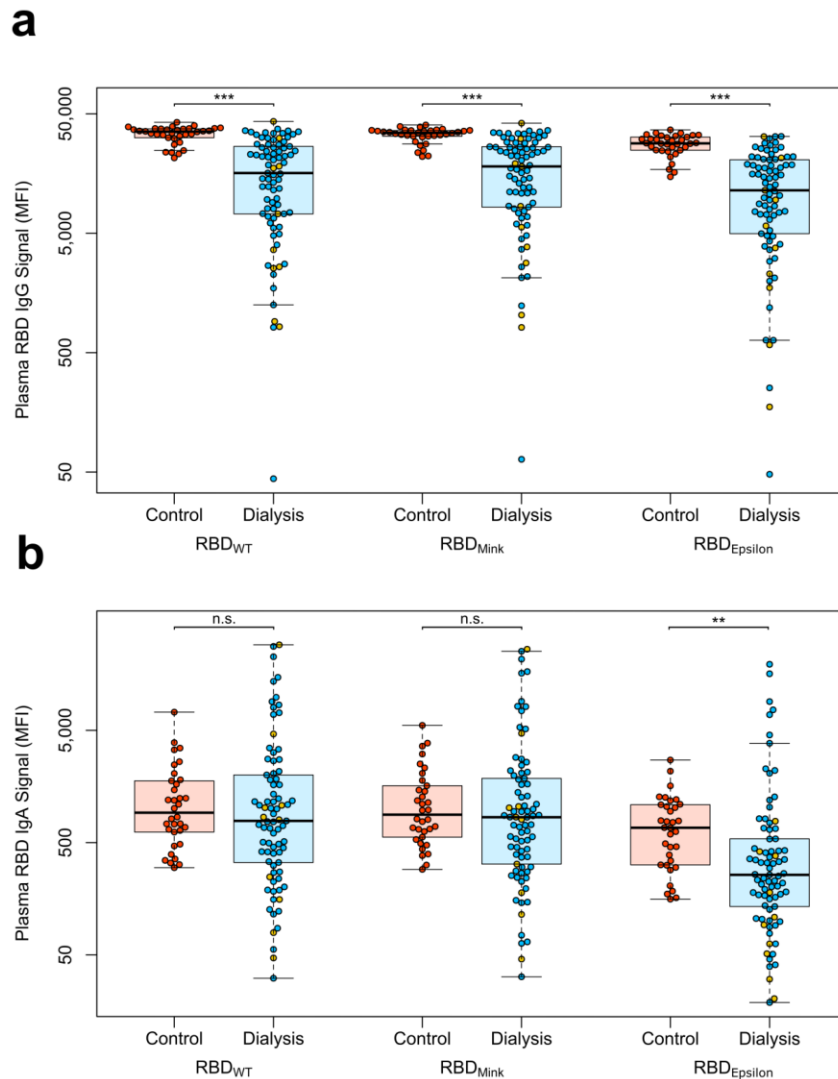
Fig. S1. Binding capacity of antibodies from plasma after vaccination with Pfizer BNT162b2 for RBDs of VoC B.1.429 (Epsilon) and Cluster 5 (Mink).
Plasma IgG (a) and IgA response (b) towards the indicated SARS-CoV-2 VoC Cluster 5 (Mink) and B.1.429 (Epsilon) from controls (red circles, n=34), individuals on maintenance haemodialysis (blue circles, n=71) and haemodialysed individuals on immunosuppressive medication (yellow circles, n=10) 21 days post second vaccination was measured using MULTICOV-AB. Data is displayed as median fluorescence intensity (MFI). Boxes represent the median, 25th and 75th percentiles, whiskers show the largest and smallest non-outlier values. Outliers were determined by 1·5 times IQR. Statistical significance was calculated by Mann-Whitney-U (two-sided). Significance was defined as *<0·01, **<0·001, ***<0·0001 or n.s.>0·01. Binding towards wild-type RBD (B.1) is again displayed for clarity and comparison.
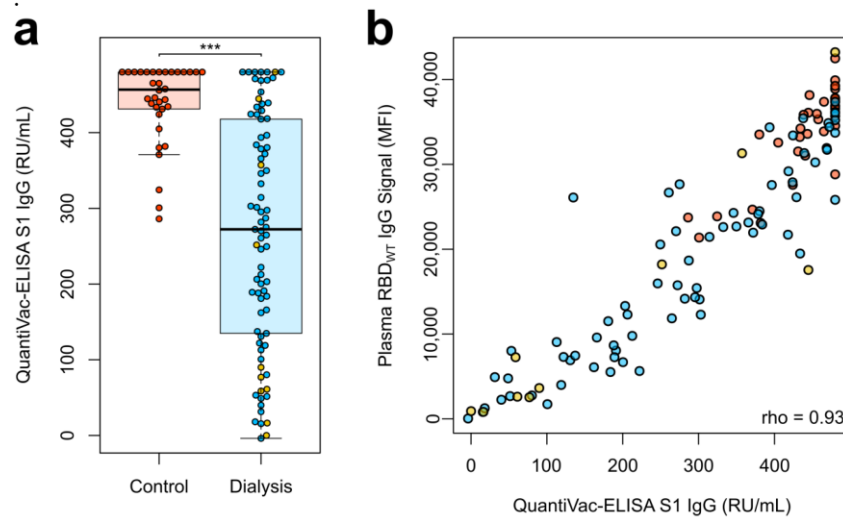
Fig. S2. Quantitative IgG titres in plasma after vaccination with Pfizer BNT162b2.
(a) Spike subdomain 1 (S1)-plasma IgG from controls (red circles, n=34), individuals on maintenance haemodialysis (blue circles, n=71) and haemodialysed individuals on immunosuppressive medication (yellow circles, n=10) 21 days post second vaccination were analysed using the QuantiVac-ELISA from Euroimmun (RU/mL). Samples that were classified as above upper or below the lower limit of detection of the assay are shown at the respective limit. Boxes represent the median, 25th and 75th percentiles, whiskers show the largest and smallest non-outlier values. Outliers were determined by 1·5 times IQR. Statistical significance was calculated by two-sided Mann-Whitney-U test. Significance was defined as *<0·01, **<0·001, ***<0·0001 or n.s.>0·01. (b) Correlation of MULTICOV-AB wild-type RBD B.1-IgG and Euroimmun QuantiVac Spike S1-IgG is shown across the study cohort. Correlation was calculated using Spearman´s coefficient.
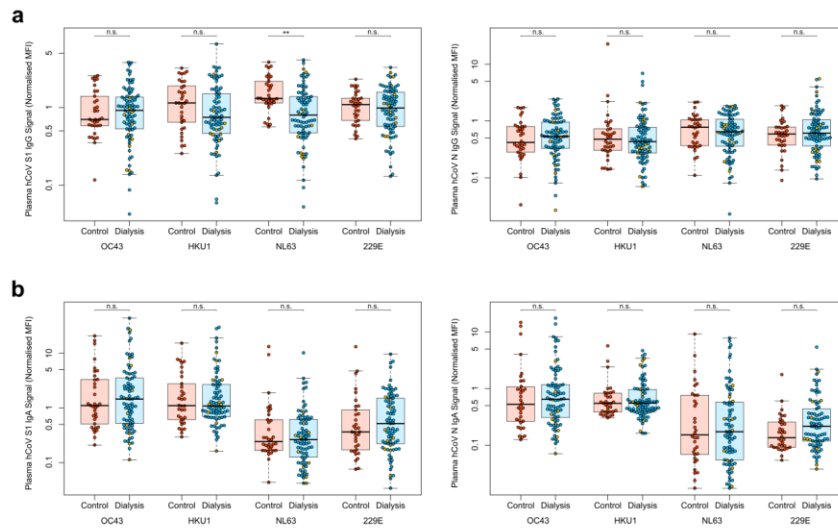
Fig. S3. Humoral immune response towards endemic coronaviruses in the vaccination cohort.
Plasma IgG (a) or IgA (b) levels towards S1 (left panel) or nucleocapsid (N, right panel) antigens were measured using MULTICOV-AB. Data for controls (red circles, n=34), individuals on maintenance haemodialysis (blue circles, n=71) and haemodialysed individuals on immunosuppressive medication (yellow circles, n=10) is shown as normalised MFI using quality control samples for IgG and IgA, respectively. Boxes represent the median, 25th and 75th percentiles, whiskers show the largest and smallest non-outlier values. Outliers were determined by 1·5 times IQR. Statistical significance was calculated by two-sided Mann-Whitney-U test. Significance was defined as *<0·01, **<0·001, ***<0·0001 or n.s.>0·01.
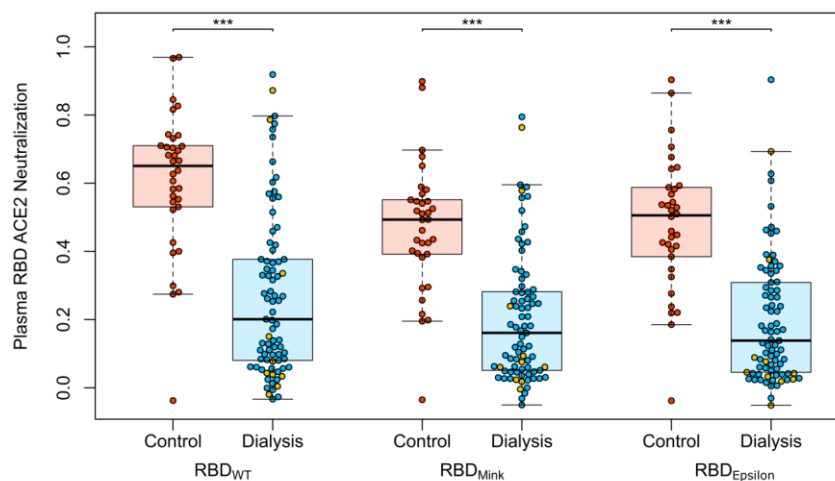
Fig. S4. Neutralizing capacity of plasma IgG after vaccination with Pfizer BNT162b2 for RBDs of VoC B.1.429 (Epsilon) and Cluster 5 (Mink).
Neutralizing capacity of plasma IgG towards the indicated SARS-CoV-2 VoC Cluster 5 (Mink) and B.1.429 (Epsilon) from controls (red circles, n=34), individuals on maintenance haemodialysis (blue circles, n=71) and haemodialysed individuals on immunosuppressive medication (yellow circles, n=10) 21 days post second vaccination was measured using an ACE2-RBD competition assay. Neutralization capacity is displayed as ratio where 1 indicates maximum neutralization and 0 no neutralization. Boxes represent the median, 25th and 75th percentiles, whiskers show the largest and smallest non-outlier values. Outliers were determined by 1·5 times IQR. Statistical significance was calculated by two-sided Mann-Whitney-U test. Significance was defined as *<0·01, **<0·001, ***<0·0001 or n.s.>0·01. Neutralization towards the wild-type RBD (B.1) is again displayed for clarity and comparison.
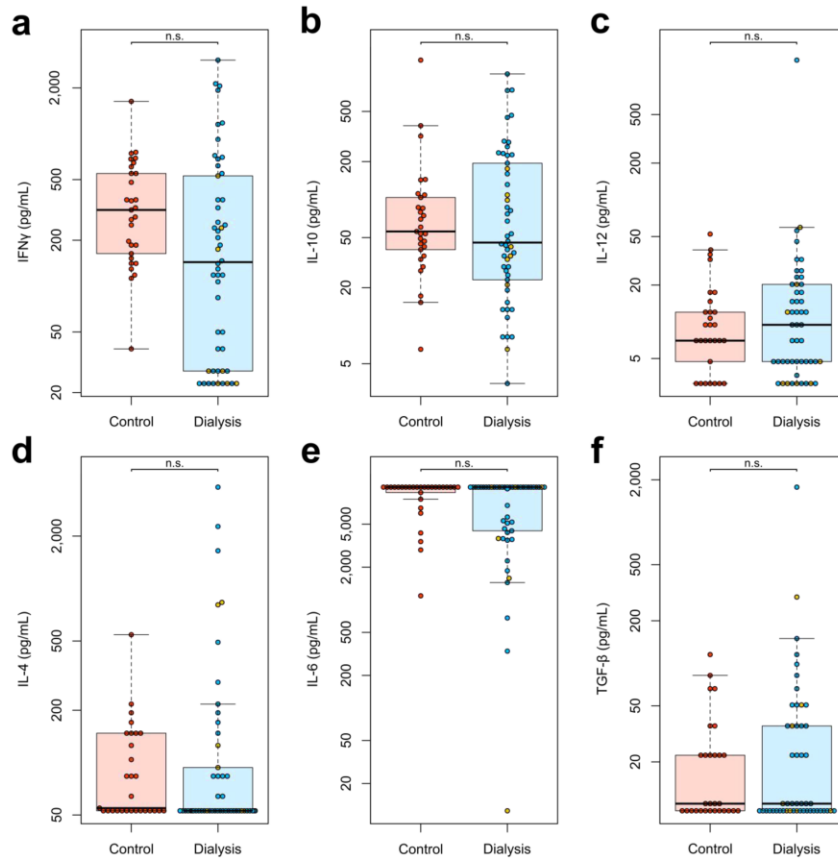
Fig. S5. Cytokine responses from PBMCs after *ex vivo* stimulation using a Spike S1-specific peptide pool. Whole blood from vaccinated controls (red circles, n=34), individuals on maintenance haemodialysis (blue circles, n=71) and haemodialysed individuals on immunosuppressive medication (yellow circles, n=10) 21 days post second vaccination was *ex vivo* stimulated using a SARS-CoV-2 spike S1-specific peptide pool. Supernatant fractions were analysed by bead-based multiplex-cytokine assay (pg/mL) for IFNγ (a), IL-10 (b), IL-12 (c), IL-4 (d), IL-6 (e) and TGF-β (f). Bead based-cytokine measurements (b-f) were performed with samples from 29 control, 42 haemodialysed and 8 haemodialysed individuals on immunosuppressive medication. Samples that were classified as above upper or below the lower limit of detection of the assay are shown at the respective limit. Boxes represent the median, 25th and 75th percentiles, whiskers show the largest and smallest non-outlier values. Outliers were determined by 1·5 times IQR. Statistical significance was calculated by two-sided Mann-Whitney-U test. Significance was defined as *<0·01, **<0·001, ***<0·0001 or n.s.>0·01.

Table S1. MULTICOV-AB antigen panel.

Virus	Antigen	Manufacturer	Product number
SARS-CoV-2	Spike Trimer	NMI	-
SARS-CoV-2	RBD B.1 (wild-type)	NMI	-
SARS-CoV-2	Nucleocapsid	Aalto	6404-b
SARS-CoV-2	RBD B.1.351 (Beta)	NMI	
SARS-CoV-2	RBD B.1.1.7 (Alpha)	NMI	
SARS-CoV-2	RBD Cluster 5 (Mink)	NMI	
SARS-CoV-2	RBD B.1.429 (Epsilon)	NMI	
hCoV-OC43	S1 domain	NMI	-
hCoV-OC43	Nucleocapsid	NMI	-
hCoV-HKU1	S1 domain	NMI	-
hCoV-HKU1	Nucleocapsid	NMI	-
hCoV-NL63	S1 domain	NMI	-
hCoV-NL63	Nucleocapsid	NMI	-
hCoV-229E	S1 domain	NMI	-
hCoV-229E	Nucleocapsid	NMI	-

Table S2. Causative kidney disease for dialysis: ANCA - Anti-Neutrophilic Cytoplasmic Autoantibody.

Characteristics	Haemodialysis group (n=81)
Diagnosis (n, %)	
Autosomal dominant polycystic kidney disease	11 (13·58)
Chronic glomerulonephritis	6 (7·41)
Diabetic nephropathy	13 (16·05)
Focal segmental glomerulosclerosis	5 (6·17)
IgA nephropathy	9 (11·11)
Interstitial nephropathy	6 (7·41)
Nephrosclerosis	18 (22·22)
Acute toxic tubular epithelial damage syndrome	1 (1·23)
Primary amyloidosis	1 (1·23)
ANCA-associated vasculitis	1 (1·23)
Cardiorenal syndrome	2 (2·47)
Medullary cystic kidney disease	1 (1·23)
Membranous glomerulonephritis	1 (1·23)
Kidney dysplasia	1 (1·23)
Obstructive nephropathy	1 (1·23)
Reflux nephropathy	1 (1·23)
Septic organ failure	1 (1·23)
Cystic kidney disease	1 (1·23)
Cyclosporin intoxication	1 (1·23)

Table S3. Medication of vaccinated study participants.

Characteristics	Non-dialysis control group (n=34)	Haemodialysis group (n=81)
Medication (n, %)		
Angiotensin-converting enzyme inhibitors	2 (5·88)	25 (30·86)
Statins	0 (0)	47 (58·02)
Angiotensin II Receptor Blockers	9 (26·47)	26 (32·10)
Vitamin D Supplements	16 (47·06)	80 (98·77)
Immunosuppressants (dosing range per day)		
Prednisolone (2-7·5 mg)	0	5 (6·17)
Prednisolone (50 mg) day 6-14 post 2nd vaccination	0	1 (1·23)
Prednisolone (5 mg), Tacrolimus (0·5-2 mg)	0	2 (2·47)
Prednisolone (5 mg), Tacrolimus (12 mg), Mycophenolatmofetil (500 mg)	0	1 (1·23)
Hydrocortisone (20 mg)	0	1 (1·23)

Appendix VII: Diminishing Immune Responses against Variants of Concern in Dialysis Patients 4 Months after SARS-CoV-2 mRNA Vaccination

Alex Dulovic*, Monika Strengert*, Gema Morillas Ramos*, **Matthias Becker**, Johanna Griesbaum, Daniel Junker, Karsten Lürken, Andrea Beigel, Eike Wrenger, Gerhard Lonnemann, Anne Cossmann, Metodi V. Stankov, Alexandra Dopfer-Jablonka, Philipp D. Kaiser, Bjoern Traenkle, Ulrich Rothbauer, Gérard Krause, Nicole Schneiderhan-Marra & Georg M.N. Behrens

  * = Authors contributed equally

Diminishing Immune Responses against Variants of Concern in Dialysis Patients 4 Months after SARS-CoV-2 mRNA Vaccination

Alex Dulovic,[1] Monika Strengert,[1] Gema Morillas Ramos,[1] Matthias Becker, Johanna Griesbaum,
Daniel Junker, Karsten Lürken, Andrea Beigel, Eike Wrenger, Gerhard Lonnemann, Anne Cossmann,
Metodi V. Stankov, Alexandra Dopfer-Jablonka, Philipp D. Kaiser, Bjoern Traenkle,
Ulrich Rothbauer, Gérard Krause,[2] Nicole Schneiderhan-Marra,[2] Georg M.N. Behrens[2]

Patients undergoing chronic hemodialysis were among the first to receive severe acute respiratory syndrome coronavirus 2 (SARS-CoV-2) vaccinations because of their increased risk for severe coronavirus disease and high case-fatality rates. By using a previously reported cohort from Germany of at-risk hemodialysis patients and healthy donors, where antibody responses were examined 3 weeks after the second vaccination, we assessed systemic cellular and humoral immune responses in serum and saliva 4 months after vaccination with the Pfizer-BioN-Tech BNT162b2 vaccine using an interferon-γ release assay and multiplex-based IgG measurements. We further compared neutralization capacity of vaccination-induced IgG against 4 SARS-CoV-2 variants of concern (Alpha, Beta, Gamma, and Delta) by angiotensin-converting enzyme 2 receptor-binding domain competition assay. Sixteen weeks after second vaccination, compared with 3 weeks after, cellular and humoral responses against the original SARS-CoV-2 isolate and variants of concern were substantially reduced. Some dialysis patients even had no detectable B- or T-cell responses.

Persistence of vaccination-induced cellular and humoral immune responses is crucial to prevent severe acute respiratory syndrome coronavirus 2 (SARS-CoV-2) infection or at least provide protection against severe coronavirus disease (COVID-19) that requires hospitalization. As in many other countries, the SARS-CoV-2 vaccination strategy in Germany was based on prioritization by occupation, underlying medical conditions, or advanced age (1). Although those priority groups have been vaccinated, a debate has emerged as to whether a third booster dose may be necessary to maintain or raise levels of protection within some of these groups. Decisions on whether to recommend a third dose needed to be made within a short timeframe, because SARS-CoV-2 infection case numbers were expected to increase again in the upcoming cold season, as previously observed in late 2020 (2). To date, however, data are lacking regarding the longevity of vaccination responses, and most published studies only provide follow-up data until 3 months after the second dose (3). Only 2 studies report data on extended time frames of 6 months after a completed 2-dose scheme (4,5), and, to our knowledge, no studies have considered follow-ups in patients receiving chronic hemodialysis. Data on the actual effect of a third dose are equally scarce and, so far, limited to organ transplant recipients, where a third dose substantially increased antibody

[1]These authors contributed equally to this article.
[2]These authors contributed equally to this article.

RESEARCH

responses (*6*). In addition, protection offered by first-generation vaccines is reduced for SARS-CoV-2 variants of concern (VOCs) (*7*), which now account for most infections worldwide (*8*), making the decision of whether a third dose is advisable even more critical for those with underlying conditions, immunodeficiencies, or an increased exposure risk (e.g., healthcare workers).

One particular risk group for SARS-CoV-2 infection and severe COVID-19 disease is hemodialysis patients; currently, ≈80,000 persons requiring regular renal replacement therapy in Germany (*9*). Their various underlying medical conditions and dialysis therapy often lead to a state of generalized immunosuppression (*10*). At the same time, these patients bear a continuous exposure risk because of the regular need for in-center hemodialysis therapy, which prevents them from self-isolating or reducing contacts to avoid infection. We and others have identified impaired cellular and humoral responses towards several viral vaccinations (e.g., SARS-CoV-2, influenza A, or hepatitis B) (*10–13*); however, there is a lack of longitudinal vaccination response studies against SARS-CoV-2 within this population. To guide future vaccination strategies as to whether additional booster vaccinations for at-risk groups to prevent severe COVID-19 are required, we provide follow-up data for a previously reported cohort of 76 persons receiving hemodialysis and 23 healthcare workers with no underlying conditions (*13*) for systemic and mucosal B- and T-cell responses 16 weeks after full BNT162b2 vaccination and the neutralizing potency of vaccination-induced antibodies. Because of the emergence of VOCs, and because all currently licensed vaccines are formulated against the original wild-type isolate (B.1), we also examined antibody binding and neutralization toward the Alpha (B.1.1.7), Beta (B.1.351), Gamma (P.3) and Delta (B.1.617.2) VOCs.

Methods

Study Design and Sample Collection

We collected blood samples by using vascular access before the start of dialysis or by venipuncture for the control population 16 weeks after the standard 2-dose vaccination with a 21-day interval of BNT162b2 (Pfizer-BioNTech, https://www.pfizer.com) was completed (T2). An analysis of samples from this population that were collected 3 weeks after the second dose of BNT162b2 (T1) has been published previously (*13*). A total of 76 patients on maintenance hemodialysis and 23 healthcare workers from the same dialysis center participated in the longitudinal follow-up (*13*). Demographic characteristics (e.g., age and sex), body mass index, time on dialysis, use of immunosuppressive medications, and anti-S1 domain IgG levels at T1 of persons who did not provide a sample at T2 were not substantially different compared with persons included in this analysis (Table; Appendix Table 1, 2, https://wwwnc.cdc.gov/EID/article/28/4/21-1907-App1.pdf). We obtained plasma by using an S-Monovette lithium heparin blood collection kit (Sarstedt, https://www.sarstedt.com). We used whole-blood samples immediately for an interferon-γ (IFN-γ) release assay (IGRA). To inactivate potential pathogens, we treated collected saliva samples with Tri (n-butyl) phosphate for a final concentration of 0.3% and Triton X-100 for a final concentration of 1%.

Ethics Considerations

The study was approved by the Internal Review Board of Hannover Medical School (approval number

Table. Characteristics of participants in a study of immune response against variants of concern in dialysis patients 4 months after SARS-CoV-2 mRNA vaccination*

Characteristic	Nondialysis control group	Hemodialysis group	p value for difference between groups
No. (%) patients	23 (100)	76 (100)	NA
Median age, y (IQR)	55 (14)	70.5 (18.25)	2.78×10^{-9}
Sex			1.01×10^{-2}†
M	6 (26.09)	43 (56.58)	
F	17 (73.91)	33 (43.42)	
Median days since start of hemodialysis (IQR)	NA	1,337 (1,686.5)	NA
Using immunosuppressive medication	0	10 (13.16)	6.77×10^{-2}
Underlying condition			
Obesity, BMI >30‡	4 (17.39)	16 (21.05)	8.68×10^{-1}
Diabetes mellitus	0	19 (25)	7.30×10^{-3}
Cardiovascular disease	0	35 (46.05)	2.93×10^{-5}

*Values are no. (%) except as indicated. Percentages are for total group. BMI, body mass index; IQR, interquartile range; NA, not applicable; SARS-CoV-2, severe acute respiratory syndrome coronavirus 2.
†p value reflects difference in male-to-female ratios between the two groups, not differences explicitly for either male or female persons.
‡BMI for 1 person was not known.

8973_BO-K_2020). We obtained written informed consent from all participants before the start of the study.

Bead Coupling

We coupled antigens to spectrally distinct MagPlex beads (Luminex, https://www.luminexcorp.com) by using EDC/s-NHS coupling for all standard (MULTI-COV-AB) antigens (14). We coupled receptor-binding domains (RBDs) from VOCs by using Anteo coupling (AnteoTech, https://www.anteotech.com) according to the manufacturer's instructions (15).

MULTICOV-AB

We analyzed IgG and IgA binding and levels by using MULTICOV-AB, a multiplex coronavirus immunoassay, as previously described (14). For our study, we used a panel of recombinant proteins as antigens (Appendix Table 3). In brief, we immobilized antigens on spectrally distinct populations of MagPlex beads either by EDC/s-NHS coupling (14) or by Anteo coupling according to the manufacturer instructions (15). We then incubated the combined MagPlex beads with samples. After conducting a wash step to remove unbound antibodies, we detected IgG or IgA with either R-phycoerythrin labeled goat anti-human IgG (Jackson ImmunoResearch, https://www.jacksonimmuno.com) or IgA (Jackson ImmunoResearch) as secondary antibodies. After conducting another wash step and bead resuspension, we measured samples once on a FLEXMAP 3D instrument (Luminex) by using the following settings: timeout, 80 s; gate, 7,500–15,000; reporter gain, standard photomultiplier tube; 40 events. Raw median fluorescence intensity (MFI) values or normalized values (MFI/MFI of quality control [QC] samples) (15) are reported. Three QC samples were measured per individual plate to monitor MULTICOV-AB performance. We measured all samples once.

Angiotensin-Converting Enzyme 2 Receptor Binding Domain Competition Assay

We carried out an angiotensin-converting enzyme 2 receptor-binding domain (ACE2-RBD) competition assay as previously described (15; D. Junker et al., unpub. data, https://doi.org/10.1101/2021.08.20.21262328) to determine IgG neutralization capacity against SARS-CoV-2 wild-type and the VOCs. For this assay, we combined biotinylated ACE2 with individual samples (and as a control, ACE2 alone) and incubated with the previously described MULTICOV-AB bead mix. Before and after ACE2 detection with Streptavidin-PE (Moss, Fisher Scientific, https://www.fishersci.com), we conducted washes. We measured samples once on a FLEXMAP 3D instrument with the same settings as MULTICOV-AB and analyzed them by using normalization of MFI values against the control. We considered samples with a neutralization ratio <0.2 as nonneutralizing. This cutoff is based on comparison to a classic virus neutralization test (D. Junker et al., unpub. data).

Euroimmun ELISA QuantiVac

As a control for the MULTICOV-AB results, we also analyzed plasma samples by using the Anti-SARS-CoV-2 QuantiVac ELISA IgG (Euroimmun, https://www.euroimmun.com). Samples were measured as previously described (13). We measured all samples once.

IGRA

We analyzed SARS-CoV-2–specific T-cell responses from whole blood by measuring IFN-γ production after stimulation with a peptide pool from the SARS-CoV-2 spike S1 with the SARS-CoV-2 Interferon Gamma Release Assay (Euroimmun) and the IFN-γ ELISA (Euroimmun), as previously described (13). We subtracted background signals from negative controls and calculated final results in milli-IU (mIU) per milliliter by using standard curves. Results from positive and negative controls were not statistically significantly different between timepoints T1 and T2. We considered IFN-γ concentrations >200 mIU/mL as reactive. We defined this arbitrary cutoff by using average background IFN-γ activity without antigen-stimulation in all samples of T1 multiplied with 10 for the threshold for IGRA positive. Using this cutoff, we found negative IGRA results in all of the 15 control samples (prepandemic persons) (16). The upper limit of reactivity was 2,000 mIU/mL.

Data Analysis and Statistics

We matched sample metadata and collected results from different assay platforms in Microsoft Excel 2016 (https://www.microsoft.com). We used Graph-Pad Prism 8.4.3 (https://www.graphpad.com) for statistical analysis. We generated figures in RStudio 1.2.5001 running R 3.6.1 (https://www.rstudio.com). We used the beeswarm add-on package to visualize data as strip charts with overlaying boxplots and to create nonoverlaying datapoints and used the RcolorBrewer add-on to generate specific colors for plots. We then edited the figures by using Inkscape 0.92.4 (https://inkscape.org).

269

Results

Substantial Decrease in Antibody Titers from 3 Weeks to 4 Months Postvaccination

Because antibody levels are considered a proxy for protection, we initially examined the seroreversion rate by using MULTICOV-AB (*14*), a previously published bead-based multiplex immunoassay that simultaneously analyses >20 different SARS-CoV-2 antigens, including the RBDs of VOCs and the endemic human coronaviruses. Similar to findings from our previous report (*13*), RBD IgG responses within the dialysis group (median normalized MFI 4.26 among 76 patients) toward SARS-CoV-2 wild-type RBD were significantly reduced compared with those for the control group (median

normalized MFI 13.6 among 23 persons; p<0.001) (Figure 1, panel A) 16 weeks after complete vaccination (T2). Compared with titer levels at 3 weeks after the second dose (T1), at 16 weeks after (T2), antibody titers had significantly decreased, by 61% in the control group and 75% in the dialysis group (p<0.001) (Figure 1, panel A). RBD IgG levels measured by MULTICOV-AB were additionally verified with a commercial quantitative in vitro diagnostic antibody test (Spearman rank 0.956) (Appendix Figure 1). Although none of the samples of the control group were classified as seronegative (titer below the cutoff) (Appendix Figure 2), 19.7% (15/76) of dialysis samples were defined as such 16 weeks after the second dose (T2), which constitutes a substantial increase from 3 weeks after second vaccination (T1),
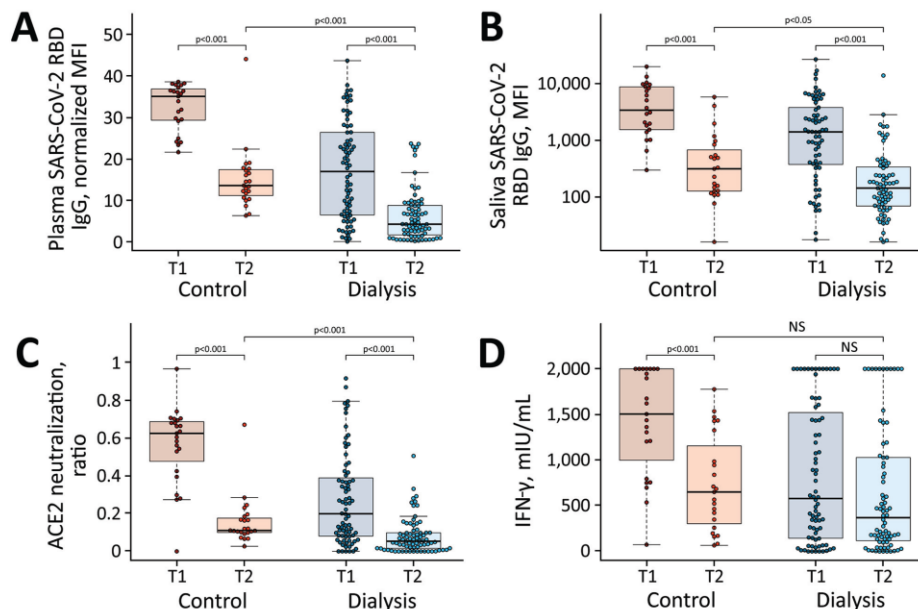
Figure 1. Significant decrease in humoral and cellular responses induced by Pfizer-BioNTech vaccine BNT162b2 (https://www.pfizer.com) against SARS-CoV-2 from 3 weeks to 16 weeks after second vaccination, observed in a study of immune response against variants of concern in dialysis patients 4 months after SARS-CoV-2 mRNA vaccination. A) IgG response in plasma; B) IgG response in saliva; C) neutralizing capacity toward SARS-CoV-2 wild type B.1; D) T-cell response measured by IFN-γ release assay. Blue circles indicate dialysis patients (n = 76) and red circles controls (n = 23). Samples were taken 3 weeks (T1) and 16 weeks (T2) after vaccination. Saliva (panel B) has reduced sample numbers in both groups because of issues in sample collection (T1 control, n = 22; T1 dialysis, n = 69; T2 control, n = 23; T2 dialysis. n = 71). T1 timepoint data has been published previously (*13*) and is reproduced here for clarity. Horizontal lines within boxes indicate medians; box tops and bottoms indicate the 25th and 75th percentiles; whiskers show the largest and smallest nonoutlier values. Outliers were determined by 1.5 times interquartile range. Statistical significance was calculated by Wilcoxon matched-pairs signed rank test when comparing T1 and T, and 2-sided Mann–Whitney–U test when comparing control and dialysis groups. ACE2, angiotensin-converting enzyme 2; IFN-γ, interferon γ; MFI; median fluorescence intensity; NS, not significant; RBD, receptor-binding domain; SARS-CoV-2, severe acute respiratory syndrome coronavirus 2; T1, timepoint 1; T2, timepoint 2.

270

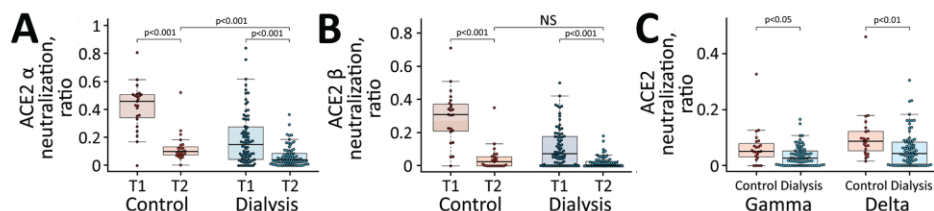**Figure 2.** Reduced neutralizing capacity against SARS-CoV-2 variants of concern observed in a study of immune response against variants of concern in dialysis patients 4 months after SARS-CoV-2 mRNA vaccination. Neutralizing capacity of plasma IgG toward SARS-CoV-2 variants of concern Alpha (A), Beta (B), and Gamma and Delta (C) in the dialysis (blue circles, n = 76) and control (red circles, n = 23) groups 16 weeks after second vaccination with Pfizer-BioNTech vaccine BNT162b2 (https://www.pfizer.com). Neutralization capacity is displayed as ratio, where 1 indicates maximum neutralization and 0 no neutralization. Horizontal lines within boxes indicate medians; box tops and bottoms indicate the 25th and 75th percentiles; whiskers show the largest and smallest nonoutlier values. Outliers were determined by 1.5 times interquartile range. Statistical significance was calculated by 2-sided Mann–Whitney–U test. ACE2, angiotensin-converting enzyme 2; NS, not significant; SARS-CoV-2, severe acute respiratory syndrome coronavirus 2; T1, timepoint 1; T2, timepoint 2.

at which point only 5.3% (4/76) of samples were seronegative. When examining plasma titers against nucleocapsid, we did not observe any dialysis patients, other than one who had a PCR-confirmed infection before the first dose, having a value above the cutoff that would indicate infection.

To evaluate whether this reduction in plasma RBD IgG was also present at the mucosal site, we profiled the local antibody response in saliva by using MULTI-COV-AB. As observed in plasma, a significant reduction occurred in saliva RBD IgG titers in the dialysis (median 143 among 71 patients) compared with the control group (median 313.5 among 23 persons) (p = 0.02) (Figure 1, panel B). When comparing saliva RBD IgG levels at T1 to those at T2, we observed a statistically significant decline in both groups (p<0.001) (Figure 1, panel B), suggesting that the antibodies have potentially lost competence to prevent transmission if infected. When examining RBD IgA, we observed a significant difference in titers between persons in the control and dialysis groups (p = 0.003) (Appendix Figure 3, panel A); 47.8% of controls and 75% of dialysis patients were classified as seronegative. This more pronounced reduction in IgA versus IgG levels most likely represents the shorter IgA half-life. Saliva RBD IgA tended to be higher in the dialysis group, although not significantly (p = 0.051) (Appendix Figure 3, panel B).

Decreased Neutralization Capacity as Time Postvaccination Increased

We next examined whether neutralization potential was also hindered because solid evidence exists on the protective role for neutralizing serum antibodies (17). By using an ACE2–RBD competition assay, which assesses neutralization potency toward SARS-CoV-2

wild-type and the circulating Alpha, Beta, Gamma, and Delta VOCs, we found that neutralization against wild-type SARS-CoV-2 RBD was significantly reduced in the dialysis group compared with the controls (p<0.001) (Figure 1, panel C) 16 weeks after complete vaccination. We found that 82.6% (19/23) of control samples and 89.5% (68/76) of dialysis patient samples were below the 0.2 threshold, which indicates the absence of neutralizing activity (Appendix Figure 2), a threshold is based on information provided for other available ACE2 competition assays (18). This difference represents a substantially significant reduction (p<0.001 for both groups) in neutralizing activity compared with 3 weeks after second vaccination, at which point only 4.3% (1/23) of the control samples and 50.0% (38/76) of the dialysis patient samples were below the threshold (Figure 1, panel C; Appendix Figure 2).

Reduced T-cell Response after Vaccination in Dialysis Patients and Decrease Over Time

Because some persons might be able to control and clear SARS-CoV-2 infections with a strong T-cell response alone, we examined spike-specific SARS-CoV-2 T-cell responses by using a commercially available IGRA. Although absolute mean IFN-γ responses in the dialysis group compared with the control group tended to be lower (median 370 vs. 651 mIU/mL), this difference was not significant (p = 0.13) (Figure 1, panel D). In the control group, IFN-γ release after restimulation declined significantly from the first timepoint (median 1,505; p<0.001) (Figure 1, panel D), whereas for dialysis patients, this decline was not significant (median 580; p = 0.13) (Figure 1, panel D). This difference is probably attributable to most control samples being at the assay's upper limit

of detection at the first timepoint, when the dialysis samples already showed reduced IFN-γ release. Overall, the number of nonresponders was higher in the hemodialysis group (40.8% [31/76]) than the control group (21.7% [5/23]) (Appendix Figure 2). A lack of serologic response appears to be more driven by T-cell immunity than B-cell immunity; 2.6% (2/76) of the dialysis group having a T-cell response but no B-cell response, compared with 23.6% (18/76) who had a B-cell response but no T-cell response. In total, 17.1% (13/76) of the dialysis group were classified as complete nonresponders because of the absence of detectable SARS-CoV-2 wild-type B- and T-cell responses, compared with none in the control group.

Significantly Reduced Antibody Binding and Neutralization Capacity against VOCs

Having characterized response against wild-type SARS-CoV-2, we then assessed humoral response against the VOCs Alpha, Beta, Gamma, and Delta. As shown with classical cell-culture based virus neutralization assays (7), neutralization responses were also reduced for all VOCs compared with wild-type when we used the previously described ACE2-RBD competition assay. Compared levels at with the initial timepoint, neutralization decreased significantly for the Alpha and Beta VOCs (p<0.001 for both) (Figure 2, panel A, B). We were unable to determine these changes for Gamma and Delta because these variants were not measured in the initial analysis. In a comparison between the dialysis and the control cohort, dialysis patients had significantly reduced neutralization against Alpha (p<0.001) (Figure 2, panel A), Gamma (p = 0.014) (Figure 2, panel C), and Delta (p = 0.002) (Figure 2, panel C) but not for Beta (p = 0.08) (Figure 2, panel B). The number of nonresponders was variable between the different strains although consistently high; 87.0% of the control group and 93.4% of the dialysis group were considered nonresponders against Alpha, 95.7% of the control group and 100% of the dialysis group against Beta and Gamma, and 95.7% of the control group and 96.1% of dialysis group against Delta.

Discussion

After our initial study (13), which focused on humoral and cellular responses 3 weeks after administering the second BNT162b2 vaccination, we provide longitudinal data for 4 months after the second dose. In comparison with other vaccine studies, which have mostly examined peak humoral response within 1 month or alternative prime-boost vaccination schedules with BNT162b2 (12), our data reveal a

substantial decrease in the subsequent months in hemodialysis patients and healthy controls. Overall, the decline in neutralizing anti–spike RBD antibodies was comparable in both groups, and the difference between groups was mostly driven by differences in the magnitude of the initial humoral response. Although this decrease is expected and can be attributed to the memory phase, the extent of the reduction was unpredicted because it resulted in a substantial proportion of persons being classified as seronegative. The reduction of salivary antibodies is particularly important because their presence has been linked to reduced transmission potential (15). This pattern of reduced antibody binding with increasing time postvaccination was also reflected in diminishing neutralization potential.

Most persons tested were classified below our defined neutralization threshold for wild-type RBD with an almost complete nonresponder rate against Delta, which was the dominant strain in many parts of the world at the time of our analysis (8). Although this finding does not automatically translate to a failure of vaccine efficacy, given that any active challenge of the immune system should result in expansion of memory B- and T-cell populations along with increased (neutralizing) antibody titers, it does suggest nevertheless that active protection against infection may be reduced. Although a recent study by Pfizer (4) indicated that BNT162b2 vaccine efficacy did only slightly decrease 6 months postvaccination in the study cohort (from 95% to 91%) in fully immunocompetent persons, data from vaccinations in Israel identified a reduction in efficacy to 40% (19). In combination with our data, where 17.1% of the dialysis cohort were classified as having no evidence for vaccine-elicited T- and B-cell immunity after 4 months, the Pfizer study findings suggest that vaccine efficacy may be even further reduced within this patient group. For dialysis patients, this finding is particularly concerning because they often have underlying conditions that put them at additional risk for severe COVID-19 (10). The lack of a considerable SARS-CoV-2 specific T-cell response in dialysis patients may result from chronic inflammatory conditions, leading to T-cell exhaustion and suppression of IFN-γ levels (20). Differences in anti–SARS-CoV-2 T-cell kinetics between groups presumably reflect difference in the magnitude of T-cell responses after boost and during the contraction phase. To what extent T-cell immunity contributes to protection from COVID-19 and whether our IGRA results below a cutoff provide evidence for the lack of effective adaptive T-cell immunity, requires further investigation. However, we should state that

although we see reductions in titer, neutralizing activity, and T-cell responses, we did not see any new infections by T2 within our cohort.

Our study is limited by the relatively small sample size of persons, who were not matched by age or sex. However, the sample number and compromised matching is consistent with similar studies on dialysis vaccine responses (*12*). Although studies have indicated that differences exist in protection and antibody responses (*21*) after different COVID-19 vaccination schedules, our study of Pfizer's BNT162b2 represents a real-world situation for most dialysis patients. Because of reduced anti-spike responses 4 weeks postvaccination in patients with other chronic conditions (*6*), these groups should undergo careful monitoring to determine whether their responses also decrease substantially over time.

Taken together, our results strongly argue that all persons undergoing chronic hemodialysis should be preferably administered a third dose of the BNT162b2 vaccine. Recent studies on administering a third dose to dialysis patients and transplant recipients has identified strong increases in humoral responses after vaccination, and a reduced percentage of recipients are considered nonresponders (*22–25*). However, longitudinal follow-up studies will be needed in early 2022 to monitor the rate of antibody decay after administration of a third dose in these and other vulnerable groups.

About the Author
Dr. Dulovic is a scientist in the Multiplex Immunoassay Group at the Natural and Medical Sciences Institute at the University of Tübingen. He has a background in molecular biology and genetics of parasitic nematodes and currently works on serologic assay development for a range of pathogens, including SARS-CoV-2, hepatitis virus, and influenza virus.

References
1. European Centre for Disease Control and Prevention. Overview of the implementation of COVID-19 vaccination strategies and deployment plans in the EU/EEA. 2021 [cited 2021 Aug 18]. https://www.ecdc.europa.eu/en/publications-data/overview-implementation-covid-19-vaccination-strategies-and-deployment-plans
2. Haab BB. Methods and applications of antibody microarrays in cancer research. Proteomics. 2003;3:2116–22. https://doi.org/10.1002/pmic.200300595
3. Ibarrondo FJ, Hofmann C, Fulcher JA, Goodman-Meza D, Mu W, Hausner MA, et al. Primary, recall, and decay kinetics of SARS-CoV-2 vaccine antibody responses. ACS Nano. 2021;15:11180–91. https://doi.org/10.1021/acsnano.1c03972
4. Thomas SJ, Moreira ED Jr, Kitchin N, Absalon J, Gurtman A, Lockhart S, et al.; C4591001 Clinical Trial Group. Safety and efficacy of the BNT162b2 mRNA Covid-19 vaccine through 6 months. N Engl J Med. 2021;385:1761–73. https://doi.org/10.1056/NEJMoa2110345
5. Doria-Rose N, Suthar MS, Makowski M, O'Connell S, McDermott AB, Flach B, et al.; mRNA-1273 Study Group. Antibody persistence through 6 months after the second dose of mRNA-1273 vaccine for Covid-19. N Engl J Med. 2021;384:2259–61. https://doi.org/10.1056/NEJMc2103916
6. Kamar N, Abravanel F, Marion O, Couat C, Izopet J, Del Bello A. Three doses of an mRNA Covid-19 vaccine in solid-organ transplant recipients. N Engl J Med. 2021;385:661–2. https://doi.org/10.1056/NEJMc2108861
7. Altmann DM, Boyton RJ, Beale R. Immunity to SARS-CoV-2 variants of concern. Science. 2021;371:1103–4. https://doi.org/10.1126/science.abg7404
8. Heyse S, Vogel H, Sänger M, Sigrist H. Covalent attachment of functionalized lipid bilayers to planar waveguides for measuring protein binding to biomimetic membranes. Protein Sci. 1995;4:2532–44. https://doi.org/10.1002/pro.5560041210
9. Girndt M, Trocchi P, Scheidt-Nave C, Markau S, Stang A. The prevalence of renal failure. Results from the German Health Interview and Examination Survey for Adults, 2008–2011 (DEGS1). Dtsch Arztebl Int. 2016;113:85–91.
10. Windpessl M, Bruchfeld A, Anders HJ, Kramer H, Waldman M, Renia L, et al. COVID-19 vaccines and kidney disease. Nat Rev Nephrol. 2021;17:291–3. https://doi.org/10.1038/s41581-021-00406-6
11. Schrezenmeier E, Bergfeld L, Hillus D, Lippert J-D, Weber U, Tober-Lau P, et al. Immunogenicity of COVID-19 tozinameran vaccination in patients on chronic dialysis. Front Immunol. 2021;12:690698. https://doi.org/10.3389/fimmu.2021.690698
12. Carr EJ, Wu M, Harvey R, Wall EC, Kelly G, Hussain S, et al.; Haemodialysis COVID-19 consortium; Crick COVID Immunity Pipeline. Neutralising antibodies after COVID-19 vaccination in UK haemodialysis patients. Lancet. 2021;398:1038–41. https://doi.org/10.1016/S0140-6736(21)01854-7
13. Strengert M, Becker M, Ramos GM, Dulovic A, Gruber J, Juengling J, et al. Cellular and humoral immunogenicity of a SARS-CoV-2 mRNA vaccine in patients on haemodialysis.

EBioMedicine. 2021;70:103524. https://doi.org/10.1016/j.ebiom.2021.103524

14. Becker M, Strengert M, Junker D, Kaiser PD, Kerrinnes T, Traenkle B, et al. Exploring beyond clinical routine SARS-CoV-2 serology using MultiCoV-Ab to evaluate endemic coronavirus cross-reactivity. Nat Commun. 2021;12:1152. https://doi.org/10.1038/s41467-021-20973-3

15. Becker M, Dulovic A, Junker D, Ruetalo N, Kaiser PD, Pinilla YT, et al. Immune response to SARS-CoV-2 variants of concern in vaccinated individuals. Nat Commun. 2021;12:3109. https://doi.org/10.1038/s41467-021-23473-6

16. Stankov MV, Cossmann A, Bonifacius A, Dopfer-Jablonka A, Ramos GM, Gödecke N, et al. Humoral and cellular immune responses against severe acute respiratory syndrome coronavirus 2 variants and human coronaviruses after single BNT162b2 vaccination. Clin Infect Dis. 2021;73:2000–8. https://doi.org/10.1093/cid/ciab555

17. Khoury DS, Cromer D, Reynaldi A, Schlub TE, Wheatley AK, Juno JA, et al. Neutralizing antibody levels are highly predictive of immune protection from symptomatic SARS-CoV-2 infection. Nat Med. 2021;27:1205–11. https://doi.org/10.1038/s41591-021-01377-8

18. Lopez E, Haycroft ER, Adair A, Mordant FL, O'Neill MT, Pymm P, et al. Simultaneous evaluation of antibodies that inhibit SARS-CoV-2 variants via multiplex assay. JCI Insight. 2021;6:e150012. https://doi.org/10.1172/jci.insight.150012

19. Ng JH, Ilag LL. Biochips beyond DNA: technologies and applications. Biotechnol Annu Rev. 2003;9:1–149. https://doi.org/10.1016/S1387-2656(03)09001-X

20. Hartzell S, Bin S, Cantarelli C, Haverly M, Manrique J, Angeletti A, et al. Kidney failure associates with T cell exhaustion and imbalanced follicular helper T cells. Front Immunol. 2020;11:583702. https://doi.org/10.3389/fimmu.2020.583702

21. Garcia P, Anand S, Han J, Montez-Rath ME, Sun S, Shang T, et al. COVID-19 vaccine type and humoral immune response in patients receiving dialysis. J Am Soc Nephrol. 2022;33:33–7. https://doi.org/10.1681/ASN.2021070936

22. Ducloux D, Colladant M, Chabannes M, Yannaraki M, Courivaud C. Humoral response after 3 doses of the BNT162b2 mRNA COVID-19 vaccine in patients on hemodialysis. Kidney Int. 2021;100:702–4. https://doi.org/10.1016/j.kint.2021.06.025

23. Hall VG, Ferreira VH, Ku T, Ierullo M, Majchrzak-Kita B, Chaparro C, et al. Randomized trial of a third dose of mRNA-1273 vaccine in transplant recipients. N Engl J Med. 2021;385:1244–6. https://doi.org/10.1056/NEJMc2111462

24. Massa F, Cremoni M, Gérard A, Grabsi H, Rogier L, Blois M, et al. Safety and cross-variant immunogenicity of a three-dose COVID-19 mRNA vaccine regimen in kidney transplant recipients. EBioMedicine. 2021;73:103679. https://doi.org/10.1016/j.ebiom.2021.103679

25. Stervbo U, Blazquez-Navarro A, Blanco EV, Safi L, Meister TL, Paniskaki K, et al. Improved cellular and humoral immunity upon a second BNT162b2 and mRNA-1273 boost in prime-boost vaccination no/low responders with end-stage renal disease. Kidney Int. 2021;100:1335–7. https://doi.org/10.1016/j.kint.2021.09.015

Address for correspondence: Gérard Krause, Helmholtz Center for Infection Research, Inhoffenstrasse 7, 38124 Braunschweig, Germany; email: gerard.krause@helmholtz-hzi.de; Nicole Schneiderhan-Marra, Natural and Medical Sciences Institute at the University of Tübingen, Markwiesenstrasse 55, 72770 Reutlingen, Germany; email: nicole.schneiderhan@nmi.de; Georg M.N. Behrens, Hannover Medical School, Carl-Neuberg-Straße 1, 30625 Hannover, Germany; email: behrens.georg@mh-hannover.de

274

Diminishing Immune Responses against Variants of Concern in Dialysis Patients 4 Months after SARS-CoV-2 mRNA Vaccination

Appendix

Appendix Table 1. Therapeutic indication for hemodialysis*

Diagnosis	No. patients (%) in hemodialysis group
Total	76 (100)
Autosomal dominant polycystic kidney disease	11 (14.47)
Chronic glomerulonephritis	6 (7.90)
Diabetic nephropathy	11 (14.47)
Focal segmental glomerulosclerosis	5 (6.59)
IgA nephropathy	8 (10.53)
Interstitial nephropathy	6 (7.90)
Nephrosclerosis	16 (21.05)
Acute toxic tubular epithelial damage syndrome	1 (1.32)
Primary amyloidosis	1 (1.32)
ANCA-associated vasculitis	1 (1.32)
Cardiorenal syndrome	2 (2.64)
Medullary cystic kidney disease	1 (1.32)
Membranous glomerulonephritis	1 (1.32)
Kidney dysplasia	1 (1.32)
Obstructive nephropathy	1 (1.32)
Reflux nephropathy	1 (1.32)
Septic organ failure	1 (1.32)
Cystic kidney disease	1 (1.32)
Cyclosporin intoxication	1 (1.32)

*ANCA, antineutrophilic cytoplasmic autoantibody.

Appendix Table 2. Medication of vaccination cohort

Medication	No. (%)	
	Nondialysis control group	Hemodialysis group
Total	23 (100)	76 (100)
Angiotensin-converting enzyme inhibitors	2 (8.70)	22 (28.95)
Statins	0 (0)	45 (59.21)
Angiotensin II Receptor Blockers	5 (21.74)	25 (32.89)
Vitamin D Supplements	12 (52.17)	75 (98.68)
Immunosuppressants (dosing range per day)*		
Prednisolone (2–7.5 mg)	0	5 (6.59)
Prednisolone (50 mg) day 6–14 post 2nd vaccination	0	1 (1.32)
Prednisolone (5 mg), Tacrolimus (0.5–2 mg)	0	2 (2.64)
Prednisolone (5 mg), Tacrolimus (12 mg), Mycophenolatmofetil (500 mg)	0	1 (1.32)
Hydrocortisone (20 mg)	0	1 (1.32)

*Therapeutic indication for immunosuppression were in four patients a kidney transplant (one had received an additional liver transplant), polymyositis, polyarthritis, vasculitis and chronic obstructive pulmonary disease.

Appendix Table 3. MULTICOV-AB antigen panel

Virus	Antigen	Manufacturer	Product number
SARS-CoV-2	Spike Trimer	NMI	–
SARS-CoV-2	RBD B.1 (wild-type)	NMI	–
SARS-CoV-2	Nucleocapsid	Aalto	6404–b
SARS-CoV-2	S1 domain	NMI	–
SARS-CoV-2	S2 domain	NMI	–
SARS-CoV-2	RBD B.1.1.7 (Alpha)	NMI	–
SARS-CoV-2	RBD B.1.351 (Beta)	NMI	–
SARS-CoV-2	RBD P.3 (Gamma)	NMI	–
SARS-CoV-2	RBD B.1.617.2 (Delta)	NMI	–
hCoV-OC43	S1 domain	NMI	–
hCoV-OC43	Nucleocapsid	NMI	–
hCoV-HKU1	S1 domain	NMI	–
hCoV-HKU1	Nucleocapsid	NMI	–
hCoV-NL63	S1 domain	NMI	–
hCoV-NL63	Nucleocapsid	NMI	–
hCoV-229E	S1 domain	NMI	–
hCoV-229E	Nucleocapsid	NMI	–

Appendix Figure 1. Quantitative plasma IgG titers 16 weeks after vaccination with Pfizer BNT162b2. A) Spike S1-specific plasma IgG (RU/mL) from control group (red, n = 23) and dialysis group (blue, n = 76) were analyzed 16 weeks post-second dose of Pfizer BNT162b2 using the QuantiVac-ELISA (Euroimmun). Samples above upper or below the ELISA's limits of detection are shown at the corresponding limit. Boxes represent the median, 25th and 75th percentiles, whiskers show the largest and smallest non-outlier values. Outliers were determined by 1.5 times IQR. Statistical significance was calculated by two-sided Mann-Whitney-U test. Significance was defined as ***<0.001. B) Correlation of MULTICOV-AB wild-type RBD B.1-IgG and QuantiVac Spike S1-IgG across the study population. Spearman's rank was used for correlation analysis.
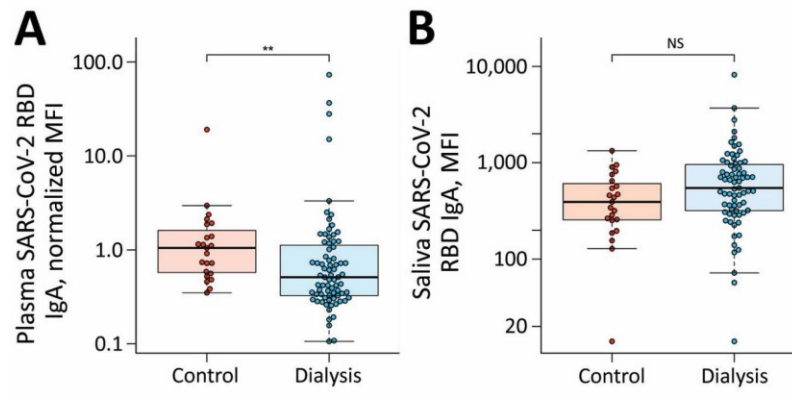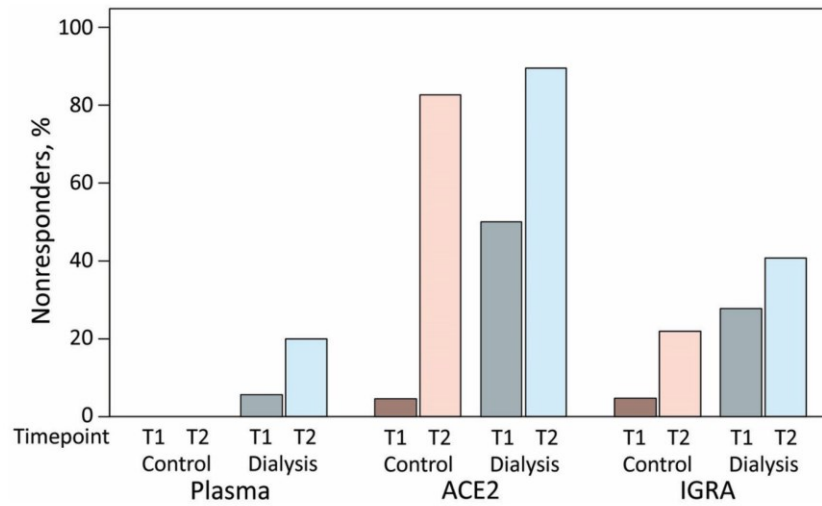
Reference

1. Strengert M, Becker M, Ramos GM, Dulovic A, Gruber J, Juengling J, et al. Cellular and humoral immunogenicity of a SARS-CoV-2 mRNA vaccine in patients on haemodialysis. EBioMedicine. 2021;70:103524. PubMed https://doi.org/10.1016/j.ebiom.2021.103524

Appendix VIII: Longitudinal cellular and humoral immune responses after triple BNT162b2 and fourth full-dose mRNA-1273 vaccination in haemodialysis patients

Matthias Becker*, Anne Cossmann*, Karsten Lürken, Daniel Junker, Jens Gruber, Jennifer Juengling, Gema Morillas Ramos, Andrea Beigel, Eike Wrenger, Gerhard Lonnemann, Metodi V. Stankov, Alexandra Dopfer-Jablonka, Philipp D. Kaiser, Bjoern Traenkle, Ulrich Rothbauer, Gérard Krause, Nicole Schneiderhan-Marra, Monika Strengert, Alex Dulovic & Georg M.N. Behrens

* = Authors contributed equally

Check for updates

Longitudinal cellular and humoral immune responses after triple BNT162b2 and fourth full-dose mRNA-1273 vaccination in haemodialysis patients

Matthias Becker[1†], Anne Cossmann[2†], Karsten Lürken[3],
Daniel Junker[1], Jens Gruber[1], Jennifer Juengling[1],
Gema Morillas Ramos[2], Andrea Beigel[3], Eike Wrenger[3],
Gerhard Lonnemann[3], Metodi V. Stankov[2],
Alexandra Dopfer-Jablonka[2,4], Philipp D. Kaiser[1],
Bjoern Traenkle[1], Ulrich Rothbauer[1,5], Gérard Krause[4,6,7],
Nicole Schneiderhan-Marra[1], Monika Strengert[6,7*†],
Alex Dulovic[1*†] and Georg M. N. Behrens[2,4,8*†]

[1]NMI Natural and Medical Sciences Institute at the University of Tübingen, Reutlingen, Germany,
[2]Department for Rheumatology and Immunology, Hannover Medical School, Hannover, Germany,
[3]Department of Internal Medicine and Nephrology, Dialysis Centre Eickenhof, Langenhagen, Germany,
[4]German Centre for Infection Research (DZIF), partner site Hannover-Braunschweig, Hannover, Germany,
[5]Pharmaceutical Biotechnology, University of Tübingen, Tübingen, Germany, [6]Department Epidemiology,
Helmholtz Centre for Infection Research, Braunschweig, Germany, [7]TWINCORE GmbH, Centre for
Experimental and Clinical Infection Research, a joint venture of the Hannover Medical School and the
Helmholtz Centre for Infection Research, Hannover, Germany, [8]CiiM – Centre for Individualized Infection
Medicine, Hannover, Germany

Haemodialysis patients respond poorly to vaccination and continue to be at-risk
for severe COVID-19. Therefore, dialysis patients were among the first for which a
fourth COVID-19 vaccination was recommended. However, targeted information
on how to best maintain immune protection after SARS-CoV-2 vaccinations in at-
risk groups for severe COVID-19 remains limited. We provide, to the best of our
knowledge, for the first time longitudinal vaccination response data in dialysis
patients and controls after a triple BNT162b2 vaccination and in the latter after a
subsequent fourth full-dose of mRNA-1273. We analysed systemic and mucosal
humoral IgG responses against the receptor-binding domain (RBD) and ACE2-
binding inhibition towards variants of concern including Omicron and Delta with
multiplex-based immunoassays. In addition, we assessed Spike S1-specific T-cell
responses by interferon γ release assay. After triple BNT162b2 vaccination, anti-
RBD B.1 IgG and ACE2 binding inhibition reached peak levels in dialysis patients,
but remained inferior compared to controls. Whilst we detected B.1-specific ACE2
binding inhibition in 84% of dialysis patients after three BNT162b2 doses, binding
inhibition towards the Omicron variant was only detectable in 38% of samples and

281

declining to 16% before the fourth vaccination. By using mRNA-1273 as fourth dose, humoral immunity against all SARS-CoV-2 variants tested was strongly augmented with 80% of dialysis patients having Omicron-specific ACE2 binding inhibition. Modest declines in T-cell responses in dialysis patients and controls after the second vaccination were restored by the third BNT162b2 dose and significantly increased by the fourth vaccination. Our data support current advice for a four-dose COVID-19 immunisation scheme for at-risk individuals such as haemodialysis patients. We conclude that administration of a fourth full-dose of mRNA-1273 as part of a mixed mRNA vaccination scheme to boost immunity and to prevent severe COVID-19 could also be beneficial in other immune impaired individuals. Additionally, strategic application of such mixed vaccine regimens may be an immediate response against SARS-CoV-2 variants with increased immune evasion potential.

Introduction

To date, SARS-CoV-2 vaccinations reassuringly provide some degree of protection from severe COVID-19 independent of the currently circulating variants of concern (VoC) for the majority of healthy individuals (1). However, weaker immunogenicity and a faster decline in protection levels to standard two-dose or three-dose booster SARS-CoV-2 immunisation schemes have been widely demonstrated in immunocompromised individuals such as solid organ transplant recipients (2), dialysis patients (3) or patients suffering from other severe chronic conditions such as cancer (4). Starting in mid-2021 and more widely since the beginning of 2022, several countries recommended a fourth dose of SARS-CoV-2 mRNA vaccines for immunosuppressed populations at-risk for severe COVID-19 disease and older individuals to maintain levels of immune protection (5–8). This was driven by weaker peak vaccine responses and waning immunity in those individuals as well as continued evolution of SARS-CoV-2 variants with increasing levels of immune evasion potential as demonstrated for Omicron VoC subspecies BA.1, BA.4, BA.5, and BA.2.12.1 (9–12).

Recent studies reported improved SARS-CoV-2 humoral and cellular responses not only towards the original SARS-CoV-2 B.1 isolate but also Delta and Omicron VoC after a fourth vaccination in haemodialysis patients receiving either mRNA vaccines or vector-based formulations in combination with mRNA vaccines (13–15). However, targeted data on the most efficient dosing and

vaccination scheme or even predictors of vaccination success in haemodialysis patients at-risk of severe COVID-19 and its associated mortality is limited. We aimed to comprehensively examine the magnitude and kinetics of both cellular and humoral immunity towards the most recently dominating Delta and Omicron variant's in a well-controlled longitudinal cohort of haemodialysis patients. These patients received a triple dose of BNT162b2 followed by a full-dose of mRNA-1273. Healthcare workers vaccinated three times with BNT162b2 served as controls. Our data provide preliminary evidence that in addition to heterologous vector- and mRNA-based vaccination schemes also heterologous mRNA vaccine regimens may become strategically beneficial for achieving efficient immunity against SARS-CoV-2 in immunosuppressed patients.

Methods

Study design and sample collection

This is a follow-up study in haemodialysis patients and control individuals, for which the results for haemodialysis patients after a complete two-dose BNT162b2 vaccination (16) and subsequent decline (17) have been previously reported. Blood samples were taken before start of dialysis treatment (n=50) or from healthcare workers (n=33), who participated in the COVID-19 contact (CoCo) study served (18) as non-dialysed control population. To be included in the study, participants had to be over the age of 18 and able to give

282

written informed consent. For the current analysis, we only considered dialysis patients for which results from all time points after either three or four vaccine doses were available. All participants received the standard two-dose regimen of BNT162b2 three weeks apart, followed by a third BNT162b2 vaccination about six (dialysis) or 8.5 months (controls) after the second vaccination. Only dialysis patients were vaccinated a fourth time with 100 µg mRNA-1273 four months after the last BNT162b2 vaccination. The vaccination schedule and blood collection time points are depicted in Figure 1 and Figure S1. Participants with SARS-CoV-2 infection diagnosed by either PCR or anti-nucleocapsid IgG determined by MULTICOV-AB multiplex measurement (19) were excluded from the analysis. Demographic characteristics and medical information are listed in Tables 1, S1, S2. Plasma was obtained from lithium heparin blood (S-Monovette Plasma, Sarstedt, Germany). Whole blood samples were used immediately for interferon γ release assay (IGRA). For saliva collection, all individuals spat directly into a collection tube. To inactivate replication-competent SARS-CoV-2 virus particles potentially present in saliva samples, Tri(n-butyl) phosphate (TnBP) and Triton X-100 were added to final concentrations of 0.3% and 1%, respectively (20). Both plasma and saliva samples were frozen and stored at −80°C until further use.

MULTICOV-AB

IgG binding and levels were analysed using MULTICOV-AB, a multiplex coronavirus immunoassay which contains the trimeric Spike B.1, its subdomains (S1, S2, RBD), nucleocapsid B.1 and RBDs of Delta and Omicron BA.1 antigens as previously described (9, 19). Briefly, antigens were immobilised on spectrally distinct populations of MagPlex beads (Cat #MC10XXX-01, Luminex Corporation) either by EDC/s-NHS

coupling (21) or by Anteo coupling (Cat #A-LMPAKMM-10, Anteo Tech Reagents) following the manufacturer's instruction (19). The combined MagPlex beads were then incubated with samples at an effective dilution of 1:3200 for plasma and of 1:12 for saliva. After a wash step to remove unbound antibodies, IgG was detected with R-phycoerythrin labelled goat-anti-human IgG (Jackson ImmunoResearch Labs, Cat #109-116-098, Lot #148837, RRID: AB_2337678) as secondary antibody. After another wash step and bead resuspension, samples were measured once on a FLEXMAP 3D instrument (Luminex Corporation) using the following settings: Timeout 80 sec, Gate: 7500-15000, Reporter Gain: Standard PMT, 50 events. Raw median fluorescence intensity (MFI) values or normalised values (MFI/MFI of quality control (QC) samples (19, 22) are reported. Three QC samples were measured per individual plate to monitor MULTICOV-AB performance.

RBDCoV-ACE2

RBDCoV-ACE2, a multiplex competitive inhibition assay, was performed as previously described (23) as surrogate assay to determine immunoglobulin neutralisation capacity against SARS-CoV-2 B.1 isolate and variants of concern. For this, biotinylated ACE2 was combined with individual samples (and as a control, ACE2 alone) and incubated with the above mentioned MULTICOV-AB bead mix. Before and after ACE2 detection with Strep-PE (Cat #SAPE-001, Moss), washes were carried out. Samples were measured once on a FLEXMAP 3D instrument with the same settings as MULTICOV-AB and analysed by normalisation of MFI values against the control. 100% ACE2 binding inhibition indicates maximum binding inhibition. Responders for ACE2 binding inhibition are classified as above a 20% ACE2 binding threshold as described in Junker et al. (23).

FIGURE 1
Participant recruitment scheme for longitudinal vaccination response analysis in haemodialysis patients after triple BNT162b2 and fourth full-dose mRNA-1273. Patients on haemodialysis (n = 50) and healthcare workers as controls (n = 33) were triple-vaccinated with BNT162b2 (green syringe) followed by a 100 µg (full) dose of mRNA-1273 (blue syringe) for dialysed individuals only. Sampling and vaccination schedule is given in days and weeks as indicated.
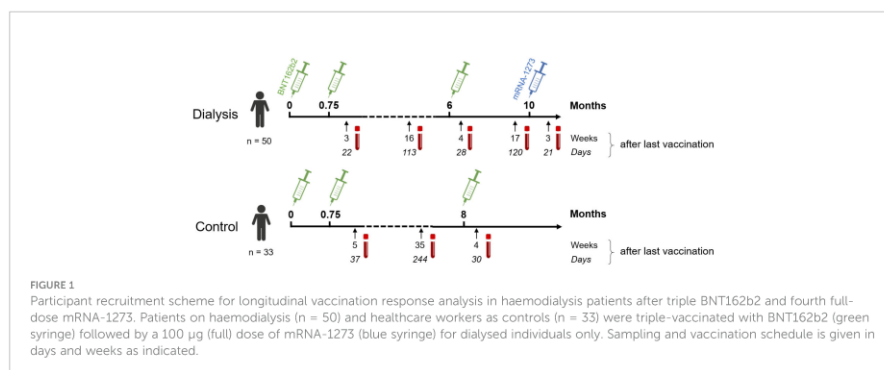
283

TABLE 1 Characteristics of study population.

Characteristics	Haemodialysis group (n = 50)	Non-dialysis control group (n =33)	p-value for difference between groups
Age (years), median (IQR)	69.5 (60–79)	42 (32–55)	$1.08*10^{-11}$
Sex (female: n, %)	19 (38.0)	23 (69.7)	$9.26*10^{-3}$
Days since start of haemodialysis (median, IQR)	1263 (753-2314)	n. a.	n. a.
Immunosuppressive medication (n, %)			
2021 (Vaccine dose 1-3)*	7 (14.0)	0 (0.0)	n. a.
2022 (Vaccine dose 4)*	6 (12.0)	n. a.	n. a.
Co-morbidities			
Obesity (BMI, >30)	12 (24.0)	NA	n. a.
Diabetes mellitus (n, %)	14 (28.0)	1 (3.0)	$9.27*10^{-3}$
Cardiovascular disease (n, %)	21 (42.0)	2 (6.1)	$8.69*10^{-4}$
Cancer (n, %)	1 (2.0)	0 (0.0)	n. a.
Chronic conditions (n, %)			
Ulcerative colitis (n, %)	0 (0.0)	1 (3.0)	n. a.
Goiter (n, %)	0 (0.0)	1 (3.0)	n. a.
Hashimoto's thyroiditis (n, %)	0 (0.0)	1 (3.0)	n. a.
Hypothyroidism (n, %)	0 (0.0)	1 (3.0)	n. a.
Other	0 (0.0)	1 (3.0)	n. a.

*Participants on medication when vaccinated and sampled.
IQR, Inter Quartile Range; BMI, Body Mass Index; n, absolute numbers per group; NA, Information not available; n. a., not applicable.

Anti-SARS-CoV-2 QuantiVac ELISA

Plasma samples were additionally analysed using the Anti-SARS-CoV-2-QuantiVac-ELISA IgG (Cat #EI 2606-9601-10G, Euroimmun) as previously described (16).

Interferon γ release assay

SARS-CoV-2-specific T-cell responses from whole blood were analysed by measuring IFNγ production after stimulation with a peptide pool from the SARS-CoV-2 Spike S1 with the SARS-CoV-2 Interferon Gamma Release Assay (Cat #ET-2606-3003, Euroimmun) and the IFNγ ELISA (Cat #EQ-6841-9601, Euroimmun) according to the manufacturer's description and as previously evaluated against alternative assays for antigen-specific T-cell reactivity using intracellular cytokine staining or enzyme linked immuno spot assay (24, 25). Background signals from negative controls were subtracted and final results calculated in mIU/mL using standard curves. IFNγ concentrations >200 mIU/mL were considered as reactive. We defined this arbitrary cut-off by using average background IFNγ activity without antigen-stimulation in all samples multiplied with 10 for the threshold for IGRA-positive. Using this cut-off, we found in all of the 15 controls taken from independent

individuals before the COVID-19 pandemic negative IGRA results (26). The upper limit of reactivity was 16,000 mIU/mL.

Data analysis and statistics

RStudio (Version 1.2.5001), with R (version 3.6.1) was used for data analysis and figure generation. Additionally, the R add-on package "beeswarm" was utilised to visualise data as stripcharts with overlaying boxplots and to create non-overlaying data points. A second R add-on package "gplots" was used to generate specific colours for plots. Figures were exported from RStudio and then edited using Inkscape (Inkscape 1.2). Spearman's rho coefficient was calculated to determine correlation between IGRA results and ACE2 binding inhibition using the "cor" function from R's "stats" library. Mann-Whitney-U test and Wilcoxon test were used to determine difference of signal distributions between dialysed and control groups for unpaired and paired samples, respectively using the "wilcox.test" function from R's "stats" library. To assess differences in the study population, Pearson's Chi-squared test with Yates' continuity correction was used for categorical characteristics using the "chisq.test" function from R's "stats" library and Mann-Whitney-U test as above was used for difference in age. The type of statistical analysis performed

284

(when appropriate) is listed in the figure legends. Pre-processing of data such as matching sample metadata and collecting results from multiple assay platforms was performed in Excel 2016.
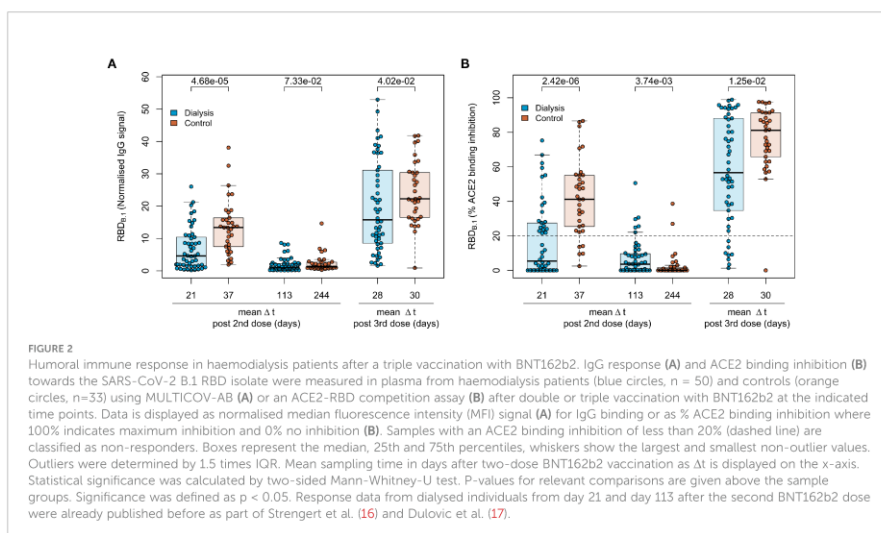
Results

Inferior humoral responses in haemodialysis patients after triple BNT162b2 vaccination

To characterise the vaccination response after the third BN162b2 vaccination in 50 patients on maintenance haemodialysis, we had followed immunoglobulin levels longitudinally after the second dose of BNT162b2 using MULTICOV-AB, a multiplex immunoassay containing antigens from the Spike protein of SARS-CoV-2 and selected variants of concern (9). As a novel control group, 33 samples from healthcare workers with triple BNT162b2 vaccination were used for comparison. Detailed information on the study populations can be found in Tables 1, S1, S2. Consistent with our previous reports (16, 17), IgG responses towards the original B.1 isolate in vaccinated dialysis patients were significantly reduced ($p=4.68*10^{-5}$, Mann-Whitney-U test) when compared to the control group and declined after the second vaccination to comparable levels in both groups ($p=7.33*10^{-2}$, Mann-Whitney-U test, Figure 2A). A third BNT162b2 vaccination about six to eight months after the second increased the peak IgG RBD B.1 response in both groups but with

higher variability in dialysis patients ($p=4.02*10^{-2}$, Mann-Whitney-U test, Figure 2A). As an additional control, quantitative S1 IgG titres were measured using a commercial assay (Figure S2), which led to a very similar pattern of significantly diminished antibody responses in dialysis patients compared to non-dialysed individuals after the second BNT162b2 dose, declining titres and a robust peak response increase after the third vaccination. There was no significant difference in male or female individuals and we did not find any association to age. Regarding the decline in anti-S IgG after the third dose, we were able to measure this in only n=10 of the control group at a comparable time point after vaccination to the haemodialysis group (Figure S3). Dialysis patients showed a mean 3-fold reduction in anti-S IgG levels 121 days (range 119-129 days) after the third vaccination (from mean 2,314 BAU/mL to mean 771 BAU/mL). This was almost identical to the 3.2-fold decline in healthy controls (from mean 5,430 BAU/mL to mean 1, 662 BAU/mL), although the time point for the follow up was somewhat later.

For a functional characterisation of vaccine-induced antibodies towards the original B.1 RBD isolate, we used RBDCoV ACE2 - a multiplex competitive inhibition assay (23). ACE2 binding inhibition was significantly reduced in dialysed compared to non-dialysed individuals ($p=2.42*10^{-6}$, Mann-Whitney-U test) after the second vaccination (Figure 2B). Responses were comparably diminished in both groups four to eight months after the second vaccination, with only 12% and 6% of samples being above the 20% responder threshold in patients on haemodialysis and controls, respectively. However, comparable to IgG binding levels, the

FIGURE 2

Humoral immune response in haemodialysis patients after a triple vaccination with BNT162b2. IgG response **(A)** and ACE2 binding inhibition **(B)** towards the SARS-CoV-2 B.1 RBD isolate were measured in plasma from haemodialysis patients (blue circles, n = 50) and controls (orange circles, n=33) using MULTICOV-AB **(A)** or an ACE2-RBD competition assay **(B)** after double or triple vaccination with BNT162b2 at the indicated time points. Data is displayed as normalised median fluorescence intensity (MFI) signal **(A)** for IgG binding or as % ACE2 binding inhibition where 100% indicates maximum inhibition and 0% no inhibition **(B)**. Samples with an ACE2 binding inhibition of less than 20% (dashed line) are classified as non-responders. Boxes represent the median, 25th and 75th percentiles, whiskers show the largest and smallest non-outlier values. Outliers were determined by 1.5 times IQR. Mean sampling time in days after two-dose BNT162b2 vaccination as Δt is displayed on the x-axis. Statistical significance was calculated by two-sided Mann-Whitney-U test. P-values for relevant comparisons are given above the sample groups. Significance was defined as p < 0.05. Response data from dialysed individuals from day 21 and day 113 after the second BNT162b2 dose were already published before as part of Strengert et al. (16) and Dulovic et al. (17).
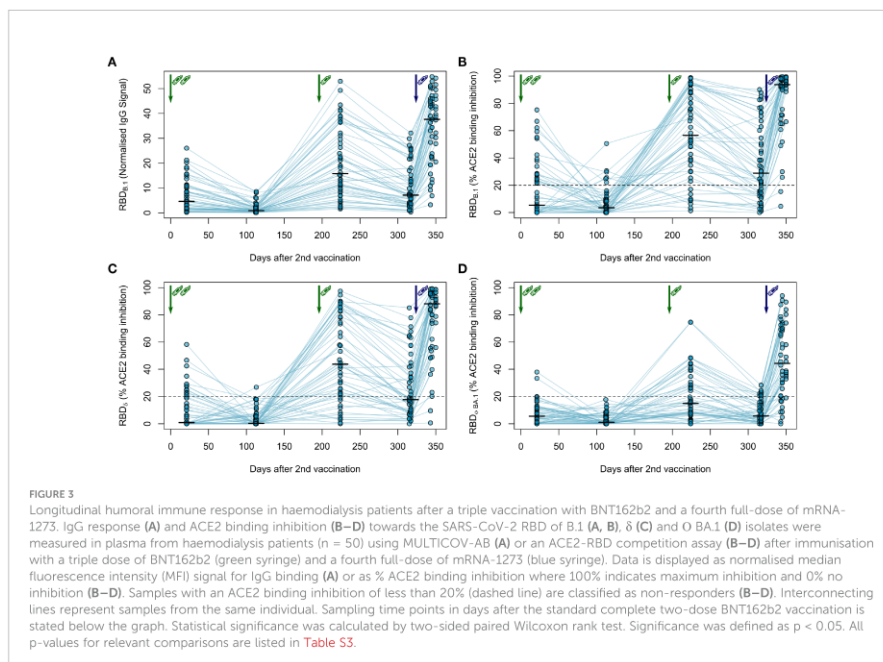
285

third BNT162b2 vaccination restored and even augmented ACE2 binding inhibition against the B.1 variant in both populations.

Strong immune responses after a fourth mRNA-1273 vaccination in haemodialysis patients

Next, we followed the anti-Spike RBD IgG levels in haemodialysis patients after the third vaccination over time and after a fourth vaccination with a full 100 µg dose of mRNA-1273, which was considered by German guidelines for immunocompromised individuals. As expected, IgG responses against the original B.1 isolate had again declined within approximately 4 months after the third vaccination (Figure 3A; Figure S2) as did the ACE2 binding inhibition activity as a surrogate for virus neutralisation (Figure 3B). Whilst the decline was not as severe as after the second BNT162b2 dose with now 64% of samples remaining above the 20% ACE2 binding inhibition threshold, only the fourth vaccination with mRNA-1273 markedly raised both anti-Spike RBD IgG levels (Figures 3A, S2; Table S3 for a complete

statistical evaluation) and ACE2 binding inhibition (Figure 3B) towards the B.1 isolate above levels seen at peak response after the second and third dose of BNT162b2. 96% of samples from individuals on haemodialysis were now classified as above the 20% ACE2 responder threshold. Further, we also analysed the longitudinal development of ACE2 binding inhibition towards the dominantly circulating SARS-CoV-2 of 2021 (Delta) and 2022 (Omicron) (Figures 3C, D). ACE2 binding inhibition towards the Delta variant was slightly reduced over time compared to levels observed with the B.1 isolate. Overall, the third dose resulted in a clear increase in Delta ACE2 responder rates from 24% after two-dose BNT162b2 scheme to 64%, which was further increased to 94% after the subsequent dose of mRNA-1273 (Figure 3C). Importantly, neutralisation against the Omicron BA.1 variant, which was largely absent after the second vaccination and only transiently above threshold in 38% of dialysis patients after the third vaccination, reached high levels of ACE2 binding inhibition with an 80% responder rate at peak response after the fourth vaccination with mRNA-1273. This coincided with Omicron being the dominant SARS-CoV-2 variant circulating in Germany (Figure 3D).

We also analysed IgG binding longitudinally after a triple dose of BNT162b2 towards the RBD of B.1, Delta and Omicron

FIGURE 3
Longitudinal humoral immune response in haemodialysis patients after a triple vaccination with BNT162b2 and a fourth full-dose of mRNA-1273. IgG response (A) and ACE2 binding inhibition (B–D) towards the SARS-CoV-2 RBD of B.1 (A, B), δ (C) and O BA.1 (D) isolates were measured in plasma from haemodialysis patients (n = 50) using MULTICOV-AB (A) or an ACE2-RBD competition assay (B–D) after immunisation with a triple dose of BNT162b2 (green syringe) and a fourth full-dose of mRNA-1273 (blue syringe). Data is displayed as normalised median fluorescence intensity (MFI) signal for IgG binding (A) or as % ACE2 binding inhibition where 100% indicates maximum inhibition and 0% no inhibition (B–D). Samples with an ACE2 binding inhibition of less than 20% (dashed line) are classified as non-responders (B–D). Interconnecting lines represent samples from the same individual. Sampling time points in days after the standard complete two-dose BNT162b2 vaccination is stated below the graph. Statistical significance was calculated by two-sided paired Wilcoxon rank test. Significance was defined as p < 0.05. All p-values for relevant comparisons are listed in Table S3.

286

BA.1 VoC in saliva of haemodialysis patients to determine protection levels at the primary side of SARS-CoV-2 replication. Although anti-RBD specific IgG was readily detectable both in the peak and plateau response phase following the complete two-dose and the third booster dose of BNT162b2, IgG binding towards the Delta and Omicron BA.1 RBD was significantly reduced compared to the B.1 RBD across all time points (Figure S4). Interestingly, saliva responses across vaccinated individuals were much more widespread in saliva than in plasma.

As clinical studies suggested that both cellular and humoral response can confer protection from COVID-19 (27), we also assessed vaccination-induced T-cell responses by IFNγ release assay longitudinally. Overall, these responses were more stable over time (Figure 4A). After two BNT162b2 vaccinations, IFNγ release after in vitro re-stimulation was readily detectable in haemodialysis patients, but declined slightly thereafter. The third BNT162b2 vaccination increased cellular responses to levels comparable to after the second vaccination. Similar to the humoral responses, the fourth vaccination with mRNA-1273 further increased IFNγ release after Spike S1 peptide restimulation of T-cells (Figure 4A; Table S3 for a complete statistical evaluation).

Finally, we correlated B- and T-cell responses after each vaccination within our longitudinal cohort of haemodialysis patients. We overall observed moderate correlation between peak T-cell responses (measured by IGRA) and B-cell responses [determined by % ACE2 binding inhibition of the B.1 variant (Spearman's rho=0.561, Figure 4B, upper panel)], which did not increase after the third (Spearman's rho=0.405) and fourth (Spearman's rho=0.371) vaccination. We further described responder rates for T- and B-cell response by a combined cut-off as displayed in Figure 4B. Notably, responder rates among haemodialysis patients strongly increased to 72% after the triple BNT162b2 dose and further to 86% after the fourth full-dose mRNA-1273. Importantly, whilst we observed a similar trend for the correlation coefficient between Delta and Omicron BA.1 % ACE2 binding inhibition and T-cell responses (Figure 4B; middle and lower panel, Table S3 for a complete statistical evaluation), dual cellular (>200mIU/mL) and humoral (>20% ACE inhibition) responders levels equally strongly increased for both VoC after the third and fourth vaccination to a final 84% and 74%, respectively.
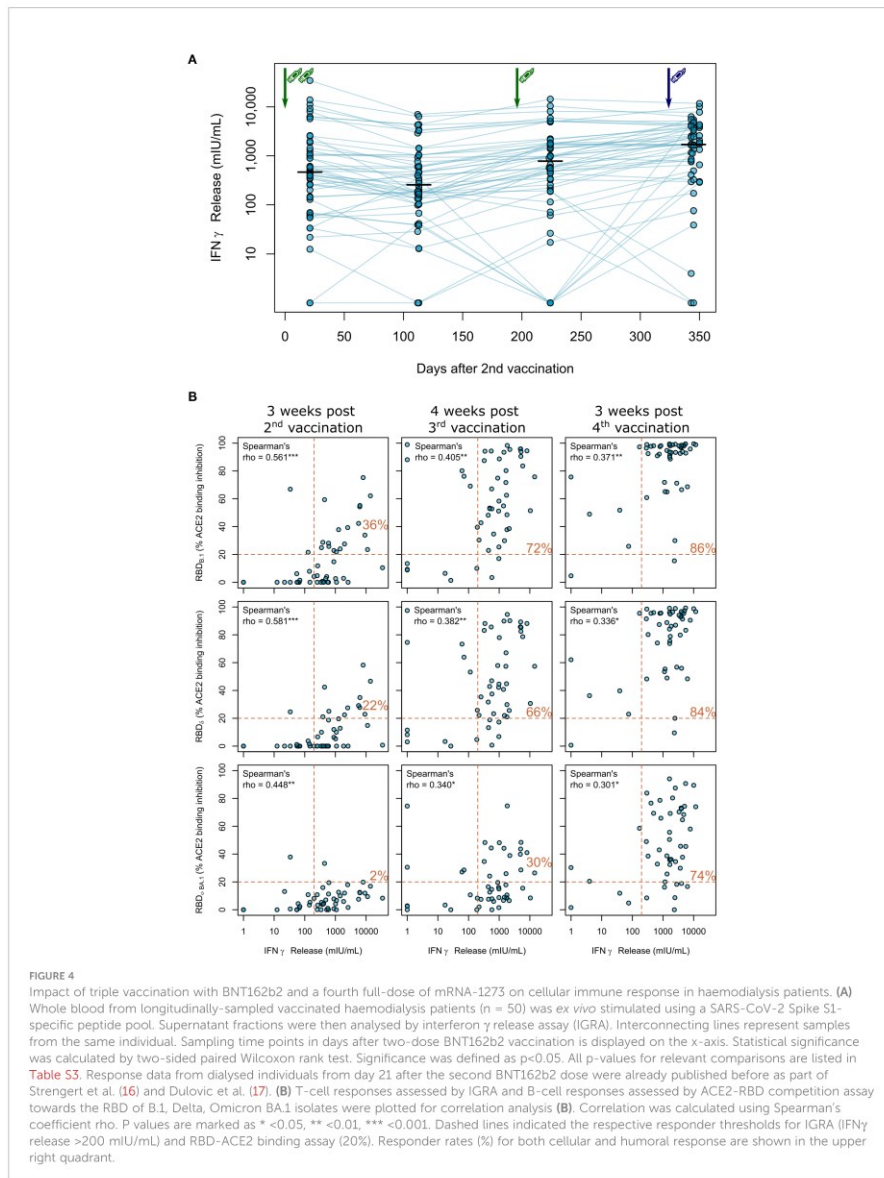
Discussion

Although overall case mortality rates for SARS-CoV-2 have significantly decreased since the initial wave of the pandemic, maintaining high levels of vaccine-induced protection is of paramount importance for at-risk individuals for severe COVID-19 such as haemodialysis patients. Ensuring that these

and other similarly vulnerable individuals are sufficiently protected remains challenging, with high case numbers throughout 2022 as a result of successive occurrence of Omicron subvariants. Despite clear recommendations on the need for a fourth dose, worryingly this fourth dose uptake among haemodialysis patients has decreased compared to the first three doses, with disparities among demographic groups remaining in place (28). At present, recommendations by the German Standing Committee on Vaccination (STIKO) clearly endorse a fourth SARS-CoV-2 vaccine dose including a full dose of mRNA-1273 for immunocompromised individuals (5), which contrasts WHO guidelines recommending 50 µg mRNA-1273 for fourth vaccinations (29).

Several studies report of superior immunity after initial mRNA-1273 prime/boost vaccination when compared to BNT162b2 in haemodialysis patients (30, 31) or in the general population (32–34) and further improved humoral responses after triple vaccination in dialysis patients (35–39). Third dose vaccination with mRNA-1273 or BNT162b2 provided comparable protection against symptomatic SARS-CoV-2 infection in the general population, although differences between both vaccines were observed after the second dose (40). Finally, Caillard et al. found that a four-dose mRNA-1273 compared to a four-dose BNT162b2 results in increased levels of binding antibodies in kidney transplant recipients (41). In general, COVID-19 vaccine-induced humoral immune responses tend to be higher in females and lower in elderly people. Differences in anti-S IgG were prominent after the second but not after the third vaccination, whilst males remained to have inferior neutralisation activity even after the third vaccination (42). We did not find such association most likely due to the smaller samples size of our cohort.

Two studies found more durable neutralising antibody titers four or six months after a third dose of mRNA vaccine compared to two doses (43, 44). For the BNT162b2 vaccine the decline was 1.6-fold at four months. These findings indicate robust long-lived antibody production after three doses, but the durability of neutralising activity against different SARS-CoV-2 variants could be variable (43). In a third study in an Israeli population receiving the BNT162b2 vaccine, the decline over approximately four months after the third dose was much higher (5.5-fold). We observed an about 3-fold decline in both groups, which is in line with the current literature and indicates that the peak anti-S IgG responses are the main drivers for the differences between groups over time and that the anti-S IgG kinetics are likely similar in dialysis patients and controls. However, conclusions about durability of antibody responses after 3-doses mRNA vaccination remain uncertain, particularly after combination of different vaccines (45). With regard to the T-cell responses, we (24, 25, 46, 47) and others (48, 49) have described that Spike-specific T-cell responses (CD4+ or CD8+ T-lymphocytes) after infection or prime/boost vaccination are more stable as compared to the respective humoral responses in healthy

287

FIGURE 4

Impact of triple vaccination with BNT162b2 and a fourth full-dose of mRNA-1273 on cellular immune response in haemodialysis patients. **(A)** Whole blood from longitudinally-sampled vaccinated haemodialysis patients (n = 50) was *ex vivo* stimulated using a SARS-CoV-2 Spike S1-specific peptide pool. Supernatant fractions were then analysed by interferon γ release assay (IGRA). Interconnecting lines represent samples from the same individual. Sampling time points in days after two-dose BNT162b2 vaccination is displayed on the x-axis. Statistical significance was calculated by two-sided paired Wilcoxon rank test. Significance was defined as p<0.05. All p-values for relevant comparisons are listed in Table S3. Response data from dialysed individuals from day 21 after the second BNT162b2 dose were already published before as part of Strengert et al. (16) and Dulovic et al. (17). **(B)** T-cell responses assessed by IGRA and B-cell responses assessed by ACE2-RBD competition assay towards the RBD of B.1, Delta, Omicron BA.1 isolates were plotted for correlation analysis **(B)**. Correlation was calculated using Spearman's coefficient rho. P values are marked as * <0.05, ** <0.01, *** <0.001. Dashed lines indicated the respective responder thresholds for IGRA (IFNγ release >200 mIU/mL) and RBD-ACE2 binding assay (20%). Responder rates (%) for both cellular and humoral response are shown in the upper right quadrant.

individuals. Thus, vaccine-induced long-lasting T-cell memory after two or three COVID-19 vaccination are most likely not a specific response in dialysis patients COVID-19 (45). The IGRA employed in this study reliably detects vaccine-induced Spike-specific T-cell responses and showed good correlation to other techniques for studying post-vaccination T-cell immunity including ELISpot and intracellular cytokine staining (24, 26).

Potential causes for our observations may include the higher dose of mRNA-1273. Similar doses of mRNA-1273 (25 µg) to the BNT162b2 dose (30 µg) generated comparable Spike-specific memory CD4 T-cell frequencies to natural infection and about half as strong as those seen with high-dose vaccination (100 µg) indicating that differences between cellular and humoral immunity after two mRNA vaccines most likely result from the different doses of the vaccine (48). In addition, Spike and RBD IgG+ memory B-cell frequencies increase between 3 and 6 months after immunisation with mRNA vaccine (50) and germinal centers appear to be central to the immune responses to COVID-19 vaccines (45). Kidney transplant recipients, unlike healthy subjects, presented deeply blunted SARS-CoV-2-specific germinal center B-cell responses coupled with severely hindered neutralising antibody responses. These data indicate impaired germinal center-derived immunity in immunocompromised individuals (51). Germinal centers can persist and be productive for more than six months after two doses of COVID-19 mRNA vaccines and that the quality of neutralising antibodies can improve over three to six months (52). We speculate that diminished B-cell memory generation and germinal center formation is one feature of the immune dysfunction in dialysis patients and that repetitive vaccination, mix of mRNA vaccines or increase in vaccine dose may help to overcome these limitations. Finally, we specifically looked at dialysis patients with IGRA results below threshold after the third vaccination (n=12), of which almost all were among individuals with lowest IGRA results also after the second and fourth vaccination. We classified these as "low responders", since also their anti-S IgG responses were persistently very low. These low responders comprised all patients with organ-transplantation (n=4) and 7 out of 8 individuals with immunosuppressive therapy at the time of the third vaccination. We found no other association to co-morbidities or clinical conditions in the low responder subgroup. Thus, immunosuppression as listed in Table S2 is a further explanation for the inferior humoral and cellular vaccine response in many of the low responders.

We can only speculate about the effects of mixing mRNA-based vaccines. Janssen et al. compared heterologous and homologous mRNA-1273 and BNT162b2 vaccination after the respective first vaccination in a randomised trial (53). They found the geometric mean titers of anti-Spike IgG antibodies for each heterologous regimen to be higher relative to the corresponding homologous regimen. This is consistent with data from Israel (54) and the COV-BOOST study (55), in which even half-dose mRNA-1273 as fourth dose after triple BNT162b2 vaccination

appeared to have higher immunogenicity than full-dose BNT162b2. The authors suggested that this result might be due to a heterologous schedule effect or the vaccine dose. Interestingly, differences between both mRNA vaccines could be more complex, since mRNA-1273 is reported to induce higher concentrations of RBD- and N-terminal domain-specific IgA and more antibodies eliciting neutrophil phagocytosis and natural killer cell activation as compared to BNT162b2 (56).

Our study is, to our knowledge, the only study examining the longitudinal humoral and cellular immune response towards the most recent SARS-CoV-2 isolates in haemodialysis patients after administration of consistent vaccination regimens starting with a triple dose of BNT162b2 followed by a fourth full-dose of mRNA-1273. Whilst other studies principally support the beneficial impact of a fourth vaccination dose on both antibody titers and neutralising potency towards SARS-CoV-2 B.1 and VoC isolates, often various vaccination regimens including heterologous vector-based/mRNA regimens were pooled in cohorts (14) or vaccine dosages not provided (13).

Our data provide solid evidence that the triple vaccination resulted in mean antibody concentration and neutralising activity above levels to after the second vaccination. Interestingly, we identified significant further increases in both humoral and cellular response rates following the fourth dose, compared to the second and third. The increase in response rate from 30% to 74% from third to fourth dose for Omicron is particularly important considering it comprises almost all currently circulating variants of SARS-CoV-2. We consider this as a valid argument for a fourth vaccination in at-risk patients, especially, since T-cell immunity elicited by current vaccines is also effective against VoC including Omicron (57–59). The large range in both humoral and cellular responses illustrates however the variable nature of SARS-CoV-2 vaccination responses in dialysis patients and may be of relevance for identifying individuals with inferior responses in need for further doses.

Our study has several limitations. The number of participants within our cohort was limited, with only 50 patients on haemodialysis and a further 33 control participants, although our sample size is larger than similar studies examining the effect of the fourth dose within haemodialysis patients (15). The use of longitudinal cohort also allows us to directly identify the responses and their decline following each individual dose. Unfortunately, we were unable to obtain samples post-fourth dose for our control population, since many individuals were meanwhile infected with Omicron, additional booster vaccinations are not generally recommended and a full dose mRNA-1273 vaccination would be the unlikely regimen for the healthy controls. Although our control group was well-matched for sample collection at peak antibody levels after the second and third vaccination, they were not optimally matched for age and gender. A potential limitation of our study is that we used only peptides from a single SARS-

CoV-2 S1 protein for T-cell analysis, not taking into account reactivity against other variants including Omicron. To investigate the extent to which substitutions in spike and non-spike proteins affect T-cell recognition, several studies examined T-cells in vaccinated and convalescent individuals (49, 60–62). Overall, these studies show a high degree of preservation of T-cell epitopes between the ancestral strain, Omicron and other variants of concern. However, the degree of cross-reactivity varied among individuals, possibly as a consequence of genetic aspects of antigen presentation. Finally, it would have been interesting to directly compare homologous fourth BNT162b2 dose to mRNA-1273 in haemodialysis patients and to assess the reactogenicity, but this would have required a prospective study design for an interventional study.

Overall, a fourth full-dose of the mRNA-1273 vaccine elicits improved cellular and humoral responses compared to the triple BNT162b2 vaccination and appears to be an advisable strategy for immunocompromised patients, such as haemodialysis patients. Nevertheless, the decline after fourth vaccination and the effectivity against emerging SARS-CoV-2 variants will have to be monitored to assess the immune response duration and requirement for further booster vaccinations.

Data availability statement

The raw data supporting the conclusions of this article will be made available by the authors, without undue reservation.

Ethics statement

The studies involving human participants were reviewed and approved by the Internal Review Board of Hannover Medical School (MHH, approval number 8973_BO-K_2020, amendment Dec. 2020). The patients/participants provided their written informed consent to participate in this study.

Author contributions

GMNB, NS-M, AD, and MS conceived the study. MB, AD, MS, AD-J, GMNB, AC, NS-M, DJ, and MVS designed the experiments. NS-M, MS, GMNB, AD-J, and GK procured funding. GR, JG, JJ, DJ, and MVS performed experiments. KL, AB, EW, GL, AC, and GMNB collected samples or organised their collection. PK, BT, and UR produced and designed recombinant assay proteins. MB, KL, AD, MS, GR, MVS, and AC performed data collection and analysis. MB generated the figures. MB, MS, AD, and GMNB verified the underlying data. GMNB and MS wrote the first draft of the manuscript with input from MB, AC, KL, and AD. All authors critically reviewed and approved the final manuscript.

Conflict of interest

NS-M was a speaker at Luminex user meetings in the past. The Natural and Medical Sciences Institute at the University of Tübingen is involved in applied research projects as a fee for services with the Luminex Corporation. GMNB was a speaker on a symposium sponsored by Moderna.

The remaining authors declare that the research was conducted in the absence of any commercial or financial relationships that could be construed as a potential conflict of interest.

Publisher's note

All claims expressed in this article are solely those of the authors and do not necessarily represent those of their affiliated organizations, or those of the publisher, the editors and the reviewers. Any product that may be evaluated in this article, or claim that may be made by its manufacturer, is not guaranteed or endorsed by the publisher.

Supplementary material

The Supplementary Material for this article can be found online at: https://www.frontiersin.org/articles/10.3389/fimmu.2022.1004045/full#supplementary-material

290

References

1. Zeng B, Gao L, Zhou Q, Yu K, Sun F. Effectiveness of COVID-19 vaccines against SARS-CoV-2 variants of concern: A systematic review and meta-analysis. *BMC Med* (2022) 20(1):200. doi: 10.1186/s12916-022-02397-y

2. Manothummetha K, Chuleerarux N, Sanguankeo A, Kates OS, Hirankarn N, Thongkam A, et al. Immunogenicity and risk factors associated with poor humoral immune response of SARS-CoV-2 vaccines in recipients of solid organ transplant: A systematic review and meta-analysis. *JAMA Netw Open* (2022) 5(4):e226822. doi: 10.1001/jamanetworkopen.2022.6822

3. Galmiche S, Luong Nguyen LB, Tartour E, de Lamballerie X, Wittkop L, Loubet P, et al. Immunological and clinical efficacy of COVID-19 vaccines in immunocompromised populations: A systematic review. *Clin Microbiol Infect* (2022) 28(2):163–77. doi: 10.1016/j.cmi.2021.09.036

4. Kuderer NM, Lyman GH. COVID-19 vaccine effectiveness in patients with cancer: remaining vulnerabilities and uncertainties. *Lancet Oncol* (2022) 23(6):693–5. doi: 10.1016/S1470-2045(22)00252-2

5. Epidemiologisches Bulletin.Ständige Impfkommission: Beschluss der STIKO zur 20. Aktualisierung der COVID-19-Impfempfehlung. *Epid Bull* (2022) 21:3–19. doi: 10.25646/10076.2

6. *Update: FDA authorizes additional vaccine dose for certain immunocompromised individuals* (2021). Available at: https://www.fda.gov/news-events/press-announcements/coronavirus-covid-19-update-fda-authorizes-additional-vaccine-dose-certain-immunocompromised.

7. *Direction générale de la santé DGS precisions sur la vaccination IMD*. Available at: https://solidarites-sante.gouv.fr/IMG/pdf/dgs_urgent_52_precisions_sur_la_vaccination_imd.pdf.

8. Burki TK. Fourth dose of COVID-19 vaccines in Israel. *Lancet Respir Med* (2022) 10(2):e19. doi: 10.1016/S2213-2600(22)00010-8

9. Junker D, Becker M, Wagner TR, Kaiser PD, Maier S, Grimm TM, et al. Antibody binding and ACE2 binding inhibition is significantly reduced for both the BA1 and BA2 omicron variants. *Clin Infect Dis* (2022), ciac498. doi: 10.1093/cid/ciac498

10. van Gils MJ, Lavell A, van der Straten K, Appelman B, Bontjer I, Poniman M, et al. Antibody responses against SARS-CoV-2 variants induced by four different SARS-CoV-2 vaccines in health care workers in the Netherlands: A prospective cohort study. *PloS Med* (2022) 19(5):e1003991. doi: 10.1371/journal.pmed.1003991

11. Gruell H, Vanshylla K, Korenkov M, Tober-Lau P, Zehner M, Münn F, et al. SARS-CoV-2 Omicron sublineages exhibit distinct antibody escape patterns. *Cell Host Microbe* (2022) 30(9):1231–1241.e6. doi: 10.1101/2022.04.06.487257

12. van der Straten K, Guerra D, van Gils MJ, Bontjer I, Caniels TG, van Willigen HDG, et al. Antigenic cartography using sera from sequence-confirmed SARS-CoV-2 variants of concern infections reveals antigenic divergence of Omicron. *Immunity.* (2022) 55(9):1725–1731.e4. doi: 10.1016/j.immuni.2022.07.018

13. Anft M, Blazquez-Navarro A, Frahnert M, Fricke L, Meister TL, Roch T, et al. Inferior cellular and humoral immunity against omicron and delta variants of concern compared with SARS-CoV-2 wild type in hemodialysis patients immunized with 4 SARS-CoV-2 vaccine doses. *Kidney Int* (2022) 102(1):207–8. doi: 10.1016/j.kint.2022.05.004

14. Cheng CC, Platen L, Christa C, Tellenbach M, Kappler V, Bester R, et al. Improved SARS-CoV-2 neutralization of Delta and Omicron BA.1 variants of concern after fourth vaccination in hemodialysis patients. *Vaccines (Basel)* (2022) 10(8):1328. doi: 10.3390/vaccines10081328

15. Housset P, Kubab S, Hanafi L, Pardon A, Vittoz N, Bozman D-F, et al. Humoral response after a fourth "booster" dose of a coronavirus disease 2019 vaccine following a 3-dose regimen of mRNA-based vaccination in dialysis patients. *Kidney Int* (2022) 101(6):1289–90. doi: 10.1016/j.kint.2022.04.006

16. Strengert M, Becker M, Ramos GM, Dulovic A, Gruber J, Juengling J, et al. Cellular and humoral immunogenicity of a SARS-CoV-2 mRNA vaccine in patients on haemodialysis. *EBioMedicine*. (2021) 70:103524. doi: 10.1016/j.ebiom.2021.103524

17. Dulovic A, Strengert M, Ramos GM, Becker M, Griesbaum J, Junker D, et al. Diminishing immune responses against variants of concern in dialysis patients 4 months after SARS-CoV-2 mRNA vaccination. *Emerg Infect Dis* (2022) 28(4):743–50. doi: 10.3201/eid2804.211907

18. Behrens GMN, Cossmann A, Stankov MV, Schulte B, Streeck H, Förster R, et al. Strategic anti-SARS-CoV-2 serology testing in a low prevalence setting: The COVID-19 contact (CoCo) study in healthcare professionals. *Infect Dis Ther* (2020) 9(4):837–49. doi: 10.1007/s40121-020-00334-1

19. Becker M, Dulovic A, Junker D, Ruetalo N, Kaiser PD, Pinilla YT, et al. Immune response to SARS-CoV-2 variants of concern in vaccinated individuals. *Nat Commun* (2021) 12(1):3109. doi: 10.1038/s41467-021-23473-6

20. Rabenau HF, Biesert L, Schmidt T, Bauer G, Cinatl J, Doerr HW. SARS-coronavirus (SARS-CoV) and the safety of a solvent/detergent (S/D) treated immunoglobulin preparation. *Biologicals*. (2005) 33(2):95–9. doi: 10.1016/j.biologicals.2005.01.003

21. Becker M, Strengert M, Junker D, Kaiser PD, Kerrinnes T, Traenkle B, et al. Exploring beyond clinical routine SARS-CoV-2 serology using MultiCoV-ab to evaluate endemic coronavirus cross-reactivity. *Nat Commun* (2021) 12(1):1152. doi: 10.1038/s41467-021-20973-3

22. Planatscher H, Rimmele S, Michel G, Potz O, Joos T, Schneiderhan-Marra N. Systematic reference sample generation for multiplexed serological assays. *Sci Rep* (2013) 3:3259–64. doi: 10.1038/srep03259

23. Junker D, Dulovic A, Becker M, Wagner TR, Kaiser PD, Traenkle B, et al. COVID-19 patient serum less potently inhibits ACE2-RBD binding for various SARS-CoV-2 RBD mutants. *Sci Rep* (2022) 12(1):7168. doi: 10.1038/s41598-022-10987-2

24. Barros-Martins J, Hammerschmidt SI, Cossmann A, Odak I, Stankov MV, Morillas Ramos G, et al. Immune responses against SARS-CoV-2 variants after heterologous and homologous ChAdOx1 nCoV-19/BNT162b2 vaccination. *Nat Med* (2021) 27(9):1525–9. doi: 10.1038/s41591-021-01449-9

25. Behrens GMN, Barros-Martins J, Cossmann A, Ramos GM, Stankov MV, Odak I, et al. BNT162b2-boosted immune responses six months after heterologous or homologous ChAdOx1nCoV-19/BNT162b2 vaccination against COVID-19. *Nat Commun* (2022) 13(1):4872. doi: 10.1038/s41467-022-32527-2

26. Stankov MV, Cossmann A, Bonifacius A, Dopfer-Jablonka A, Ramos GM, Godecke N, et al. Humoral and cellular immune responses against severe acute respiratory syndrome coronavirus 2 variants and human coronaviruses after single BNT162b2 vaccination. *Clin Infect Dis* (2021) 73(11):2000–8. doi: 10.1093/cid/ciab555

27. Forni G, Mantovani A, Forni G, Mantovani A, Moretta L, Rappuoli R, et al. COVID-19 vaccines: where we stand and challenges ahead. *Cell Death Differentiation.* (2021) 28(2):626–39. doi: 10.1038/s41418-020-00720-9

28. Parker EPK, Tazare J, Hulme WJ, Bates C, Beale R, Carr EJ, et al. Factors associated with COVID-19 vaccine uptake in people with kidney disease: An OpenSAFELY cohort study. *medRxiv.* (2022), 2022.06.14.22276391. doi: 10.1101/2022.06.14.22276391

29. WHO. *The moderna COVID-19 (mRNA-1273) vaccine: what you need to know* (2022). Available at: https://www.who.int/news-room/feature-stories/detail/the-moderna-covid-19-mrna-1273-vaccine-what-you-need-to-know.

30. Van Praet J, Reynders M, De Bacquer D, Viaene L, Schoutteten MK, Caluwé R, et al. Predictors and dynamics of the humoral and cellular immune response to SARS-CoV-2 mRNA vaccines in hemodialysis patients: A multicenter observational study. *J Am Soc Nephrol* (2021) 32(12):3208. doi: 10.1681/ASN.2021070908

31. Yau K, Chan CT, Abe KT, Jiang Y, Atiquzzaman M, Mullin SI, et al. Differences in mRNA-1273 (Moderna) and BNT162b2 (Pfizer-BioNTech) SARS-CoV-2 vaccine immunogenicity among patients undergoing dialysis. *Can Med Assoc J* (2022) 194(8):E297. doi: 10.1503/cmaj.211881

32. Dulovic A, Kessel B, Harries M, Becker M, Ortmann J, Griesbaum J, et al. Comparative magnitude and persistence of humoral SARS-CoV-2 vaccination responses in the adult population in Germany. *Front Immunol* (2022) 13. doi: 10.3389/fimmu.2022.828053

33. Montoya JG, Adams AE, Bonetti V, Deng S, Link NA, Pertsch S, et al. Differences in IgG antibody responses following BNT162b2 and mRNA-1273 SARS-CoV-2 vaccines. *Microbiol spectrum.* (2021) 9(3):e0116221. doi: 10.1128/Spectrum.01162-21

34. Steensels D, Pierlet N, Penders J, Mesotten D, Heylen L. Comparison of SARS-CoV-2 antibody response following vaccination with BNT162b2 and mRNA-1273. *Jama.* (2021) 326(15):1533–5. doi: 10.1001/jama.2021.15125

35. Benning L, Klein K, Morath C, Bartenschlager M, Kim H, Buylaert M, et al. Neutralizing antibody activity against the B.1.617.2 (delta) variant before and after a third BNT162b2 vaccine dose in hemodialysis patients. *Front Immunol* (2022) 13. doi: 10.3389/fimmu.2022.840136

36. Espi M, Charmetant X, Barba T, Mathieu C, Pelletier C, Koppe L, et al. A prospective observational study for justification, safety, and efficacy of a third dose of mRNA vaccine in patients receiving maintenance hemodialysis. *Kidney Int* (2022) 101(2):390–402. doi: 10.1016/j.kint.2021.10.040

37. Tillmann F-P, Figiel L, Ricken J, Still H, Korte C, Plaßmann G, et al. Effect of third and fourth mRNA-based booster vaccinations on SARS-CoV-2 neutralizing antibody titer formation, risk factors for non-response, and outcome after SARS-CoV-2 omicron breakthrough infections in patients on chronic hemodialysis: A

291

prospective multicenter cohort study. *J Clin Med* (2022) 11(11):3187–201. doi: 10.3390/jcm11113187

38. Patyna S, Eckes T, Koch BF, Sudowe S, Oftring A, Kohmer N, et al. Impact of moderna mRNA-1273 booster vaccine on fully vaccinated high-risk chronic dialysis patients after loss of humoral response. *Vaccines* (2022) 10(4):585–94. doi: 10.3390/vaccines10040585

39. Bensouna I, Caudwell V, Kubab S, Acquaviva S, Pardon A, Vittoz N, et al. SARS-CoV-2 antibody response after a third dose of the BNT162b2 vaccine in patients receiving maintenance hemodialysis or peritoneal dialysis. *Am J Kidney Diseases.* (2022) 79(2):185–92.e1. doi: 10.1053/j.ajkd.2021.08.005

40. Niesen Michiel JM, Matson R, Puranik A, O'Horo John C, Pawlowski C, Vachon C, et al. Third dose vaccination with mRNA-1273 or BNT162b2 vaccines improves protection against SARS-CoV-2 infection. *PNAS Nexus* (2022) 1(2): pgac042. doi: 10.1093/pnasnexus/pgac042

41. Benotmane I, Gautier G, Perrin P, Olagne J, Cognard N, Fafi-Kremer S, et al. Antibody response after a third dose of the mRNA-1273 SARS-CoV-2 vaccine in kidney transplant recipients with minimal serologic response to 2 doses. *JAMA.* (2021) 326(11):1063–5. doi: 10.1001/jama.2021.12339

42. Lustig Y, Gonen T, Meltzer L, Gilboa M, Indenbaum V, Cohen C, et al. Superior immunogenicity and effectiveness of the third compared to the second BNT162b2 vaccine dose. *Nat Immunol* (2022) 23(6):940–6. doi: 10.1038/s41590-022-01212-3

43. Pajon R, Doria-Rose NA, Shen X, Schmidt SD, O'Dell S, McDanal C, et al. SARS-CoV-2 omicron variant neutralization after mRNA-1273 booster vaccination. *N Engl J Med* (2022) 386(11):1088–91. doi: 10.1056/NEJMc2119912

44. Xia H, Zou J, Kurhade C, Cai H, Yang Q, Cutler M, et al. Neutralization and durability of 2 or 3 doses of the BNT162b2 vaccine against omicron SARS-CoV-2. *Cell Host Microbe* (2022) 30(4):485–8.e3. doi: 10.1016/j.chom.2022.02.015

45. Sette A, Crotty S. Immunological memory to SARS-CoV-2 infection and COVID-19 vaccines. *Immunol Rev* (2022) 310(1):27–46. doi: 10.1111/imr.13089

46. Bonifacius A, Tischer-Zimmermann S, Dragon AC, Gussarow D, Vogel A, Krettek U, et al. COVID-19 immune signatures reveal stable antiviral T cell function despite declining humoral responses. *Immunity.* (2021) 54(2):340–54.e6. doi: 10.1016/j.immuni.2021.01.008

47. Guerrera G, Picozza M, D'Orso S, Placido R, Pirronello M, Verdiani A, et al. BNT162b2 vaccination induces durable SARS-CoV-2-specific T cells with a stem cell memory phenotype. *Sci Immunol* (2021) 6(66):eabl5344. doi: 10.1126/sciimmunol.abl5344

48. Mateus J, Dan JM, Zhang Z, Rydyznski Moderbacher C, Lammers M, Goodwin B, et al. Low-dose mRNA-1273 COVID-19 vaccine generates durable memory enhanced by cross-reactive T cells. *Science* (2021) 374(6566):eabj9853. doi: 10.1126/science.abj9853

49. Tarke A, Coelho CH, Zhang Z, Dan JM, Yu ED, Methot N, et al. SARS-CoV-2 vaccination induces immunological T cell memory able to cross-recognize variants from alpha to omicron. *Cell.* (2022) 185(5):847–59.e11. doi: 10.1016/j.cell.2022.01.015

50. Zhang Z, Mateus J, Coelho CH, Dan JM, Moderbacher CR, Galvez RI, et al. Humoral and cellular immune memory to four COVID-19 vaccines. *Cell.* (2022) 185(14):2434–51.e17. doi: 10.1016/j.cell.2022.05.022

51. Lederer K, Bettini E, Parvathaneni K, Painter MM, Agarwal D, Lundgreen KA, et al. Germinal center responses to SARS-CoV-2 mRNA vaccines in healthy and immunocompromised individuals. *Cell.* (2022) 185(6):1008–24.e15. doi: 10.1016/j.cell.2022.01.027

52. Turner JS, O'Halloran JA, Kalaidina E, Kim W, Schmitz AJ, Zhou JQ, et al. SARS-CoV-2 mRNA vaccines induce persistent human germinal centre responses. *Nature.* (2021) 596(7870):109–13. doi: 10.1038/s41586-021-03738-2

53. Janssen C, Cachanado M, Ninove L, Lachatre M, Michon J, Epaulard O, et al. Immunogenicity and reactogenicity of heterologous and homologous mRNA-1273 and BNT162b2 vaccination: A multicenter non-inferiority randomized trial. *eClinicalMedicine.* (2022) 48:101444. doi: 10.1016/j.eclinm.2022.101444

54. Regev-Yochay G, Gonen T, Gilboa M, Mandelboim M, Indenbaum V, Amit S, et al. Efficacy of a fourth dose of covid-19 mRNA vaccine against omicron. *New Engl J Med* (2022) 386(14):1377–80. doi: 10.1056/NEJMc2202542

55. Munro APS, Janani L, Cornelius V, Aley PK, Babbage G, Baxter D, et al. Safety and immunogenicity of seven COVID-19 vaccines as a third dose (booster) following two doses of ChAdOx1 nCov-19 or BNT162b2 in the UK (COV-BOOST): a blinded, multicentre, randomised, controlled, phase 2 trial. *Lancet* (2021) 398(10318):2258–76. doi: 10.1016/S0140-6736(21)02717-3

56. Kaplonek P, Cizmeci D, Fischinger S, A-r C, Suscovich T, Linde C, et al. mRNA-1273 and BNT162b2 COVID-19 vaccines elicit antibodies with differences in fc-mediated effector functions. *Sci Trans Med* (2022) 14(645):eabm2311. doi: 10.1126/scitranslmed.abm2311

57. De Marco L, D'Orso S, Pirronello M, Verdiani A, Termine A, Fabrizio C, et al. Assessment of T-cell reactivity to the SARS-CoV-2 omicron variant by immunized individuals. *JAMA Network Open* (2022) 5(4):e2210871–e. doi: 10.1001/jamanetworkopen.2022.10871

58. Jung MK, Jeong SD, Noh JY, Kim D-U, Jung S, Song JY, et al. BNT162b2-induced memory T cells respond to the omicron variant with preserved polyfunctionality. *Nat Microbiol* (2022) 7(6):909–17. doi: 10.1038/s41564-022-01123-x

59. Jergović M, Coplen CP, Uhrlaub JL, Beitel SC, Burgess JL, Lutrick K, et al. Cutting edge: T cell responses to B.1.1.529 (Omicron) SARS-CoV-2 variant induced by COVID-19 infection and/or mRNA vaccination are largely preserved. *J Immunol* (2022) 208(11):2461–5. doi: 10.4049/jimmunol.2200175

60. Naranbhai V, Nathan A, Kaseke C, Berrios C, Khatri A, Choi S, et al. T Cell reactivity to the SARS-CoV-2 omicron variant is preserved in most but not all individuals. *Cell.* (2022) 185(6):1041–51.e6. doi: 10.1016/j.cell.2022.01.029

61. Keeton R, Tincho MB, Ngomti A, Baguma R, Benede N, Suzuki A, et al. T Cell responses to SARS-CoV-2 spike cross-recognize omicron. *Nature.* (2022) 603 (7901):488–92. doi: 10.1038/s41586-022-04460-3

62. GeurtsvanKessel CH, Geers D, Schmitz KS, Mykytyn AZ, Lamers MM, Bogers S, et al. Divergent SARS-CoV-2 omicron-reactive T and b cell responses in COVID-19 vaccine recipients. *Sci Immunol* (2022) 7(69):eabo2202. doi: 10.1126/sciimmunol.abo2202

292

Supplementary Material

Longitudinal cellular and humoral immune responses after triple BNT162b2 and fourth full-dose mRNA-1273 vaccination in haemodialysis patients

Matthias Becker[1,#], Anne Cossmann[2,#], Karsten Lürken[3], Daniel Junker[1], Jens Gruber[1], Jennifer Juengling[1], Gema Morillas Ramos[1], Andrea Beigel[3], Eike Wrenger[3], Gerhard Lonnemann[3], Metodi V. Stankov[2], Alexandra Dopfer-Jablonka[2,4], Philipp D. Kaiser[1], Bjoern Traenkle[1], Ulrich Rothbauer[1,5], Gérard Krause[4,6,7], Nicole Schneiderhan-Marra[1], Monika Strengert[6,7,*], Alex Dulovic[1,*], Georg M.N. Behrens[2,4,8,*]

Author Affiliations
1. NMI Natural and Medical Sciences Institute at the University of Tübingen, Reutlingen, Germany
2. Department for Rheumatology and Immunology, Hannover Medical School, Hannover, Germany
3. Dialysis Centre Eickenhof, Langenhagen, Germany
4. German Centre for Infection Research (DZIF), partner site Hannover-Braunschweig, Germany
5. Pharmaceutical Biotechnology, University of Tübingen, Tübingen, Germany
6. Helmholtz Centre for Infection Research, Braunschweig, Germany
7. TWINCORE GmbH, Centre for Experimental and Clinical Infection Research, a joint venture of the Hannover Medical School and the Helmholtz Centre for Infection Research, Hannover, Germany
8. CiiM - Centre for Individualized Infection Medicine, Hannover, Germany

#,* these authors contributed equally to this work.
* corresponding authors.

Corresponding authors contact details:
Monika Strengert, Phone number: +49 (0)531 3103 Email address: monika.strengert@helmholtz-hzi.de, Postal address: Inhoffenstraße 7, 38124 Braunschweig, Germany.
Alex Dulovic, Phone number: +49 (0)7121 51530 580, Email address: alex.dulovic@nmi.de, Postal address: Markwiesenstraße 55, 72770 Reutlingen, Germany.
Georg M.N. Behrens, Phone number: +49 (0)511 532 5337, Email address: behrens.georg@mh-hannover.de, Postal address: Carl-Neuberg-Straße 1, 30625 Hannover, Germany.
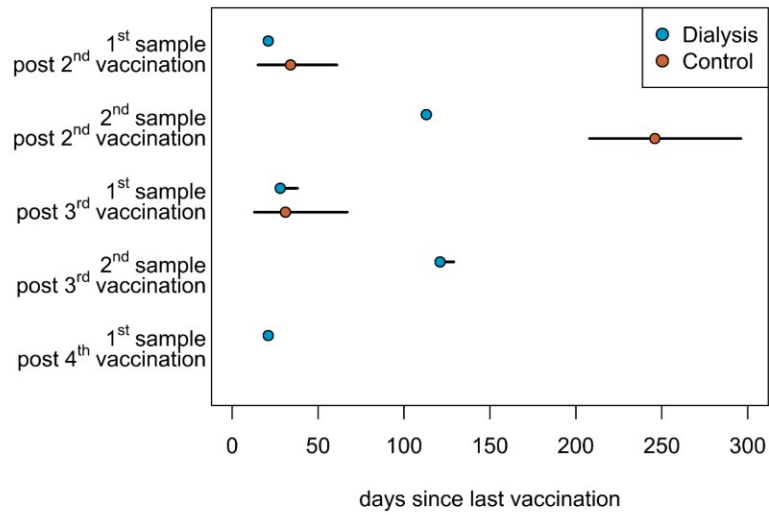
Figure S1. Sampling time points after COVID-19 vaccination in the study population.
Graphic display of median and absolute range of sampling times after the indicated vaccination of haemodialysis patients (n=50, blue circles) and healthcare workers (n=33, orange circles), who served as controls. Controls were triple-vaccinated with BNT162b2 (vaccination 1-3) whereas haemodialysed individuals received an additional full-dose of mRNA-1273 (vaccination 4).
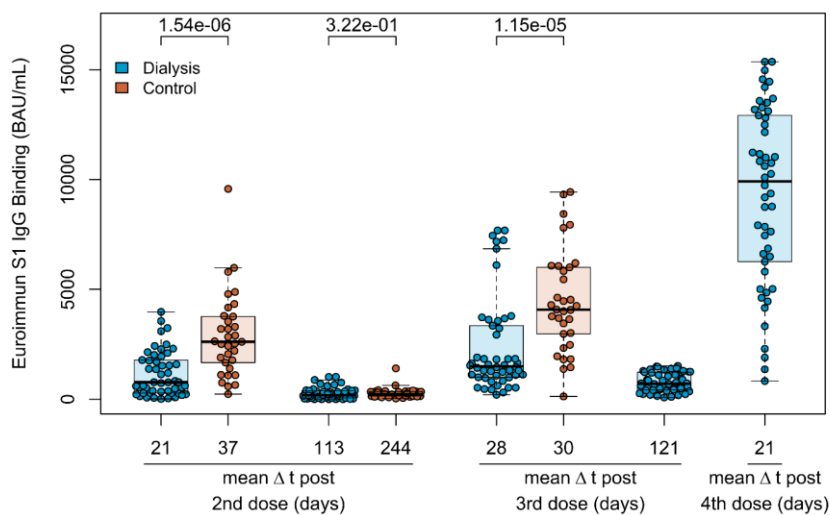
1

Figure S2. Development of quantitative plasma IgG titres after COVID-19 vaccination.
Spike subdomain 1 (S1)-plasma IgG from haemodialysis patients (blue circles, n=50) and controls (orange circles, n=33) were analysed using the QuantiVac-ELISA from Euroimmun (BAU/mL) after a triple vaccination with BNT162b2. For haemodialysed individuals, S1 IgG titres are additionally shown after a fourth 100 μg (full) dose of mRNA-1273. Mean sampling time in days after the respective vaccination is displayed as Δt on the x-axis. Boxes represent the median, 25th and 75th percentiles, whiskers show the largest and smallest non-outlier values. Outliers were determined by 1.5 times IQR. Statistical significance was calculated by two-sided Mann-Whitney-U test. P-values for relevant comparisons are given above the sample groups. Significance was defined as p<0.05. Response data from dialysed individuals from day 21 and day 113 after the second BNT162b2 dose were already published before as part of Strengert *et al.* (1) and Dulovic *et al.* (2).
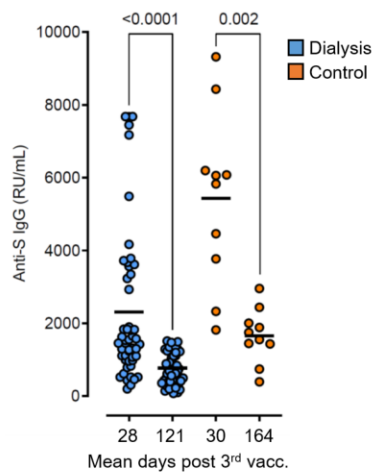
2

Figure S3. Decline in anti-S1 IgG after the third vaccination.
Spike subdomain 1 (S)-plasma IgG of dialysis patients (n=50) and a subgroup of healthy controls (n=10) after the third vaccination. Note that the second time point was slightly different with mean 121 days (range 119-129 days) for dialysis patients and mean 164 days (range 112-223 days) in healthy controls. Reduction mean anti-S1 IgG in dialysis patients and the control group was 3-fold and 3.2-fold, respectively. Statistical significance was calculated by two-sided paired Wilcoxon rank test. Significance was defined as p<0.05.
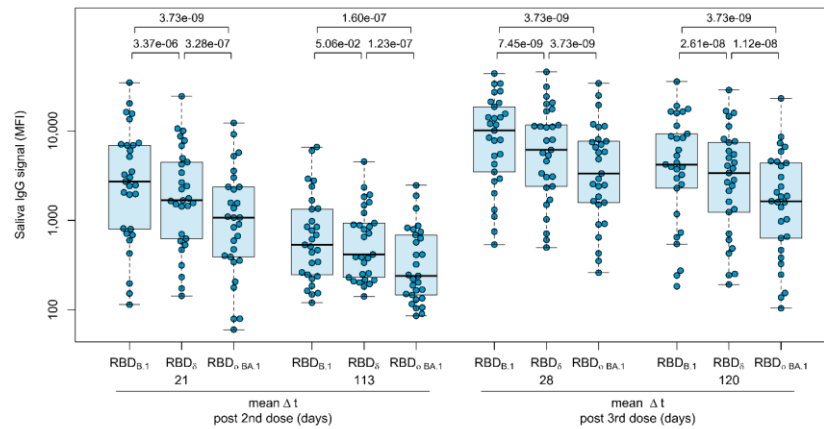
3

Figure S4. Mucosal immune response in haemodialysis patients after triple vaccination with BNT162b2. IgG response in saliva of haemodialysis patients (n=29) towards the SARS-CoV-2 RBD of B.1, Delta and Omicron BA.1 isolates were measured using MULTICOV-AB. Data is displayed as median fluorescence intensity (MFI) signal for IgG binding. Sampling time points in days after a completed standard two-dose BNT162b2 vaccination is stated on the x-axis. Statistical significance was calculated by two-sided paired Wilcoxon rank test. Significance was defined as p<0.05. P-values for relevant comparisons are given above the sample groups. Response data from dialysed individuals from day 21 and day 113 after the second BNT162b2 dose were already published before as part of Strengert *et al.* (1) and Dulovic *et al.* (2).

4

Table S1. Indication for haemodialysis in the study population.

Characteristics	Haemodialysis group (n=50)
Diagnosis (n, %)	
Autosomal dominant polycystic kidney disease	7 (14.0)
Chronic glomerulonephritis	3 (6.0)
Diabetic nephropathy	8 (16.0)
Focal segmental glomerulosclerosis	3 (6.0)
IgA nephropathy	7 (14.0)
Interstitial nephritis	4 (8.0)
Nephrosclerosis	11 (22.0)
Acute toxic tubular epithelial damage syndrome	1 (2.0)
Anti-Neutrophilic Cytoplasmic Autoantibody (ANCA)-associated vasculitis	1 (2.0)
Medullary cystic kidney disease	1 (2.0)
Membranous glomerulonephritis	1 (2.0)
Kidney dysplasia	1 (2.0)
Obstructive nephropathy	1 (2.0)
Cystic kidney disease	1 (2.0)
Cyclosporin intoxication	1 (2.0)

5

Table S2. Medication of study participants. NA - Information not available.

Medication (n, %)	Haemodialysis group (n=50)	Non-dialysis control group (n=33)
Angiotensin-converting enzyme inhibitor	15 (30.0)	2 (6.1)
Statins	28 (56.0)	0 (0.0)
Angiotensin II Receptor Blocker	16 (32.0)	1 (3.0)
Vitamin D Supplements	49 (98.0)	NA
L-Thyroxine	0 (0.0)	3 (9.1)
Ca^{2+} channel antagonist	0 (0.0)	2 (6.1)
5-aminosalicylic acid	0 (0.0)	1 (3.0)
DPP4 inhibitor + metformin	0 (0.0)	1 (3.0)
Factor Xa inhibitor	0 (0.0)	1 (3.0)
Immunosuppressants (dosing range per day)		
Prednisolone (2 mg; every second day)	1 (2.0)	0 (0.0)
Prednisolone (5 mg)*	2 (4.0)	0 (0.0)
Prednisolone (7.5 mg)	1 (2.0)	0 (0.0)
Prednisolone (5 mg), Tacrolimus (1-2 mg)	2 (4.0)	0 (0.0)
Prednisolone (5 mg), Tacrolimus (12 mg), Mycophenolatmofetil (500 mg)**	1 (2.0)	0 (0.0)
Hydrocortisone (20 mg)	1 (2.0)	0 (0.0)
5-Fluorouracil***	1 (2.0)	0 (0.0)

* One patient discontinued prednisolone 128 days after the second and 68 days before the third BNT162b2 dose.
** Mycophenolatmofetil discontinued 166 days after the second and 30 days before the third BNT162b2 dose.
*** First treatment cycle started 63 days before the fourth vaccination with mRNA-1273.

6

Table S3. Statistical comparison of longitudinal cellular and humoral vaccination responses in haemodialysis patients.

Assay	Variant	Figure	Sample 1 vs 2	Sample 1 vs 3	Sample 3 vs 4	Sample 3 vs 5
MULTICOV-AB	B.1	3a	$1.51*10^{-9}$	$1.61*10^{-9}$	$2.44*10^{-9}$	$1.05*10^{-9}$
RBDCoV-ACE2	B.1	3b	0.005	$7.79*10^{-10}$	$4.38*10^{-9}$	$7.79*10^{-10}$
RBDCoV-ACE2	Delta	3c	0.013	$1.15*10^{-9}$	$1.20*10^{-8}$	$7.79*10^{-10}$
RBDCoV-ACE2	Omicron BA.1	3d	0.002	$3.52*10^{-7}$	$8.48*10^{-7}$	$1.15*10^{-9}$
IGRA	B.1	4a	$1.38*10^{-5}$	0.564	NA	0.0005

References

1. Strengert M, Becker M, Ramos GM, Dulovic A, Gruber J, Juengling J, et al. Cellular and humoral immunogenicity of a SARS-CoV-2 mRNA vaccine in patients on haemodialysis. EBioMedicine. 2021;70:103524.
2. Dulovic A, Strengert M, Ramos GM, Becker M, Griesbaum J, Junker D, et al. Diminishing Immune Responses against Variants of Concern in Dialysis Patients 4 Months after SARS-CoV-2 mRNA Vaccination. Emerg Infect Dis. 2022;28(4):743-50.

7